Thomas White · Matthias Jonas
Zbigniew Nahorski · Sten Nilsson *Editors*

Greenhouse Gas Inventories

Dealing With Uncertainty

Springer

Foreword

At the beginning of the 1970s, at the height of the Cold War, it was believed that the scientific community could be an important element of future détente between the main political superpowers, the Soviet Union and the United States, and their allies in the Eastern and Western political blocs. It was therefore decided to establish a scientific institution whose main aim would be to build bridges between these two competing political and economic systems. The International Institute for Applied Systems Analysis (IIASA) was founded in 1972 by 12 countries. Poland, represented by the Polish Academy of Sciences (SRI PAS), was one of the founding countries of IIASA and has continuously collaborated with the Institute ever since.

Polish scientists joined the international scientific community of IIASA with great enthusiasm. Working with leading scientists from different countries helped Poland to establish new areas of scientific activity focused on interdisciplinary research. As a result of cooperation with IIASA, Poland has initiated large research programs to address problems such as the development of rural areas and the establishment of rational water policies. The important Polish contribution to the work of IIASA has also been noteworthy, especially in the application of optimization methods for solving complex decision problems.

After the breakdown of the Communist system the role of IIASA changed. IIASA now applies its main asset—expertise in solving complex problems using rigorous scientific methodology—to tackling problems of regional and global dimensions. Polish scientists working in IIASA's multinational teams have been involved in many important research activities such as efforts against transboundary air pollution. Polish scientific expertise, especially in the area of building mathematical and computer models of complex phenomena, has contributed to important research programs at IIASA addressing problems related to climatic change. As the impact of human activities on climate, especially those related to energy generation and consumption, is of great importance to Poland, the Polish scientific community is determined to continue their research engagement in this important field.

The present book is an example of the cooperative activities of IIASA and Polish researchers. It is an outcome of the 2nd Workshop on Uncertainties of Greenhouse Gas Inventories, the second of the three triennial Workshops organized by IIASA and the Systems Research Institute, Polish Academy of Sciences. The first Workshop took place in Warsaw, Poland, in 2004, the second in Laxenburg, Austria, in 2007, and the third in Lviv, Ukraine, in 2010 with the support of the Lviv Polytechnic National University. This series of Workshops, devoted to topical investigations on the impacts of human activities on climatic changes represents an important contribution of IIASA and Polish researchers cooperation to the world community.

May I wish the IIASA and the worldwide scientific community every success in their future cooperative endeavors.

Professor Michał Kleiber
President of the Polish Academy of Sciences

Warszawa
January 25, 2011

Climatic Change (2010) 103:3–18
DOI 10.1007/s10584-010-9922-6

Benefits of dealing with uncertainty in greenhouse gas inventories: introduction

Matthias Jonas · Gregg Marland · Wilfried Winiwarter · Thomas White · Zbigniew Nahorski · Rostyslav Bun · Sten Nilsson

Received: 7 April 2010 / Accepted: 15 June 2010 / Published online: 15 July 2010

Abstract The assessment of greenhouse gases emitted to and removed from the atmosphere is high on the international political and scientific agendas. Growing international concern and cooperation regarding the climate change problem have increased the need for policy-oriented solutions to the issue of uncertainty in, and related to, inventories of greenhouse gas (GHG) emissions. The approaches to addressing uncertainty discussed in this Special Issue reflect attempts to improve national inventories, not only for their own sake but also from a wider, systems analytical perspective—a perspective that seeks to strengthen the usefulness of national inventories under a compliance and/or global monitoring and reporting framework. These approaches demonstrate the benefits of including inventory uncertainty in policy analyses. The authors of the contributed papers show that considering uncertainty helps avoid situations that can, for example, create a false sense of certainty or lead to invalid views of subsystems. This may eventually prevent related errors from showing up in analyses. However, considering uncertainty does

M. Jonas (✉) · W. Winiwarter · S. Nilsson
International Institute for Applied Systems Analysis, Schlossplatz 1, 2361 Laxenburg, Austria
e-mail: jonas@iiasa.ac.at

G. Marland
Carbon Dioxide Information Analysis Center, Oak Ridge National Laboratory, Oak Ridge, TN, USA

W. Winiwarter
AIT Austrian Institute of Technology, Vienna, Austria

T. White
Canadian Forest Service, Victoria, BC, Canada

Z. Nahorski
Systems Research Institute, Polish Academy of Sciences, Warsaw, Poland

R. Bun
Lviv Polytechnic National University, Lviv, Ukraine

not come for free. Proper treatment of uncertainty is costly and demanding because it forces us to make the step from "simple to complex" and only then to discuss potential simplifications. Finally, comprehensive treatment of uncertainty does not offer policymakers quick and easy solutions. The authors of the papers in this Special Issue do, however, agree that uncertainty analysis must be a key component of national GHG inventory analysis. Uncertainty analysis helps to provide a greater understanding and better science helps us to reduce and deal with uncertainty. By recognizing the importance of identifying and quantifying uncertainties, great strides can be made in ongoing discussions regarding GHG inventories and accounting for climate change. The 17 papers in this Special Issue deal with many aspects of analyzing and dealing with uncertainty in emissions estimates.

1 Introduction

Accounting for greenhouse gas (GHG) emissions has emerged as an issue of considerable interest. While the scientific community is working for understanding of geochemical cycles, public policy is aiming to limit and decrease emissions and thereby to mitigate global climate change. The issues of monitoring and verification of international or subnational commitments to reducing emissions are receiving increasing attention (e.g., NRC 2010).

Markets for trading emission permits are emerging. Decision makers are very interested in understanding the risks of increasing emissions and the opportunities for mitigation. An earlier collection of papers (Lieberman et al. 2007) raised many of the issues associated with uncertainty in emissions accounting and this is the continuing concern of this special volume of research papers.

The current task under the United Nations Framework Convention on Climate Change (UNFCCC) is to agree on a climate treaty that comes into force in 2012, the year in which commitments under the Kyoto Protocol will cease (FCCC 2009a, b). Leaders of the world's major industrialized countries have formally agreed, in the wake of the 2009 UN climate change conference in Copenhagen, that the average global temperature should not increase by more than 2°C from its preindustrial level (FCCC 2009c; Schiermeier 2009; WBGU 2009a, b). Compliance with this temperature target can be expressed equivalently in terms of limiting cumulative GHG emissions, for example, up to 2050, while considering the risk of exceeding this target (Meinshausen et al. 2009). The emission reductions required are substantial: 50–80% below the 1990 level at the global scale, with even greater reductions for industrialized countries (EU 2009; Schiermeier 2009; WBGU 2009b).[1]

Given the formidable task ahead, we are confronted with the uncertainty inherent in estimating emissions and the challenges involved in monitoring commitments and supporting markets for emissions trading. What are the benefits of dealing directly with uncertainty?

[1]Emission reductions for industrialized countries until 2050 typically range in the order of 70–90% below their 1990 levels if the cumulative GHG emissions constraint of Meinshausen et al. (2009) for a 2°C temperature increase (with a risk of 10–43% of exceeding it) is expressed on a per-capita basis, with global population projected for 2050 taken from http://www.iiasa..ac.at/Research/POP/proj07/index.html.

The answer to this question, given by the participants of the 2nd International Workshop on Uncertainty in Greenhouse Gas Inventories, held 27–28 September 2007, in Laxenburg, Austria, was unanimous: we need to make use of uncertainty analysis in developing clear understanding and informed policy. Uncertainty matters, and is key to many issues upstream and downstream of emission inventories. Dealing proactively with uncertainty allows useful knowledge to be generated that the international community of countries would wish to have at hand before negotiating international environmental agreements such as the Kyoto Protocol or its successor. Generating this knowledge and understanding should not wait until countries agree on a formula that will translate an approved global emissions constraint to the sub-global level and allocate global emission shares to countries.

This Special Issue of *Climatic Change* brings together 17 key papers presented at the 2nd Uncertainty Workshop, which was jointly organized by the Austrian-based International Institute for Applied Systems Analysis (http://www.iiasa.ac.at/) and the Systems Research Institute of the Polish Academy of Sciences (http://www.ibspan.waw.pl/). This collection of insights and techniques captures recent thinking on why and how dealing properly with uncertainty is important as we confront the legal and technical issues of trying to mitigate global climate change. In this introduction we describe the overall setting of the Workshop and provide an introduction to the individual contributions and to the group consensus. The latter grew from the various scientific discussions and retreats during the Workshop. The participants at the 2nd Uncertainty Workshop sensed the increasing awareness of the importance of dealing with uncertainty. Moreover, methods for dealing with uncertainty are improving through research efforts such as those summarized in this volume.

2 The challenges of dealing with uncertainty are still with us

Under the UNFCCC, developed-country parties to the Convention (so-called Annex I countries) have, since the mid-1990s, published annual or periodic national inventories of GHG emissions and removals. Policymakers use these inventories to develop strategies and policies for emission reductions and to track the progress of those strategies and policies. Where formal commitments to limit emissions exist, regulatory agencies and corporations rely on emission inventories to establish compliance records. Scientists, businesses, other interest groups, and the public use inventories to better understand the sources and trends in emissions (see also, Lieberman et al. 2007: 1–4).

However, GHG inventories (whether at the global, national, corporate, or other level) contain uncertainties for a variety of reasons, and these uncertainties have important scientific, economic, and policy implications. The uncertainty of emissions estimates can be dealt with proactively. Proper treatment of uncertainty affects everything from our understanding of the physical system to the politics of mitigation agreements and the economics of mitigation strategies. A comprehensive and consistent understanding of, and a framework for dealing with, the uncertainty of emissions estimates has a large impact on the functioning and effectiveness of the Kyoto Protocol and its awaited successor.

Central to policy concerns and the present discussion alike is the need for a better definition of the role of uncertainty analyses in national GHG inventories, as well as

in other inventories (e.g., for mitigation projects) falling under the purview of international or national regulatory schemes. At present, parties to the UNFCCC listed in Annex I (industrialized countries and countries undergoing economic transition) are obliged to include in the reporting of their annual inventories direct or alternative estimates of the uncertainty associated with these emissions and removals, consistent with the good practice guidance reports of the Intergovernmental Panel on Climate Change (IPCC) (FCCC 2006a; Penman et al. 2000, 2003). Inventory uncertainty is monitored, but not regulated, under the Kyoto Protocol. International schemes such as European Union (EU) emissions trading or that established by the Kyoto Protocol, if they are to function as binding agreements, must be able to demonstrate that estimates regarding emission changes are not only measurable but also that they outstrip the uncertainty metric with which they are associated.

3 The key arguments for dealing proactively with uncertainty are becoming increasingly relevant

It makes a big difference to the framing of policies whether or not uncertainty is considered either reactively, because there is a need to do so, or proactively, because impediments are anticipated. Uncertainty estimates are not intended to dispute the validity of national GHG inventories; however, grasping the uncertainty of emission estimates serves to underscore the lack of accuracy that characterizes many source and sink categories. There is wide agreement that the consideration of uncertainty can help to identify opportunities for improvements in data measurement, data collection, and calculation methodology. But it is only by identifying elements of high uncertainty that actual methodological changes can be introduced to address them. Currently, most countries that perform uncertainty analyses do so for the express purpose of improving their future estimates; and the rationale is generally the same at the corporate and other levels. Estimating uncertainty helps to prioritize resources and to take precautions against undesirable consequences, thus establishing a more robust foundation on which to base policy.

The issues of concern at the 2nd Uncertainty Workshop continued to be rooted in the level of confidence with which national emission inventories can be performed. The research papers presented at the Workshop demonstrate that these concerns go beyond verification, compliance, and trading of GHG emissions, which were the issues of concern covered by Lieberman et al. (2007). The topics addressed at the 2nd Uncertainty Workshop covered:

1. Achieving reliable GHG inventories at national and sector scales and reporting uncertainties reliably at, and across, these scales (see especially the papers by Winiwarter and Muik 2010; Szemesová and Gera 2010; and van Oijen and Thomson 2010)
2. Bottom-up versus top-down GHG emission analyses (see especially the papers by Ciais et al. 2010; Rivier et al. 2010; Verstraeten et al. 2010; Shvidenko et al. 2010; and Gusti and Jonas 2010)
3. Reconciling short-term emission commitments and long-term concentration targets; and detecting and analyzing GHG emission changes vis-à-vis uncertainty, and addressing compliance (see especially the papers by Jonas et al. 2010; and Bun et al. 2010a)

4. Issues of scales of GHG inventories (see especially the papers by Bun et al. 2010b; Leip 2010; and Horabik and Nahorski 2010); and
5. Trading emissions (see especially the papers by Ermolieva et al. 2010; Stańczak and Bartoszczuk 2010; Nahorski and Horabik 2010; and Pickl et al. 2010)

All five topics were discussed individually and in depth at the Workshop. However, the interlinked and interdisciplinary setting of the Workshop allowed for scientific retreats during which all topics could be reviewed in context and from a holistic perspective, which allowed insights to emerge that could be fully scrutinized. This made it possible to strike a balance in dealing with topics that were seen as controversial.

4 The topics addressed

4.1 Achieving reliable GHG inventories

The comparison of inventories across countries or regions within countries, and across sectors received wide attention. There are a number of approaches to testing the quality of our uncertainty knowledge, to putting the uncertainty estimates of countries into context, and to helping us to understand the differences in estimates. Typically, only a few emission sources dominate the overall uncertainty of national emissions inventories. While, in general, the economic structure of a country influences the emission sources that contribute to uncertainty, there is currently only one major source that is uniquely uncertain for all countries: the nitrous oxide (N_2O) emissions from soils. The dominance of one source has consequences for calculating uncertainty, especially with regard to splitting the source into direct and indirect emissions following the IPCC GHG inventory guidelines (Eggleston et al. 2006, vol. 4). Winiwarter and Muik (2010) argue, based on their in-depth study on Austria, that the split sources need to be considered as being statistically interdependent, a fact that cannot be considered by the simpler methodology recommended by IPCC for uncertainty assessment, namely, the error propagation approach. When this interdependency is covered in a more elaborate Monte Carlo algorithm, the overall national GHG inventory uncertainty increases. Results thus need to be understood in a methodology-dependent context, making it even more difficult to provide meaningful comparisons between countries unless methodologies are laid open in detail. In general, correlating uncertainty properly appears to be more important than switching from less- to more-sophisticated tiers in analyzing uncertainty.

Uncertainty is inherently higher for some GHGs and sectors of an inventory than for others. Estimates of N_2O emissions tend to be more uncertain than those of methane (CH_4) and CO_2. As another example, the landfill (see Szemesová and Gera 2010) and the land use, land use change, and forestry (LULUCF) sectors[2] have higher uncertainties than other sectors. Wetlands are a typical example of a sector with high uncertainty. The emissions from wetlands can be sizable and are highly uncertain; not least because transient environmental conditions, anthropogenic or natural, can turn wetlands from a GHG source into a GHG sink, and vice versa

[2]Another and alternative acronym introduced by the 2006 IPCC Guidelines for National Greenhouse Gas Inventories (IPCC 2006: vol. 4) is AFOLU (agriculture, forestry and other land use).

(Eggleston et al. 2006: vols. 4, 5; Pandey et al. 2007). It is important to recognize the existence of these higher relative uncertainties. They raise the possibility that some components of a GHG inventory could be treated differently from others in the design of future policy agreements. Furthermore, limiting the reporting of GHG emissions and removals under the current inventory framework to anthropogenic sources and sinks creates additional difficulties, including uncertainty regarding the proper designation of which particular activities are anthropogenic and which are natural (see also full GHG accounting below). Alternative *modi operandi*, could include, for example, (1) the option of not pooling subsystems, including sources and sinks, with different relative uncertainties, but treating them individually and differently; and (2) the option of not splitting the terrestrial biosphere into directly human-impacted (managed) and not-directly human-impacted (natural) parts to avoid, among other things, sacrificing bottom-up/top-down verification, as there is no atmospheric measurement that can discriminate between the two (Jonas et al. 2009).

How to approach GHGs and sectors individually and differently was certainly not explored in the framing of the Kyoto Protocol. It is essential to bear in mind that inventorying the more certain GHG emissions from a specific sector on a corporate level can be a huge challenge. Accurately inventorying the upstream and downstream emissions of globally operating oil and gas companies serves as a good example of the inventory challenges involved. During recent years, these companies have become quite aware of their need for high quality data and harmonized measurements, monitoring, and uncertainty assessment methods; they have also realized the need to develop their own, tailored guidelines that will facilitate compliance with diverse GHG regimes (API 2004; IPIECA 2003, 2009).

The LULUCF sector with its spatially distributed emissions provides by far the largest challenges for emissions accounting (e.g., N_2O from soils or from wetlands, together with CO_2 and CH_4). The LULUCF sector's list of crucial issues is unusually long—it is difficult to squeeze them into the inventory framework considered under the Kyoto Protocol. A major reason is that the mechanisms driving changes in carbon inventories reflect both natural ecosystem processes and the direct and indirect effects of human actions. The tools for quantifying impacts of the direct effects of humans and of certain ecosystem processes are quite mature. Bayesian approaches, for example, are powerful but under-utilized tools, not only for reducing parameter errors but for combining different kinds of information and integrating across different approaches to provide a single answer. Van Oijen and Thomson (2010) make use of a Bayesian approach to account for the spatial heterogeneity in soils and weather to calculate conifer forest productivity and carbon sequestration for the whole of the United Kingdom.

Except from these specific processes, however, a wide range of indirect ecosystem responses still require significantly improved characterization in order to be adequately quantified and attributed (Field 2007). Progress in attributing and projecting changes in large-scale carbon balances—their dynamics cover a wide range of time scales—will require fundamental advances in understanding and modeling the interactions between human and ecosystem processes. Inventory techniques for quantifying ecosystem carbon stocks and stock changes are improving, as they develop from being a foundation for assessing harvestable forest resources toward being a set of general tools for supporting carbon accounting. The challenges, however, in moving from timber industry statistics to general carbon accounting are daunting and far

from being completely resolved. The advances required include not only the ability to quantify the carbon in soils and non-marketable components of the vegetation but also the ability to extend the analysis to ecosystem types not covered in traditional forest inventories. Remote sensing with LIDAR and RADAR are among the most promising techniques for efficiently extending inventories to poorly characterized ecosystems, including tropical forests, savannas, shrublands, and tundra (see, e.g., Stanford University's Carnegie Airborne Observatory: http://cao.stanford.edu).

Attributing changes in ecosystem carbon stocks to particular mechanisms is complicated. However, neither inventory techniques nor simulation models are well positioned to unravel the diversity of complex mechanisms and the range of possible interactions among these mechanisms.

4.2 Bottom-up versus top-down GHG emission analyses

Top-down accounting takes the atmosphere perspective. The atmosphere mixes and integrates surface fluxes that vary spatially and temporally. Top-down accounting relies on observations of atmospheric CO_2 concentrations (and those of other GHGs), changes in concentrations, atmospheric circulation, and atmospheric modeling to infer net fluxes from land and ocean sources, and their regional distributions. Bottom-up accounting takes the opposite perspective. It relies on observations of stock changes or net fluxes at the Earth's surface and infers the changes in the atmosphere. Full carbon (and GHG) accounting—estimating all land-based fluxes, whether human-induced or not—is necessary to reconcile the top-down and bottom-up approaches. However, this comparison is not straightforward and must be done with caution (see also Denman et al. 2007: Section 7.3.2.3).

Atmospheric inversions have proven to be a useful top-down approach for quantifying carbon fluxes at large scales. Inversions allow the mismatch between modeled and observed concentrations to be minimized, and thus measurement and model errors to be accounted for. In inversions, fossil fuel emissions are typically believed to be perfectly known so that their contribution to the CO_2 concentration in the atmosphere can be easily modeled and subtracted to solve for the remainder, the regional distribution of land and ocean fluxes. However, for the majority of countries the foundations of this assumption are weak (Marland 2008). The uncertainty number (6–10% for the global total of emissions, based on a 90% confidence interval) that Marland and Rotty (1984) published for global fossil-fuel CO_2 emissions in 1982 is not often considered and has never been formally reworked.

Ciais et al. (2010) review the potentials and perspectives of atmospheric inversion to anticipate its emerging limitations in terms of extending atmospheric inversion to smaller scales, for example, inadequate as well as insufficient data and resolving atmospheric transport in global models, Atmospheric inversion is seen as playing a role as one of several observing strategies for the global carbon cycle, especially in detecting carbon cycle feedbacks resulting from climate change and other large-scale signals. Atmospheric inversions are envisioned as a continuing complement to surface flux models or surface observations and inventories.

Rivier et al. (2010) demonstrate the usefulness of the atmospheric inversion approach, if used at large scales, to advance our understanding of the carbon cycle regionally and its relevance to mitigation policies at these scales. The authors perform a CO_2 monthly inversion for the years 1988–2001 to estimate the net

ecosystem exchange (NEE) for the whole of Europe, revealing a small sink of −0.1 ± 0.4 Gt C/y (based on a 68% confidence interval). Their regional analysis shows a "flux dipole" with a strong annual carbon sink in the southwest and a small annual source in the northeast of Europe, while their seasonal analysis shows a shift over time in the period of maximum carbon uptake from June to July.

While remote sensing is being used more often to assess ecosystem carbon fluxes, its use is still infrequent. In their study, Verstraeten et al. (2010) illustrate how remotely sensed soil moisture data (soil water index) can be integrated into an already existing carbon balance model. Their integration exercise underlines the important impact that soil moisture has on the magnitude as well as on the spatial pattern of carbon exchange. Estimated net ecosystem production (NEP) decreases in many areas when soil moisture is fully taken into account, shifting some European countries from being an apparent sink to being an apparent source of carbon.

Full GHG accounting, meaning the full accounting of all emissions and removals, including all greenhouse gases, is a prerequisite for reducing uncertainties in our understanding of the global climate system. A verified full carbon accounting, including all sources and sinks of both the technosphere and the biosphere, considered continuously over time, would allow the research and inventory communities to:

- Present a real picture of emissions and removals at national to continental scales;
- Avoid ambiguities generated by such terms as "managed biosphere," "base-line activities," "additionality," etc.; and,
- Perhaps most importantly, provide reliable and comprehensive estimates of uncertainties that cannot necessarily be achieved using the current approach under the UNFCCC and the Kyoto Protocol, which provide for only partial accounting of GHG sources and sinks. It is virtually impossible to estimate the reliability of any system output if only part of the system is considered.

Shvidenko et al. (2010) explore the limits of employing a full carbon accounting (FCA) approach in support of the Kyoto Protocol. By integrating all available information sources, including empirical landscape-ecosystem approaches and process-based vegetation models, the authors show that the net biome production of their study region, a large boreal forest ecosystem region in Siberia, can be constrained and estimated with relative uncertainty of as little as ∼60–80% and, by way of comparison, its net ecosystem production with uncertainty of ∼35–40% (based on a 90% confidence interval). Although the authors emphasize the substantial effort needed in applying such a multiply constrained systems approach, this must be considered as a very useful way of cross checking partial carbon accounts that are reported under the UNFCCC and that follow incomplete system views. It would thus be up to policymakers to decide how the FCA is used; that is, to decide whether the results of FCA should be used for "crediting" in the sense of the Kyoto Protocol (i.e., for compliance) or only for "accounting," as under the UNFCCC currently.

This perception is strengthened by Gusti and Jonas (2010) who address the gap that still exists between bottom-up and top-down in accounting for net carbon dioxide emissions. Their study focus is on the terrestrial biosphere of Russia, a signatory state to the Kyoto Protocol, and large enough to be resolved in a bottom-up/top-down exercise. For the whole of Russia during 1988–1992, the authors estimate an atmospheric loss, or net flux to Russia's terrestrial biosphere (uptake) with uncertainty of the order of 100% (based on a 90% confidence interval).

4.3 Reconciling short-term emission commitments and long-term concentrations targets; and detecting and analyzing GHG emission changes vis-à-vis uncertainty, and addressing compliance

The consideration of uncertainty can help to identify opportunities for improvement in data measurement, data collection, and calculation methodology, for resources to be prioritized and precautions to be taken against undesirable consequences, and thus for a more robust foundation for policy to be laid.

However, this may not be the full extent of the utility of uncertainty analysis. Another still widely debated rationale for performing uncertainty analysis is to provide a policy tool, a means to adjust inventories or analyze and compare emission changes so as to be able to determine compliance or the value of a transaction. While some experts find the quality of uncertainty data associated with national inventories insufficient for these purposes, others offer justification for conducting uncertainty analyses to inform and enforce policy decisions. Some experts suggest revising the system of accounting on which current reduction schemes are based, while others seek to incorporate uncertainty measurements into emission and emission change analysis procedures. The latter could offer policymakers enhanced knowledge and additional insights on which to base GHG emission reduction measures.

In the literature on climate change policy modeling at the national and international scale, there has been virtually no treatment of uncertainty in GHG inventories (inventory uncertainty is monitored, but not regulated, under the Kyoto Protocol). The only provision under the UNFCCC is for adjustments in emissions to be made for missing or misreported data (FCCC 2006b: Decision 20/CMP.1). This raises questions as to what the benefits are of including inventory uncertainty in policy analysis, and also of accounting for it in the implementation of policy, as opposed to just controlling those emissions that can be definitely reported.

The consequence of including inventory uncertainty in policy analysis has not been quantified to date. The benefit would be both short-term and long-term, for example, an improved understanding of compliance (already a research focus) or of the sensitivity of climate stabilization goals to the range of possible emissions, given a single reported emissions inventory. That is, given that emissions paths are sensitive to starting conditions and uncertain relative to what is being mandated, what is the probability that long-term targets might be missed? Further efforts in the latter direction are critical for addressing the practical concerns of policymakers.

The current policy approach of ignoring inventory uncertainty altogether, whether at the country, sector, corporate, or other level, is problematical. Emission reductions are activity- and gas-dependent and can range widely. Biases (discrepancies between true and reported emissions) are not uniform across space and time and can discredit flux-difference schemes which tacitly assume that biases cancel out. Human impact on nature is not necessarily constant and/or negligible and can jeopardize a partial GHG accounting approach that is not a logical subset of, and safeguarded by, a full GHG accounting approach. Thus, the legitimate concern is that a policy agreement is trying to tie down a system that is considered certain but is not truly controlled. Being aware, and knowing, of the uncertainties involved will help to strengthen political decision making. Of course, uncertainties are frequently reported, even by experts, with a false sense of uncertainty. But practice will allow the expert community involved to deal with uncertainty increasingly more accurately. The logical step for

policymakers would be to decide whether the post-Kyoto agreement will have good and clear rules to incorporate uncertainty and which parts of an emissions inventory will undergo stringent compliance while accounting for uncertainty, as opposed to consistent reporting under a global monitoring framework.

Such a step is overdue, as underlined by ongoing research that aims to improve our understanding of compliance under uncertainty and to make use of uncertainty at the scale of and across countries. Jonas et al. (2010) apply and compare six techniques to analyze the uncertainty in the emissions changes that countries agreed to realize by the end of the Kyoto Protocol's first commitment period, 2008–2012. The techniques all perform differently and can thus have a different impact on the design and execution of emission control policies. However, any of the techniques, if implemented, could "make or break" claims of compliance, especially in cases where countries claim fulfillment of their commitments to reduce or limit emissions. Jonas and collaborators argue that a single best technique cannot yet be identified, the main reason for this being that the techniques suffer from shortfalls that are not scientific but are related to the way the Protocol has been framed and implemented politically: (1) the overall neglect of uncertainty confronting experts with the situation that for most countries the agreed emission changes are of the same order of magnitude as the uncertainty that underlies their combined CO_2 equivalent emissions; and (2) the introduction of nonuniform emission reduction commitments from country to country. However, the two shortfalls could be easily overcome under a political regime that plans with foresight and prudence.

Bun et al. (2010a) apply one of the aforementioned techniques in an educational exercise, which allows the GHG inventories of countries under the Kyoto Protocol to be examined from the perspective of supply and demand of emission credits (allowances) in an emissions change-uncertainty context rather than in an emissions-only context. The applied boundary condition—countries balance their supply and demand among each other—facilitates the focus but does not limit the authors' conclusions. They show that, when taking uncertainty into account, not all of the countries are credible emission sellers, as the risk remains that these countries' true (but unknown) emissions exceed allowed levels. Limiting this risk considerably influences the countries' supply–demand balance. Countries can sell less, and must buy more, emission allowances if the risk is decreased that the countries' emissions exceed allowed levels. Considering uncertainty can also be seen as bringing the future closer to the present. Some countries—notably, Russia and Ukraine—can sell much of their emissions allowances, as GHG emissions in these countries are far below their agreed Kyoto targets. However, their collective GHG emissions have increased since around 2000, and appear likely to increase unabated and to exceed their Kyoto targets in the near future, which is when the supply of allowances is exhausted. This situation, the break-down of the supply side, will arise much sooner if uncertainty is considered.

4.4 Issues of scales of GHG inventories

Studying GHG inventories across spatial and temporal scales, including upscaling and downscaling, is not only carried out to achieve better insight into emissions but can also help in identifying errors in regional inventories (e.g., with regard

to LULUCF) and validating inventory procedures from a consistency point of view. Operating with data across scales of heterogeneous quality, including inventory data, is becoming commonplace. Research needs seem to be understood, such as the development of spatio-temporally resolved emission factors and their dependencies. However, although it is recognized that working across scales also requires knowledge of uncertainty, the benefits of actually including uncertainty are less explored and understood, particularly the newly involved boundary conditions and forthcoming research needs. The following papers serve as examples of the benefits that can be gained from explicitly including uncertainty in spatio-temporal analyses.

To provide a basis for regionally targeted mitigation measures, Bun et al. (2010b) spatially reference GHG emissions and removals, including their uncertainties, across the territory of the Ukraine. This allows GHGs and their uncertainties to be analyzed individually by region, gas, sector, etc. and tested against approaches—including Monte Carlo analyses—that capture emission factors, activity data, etc., and uncertainties nationally in the form of single numbers or distributions. The difference in relative uncertainty (~2%, based on a 95% confidence interval) found for the energy sector of the Lviv region is noteworthy.

Leip (2010) presents a new methodology to estimate the uncertainties for the categories subsumed under the agriculture sector in the GHG inventory of the European Community (EU15). This methodology allows a more transparent comparison of the uncertainty of GHG inventories across countries and could thus be used to focus on efforts to improve GHG emission estimates at a supra-national level. Not surprisingly, N_2O emissions from agricultural soils are found to dominate the uncertainty not only of the agricultural sector, but also of the overall GHG inventory for many countries. The author's analysis also shows that differences in the countries' uncertainty data are mainly based on different input data for the calculations. Thus, the challenge is to put uncertainty estimates for activity data and emission factors on a solid and common basis, and to harmonize the concepts underlying the uncertainty assessment.

Horabik and Nahorski (2010) study spatially distributed inventory data for N_2O emissions from municipalities in southern Norway, tackling situations where inventory extensions beyond their present coverage have to be developed using, as proxy data, emission activities which are more frequently available than activity data themselves. Examining the spatial covariance in the data—the authors use a conditional autoregressive model—it is possible to compensate for the weaker explanatory power of proxy information and thus to improve inventory accuracy. Formally, the spatial extension of inventories is treated as a prediction task within a statistical framework. Compared to a non-spatial approach, a 15% reduction in the mean square prediction error was obtained.

4.5 Trading emissions

With uncertainty in GHG emissions inventories that can be quite large and can vary significantly by country, gas, sector, source and/or sink, the focus of international agreements and mitigation activities is still on achieving maximum benefit with minimum economic cost. Thus international and national programs provide for the

trading of emissions "permits." Inventory uncertainty is not considered to have a bearing on emissions trading. However, if reliably and quantitatively assessed uncertainty were to be incorporated, a host of questions would arise: How can trading systems account for uncertainty and yet ensure that trading really does provide both environmental and economic benefits? Can methods for incorporating uncertainty be easily standardized? Is a price mechanism better able to deal with uncertainty than a cap and trade system? Can uncertain CO_2 emissions from fossil-fuel use in one country be credibly and economically offset with uncertain reductions in CH_4 emissions from agriculture in another country? Can trading or offset systems, or emission taxes, be designed to recognize or deal with the issues of uncertainty? The papers in this series focus largely on issues of trading emissions permits and the role of uncertainty.

Ermolieva et al. (2010) make use of a basic multi-agent, stochastic model of emissions trading to analyze the stability and robustness of carbon markets, while taking into account the uncertainty in estimates of natural and human-related emissions. The authors' concern is that trading markets do not necessarily minimize abatement costs or comply with environmental targets because the markets respond to stochastic "disequilibrium" price signals that are often driven by market speculations and bubbles. The authors' computer-based model allows emission trading to be studied from a decentralized equilibrium perspective, that is, when trading partners themselves choose, without revealing their knowledge on costs and uncertainties, the optimal level of technological abatement and the traded amount under the condition of minimized costs and compliance with long-term environmental constraints.

It is generally perceived that implementing a system of tradable emission permits will allow a seller with low abatement costs to sell permits to a buyer with high abatement costs, thus equalizing marginal abatement costs. Stańczak and Bartoszczuk (2010) simulate the trading process while accounting for the transaction prices of emission permits. With the goal of minimizing the cost of meeting emissions commitments or trading agreements, negotiated permit prices will result in trades when the cost of permits is lower than the cost of reductions for the buyer and vice versa for the seller. The aim of the paper is to simulate by taking uncertainty into account the evolution of prices on the basis of an iterative trading procedure, for which the authors make use of an evolutionary (multi-heuristic) algorithm.

The issue of compliance with emission restrictions or trading agreements is accentuated when there is high uncertainty in emission inventories. High uncertainty can lead to undershooting (i.e., keeping emissions well below the agreed target) in order to decrease the risk of non-compliance; hence, improved precision may not only mean more reliable inventories but also lower costs for compliance. In deriving new rules for checking compliance or for emissions trading, Nahorski and Horabik (2010) are particularly concerned about instances where the uncertainty is asymmetric. Right-skewed asymmetry is typically observed in uncertainty distributions that are obtained from Monte Carlo simulations when reported emission values are used. This leads to biased compliance; it is more likely that true emissions are higher than reported emissions and less likely that they are lower. The authors consider asymmetric distributions and apply fuzzy numbers to more precisely determine the required level of emission reductions necessary to yield a high likelihood of meeting reduction or trading commitments.

Trading of emission permits requires there to be some sort of cooperative behavior and trading markets. Pickl et al. (2010) discuss the problem of uncertainty in transaction relationships and note that the mere existence of formal markets reduces uncertainty by providing for a more structured relationship among economic agents. Markets permit stable expectations about the economic outcome of transactions. The authors describe a macro-economic game model for exploring interactive, cooperative resource planning, including uncertain emissions trading.

Box 1 Rationale for improving and conducting uncertainty analyses (revised)

- Calculations of greenhouse gas (GHG) emissions contain uncertainty for a variety of reasons such as the lack of availability of sufficient and appropriate data and the techniques for processing them.
- Understanding the basic science of GHG gas sources and sinks requires an understanding of the uncertainty in their estimates.
- Schemes to reduce human-induced global climate impact rely on confidence that inventories of GHG emissions allow the accurate assessment of emissions and emission changes. To ensure such confidence, it is vital that the uncertainty present in emissions estimates is transparent. Clearer communication of the forces underlying inventory uncertainty may be needed so that the implications are better understood.
- Uncertainty estimates are not necessarily intended to dispute the validity of national GHG inventories, but they can help improve them.
- Uncertainty is higher for some aspects of a GHG inventory than for others. For example, past experience shows that, in general, methods used to estimate nitrous oxide (N_2O) emissions are more uncertain than methane (CH_4) and much more uncertain than carbon dioxide (CO_2). If uncertainty analysis is to play a role in cross-sectoral or international comparison or in trading systems or compliance mechanisms, then approaches to uncertainty analysis need to be robust and standardized across sectors and gases, as well as among countries.
- Uncertainty analysis helps to understand uncertainties: better science helps to reduce them. Better science needs support, encouragement, and greater investment. Full carbon accounting (FCA), or full accounting of emissions and removals, including all GHGs, in national GHG inventories is important for advancing the science.
- FCA is a prerequisite for reducing uncertainties in our understanding of the global climate system. From a policy viewpoint, FCA could be encouraged by including it in reporting commitments, but it might be separated from negotiation of reduction targets. Future climate agreements will be made more robust, explicitly accounting for the uncertainties associated with emission estimates.

Source: IIASA (2007)

5 Conclusions

The approaches to addressing uncertainty discussed in this Special Issue attempt to improve national inventories, not only for their own sake but also from a wider, systems analytical perspective that seeks to strengthen their usefulness under a compliance and/or global monitoring and reporting framework. They thus show what the challenges and benefits are of including inventory uncertainty in policy analysis. The issues that are raised by the authors featured in this Special Issue, and the role that uncertainty analysis plays in many of their arguments and/or proposals, highlight the importance of such efforts. While the IPCC clearly stresses the value of conducting uncertainty analyses and offers guidance on executing them, the arguments made here in favor of performing these studies go well beyond any suggestions made by the IPCC to date. Several reasons for continuing to improve and standardize the research and estimation methodologies that lead to quantifiable estimates of uncertainty associated with GHG inventories are noted in the text box above (Box 1). These were identified during Workshop discussions and retreats, and are covered in detail by the expanded papers that appear in this Special Issue. The most important of the reasons compiled in Box 1 have been taken from a policy brief prepared as an immediate output of the 2nd Uncertainty Workshop (http://www.iiasa.ac.at/Admin/PUB/policy-briefs/pb01-web.pdf).

Acknowledgements The authors would like to thank Cynthia Festin from IIASA's Forestry Program and Joanna Horabik from the Systems Research Institute of the Polish Academy of Sciences for organizing the 2nd International Workshop on Uncertainty in Greenhouse Gas Inventories; Iain Stewart, Kathryn Platzer, and Anka James of IIASA's Communications Department for their support and editorial work in publishing this Special Issue; and Linda Foith of IIASA's Office of Sponsored Research Department for administering the financial support. This Special Issue was made possible through the financial support of the Polish Member Organization to IIASA; the Royal Swedish Academy of Agriculture and Forestry; the Cultural Department, Science and Research Promotion, of the City of Vienna; and the State of Lower Austria.

References

API (2004) Compendium of greenhouse gas emissions methodologies for the oil and gas industry. Compendium, American Petroleum Institute, Washington, p 489. Available at: http://www.api.org/ehs/climate/new/upload/2004_COMPENDIUM.pdf

Bun A, Hamal K, Jonas M, Lesiv M (2010) Verification of compliance with GHG emission targets: annex B countries. Clim Change. doi:10.1007/s10584-010-9906-6

Bun R, Hamal K, Gusti M, Bun A (2010) Spatial GHG inventory on regional level: accounting for uncertainty. Clim Change. doi:10.1007/s10584-010-9907-5

Ciais P, Rayner P, Chevallier F, Bousquet P, Logan M, Peylin P, Ramonet M (2010) Atmospheric inversions for estimating CO2 fluxes: methods and perspectives. Clim Change. doi:10.1007/s10584-010-9909-3

Denman KL, Brasseur G, Chidthaisong A, Ciais P, Cox PM, Dickinson RE, Hauglustaine D, Heinze C, Holland E, Jacob D, Lohmann U, Ramachandran S, da Silva Dias PL, Wofsy SC, Zhang X (2007) Couplings between changes in the climate system and biogeochemistry. In: Solomon S, Qin D, Manning M, Chen Z, Marquis M, Averyt KB, Tignor M, Miller HL (eds) Climate change 2007: the physical science basis. Contribution of working Group I to the fourth assessment report of the Intergovernmental Panel on Climate Change. Cambridge University Press, Cambridge, pp 499–587. Available at: http://ipcc-wg1.ucar.edu/wg1/wg1-report.html

Eggleston HS, Buendia L, Miwa K, Ngara, T, Tanabe K. (eds) (2006) 2006 IPCC guidelines for national greenhouse gas inventories. Prepared by the National Greenhouse Gas Inventories Programme. Institute for Global Environmental Strategies (IGES), Hayama, Kanagawa, Japan. Available at: http://www.ipcc-nggip.iges.or.jp/public/2006gl/index.html

Ermolieva T, Ermoliev Y, Fischer G, Jonas M, Makowski M, Wagner F (2010) Carbon emission trading and carbon taxes under uncertainties. Clim Change. doi:10.1007/s10584-010-9910-x

EU (2009) Decision no 406/2009/EC of the European Parliament and of the Council of 23 April 2009 on the effort of Member States to reduce their greenhouse gas emissions to meet the community's greenhouse gas reduction commitments up to 2020. Official Journal of the European Union, L 140, 52(5 June 2009), 136–148. ISSN: 1725-2555. Available at: http://eur-lex.europa.eu/JOHtml.do?uri=OJ:L:2009:140:SOM:EN:HTML

FCCC (2006a) Updated UNFCCC reporting guidelines on annual inventories following incorporation of the provisions of decision 14/CP.11. Report FCCC/SBSTA/2006/9, UN Framework Convention on Climate Change (FCCC), Bonn, Germany, p 93. Available at: http://unfccc.int/resource/docs/2006/sbsta/eng/09.pdf

FCCC (2006b) Report of the conference of the parties serving as the meeting of the parties to the Kyoto Protocol on its first session, held at Montreal from 28 November to 10 December 2005. Addendum. Part two: action taken by the conference of the parties serving as the meeting of the parties to the Kyoto Protocol on its first session. Report FCCC/KP/CMP/2005/8/Add.3, UN Framework Convention on Climate Change (FCCC), Bonn, Germany, p 103. Available at: http://unfccc.int/resource/docs/2005/cmp1/eng/08a03.pdf

FCCC (2009a) Copenhagen—background information. Fact sheet, UN Framework Convention on Climate Change (FCCC), Bonn, p 3. Available at: http://unfccc.int/files/press/application/pdf/fact_sheet_copenhagen_background_information.pdf

FCCC (2009b) Why is an international climate change deal so important? Fact sheet, UN Framework Convention on Climate Change (FCCC), Bonn, p 2. Available at: http://unfccc.int/files/press/fact_sheets/application/pdf/fact_sheet_climate_deal.pdf

FCCC (2009c) Copenhagen accord. Advance unedited version of decision-/CP.15, UN Framework Convention on Climate Change (FCCC), Bonn, p 6. Available at: http://unfccc.int/files/meetings/cop_15/application/pdf/cop15_cph_auv.pdf

Field CB (2007) Natural versus anthropogenic control of ecosystem carbon stocks. In: Proceedings, 2nd international workshop on uncertainty in greenhouse gas inventories, 27–28 September, Laxenburg, Austria, pp 59–60. Available at: http://www.ibspan.waw.pl/ghg2007/GHG-total.pdf

Gusti M, Jonas M (2010) Terrestrial full carbon account for Russia: revised uncertainty estimates and their role in a bottom-up/top-down accounting exercise. Clim Change. doi:10.1007/s10584-010-9911-9

Horabik J, Nahorski Z (2010) A statistical model for spatial inventory data: a case study of N_2O emissions in municipalities of southern Norway. Clim Change. doi:10.1007/s10584-010-9913-7

IIASA (2007) Uncertainty in greenhouse gas inventories. IIASA Policy Brief #01, International Institute for Applied Systems Analysis, Laxenburg. Available at: http://www.iiasa.ac.at/Publications/policy-briefs/pb01-web.pdf

IPCC (2006) 2006 IPCC guidelines for national greenhouse gas inventories. In: Eggleston HS, Buendia L, Miwa K, Ngara T, Tanabe K (eds) Intergovernmental Panel on Climate Change (IPCC), National Greenhouse Gas Inventories Programme, Institute for Global Environmental Strategies, Hayama, Kanagawa, Japan. Available at: http://www.ipcc-nggip.iges.or.jp/public/2006gl/index.html

IPIECA (2003) Petroleum industry guidelines for reporting greenhouse gas emissions. Guidelines, International Petroleum Industry Environmental Conservation Association, London, p 81. Available at: http://www.ipieca.org/activities/climate_change/downloads/publications/ghg_guidelines.pdf

IPIECA (2009) Addressing uncertainty in oil and natural gas industry greenhouse gas inventories. Guidelines pilot test version, International Petroleum Industry Environmental Conservation Association, London, p 186. Available at: http://www.api.org/ehs/climate/response/upload/Addressing_Uncertainty.pdf

Jonas M, White T, Marland G, Lieberman D, Nahorski Z, Nilsson S (2009) Dealing with uncertainty in GHG inventories: how to go about it? In: Marti K, Ermoliev Y, Makowski M (eds) Coping with uncertainty: robust solutions. Springer, Berlin, Germany, p 277. ISBN: 978-3-642-03734-4], 229–245

Jonas M, Gusti M, Jęda W, Nahorski Z, Nilsson S (2010) Comparison of preparatory signal analysis techniques for consideration in the (post-) Kyoto policy process. Clim Change. doi:10.1007/s10584-010-9914-6

Lieberman D, Jonas M, Nahorski Z, Nilsson S (eds) (2007) Accounting for climate change. Uncertainty in greenhouse gas inventories—verification, compliance, and trading. Springer, Dordrecht, Netherlands, p 159. ISBN: 978-1-4020-5929-2 [Reprint: Water Air Soil Pollut.:

Focus, 2007, 7(4–5). ISSN: 1567-7230]. Available at: http://www.springer.com/environment/global+change+-+climate+change/book/978-1-4020-5929-2
Leip A (2010) Quantitative quality assessment of the greenhouse gas inventory for agriculture in Europe. Clim Change. doi:10.1007/s10584-010-9915-5
Marland G (2008) Uncertainties in accounting for CO_2 from fossil fuels. J Ind Ecol 12(2):136–139. doi:10.1111/j.1530-9290.2008.00014.x
Marland G, Rotty RM (1984) Carbon dioxide emissions from fossil fuels: a procedure for estimation and results for 1950–1982. Tellus 36B(4):232–261. doi:10.1111/j.1600-0889.1984.tb00245.x
Meinshausen M, Meinshausen N, Hare W, Raper SCB, Frieler K, Knutti R, Frame DJ, Allen MR (2009) Greenhouse-gas emission targets for limiting global warming to 2°C. Nature 458:1158–1162. doi:10.1038/nature08017
Nahorski Z, Horabik J (2010) Compliance and emission trading rules for asymmetric emission uncertainty estimates. Clim Change. doi:10.1007/s10584-010-9916-4
NRC (2010) Verifying greenhouse gas emissions: methods to support international climate agreements. Report, National Research Council, National Academies Press, Washington, D.C., United States of America, p 132. Available at: http://www.nap.edu/catalog.php?record_id=12883 (prepublication version)
Oijen Mv, Thomson A (2010) Toward Bayesian uncertainty quantification for forestry models used in the United Kingdom Greenhouse Gas Inventory for land use, land use change, and forestry. Clim Change. doi:10.1007/s10584-010-9917-3
Pandey JS, Wate SR, Devotta S (2007) Development of emission factors for GHGs and associated Uncertainties. In: Proceedings, 2nd international workshop on uncertainty in greenhouse gas inventories, 27–28 September, Laxenburg, Austria, pp 163–168. Available at: http://www.ibspan.waw.pl/ghg2007/GHG-total.pdf
Penman J, Kruger D, Galbally I, Hiraishi T, Nyenzi B, Emmanuel S, Buendia L, Hoppaus R, Martinsen T, Meijer J, Miwa K, Tanabe K (eds) (2000) Good practice guidance and uncertainty management in national greenhouse gas inventories. Institute for Global Environmental Strategies, Hayama, Kanagawa, Japan. Available at: http://www.ipcc-nggip.iges.or.jp/public/gp/english/
Penman J, Gytarsky M, Hiraishi T, Krug T, Kruger D, Pipatti R, Buendia L, Miwa K, Ngara T, Tanabe K, Wagner F (eds) (2003) Good practice guidance for land use, land-use change and forestry. Institute for Global Environmental Strategies, Hayama, Kanagawa, Japan. Available at: http://www.ipcc-nggip.iges.or.jp/public/gpglulucf/gpglulucf.htm
Pickl S, Kropat E, Hahn H (2010) The impact of uncertain emission trading markets on interactive resource planning processes and international emission trading experiments. Clim Change. doi:10.1007/s10584-010-9912-8
Rivier L, Peylin P, Ciais P, Gloor M, Rödenbeck C, Geels C, Karstens U, Bousquet P, Brandt J, Heimann M, Aerocarb experimentalists (2010) European CO_2 fluxes from atmospheric inversions using regional and global transport models. Clim Change. doi:10.1007/s10584-010-9908-4
Schiermeier Q (2009) G8 climate target questioned. Nature 460(7253), 16 July:313. doi:10.1038/460313a
Shvidenko A, Schepaschenko D, McCallum I, Nilsson S (2010) Can the uncertainty of full carbon accounting of forest ecosystems be made acceptable to policy makers? Clim Change. doi:10.1007/s10584-010-9918-2
Stańczak J, Bartoszczuk P (2010) CO_2 emission trading model with trading prices. Clim Change. doi:10.1007/s10584-010-9905-7
Szemesová J, Gera M (2010) Uncertainty analysis for estimation of landfill emissions and data sensitivity for the input variation. Clim Change. doi:10.1007/s10584-010-9919-1
Verstraeten WW, Veroustraete F, Wagner W, Roey Tv, Heyns W, Verbeiren S, Feyen J (2010) Remotely sensed soil moisture integration in an ecosystem carbon flux model. The spatial implication. Clim Change. doi:10.1007/s10584-010-9920-8
WBGU (2009a) Climate change: why 2°C? Factsheet 2/2009, German Advisory Council on Global Change (WBGU), Berlin, Germany. ISBN: 3-936191-33-6. Available at: http://www.wbgu.de/wbgu_factsheet_2_en.html
WBGU (2009b) Solving the climate dilemma: the budget approach. Special Report, German Advisory Council on Global Change (WBGU), Berlin, Germany, p 55. ISBN: 978-3-936191-27-1. Available at: http://www.wbgu.de/wbgu_sn2009_en.pdf
Winiwarter W, Muik B (2010) Statistical dependence in input data of national greenhouse gas inventories: effects on the overall inventory uncertainty. Clim Change. doi:10.1007/s10584-010-9921-7

Climatic Change (2010) 103:19–36
DOI 10.1007/s10584-010-9921-7

Statistical dependence in input data of national greenhouse gas inventories: effects on the overall inventory uncertainty

Wilfried Winiwarter · Barbara Muik

Received: 5 January 2009 / Accepted: 15 June 2010 / Published online: 14 July 2010

Abstract An uncertainty assessment of the Austrian greenhouse gas inventory provided the basis for this analysis. We isolated the factors that were responsible for the uncertainty observed, and compared our results with those of other countries. Uncertainties of input parameters were used to derive the uncertainty of the emission estimate. Resulting uncertainty using a Monte Carlo approach was 5.2% for the emission levels of 2005 and 2.4 percentage points for the 1990–2005 emission trend. Systematic uncertainty was not assessed. This result is in the range expected from previous experience in Austria and other countries. The determining factor for the emission level uncertainty (not the trend uncertainty) is the uncertainty associated with soil nitrous oxide N_2O emissions. Uncertainty of the soil N_2O release rate is huge, and there is no agreement even on the magnitude of the uncertainty when country comparisons are made. In other words, reporting and use of N_2O release uncertainty are also different between countries; this is important, as this single factor fully determines a country's national greenhouse gas inventory uncertainty. Inter-country comparisons of emission uncertainty are thus unable to reveal much about a country's inventory quality. For Austria, we also compared the results of the Monte Carlo approach to those obtained from a simpler error propagation approach, and find the latter to systematically provide lower uncertainty. The difference can be explained by the ability of the Monte Carlo approach to account for statistical dependency of input parameters, again regarding soil N_2O emissions. This is in contrast to the results of other countries, which focus less on statistical dependency

W. Winiwarter (✉)
AIT Austrian Institute of Technology, 1220 Vienna, Austria
e-mail: wilfried.winiwarter@ait.ac.at

W. Winiwarter
IIASA, 2361 Laxenburg, Austria

B. Muik
Umweltbundesamt, 1090 Vienna, Austria

when performing Monte Carlo analysis. In addition, the error propagation results depend on treatment of skewed probability distributions, which need to be translated into normal distributions. The result indicates that more attention needs to be given to identifying statistically dependent input data in uncertainty assessment.

1 Introduction

Maintaining greenhouse gas (GHG) inventories is a key requirement of international efforts to combat global climate change. We need to understand the quantities and the sources of GHG fluxes to the atmosphere to be able to devise measures to reduce them. Information about data reliability is also required; thus uncertainty estimates are an essential element of a complete emission inventory.

Uncertainty analysis is useful in many respects (Lieberman et al. 2007). It helps with analyzing and revising an inventory, provides information about the most important factors contributing to uncertainty, and thus assesses which parts of the inventory require the most urgent improvements. It is not able or intended to dispute the validity of the inventory estimates. However, comparing uncertainty across countries helps the comparability of the inventories as such to be judged, as well as the "tradability" of the respective emissions.

Ideally, emission estimates and uncertainty ranges would both be derived from source-specific measured data. In practice, estimates are often based on the known characteristics of sources taken to be representative of the data population. Sometimes, uncertainty and statistical distributions can be determined empirically, based on a large number of specific measurements. Often, however, expert judgement will be necessary to define the uncertainty ranges.

The assessment and propagation of uncertainties in emission inventories have been described in detail in IPCC (2000, 2006). The mathematical algorithms used allow information to be added up in such a way that the relative uncertainty of the parameter combination (as a percentage of the mean value) becomes lower than the relative uncertainty of any of the input parameters. A precondition for applying such algorithms is that statistically independent data should be used, that is, data whose random variation does not simultaneously affect another input parameter. One can say that such parameters need to provide additional information, or, in mathematical terms, that parameters must not be correlated.

The advantage of going into statistically independent detail is often implicitly taken advantage of when a problem is disassembled into sub-problems and the sub-results are being recombined. Such a procedure will allow the overall uncertainty to be reduced (on a relative basis). Nevertheless, it is not always the most detailed level that yields the results of lowest uncertainty. If measurements or assessments at the most detailed level are difficult, a more comprehensive level of information may provide the lower overall uncertainty.

Thus, optimizing the approach requires input information to be collected at the most detailed level at which an inventory can be prepared. Attaching uncertainty data should then be done at a level where greatest confidence can be expected regarding the data. This may be at the most detailed level; but uncertainty data will more often not be available, or an approach using balances at a more aggregate level (energy balance, solvent balance) will provide lower uncertainty. To obtain adequate

results, error propagation may be performed at the most reliable level of information available.

For this paper, we use the results of a recent study on the uncertainties in the Austrian GHG inventory (Winiwarter 2008). The work is based on a previous assessment for Austria (Winiwarter and Rypdal 2001; Winiwarter and Orthofer 2000). Similar assessments, which are a reporting requirement under the United Nations Framework Convention on Climate Change (UNFCCC), have been published for a variety of countries, for example, the United Kingdom (Baggott et al. 2005), Finland (Monni et al. 2004), the Netherlands (Ramirez et al. 2008), and Luxembourg (Winiwarter and Köther 2008).

To understand how the methods chosen influence the results, and which parameters are in general (not nationally) most important for describing the overall uncertainty, we draw on the similarities and differences between the respective exercises and the numerical values that are available in detail for Austria.

2 Methodology: how to assess the uncertainty of national emission inventories

2.1 Selection of input data

We demonstrate the general principles according to a description of the system in Austria. The Austrian national inventory system ("OLI") contains a compilation of emissions of air pollutants and greenhouse gases. Results from OLI feed into national reports on air pollution emissions (required under the framework of United Nations Economic Commission for Europe [UNECE] protocols) and greenhouse gas reporting to the UNFCCC and the European Commission. To allow these quite different tasks, OLI provides emission factors and activity data for a large number of sectors and sector/fuel combinations. In this study we use OLI data for 559 individual sectors or sector/fuel combinations (activity data, emission factors for CO_2, CH_4, and N_2O). Additionally, 24 sector/gas combinations for fluorinated gases (F-gases) are evaluated. Not all, but many, of these detailed input data are relevant for the GHG inventory. We will refer to this information as the "base level" of OLI, even if some of the emission factors or activity numbers presented may derive from more detailed emission models. Starting from the "base level" enables us to perform a consistent uncertainty analysis.

Within the framework of this project we had to attribute quantitative information on uncertainty to this input data. All the details of this task have been laid out in the background report (Winiwarter 2008). Linking was performed on the OLI base level, but most uncertainty information was available at a more aggregate level. For aggregate information the same uncertainty was attributed to all input entries concerned, with this input being considered a statistically dependent entity. Uncertainty information was collected both for emission factors and for activities associated with the respective emission source. Uncertainty of total emissions was used only when this more detailed information was not available.

Uncertainty information was taken from national studies, from international information (like, for example, the reports of the Intergovernmental Panel on Climate Change [IPCC]), from data variations in the literature, and from national experts. Structured interviews were not held, but information collected previously

in structured interviews (Winiwarter and Orthofer 2000) could still be made use of. As will be explained in Section 2.3, special attention was given to covering statistical dependence (correlation) of source categories.

In all input and output parameters, uncertainty has been expressed as a normal or lognormal probability density function. In line with IPCC requirements, the uncertainty range is presented as the range with 95% probability of a given value being within its boundaries. Thus the boundaries were given as the 2.5 and 97.5 percentiles of the respective distribution. For a normal distribution, this is ±2 standard deviations (SD) from the mean.

As information on uncertainty is often very sparse, we had already considered information on reasonable upper and lower limits of a value as being sufficient to describe a full distribution. Consistent with the procedure above we understand a reasonable range (lower limit to upper limit) to contain 95% of all possible values; thus the total difference is interpreted as 4 SD. As Winiwarter and Rypdal (2001) have shown that the type of distribution used does not strongly influence the results in a wide range of cases, we chose to transform distributions into normal or lognormal distributions rather than using other distribution types. Lognormal distributions were required to cover realistic cases of very large uncertainties (i.e., uncertainties higher than 100%, which were physically limited by zero as the lower end of range [strongly skewed distributions]).

2.2 Error propagation vs. Monte Carlo simulation

Error propagation is a technique that allows the uncertainty associated with the result of a mathematical function to be estimated, based on the function's input uncertainties. Explicit equations for error propagation can be set under a number of preconditions only (IPCC 2000):

- The function consists of additive and multiplicative terms only;
- Uncertainty for each input parameter is normally distributed (i.e., lognormal or other distributions are not modeled);
- Input data are not correlated; and
- Standard deviation does not exceed 30% of the mean.

IPCC (2000) provides a standard template to perform error propagation. This template has been utilized by a number of countries under their obligation to submit national greenhouse gas inventories. This approach is, in accordance with these guidelines, often also referred to as the "Tier 1" uncertainty calculation. Using the template requires assumptions to be applied on a conversion of lognormally distributed parameters to a normal distribution.

A Monte Carlo simulation is based on repeating the actual inventory calculation a number of times. For each replicate, input parameters are varied and (multiple) output is recorded. Variation of input is performed randomly, according to predefined boundary values and probability density functions. The set of individual output data will again follow its own probability density and thus provide the resulting uncertainty, strictly based on the input uncertainty.

Moreover, as correlating inputs and outputs are stored, it is possible to calculate regressions. The regression allows the sensitivity of the result toward an input

parameter to be obtained, thus indicating which input is responsible for the result and to what extent.

Emission inventories are fairly easy to calculate and require only little computation time, such that even a few thousand replicates will not require more than a few minutes. Commercial software packages are available that couple with standard spreadsheet programs. This facilitates application on a standard PC. Within this project, we use the software "@RISK" from Palisade Co. (www.palisade.com). The standard tools of these software packages allow many different kinds of probability density functions to be defined and used, as well as the specification of full and even partial correlation between parameters. This also allows for coupling of inputs to a level of detail where uncertainty is assumed to be the smallest. Because of the simplicity of use, many countries have also successfully implemented the Monte Carlo approach (termed: "Tier 2" uncertainty calculation). Respective reports have been published, among others, by Charles et al. (1998), Winiwarter and Rypdal (2001), Monni et al. (2004), and Ramirez et al. (2008). In this paper we provide some specific comparisons between the results of Tier 1 vs. Tier 2 approaches. The methodologies as such are well established and do not require further specification.

2.3 Considering correlated uncertainties

In the standard methodology to estimate uncertainties of an emission inventory, uncertainties are derived for an emission factor or activity number of a specific source category, and as they are assessed independently they are treated as being statistically independent. This procedure is implemented in the IPCC template of "Tier 1" uncertainty calculation, which by its nature would not allow treatment of correlated variables to estimate the uncertainty of emission levels. We do not deem this approach to be the most appropriate representation of the situation Instead, in this study we attempt to identify indications that hint at correlation within parameters. These indications could then be used only in the "Tier 2" approach.

In the case of activities, we regard input information as correlated if derived from data originally collected at a lower level of detail. This is the case for energy balances. All energy activities related to solid fuels, whether in the industry sector or used for domestic heating, are thus considered correlated with respect to their uncertainty. Likewise, we consider liquid fuels used in transport or power plants to be statistically dependent—the same goes for gaseous fuels or biofuels. We treat solvent balances in the same way as fuel balances.

For emission factors, one indication to be used is the value of the emission factor. If two emission factors used in different areas have the same value (e.g., in combustion for different source categories but using the same fuel), there should be a suspicion that these emission factors have been derived from the same set of measurements, and thus uncertainties should be seen as correlated. This has happened in the case of Austria, as shown by an inspection of the original source of emission factors, but it need not be the case generally. Two emission factors could have been assessed fully independently, and still have arrived at the identical value.

Moreover, two emission factors could have different values, but with the uncertainty being most strongly affected by just one parameter. Such a case is visible when national Austrian emission factors for CH_4 from combustion processes are inspected. Measured quantities are emissions of total hydrocarbons and assumptions on the

fraction of CH_4 in total hydrocarbons (Orthofer 1991) drive the overall uncertainty. Thus it is also clear in this case that emission factors are correlated. We also assumed this to be the case for N_2O from soil nitrogen (direct and indirect emissions), as the underlying processes are the same. When specifically considering the indirect emissions that occur because of volatilization loss of nitrogen, assumptions on subsequent N_2O formation are based on exactly the same assumptions as those used for direct nitrogen application (IPCC 2000). However, in order to account for the unknown pathways of nitrogen, which also include leaching to groundwater or runoff in surface water, uncertainty for indirect emissions was considered higher, as it also contained other components contributing to uncertainty. Thus one could also argue that those other components are independent and that only partial correlation should be considered—an argument that we do not apply here, as it seems impossible to assess the degree of such a partial correlation.

3 Results

3.1 Tasks

Estimating uncertainty does not yield just one result. Following the guidance of IPCC (2000), uncertainties have been derived for the total GHG inventory (as CO_2 equivalents) as level uncertainty for 2005 and for the base year 1990, and for the trend uncertainty between those years. Moreover, the same results are available specifically for each of the six gases in the "Kyoto basket." Individual uncertainty estimates have been provided for the 40 key sources of the Austrian inventory (it is only for the respective gas(es) that this source category is "key") and for the combined non-key sources (aggregated for all non-key source emissions of each gas). Key sources have been identified according to the procedures developed by IPCC (2000), which also guides which source categories should be used. A key source category is thus one that is prioritized within the national inventory system because its estimate has a significant influence on the total GHG inventory in terms of the absolute level of emissions, the trend in emissions, or both.

Separate uncertainty calculations were performed using a spreadsheet prepared specifically according to the "Tier 1" approach (IPCC 2000) and with a Monte Carlo approach fully considering statistical dependence of detailed input data as described above ("Tier 2" approach). The same input uncertainty information was used as much as possible. It should be noted that the "Monte Carlo" approach, averaging a large number of randomly varied input data, may exhibit slightly different results in total emissions as well as source category emissions in comparison with a direct calculation. The physical meaning of this difference is similar to a rounding error and may be ignored. For the present evaluation we used 10,000 iterations and standard Monte Carlo (random) sampling.

3.2 Results using the Tier 1 (error propagation) approach

The results of the error propagation approach are strictly limited to the key sources and the potential of the IPCC spreadsheet used. Table 1 presents the resulting spreadsheet. An extension to other sources than the 40 key sources is in theory

Table 1 Tier 1 (error propagation) uncertainty calculation and reporting, according to Table 6.1 of IPCC (2000) for Austria, 2005

A	B	C	D	E	F	G	H	I	J	K	L	M
IPCC source category	Gas	Base year emissions 1990	Year 2005 emissions	Activity data uncertainty	Emission factor uncertainty	Combined uncertainty	Combined uncertainty as % of total national emissions in 1990	Type A sensitivity	Type B sensitivity	Uncertainty in trend in national emissions introduced by emission factor uncertainty	Uncertainty in trend in national emissions introduced by activity data uncertainty	Uncertainty introduced into the trend in total national emissions
		Input data	Input data	Input data	Input data							
		Gg CO_2 equivalent	Gg CO_2 equivalent	%	%	%	%	%	%	%	%	%
1 A 1 a liquid: public electricity and heat production	CO_2	1,229	1,083	0.5	0.5	0.7	0.01	−0.00	0.01	−0.0024	0.0100	0.01
1 A 1 a other: public electricity and heat production	CO_2	118	490	10.0	20.0	22.4	0.12	0.00	0.01	0.0917	0.0907	0.13
1 A 1 a solid: public electricity and heat production	CO_2	6,247	5,844	0.5	0.5	0.7	0.05	−0.02	0.08	−0.0101	0.0541	0.05
1 A 1 b liquid: petroleum refining	CO_2	1,957	2,151	0.5	0.3	0.6	0.01	−0.00	0.03	−0.0006	0.0199	0.02
1 A 2 mobile-liquid: manufacturing industries and construction	CO_2	1,018	1,161	3.0	0.5	3.0	0.04	−0.00	0.02	−0.0003	0.0645	0.06
1 A 2 other: manufacturing industries and construction	CO_2	375	849	10.0	20.0	22.4	0.21	0.01	0.01	0.1061	0.1570	0.19
1 A 2 solid: manufacturing industries and construction	CO_2	5,014	5,602	1.0	0.5	1.1	0.07	−0.00	0.07	−0.0021	0.1036	0.10

Table 1 (continued)

A	B	C	D	E	F	G	H	I	J	K	L	M
IPCC source category	Gas	Base year emissions 1990	Year 2005 emissions	Activity data uncertainty	Emission factor uncertainty	Combined uncertainty	Combined uncertainty as % of total national emissions in 1990	Type A sensitivity	Type B sensitivity	Uncertainty in trend in national emissions introduced by emission factor uncertainty	Uncertainty in trend in national emissions introduced by activity data uncertainty	Uncertainty introduced into the trend in total national emissions
		Input data	Input data	Input data	Input data							
		Gg CO_2 equivalent	Gg CO_2 equivalent	%	%	%	%	%	%	%	%	%
1 A 2 stat-liquid: manufacturing industries and construction	CO_2	2,883	1,920	3.0	0.5	3.0	0.06	−0.02	0.03	−0.0097	0.1066	0.11
1 A 3 a jet kerosene: civil aviation	CO_2	24	209	3.0	3.0	4.2	0.01	0.00	0.00	0.0071	0.0116	0.01
1 A 3 b diesel oil: road transportation	CO_2	4,013	16,645	3.0	3.0	4.2	0.78	0.16	0.22	0.4668	0.9238	1.04
1 A 3 b gasoline: road transportation	CO_2	7,911	6,393	3.0	3.0	4.2	0.30	−0.04	0.08	−0.1162	0.3548	0.37
1 A 3 b gasoline: road transportation	N_2O	219	149	3.0	70.0	70.1	0.12	−0.00	0.00	−0.1013	0.0082	0.10
1 A 4 biomass: other sectors	CH_4	315	244	10.0	50.0	51.0	0.14	−0.00	0.00	−0.0842	0.0451	0.10
1 A 4 mobile-diesel: other sectors	CO_2	1,379	1,472	3.0	0.5	3.0	0.05	−0.00	0.02	−0.0010	0.0817	0.08
1 A 4 other: other sectors	CO_2	239	72	10.0	20.0	22.4	0.02	−0.00	0.00	−0.0552	0.0132	0.06
1 A 4 solid: other sectors	CO_2	2,654	562	1.0	0.5	1.1	0.01	−0.03	0.01	−0.0168	0.0104	0.02
1 A 4 stat-liquid: other sectors	CO_2	7,319	7,125	3.0	0.5	3.0	0.24	−0.02	0.09	−0.0100	0.3955	0.40

1 A gaseous: fuel combustion (stationary)	CO_2	11,169	18,510	2.0	0.5	2.1	0.42	0.07	0.24	0.0346	0.6849	0.69
1 B 2 b: natural gas	CH_4	273	552	4.2	14.1	14.7	0.09	0.00	0.01	0.0423	0.0429	0.06
2 A 1: cement production	CO_2	2,033	1,797	5.0	2.0	5.4	0.11	−0.01	0.02	−0.0159	0.1663	0.17
2 A 2: lime production	CO_2	396	579	20.0	5.0	20.6	0.13	0.00	0.01	0.0072	0.2141	0.21
2 A 3: limestone and dolomite use	CO_2	222	291	19.6	2.0	19.7	0.06	0.00	0.00	0.0007	0.1053	0.11
2 A 7 b: sinter production	CO_2	481	310	2.0	5.0	5.4	0.02	−0.00	0.00	−0.0170	0.0115	0.02
2 B 1: ammonia production	CO_2	517	503	2.0	4.6	5.0	0.03	−0.00	0.01	−0.0065	0.0186	0.02
2 B 2: nitric acid production	N_2O	912	274	3.0	20.0	20.2	0.06	−0.01	0.00	−0.2104	0.0152	0.21
2 C 1: iron and steel production	CO_2	3,546	4,995	0.5	0.5	0.7	0.04	0.01	0.07	0.0052	0.0462	0.05
2 C 3: aluminium production	CO_2	158	0	2.0	0.5	2.1	0.00	−0.00	0.00	−0.0012	–	0.00
2 C 3: aluminium production	PFCs	1,050	0	0.0	50.0	50.0	0.00	−0.02	0.00	−0.8123	–	0.81
2 C 4: SF_6 used in Al and Mg foundries	SF6	253	0	0.0	5.0	5.0	0.00	−0.00	0.00	−0.0196	–	0.02
2 F 1/2/3/4/5: ODS substitutes	HFCs	21	908	0.0	54.0	54.0	0.54	0.01	0.01	0.6237	–	0.62
2 F 7: semiconductor manufacture	FCs	133	291	0.0	11.2	11.2	0.04	0.00	0.00	0.0195	–	0.02
2 F 9: other sources of SF_6	SF6	127	82	0.0	56.0	56.0	0.05	−0.00	0.00	−0.0498	–	0.05
3: solvent and other product use	CO_2	283	177	5.0	10.0	11.2	0.02	−0.00	0.00	−0.0205	0.0164	0.03
4 A 1: cattle	CH_4	3,561	3,029	10.0	20.0	22.4	0.75	−0.02	0.04	−0.3091	0.5605	0.64
4 B 1: cattle	N_2O	908	789	10.0	100.0	100.5	0.88	−0.00	0.01	−0.3727	0.1460	0.40

Table 1 (continued)

A	B	C	D	E	F	G	H	I	J	K	L	M
IPCC source category	Gas	Base year emissions 1990	Year 2005 emissions	Activity data uncertainty	Emission factor uncertainty	Combined uncertainty	Combined uncertainty as % of total national emissions in 1990	Type A sensitivity	Type B sensitivity	Uncertainty in trend in national emissions introduced by emission factor uncertainty	Uncertainty in trend in national emissions introduced by activity data uncertainty	Uncertainty introduced into the trend in total national emissions
		Input data	Input data	Input data	Input data							
		Gg CO_2 equivalent	Gg CO_2 equivalent	%	%	%	%	%	%	%	%	%
4 B 1: cattle	CH_4	587	459	10.0	70.0	70.7	0.36	−0.00	0.01	−0.2156	0.0849	0.23
4 B 8: swine	CH_4	448	397	10.0	70.0	70.7	0.31	−0.00	0.01	−0.1215	0.0734	0.14
4 D 1: direct soil emissions	N_2O	1,760	1,518	5.0	150.0	150.1	2.52	−0.01	0.02	−1.1051	0.1404	1.11
4 D 3: indirect emissions	N_2O	1,310	1,086	5.0	150.0	150.1	1.80	−0.01	0.01	−0.9077	0.1005	0.91
6 A: solid waste disposal on land	CH_4	3,377	1,880	12.0	25.0	27.7	0.58	−0.03	0.02	−0.6909	0.4173	0.81
National total		76,439	90,395				3.59					2.55

The emissions of the key source categories cover 96.7% and 96.9% of the total GHG emissions (1990 and 2005, respectively)

possible, but in the Austrian inventory, as sources can only be dealt with individually, this would mean adding more than 100 sources.

As error propagation requires the use of normal distributions, the proper implementation of variables characterized by a skewed distribution necessarily requires an arbitrary choice. Especially regarding sources that will eventually contribute significantly to overall uncertainty, this choice can be quite important. Using the range of 0.3 to 3 times the emission factor for N_2O from soils, we chose to apply an uncertainty of 150%.

This appears to be in contrast to guidance provided by IPCC (2000): "If uncertainty is known to be highly asymmetrical, enter the larger percentage difference between the mean and the confidence limit." However, that statement clearly refers to distributions where standard deviations do not exceed 30% of the mean. Although it does not seem useful to represent a given distribution by a normal distribution which, though it follows the guidance, does not represent the occurrence of events of the original distribution (e.g., negative emissions), we also tested the results for an uncertainty of 200% (consistent with the factor 3 increase). In that case, the overall uncertainties would have been 4.51% (level) and 2.85 percentage points (trend) instead of 3.59% and 2.55 percentage points as identified in Table 1.

3.3 Results using the Tier 2 (Monte Carlo) approach

While the iterations representing the Monte Carlo approach are being performed, all randomly selected input data are recorded, as are all the respective results of calculations for a predefined set of output parameters. Here we selected the following outputs (for all three cases: base year 1990, target year 2005, and the difference between them), listed in detail in the background report (Winiwarter 2008):

- Emissions of each of 40 key sources (key gas only);
- Totals of all non-key source emissions (for each of six gases);
- Emission totals (for each of six gases);
- GHG totals as reported to the UNFCCC (different gases added according to their greenhouse warming potential, in CO_2 eq.); and
- National GHG totals, including land use, land use change, and forestry (LULUCF), and international bunker fuels.

As the whole set of data (10,000 individual results) is available for both outputs and inputs, the respective probability distributions can also be derived. Standard deviation, and thus uncertainty (here defined as 2 SD), is just one result of such a probability distribution, and is available for each of the outputs.

We merely display the main results of the Monte Carlo analysis of the Austrian GHG inventory (Table 2). Uncertainty is presented for each gas and for the level of target year 2005 (as a percentage) as well as for the trend (in percentage points relative to the total base year emissions). Detailed results by source category, using the original IPCC version of the table, are available from the background report (Winiwarter 2008).

In addition to overall uncertainties, the Monte Carlo approach also allows contributions to the overall variance of the results to be differentiated, using the correlation of input to output parameters. This result (Fig. 1) denotes the emission factor of soil

Table 2 Key results of the Austrian GHG inventory uncertainty 2005—Monte Carlo approach

Random uncertainty		CO_2	CH_4	N_2O	PFC	HFC	SF_6	Total GHG emissions
1990	Mean value	61.94	9.18	6.26	1.08	0.02	0.50	78.98
	Standard deviation	0.41	0.72	2.64	0.27	0.01	0.04	2.78
	Uncertainty (2 SD) (%)	1.3	15.6	84.3	49.1	49.9	16.6	7.0
2005	Mean value	79.65	7.06	5.24	0.12	0.91	0.29	93.26
	Standard deviation	0.65	0.53	2.26	0.01	0.24	0.03	2.41
	Uncertainty (2 SD) (%)	1.6	14.9	86.4	11.3	53.5	23.9	5.2
Trend	Difference	17.72	−2.12	−1.02	−0.97	0.89	−0.22	14.28
	Uncertainty of trend (percentage points)	2.10	8.00	13.05	49.12	21.20	21.40	2.37

N_2O emissions as clearly the most important factor influencing results, followed by transport activities, and the emission factor for N_2O related to manure handling.

3.3.1 Overall results comparing the two approaches

It is obvious that the level of uncertainty presented for a specific source category would not differ strongly between the error propagation and the Monte Carlo approach, which have basically the same set of assumptions. Moreover, the sectoral combined uncertainties of the underlying template-derived tables (see Winiwarter 2008) agree. The highest contributions to overall uncertainty, both according to the Monte Carlo analysis (Fig. 1) and to the error propagation template (column H in Table 1), are in the agricultural sector (nitrous oxide from soils, direct as well as indirect emissions, covered as one item in the Monte Carlo approach; somewhat smaller are the contributions from cattle emissions). Other sectors that are exposed to high uncertainties with respect to total emissions are transport (specifically transport using diesel fuels) and the waste sector. Other sectors of energy consumption

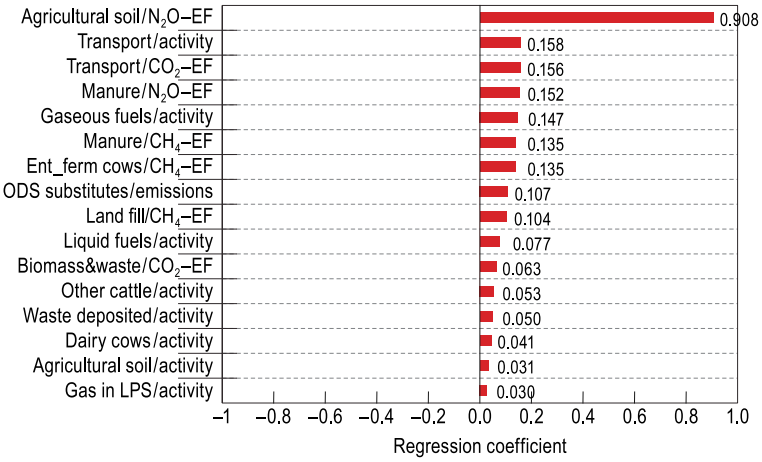

Fig. 1 Contribution of input parameters to the uncertainty of the Austrian 2005 emission levels

or industry exhibit smaller uncertainty with respect to the total, with the exception of substitutes for ozone-depleting substances (ODS). A slight deviation becomes evident between the approaches (e.g., in the agricultural sector, where N_2O emissions from manure rank higher in the error propagation approach because of inadequate treatment of skewed distributions).

Distinct discrepancies appear when the national totals are compared. At 5.17%, total uncertainty of the Monte Carlo approach is about 1.5 times that of the simpler error propagation approach (3.59%). As already indicated above, this difference is in part due to decisions affecting treatment of skewed distributions. The inability of the Tier 1 approach to deal with skewed distributions has already been identified by IPCC (2000) as a major reason for differences.

However, data shown here imply a more essential reason for discrepancy. The IPCC Tier 1 equations implicitly assume that all source categories referred to in the table are fully independent. When these equations are applied, error propagation takes advantage of this seemingly independent information, such that overall error decreases. This is different from data treatment according to the Monte Carlo approach. Overall relative error decreases in a much less pronounced way, which reflects the statistical dependence of data more adequately. Overall uncertainty in error propagation is thus lower.

Statistical dependence has been assumed in the Monte Carlo approach, in the energy sector, and for N_2O emissions from soil (direct emissions vs. indirect emissions). It is also possible to mimic statistical dependence for soil N_2O emissions in the error propagation approach, simply by adding direct and indirect emissions into one single source category. Doing this will increase level uncertainty to 4.69%. This is close to the 5.15% of the Monte Carlo approach and higher than the 4.51% obtained with a formally justified but unrealistic conversion of a skewed distribution into a normal distribution (see Section 3.2).

A very similar general situation can be seen for trends (Table 1 and Fig. 2, respectively). Source categories that display large level uncertainties are also often

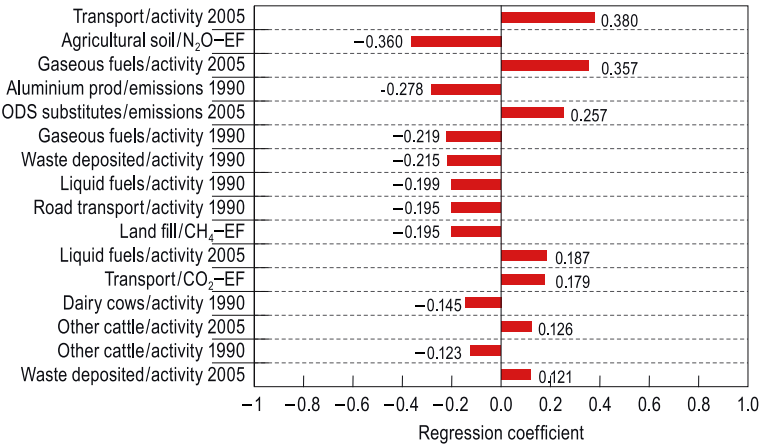

Fig. 2 Contribution of input parameters to the uncertainty of the Austrian emission trends for the 1990–2005 period

important for trend uncertainty, and results are comparable between the two approaches. In the case of trend uncertainty, however, transport and agriculture (soils) play an equally important role. The activity change in gaseous fuels between 1990 and 2005 is sufficiently large to put this element, even at quite small relative uncertainty, among the source categories that contribute most strongly to overall uncertainty. To a lesser extent, this is also the case for ODS substitutes. It is interesting to note that among industrial emissions, perfluorocarbon (PFC) emissions from aluminium production can be identified as a major contributor to trend uncertainty: Austrian aluminium production, in 1990 an important source, had been completely phased out by the reference year 2005. Non-key sources do not seem to contribute to overall trend uncertainty, not even when aggregated. Using the error propagation approach, sectoral trend uncertainties tend to be higher with respect to emissions, as less advantage is taken of error reduction due to exclusion of correlated emission factors. This effect does not remain very visible for total trend uncertainty, which is 2.55 percentage points—very similar to the 2.37 percentage points from the Monte Carlo approach.

4 Austrian results in comparison to other published uncertainty estimates of national GHG inventories

Results from a number of recent uncertainty estimates of national GHG inventories have been compiled in Tables 3 and 4. All these countries have high quality statistical information. One would thus not expect differences in the uncertainty level of a specific input parameter. Instead, differences should be expected mainly when situations differ. This is, for example, the case for Finland, where uncertainty regarding CO_2 emissions from peatland contributes to the enhanced uncertainty in CO_2 emissions (Monni et al. 2004). The latest estimations by Statistics Finland (2007), excluding CO_2 emissions from peatland, show an uncertainty for CO_2 that agrees quite well with that of other countries. Uncertainty associated with CH_4 also seems to be well adjusted between countries. Some differences appear because of the use of default vs. country-specific model parameters in the calculation of CH_4 emissions from solid waste disposal sites.

Table 3 Results of recent national GHG inventory uncertainty assessment (tier 2)

Random uncertainty for reference (most recent) year (all given as 2 SD)	Country	CO_2 (%)	CH_4 (%)	N_2O (%)	PFC (%)	HFC (%)	SF_6 (%)	Total GHG emissions (%)
This study	AT	1.6	15	86	11	54	24	5.2
Ramirez et al. (2008)	NL	1.5	15	42	28[a]			3.9
USEPA (2007)[b]	US	3.5	13	20	11[a]			3
Baggott et al. (2005)	UK	2.4	13	226	13	21	16	14
Monni et al. (2004)[b]	FI	5.0	19.5	36.5	42.5[a]			5.5
Statistics Finland (2007)[b]	FI	3	21	50	16[a]			5.5

[a] Combined for all F-gases

[b] All data originally presented with upper and lower limit estimates—here averaged

Table 4 Results of recent national GHG inventory uncertainty assessment using error propagation (tier 1) as submitted to UNFCCC (all submissions are available at unfccc.int)

Country	Source	CO_2 (%)	CH_4 (%)	N_2O (%)	F-gas (%)	Total (%)
AT	Umweltbundesamt (2007)	1.4	14.9	76.4	38.6	3.7
NL[a]	MNP (2006)	1.9	18	45	27	4.3
UK[b]	Baggott et al. (2007)	2.0	20.3	270.9	16.5	16.4
FI	Statistics Finland (2007)	2.6	22.0	70.2	23.1	7.1

[a]Same inventory as Ramirez et al. (2008)

[b]Percentages are calculated by authors on basis of the NIR

Even for F-gases, the level of agreement is remarkable: differences depend mainly on the contribution of emissions from production processes that are usually associated with lower uncertainties than on emissions from the consumption of F-gases as ODS substitutes.

Again, as already described by Rypdal and Winiwarter (2001), the uncertainty in N_2O emissions deriving from soil emissions clearly exhibits the largest variability. As the actual processes that cause formation of N_2O in soil are still far from being fully understood, differences definitely do not result from different situations in different countries, but reflect the priorities of the experts assessing the uncertainty. Further work, for example, through the application of detailed biophysical soil modeling, will be required to resolve this issue.

Differences in uncertainty are also seen in total GHG emissions. In almost all cases, these differences are associated with soil N_2O (except for Finland, where the contribution of CO_2 from peatland is also significant, as mentioned above). Irrespective of all other figures, high N_2O uncertainty is associated with high overall uncertainty and vice versa. This result proves that the magnitude of uncertainty associated with a national greenhouse gas inventory mainly depends on the uncertainty of soil N_2O which, because of a lack of measured data, depends very much on the judgment of the experts assessing the uncertainty.

Only a few countries provide results from both error propagation and Monte Carlo uncertainty analysis. Here we compare the Austrian results with those of Finland, the Netherlands, and the United Kingdom (UK). In all countries except Austria, the Monte Carlo approach yields lower uncertainties for total national emissions than the error propagation approach (see Table 4). One explanation for this, at least in Finland (Statistics Finland 2007), is the use of skewed distributions in the Monte Carlo analysis, where for error propagation the larger difference between the mean and the confidence limit was systematically applied. This transformation from a skewed distribution is in line with guidance provided by IPCC (2000), except that this guidance is strictly limited to distributions that have standard deviations of 30% or less of the mean value. As discussed in Section 3.2, however, the actual distribution and the normal distribution chosen this way will have little in common for skewed distributions with standard deviations much larger than 30%. The method of choosing a representation of this skewed distribution will thus have an influence on the outcome.

Furthermore, the Monte Carlo analyses presented in general do not focus on recognizing correlated inputs. This methodical advantage of a Monte Carlo analysis

is thus not fully taken advantage of and results have the same shortcomings, leading to a systematic underestimation of the overall error.

5 Discussion: how statistical dependence affects uncertainty estimates

According to IPCC (2000), inventory agencies are encouraged to identify key sources using the results of the uncertainty analysis (Tier 2 key category analysis). The basic idea behind identifying key sources is to focus resources during inventory compilation. Thus, an uncertainty evaluation that requires additional resources will be focused on sources of major importance, and non-key sources will be investigated in less detail. In the Austrian inventory 151 sources are identified for analysis, of which 40 are identified as key. A detailed investigation of more than 100 sources that account for less than 5% of total national GHG emissions would thus contradict the concept described by IPCC (2006), namely, to focus limited resources on where they can be applied most usefully.

Moreover, following the arguments presented above, separate consideration of each emission source may not be advisable, at least as long as data are statistically dependent and derive from the same or a similar set of input information. We have shown that, in the calculation algorithms, treating dependent data as independent leads to a decrease of the overall uncertainty, which does not reflect the real situation. While in the case of Austria (and probably in many GHG inventories) the conclusions in terms of priority setting are not affected, the numerical values as such are affected and make it difficult to compare the results between two different countries or between two different studies within a country. An appropriate consideration of statistical dependencies is thus important.

We regard this mathematical artifact as more significant than that created by artificial choices during the translation of skewed distributions into error propagation analysis (lower, higher, mean value). This is because, in those cases, the reasons for a discrepancy are more obvious. In the case of statistical dependency, the problem remains, not only when comparing inventories and assessing overall uncertainties for a larger set of countries (Leip 2010) but also when inventory uncertainty is to be combined with uncertainty from, for example, economic parameters (Nahorski and Horabik 2010). While in the latter case the chances are higher that no dependence will be observed, it will still be worthwhile accounting for common underlying factors that may be found in very generic parameters, such as ambient temperature, which can affect very different areas. This underlines the importance of truly independent data, for example, in the form of measurements, as a method of further reducing uncertainties associated with reported inventory data on greenhouse gases (see Theloke et al. 2007, for such a validation approach).

6 Conclusion

Uncertainty analysis is important for national inventory compilers to understand the complexity connected with data quality. One should not expect, however, that the results in terms of overall uncertainty allow conclusions to be drawn on the inventory quality.

We attribute the differences between the datasets of one country (Austria), as compared with those of several other countries for which Monte Carlo type uncertainty assessments are available, to:

- Differences in economic structure: countries in which highly uncertain sources (specifically, emissions of N_2O from soils as a consequence of agricultural nitrogen application) are prevalent will exhibit higher uncertainties than those with a very high share of energy-related emissions.
- Methodological differences: the importance of correlation in assessing overall uncertainties needs to be recognized, especially regarding the most important contributors to overall uncertainty (N_2O from soils).
- Choice of parameters describing uncertainty: especially for uncertain sources (N_2O from soils) little firm evidence is available on the uncertainty distribution, too. The choice of parameters may also reflect the transformation of a highly skewed distribution into a normal distribution which is needed to perform error propagation calculations.

Obviously, input assumptions of uncertainty assessment will strongly drive the result in terms of overall uncertainty. To cover such artifacts, we have previously recommended (Winiwarter 2007) the application of harmonized approaches in emission assessment and uncertainty evaluation instead of using country-specific approaches. Harmonization will allow country results to be made comparable.

Nevertheless, it is interesting to see that the overall order of source contributions is not very different, despite the large differences in the approaches between countries. Thus, qualitatively, agreement between the different approaches remains, and the order of sources in terms of their contribution to overall uncertainty is also similar. The largest of these contributors, in all cases, remains N_2O from soils.

We may conclude that the differences between source categories are so large that they are qualitatively identified independently of the methodology chosen. The quantitative result in terms of overall uncertainty, however, is driven to such a large extent by the approach taken that its numerical value should not be used for direct comparison. The extent of statistical dependence of input parameters needs to be better described and elucidated, before the full benefit of an uncertainty analysis can be obtained.

References

Baggott SL, Brown L, Milne R et al (2005) UK greenhouse gas inventory 1990 to 2003. Annual report for submission under the Framework Convention on Climate Change. AEA Technology, Didcot

Baggott SL, Cardenas L, Garnett E et al (2007) UK greenhouse gas inventory 1990 to 2005. Annual report for submission under the Framework Convention on Climate Change, Report AEAT/ENV/R/2429. AEA Technology, Didcot

Charles D, Jones BMR, Salway AG et al (1998) Treatment of uncertainties for national estimates of greenhouse gas emissions, AEAT-2688-1. AEA Technology, Culham

IPCC (2000) Good practice guidance and uncertainty management in national greenhouse gas inventories. Intergovernmental Panel on Climate Change, National Greenhouse Gas Inventories Programme, Hayama

IPCC (2006) 2006 IPCC guidelines for national greenhouse gas inventories. In: Eggleston HS, Buendia L, Miwa K, Ngara T, Tanabe K (eds) IGES, Hayama (prepared by the National Greenhouse Gas Inventories Programme)

Leip A (2010) Quantitative quality assessment of the greenhouse gas inventory for agriculture in Europe. Clim Change. doi:10.1007/s10584-010-9915-5
Lieberman D, Jonas M, Winiwarter W et al (2007) Accounting for climate change: introduction. Water Air Soil Pollut Focus 7:421–424
MNP (2006) Greenhouse gas emissions in the Netherlands 1990–2004. National Inventory Report 2006, MNP report 500080 001. Netherlands Environmental Assessment Agency (MNP), Bilthoven
Monni S, Syri S, Savolainen I (2004) Uncertainties in the Finnish greenhouse gas emission inventory. Environ Sci Policy 7(2):87–98
Nahorski Z, Horabik J (2010) Compliance and emission trading rules for nonsymmetric emission uncertainty estimates. Clim Change. doi:10.1007/s10584-010-9916-4
Orthofer R (1991) Abschätzung der Methan-Emissionen in Österreich, report OEFZS-4586. Forschungszentrum Seibersdorf, Seibersdorf
Ramirez A, de Keizer C, van der Sluijs JP et al (2008) Monte Carlo analysis of uncertainties in the Netherlands greenhouse gas emission inventory for 1990–2004. Atmos Environ 42:8263–8272
Rypdal K, Winiwarter W (2001) Uncertainties in greenhouse gas inventories—evaluation, comparability and implications. Environ Sci Policy 4:107–116
Statistics Finland (2007) Greenhouse gas emissions in Finland 1990–2005. National Inventory Report to the UNFCCC. Statistics Finland, Helsinki
Theloke J, Pfeiffer H, Pregger T et al (2007) Development of a methodology for temporal and spatial resolution of greenhouse gas emission inventories for validation. In: Proceedings of the 2nd international workshop on uncertainty in greenhouse gas inventories, 27–28 September 2007. International Institute for Applied Systems Analysis, Laxenburg, Austria, pp 203–208
Umweltbundesamt (2007) Austria's National Inventory Report 2007, submission under the United Nations Framework Convention on Climate Change. Report REP-0084, Umweltbundesamt, Vienna, Austria
US EPA (2007) Inventory of U.S. greenhouse gas emissions and sinks: 1990–2005. USEPA #430-R-07-002. US Environmental Protection Agency, Washington
Winiwarter W (2007) National greenhouse gas inventories: understanding uncertainties vs. potential for improving reliability. Water Air Soil Pollut Focus 7:443–450
Winiwarter W (2008) Quantifying uncertainties of the Austrian Greenhouse Gas Inventory. Report ARC-sys-0154. Austrian Research Centers GmbH-ARC, Vienna. Available at http://systemsresearch.ac.at/FTP/winiwarter/papers/ARC_sys_0154.pdf. Accessed 9 November 2009
Winiwarter W, Köther T (2008) Uncertainty related to Luxembourg's National Greenhouse Gas Inventory. Report ARC-sys-0162. Austrian Research Centers GmbH-ARC, Vienna. Available at http://systemsresearch.ac.at/FTP/winiwarter/papers/ARC_sys_0162.pdf. Accessed 9 November 2009
Winiwarter W, Orthofer R (2000) Unsicherheit der Emissionsinventur für Treibhausgase in Österreich. Seibersdorf Research Report OEFZS-S-0072, Österreichisches Forschungszentrum Seibersdorf GmbH, Seibersdorf (Austria). Available at http://systemsresearch.ac.at/FTP/winiwarter/papers/arcs0072.pdf. Accessed 9 November 2009
Winiwarter W, Rypdal K (2001) Assessing the uncertainty associated with national greenhouse gas emission inventories: a case study for Austria. Atmos Environ 35:5425–5440

Climatic Change (2010) 103:37–54
DOI 10.1007/s10584-010-9919-1

Uncertainty analysis for estimation of landfill emissions and data sensitivity for the input variation

J. Szemesova · M. Gera

Received: 5 January 2009 / Accepted: 15 June 2010 / Published online: 17 July 2010

Abstract Results of research and practical experience confirm that stabilization of GHG concentrations will require a tremendous effort. One of the sectors identified as a significant source of methane (CH_4) emissions are solid waste disposal sites (SWDS). Landfills are the key source of CH_4 emissions in the emissions inventory of Slovakia, and the actual emission factors are estimated with a high uncertainty level. The calculation of emission uncertainty of the landfills using the more sophisticated Tier 2 Monte Carlo method is evaluated in this article. The software package that works with the probabilistic distributions and their combination was developed with this purpose in mind. The results, sensitivity analysis, and computational methodology of the CH_4 emissions from SWDS are presented in this paper.

1 Introduction

The results of both research and practical experience confirm that stabilization of greenhouse gas (GHG) concentrations will require a tremendous effort. Without a limitation of emissions, atmospheric concentrations of CO_2 will grow from an expected 385 ppm in 2008 to 490–1,260 ppm in 2100, representing a 75–350% increase over 1750 (IPCC 2007). To stabilize concentrations at the 450 ppm level, GHG emissions need to fall to below the level of the reference year 1990 in the next decade.

The concentration of methane (CH_4) in the atmosphere has increased 250% in the industrial era. CH_4 contributes up to 20% of anthropogenic GHG emissions. The

J. Szemesova (✉)
Slovak Hydrometeorological Institute, Jeseniova 17, Bratislava, Slovakia
e-mail: janka.szemesova@shmu.sk

M. Gera
Faculty of Mathematics, Physics and Informatics, Comenius University,
Mlynska dolina, 842 48, Bratislava, Slovak Republic
e-mail: mgera@fmph.uniba.sk

rapid growth in CH_4 concentration has been caused by intensive farming, livestock production, coal mining, transport, utilization of natural gas, and solid waste disposal sites. The life span of CH_4 in the atmosphere is 10–12 years. Total annual emissions are about 0.4 billion tonnes of CH_4 and represent a stable annual increment (IPCC 2007).

CH_4 is one of the most important greenhouse gases, with around 20 times higher global warming potential (GWP) per 100 years than CO_2. The main sources of CH_4 emissions with a high level of uncertainty are solid waste landfills. There are several methods available for estimating CH_4 emissions from solid waste disposal sites (SWDS). The most sophisticated method with a higher tier of accuracy is the kinetic approach, which takes into account that CH_4 is emitted over a long period of time rather than all at once. The kinetic approach thus needs to consider various factors influencing the rate and extent of CH_4 generation and release from SWDS. The equations presented in IPCC manuals form the basis for first order decay (FOD) method kinetics and come from the *Revised 1996 IPCC Guidelines for National Inventories: Reference Manual* (IPCC 1996). The *IPCC Good Practice Guidance and Uncertainty Management in National Greenhouse Gas Inventories* (IPCC 2000) provides further details on the FOD method, mainly through defining FOD model parameters in terms that are familiar to users of the default method Tier 1.

The waste sector is the source of greenhouse gas emissions from three main categories as follows:

- Solid waste disposal (CH_4);
- Waste water treatment (CH_4, N_2O);
- Waste incineration in combustion plants and non-controlled waste incineration (CO_2).

Solid waste disposal is a significant source of CH_4 emissions in Slovakia; these are generated during the decomposition of organic materials present in the waste under anaerobic conditions. Methane emissions from the landfills are the key source in the emission inventory of Slovakia and with regard to the actual emission factors, these are estimated with a high degree of uncertainty. Total emissions of CH_4 from SWDS have been increasing since the 1990 base year and represent at present about 45 Gg CH_4 per year NIR 2007 with default set at Tier 1 with a 50% degree of uncertainty (IPCC 2000). Waste disposal is the main method of waste treatment in Slovakia, with more than 80% of municipal waste being placed in landfills. For the purposes of individual greenhouse gases inventories, waste disposal represents a single category. However, for calculation purposes, there is a need to differentiate, if the waste is characterized as:

- Mixed municipal waste (methodology Tier 2, first order decomposition formula);
- Industrial waste and other waste flows (methodology Tier 1, default balance);
- Municipal wastewater and sludge treatment and release;
- Industrial wastewater and sludge treatment and release.

Mixed municipal solid waste disposals represent the vast majority of emissions, making up more than 80% of waste. For this reason this study has focused on

municipal waste disposal. Waste streams can be used as an approach to model landfill gas generation rate curves for an individual landfill. They can also be used to model the gas generation for a set of SWDS to develop the country emissions estimates; or it can be applied in a more general way to entire regions.

CH_4 emissions from landfills in Slovakia were estimated with first order decay (FOD) method Tier 2 methodology in line with the advice of the expert review team of the UNFCCC Secretariat and the European Commission. All time series were recalculated to 1960, and the entire methodological approach was changed.

Three versions of the FOD method presented (Farkas 2006), were considered for the Tier 2 method for estimation of CH_4 emissions from SWDS in Slovakia. A comparison between the situation in Slovakia and other countries applied the Tier 2 approach (Finland, Austria) identifies several differences:

- Most countries use site-specific data. CH_4 emissions are calculated for each SWDS (or group of SWDS) separately and the results are then summed to obtain the national CH_4 emission estimation. This approach cannot yet be applied in Slovakia, as the data collected on municipal solid waste (MSW) do not include the necessary SWDS characterization, as outlined above;
- Historical data on MSW management and disposal are more detailed than the data available in Slovakia;
- Data on MSW fractions are collected in a more systematic and regular way than in Slovakia.

The second version of the FOD method was selected as the most appropriate approach, as it is defined (IPCC 2000). This decision was based on recommendations from a previous review of Slovakia under the UNFCCC and is also supported for the following reasons:

- The parameters used are better defined and allow direct comparison with the Tier 1 method;
- Some of the parameters used are defined as time variables. This allows the waste sector transformation in Slovakia in the 1992–2000 period to be modeled.

The uncertainty of the CH_4 emission estimation is due mainly to the uncertainty regarding the input of statistical data. Another source of uncertainty is the applied default emission factors (EF). An additional error in calculations may occur as a result of the less exact methods used. The calculation of landfill emission uncertainty by the more sophisticated Tier 2 Monte Carlo method is evaluated in this paper.

2 The Monte Carlo method

In some cases it is difficult to find a purely analytical solution to problems being investigated. Where data are significantly inaccurate, the statistical approach is used, which helps us include uncertainty in the final assumption. To know the final margin of uncertainty of the processes observed, the fluctuation of the analyzed variables that entered the examined interdependent processes ultimately needs to be estimated. Using a classical statistical approach, it can be difficult in some cases

to obtain reasonable final information about the consequential uncertainty of the processes investigated. One method that allows us to implement all the uncertainty in the final analyses is the Monte Carlo method. Many examples of the application of this method can be found in the literature of different areas of study. In many cases where the Monte Carlo method is applied, the process investigated is simulated directly. The Monte Carlo theory is applied here in a general, well known format. There is no need to describe the behavior of the system investigated, which can be advantageous in some complicated systems. The only important requirement is for the system to be able to be described by probability density functions (PDFs). We will assume that the properties of a system can be described by PDFs. Once these are known, the Monte Carlo simulation can proceed by random sampling technique from the PDFs. This approach works using a generator of random numbers with the properties of the PDF. Many trials are then performed, and the expected result is obtained as an average of the number of values. In this case the statistical structure, variance, kurtosis, and other higher statistical moments of the simulated result can be predicted. An estimation of the number of Monte Carlo trials needed to obtain a result with an expected error can be achieved from these characteristics.

The Monte Carlo method is based on the generation of multiple trials to determine the expected value of a random value. It can be said in our case that this method is the combination of the uncertainties of the probability distribution functions for the activity data (AD) and for the emission factors (EFs). The total emissions are then computed as a combination of random numbers for the appropriate distribution function for the assigned greenhouse gases. The advantage of this method is the allowance for asymmetry in the statistical distribution (the default Tier 1 method does not allow asymmetry). This advanced method is useful for data manipulation, as long as proper input data quality is provided. It can usually be assumed that higher tier methods are associated with lower input data uncertainties (Rypdal and Winiwarter 2001).

In practice, process uncertainties vary from a few percent to orders of magnitude, and they may be correlated. This is not consistent with the simplified assumptions applied in the Tier 1 method (the variables are uncorrelated with the standard deviation of less than about 30% of the mean). The Tier 1 method assumes that: the number of emission and uptake terms is large; no single term dominates the sum; and the emissions and uptakes are independent. If this is so, the sum of the variances of all the terms equals the variance of the total inventory, and the distribution of total emissions is normal. Thus, the interval defined by approximately two standard deviations from either side of the mean is the 95% confidence interval of the inventory.

In Tier 1, the uncertain quantities are usually added together. In this case, with respect to the limitation, it can be assumed that the standard deviation of the sum is the square root of the sum of the squares of the standard deviations of the quantities that are added, with the standard deviations all expressed in absolute terms (this rule is exact for uncorrelated variables).

Next, in Tier 1, the uncertain quantities are multiplied together, and the same rule applies as in the previous case, except that the standard deviations must all be expressed as fractions of the appropriate mean values (this rule is approximate for all random variables) (IPCC 2000).

In spite of the simplified limitations to approximate results with Tier 1, the method also obtains in cases that go beyond the circumstances mentioned.

In contrast to the previous difficulties, the Monte Carlo method can combine uncertainties with any probability distribution (non-Gaussian), range (large variances), and correlation structure (IPCC 2000). The Monte Carlo method could be the method of choice in these cases.

The practice shows that, in some cases, the Tier 1 method could yield results with a lower uncertainty than the higher-tier methods. In this situation, the limitation and statistical simplification of the Tier 1 method should be known. It is important to understand that the Tier 1 method offers only rough and approximate results. It gives informative data, which serve as the background for more sophisticated analyses. On the other side, the Tier 1 method could be a unique starting point for obtaining solid results in the absence of quality input data (high variance of examined processes, etc.).

3 Landfill CH_4 emissions

Ideal information for estimating uncertainties includes (IPCC 2000):

- The arithmetic mean (the mean) of the data set;
- The standard deviation of the data set (the square root of the variance);
- The standard deviation of the mean (the standard error of the mean);
- The probability distribution of the data;
- Covariance of the input quantity with other input quantities used in the inventory calculations.

This information, which is based on measurement, on an empirical data source, or on expert-assessed data is sufficient to define the probability distribution for statistical analysis and for specification of a 95% confidence interval.

During the inventory the uncertainty source can be identified from different processes (IPCC 2000), as follows:

- Uncertainties from definitions (e.g., incomplete/unclear meaning or faulty definition of an emission or uptake);
- Uncertainties from natural variability of the process that produces an emission or uptake;
- Uncertainties resulting from assessment of the process or quantity, including the method and depending on it.

In Slovakia, the second variant of the FOD method was chosen (IPCC 2000) and the Tier 2 approach was also used (Tier 1 approach was also calculated) for the inventory to simulate CH_4 emissions from landfill. More details can be seen in publication (Farkas 2006). Emissions of CH_4 from waste disposal sites depend mainly on the factors, as well as other parameters from the emission inventory, that change from year to year (amount of waste landfill, meteorological conditions, population growth, composition of waste, etc.) and from previous years (management style of sites, etc.), which contribute CH_4 from deeper layers to the emissions in the inventory

year. It is obvious that total emissions are dependent on many factors, which vary from year to year. The formulas, which describe these emissions, have the form:

$$L_0(x) = \frac{16}{12} MCF(x)\,DOC(x)\,DOCF(x)\,F(x)$$

$$Fk(x,t) = (1 - e^{-k})e^{-k(t-x)}$$

$$MSWL(x) = MSWT(x)\,MSWF(x)$$

$$Q_t(x,t) = Fk(x,t)\,MSWL(x)\,L_0(x) \tag{1}$$

$$Q_T(t) = \sum_x (Q_t(x,t) - R(x))(1 - OX(x)) \tag{2}$$

where variable t identifies the year of emission inventory, variable x identifies the year of waste added to the dump, $L_0(x)$ represents the CH_4 generation potential (Gg CH_4/Gg waste), $MCF(x)$ is related to the CH_4 correction factor in the year x (fraction), $DOC(x)$ is related to the degradable organic carbon in the year x (Gg C/Gg waste), $DOCF(x)$ represents the dissimilated fraction of $DOC(x)$, $F(x)$ represents the fraction by volume of the CH_4 in the landfill gas, $Fk(x)$ represents the gas leakage from the deeper dump layers (the normalization factor which corrects the summation), k is related to the CH_4 generation rate constant (1/year), $MSWT(x)$ is the total municipal solid waste, $MSWF(x)$ is the fraction of $MSWT$ disposed of in the year x, $R(x)$ is related to the recovered CH_4 in the inventory year t (Gg/year), $OX(x)$ is the oxidation factor (fraction) and Q_t, Q_T represent the CH_4 generated in the year t (Gg/year) from the waste layer storage in the year x and the CH_4 generated in the year t (Gg/year) from all layers, respectively.

Using formulas 1 and 2, one can interpret that formula 1 and term Qt represent the contribution of emissions from the waste layer added in the year x to the year of inventory t. It means that the result for the inventory year t is computed by formula 2, which performs the summation of the CH_4 submission from different layers stored in different years.

The model presented computes cumulative uncertainties of emissions from layers of landfills deposited from 1960. The function Fk represents the contribution to emissions of deposited layers during the years observed. The exponential character of function Fk ensures appropriate estimation of annual emissions.

Every parameter entered into the presented formulas has its own uncertainty. To know the resulting uncertainty for CH_4 generation from waste disposal sites, a complex method must be used, which appropriates and combines all the uncertainties. The Monte Carlo method is convenient for uncertainty problem solving. One requirement is to know the distribution function of uncertainties. This approach allows us, using computing power, to simulate the complete properties of the final probability distribution function and to obtain the required statistical characteristics. In this point, one should pay attention to the way in which the uncertainties are specified. If measurement data are available, the situation is solvable. If these data are absent, there is a special estimation by the waste expert. There are special recommendations in the literature (IPCC 2000) regarding how to make this estimation. Reasoning and detailed explanations of expert estimation can be found

(Farkas 2006; NIR 2008). The parameter settings for the terms used can be seen in Table 1.

It is clear from Eqs. 1, 2 and Table 1 that the Tier 1 approach is below the method limits and that its result should be interpreted carefully. The formulas are not simple; the time dependence and the nonlinear features they contain are important, and the standard deviations of some input parameters are >30% of the mean value. In this case the computation uncertainty with Tier 1 could provide only informative results.

A variety of inputs, two parametric distributions, three parametric distribution functions, and empirical probability profiles are utilized (Monni 2004; Monni et al. 2004) for specification of the probability distribution of AD and EF).

To solve Eqs. 1 and 2 with the Monte Carlo method, specified uncertainty parameters were used. The profiles of the PDF functions are obtained after an expert consultation and in line with the recommendations of the IPCC Guidelines. The result of the efforts entailed in setting the PDFs is summarized in Table 1. The country-specific value for the mean values and confidence interval in Table 1 were estimated by a waste sector expert in UNFCCC Decision 20/CP.7 (2001). More details can be seen in literature (Farkas 2006). If measured data are absent, PDF shapes are chosen in the simplest possible form. In a situation where the expert estimation is too great to fit the possibilities, the empirical PDF can be used. This approach is preferable if the main properties of the parameters examined are to be retained, instead of the data being adapted to satisfy the PDF properties. This problem is discussed later.

The value of some parameters in Table 1 should be explained. Parameter F, which can be seen in Eqs. 1 and 2, is split into variables with different confidence intervals in pre-1994 and post-1994 years. The *MCF* parameters are defined analogically. The difference in comparison with the previous case is that the mean value is also changed. For this reason, the data to 1993 and in 1994–2001 should be resolved. In 1994–2001, the mean value is linearly interpolated between pre-1994 and post-2001 data values. The variability is correspondingly modified. After 2001 the table values are valid. The *MSWL* parameter which is a product of the multiplication of *MSWT* and *MSWF* requires a special explanation. In this case we exploit the possibility of easily transforming the standard normal distribution into the normal distribution.

Table 1 Probability distribution functions and their basic characteristics, the mean value, and 95% confidence interval expressed with two percentage values relative to the mean value

Category	Mean value	Confidence interval	Distribution function
k	0.065	−45% : 230%	Empirical
$F(x)$ (until 1994)	0.500	−20% : 20%	Normal
$F(x)$ (after 1994)	0.500	−2.0% : 20%	Empirical
MSWL			Stand. normal
DOCF	0.600	−30% : 28%	Triangular
DOCX	0.120	−50% : 20%	Empirical
MCF (until 1994)	1.000	−30% : 4%	Empirical
MCF (after 2001)	0.600	−50% : 60%	Triangular
OX	0.050	−95% : 100%	Triangular

The units of the parameters are defined in the text ($\sigma = 1$ for standard normal distribution). Source: The confidence interval in values and PDFs were taken from Farkas (2006). Parameters estimation considered IPCC default recommended values and country specific circumstances. Presented parameters were reviewed during in-country reviews of Slovakia in 2007 and 2009

The *MSWL* parameter is varied significantly during the 1960–2005 period we analyze (Fig. 1b). The uncertainty of *MSWL* data has the standard normal distribution. These properties of PDF and *MSWL* annual values are applied to construct the final form of PDF. The *MSWL* uncertainty to 1995 was taken to be 50% of the mean value. After 1995 the uncertainty of *MSWL* was taken to be 10% of the mean value. The variation of the mean value of *MSWL* can be seen in Fig. 1b. The annual *DOCX* value is linearly changed from value 0.06 in 1960 to value 0.12 in 1990. After 1990 this parameter has a constant value. The *DOCX* value in a given year is calculated as an average of *DOC* values for different housing quality based on statistical information about the type of household heating (Farkas 2006). The values from the table are valid for the *OX* parameter only in the period 1994–2005. Beyond this time the zero value is assumed.

To estimate the total emissions for a chosen year, the formulas presented here can be used. The situation starts to become complicated when the assumption of the input data uncertainty takes place. Formulas 1 and 2 show the relatively complicated relation between the terms in these functions. There starts to be hardly any computation of the interaction of uncertainties. For that reason the simplified linear analysis is performed in advance.

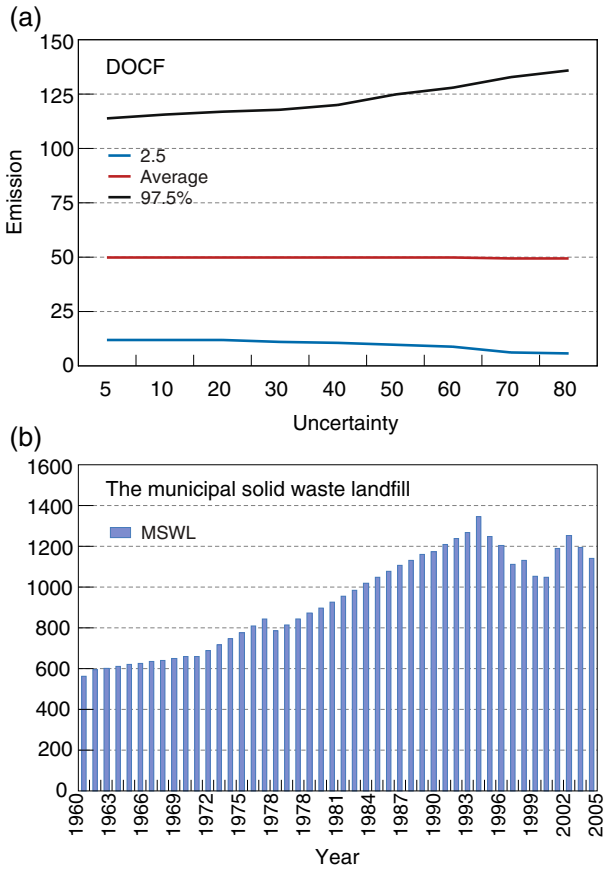

Fig. 1 **a** The *DOCF* parameter sensitivity to the normal PDF uncertainty variation; **b** the municipal solid waste landfill (*MSWL*) mean value variation during the 1960–2005 period

It can be assumed that our emission production is expressed by function $F(Xi)$, where Xi are the factors affecting the sequential result of emissions (i = 1…N, N represents the number of factors). Every factor has its own uncertainty $\delta(Xi)$, which depends on several sources. In some situations it is impossible to express the variation of these sources in a function value. It is possible only to express the interval of the eventual values and their statistical behavior. In this case the values Xi can be interpreted as per the data set. For example, factor X_1 will be represented by random values from the expected range of values. The function value and their uncertainties can be expressed as:

$$F(X_i) = F(+\delta(X_i)), \tag{3}$$

where $\overline{X}_i$ represents the mean (expected value) or the special chosen value from the possible range of Xi values. It depends on algorithm solution. The question is how the uncertainties of X_i values will affect the function value $F(Xi)$. The interest is focused on finding the expression for $\delta\,(F(Xi))$. Assume that X_i are random variables. For example, let X_1 have normal distribution $X_1 \sim N(\mu_1, \sigma_1)$ and $X_2 \sim N(\mu_2, \sigma_2)$. There are independent random variables. For addition, $F(X_1 + X_2) \sim N(\mu_1 + \mu_2, \sigma_1^2 + \sigma_2^2)$ can be expected. For multiplication, the situation is complicated; assume that $\mu_1 = \mu_2 = 0$. For this situation the result can be written in the form: $\mathrm{F}(X_1 X_2) \sim \frac{1}{\sigma_1\sigma_2} J_0\left(\frac{|X_1 X_2|}{\sigma_1\sigma_2}\right)$, where J_0 is the modified Bessel function of the second kind. For exponential distribution, which is a special case of gamma distribution, one can obtain, after multiplication of the exponential distribution, the Weibull distribution: $X_1 \sim$ Exponential$(\lambda^{-\gamma})$ and than $F(X_1^{1/\gamma}) \sim$ Weibull (γ, λ), (γ, λ are the parameters affecting the shape of PDF). It can be seen from these examples that the direct computation of $\delta\,(F(Xi))$ is possible only in special cases.

To estimate the properties of $\delta\,(F(Xi))$, the error propagation can be analyzed by linearized theory. Consider the term grouped with the first derivative of Taylor's series for $F(Xi)$. It can be written as:

$$\left|F(X_i) - F\left(\overline{X}_i\right)\right| \leq \sum_i \left|X_i - \overline{X}_i\right| \left|\frac{\partial F\left(\overline{X}_i\right)}{\partial X_i}\right|,$$

or it can be expressed in an equivalent form, where the prime marks derivative:

$$|\delta\ F\,(X_i)| \cong \sum_i |\delta\,(X_i)| \left|F'\left(\overline{X}_i\right)\right|. \tag{4}$$

Using the same approach, it is possible to take the formula for the variance:

$$Var\left[\delta\ F\,(X_i)\right] \cong \sum_j \sum_i Cov\left[\delta\,(X_i)\,, \delta\left(X_j\right)\right] \left|\frac{\partial F\left(\overline{X}_i\right)}{\partial X_i}\right| \left|\frac{\partial F\left(\overline{X}_j\right)}{\partial X_j}\right|. \tag{5}$$

This simplified approach allows us to refuse the complicated behavior of function $F(Xi)$ and compute its uncertainty as a linear combination of the uncertainty of its variables, see formula 4. For variance, there is no linear relation, but when

correlations between factors X_i are suppressed and $X_i \sim N(\mu_i, \sigma_i)$, then a non-central chi-square distribution can be assumed for $\delta\,(F(Xi))$.

This simple approach has limited applicability. It shows the error spreading and forms a scheme of uncertainty interactions. Without the generality lost, formula 4 can be prescribed into the applicable form:

$$|\delta\ F\,(X_i)| \cong \sum_i \left|\frac{\delta\,(X_i)}{\overline{X}_i}\right| \left|\overline{X}_i F'\left(\overline{X}_i\right)\right|,$$

or with introduction of new functions:

$$|\delta\ F\,(X_i)| \cong \sum_i \left|\frac{\delta\,(X_i)}{\overline{X}_i}\right| \left|G\left(\overline{X}_i\right)\right|, \tag{6}$$

where $G(\overline{X}_i) = \overline{X}_i F'(\overline{X}_i)$. This expression shows the linearized form of the uncertainty combination. When a value that represents the 95% confidence interval is substituted for $\delta(Xi)$, the ratio $(X_i)/\overline{X}_i$ it represent the percentage contribution to the total uncertainty. The result is a linear combination of these percentage submissions. In the linear dependence of $F(\overline{X}_i)$ the solution is modified to the form:

$$|\delta\ F\,(X_i)| \cong \sum_i \left|\frac{\delta\,(X_i)}{\overline{X}_i}\right| \left|F\left(\overline{X}_i\right)\right|. \tag{7}$$

In this case the total error of the above formula is an addition of particular terms, which occur in the function defined by expression 1 or 2. From this it can be seen that the linearized approach is effective for use only in the case when $|G(\overline{X}_i)| << 1$. On the other hand, it shows us that PDFs of $\delta(Xi)$ can play an important role within the process of uncertainty combination. It is clear from this knowledge that one cannot simply sum together the errors from $\delta(Xi)$ without investigation of the probability distribution function of $\delta(Xi)$. The application of initialization records from the applied values to the FOD model confirms the concerns from the linear theory limitations (Szemesová and Gera 2007b). These results, formulas 5, 6, or 7 are close to the Tier 1 uncertainty computation. The knowledge obtained by the linear approach requires the use of a sophisticated model for improved description of uncertainty.

The software package, which works with the probabilistic distributions and their combination, was developed for the resulting uncertainty computation. Together with the AuvTool software, they create useful tools for uncertainty estimation. The following statistical distributions are supported in the developed packages: Gumbel, Exponential, Weibull, Lognormal, Uniform, Triangular, Beta, Binomial, Negative binomial, Chi-square, Noncentral chi-square, F, Noncentral F, Gamma, T, Noncentral T, Normal, Poisson, and empirical.

The above-mentioned PDFs and their statistical properties are well known, apart from the empirical distribution. The probability function for the model parameters was presented in the above text. When the data obtained are used for development of distributions, it is important to determine if the data are a random, representative sample, for instance, a sample from a population. To obtain the 95% confidence

limit, some additional information about the data set is needed. Use of the PDF properties or the cumulative distribution function (CDF) allows us to obtain additional information about the percentiles and data properties. With this knowledge the propagation of uncertainties can be analyzed and the values for the confidence interval determined.

In some cases it is necessary to construct the empirical distributions that supply the analytical properties of PDF or CDF. There are many instances in the literature where the use of analytical distribution is preferred to empirical distribution. According to these, the empirical probability distributions are unwieldy, and there are proposals to replace them with an analytical function, either with CDF or with PDF. It can be seen in the text below that, in some cases, adherence to the empirical distribution is more advantageous than being forced to find the analytical function. For example, in many cases, several functions can fit the empirical data satisfactorily within given probability criteria. These different functions can have different distributions at the extremes where there are few or no data to constrain them, and the choice of one function over another can systematically change the outcome of an uncertainty analysis (IPCC 2000).

For these reasons, there are some recommendations in the literature regarding how to construct a PDF or a CDF. These recommendations become important especially when there are some degrees of freedom for PDF construction: usually this happens when expert recommendations are important and an insufficient amount of data is available.

When empirical data are available, the first choice should be to assume the normal distribution of the data (either in a complete or truncated form to avoid negative values, if these would be unrealistic), unless the scatter plotting of the data suggests a better fit to another distribution. When an expert judgment is used, the distribution function adopted should be normal or lognormal or as in the previous case, supplemented by uniform or triangular distributions. Other distributions are used only where there are compelling reasons to do so, either through empirical observations or resulting from an expert judgment backed up by a theoretical argument (IPCC 2000).

In some special cases, for example, when a strong skew in the PDF is desired by the expert assessment, empirical distribution has to be constructed. It is for this reason that we have developed the methodology. In order to know all the above-mentioned recommendations regarding how to construct the PDF, the empirical distribution is constructed as required and these are requirements that should be observed strictly. First, monotonous properties before and after one global maximum on the examined interval are demanded. Probability decomposition is assigned by the confidence interval values (in our case 95%), known from the expert entry. The mean value for the data set is also assigned. These requirements create relations that allow us to construct a system of equations that describes these objectives. In the system there can be a few free parameters that allow us to modify the shape of the probability function. The number of tuned parameters is dependent on the number of subintervals (related to the density of points at which the function values are computed). For a better illustration of the empirical behavior, the $DOC(x)$ parameter is presented in Fig. 2a, b.

In this case, it should be effective, with respect to the previous recommendations regarding PDF construction, to take this data sample and construct the desired

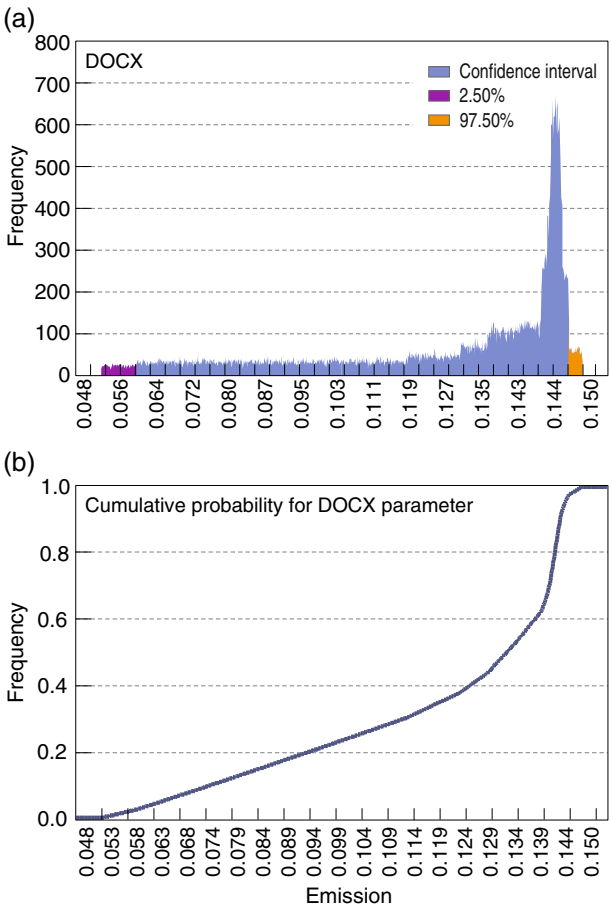

Fig. 2 **a** The probability density function is generated by the empirical function; **b** the cumulative probability function for the *DOCX* parameter is presented. The mean value is 0.120, the confidence interval −50%:20% relative to the mean value (0.060:0.144)

analytical distributions using a method such as the statistical parameter estimation method, Method of Matching Moment (MoMM), and Maximum Likelihood Estimation (MLE). In special cases, our suggestion, based on experience, is to adhere to the empirical form of data (high skew) because the continuous analytical form, which approximates our empirical distribution, can change the desired statistical criteria significantly (the confidence interval or average differ from the initial conditions).

Where an expert determines the confidence interval, the creation of the PDF procedure could force us to modify these input parameters. It can be deduced from Fig. 1a that the uncertainty changes are not linear and that the influence on total uncertainty of value changes to the PDF function should be investigated in advance. To prevent manipulation of input values, which represent the confidence interval or the mean value, it is preferable, as explained above, to use the empirical PDF. This approach will satisfy the expert requirements absolutely.

With this knowledge, the PDFs from the parameters entered (Table 1) are constructed (the result can be seen in Table 2) and they are applied consecutively

Table 2 Statistical characteristics for the last seven computed inventory years, mean value of emissions (Gg/year), average emission (Gg/year), standard deviation (Gg/year), and 95% confidence interval are expressed with two values 2.50% and 97.50%

CH_4/year	1999	2000	2001	2002	2003	2004	2005
Median	42.6329	43.7533	43.7509	50.0221	53.0137	50.7267	48.7324
Average	42.2509	43.1205	43.0749	49.2063	52.1081	49.8123	47.8165
SD	15.9239	16.2150	16.1070	18.3016	19.2825	18.3440	17.5280
2.50%	11.2803	11.0346	11.0738	12.7138	13.5350	13.0018	12.5398
Percent	−73.3016	−74.4099	−74.2918	−74.1623	−74.0251	−73.8985	−73.7751
97.50%	74.4430	75.5031	75.0564	85.3523	90.0037	85.6646	81.8976
Percent	76.1927	75.0979	74.2461	73.4580	72.7251	71.9748	71.2749
Abs. min	1.0869	1.0628	1.0799	1.2545	1.3506	1.3122	1.2800
Abs. max	114.3017	111.8264	111.0865	126.2310	133.0095	126.5504	120.9383

The relative percentage values related to the mean value are also presented. The following absolute minimum and absolute maximum are shown

to the FOD. After application of the Monte Carlo method in the FOD model, the final probability distributions are obtained for each inventory year. This approach allows us to see the detailed variation and combination of the input parameters and their distribution functions. As shown, the interactions of the PDFs are not simple.

With respect to the knowledge obtained, using Eqs. 1 and 2, together with the probability parameters settings in Table 1, the final statistics for total CH_4 emissions for the chosen period (1960–2005) can be seen in Fig. 3. The result shown is for 60,000 trials. The number of trials has an influence on the precision of the result. Table 2 is added for more specific results for the last 7 years.

Where measured data are absent, it can be useful to know which parameter entered into Eqs. 1 and 2 is more sensitive to the assigned values and their accuracy, which is determined by an expert. Likewise, the PDF type influence for the parameters could be investigated in a similar manner. These facts allow us to focus our interest on the sensitivity of the parameters and to analyze their dependence more carefully. The applied uncertainty values for the sensitivity testing of parameters in Table 1 are chosen from 10% to 50%, for selected parameter *DOCF* 10% to 80% in Fig. 1a. These intervals are selected to demonstrate the total uncertainty dependences of the model and do not directly correspond to the values in Table 1.

To see the influence of the PDFs changes on the total emissions, we try to modify the PDF profiles for every input parameter, as defined in Table 1 (source: IPCC default values and expert estimation). At the beginning of our analysis, each profile was changed into the normal or uniform distribution. The mean values were retained, but the uncertainties were changed. The symmetrical uncertainties were used in the first step of the analysis for input parameters. The first four rows in Table 3 represent this assumption. Abbreviation "Nor." expresses the normal distribution and "Uni." the uniform distribution. The number following expresses the symmetrical uncertainty specification for all the parameters contributing to total CH_4 emissions (for example, number 10 means that the parameter K and other parameters are varied by ±10% about the mean value). The last row was introduced for comparison. It represents the original setting from Table 1.

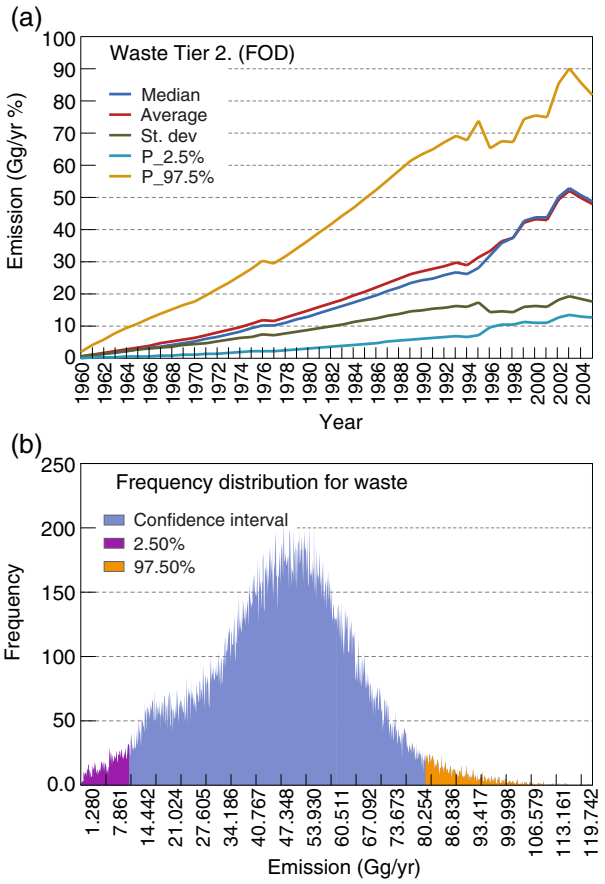

Fig. 3 **a** The variation of the median, average, standard deviation, and 95% confidence interval are expressed by the values during the period 1960–2005; **b** the frequency distribution function for waste for the year 2005 is shown

A different approach should be used to analyze the influence of the parameter on the degree of uncertainty on the aggregate emissions, which is, in our case, offered by formula 7. The uncertainty magnitude for some parameters (Table 1) is several times higher than the mean value. This property does not allow the results from the linearized theory to be used directly. The results for the sensitivity of input parameters are simply validated with the method, which examines the uncertainty

Table 3 Statistical characteristics for different PDF settings for the year 2005, the mean value of emissions (Gg/year), the average emissions (Gg/year), the standard deviation (Gg/year), and the 95% confidence interval are expressed using two relative percentage values 2.50% and 97.50% (the following absolute minimum and absolute maximum are shown)

CH_4/Par.	Median	Average	SD	2.50%	Percent	97.50%	Percent	Abs. min	Abs. max
Nor.10	49.1889	49.4552	5.6646	39.1089	−20.9206	61.2238	23.7964	28.1715	77.1365
Nor.50	42.4680	48.7127	29.8443	10.1810	−79.1000	123.8633	154.2732	0.0000	291.8520
Uni.10	49.0160	49.4153	6.7636	37.3642	−24.3875	63.6923	28.8917	30.2680	76.5576
Uni.50	38.3450	48.2823	36.2270	8.3265	−82.7546	145.1353	200.5973	2.1156	318.7652
Tabular	48.7324	47.8165	17.5280	12.5398	−73.7751	81.8976	71.2749	1.2800	120.9383

fluctuation of the chosen parameter and the total uncertainty. The results of choosing this example of sensitivity can be seen in Table 4 and in Fig. 4.

Tables 3 and 4 are compared for the sensitivity analysis. It is convenient to compare the row "Nor.50" with the chosen statistics from Table 3 and statistics in Table 4. Each row in Table 4 shows the influence of the relevant parameter on the total emission computation. It can be seen that the variation of parameter K has a less significant influence on the total level of emissions. This result was obtained with the normal PDF setting for all parameters and with the change of uncertainty level from ±50% to ±10% for the given parameter. Other parameters show a similar dependence on the uncertainty of total emissions; more details can be seen in publication (Szemesová and Gera 2007a).

We can assume that other parameters, except K parameters concerning the equation structure 1 and 2, will have some variation and influence on the aggregate uncertainty. Examination of the normal PDF was chosen so as to be closer to the Tier 1 approach as though distribution were normal (example in Table 4, other obtained results are not presented here).

This analysis shows that the asymmetry allowance in (Szemesová and Gera 2007c) could be an important feature in our formula and have the strongest influence on the total uncertainty. The asymmetrical PDF could better represent the uncertainty. The normal distribution does not allow asymmetry. For this reason, one can see the disadvantage of the Tier 1 method, which works with symmetric uncertainty. The better choice for the uncertainty specification would thus seem to be the use of a simple PDF in the absence of measured data. For example, a triangular PDF, which allows asymmetry, has features that help us better compute total uncertainty. Use of the symmetric PDF could artificially overestimate the total uncertainty. On the other hand, introduction of a detailed structure to better describe real processes, instead of using simplified models, can introduce greater uncertainties (IPCC 2000). This approach, at first glance, could initiate some reflection regarding the need to develop these sophisticated methods. But we should bear in mind that accurate observation of the problem helps us eliminate further uncertainties.

It should be noted, when interpreting the results obtained, that the parameter uncertainty changes over the years in the FOD model. Similarly, the mean value of some parameters changes during the inventory period analyzed. These features do

Table 4 Statistical characteristics for normal PDF setting for different parameters settings; the parameter sensitivity is analyzed for the year 2005, the mean value (Gg/year), the average (Gg/year), the standard deviation (Gg/year), and the 95% confidence interval are expressed using two relative percentage values 2.50% and 97.50%

CH_4/Par.	Median	Average	SD	2.50%	Percent	97.50%	Percent	Abs. min	Abs. max
DOCX	43.8849	48.7868	26.6149	11.8784	−75.6525	113.7061	133.0671	0.0000	337.3469
MCF	43.7599	48.7756	26.4652	11.9973	−75.4031	113.5155	132.7302	0.0000	244.4157
K	43.3046	49.6141	30.2694	10.5004	−78.8359	126.0141	153.9885	0.0000	308.2557
F	43.7599	48.7756	26.4652	11.9973	−75.4031	113.5155	132.7302	0.0000	244.4157
DOCF	43.8373	48.7171	26.4684	12.0842	−75.1951	113.4445	132.8639	0.0000	288.6757
MSWL	43.8908	48.7435	26.5507	11.9458	−75.4926	112.7903	131.3958	0.0852	248.8542

The following absolute minimum and absolute maximum are shown. For the total uncertainty with normal PDF, there are the input parameters with ±50% uncertainty, apart from the parameter in the first row of the table. The uncertainty of this parameter is only ±10% above the mean value

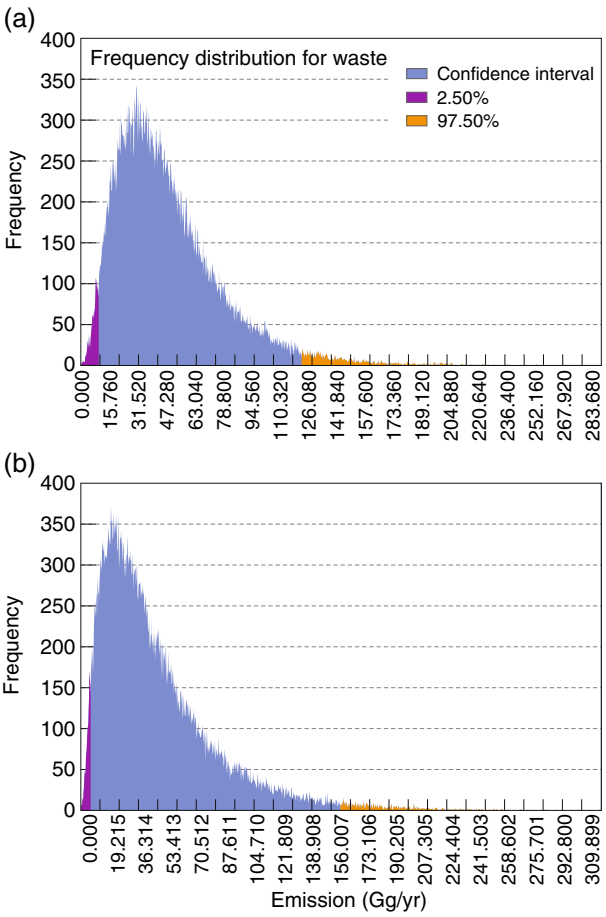

Fig. 4 **a** Are the total emissions of CH_4 for the year 2005 for the normal parameter distribution with a 50% degree of uncertainty for all parameters; **b** the same is shown for the uniform parameter distribution with 50% of uncertainties for all parameters

not allow simple result analyses. Our results show that application of the linearized approach is not useful in our case. The Monte Carlo method provides an effective method for obtaining the statistical structure of the CH_4 emissions from waste disposal sites. It should be noted that the FOD model works with many parameters. The parameter interaction can be seen in formulas 1 and 2. Each uncertainty parameter has a different sensitivity to the computation of total uncertainty. In addition to other dependences, parameter K depends on the amount of precipitation. Because of climate changes, the precipitation allocation (temporal distribution during the year and spatial distribution) will be changed. In the future a different climatic scenario will be assumed, with a more than a 30% variation when compared with the current state of precipitation. The duration of arid and wet seasons will also change. It can be assumed that these conditions will have an influence on disposal site processes. This can influence the mean value of the parameters, or it can change the uncertainty of this parameter and, consecutively, influence the total CH_4 emission estimation in the future. The expected improvements in the future in landfill management can minimize the level of uncertainty of the parameters entered in our study.

4 Conclusion

The main topic of this paper was description of the uncertainty of the CH_4 emissions produced by solid waste disposal sites in Slovakia. Based on our analyses, the emissions uncertainty would appear to be strongly dependent on the PDF setting. These features were identified by the FOD model investigation by simple linear analyses of the uncertainty of total emissions and, in the second case, by changing the PDF setting. Data accuracy plays an important role in the computation of total uncertainty Increase in partial uncertainties for the input factors increases total uncertainties nonlinearly. Where asymmetry is allowed, total uncertainty could be smaller than the uncertainties of single input parameters. Variation in parameter K is seen to have a less significant influence on total emissions than in other parameters. This result was obtained with normal PDF setting for all the parameters and with a change of uncertainty level from ±50% to ±10% for a given parameter. Other parameters except K parameter show a similar dependence on total emission uncertainty. This approach shows that the more important feature, which has the stronger influence on the total uncertainty, is the asymmetry allowance. The result from our study is that total uncertainty was increased comparably to the IPCC default recommended value to the value about ±70% (year 2005). The default value is 50% for the total CH_4 emissions from SWDS. This uncertainty growth is not a failure of Tier 2 against Tier 1, the applicability of which was discussed in the text above. On the contrary, Tier 2 provides the deeper analysis and describes the reality more accurately. It means that actual uncertainty is close to the Tier 2 result and improvement could be achieved by a decrease in input uncertainty parameters. In spite of the high levels of inaccuracy of the input data in the beginning of the period examined (this uncertainty has an influence on the current uncertainty) a relatively useful result based on sophisticated method is obtained. Another result from our analysis is that the CH_4 emissions from the *MSWDs* are the important key category. Specification and identification of the key categories are important for the economy and for government institutions to obtain an overview of the important emission categories, the emission of CH_4 from the underlayer, and many other factors like meteorological conditions, management of the waste sites, and policies and measures that were included in the uncertainty computation. These dependences are expressed in the FOD model, which was solved by Monte Carlo simulation. A propagation of emission computation uncertainty during the analyzed period was obtained.

References

Farkas J (2006) Methane emissions from solid waste disposal sites in 2005. Integrated Skills Ltd, Bratislava. Available at http://www.ghg-inventory.gov.sk

IPCC (1996) Revised 1996 IPCC guidelines for national greenhouse gas inventory, vols 1–3. Available at http://www.ipcc-nggip.iges.or.jp/public/gl/invs1.htm/

IPCC (2000) Good practice guidance and uncertainty management in national GHGs inventories. Available at http://www.ipcc-nggip.iges.or.jp/public/gp/english/

IPCC (2007) Fourth assessment report: climate change. Available at http://www.ipcc.ch/and_data/publications_ipcc_fourth_assessment_report_synthesis_report.htm

Monni S (2004) Uncertainties in the Finnish 2002 Greenhouse Gas Emission Inventory. VTT Working Papers 5

Monni S, Syri S, Savolainen I (2004) Uncertainties in the Finnish greenhouse gas inventory. Environ Sci Policy 7:87–98

National Inventory Reports for GHG Inventory (2008) Available at http://ghg-inventory.shmu.sk
Rypdal k, Winiwarter W (2001) Uncertainties in greenhouse gas emission inventories. Evaluation, comparability and implications. Environ Sci Policy 4:107–116
Szemesová J, Gera M (2007a) Uncertainty analysis for estimation of landfill emissions and data sensitivity for input variation. Paper presented to 2nd international workshop on uncertainty in greenhouse gas inventories. International Institute for Applied Systems Analysis, Laxenburg, Austria
Szemesová J, Gera M (2007b) Emission estimation of solid waste disposal sites according to the uncertainty analysis methodology. International Scientific Conference on Bioclimatology and Natural Hazards
Szemesová J, Gera M (2007c) Uncertainty analysis for estimation of landfill methane emissions. Contrib Geophys Geod 37(3):251–265
UNFCCC Decision 20/CP.7 (2001) Guidelines for national systems under Article 5, Paragraph 1, of the Kyoto Protocol

Climatic Change (2010) 103:55–67
DOI 10.1007/s10584-010-9917-3

Toward Bayesian uncertainty quantification for forestry models used in the United Kingdom Greenhouse Gas Inventory for land use, land use change, and forestry

Marcel van Oijen · Amanda Thomson

Received: 5 January 2009 / Accepted: 15 June 2010 / Published online: 14 July 2010

Abstract The Greenhouse Gas Inventory for the United Kingdom currently uses a simple carbon-flow model, CFLOW, to calculate the emissions and removals associated with forest planting since 1920. Here, we aim to determine whether a more complex process-based model, the BASic FORest (BASFOR) simulator, could be used instead of CFLOW. The use of a more complex approach allows spatial heterogeneity in soils and weather to be accounted for, but places extra demands on uncertainty quantification. We show how Bayesian methods can be used to address this problem.

1 Introduction

Quantifying a greenhouse gas (GHG) inventory is a problem of incomplete information. As no amount of data collection will provide us with a full inventory of all fluxes in a region, additional calculations and assumptions are required. In the case of land use, land use change, and forestry (LULUCF) in the United Kingdom (UK), process-based models are used to quantify net carbon dioxide (CO_2) emissions associated with afforestation, reforestation, and deforestation, based on forestry data and soil type information (Thomson and van Oijen 2007). The model currently used for forests planted after 1920 is CFLOW (Dewar and Cannell 1992; Thomson and van Oijen 2007). CFLOW is a simple compartmental model for the carbon cycle which uses measured wood productivity as input and calculates the flows of carbon to tree parts and soil, with different turnover rates being used for the various compartments. A similar approach, with a similar model (CARBWARE), is used in the GHG Inventory for Ireland (Black, pers. comm. 2007). Here, we investigate

M. van Oijen (✉) · A. Thomson
Centre for Ecology and Hydrology (CEH-Edinburgh),
Bush Estate, Penicuik, EH26 0QB, UK
e-mail: mvano@ceh.ac.uk

the scope for partly or completely replacing CFLOW with a more complex process-based model, the BASic FORest (BASFOR) simulator, that can better take into account the spatial distribution of climate and soil properties across the UK—and how this replacement would affect the process of quantifying uncertainties in the UK Inventory. Besides spatial variation in environmental drivers, process-based models can also calculate the effects of inter-annual variation in weather conditions, such as the irregular occurrence of drought years. However, we shall focus on the spatial variation in this contribution.

A major problem with the use of complex models is incomplete knowledge of input variables as well as model parameters. This causes uncertainty in the model outputs which needs to be quantified and reported in an inventory. The basis of the method for uncertainty quantification used in this work is the Good Practice Guidance, Methodological Tier 2, of the Intergovernmental Panel on Climate Change (IPCC) (Penman et al. 2003). We first quantify the uncertainties associated with model parameters used in the inventory calculation by expressing them as probability distribution functions (PDFs). Then, representative samples are taken from the PDFs to propagate parameter uncertainty forward through the calculations. This results in representative samples of the desired output variables. There are excellent examples of the use of this method for uncertainty quantification (Monni et al. 2007; Peltoniemi et al. 2006). Although the method is relatively straightforward, it needs to be applied with caution. Knowledge about parameters is generally incomplete; they interact, and uncertainty may propagate nonlinearly in the calculations. If the only source of information utilized for the PDFs is direct measurement or expert opinion, the resulting output uncertainty may be overly high (van Oijen et al. 2005). To prevent the generation of inventory uncertainty estimates that are unrealistically high, or even unusable in practice, we need to reduce uncertainties where possible, but we also need to combine direct and indirect information when estimating uncertainties. Here, we use Bayesian calibration to incorporate as much information into our PDFs as possible (Patenaude et al. 2008; van Oijen et al. 2005). Bayesian calibration is the application to parameter pdf estimation of Bayes' Theorem:

$$\mathrm{p}(\theta|\mathrm{D}) = \mathrm{c}\,\mathrm{p}(D|\theta)\mathrm{p}(\theta), \tag{1}$$

where $\mathrm{p}(\theta|\mathrm{D})$ is the so-called posterior pdf for our parameters θ after incorporating new direct or indirect information D, $\mathrm{p}(\theta)$ is the prior pdf for θ that we had before arrival of the new information D, $\mathrm{p}(\mathrm{D}|\theta)$ is the likelihood of D for given values of θ, and c is proportionality constant. Bayes' Theorem is valuable for the inventory because it is often relatively easy to quantify the likelihood $\mathrm{p}(\mathrm{D}|\theta)$ of new information, in which case the Theorem tells us immediately how our uncertainty about the parameters θ decreases because of that information. Useful information D could be measurements of carbon stock changes or emissions (i.e., the key output variables of interest in the inventory), but also equally well measurements of any other variables that play a role in the inventory calculation such as litter fall rates or soil organic matter (SOM) decomposition rates that are intermediate variables in the calculations of the carbon pools and fluxes. The method thus not only propagates uncertainty in inputs and parameters to model outputs, but also uses data on output variables to reduce the uncertainty in inputs and parameters. Finally, an additional

benefit of the method is that the posterior distribution generated by the Bayesian calibration includes appropriate correlations between all parameters—which would be hard to establish otherwise (Winiwarter and Muik 2010).

Here we will demonstrate the application of Bayesian calibration to BASFOR and show predictions of carbon sequestration, including their uncertainty for the time periods 1920–2000 and 2000–2080. From the model results, we calculate coefficients of sensitivity to environmental change. We discuss how the coefficients could be added to the model currently used in the UK Inventory (i.e., CFLOW), as a possibly simple way of sensitizing that model—and thereby the Inventory—to spatio-temporal patterns of atmospheric CO_2, nitrogen (N) deposition, and climate.

2 Methods

In this study, the parameters of the BASFOR model were calibrated using data for two Sitka spruce plantations in the UK. After calibration, the model was run for the whole of the UK at 20 × 20 km resolution for both current and future environmental conditions. For each of the 655 grid cells, flux rates per unit of forested area were calculated. The study did not quantify total fluxes per grid cell, which would have required information about planting areas, as the primary objective was to quantify uncertainties at the level of the forest stand. This section describes the different elements in the approach: the model (Section 2.1), the data (Section 2.2), and the method of Bayesian calibration (Section 2.3).

2.1 BASFOR model

The BASic FORest simulator, BASFOR, is a process-based forest model that simulates carbon and nitrogen cycling in trees, soil organic matter, and litter (van Oijen et al. 2005, 2010). It simulates the response of trees and soil to radiation, temperature, precipitation, humidity, wind speed, atmospheric CO_2 and N deposition, and thinning regime. The model has 11 state variables, representing carbon and nitrogen pools in trees and soil, and 32 parameters controlling the rate of physiological processes and morphological characteristics. Net carbon uptake by the trees is simulated by multiplying light absorption, calculated using Beer's Law, with a light-use efficiency that depends on temperature and the water and nitrogen status of the trees. Uptake of water and nitrogen depends on the balance between tree demand and soil supply. The model is deterministic and is solved by Euler integration with a time step of 1 day.

BASFOR is more complex than CFLOW, the model currently being used in the UK GHG Inventory. CFLOW simulates the pools and fluxes of carbon in the tree–soil system, whereas BASFOR also simulates pools and fluxes of nitrogen and water. The input requirements of the two models also differ. Forest volumetric yield class is input to the CFLOW model, and information on wood density and biomass expansion factors is needed to convert yield class into carbon uptake rates. BASFOR does not require tree productivity as input, but calculates net primary productivity (NPP) dynamically as a function of the current state of the trees and the environmental conditions, including the thinning regime of the stands.

2.2 Data

2.2.1 Weather data

Weather data for the periods 1920–2000 and 2000–2080 were taken from the *UK Climate Impacts Programme* (UKCIP) climate scenarios (Hulme and Jenkins 1998). For future weather, only the "medium–high" scenario was used. The data are given for a regular spatial grid of 655 cells of 20 × 20 km each. The scenarios show that current spatial gradients in the UK for temperature and precipitation are dominated by latitudinal and longitudinal effects, respectively. Future warming is expected to show a decreasing pattern from the southeast to the northwest.

2.2.2 Atmospheric CO_2

Atmospheric CO_2 concentration has increased from around 300 ppm in 1920 to current levels of close to 380 ppm, with an average for the period 1920–2000 of 325 ppm. For the average CO_2 level in the period 2000–2080 under the Special Report on Emissions Scenarios (SRES) IS92a, the Bern model (Joos et al. 1996) predicts a value of 480 ppm.

2.2.3 N deposition

Early twentieth century levels of N deposition were low across Europe (<3 kg N ha^{-1} $year^{-1}$) (Galloway 1985). Data and calculations by the Co-operative Programme for Monitoring and Evaluation of the Long-Range Transmission of Air Pollutants in Europe (EMEP) show increasing N deposition values during most of the twentieth century, with maxima reached around 1990 (van Oijen et al. 2008). The 1999 Gothenburg Protocol to Abate Acidification, Eutrophication and Ground-level Ozone sets emission ceilings for 2010 for NO_x, ammonia, and other pollutants. Hence, we assumed continued reductions of N deposition until the year 2010, with deposition remaining constant thereafter. These temporal patterns were spatially disaggregated using the 2004 UK deposition map (R.I. Smith, personal communication).

2.2.4 Soils

Data on soil nitrogen, carbon, and plant-available water content were taken from the global soils database produced by the Data and Information Services of the International Geosphere–Biosphere Programme (Global Soil Data Task 2000). The data are at a resolution of 5 × 5 arc minutes.

2.2.5 Tree data from Dodd Wood and Rheola sites

Forest Research UK provided data on soil characteristics and destructive measurements of tree growth from two Sitka spruce stands for use in model calibration (Fig. 1) (R. Matthews and P. Taylor, personal communication). The sites were Dodd Wood (54.64° N, 3.17° W, alt. 381 m, indurated brown earth sandy soil) and Rheola (51.74° N, 3.68° W, alt. 220 m, brown earth soil). Trees were planted in 1927 and 1935, respectively, and management followed a 5-year thinning cycle on both sites, starting 24 and 28 years, respectively, after planting. In each thinning year, data were gathered on standing and removed stem volume and on standing and removed whole tree biomass. At the last thinning, biomass fractions in leaves, branches, stems, and

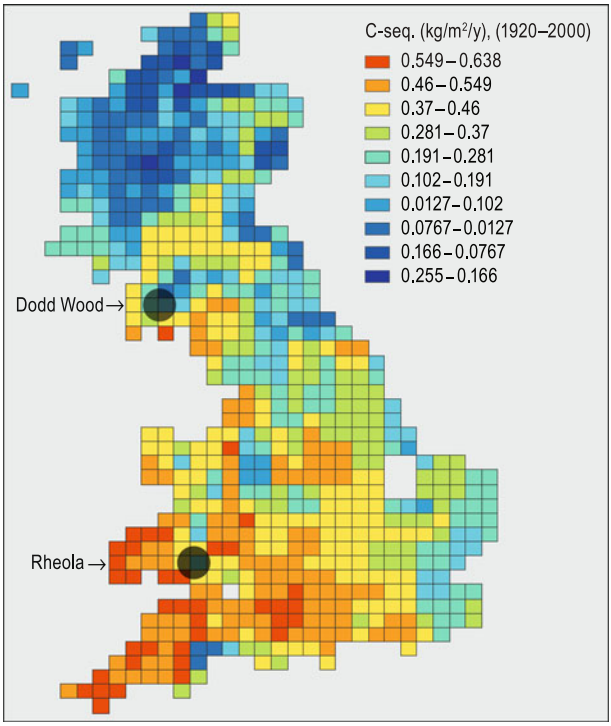

Fig. 1 Simulated average annual C-sequestration (in soil, living trees and wood products) for 1920–2000. Results from model BASFOR following Bayesian calibration on data from Sitka spruce plantations at Dodd Wood and Rheola

roots were estimated using site-specific biomass expansion factors. In total there were 52 data points for Dodd Wood and 44 for Rheola, for each of which a measurement uncertainty of 20% was estimated.

2.3 Bayesian calibration and uncertainty quantification

The parameters of the BASFOR model were quantified by means of Bayesian calibration (van Oijen et al. 2005), using the Forest Research UK data for Dodd Wood and Rheola. The procedure began with quantification of the uncertainty about the parameter values in the form of a prior probability distribution. In the absence of detailed data on Sitka spruce, the prior distribution was based on literature data on conifer growth (Table 1) (Levy et al. 2004; van Oijen et al. 2005). The Forest Research data on model output variables were used to update the parameter distribution by application of Bayes' Theorem (Eq. 1). This yielded a posterior, calibrated probability distribution for the parameters. As BASFOR is a nonlinear model, the posterior distribution could not be determined analytically. We therefore used a Markov Chain Monte Carlo (MCMC) approach, the Metropolis algorithm (Robert and Casella 1999), to generate a representative sample from the posterior distribution (for computer code, see http://nora.nerc.ac.uk/6087/). The calibration was carried out in two steps. In the first MCMC, the prior distribution was updated using the Dodd Wood data. The parameter sample generated by this step was approximated by a truncated normal distribution which was further modified

Table 1 Prior and posterior probability distributions for parameters of BASFOR

Parameter vector			Prior probability distribution			Posterior probability distribution	
Symbol	Unit	Meaning	Lower limit	Upper limit	Mean	Mean	CV
$C_{B,0}$	($kg\ m^{-2}$)	Initial value branch C	0.00005	0.005	0.0012	0.0010	0.18
$C_{L,0}$	($kg\ m^{-2}$)	Initial value leaf C	0.0001	0.01	0.0024	0.0015	0.38
$C_{R,0}$	($kg\ m^{-2}$)	Initial value root C	0.0001	0.01	0.0024	0.0017	0.16
$C_{S,0}$	($kg\ m^{-2}$)	Initial value stem C	0.00005	0.005	0.0012	0.00090	0.34
B	(–)	CO_2-response factor	0.4	0.6	0.50	0.52	0.06
$CO_{2,0}$	(ppm)	CO_2-response base level	320	380	350	362	0.02
f_B	(–)	Allocation to branches	0.25	0.30	0.28	0.29	0.02
$f_{L,max}$	(–)	Maximum allocation to leaves	0.27	0.37	0.31	0.29	0.03
f_S	(–)	Allocation to stem	0.25	0.30	0.28	0.28	0.01
Γ	(–)	Respiration fraction	0.4	0.6	0.50	0.48	0.06
k_{CA}	(m^2)	Crown area allometric normalization constant	5	15	10	11	0.12
$k_{CA,exp}$	(–)	Crown area allometric exponent	0.30	0.45	0.38	0.36	0.07
k_h	(m)	Tree height allometric normalization constant	4	12	6.6	7.5	0.07
$k_{h,exp}$	(–)	Tree height allometric exponent	0.2	0.3	0.25	0.26	0.04
LAI_{max}	($m^2\ m^{-2}\ mm^{-1}$)	Maximum LAI	4	10	5.7	6.3	0.06
LUE_0	($kg\ MJ^{-1}$)	Light-use efficiency	0.001	0.003	0.0020	0.0014	0.10
$NC_{L,max}$	($kg\ kg^{-1}$)	Maximum N/C ratio leaves	0.02	0.05	0.038	0.028	0.12
$NC_{R,con}$	($kg\ kg^{-1}$)	N/C ratio roots	0.02	0.04	0.030	0.023	0.06
$NC_{W,con}$	($kg\ kg^{-1}$)	N/C ratio woody parts	0.0005	0.002	0.0011	0.00080	0.23
SLA	($m^2\ kg^{-1}$)	Specific leaf area	5	40	14.2	6.0	0.05
T_{opt}	(°C)	Temperature optimum	12	28	20	19	0.12
$TC_{L,max}$	(d)	Maximum survival time coefficient leaves	365	1460	791	1048	0.09
δ	($kg\ C\ m^{-3}$)	Wood density	150	250	203	182	0.04

The prior is skewed or symmetrically beta-distributed between specified lower and upper limits. The posterior, derived using data from Dodd Wood and Rheola, is not analytical and is characterized here by the mean values of the marginal parameter probability distribution and the coefficients of variation (CV = standard deviation/mean). The posterior correlation matrix is not shown

in the second MCMC using the Rheola data. Note that, in Bayesian calibration, the order in which two or more data sets are processed does not affect the final posterior distribution. After calibration, the predictive uncertainty of the model was quantified by running the model with different parameter settings sampled from the posterior distribution ($n = 5$). The sample size was kept small to allow uncertainty quantification for each of the 655 grid cells covering the UK. It was verified that deleting any of the five parameter vectors from the sample changed the average value of sequestration by <2%.

The calibration was applied only to model parameters. Uncertainty associated with model drivers (CO_2, temperature, N deposition) was assessed in only a preliminary way by varying their values for the Dodd Wood site and quantifying forward propagation of the variation to model output. Model drivers consist of long time series, and formally including them in the Bayesian calibration would have required determination of a joint prior distribution encompassing daily values of each variable, which was beyond the scope of this study. Moreover, no attempt was made to quantify uncertainty relating to the structure of the model itself.

3 Results

3.1 Bayesian calibration and uncertainty quantification

Table 1 lists the major parameters of BASFOR, with their prior uncertainty before application of data from UK forests, and their posterior uncertainty after Bayesian calibration. For most parameters, prior uncertainty was large (i.e., lower and upper limits were far apart). Figure 2 (black dotted lines) shows for four model output variables (tree and soil carbon, tree height, and total produced wood volume) how the prior parameter uncertainty caused uncertainty in model outputs at the Dodd Wood site. For example, the uncertainty interval (two standard deviations wide) for tree carbon at the end of the 80-year rotation ranged from below 40 to above 80 tonnes carbon ha^{-1}. Table 1 and Fig. 2 also show to what extent uncertainties were reduced by the Bayesian calibration using the data from the Dodd Wood and Rheola sites, described above. The marginal posterior probability distributions for the parameters were much narrower than the prior distributions, as can be seen from the small coefficients of variation. The data from the two forest sites were not equally informative for all parameters, with coefficients of variation (CV) for three parameters—initial leaf and stem carbon content and the nitrogen to carbon (N/C) ratio of wood—exceeding 20%. However, the red unbroken lines in Fig. 2 show that overall parameter uncertainty had been reduced enough to significantly reduce output uncertainty for the four selected variables.

3.2 C sequestration 1920–2000

The calibrated model was applied to calculate UK-wide C sequestration between 1920 and 2000 for a standardized Sitka spruce rotation with a five-yearly thinning interval (Fig. 1). C sequestration was defined as the average annual total accumulation of carbon in soil, standing biomass, and wood removed at thinnings. Product decay was not accounted for. Calculated sequestration rates were highest

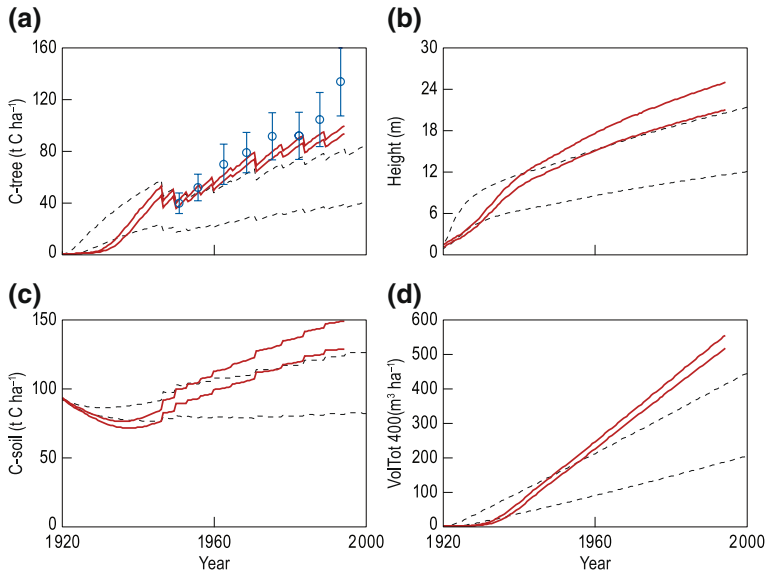

Fig. 2 Prior (*black*, *dotted lines*) and posterior (*red*, *unbroken lines*) model output uncertainty for conifer forests planted in 1920 under Dodd Wood environmental conditions. Pairs of lines are separated by two standard deviations. Output variables are tree and soil carbon content, tree height and cumulative wood volume production. *Blue circles and vertical lines* data with estimated measurement error

in the southwest of the country, which combines moderately high temperature and precipitation. The far north is identified by the model as an area of net C source rather than a sink (Fig. 1). The spatial pattern of C sequestration was not closely related to the spatial distribution of atmospheric N deposition and soil nitrogen. The propagation of parameter uncertainty to uncertainty about C sequestration rates was calculated by randomly taking five parameter vectors from the posterior parameter probability distribution (Table 1) and calculating the standard deviation for the five resulting output sets. Figure 3 shows the resulting map of sequestration uncertainty. The spatial pattern of sequestration uncertainty differed strongly from that of sequestration itself, with Figs. 1 and 3 showing only a weak correlation ($r = -0.25$). This means that the coefficient of variation for carbon sequestration, induced by parameter uncertainty alone, varies among different growing conditions.

3.3 C sequestration, 2000–2080

The same calculations of C sequestration were repeated for the environmental conditions expected for the period 2000–2080. Figure 4 shows the spatial distribution of expected changes in sequestration relative to 1920–2000. The changes are not closely related to the magnitude of expected changes in temperature, as their spatial patterns differ. However, some degree of warming is expected across the whole country, causing C sequestration to increase mainly in the higher, colder regions of Wales, northern England, and Scotland, and to decrease in southern England.

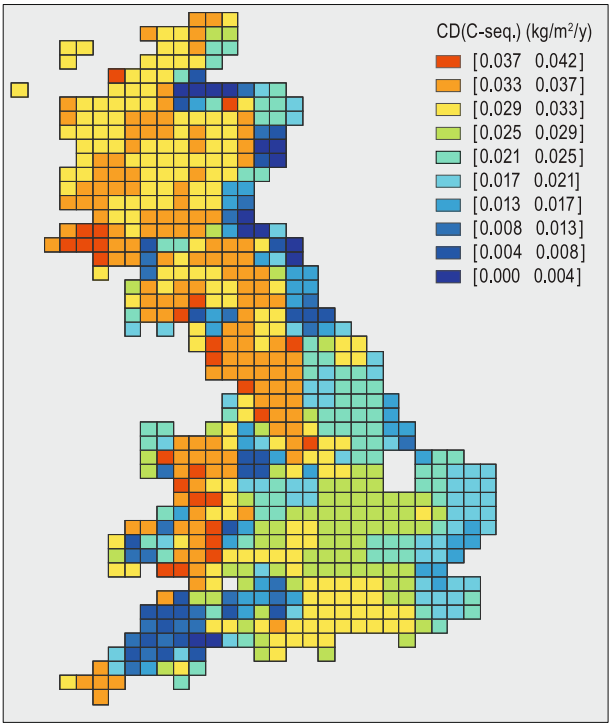

Fig. 3 Uncertainty (standard deviation) in simulated average annual C-sequestration (in soil, living trees and wood products) for 1920–2000. Results from model BASFOR

3.4 Analysis in terms of environmental change factors: climate, CO_2, N deposition

The above-mentioned UK-wide assessments of the effects of environmental change on expected C sequestration rates in conifer forests did not separate out the effects of the different environmental factors that are subject to change. For the purpose of such analysis, we ran additional simulations for the Dodd Wood site with a range of temperatures, atmospheric CO_2 concentrations, and N deposition rates in a full-factorial setup. The ranges of these factors were not intended to represent uncertainty; they served only as input to a sensitivity analysis encompassing the full range of conditions from 1920 to 2080. Average temperature was varied from 6.8°C to 9.9°C (which amounts to expanding the UKCIP estimates for the site for 1920–2000 and 2000–2080 by one degree on either side of the range); atmospheric CO_2 was varied from 320 to 480 ppm (corresponding to changes estimated by the Bern model using the IS92a emission scenarios for 1920–2000 and 2000–2080); and N deposition was varied from 0 to double the 1920–2000 average value of 8.0 kg N ha^{-1} $year^{-1}$. Table 2 summarizes the results of application of the model for these environmental conditions. The first data column of the table lists the average values of yield class and annual C sequestration rate across the set of environmental conditions considered, with standard deviations indicating the uncertainty arising from both the variation in environmental conditions and the parametric uncertainty determined previously. The final three data columns of Table 2 give the average effect on yield class and sequestration of changes in temperature, CO_2, and N deposition, with uncertainties. At the site examined, Dodd Wood, changes in each of the three environmental

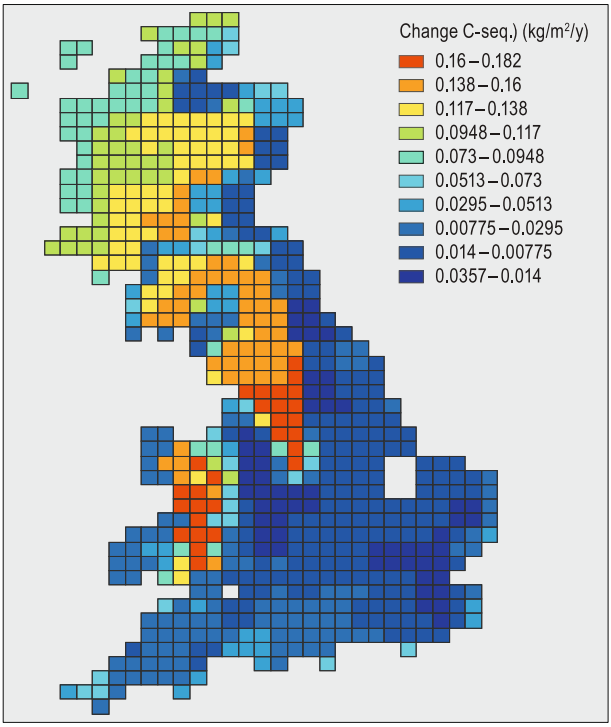

Fig. 4 Simulated change in average annual C-sequestration (in soil, living trees, and wood products) from 1920–2000 to 2000–2080. Results from model BASFOR

factors have an effect on the output variables, but with the strongest effect (relative to its expected degree of change) being for CO_2. The analysis further suggests that C sequestration rates are likely to increase to a similar extent in soils and in tree biomass.

Table 2 Simulated change in average yield class and annual C sequestration at the Dodd Wood site due to changes in temperature and CO_2 and N deposition

Ecosystem variable	Dodd Wood value	Impact of environmental change		
		Effect of temperature (per °C)	Effect of $[CO_2]$ (per 100 ppm)	Effect of N deposition (per 10 kg N ha^{-1} $year^{-1}$)
Yield class (m^3 ha^{-1} $year^{-1}$)	7.91 ± 1.11	0.18 ± 0.05	1.32 ± 0.38	0.74 ± 0.26
C sequestration (t C ha^{-1} $year^{-1}$)	3.99 ± 0.64	0.10 ± 0.03	0.76 ± 0.21	0.41 ± 0.14
C sequestration, soil (t C ha^{-1} $year^{-1}$)	1.58 ± 0.31	0.05 ± 0.01	0.36 ± 0.10	0.18 ± 0.07
C sequestration, trees and products (t C ha^{-1} $year^{-1}$)	2.41 ± 0.34	0.05 ± 0.02	0.40 ± 0.12	0.23 ± 0.07

The standard deviations are due to uncertainty in parameterization and to variation in interacting environmental factors, but not including soil characteristics

4 Discussion and conclusions

4.1 Bayesian calibration and data quality

This study has investigated methods that may be used to improve the construction of the UK GHG Inventory. The process-based forest model BASFOR was parameterized efficiently using Bayesian calibration. The method is probabilistic in that it uses information from data to update the probability distribution for parameters. The calibration thus allowed subsequent uncertainty to be quantified when the model was used to calculate UK-wide conifer forest productivity and C sequestration.

The Bayesian procedure depends on the availability of good data. Data for which measurement uncertainty is considered to be high are not very informative, for example, the likelihood $p(D|\theta)$ is a relatively flat function of the parameters θ. In the calibration, such data will not strongly modify the parameter distribution. As there was considerable uncertainty in the forest data used here, posterior model outputs tended to be intermediate between the prior outputs and the data (Fig. 2). The prior information helps prevent overfitting of the data.

Data that are biased will lead to bias in parameterization. Our soil nitrogen data in particular were taken from a global database of low resolution (Global Soil Data Task 2000) and they showed surprisingly high values for the UK, suggesting that forests tend to be nitrogen-saturated and therefore unresponsive to N deposition. As these data were the only source of information on soil nitrogen content available to us, we were unable to decide if they represented overestimates. Using these data, we found relatively low sensitivity on the part of UK forest productivity and C sequestration rates to soil nitrogen content and atmospheric N deposition, as opposed to the high values calculated for sensitivity to changes in temperature and atmospheric CO_2 concentration. As explained, this finding may be an artifact from the use of the IGBP-DIS dataset with its possibly overestimated values of nitrogen contents of UK soils, leading to apparent nitrogen saturation (van Oijen and Jandl 2004).

Although our joint prior pdf reflected uncertainty about conifer forests in general, the posterior pdf—as well as the sequestration values shown in Figs. 1, 3 and 4—are specific to Sitka spruce, as only data from this species were used in the Bayesian calibration.

4.2 Spatial distribution of uncertainties

Uncertainties, expressed both in absolute terms (Fig. 3) and as coefficients of variation (compare Figs. 1 and 3) showed distinct spatial trends across the country. Uncertainty with regard to carbon sequestration was highest in northern and western parts of the country. Spatial variation in inventory uncertainty is a well known phenomenon, typically associated with spatial variation in economic activity (Bun et al. 2010). However, our study is restricted to a single activity, forestry, and the spatial distribution is exclusively the result of heterogeneity in environmental conditions. This is a finding of significance for the UK GHG Inventory, as it suggests that a simple approach to forestry-related uncertainty (e.g., assuming uncertainty to be a fixed percentage of the absolute flux rate) is unfeasible across regions of this magnitude. Thus, when a GHG Inventory is being determined for forestry GHG

fluxes, not only the calculation of main effects, but also uncertainty quantification needs to be carried out in a spatially disaggregated manner.

4.3 The impacts of changes in environmental factors

The use of a process-based model for calculating C sequestration, rather than the semi-empirical model CFLOW currently used in the UK GHG Inventory, allowed us to analyze the contribution of changes in temperature and CO_2 and N deposition to changes in sequestration. Elevated CO_2 was found to have a particularly strong effect on sequestration. In the future, C sequestration is expected to decrease in southern England and increase in the currently coldest parts of the country, which is consistent with studies by Broadmeadow et al. (2005) using a different model. However, given the likely poor quality of the soils data our analysis should be seen as a proof of concept for the methodology rather than as a high-probability identification of a key environmental variable. Furthermore, the factor analysis was applied only to a single site and should be repeated for the whole of the UK.

4.4 The use of process-based models in GHG inventories

Relatively complex models like BASFOR provide more detailed outputs than simple compartmental carbon models can provide. These outputs include fluxes of carbon within trees and how they respond over time to the changes in the environment at different locations. Furthermore, this study has shown that Bayesian calibration may be an efficient method of calibrating such parameter-rich models, while simultaneously quantifying uncertainties in parameters and outputs. In our test of the approach, we used the model BASFOR, but many process-based forest models exist that simulate the carbon cycle (for one comparison of such models see van Oijen et al. 2008), and could be selected for this purpose. Using process-based models in a GHG inventory may therefore be an attractive proposition. However, this study has also shown how the extra demand that complex models place on input information may lead to biased outputs if no good-quality data are available—with soil fertility being a prime example.

Instead of using the complex models directly in the UK Inventory, we were able to restrict ourselves to using their output. From the output of BASFOR, we calculated response factors that quantify the impact of environmental change on flux rates (Table 2). Black (pers. comm. 2007) found that uncertainties in the Irish Inventory—whose calculation scheme is similar to that of the UK Inventory—were mainly associated with incomplete information about annual biomass increments as derived from yield tables. The yield class response factors we calculated (Table 2) could conceivably be added to the currently used CFLOW model to provide a more realistic spatial distribution and inter-annual variability of the annual increments. However, the presence of nonlinear individual and interactive effects limits the scope for using the response factors. For example, because of nonlinearity, the yield class temperature response factor of 0.18 ± 0.05 (m^3 ha^{-1} $year^{-1}$) $(°C)^{-1}$ does not necessarily apply outside the Dodd Wood area. This has implications for the way in which we can use results from the process-based modeling to derive modifiers for the yield class values that are used as input for the carbon inventory calculations using CFLOW. The yield class modifiers likely need to be complex multivariate functions

of the set of different environmental factors. However, we may calculate such functions if we redo the current factor analysis at a UK-wide scale and with improved input information. We aim to do this alongside quantification of the uncertainties from incomplete knowledge of parameters, environmental drivers, and model structure.

Acknowledgements We thank Robert Matthews and Paul Taylor (Forest Research, Alice Holt) for providing information about the Sitka spruce stands at Dodd Wood and Rheola, and Ron Smith (CEH-Edinburgh) for providing information on the spatial distribution of N-deposition across the UK.

References

Broadmeadow MSJ, Ray D, Samuel CJA (2005) Climate change and the future for broadleaved tree species in Britain. Forestry 78:145–161

Bun R, Hamal K, Gusti M et al (2010) Spatial GHG inventory on regional level: accounting for uncertainty. Clim Change. doi:10.1007/s10584-010-9907-5

Dewar RC, Cannell MGR (1992) Carbon sequestration in the trees, products and soils of forest plantations—an analysis using UK examples. Tree Physiol 11:49–71

Galloway JN (1985) The deposition of sulphur and nitrogen from the remote atmosphere. In: Galloway JN, Charlson RJ, Andrew MO et al (eds) Biogeochemical cycling of sulphur and nitrogen in the remote atmosphere. NATO ASI Series D. Reidel, Dordrecht

Global Soil Data Task (2000) Global gridded surfaces of selected soil characteristics (IGBP-DIS). International Geosphere–Biosphere programme—Data and information services. Available at http://www.daac.ornl.gov

Hulme M, Jenkins GJ (1998) Climate change scenarios for the United Kingdom: scientific report. KCIP Technical report no 1, Climatic Research Unit, Norwich, 80 pp. Available at http://www.cru.uea.ac.uk/link/ukcip/ukcip_report.html

Joos F, Bruno M, Fink R et al (1996) An efficient and accurate representation of complex oceanic and biospheric models of anthropogenic carbon uptake. Tellus 48B:397–416

Levy PE, Wendler R, van Oijen M et al (2004) The effects of nitrogen enrichment on the carbon sink in coniferous forests: uncertainty and sensitivity analyses of three ecosystem models. Water Air Soil Pollut Focus 4:67–74

Monni S, Peltoniemi M, Palosuo T et al (2007) Uncertainty of forest carbon stock changes—implications to the total uncertainty of GHG inventory of Finland. Clim Change 81:391–413

Patenaude G, Milne R, van Oijen M et al (2008) Integrating remote sensing datasets into ecological modelling: a Bayesian approach. Int J Remote Sens 29:1295–1315

Peltoniemi M, Palosuo T, Monni S et al (2006) Factors affecting the uncertainty of sinks and stocks of carbon in Finnish forests soils and vegetation. For Ecol Manag 232:75–85

Penman J, Gytarsky M, Hiraishi T et al (eds) (2003) Good practice guidance for land use, land-use change and forestry, IGES/IPCC. Available at http://www.ipcc-nggip.iges.or.jp

Robert CP, Casella G (1999) Monte Carlo statistical methods. Springer, New York, pp xxi + 507

Thomson AM, van Oijen M (eds) (2007) Inventory and projections of UK emissions by sources and removals by sinks due to land use, land use change and forestry. Centre for Ecology and Hydrology/DEFRA, London, 197 pp

van Oijen M, Jandl R (2004) Nitrogen fluxes in two Norway spruce stands in Austria: an analysis by means of process-based modelling. Austrian J For Sci 12:167–182

van Oijen M, Rougier J, Smith R (2005) Bayesian calibration of process-based forest models: bridging the gap between models and data. Tree Physiol 25:915–927

van Oijen M, Ågren GI, Chertov O et al (2008) Application of process-based models to explain and predict changes in European forest growth. In: Kahle HP, Karjalainen T, Schuck A et al (eds) Causes and consequences of forest growth trends in Europe. Brill, Leiden, pp 67–80

van Oijen M, Dauzat J, Harmand J-M et al (2010) Coffee agroforestry systems in Central America: II. Development of a simple process-based model and preliminary results. Agroforest Syst. doi:10.1007/s10457-010-9291-1

Winiwarter W, Muik B (2010) Statistical dependences in input data of national GHG emission inventories: effects on the overall GHG uncertainty and related policy issues. Clim Change. doi:10.1007/s10584-010-9921-7

Climatic Change (2010) 103:69–92
DOI 10.1007/s10584-010-9909-3

Atmospheric inversions for estimating CO_2 fluxes: methods and perspectives

P. Ciais · P. Rayner · F. Chevallier · P. Bousquet · M. Logan · P. Peylin · M. Ramonet

Received: 5 January 2009 / Accepted: 15 June 2010 / Published online: 20 July 2010

Abstract We provide a review description of atmospheric inversion methods for the determination of fluxes of long-lived trace gases based on measurements of atmospheric concentration. Emphasis is given to technical aspects of inversion settings, which are crucial to inter-compare and understand inversion results. We briefly sketch the formalism used in such methods, then provide a summary of major currents in research and contemporary problems. Most attention is given to carbon dioxide (CO_2) which poses the threat of future climate change. Therefore, there is keen interest in better understanding where and when CO_2 emitted by the combustion of fossil fuels is reabsorbed by land ecosystems and oceans. Using the information contained in concentration fields observed from ground-based networks and from upcoming satellite observations in order to constrain the geographic distribution of surface fluxes is an inverse problem; it consists of finding a set of fluxes that optimally matches the observations available. We review the application of inverse methods to quantify the distribution of the sources and sinks of CO_2 at the surface of the Earth based on global measurements of atmospheric concentration and three-dimensional models of atmospheric transport. We describe the use of top–down atmospheric inversion methods in terms of numerical transport modeling and atmospheric observation networks, and detail some of the currently important issues in assigning uncertainties.

P. Ciais (✉) · P. Rayner · F. Chevallier · P. Bousquet · M. Logan · P. Peylin · M. Ramonet
Unité Mixte de Recherche LSCE, CEA-CNRS-UVSQ, Bâtiment 709,
CE Orme des Merisiers, 91191 Gif sur Yvette, France
e-mail: philippe.ciais@cea.fr

P. Peylin
Unité Mixte de Recherche BioMCo, INRA-CNRS-INAPG, Université Paris 6,
Bâtiment EGER, 78850 Thivernal-Grignon, France

1 Introduction

Quantitative understanding of the sources and sinks of chemically and radiatively important trace gases and aerosols is essential to assess human impact on the environment. Observations of atmospheric concentrations provide the basic data for inferring sources and sinks at the Earth's surface, or in the atmosphere. For conservative tracers, which stay inert once emitted, the influence of surface fluxes is modified only by atmospheric transport, which tends to integrate over regional and continental scales. The concentrations of reactive species such as aerosols or chemicals are also influenced by being produced or destroyed via chemical reactions or physical processes in the atmosphere.

Starting from a set of atmospheric concentration observations, and using a model of atmospheric transport and chemistry, it is possible to infer information on the distribution of sources and sinks at the surface. This process is known as inverse modeling of atmospheric transport. Inverse modeling consists of finding a set of statistically optimal fluxes, which satisfies all available pieces of information (measurements and prior inventories) within their respective uncertainties. This approach has been applied to various problems, ranging from the relatively small scale when determining pollution emissions from a factory or a city (e.g., Vautard et al. 1998) to inferring the emissions of industrialized regions within a continent (e.g., Manning et al. 2003), and the global distribution of sources and sinks of long-lived species such as CO_2 (e.g., Enting et al 1995; Bousquet et al. 2000; Rödenbeck et al. 2003a, b), methane (Hein et al. 1997; Houweling et al. 1999; Bousquet et al. 2006), or carbon monoxide (Petron et al. 2002; Arellano et al. 2006).

The focus of this review is on technical aspects of inversion settings, which are crucial to intercomparison and comprehension of inversion results. In the following, we describe the principles of inverse modeling of atmospheric transport applied to quantification of the sources and sinks of carbon dioxide (CO_2). The formalism is only slightly complicated by reactive trace gases of moderately long lifetimes like methane (CH_4; 8 years). The rising concentration of CO_2 is the main factor increasing the Earth's greenhouse effect. Atmospheric CO_2 concentrations have risen by 38% since pre-industrial times and are now at their highest for the past 25 million years. The increase in CO_2 is driven by the combustion of fossil carbon in gas, oil, and coal deposits to produce energy, as well as by the clearing of forests to establish arable or pasture lands (deforestation). Levels of CO_2 are, however, tempered by uptake by land ecosystems and by the oceans. Although a detailed description of the carbon cycle is not within the scope of this paper, we recall that roughly half of the yearly anthropogenic emissions accumulate on average in the atmosphere, while the other half ends up being sequestered by land and oceans. Where and when the uptake of anthropogenic CO_2 takes place is a high research priority for understanding the global carbon cycle, as well as for designing verification systems to monitor the effectiveness of emission controls or emission reduction policies aiming to curb the atmospheric increase of CO_2 (e.g., Kyoto Protocol).

Land ecosystems and oceans are active carbon reservoirs, which exchange large fluxes of CO_2 with the atmosphere in both directions, the fluxes being driven by a myriad of bio-geochemical processes. The probability of having a source or a sink of CO_2 at the surface of the globe is non-zero everywhere, except over ice and deserts. Further, the CO_2 surface sources can vary in time (1) diurnally, such as during uptake

and release of CO_2 over vegetation canopies, (2) seasonally, from one year to the next, and (3) also evolve on a longer-term basis in response to changing CO_2, climate, and other factors.

The paper is divided into three main sections. First, we recall inverse modeling principles and general issues relative to the problem of inverting CO_2 fluxes over the globe. Then we review the key technical settings of atmospheric inversions: the a priori flux information, the atmospheric measurements, and the model of atmospheric tracer transport. In the third part, the Bayesian synthesis inversion technique, most currently applied for inferring CO_2 sources and sinks, is discussed in more detail, together with issues related to atmospheric transport uncertainties, observational errors, settings of the inverse problem in terms of spatial and temporal resolution, and how those propagate into the solution of Bayesian inversions.

2 Inverse modeling principles

In this section, we provide a general background on inversion modeling principles relevant for inversion of CO_2 fluxes using CO_2 concentration data. Figure 1a illustrates a dynamical system, corresponding to a model with errors. In the case of CO_2, this would be a perfect atmospheric tracer transport model, able to reproduce the CO_2 concentration of any point of the atmosphere t any time. The model allows us to simulate the state of the system Y, according to some initial conditions Y_i and input parameters x. In the case of CO_2 inversions, Y is a time-varying field of atmospheric CO_2 concentration and x is a time-varying field of surface CO_2 fluxes. The model is deterministic, so that at each time step t, Y takes a unique value according to x and Y_i. The output Y of the model is a vector characterizing the dynamic state of the system at each time step (i.e., the atmospheric CO_2 concentration distribution). If we define H_{t+1} the explicit function that describes the dynamic evolution of the system between t and $t + 1$, and O_t, the function describing the relationship between the state of the system Y and the output data y at time t, one can write:

$$Y(t_i) = Y_i \tag{1}$$

$$Y_{t+1} = H_{t+1}(Y_t, x_{t+1}) \tag{2}$$

$$y_t = O_t(Y_t) \tag{3}$$

Practically, H_{t+1} is a numerical transport model, and O_t is an "observation operator" sampling the distribution of CO_2 where and when observations are collected. Usually in physical problems there are uncertainties regarding the initial conditions called Ψ_i, on input parameters called ξ, and on the dynamical model H. Then at each time t, the state of the system becomes associated with an uncertainty Ψ_t that propagates into an uncertainty in its output Ψ_t. Therefore the set of equations above become:

$$Y_i = Y(t_i) + \Psi_i \tag{4}$$

$$x = x_b + \xi, \tag{5}$$

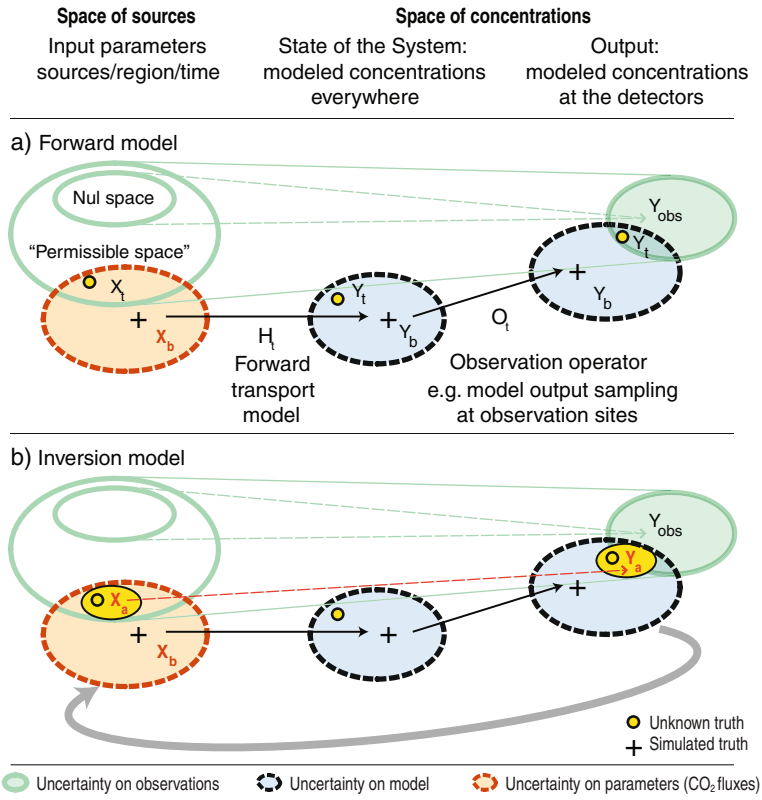

Fig. 1 **a** Information flow in a forward atmospheric transport model with errors compared with the available CO_2 concentration observations, **b** Same for an atmospheric inversion model where an optimal set of parameters (surface CO_2 fluxes, x) is determined from the available concentration observations within their errors. *H* represents the transport model used to simulate concentrations everywhere in the atmosphere. *O* is observation operator in which the modeled CO_2 distribution is sampled at the time and location of the actual observations

$$Y = H_{t+1}(Y_t, x_{t+1}) + \Psi_{t+1} \tag{6}$$

$$y_t = O_t(Y_t) + \Psi_t \tag{7}$$

The diagram in Fig. 1a includes an uncertainty ξ, regarding the unknown CO_2 flux parameters x_b and the modelled CO_2 concentration output y. The "+" signs in Fig. 1 describe the simulated values, and the ellipses describe the associated errors. The yellow circles show the true values of the variables, assuming that these are known. In the example of Fig. 1, the model H and the setting of x to an a priori value x_b with an uncertainty ξ, is not unrealistic, as $x_b + \xi$, encompasses the true value. If we now suppose that the system is a representation of a real world phenomenon and that some of its characteristics can be measured, the set of observations (e.g., at observing stations), is called y_{obs}. Depending upon the measurement accuracy and other factors, a data error pertains to y_{obs} if we assume that the observations at time t relate to the characteristics described in the vector Y. The ellipse in green around y_{obs} represents

the data error. As neither the measurements nor the model simulations are perfect, we expect y and y_{obs} to differ. In the example of Fig. 1, varying the input parameters x through the model structure allows y to better match the observations within their errors.

Inverse modeling consists of adjusting the input CO_2 fluxes parameters x from their a priori settings x_b so as to minimize the distance between the optimized CO_2 concentrations called y_a and the observed concentrations y_{obs} within their errors. This is illustrated in Fig. 1b. The optimized value of x, called x_a, is referred to as the a posteriori, or analyzed, set of CO_2 flux parameters. The distance between y and y_{obs} is called the innovation. One can also see in Fig. 1b that, resulting from the inversion, uncertainties on both the optimized state of the system y_a and the optimized parameters x_a are reduced (ellipses in yellow), as compared to their a priori values, thanks to the information content carried by the observations.

Note that in the forward problem of Fig. 1a, several input parameters x may exist that would match the observation within their errors. All those solutions form the "null space" of the parameters, which contains the truth as well as the analyzed parameters x_a. The null space is shown as a thin ellipse in Fig. 1. When the inverse problem is ill-constrained, for instance, because of scarce or inadequate observations compared to the CO_2 fluxes to be solved for, then the null space becomes very large. Given an a priori value x_b of the CO_2 fluxes to be optimized x, optimizing the value of x against observations results in determining the portion of the null space that is compatible with the a priori value of x_b, taking into account its uncertainties.

3 The inverse problem of CO_2 sources and sinks and its components

We briefly describe in this section the components of the geophysical problem involved in finding an optimal value for CO_2 sources and sinks at the surface of the Earth that best matches a set of atmospheric concentration observations (given an a priori distribution of the fluxes and of observational errors) using a numerical model of atmospheric transport. We review briefly in the following the nature of the different components of the inverse problem: a priori fluxes and errors, observations, and transport model. In this problem, input parameters are the fluxes we wish to determine and the output of the model is a set of simulated concentrations, which we will compare to observations.

3.1 A priori flux information

Having said in the introduction that both oceans and land surface exchange CO_2 in both directions (uptake and release), we will search for the space and time distribution of the net CO_2 fluxes, components of the vector x, expressed in molC per unit area per unit time. The net flux results from the superposition of all directional fluxes corresponding to different processes.

The anthropogenic CO_2 source to the atmosphere due to the combustion of fossil fuel carbon stores (coal, gas, oil) is accurately known globally within 5% from energy statistics (Andres et al. 1996; Brenkert 1998; Marland et al. 2001).

Anthropogenic emissions are the main perturbation of the carbon cycle that causes CO_2 to increase. Although the total fossil CO_2 source of developed countries is accurately determined (±2%), there are large uncertainties regarding how those emissions are distributed in space and time over industrial regions depending on car traffic, electricity, heating, and other residential use. One example of the fossil fuel emissions distribution is given in Fig. 2a (data available from http://www.rivm.nl/edgar/model/v32ft2000edgar/edgv32ft-ghg/edgv32ft-co2.jsp). Such geographic patterns of fossil fuel CO_2 sources, including their temporal variability, are needed as an a priori component of the inverse problem, on a grid that should match the spatial and temporal resolution of the atmospheric transport model.

The net CO_2 flux at the air–sea interface is driven by the partial pressure difference between CO_2 dissolved in surface waters and CO_2 in the overlying atmosphere, multiplied by an exchange coefficient describing the kinetics of the mass transfer across the interface. Although at thermodynamic equilibrium, after infinite time, the air–sea flux would be zero, in the real world there are always processes preventing this equilibrium from actually being reached. An a priori map of the global CO_2 air–sea flux patterns based on ocean surveys (e.g., Takahashi et al. 1997—related data available at http://cdiac.esd.ornl.gov/oceans/datmet.html) is given in Fig. 2b. We can see that the oceans around the equator release CO_2 to the

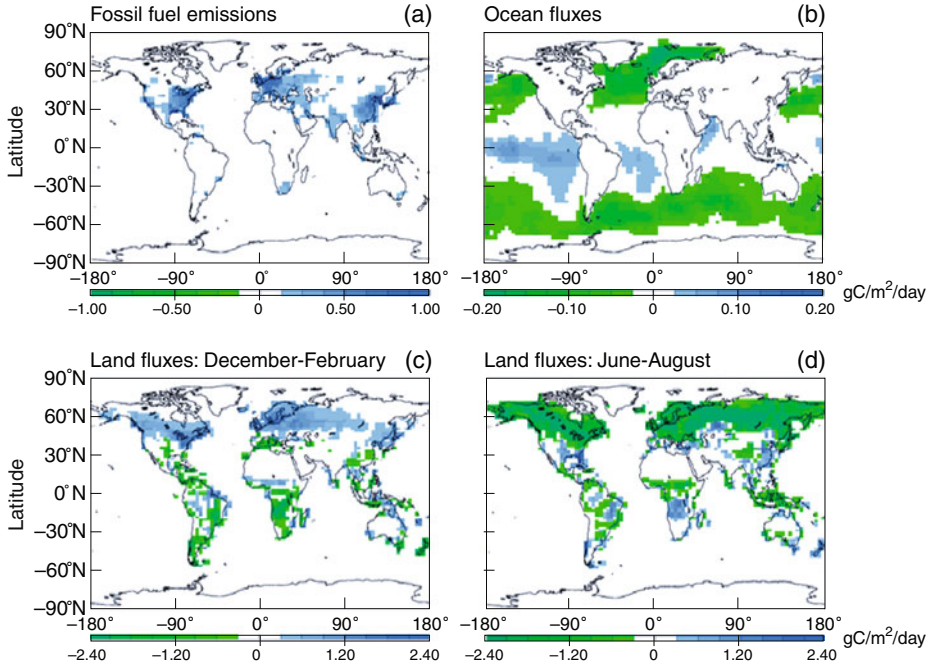

Fig. 2 **a** Distribution of mean annual fossil fuel CO_2 emissions obtained from statistics on energy consumption and spatial information on population density and anthropogenic activities (after EDGAR FT2000 database). **b** Air–sea flux (after Takahashi et al. 1997). **c** Land–atmosphere flux of CO_2 in the peak of the northern hemisphere growing season during June–August (after Krinner et al. 2005). **d** Same during the non-vegetative season in January–March

atmosphere when CO_2-enriched bottom waters outcrop to the surface in so-called upwelling regions. In contrast, cold waters in northern and southern extra-tropical gyres are net sinks of CO_2. Seasonally speaking, the air–sea flux varies according to changing biological activity and sea surface conditions (temperature, wind speed), but the seasonality of the air–sea fluxes is lower than that of vegetation-atmosphere exchange. Currently, the degree of confidence on the global ocean uptake is of the order of 30%. We have reasonable confidence in the broad structures reflected in Fig. 2b, but the air–sea CO_2 flux at the scale of ocean gyres is subject to larger a priori uncertainties, especially over the southern oceans where little oceanographic information constrains the patterns shown in Fig. 2b.

The net CO_2 flux at the top of vegetation canopies results from the superposition of CO_2 uptake by photosynthesis, when growing conditions for plants are met, and co-located release by respiration of plants and soils, including the decomposition of soil organic matter by microbes and soil fauna. In addition, when large spatial scales are being dealt with, disturbances occur which sporadically devastate ecosystems and subsequently release CO_2 to the atmosphere. Disturbance processes include combustion by fires, pest outbreaks, forest windfall, and land use changes such as the clearing of forests for agriculture occurring at large scales in the tropics (not shown in Fig. 2). Increasing attention has been paid to the importance of disturbances in addition to photosynthesis and respiration in driving the net carbon flux of ecosystems. An a priori map of the net terrestrial exchange of CO_2 is given in Fig. 2c, d, based on calculations of a global model of terrestrial ecosystems (Krinner et al. 2005—data available at http://www-lsceorchidee.cea.fr/). One can observe in Fig. 2c, d that the northern hemisphere ecosystems emit CO_2 from late fall to early spring, and absorb CO_2 from the atmosphere during the rest of the year. Large uncertainties pertain to such a priori knowledge of the terrestrial CO_2 fluxes, of the order of 100% of the mean fluxes, partly reflecting the spatially heterogeneous nature of ecosystems and the difficulties in extrapolating ground-based flux measurements up to large regions or in using global remote sensing information on vegetation condition to map the a priori fluxes. Further, the net terrestrial CO_2 flux that is sought results from a difference between gross fluxes that are at least one order of magnitude bigger, and driven by independent factors. We also note that the temporal variability of the terrestrial CO_2 fluxes is high, with a marked diurnal cycle (uptake during daytime; release at night over active vegetation), and a pronounced seasonal cycle outside the tropics, which parallels the climate conditions driving plant growth. In particular, we can also see in Fig. 2c, d that the northern hemisphere land masses consistently take up CO_2 in spring and summer, but release CO_2 in fall and winter, yielding a strong seasonal cycle of the net flux, which imprints atmospheric CO_2 distribution.

3.2 Atmospheric observations

Atmospheric surface observations consist of a global network of about 100 stations where CO_2 is measured either continuously in situ or via discrete air sampling in flask air samples (weekly snapshot measurements) that are analyzed at a central laboratory (various data and data products available from http://www.esrl.noaa.gov/gmd/ccgg/ and http://gaw.kishou.go.jp/wdcgg/products/publication.html). The observatories where CO_2 is measured continuously with good accuracy are fewer (about 30 stations) than the sites where air is sampled in flasks (100 sites). There are additional

continuous sites, but these are urban sites or their records are not calibrated to international scales. Obviously, the continuous records of CO_2 concentration contain more information than the flask data collected weekly (Carouge et al. 2010). The current network is part of an international effort that started 50 years ago with the establishment of the first two stations at the South Pole and Mauna Loa in Hawaii (Bolin and Keeling 1963). Many of the sites from the global network shown in Fig. 3 are from the United States National Oceanic and Atmospheric Administration–Earth System Research Laboratory (NOAA–ESRL) network (Conway et al. 1994). When overlaying the network geometry on top of the a priori flux patterns (Fig. 2), it is striking that the interior of the continents remains undersampled, as do key areas of the ocean such as the southern oceans. Regionally, in Western Europe and North America, the North American Carbon Program (http://www.nacarbon.org/cgi-nacp/web/investigations/inv_profiles.pl) and the CARBOEUROPE project (http://ce-atmosphere.lsce.ipsl.fr/database/index_database.html) programs have increased the network density over the past few years with eight new continuous surface stations in North America and seven new stations in Western Europe, mainly tall towers.

The reason for most stations being located over the ocean is that the fluxes and transport patterns are less variable than in the continental boundary layer, so that atmospheric sampling can best capture the air masses representative of large-scale sources and sinks at oceanic sites, minimizing local "noise". In order to take representative atmospheric measurements over land, one must at least be outside the surface layer and far from immediate source regions. Thus, historically, mountain

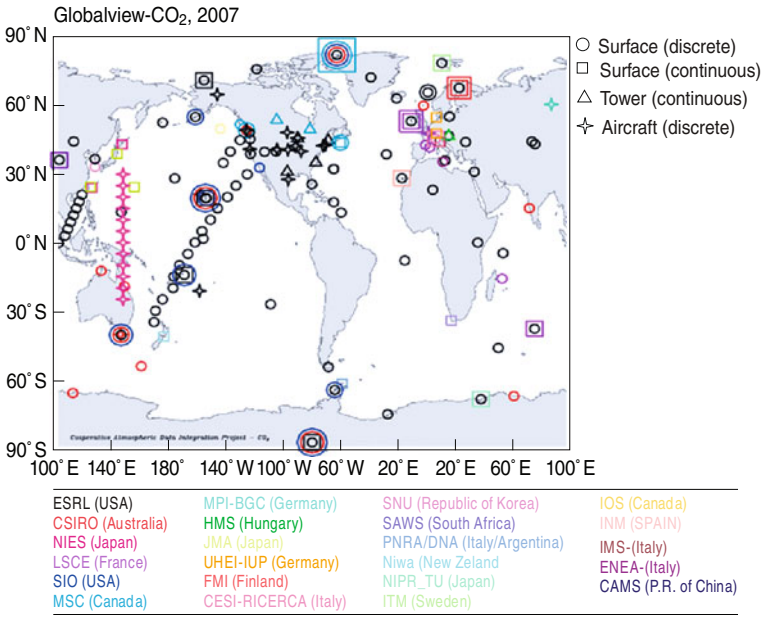

Fig. 3 Map of atmospheric stations where CO_2 observations are made routinely by means of flask sampling and continuous measurements. Each *color* corresponds to a different laboratory contributing measurements (courtesy of K. Masarie at NOAA-ESRL)

stations, aircraft vertical profiles (Tans et al. 1996) and tall towers (Bakwin et al. 1995; Gloor et al. 2001) probing up to more than 100 m into the atmosphere have been progressively added to the network. Vertical profiles are particularly useful to independently check on vertical mixing in models (Ramonet et al. 2002; Stephens et al. 2007). It is also apparent, given the large number of different unknown fluxes acting over nearly all the globe (Fig. 2) and the small number of observations (Fig. 3) that the inverse problem is severely under-determined when based upon in situ measurements.

Figure 4 illustrates the variability of the atmospheric CO_2 concentration recorded on a continuous basis for 2 years at the station of Mace Head, Ireland (Biraud et al. 2002). A long-term increase, an asymmetric seasonal cycle with a short summer time minimum and a broad maximum lasting from October to May, can be seen, which is characteristic of nearly all northern extra-tropical stations. In addition, there is synoptic variability associated with different air masses (meteorology) carrying various CO_2 concentrations when they reach the station. In the first generation of inversions (e.g., Enting 2002), only the annual or smoothed monthly mean CO_2 concentration in the network was used, but not the synoptic variability. Rödenbeck et al. (2003a, b) assimilated for the first time monthly flask data, without smoothing. The limited ability of global transport models to capture the synoptic CO_2 variability requires the use of an accurate meteorology and of high spatial resolution (e.g., Gerbig et al 2003). At most other stations where only flask sampling is available (Fig. 3), the synoptic information contained in the atmospheric signal is sparse and not obviously related to regional sources and sinks.

Important information contained in the network of stations can be visualized when plotting all concentrations as differences with the South Pole taken as a reference (Fig. 5). A positive mean annual CO_2 difference between the northern hemisphere and the southern hemisphere is noticeable. This difference reflects as zero order the release of fossil CO_2 in northern hemispheric industrial areas, but it is further reduced by land and ocean sinks north of the equator. Moreover, we observe from the data shown in Fig. 5 that the amplitude of the seasonal cycle of atmospheric CO_2 increases with northern latitude, reflecting the growing season duration and intensity

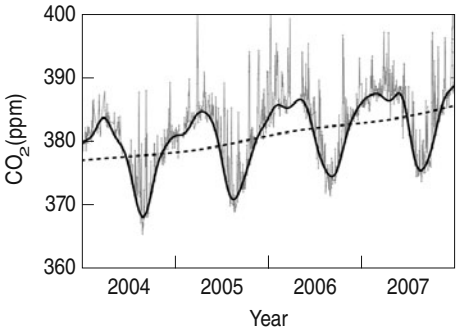

Fig. 4 Daily CO_2 mixing ratios recorded at the station of Mace Head, Ireland, for three consecutive years. *Black dots* and the *gray line* are daily means of hourly measurements. The *black curve* is the monthly smoothed concentration (from baseline values selected for marine sector winds). The *dashed curve* is a long-term deseasonalized curve showing the annual increase of CO_2 and its inter-annual variability

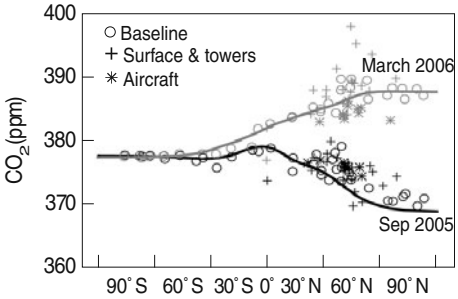

Fig. 5 Important information contained in the network of stations can be visualized when plotting all concentrations as differences with the South Pole taken as a reference. A positive mean annual CO_2 difference between the northern hemisphere and the southern hemisphere is noticeable. This difference reflects as zero order the release of fossil CO_2 in northern hemispheric industrial areas, but it is further reduced by land and ocean sinks north of the equator. Data sources are smoothed CO_2 concentration measurements from the GLOBAL VIEW-CO_2 global data product

over North American and Eurasian ecosystems (see Fig. 2c). Tropical ecosystems actively exchange CO_2 with the atmosphere, but climate conditions in the tropics are equally favorable for photosynthesis and respiration nearly all year round, so that there is little seasonality of atmospheric CO_2 in the tropical atmosphere (Fig. 5).

3.3 Atmospheric transport modeling

The function H, which projects the sources into the observation space, is linear in the case of the transport of a passive constituent. It is represented by a numerical model that solves the conservation equations of geophysical fluid mechanics (mass, momentum, energy) on a 3D grid covering the atmosphere from the surface up to typically the mid-stratosphere (~20–30 km). Note that the space–time discretization of the transport equation introduces some limited non-linearities in the function H. The transport computation is part of elaborate Atmospheric General Circulation Models (AGCM) that calculate the physical and dynamical state of the atmosphere. Large-scale advection and large-scale horizontal diffusion are transport processes that are explicitly solved in those models. Sub-grid transport processes, such as moist convection, vertical diffusion, or boundary layer mixing by turbulence are parameterized, as the resolution of AGCMs is still larger than turbulence scales. Usually, AGCM models are forced to reproduce the actual meteorology by a nudging scheme that keeps their winds in the vicinity of numerical weather prediction (NWP) analyses. Only recently have some NWP models introduced tracer transport into their systems, so that the simulated transport is directly constrained by all available observations (e.g., Engelen et al. 2009).

CO_2 is a long-lived species, and the transport model has to cover a long period of time to relate fluxes and concentrations, typically weeks, months, or even years (e.g., Bruhwiler et al. 2005). Computing time is therefore a critical issue, and methods have been developed to optimize it. First, it is noteworthy that most of the computations in AGCMs are related to processes other than the transport of passive tracers. Radiation processes are a typical example (e.g., Chevallier et al. 2000). Therefore, a significant amount of computation can be saved for the H function by isolating

the transport equations. In this approach, the AGCM is used "online" to produce a frozen archive of atmospheric mass fluxes, which is then used by an "offline" model dedicated to passive transport (e.g., Krol et al. 2005; Hourdin et al. 2006). The time step of the mass flux archive is usually about a few hours (typically 3 or 6) and intermediate fluxes are kept constant or deduced by interpolation. Another way of reducing the amount of computation consists of linearizing H. In this case, the offline or online model serves as a means to calculate the elements of the Jacobian matrix **H**. The derivatives can be approximated by finite differences or backward computations (e.g., Hourdin et al. 2006) or computed exactly using a tangent-linear model or its adjoint (Kaminski et al. 1999).

The difficulty of modeling the atmospheric transport and the diversity of the approaches introduces a significant spread of the concentrations simulated by the models at all time scales (e.g., Law et al. 1996; Geels et al. 2007; Law et al. 2008). Typical resolution of global transport models has evolved together with computer power. From coarse models in the 1980s (typically, $10° \times 10° \times 19$ vertical layers), they now have a typical resolution of 1–2° on the horizontal and 20 to 50 layers in the vertical. Some models have zooming or nesting ability that allow resolution to be downscaled by a factor of at least 2 to 4 for specific regions of interest (Frohn et al. 2002; Chevillard et al. 2002; Krol et al. 2005). Nesting consists of coupling a global model to a domain-limited model. The main advantage of nesting is the ability to use a more refined model on a specific zone, from regional to continental scales (e.g., Nicholls et al. 2004). Note that both model resolution and physical parameterizations can be refined. The main advantage of zooming is to refine model resolution in only one consistent, mass-conservative model. In any case, model resolution is a crucial point to calculate atmospheric concentrations, especially over land where horizontal resolution determines topography smoothing (compared to reality) and vertical resolution plays a major role in representing vertical mixing within and outside the planet boundary layer. Some inversions focus on specific regions with the rest of the world treated as a boundary condition adjustable by the inversion (e.g., Peylin et al. 2005; Lauvaux et al. 2008a). They can use Eulerian meso-scale models or Lagrangian models (Uliasz 1994), with resolutions down to a few kilometers.

4 Bayesian synthesis inversions

The statistical method generally adopted in atmospheric inverse modeling of CO_2 sources and sinks is based on the Bayes theorem (Tarantola 2005). In this formalism, all the information used to constrain a set of parameters, here unknown sources x, that is solved for is represented by probability density functions (PDF). The combination of those PDFs yields the PDF of vector x, from which typical characteristics such as its optimum and width can be derived. If in addition, Gaussian PDFs are assumed, as in most studies, the optimum corresponds to the minimum of a cost function $J(\mathbf{x})$ in least square sense, defined as

$$J(\mathbf{x}) = < \mathbf{H}\mathbf{x} - \mathbf{y}_o,\ \mathbf{C}_\mathbf{y}^{-1}\left(\mathbf{H}\mathbf{x} - \mathbf{y}_o\right) > + < \mathbf{x} - \mathbf{x}_b,\ \mathbf{C}_\mathbf{x}^{-1}\left(\mathbf{x} - \mathbf{x}_b\right) > \qquad (8)$$

The y_o and **Hx** vectors contain respectively observed atmospheric CO_2 mixing ratios at several geographic locations of the network and times, and the corresponding model simulations. $\mathbf{C_y}$ and $\mathbf{C_{xb}}$ are the covariance matrices of the vectors $\mathbf{y}_o$ and

$\mathbf{x}_b$ which describe the error terms Ψ and ξ in Eqs. 4 and 5. What remains is then a quadratic function of x that has a well-defined minimum.

$$\mathbf{x}_a = \mathbf{x}_b + \left(\mathbf{H}^T \mathbf{C}_y^{-1} \mathbf{H} + \mathbf{C}_{xb}^{-1}\right)^{-1} \mathbf{H}^T \mathbf{C}_y^{-1} \left(\mathbf{y}_o - \mathbf{H}\mathbf{x}_b\right) \tag{9}$$

The obtained $\mathbf{x}_a$ can be interpreted as the most likely flux estimates. The dimension of $\mathbf{x}$ is a function of the number of fluxes (regions) that are solved in space and time, plus initial condition information. Regions denote fluxes that emit or absorb tracer during a certain period of time. The maximum number of regions is the number of model grid cells, multiplied by the number of time steps for which it is relevant to solve for sources. The vector $\mathbf{x}_b$ describes the prior estimate of the sources, which comes from land ecosystem or ocean bio-geochemistry information, such as the flux maps in Fig. 2. Note that, despite some uncertainties regarding its space–time distribution, the fossil fuel source parameter is often not estimated per grid but, for example, scaled by a single parameter for simplicity. The dimension of $\mathbf{y}_o$ is the number of observations. Typically CO_2 is observed monthly at 80% of the flask stations forming the global network (Fig. 3), and continuously at the remaining 20% of stations, such as the station of Mace Head in Fig. 4.

The elements of matrix $\mathbf{H}$ are computed using a transport model. In forward mode, a transport model calculates the influence of one region on all the detectors. In practice, the transport model output is sampled at the locations, or in such a way that best represents the actual data. This might imply some averaging of the model output and the observations to provide a more robust comparison between model and data. For instance, in the daytime well-mixed boundary layer, when tracer transport takes place by turbulence, it might be preferable to average the model output on the entire well-mixed boundary layer thickness and to obtain data as representative as possible of that quantity (e.g., in situ aircraft profiles, or measurements from very tall towers).

The matrix $\mathbf{C_y}$ describes both the observational error on its diagonal terms, and the correlation among observational errors. There are several reasons for observational errors to be correlated; for instance, the observed time series are serially correlated in time by the integrative properties of the atmospheric transport, with a typical correlation time of 2–3 days at northern mid-latitudes, and so also might be their errors. For instance, there are conditions when the observations might be more contaminated by local sources unresolved by the model, and thus have correlated errors (see Lauvaux et al. 2008b).

The matrix $\mathbf{C_{xb}}$ describes the (Gaussian) uncertainties of the components of the prior source vector $\mathbf{x_b}$ for its diagonal elements. The non-diagonal terms of $\mathbf{C_{xb}}$ describe the correlations between prior source errors, as provided by some knowledge of carbon cycle processes. For instance, some error in understanding of the behavior of a particular ecosystem is likely to impact our prior estimates in the same way at many points. Importantly, the uncertainty in the analyzed flux estimates x_a is contained in the a posteriori covariance matrix $\mathbf{C_x}$. This matrix is quantified by the curvature or second derivative of the cost function J, as given by:

$$\mathbf{C_x} = \left(\mathbf{H}^T \mathbf{C_y}^{-1} \mathrm{H} + \mathbf{C_{xb}}^{-1}\right)^{-1} \tag{10}$$

We discuss below the uncertainties in each component: transport, observation error, dimension of the source vector, and how they affect the results of Bayesian inversions.

4.1 Atmospheric transport large-scale errors

Each transport model will give rise to a different version of the matrix **H**. There is no simple theory for relating variations in this matrix to variations in sources calculated in an inversion (as the inversion uses the pseudo-inverse of the matrix). However, we can use a sample of sources estimated from different transport models to illustrate how different transport parameterizations impact the inferred fluxes. Such an approach was taken in the TRANSCOM-3 study based upon 16 transport models with all other elements in the inversion fixed (Gurney et al. 2003). Figure 6 shows a comparison of different inversion results. We see from the errors reported in the Gurney et al. (2003) inversions (marked as (b) in Fig. 6) using different transport models of the TRANSCOM group, that the uncertainty of transport (gray bar in Fig. 6) is larger or equal than the posterior uncertainty (color bar in Fig. 6). The main problem is the lack of data rather than its quality, with many important regions being badly undersampled. The TRANSCOM study also sought to identify those features of model transport that contributed most to the spread among results. They discovered significant differences between models over northern-hemisphere continents (Law 1996). These differences were found to reflect differences in the covariance between the seasonality of transport and fluxes from the terrestrial biosphere. This covariance, commonly termed the *rectifier effect* (Denning et al. 1995) varies widely among atmospheric transport models and is not compensated for by other features of transport. The recent study of Stephens et al. (2007) where vertical profiles of CO_2 were used to cross validate the TRANSCOM-3 models, found that most of the current transport models have biases in transport. These biases are related to a too-weak vertical mixing in winter in the northern hemisphere, and possibly to a too-strong vertical mixing in summer. Therefore, even a sample of 16 different models can have a common bias in their simulated transport. The size of this *rectifier effect* bias is large enough to imply a reconsideration of the balance of land carbon uptake between the northern hemisphere and the tropics.

4.2 Observation errors and transport small-scale errors

Ideally, inverse modelers should assign observational errors in such a manner as to account for (1) random measurement errors, (2) systematic measurement errors such as calibration drifts, and (3) representation errors arising from the fact that at a single location, a measurement is not necessarily representative of larger grid cells that are effectively modeled. In addition, transport errors should be included in the observational error budget. These are errors in the function O and model H shown in Fig. 1, including limitations in the structure of model H itself. Indeed, both measurement and model errors represent all possible mismatches between model output and actual observations. In particular, there should be a consistency between the measurements, the assigned observation error budget, and the a priori distribution and errors of the flux in the cost function J. A necessary condition to meet this consistency is that twice the value of J at the minimum follows an χ^2 probability density with the number of observations as the number N of degree of freedom. The value of $\chi^2 = J(\mathbf{x}_a)/\mathrm{N}$ should be close to one. Failure to meet such criteria suggests a violation of the statistical assumptions underlying the Bayesian approach, in particular that the error budget setup is inconsistent with the quality of

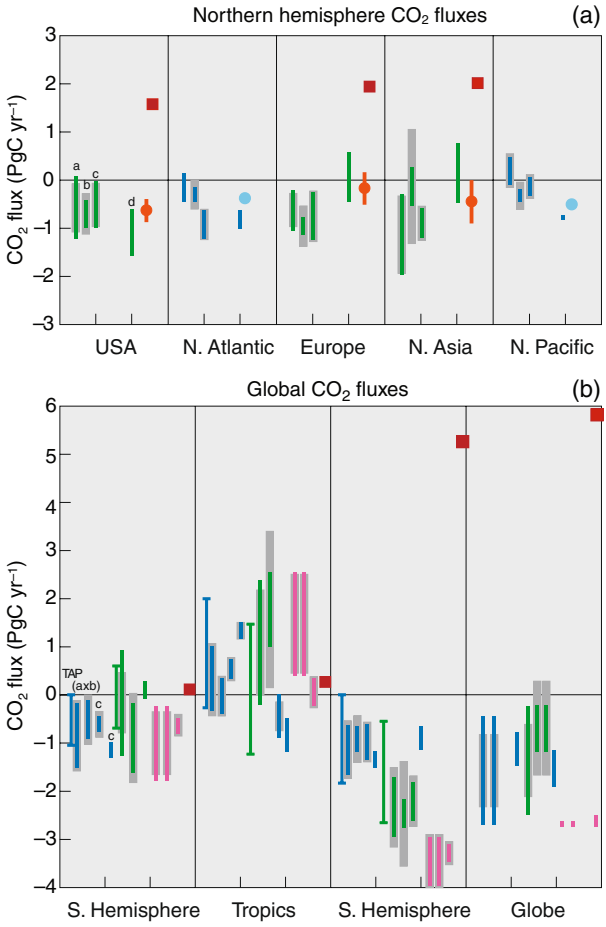

Fig. 6 Regional ocean-atmosphere and land-atmosphere CO_2 fluxes from global inversions and selected bottom–up studies. The inversion results all correspond to the period 1992–1996. **a** Regional fluxes in the northern hemisphere. **b** Regional fluxes over the globe, regrouped into three large latitude bands. *Orange* bottom–up continental-level land-atmosphere flux estimates. *Cyan* bottom–up ocean basin level flux estimates; *Blue* ocean–atmosphere fluxes from inversion models; *Green* land–atmosphere fluxes from inversion models; *Magenta* land + ocean inversion fluxes; *Red* fossil fuel emissions as being pre-substracted in the inversions. The mean flux of different inversion ensemble is reported with the random errors and the bias (range) due to different inversion settings within each ensemble. *Error boxes* show the random and systematic uncertainties of the inversions. *Colored error boxes* average of 1-sigma Gaussian random errors returned by each member of the ensemble. *Gray error boxes* spread of mean fluxes from inversions of the ensemble, with different settings. *TAR* = range of mean fluxes from the IPCC Third Assessment Report; Chapter 3, Figure 3.5; **a**–**d** = (Gurney et al. 2002) inversions using annual mean CO_2 observations with grey error from 16 transport models of the TRANSCOM group; **b** = 2003 inversions using monthly CO2 observations with grey error from 13 transport models of TRANSCOM; **c** = (Peylin et al. 2005) inversions with grey error obtained from 3 transport models × 3 discretizations in large regions × 3 inversion settings; **d** = (Rödenbeck et al. 2003b) inversions where fluxes are solved on the model grid, using monthly flask data, with the gray error from their different sensitivity inversions

the fit. Values of χ^2 less than 1 are less problematic, as they suggest that the assigned error budget is too conservative, which is always preferable.

In the northern hemisphere, random measurement errors of the in situ CO_2 measurements are generally small (<0.1 ppm) compared to the variability which is typically greater than 10 ppm (Fig. 4). In the southern hemisphere, measurement errors can be of similar magnitude compared to the variability (≈1 ppm). If the sampling frequency is high enough to allow the CO_2 observations to be averaged before they are matched them with the model output and the high frequency observations to be independent, then the measurement error can be decreased very significantly. In the case of continuous CO_2 observations, the instrumental errors σ_{inst} contribute negligibly to the monthly means if all N data are assumed to be independent with $\sigma_{mean} = \sigma_{inst}/\mathrm{sqrt(N)}$, although there are several hints that this is not the case (Gerbig et al. 2003; Bakwin et al. 1998).

Another concern is the existence of calibration offsets that add differences among different sites operated by different laboratories that are systematic and variable in time. Those offsets, as measured sporadically in inter-comparison programs, can be of the order of the gradients induced by sources. The problem is compounded by the existence of distinct regional networks (colors in Fig. 3). For example, while the largest global network, operated by NOAA is predominantly based in the northern hemisphere, the second largest network, at least historically, operated by the Commonwealth Scientific and Industrial Research Organization (CSIRO), is predominantly based in the southern hemisphere. A systematic offset between these two networks would appear as an anomalous inter-hemispheric gradient in concentration, impacting the distribution of fluxes between the hemispheres, a key target quantity for inversion studies. Strenuous efforts are under way to improve comparability among networks to limit this problem (Levin et al. 2003; Zhao and Tans 2006). The possibilities for systematic calibration offsets between stations can be explicitly accounted for in inversions and propagated to the inferred fluxes (Rödenbeck et al. 2006). Doing so does not solve the problem, but it helps quantify its negative regional impact on the fluxes.

Representation errors encompass the limitations of a model to reproduce actual measurements. These errors include the subgrid scale patterns of sources and sinks influencing a point-wise detector, and the subgrid transport. For stations located in the interior of continents near active vegetation, the heterogeneity of the nearby biospheric sources and the variability of transport imply that the representation error should be much larger than their counterparts at oceanic baseline stations. We show one example of this in Fig. 7 with vertical profiles of CO_2 in the well-mixed daytime boundary layer over a rural area in Germany. The profile indicates that there are several layers of CO_2 near the top of the well-mixed layer where entrainment mixes the air with the free atmosphere aloft and creates a discontinuity in the CO_2 concentration. Such layers and sharp discontinuities cannot be captured in models with relatively coarse vertical resolution. Therefore, either experimentalists should target measurements of the boundary layer integral of CO_2 concentration, or modelers should enlarge the observation error when only a few data points in the boundary layer are available.

The representation error is relatively hard to quantify. One could use different estimations of the surface fluxes coupled to different transport models (such as in the TRANSCOM-3 experiment) to assess the degree of uncertainty related to

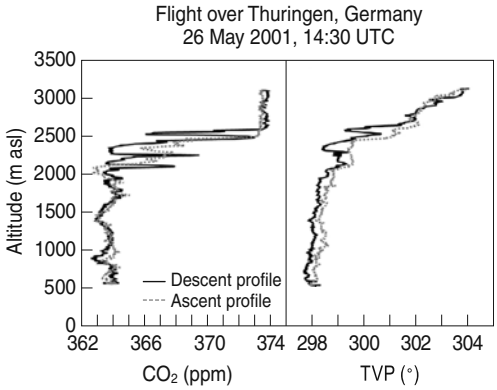

Fig. 7 Example of small-scale variability of CO_2 being sub-grid in a transport models, induced by biospheric sources and turbulent transport in the daytime convective boundary layer over Thuringen, Germany. Data are from the CAATER-1 campaign (D. Filippi, personal communication)

the transfer function between flux and concentration spaces. On the other hand, the ability of a given model to simulate the variance at each location could also be used as a proxy to derive model error. This would imply that the variance of atmospheric CO_2 within, say, a model grid box can be characterized, for instance by an intensive sampling campaign (Schmitgen et al. 2004; Gerbig et al. 2003). The results of Gerbig et al. (their figure 5) based upon an intensive campaign with over 100 vertical profiles in the eastern USA show how this representation error increases with model horizontal resolution, suggesting a minimum resolution of 20–30 km for their campaign.

To minimize the effect of representation errors, one can filter out from the data the information believed to be not representable by a model (e.g., intervals of high variability, contamination by local pollution sources). One can also sample both the model and the data toward some "baseline" conditions under which both model and observations can be more robustly compared (Ramonet and Monfray 1996; Law 1996). To do this in the best way possible, it is preferable to have continuous measurements in place so that a significant number of representative data can be retained and placed in the observation vector. For discrete measurements (flasks), a data selection procedure to screen out "local" data is often applied based on statistical criteria, flagging, for instance, as "non-background" flask measurements data that deviate by more than 3–σ from the smoothed seasonal cycle. Representation errors assigned to discrete data time series are a function of the modelers' choice for time discretization of the observation vector $\mathbf{y}_o$ (see next section). In some global inversions, monthly means of CO_2 concentration, as derived from discrete flask data, define the components of $\mathbf{y}_o$ with sub-monthly variability in flasks defining the data errors, thus encompassing the representation error linked to a model's inability to simulate synoptic and diurnal variability. In general, regional models with finer resolution show better performance than coarse-scale global models (Geels et al. 2007) provided that they are prescribed with land-atmosphere fluxes of realistic variability (Matross et al. 2006). Fine resolution models can also, to some extent, capture local mesoscale circulations, which can be driven for instance by sea breeze or by local orography over complex terrain (Sarrat et al. 2007; Pérez-Landa et al. 2007a, b).

4.3 Dimension of the source vector

The degree of temporal and spatial discretization of the source vector **x** is at the discretion of the modeler. In principle, it is recommended that the highest possible spatial and temporal resolutions be used to solve the inversion problem, the limit being the resolution of the transport model (with typically time steps of minutes and spatial scales of tens or hundreds of kilometers). This general statement refers to the inversion theory. It is separated from the main policy demand on inversions that usually focus on fluxes aggregated on yearly timescales and over countries or large regions. In practice, the memory storage induced by a large state vector and its associated error covariance matrix makes lower resolutions in space and/or in time attractive. Further, the correlations of the prior error fluxes limit the resolution of the flux increments generated by the inverse system anyway. Historically, both time and space dimensions have been dramatically reduced, with only monthly fluxes of a few large regions explicitly solved for. By doing this, the variations on smaller scales are assumed to be perfectly known. This hard constraint in the inversion degrades the observation error budget, but this has actually never been taken into account. Kaminski et al. (2001) brought the expression "aggregation error" to the attention of the community to designate the effect of this inconsistency. The recent introduction of variational methods (Chevallier et al. 2005b; Rödenbeck 2005) and ensemble methods (e.g., the CarbonTracker system http://www.esrl.noaa.gov/gmd/ccgg/carbontracker/, Peters et al. 2005) has significantly reduced the importance of this issue. These methods have also revealed the importance of the assignment of prior error correlations for the state vector, in order to avoid the unrealistic restriction of the inversion flux increments to the vicinity of the measurement location (Bocquet 2005). Prior error correlations implicitly reduce the dimension of the state vector but in a rigorous way. Eddy-covariance observations provide direct knowledge of ecosystem CO_2, water vapor, and heat fluxes on a continuous basis. These point-scale measurements can be used to estimate prior error and their correlations, the error being defined by the difference between the observed CO_2 flux and the modeled flux at the same site (more details in Chevallier et al. 2006). Although there is a network of about 300 eddy covariance ecosystem observation sites (Baldocchi et al. 2001) the sparseness of this network makes it difficult to evaluate the full space–time structure of prior flux errors in inversions. Like any other statement about prior errors, evaluation of the error correlation is dependent on the quality of a particular prior estimate. There is evidence that, with the current state of the art in terrestrial biosphere modeling, spatial error correlation lengths over land are short (not longer than a few hundred kilometers), and that temporal error correlations span weeks or even months (see Chevallier et al. 2006).

4.4 Alternative methods

The Bayesian method described above is the dominant methodology for the combination of top-down and bottom-up information, but it is not the only one. The geostatistical approach, introduced to the field by Michalak et al. (2005) and recently advanced by Gourdji et al. (2008) formulates the inversion problem differently. Flux fields are expressed as a combination of large-scale patterns and small-scale deviations. Multipliers are solved for the patterns and for the deviations. Critically,

the multipliers for the large-scale patterns are not given prior estimates, but the choice of adjustable parameters is an implicit prior setting as well. At the other extreme is the data assimilation methodology introduced by Kaminski et al. (2002) and extended by Rayner et al. (2005). Here, the bottom–up information is encapsulated in the dynamics of a process model and the state variables are a series of unknown parameters in this model. The method is radical, as it greatly reduces the dimensionality of the solution space, which is at tremendous risk of aggregation error. On the other hand the results can be used in a predictive manner and the structure of the prior error is necessary, consistent with physical understanding.

5 Future directions and carbon cycle data assimilation

Beyond the inversion surface CO_2 fluxes from concentration observations, a growing challenge is to integrate distinct streams of carbon cycle observations.

The CO_2 concentrations measured at the surface of the Earth bring limited knowledge about the surface fluxes and different ways are explored to bring additional information to the inverse systems.

Global remote-sensing of CO_2 from space is an attractive solution, which has been explored for about a decade. Existing instruments, that are sensitive to variations of CO_2 concentrations not designed to measure them, have been studied to yield CO_2 concentrations (Chédin et al. 2003; Engelen et al. 2004; Buchwitz et al. 2005). The quality of the surface fluxes inverted from them has been disappointing so far (Chevallier et al. 2005b, 2009a). Indeed, the long life time of CO_2 makes its relative variations much smaller than for shorter-lived species. Such a small variability imposes a stringent constraint on the retrieval uncertainties (random errors and biases) for the estimation of CO_2 surface fluxes (Chevallier et al. 2005a), which, to date, have not been achieved with multipurpose sounding instruments. CO_2-dedicated satellite instruments have also been designed and the first one was launched in January 2009: the Japanese Greenhouse Gases Observing Satellite (GOSAT, Yokota et al. 2004), shortly after the loss of the US Orbiting Carbon Observatory (OCO, Crisp et al. 2004) that did not reach orbit. It is too early to assess the real contribution of GOSAT to the estimation of CO_2 surface fluxes, even though theoretical simulations are promising (Chevallier et al. 2009b). Given the importance of the topic, new instruments are being prepared in the USA, in Europe, and in Japan. The dataflow that they will generate forces the inverse systems to evolve towards more industrial systems. It also poses the problem of an adequate treatment of likely correlated errors between different soundings (Chevallier 2007).

Another way to constrain the inversion of CO_2 surface fluxes consists of exploiting other types of observations in addition to atmospheric concentrations. Meeting this challenge requires both carbon cycle models with parameterizations that can capture the observations, and assimilation techniques that modify model behavior to match observations within their errors. Such techniques were initially applied long ago to the tuning of the seasonal cycle of atmospheric CO_2 concentration (e.g., Randerson et al. 1997) but the use of formal data assimilation methods allowed rapid development in the field. Examples of such applications are the estimation of phenology parameters from satellite observations (Stöckli et al. 2008), estimates of photosynthetic parameters using CO_2 and heat fluxes observed locally at

eddy-covariance sites (e.g., Santaren et al. 2007), or of a larger suite of parameters in a terrestrial model (e.g., Rayner et al. 2005). Oceanic applications are rarer, but several notable applications exist. In the wake of the 4D-VAR systems of the Numerical Weather Prediction centers described by Courtier et al. (1994), atmospheric data assimilation techniques were used in the atmospheric inverse models to analyze the concentrations and surface fluxes of CO_2 (Chevallier et al. 2005b; Baker et al. 2006; Engelen et al. 2009) and of CH_4 (Meirink et al. 2008; Pison et al. 2010). In the context of a carbon cycle data assimilation system combining models of different carbon reservoirs in a Bayesian synthesis inversion, such as the Rayner et al. (2005) study using a combined terrestrial-atmosphere model, the inversion of atmospheric CO_2 measurements is only one part of the cost function (Eq. 8) to be minimized.

Carbon cycle data assimilation applications belong to two broad categories: those that constrain the structure of the underlying model by assimilating state variables and those that estimate parameters of the model. As state variable assimilation will produce a closer fit to observations it is preferred where the best possible performance within the observing period is required (i.e., diagnostic applications to assess fluxes). Optimal estimation of parameters obviously relies on model structural qualities, but is very useful to improve the underlying behavior of the model for prognostic applications, for instance, when the goal is to project the future evolution of the system.

Most importantly, every observation such as atmospheric CO_2 concentrations, or local flux measurements, must be associated with an uncertainty, as this is necessary to weight the observation's influence on the model. Beyond this, use of any observation in a data assimilation system requires an operator that can map the internal state of the model on to the observed variable (e.g. the operator O in Section 2). Here there are practical choices to be made if the target data are themselves the result of a complex model such as a radiative transfer model retrieval in the case of remotely sensed observation.

In general it is best to bring these observation operators into the data assimilation process itself to ensure the consistency of the inverse systems. This can be difficult to represent. As an example, uncertainties in calibration can generate coherent errors that will not be captured by point-wise descriptions of errors. Experience with numerical weather prediction suggests that the generation of observational operators requires close collaboration between modelers and experts in the production of the observed variables. As a scientific task, the generation of these observation operators is equally as important as the generation of data sets of observations that use them.

6 Concluding remarks

Atmospheric inversions have proven to be a useful tool for quantifying carbon fluxes at large scales. As the research community attempts to extend this success to smaller scales it is clear that several limitations will emerge. The main limitation is the sheer lack of data. Advances in obtaining continuous, remote data at the surface (Law et al. 2002; Geels et al. 2007) or spatially dense but less precise measurements of vertically integrated concentration from satellites (e.g., Houweling et al. 2004) hold considerable promise for addressing the large data gaps. Each dataset will come with its own pitfalls. It will be hard, for example, to tie potential satellite

measurements to the global standards for long-term concentration accuracy used in the surface observations. This could lead to strong examples of the bias problems due to calibration discussed earlier. The use of continuous data, however it is obtained, will stretch our capability in transport modeling as, although synoptic concentration information contains strong signals, many of these occur at spatial and temporal resolution near the limits of current global models (Patra et al. 2008). Finally, the integration of atmospheric inversion with other forms of bio-geochemical information (e.g., Kaminski et al. 2002; Rayner et al. 2005) poses a range of methodological problems beyond those discussed here. It seems quite possible that atmospheric inversion may finally play a role as just one of several observing strategies for the underlying carbon cycle (Ciais et al. 2006) However, the integrating power of the atmosphere will, probably for a long time to come, allow it a specific role in detection of subtle but large-scale signals, such as potential feedbacks between climate change and the carbon cycle. The method will remain complementary to methods based on surface flux models or local observations.

References

Andres RJ, Marland G, Fung I, Matthews E (1996) A 1° × 1° distribution of carbon dioxide emissions from fossil fuel consumption and cement manufacture, 1950–1990. Glob Biogeochem Cycles 10:419–429

Arellano AF, Kasibhatla PS, Giglio L, van der Werf GR, Randerson JT, Collatz GJ (2006) Time-dependent inversion estimates of global biomass-burning CO emissions using Measurement of Pollution in the Troposphere (MOPITT). J Geophys Res 111:D09303. doi:10.1029/2005JD006613

Baker DF, Doney SC, Schimel DS (2006) Variational data assimilation for atmospheric CO2. Tellus, Ser B Chem Phys Meteorol 58(5):359–365

Bakwin PS, Tans PP, Zhao C, Ussler W III, Quesnell E (1995) Measurements of carbon dioxide on a very tall tower. Tellus B 47:535–549

Bakwin PS, Tans PP, Hurst DF, Zhao C (1998) Measurements of carbon dioxide on very tall towers: results from the NOAA/CMDL program. Tellus B 50:401–415

Baldocchi D, Falge E et al (2001) FLUXNET: a new tool to study the temporal and spatial variability of ecosystem-scale carbon dioxide, water vapor, and energy flux densities. Bull Am Meteorol Soc 82(11):2415–2434

Biraud S, Ciais P, Ramonet M, Simmonds P, Kazan V, Monfray P, O'Doherty S, Spain G, Jennings SG (2002) Quantification of carbon dioxide, methane, nitrous oxide and chloroform emissions over Ireland from atmospheric observations at Mace Head. Tellus B 54:1–41

Bocquet M (2005) Grid resolution dependence in the reconstruction of an atmospheric tracer source. Nonlinear Process Geophys 12:219–234

Bolin B, Keeling CD (1963) Large-scale atmospheric mixing as deduced from the seasonal and meridional variations of carbon dioxide. J Geophys Res 68:3899–3920

Bousquet P, Peylin P, Ciais P, Le Quere C, Friedlingstein P, Tans PP (2000) Regional changes in carbon dioxide fluxes on land and oceans since 1980. Science 290(5495):1342–1346

Bousquet P, Ciais P, Miller JB, Dlugokencky EJ, Hauglustaine DA, Prigent C, Van der Werf GR, Peylin P, Brunke EG, Carouge C, Langenfelds RL, Lathiere J, Papa F, Ramonet M, Schmidt M, Steele LP, Tyler SC, White J (2006) Contribution of anthropogenic and natural sources to atmospheric methane variability. Nature 443:439–443. ISI:000240798800042

Brenkert AL (1998) Carbon dioxide emission estimates from fossil-fuel burning, hydraulic cement production, and gas flaring for 1995 on a one degree grid cell basis. Available at http://cdiac.esd.ornl.gov/ndps/ndp058a.html

Bruhwiler LMP, Michalak AM, Peters W, Baker DF, Tans P (2005) An improved Kalman Smoother for atmospheric inversions. Atmos Chem Phys 5:2691–2702

Buchwitz M, De Beek R, Noël S, Burrows JP, Bovensmann H, Bremer H, Bergamaschi P, Körner S, Heimann M (2005) Carbon monoxide, methane and carbon dioxide columns retrieved from SCIAMACHY by WFM-DOAS: year 2003 initial data set. Atmos Chem Phys 5:3313–3329

Carouge C, Peylin P, Rayner PJ, Bousquet P, Chevallier F, Ciais P (2010) What can we learn from European continuous atmospheric CO_2 measurements to quantify regional fluxes. Part 2: sensitivity of flux accuracy to inverse setup. Atmos Chem Phys 10:3119–3129

Chédin A, Serrar S et al (2003) First global measurement of midtropospheric CO_2 from NOAA polar satellites: tropical zone. J Geophys Res 108(D18):4581

Chevallier F (2007) Impact of correlated observation errors on inverted CO_2 surface fluxes from OCO measurements. Geophys Res Lett 34:L24804. doi:10.1029/2007GL030463

Chevallier F, Morcrette JJ, Chéruy F, Scott NA (2000) Use of a neural-network-based long-wave radiative: transfer scheme in the EMMWF atmospheric model. Q J R Meteorol Soc 126: 761–776

Chevallier F, Engelen RJ, Peylin P (2005a) The contribution of AIRS data to the estimation of CO_2 sources and sinks. Geophys Res Lett 32:L23801. doi:10.1029/2005GL024229

Chevallier F, Fisher M, Peylin P, Serrar S, Bousquet P, Breon FM, Chedin A, Ciais P (2005b) Inferring CO_2 sources and sinks from satellite observations: method and application to TOVS data. J Geophys Res Atmos 110(D24):0148-0227, D24309. ISI:000234506500004

Chevallier F, Viovy N, Reichstein M, Ciais P (2006) On the assignment of prior errors in Bayesian inversions of CO_2 surface fluxes. Geophys Res Lett 33:L13802. doi:10.1029/2006GL026496

Chevallier F, Engelen RJ, Carouge C, Conway TJ, Peylin P, Pickett-Heaps C, Ramonet M, Rayner PJ, Xueref-Remy I (2009a) AIRS-based vs surface-based estimation of carbon surface fluxes. J Geophys Res 114:D20303. doi:10.1029/2009JD012311

Chevallier F, Maksyutov S, Bousquet P, Bréon FM, Saito R, Yoshida Y, Yokota T (2009b) On the accuracy of the CO_2 surface fluxes to be estimated from the GOSAT observations. Geophys Res Lett 36:L19807. doi:10.1029/2009GL040108

Chevillard A, Karstens U, Ciais P, Lafont S, Heimann M (2002) Simulation of atmospheric CO_2 over Europe and Western Siberia using the regional scale model. REMO Tellus 54B:872–894

Ciais P, Moore B, Steffen W, Hood M, Quegan S, Cihlar J, Raupach M, Rasool I, Doney S, Heinze H, Sabine C, Hibbard K, Schulze ED, Heimann M, Chédin A, Monfray P, Watson A, Le Quéré C, Tans PP, Dolman H, Valentini R, Arino O, Townshend J, Seufert G, Field C, Igrashi T, Goodale C, Nobre A, Inoue G, Crisp D, Baldocchi D, Tschirley J, Denning AS, Cramer W, Francey R, Wickland D (2006) A strategy to realize a coordinated system of integrated global carbon cycle observations. Integrated Global carbon observation theme. IGOS-Partnership. Available at http://ioc.unesco.org/igospartners/carbon.htm

Conway TJ, Tans PP, Waterman LS, Thoning KW, Kitzis DR, Masarie KA, Zhang N (1994) Evidence for interannual variability of the carbon cycle from the national oceanic and atmospheric administration/climate monitoring and diagnostics laboratory global air sampling network. J Geophys Res 99(D11):22831–22855

Courtier P, Thépaut J-N, Hollingsworth A (1994) A strategy for operational implementation of 4D-VAR, using an incremental approach. Q J R Meteorol Soc 120:1367–1387

Crisp D, Atlas RM, Breon F-M, Brown LR, Burrows JP, Ciais P, Connor BJ, Doney SC, Fung IY, Jacob DJ, Miller CE, O'Brien D, Pawson S, Randerson JT, Rayner P, Salawitch RJ, Sander SP, Sen B, Stephens GL, Tans PP, Toon GC, Wennberg PO, Wofsy SC, Yung YL, Kuang Z, Chudasama B, Sprague G, Weiss B, Pollock R, Kenyon D, Schroll S (2004) The orbiting carbon observatory mission. Adv Space Res Sp Iss 700–709:0273–1177. ISI:000223618200004

Denning AS, Fung I, Randall DA (1995) Strong simulated meridional gradient of atmospheric CO_2 due to seasonal exchange with the terrestrial biota. Nature 376:240–242

Engelen RJ, Andersson E, Chevallier F, Hollingsworth A, Matricardi M, McNally AP, Thépaut J-N, Watts PD (2004) Estimating atmospheric CO2 from advanced infrared satellite radiances within an operational 4D-Var data assimilation system: methodology and first results. J Geophys Res 109:D19309. doi:10.1029/2004JD004777

Engelen RJ, Serrar S, Chevallier F (2009) Four-dimensional data assimilation of atmospheric CO_2 using AIRS observations. J Geophys Res 114:D03303. doi:10.1029/2008JD010739

Enting IG (2002) Inverse problems in atmospheric constituent transport. Cambridge University Press, Cambridge

Enting IG, Trudinger CM, Francey RJ (1995) A synthesis inversion of the concentration and $\delta^{13}C$ of atmospheric CO_2. Tellus B 47:35–52

Frohn LM, Christensen JC, Brandt J (2002) Development of a high resolution nested air pollution model - the numerical approach. J Comp Physiol 179(1):68–94

Geels C, Gloor M, Ciais P, Bousquet P, Peylin P, Vermeulen AT, Dargaville R, Aalto T, Brandt J, Christensen JH, Frohn LM, Haszpra L, Karstens U, Rödenbeck C, Ramonet M, Carboni G, Santaguida R (2007) Comparing atmospheric transport models for future regional inversions

over Europe. Part 1: mapping the atmospheric CO_2 signals. Atmos Chem Phys 7:3461–3479. ISI:000248733000006

Gerbig C, Lin JC, Wofsy SC, Daube BC, Andrews AE, Stephens BB, Bakwin P, Grainger CA (2003) Towards constraining regional scale fluxes of CO2 with atmospheric observations over a continent: 2. Analysis of COBRA data using a receptor oriented framework. J Geophys Res 108:D4757. doi:10.1029/2003JD003770

Gloor M, Bakwin P, Hurst D, Lock L, Drexler R, Tans P (2001) What is the concentration footprint of a tall tower? J Geophys Res 106:17831–17840

Gourdji S, Mueller K, Schaefer K, Michalak AM (2008) Global monthly-averaged CO_2 fluxes recovered using a geostatistical inverse modeling approach: 2. Results including auxiliary environmental data. J Geophys Res 113(D21):D21115

Gurney KR, Law RM, Denning AS, Rayner PJ, Baker D, Bousquet P, Bruhwiler L, Chen YH, Ciais P, Fan S, Fung IY, Gloor M, Heimann M, Higuchi K, John J, Maki T, Maksyutov S, Masarie K, Peylin P, Prather M, Pak BC, Randerson J, Sarmiento J, Taguchi S, Takahashi T, Yuen CW (2002) Towards robust regional estimates of CO_2 sources and sinks using atmospheric transport models. Nature 415:626–630

Gurney KR, Law RM, Denning AS, Rayner PJ, Baker D, Bousquet P, Bruhwiler L, Chen Y-H, Ciais P, Fan S, Fung IY, Gloor M, Heimann M, Higuchi K, John J, Kowalczyk E, Maki T, Maksyutov S, Peylin P, Prather M, Pak BC (2003) TransCom3 CO_2 inversion intercomparison: 1. Annual mean control results and sensitivity to transport and prior flux information. Tellus 55B(2):555–579. doi:10.1034/j.1600-0560.2003.00049

Hein R, Crutzen PJ, Heimann M (1997) An inverse modeling approach to investigate the global atmospheric methane cycle. Glob Biogeochem Cycles 11:43–76

Hourdin F, Idelkadi A, Talagrand O (2006) Eulerian backtracking of atmospheric tracers: adjoint derivation, parametrization of subgrid-scale transport and numerical aspects. Q J R Meteorol Soc 132B(615):567–583

Houweling S, Kaminski T, Dentener F, Lelieveld J, Heimann M (1999) Inverse modeling of methane sources and sinks using the adjoint of a global transport model. J Geophys Res 104:26137–26160

Houweling S, Bréon FM, Aben I, Rödenbeck C, Gloor M, Heimann M, Ciais P (2004) Inverse modeling of CO_2 sources and sinks using satellite data: a synthetic inter-comparison of measurement techniques and their performance as a function of space and time. Atmos Chem Phys 4: 523–538

Ide KP, Courtier P, Ghil M, Lorenc AC (1997) Unified notation for data assimilation: operational, sequential and variational. J Meteorol Soc Jpn 75:181–189

Kaminski T, Heimann M, Giering R (1999) A coarse grid three-dimensional global inverse model of the atmospheric transport. 1. Adjoint model and Jacobian matrix. J Geophys Res 104(D15):18535–18553

Kaminski T, Rayner PJ, Heimann M, Enting IG (2001) On aggregation errors in atmospheric transport inversions. J Geophys Res 106(D5):4703–4715

Kaminski T, Knorr W, Rayner PJ, Heimann M (2002) Assimilating atmospheric data into a terrestrial biosphere model: a case study of the seasonal cycle. Glob Biogeochem Cycles 16(4):1066. doi:10.1029/2001GB001463

Krinner G, Viovy N, De Noblet-Ducoudré N, Ogee J, Polcher J, Friedlingstein P, Ciais P, Sitch S, Prentice IC (2005) A dynamic global vegetation model for studies of the coupled atmosphere-biosphere system. Glob Biogeochem Cycles 19:GB1015, 0886–6236. ISI:000227525800001

Krol M, Houweling S, Bregman B, van den Broek M, Segers A, van Velthoven P, Peters W, Dentener F, Bergamaschi P (2005) The two-way nested global chemistry-transport zoom model TM5: algorithm and applications. Atmos Chem Phys 5(2):417–432

Law RM (1996) The selection of model-generated CO_2 data: a case study with seasonal biospheric sources. Tellus 48B:474–486

Law RM, Rayner PJ, Denning AS, Erickson D, Fung IY, Heimann M, Piper SC, Ramonet M, Taguchi S, Taylor JA, Trudinger CM, Watterson IG (1996) Variations in modeled atmospheric transport of carbon dioxide and the consequences for CO_2 inversions. Glob Biogeochem Cycles 10(4). doi:10.1029/96GB01892

Law RM, Rayner PJ, Steele LP, Enting IG (2002) Using high temporal frequency data for CO_2 inversions. Glob Biogeochem Cycles 16(4):1053. doi:10.1029/2001GB001593

Law RM et al (2008) TransCom model simulations of hourly atmospheric CO_2: experimental overview and diurnal cycle results for 2002. Glob Biogeochem Cycles 22:GB3009. doi:10.1029/2007GB003050

Lauvaux T, Uliasz M, Sarrat C, Chevallier F, Bousquet P, Lac C, Davis KJ, Ciais P, Denning AS, Rayner PJ (2008a) Mesoscale inversion: first results from the CERES campaign with synthetic data. Atmos Chem Phys 8:3459–3471

Lauvaux T, Pannekoucke O, Sarrat C, Chevallier F, Ciais P, Noilhan J, Rayner PJ (2008b) Structure of the transport uncertainty in mesoscale inversions of CO_2 sources and sinks using ensemble model simulations. Biogeosciences 6:1089–1102

Levin I, Langendörfer U, Schmidt M, Facklam C, Langenfelds R, Allison C, Francey R, Jordan A, Brand WA, Neubert REM, Meijer HAJ, Holmen K (2003) EuroSiberianCarbonflux: technical Report. CO_2 intercomparison. In: Toru S (ed) Proceedings of the 11th IAEA/WMO meeting of CO_2 experts, Tokyo, Sept 2001, WMO-GAW Report, vol 148, pp 37–54. Available at http://www.wmo.ch/web/arep/gaw/gawreports.html

Manning AJ, Ryall DB, Derwent RG, Simmonds PG, O'Doherty S (2003) Estimating European emissions of ozone depleting and greenhouse gases using observations and a modeling back-attribution technique. J Geophys Res 108(D14):4405. doi:10.1029/2002JD002312

Marland G, Boden T, Andres RJ (2001) Global, regional, and national CO_2 emissions from fossil-fuel burning, cement production, and gas flaring: 1751–1998. Carbon Dioxide Information and Analysis Center, Oak Ridge National Laboratory, Oak Ridge, TN, USA, NDP-030. Available at http://cdiac.esd.ornl.gov

Matross DM, Andrews A, Pathmathevan M, Gerbig C, Lin JC, Wofsy SC, Daube BC, Gottlieb EW, Chow VY, Lee JT, Zhao C, Bakwin PS, Munger JW, Hollinger DY (2006) Estimating regional carbon exchange in New England and Quebec by combining atmospheric, ground-based and satellite data. Tellus B 58:344–358

Meirink JF, Bergamaschi P, Frankenberg C, d'Amelio MTS, Dlugokencky EJ, Gatti LV, Houweling S, Miller JB, Röckmann T, Villani MG, Krol M (2008) Four-dimensional variational data assimilation for inverse modelling of atmospheric methane emissions: analysis of SCIAMACHY observations. J Geophys Res 113:D17301. doi:10.1029/2007JD009740

Michalak AM, Hirsch A, Bruhwiler L, Gurney KR, Peters W, Tans PP (2005) Maximum likelihood estimation of covariance parameters for Bayesian atmospheric trace gas surface flux inversions. J Geophys Res 110(D24):D24107. doi:10.1029/2005JD005970

Nicholls ME, Denning AS, Prihodko L, Vidale PL, Baker I, Davis K, Bakwin P (2004) A multiple-scale simulation of variations in atmospheric carbon dioxide using a coupled biosphere-atmospheric model. J Geophys Res 109:D18117. doi:10.1029/2003JD004482

Patra PK, Law RM, Peters W, Rödenbeck C, Takigawa M, Aulagnier C, Baker I, Bergmann DJ, Bousquet P, Brandt J, Bruhwiler L, Cameron-Smith PJ, Christensen JH, Delage F, Denning AS, Fan S, Geels C, Houweling S, Imasu R, Karstens U, Kawa SR, Kleist J, Krol MCL, Lin S-J, Lokupitiya R, Maki T, Maksyutov S, Niwa Y, Onishi R, Parazoo N, Pieterse G, Rivier L, Satoh M, Serrar S, Taguchi S, Vautard R, Vermeulen AT, Zhu1 Z (2008) TransCom model simulations of hourly atmospheric CO_2. Analysis of synoptic scale variations for the period 2002–2003. Glob Biogeohem Cycles 22(4). doi:10.1029/2007GB003081

Pérez-Landa G, Ciais P, Sanz MJ, Gioli B, Miglietta F, Palau JL, Gangoiti G, Millán MM (2007a) Mesoscale circulations over complex terrain in the Valencia coastal region, Spain. Part 1: simulation of diurnal circulation regimes. Atmos Chem Phys 7:1835–1849

Pérez-Landa G, Ciais P, Gangoiti G, Palau JL, Carrara A, Gioli B, Miglietta F, Schumacher M, Millán MM, Sanz MJ (2007b) Mesoscale circulations over complex terrain in the Valencia coastal region, Spain. Part 2: modeling CO_2 transport using idealized surface fluxes. Atmos Chem Phys 7:1851–1868

Peters W, Miller JB, Whitaker J, Denning AS, Hirsch A, Krol MC, Zupanski D, Bruhwiler L, Tans PP (2005) An ensemble data assimilation system to estimate CO_2 surface fluxes from atmospheric trace gas observations. J Geophys Res 110(D24):D24304. doi:10.1029/2005JD006157

Petron G, Granier C, Khattatov B, Lamarque J-F, Yudin V, Muller J-F, Gille J (2002) Inverse modeling of carbon monoxide surface emissions using Climate Monitoring and Diagnostics Laboratory network observations. J Geophys Res 107:4761. doi:10.1029/2001JD001305

Peylin P, Rayner PJ, Bousquet P, Carouge C, Hourdin F, Heinrich P, Ciais P, AEROCARB contributors (2005) Daily CO_2 flux estimates over Europe from continuous atmospheric measurements. Part 1 inverse methodology. Atmos Chem Phys 5:3173–3186

Pison I, Bousquet P, Chevallier F, Szopa S, Hauglustaine DA (2010) Multi-species inversion of CH_4, CO and H_2 emissions from surface measurements. Atmos Chem Phys 9:5281–5297

Ramonet M, Monfray P (1996) CO_2 baseline concept in 3-D atmospheric transport models. Tellus B 48:502–520

Ramonet M, Ciais P, Nepomniachii I, Sidorov K, Neubert R, Langendorfer U, Picard D, Biraud S, Gusti M, Kolle O, Schulze E, Lloyd J (2002) Two years of aircraft based trace gas measurements over the Fyodorovskoye southern taiga forest 300km north west of Moscow. Tellus B 54:5

Randerson JT (2001) The CASA terrestrial biogeochemical model. In: Mooney HA, Canadell J (eds) Encyclopedia of global environmental change, vol 2: the earth system: biological and ecological dimensions of global environmental change. Wiley, Hoboken

Randerson JT, Thompson MV, Conway TJ, Fung IY, Field CB (1997) The contribution of terrestrial sources and sinks to trends in the seasonal cycle of atmospheric carbon dioxide. Glob Biogeochem Cycles 11:535–560

Rayner PJ, Scholze M, Knorr W, Kaminski T, Giering R, Widmann H (2005) Two decades of terrestrial carbon fluxes from a carbon cycle data assimilation system (CCDAS). Glob Biogeochem Cycles 19. doi:10.1029/2004GB002254

Rödenbeck C (2005) Estimating CO_2 sources and sinks from atmospheric mixing ratio measurements using a global inversion of atmospheric transport. Technical Report 6, Max Planck Institute for Biogeochemistry, Jena

Rödenbeck C, Houweling S, Gloor M, Heimann M (2003a) Time-dependent atmospheric CO_2 inversions based on interannually varying tracer transport. Tellus B 5:2488–2497

Rödenbeck C, Houweling S, Gloor M, Heimann M (2003b) CO_2 flux history 1982–2001 inferred from atmospheric data using a global inversion of atmospheric transport. Atmos Chem Phys 3:1919–1964

Rödenbeck C, Conway TJ, Langenfeld RI (2006) The effect of systematic measurement errors on atmospheric CO_2 inversions: a quantitative assessment. Atmos Chem Phys 6:149–161

Santaren D, Peylin P, Viovy N, Ciais P (2007) Optimizing a process-based ecosystem model with eddy-covariance flux measurements: a pine forest in southern France. Glob Biogeochem Cycles 21:2. doi:10.1029/2006GB002834

Sarrat C, Noilhan J, Lacarrere P, Donier S, Lac C, Calvet JC, Dolman AJ, Gerbig C, Neininger B, Ciais P, Paris JD, Boumard F, Ramonet M, Butet A (2007) Atmospheric CO_2 modeling at the regional scale: application to the CarboEurope Regional Experiment. Biogeosci 4:1115–1126, 0148–0227 112 D12 D12105. ISI:000247369600006

Schmitgen S, Geiss H, Ciais P, Neininger B, Brunet Y, Reichstein M, Kley D, Volz-Thomas A (2004) Carbon dioxide uptake of a forested region in southwest France derived from airborne CO_2 and CO measurements in a quasi-Lagrangian experiment. J Geophys Res 109:D14. doi:10.1029/2003JD004335

Stephens BB, Gurney KR, Tans PP, Sweeney C, Peters W, Bruhwiler L, Ciais P, Ramonet M, Bousquet P, Nakazawa T, Aoki S, Machida T, Inoue G, Vinnichenko N, Lloyd J, Jordan A, Heimann M, Shibistova O, Langenfelds RL, Steele LP, Francey RJ, Denning AS (2007) Weak northern and strong tropical land carbon uptake from vertical profiles of atmospheric CO_2. Science 316:1732–1735. ISI:000247400500043

Stöckli R, Rutishauser T, Dragoni D, O'Keefe J, Thornton PE, Jolly M, Lu L, Denning AS (2008) Remote sensing data assimilation for a prognostic phenology model. J Geophys Res 113:G04021. doi:10.1029/2008JG000781

Takahashi T, Feely RA, Weiss RF, Wanninkhof RH, Chipman DW, Sutherland ST, Takahashi TT (1997) Global air–sea flux of CO2: an estimate based on measurements of sea-air pCO_2 difference. Proc Natl Acad Sci U S A 94:8292–8299

Tans PP, Bakwin PS, Guenther DW (1996) A feasible global carbon cycle observing system: a plan to decipher today's carbon cycle based on observations. Glob Chang Biol 2:309–318

Tarantola A (2005) Inverse problem theory and methods for model parameter estimation. Society for Industrial and Applied Mathematics, Philadelphia. ISBN 0-89871-572-5

Uliasz M (1994) Lagrangian particle modeling in mesoscale applications. In: Zanetti P (ed) Environmental modelling II. Computational Mechanics, Southampton, pp 71–102

Vautard R, Beekmann M, Menut L, Lattuati M (1998) Applications of adjoint modelling in urban air pollution. In: Borrell PM, Borrell P (eds) Eurotrac 1998, Guest contribution to subproject Saturn. WIT, Southampton, pp 502–508

Yokota T, Oguma H, Morino I, Higurashi A, Aoki T, Inoue G (2004) Test measurements by a BBM of the nadir-looking SWIR FTS aboard GOSAT to monitor CO2 column density from space. In: Tsay SC, Yokota T, Ahn M-H (eds) Society of Photo-Optical Instrumentation Engineers (SPIE) conference series, vol 5652, pp 182–188

Zhao CL, Tans PP (2006) Estimating uncertainty of the WMO mole fraction scale for carbon dioxide in air. J Geophys Res 111:D08S09. doi:10.1029/2005JD006003

Climatic Change (2010) 103:93–115
DOI 10.1007/s10584-010-9908-4

European CO_2 fluxes from atmospheric inversions using regional and global transport models

L. Rivier · Ph. Peylin · Ph. Ciais · M. Gloor · C. Rödenbeck · C. Geels · U. Karstens · Ph. Bousquet · J. Brandt · M. Heimann · Aerocarb experimentalists

Received: 5 January 2009 / Accepted: 15 June 2010 / Published online: 15 July 2010

Abstract Approximately half of human-induced carbon dioxide (CO_2) emissions are taken up by the land and ocean, and the rest stays in the atmosphere, increasing the global concentration and acting as a major greenhouse-gas (GHG) climate-forcing element. Although GHG mitigation is now in the political arena, the exact spatial distribution of the land sink is not well known. In this paper, an estimation of mean European net ecosystem exchange (NEE) carbon fluxes for the period 1998–2001 is performed with three mesoscale and two global transport models, based on the integration of atmospheric CO_2 measurements into the same Bayesian synthesis inverse approach. A special focus is given to sub-continental regions of Europe making use of newly available CO_2 concentration measurements in this region. Inverse flux estimates from the five transport models are compared with independent flux estimates from four ecosystem models. All inversions detect a strong annual

L. Rivier (✉) · Ph. Ciais · Ph. Bousquet
Laboratoire des Sciences du Climat et de l'Environnement, CEA-CNRS-UVSQ, IPSL, Paris, France
e-mail: Leonard.Rivier@lsce.ipsl.fr

Ph. Peylin
Laboratoire de Biogéochimie des Milieux Continentaux, CEA-CNRS-UVSQ, IPSL, Grignon, France

M. Gloor
School of Geography, University of Leeds, Leeds LS2 9JT, UK

C. Rödenbeck · U. Karstens · M. Heimann
Max-Planck-Institut fur Biogeochemie, Jena, Germany

C. Geels · J. Brandt
National Environmental Research Institute,
University of Aarhus, Roskilde, Denmark

Aerocarb experimentalists
URL: http://aerocarb.lsce.ipsl.fr/

carbon sink in the southwestern part of Europe and a source in the northeastern part. Such a dipole, although robust with respect to the network of stations used, remains uncertain and still to be confirmed with independent estimates. Comparison of the seasonal variations of the inversion-based net land biosphere fluxes (NEP) with the NEP predicted by the ecosystem models indicates a shift of the maximum uptake period, from June in the ecosystem models to July in the inversions. This study thus improves on the understanding of the carbon cycle at sub-continental scales over Europe, demonstrating that the methodology for understanding regional carbon cycle is advancing, which increases its relevance in terms of issues related to regional mitigation policies.

1 Introduction

A precise quantification of the CO_2 fluxes exchanged between the atmosphere and surface reservoirs and of their variability is crucial for making better projections of the future evolution of the coupled land surface–climate system. Detailed and accurate knowledge of sources and sinks for atmospheric CO_2 down to continental and regional scales is also required for monitoring and assessment of the effectiveness of carbon sequestration and/or emission reduction policies, such as the Kyoto Protocol. Two complementary approaches are typically used to estimate CO_2 fluxes at regional to global scales. The bottom-up approach is based upon bio-geochemical oceanic and terrestrial carbon cycle modeling, with models being forced by input climate fields, and combined with local measurements of fluxes and/or remote sensing information of surface properties and state. The top-down approach is based on gradients in atmospheric CO_2 concentration across different measuring stations, which are combined with an atmospheric transport model, to optimize a priori distribution of fluxes in order to best fit the concentration data within their errors.

Inversion methods have been developed and applied at the global scale, making use of CO_2 flask data from a global network of predominantly oceanic stations. Using such data, it might be possible to constrain the budget of the northern hemisphere at the scale of ocean basins and large continental regions (Gurney et al. 2005), as well as the interannual variability of these fluxes (Bousquet et al. 2000; Baker et al. 2001).

Only recently, inversions have been set up to calculate CO_2 flux estimates with more details at the sub-continental scale, based upon surface CO_2 data of higher, sub-monthly, temporal frequency (Rodenbeck et al. 2003; Peters et al. 2007; Carouge et al. 2008 submitted), or based upon higher spatial density data collected during campaigns (Gerbig et al. 2003; Lauvaux et al. 2007). Yet, the scarcity of the atmospheric network over land and the large uncertainties of transport models (Geels et al. 2007) still hamper inversions from increasing the resolution and accuracy of the retrieved fluxes. Recent improvements of these two critical components might pave the way for new reliable regional estimates. Efforts are made on the experimental side to increase the density of networks, both in time and in space, over regions like western Europe (Carboeurope,[1] ICOS[2]) and North America

[1] http://wwwcarboeurope.org/

[2] http://www.icos-infrastructure.eu/

(NACP[3]). On the modeling side, several integrative efforts have been taking place to improve our understanding of the carbon cycle at all scales, including improvement of the underlying bio-geochemical flux models as well as of atmospheric transport models (CarboEurope1 and NACP3 projects for instance). In this context, the study follows two main objectives. The first is to provide an inversion-based assessment of the carbon budget of western Europe, where the continent is subdivided into few smaller regions, and for the period 1998–2001. The second is to compare inverse estimates from conventional global models to those using mesoscale models. To meet these goals, we make use of a larger number of stations over Europe than in global inversions, of an ensemble of both mesoscale models with a high spatial resolution, and of global atmospheric transport models. The inversion-based fluxes, within their errors, are compared with the independently obtained results of bottom-up studies based upon a suite of bio-geochemical models.

Increasing the spatial resolution of atmospheric inversions faces some scientific and technical difficulties (Kaminski et al. 2001), with the need to properly account for the complex spatial patterns of the fluxes and of their temporal variability (especially over Europe) and with the numerical size of the inverse problem. Correctly capturing the flux variability, especially over land, represents a great challenge for global and regional models. Furthermore, biases in transport models constitute a large source of error in the inversion of the surface CO_2 fluxes, of up to 50% in a given setup (e.g., Gloor et al. 1999). Recent testing and intercomparison experiments of transport models, like Chevillard et al. (2002), Geels et al. (2007), Law et al. (2008) suggest that mesoscale models, with their higher spatial and vertical resolution, may be able to better capture the observed CO_2 concentration high-frequency variability. Geels et al. (2007) showed for instance that mesoscale models like REMO and DEHM (see description below) with a resolution of ≈50 km tend to better capture the synoptic/diurnal variability and the vertical gradients of CO_2 in western Europe than global models with a resolution of hundreds of kilometers. Moreover, Law et al. (2008) state that. "The models giving diurnal amplitudes closer to the observed are those with higher horizontal resolution." Note also that the fact that the models are either driven or nudge to the meteorological analysis of the European Centre for Medium-Range Weather Forecasts (ECMWF) explains some of the improved representation of synoptic scale variability.

In this paper, we perform a series of Bayesian synthesis inversions with the five transport models tested by Geels et al. (2007), comprising three regional mesoscale models and two global models. The potential of the mesoscale models has been evaluated in Geels et al. (2007) with a comparison of simulated concentrations at European stations and it is now tested within an inverse approach. The same inverse procedure is applied to the different transport models, allowing us to assess the between-model differences in the retrieved fluxes, which should form part of the inversion uncertainty calculation. Mesoscale models have a limited domain, which implies a specific treatment of their boundary conditions. So far, very little use of regional models has been made in inversions, apart from short-term episode studies with fixed boundary conditions (Lauvaux et al. 2007; Zupanski et al. 2007; Gerbig et al. 2003). One originality of this study is to combine mesoscale models centered

[3] http://www.nacarbon.org/nacp/

over Europe with global models elsewhere to produce a consistent global inversion with a special focus on a few European regions. A major interest is to compare the results of the inversion with mesoscale models with those of global models.

In the following, we first describe the inversion method, focusing on the use of mesoscale models and on the assimilation of data from continental stations (Section 2). We then analyze the annual flux estimates and their seasonal variation and compare them with independent estimates from ecosystem model results (Sections 3 and 4). We discuss the sensitivity of the inversion-based European carbon budget to some critical components of the inversion, and some technical challenges linked to the use of regional models (Sections 5 and 6).

2 Atmospheric inversion setup

We performed a series of inversions for 1 year using one fixed inverse set-up but five different transport models (two global and three regional models). Below, we describe successively the overall inverse approach, the atmospheric data, the transport models, the prior fluxes and their errors, and the different sensitivity tests that were conducted.

2.1 Global inversion with increased resolution over Europe

2.1.1 Principle

We used the Bayesian synthesis inverse method (Enting 2002; Tarantola 1987). The method jointly minimizes the Euclidean distance between simulated and observed concentrations along with prior and posterior fluxes. In all cases distances are expressed as multiples of the relevant uncertainty. The method calculates the maximum likelihood estimate and uncertainty of posterior fluxes. Prior uncertainties on fluxes and data are inputs to the problem and those for the data contain the contribution from model error (Tarantola 1987, Eq. 1.43). The solution requires the sensitivity of each observation to each flux (i.e., influence functions) parameter to be optimized. The CO_2 flux distribution over the globe is arbitrarily discretized in space into source regions, and in time into a number of emitting periods fully covering the entire year. In our set up, the source regions are ten small provinces over Europe (Fig. 1) and continents/ocean gyres elsewhere. For these source regions, influence functions are simulated with the five; see regional map of different transport models for a network of 76 monitoring stations (see details, Section 2.4).

2.1.2 Spatial discretization of fluxes

The degree of spatial discretization of the CO_2 sources can vary from few large regions over the globe (Fan et al. 1998) to all the grid cells of a transport model for the most recent studies (Rodenbeck et al. 2003; Peylin et al. 2005). There is still a debate in the community on the best degree of spatial resolution to use in these calculations (Peylin et al. 2001; Bocquet 2005). Significant biases of the inversion may occur when solving for few large regions, implicitly assuming a perfectly known spatial pattern of fluxes within each region. The impacts of this aggregation error have been analyzed by Kaminski et al. (2001). On the other hand, solving for a large

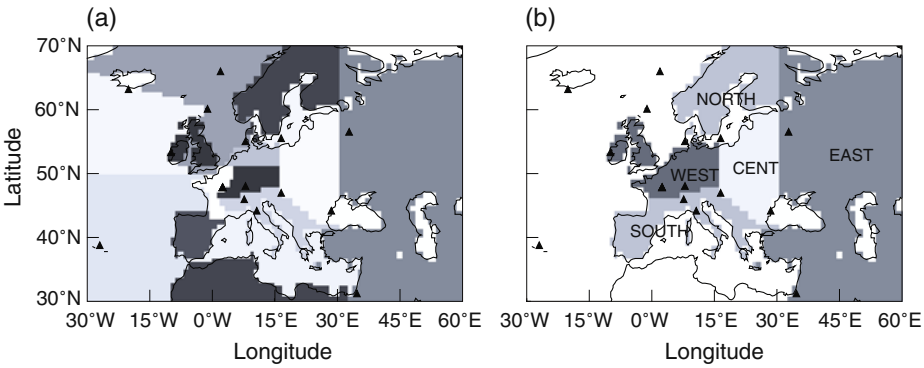

Fig. 1 Maps of regions used over Europe in this study. **a** Displays the regions used for the control inversion. **b** Displays the regions on which the results are further aggregated and discussed. *Black triangles* show the stations used in the inversions. See text for name and coordinates of the stations (Section 2.2)

number of regions, and assuming them to be independent of each other, leads to undetermined sources, given the sparseness of the atmospheric network. The use of distance-based error correlations (Carouge et al. 2008), when solving the fluxes at the resolution of the transport model, has been tested but is still being debated. In this study, we adopt a compromise, and solve for large regions over most of the world (ten land and ten ocean regions as in the Transcom-3 experiment,[4] with no error correlation) and for smaller regions over Europe and the Northeast Atlantic Ocean (ten land and five ocean regions, see Fig. 1) in order to exploit the regionally higher density of the European network.

2.1.3 Temporal discretization of fluxes

For the temporal discretization of fluxes we chose a monthly time step. Accordingly, the atmospheric data used are monthly mean CO_2 values, as in most global inversions studies, avoiding complications linked to the assimilation of high-frequency measurements. We built a monthly CO_2 climatology (mean seasonal cycle) over the period 1998–2001 forming a quasi-stationary seasonal cycle superimposed on the observed global trend for that period (see Kaminski et al. 1999 for technical details). We ignore inter-annual variations of atmospheric transport and source strengths, and solve for 12 monthly "climatological" sources over each region for the 1998–2001 period. The same "influence functions" are "recycled" in the inversion periodically over the 4 years by shifting each monthly pulse influence function 1 year forward in time and adding its results back on to the tail of the previous year influence function in order to define the "quasi-stationary influence functions" (Enting 2002; Kaminski et al. 1999). The atmospheric transport is calculated for all models by recycling the meteorological fields of 1998 and using a priori fluxes for 1998.

[4] http://www.purdue.edu/transcom/transcom.php; see regional map

2.2 Global atmospheric CO_2 measurements with new sites over Europe

Outside Europe we used a global network of 76 stations with smoothed monthly CO_2 concentrations (GLOBALVIEW-CO_2 2005), identical to the TRANSCOM network of Gurney et al. (2003), but over a different period (1998–2001 instead of 1992–1996 in Gurney et al.). Data from nine European stations operated as part of the AEROCARB EU-funded project (see location in Fig. 1) were added to this initial network. These nine stations are: Cabauw-CBW (4.92°E; 51.97°N), Monte Cimone-CMN (10.7°E; 44.18°N), H Hegyhátsál-HUN (16.65°E; 46.95°N), Mace Head-MHD (9.88°W; 53.32°N), Pallas-PAL (24.12°E; 67.97°N), Plateau Rosa-PRS (7.7°E; 45.93°N), Schauinsland-SCH (7.92°E; 47.92°N), Westerland-WES (8.32°E; 54.93°N), and Zeppelin-ZEP (11.88°E; 78.9°N). For each of these sites the raw data are processed as follows. Hourly CO_2 concentrations have been selected for daytime periods (11:00 to 16:00 LT), and combined into monthly means and errors (see below). The daytime selection reflects the fact that the transport models are not able to properly capture the nocturnal accumulation of respired CO_2 (and fossil emissions) near the ground during the growing season (Geels et al. 2007). The choice of the 1998–2001 period corresponded to the maximum availability of data.

The observation error should include not only measurement errors but also model errors and in particular those associated with the scale mismatch between the measured CO_2 concentration at one point and the simulated concentration in a large grid-box (so-called representation error, see Gerbig et al. 2003). The monthly errors were computed as the standard deviation of the CO_2 raw data over the entire year, following the assumption that transport models tend to be less reliable for sites with large concentration variability. The resulting errors vary between 0.3 ppm for a remote site (Amsterdam Island, southern ocean) and 2.47 ppm for KSN in Korea.

2.3 Global transport models and finer-scale regional transport models over Europe

We used two global models (TM3 and LMDz) and three regional models with a limited domain (REMO, DEHM, and HANK). The ensemble of models covers a representative sample of transport models used previously in various atmospheric trace gases studies, including CO_2 and air pollution transport. Their characteristics are summarized below and in Table 1 (see Geels et al. 2007, for more details).

- TM3 is a global off-line atmospheric tracer transport model (i.e., using a precomputed meteorological field) (Heimann 1996). It was run at the resolution of $5° \times 3.75°$ using 6-hourly reanalyzed meteorological fields from the European Center for Medium Range Weather Forecasting (ECMWF).
- LMDz is a Global Circulation Model (GCM), developed by the Laboratory of Dynamic Meteorology (LMD) in France (Sadourny and Laval 1984), with the possibility of a stretched horizontal grid. In this paper, we used a grid with a zoom centered over Europe, leading to a maximum resolution of $1.2° \times 0.8°$, and 19 sigma-pressure vertical layers up to 3 hPa. Model horizontal winds are relaxed toward analyzed ECMWF fields (with a time constant of 2.5 h) for the year 1998. When compared with the models used in the Transcom-1 intercomparison experiment (Law et al. 1996), LMDz tends to have a fast large-scale horizontal and vertical mixing.

Table 1 Transport model description

Model	TM3	LMDZ	REMO	DEHM	HANK
Domain	Global	Global, zoomed over Europe	Europe	Northern hemisphere	Northern hemisphere/ Europe
Resolution	4 × 5	3.75 × 2.5 1.25 × 1 in zoomed region	0.5 × 0.5	150 km × 150 km	270 km × 270 km / 90 km × 90 km
Response functions durations	2 years	2 years	3 months	4 months	3 months
Vertical levels	19	19	20	20	23
Lowest level	82 m	150 m	60 m	80 m	100 m
Boundary conditions	None: global model	None: global model	Uses TM3	Zero BC at the equator	Zero BC at the equator

- The REgional MOdel (REMO) is based on the EuropaModell (EM) of the German Weather Service (DWD) (Majewski 1991). The current version of REMO (version 4.3) is operated in a diagnostic mode where the model is started for each day at 00 UTC from the ECMWF ERA40 reanalyzes and a 30- h forecast is computed. To account for a spin-up time the first 6 h of the forecast are neglected. By restarting the model every day from analyses, the model state is forced to stay close to the ECMWF weather situation.
- The regional Danish Eulerian Hemispheric Model (DEHM) was initially developed to study long range transport of sulfur into the Arctic (Christensen 1997). The model has since then been further developed to include nesting capabilities (Frohn et al. 2002) and it has been coupled to the Fifth-Generation NCAR/Penn State Mesoscale Model (MM5) (Grell et al. 1995), which is used as a meteorological driver for the model system.
- The regional chemistry transport model HANK has been developed by Hess et al. (2000). In a modeling system with the MM5 model (Grell et al. 1995) the HANK model can be used to model the concentration fields of non-reactive and reactive constituents in the atmosphere. For this paper a polar stereographic coordinate system with coarse grid mesh centered at the North Pole that covers approximately two-thirds of the northern hemisphere is used. Within this larger domain a domain with three times finer resolution that is centered over Europe is embedded.

2.4 Calculation of the influence function of each region

Monthly influence functions of each source region are computed with a unit carbon source (1 GtC) emitted over this region during 1 month and further dispersed globally by the transport models. For the two global models, TM3 and LMDz, the influence of each source at all the stations is computed for 24 months, recycling the meteorology of 1998. Ideally, with the limited domain regional models, one would nest them in both directions into a “mother” global model for accounting in their

influence functions of the mass of CO_2 exiting at one boundary but re-entering later at another boundary, especially during fast zonal winter transport (Holton 1992).

For the stations outside the domain of each regional model, we used the influence functions calculated by TM3. For the stations inside the domain, we chose a simplified one-way nesting for computing the REMO influence functions, where REMO is prescribed with the interpolated CO_2 concentration from TM3 at the boundary of its domain. By doing this, only the influx of CO_2 from TM3 into REMO for each regional source is accounted for, but not the feedback of REMO on TM3. For computing the influence functions of DEHM and HANK, which have a larger hemispheric domain, the CO_2 boundary conditions should be less important than with REMO. Therefore, a uniform zero CO_2 concentration was initially prescribed around the equator. However, this simplification means that inverse models based on this approximation tend to underestimate CO_2 sinks/sources with progressing time with compensating sources/sinks in the southern hemisphere. We hoped that, given the fast zonal advection (Holton 1987) compared to the slow cross-equatorial transport, the influence functions from HANK and DEHM at the western European stations would be primarily determined by recent regional sources, and not by the inflow of CO_2 at the equator, so that ignoring boundary conditions would cause only a small error. We will see below (Section 6.1) that the resulting error is in fact more severe than expected in terms of inverted fluxes. With a unit source of 1 GtC emitted during 1 month, the influence functions should converge to the asymptotic value of ~0.47 ppm (1 GtC spread evenly into the whole atmosphere). In practice, the two global models were run for 24 months, but the mesoscale models were run for only 3 months for REMO and HANK, and for 4 months for DEHM because of the computing cost. The tail of each influence function from the mesoscale models was therefore extrapolated over 4 years (period chosen for the "quasi-stationary influence functions," see above) using an exponentially decreasing function of time. We discuss below (Section 6.2) the impact of this simplification on the inverted fluxes.

2.5 Prior fluxes and errors

2.5.1 Fossil fuel CO_2 emissions

The fossil fuel CO_2 emissions are assumed to be perfectly known (the associated uncertainty is considered negligible compared to that of the natural fluxes), their influence function being pre-subtracted from the CO_2 concentration data to invert the land and oceanic fluxes as residuals. The same fossil fuel CO_2 emission map of EDGARv3.2 established at $1° \times 1°$ resolution is prescribed to the five models (Olivier and Berdowski 2001), with no temporal variability. The annual fossil fuel CO_2 emissions are rescaled in each country to correspond to the year 1998, using the CDIAC country statistics. This produces a global fossil fuel CO_2 flux to the atmosphere of 6.6 GtC/year and a western Europe flux of 1.2 GtC/year (EU12 countries).

2.5.2 Air–sea exchange

The impact of a global climatological air–sea flux distribution (Takahashi et al. 1997) was pre-subtracted in each model, before inverting for monthly residual fluxes

over each ocean region (see also Gurney et al. 2005). The optimized residual ocean fluxes are given a flat spatial distribution and a zero prior value over each region (accounting for sea–ice coverage). We assigned an uncertainty of 1/12 GtC/month to each ocean flux and use no error correlation which gives 1 GtC/year uncertainty on the annual fluxes (a diagonal variance–covariance matrix is assumed).

2.5.3 Net ecosystem productivity

We used as a prior the global distribution of Net Ecosystem Production (NEP) predicted by the TURC model (Lafont et al. 2002). TURC is a diagnostic model driven by daily climate fields and 10-day mean satellite observations of the Normalized Difference Vegetation Index (NDVI) from the SPOT4 space-borne instrument. NEP is calculated globally at a resolution of $1^\circ \times 1^\circ$ as the difference between photosynthesis (GPP) and ecosystem respiration (TER) using climate input data for year 1998, and NDVI data over the period April 1998–April 1999. The TURC daily results were corrected (1) by subtracting the monthly smoothed TURC seasonal cycle of NEP at each grid point and replacing it by the smoothed seasonal cycle from the SDBM Model (Knorr and Heimann 1995) which is more realistic compared to CO_2 observations, and (2) by adding a diurnal variation of GPP based on solar radiation variations (see Geels et al. 2007 for details). The a priori error on monthly NEP in each land region is assumed to be proportional to the monthly GPP calculated by TURC. A global scaling of NEP error is applied so that the most productive region of the globe has a maximum error of ± 1 GtC/year and the least productive region has a minimum error of 0.3 GtC/year. Monthly NEP errors are derived from annual values, assuming random and independent errors (monthly error = annual error/12). As an example, the prior error for the boreal Eurasia region, is of ± 0.56 GtC/year (one sigma error). As a matter of comparison, Gusti and Jonas in this issue give the value of 0.956 GtC/year for the 90% confidence interval NBP (Net Biome Productivity) uncertainty over Russia.

2.6 Sensitivity tests

In addition to the control inversion described above (referred as CNT), we designed and applied several sensitivity tests to assess how the inversion results for European regional fluxes depend upon various inversion parameters. These sensitivity tests are summarized in Table 2 and discussed in Section 5.

3 Results: annual mean fluxes

We first discuss the differences in regional flux estimates between the five different transport models in the control (CNT) inversion described in Section 2. Although the fluxes are inverted for ten small regions in Europe, we grouped them into a smaller number of regions to discuss the estimated fluxes (see Fig. 1). Following the TRANSCOM3 analysis (Gurney et al. 2005) we define the "within model uncertainty" as the average of the estimated errors from the five inversions, and the "between-model uncertainty" as the standard deviation of the mean flux returned by each inversion. The fit to the data (not shown) was optimal and the posterior normal global normalized $\chi 2$ (twice the cost function at its minimum divided by the number

Table 2 Description of the sensitivity tests (CNT stands for control run)

Test	Spatial discretization	Atmospheric CO_2 uncertainty at European stations[a]	A priori flux error on each European region	Number of site in Europe
Inversion parameter varied	Number of regions solved for in Europe	Multiplier of monthly 1-sigma errors (σ)	Distribution of the errors between regions	Exclude 5 European stations[b]
CNT	11	$\sigma = 1$	Based on GPP	76
SR-HI	20	CNT	CNT	CNT
SR-LO	6	CNT	CNT	CNT
SD-HI	CNT	$\sigma = 2$	CNT	CNT
SD-LO	CNT	$\sigma = 0.5$	CNT	CNT
SP-EQ	CNT	CNT	0.5 GtC/year for each region	CNT
SN-LO	CNT	CNT	CNT	71

[a]We test how model-data mismatch at stations HUN, MHD, CMN, PRS, SCH, and WES might impact the spatial distribution of the estimated fluxes
[b]Stations HUN, CBW, CMN, PAL, WES have been removed so as to have a similar network to that in the Transcom inversion experiment

of observations) was around one for all models showing that the Gaussian hypothesis was coherent. After a brief analysis of large-scale continental fluxes to check the inverse results, we investigate the European fluxes where the regional models show differences (mean annual value, and the seasonal cycle of NEP).

3.1 Large-scale mean annual fluxes

3.1.1 Fluxes in broad latitude bands

First, we discuss the fluxes of the Northern Hemisphere (NH > 20°), Tropical (TROP 20°S–20°N) and Southern Hemisphere (SH < 20°) regions and compare them with previous inversion results (graph not shown). On average for the five inversions, the total CO_2 sink is partitioned about equally between land and ocean (respectively, 1.2 and 1.3 GtC/year). The latitudinal distribution of the fluxes shows (1) a large tropical source (1.0 and 1.2 GtC/year over land and ocean, respectively), and (2) a large northern hemisphere sink (1.9 and 0.9 GtC over land and ocean, respectively). This distribution is in good agreement with the results of other inversions (Gurney et al. 2003, with 13 transport models over 1992–1996; Fan et al. 1998). In Patra et al. (2006) for the period 1999–2001, the tropical sources are, respectively, 0.85 and 0.6 GtC/year for the land and the ocean and the northern hemisphere sinks are, respectively, 1.41 and 1.84 GtC/year for the land and the ocean. Rodenbeck et al. (2003) for the period 1996–1999, solving for fluxes at the TM3 model resolution, obtained a smaller tropical source of 0.3 GtC/year (−0.8 GtC/year on land and 1.1 GtC/year on the ocean) and a northern hemisphere sink of 2.1 GtC/year (0.4 and 1.7 GtC/year for land and ocean, respectively). Note that the tropical land fluxes are poorly constrained in the inversions (very few atmospheric data). In this study the large tropical land source is consistent with the use of atmospheric data during 1998–2001, with the strong 1997/1998 El Nino climate anomaly causing high fire emissions in Southeast

Asia (Page et al. 2002; Van Der Werf et al. 2004) and drought stress over tropical forests.

3.1.2 Northern hemisphere fluxes

Figure 2 compares annual NH fluxes from our five inversions to the estimates of Gurney et al. (2005) (1992–1996, "Transcom") and to the bottom-up C balance synthesis of Janssens et al. (2003) and Pacala et al. (2001) for geographic Europe and North America, respectively. Although the different estimates correspond to different time periods (see legend, Fig. 2), this comparison indicates the major discrepancies of regional carbon balances between the different approaches. Mean fluxes (cross), between-model (1-σ) error (vertical bar) and within model error (1-σ) (diamonds) are shown. Except for boreal North America, all regions are significant carbon sinks, with the highest uptake over temperate Eurasia (0.9 GtC/year) and Temperate North America (0.8 GtC/year). These values are comparable to Gurney et al. (2003) (G letter in Fig. 2), except for the partition of the Eurasian sink between boreal and temperate regions. The use of additional sites in Europe (compared to that study) tends to shift part of the boreal Eurasian carbon uptake to the temperate ecosystems, the total remaining similar to the "Transcom" study. The region boreal Eurasia shows a sink of 0.2 GtC/year. As a matter of comparison, Gusti and Jonas (this issue) find a sink of 0.95 GtC/year (Table 2) for whole of Russia (1988–1992

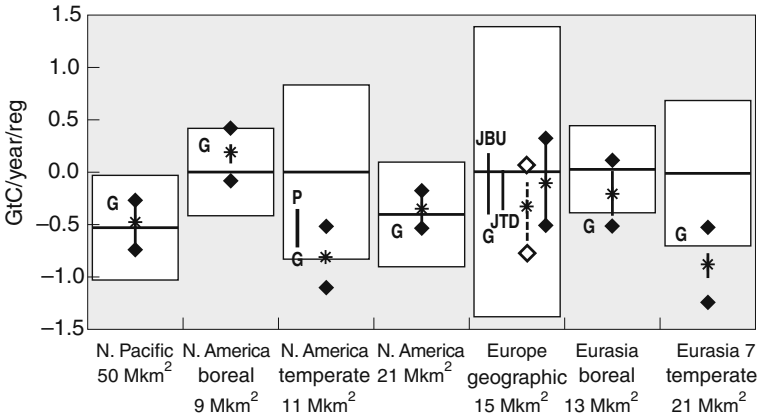

Fig. 2 Mean annual sources and uncertainties for a Northern Hemisphere breakdown. Mean estimated fluxes across models are shown by *crosses* (fossil fuel not included). *Positive values* indicate a source to the atmosphere. The prior flux estimates and their uncertainties are indicated by the *boxes*; the *central horizontal bar* indicates the prior flux estimates, and the *top* and *bottom* of the *box* give the prior flux uncertainty range. The mean estimated uncertainty across all models (the "within model" uncertainty) is indicated by the *diamonds*. The standard deviation of the models' estimated fluxes (the "between model" uncertainty) is indicated by the *vertical bar*. The P range corresponds to results from Pacala et al. (2001) (1980–1989 period); the JBU and JTD range to results from Janssens et al. (2003) (mean inversion results for the period ranging from 1980 to 1998). G letters give mean result from Gurney et al. (2003). For the "Europe Geographic" region, results on the *left* are taking into account only the three models TM3, LMDZ, and REMO; on the *right* are results considering all five models

period) For the North Pacific and North Atlantic oceans, the mean flux estimate remains close to the prior value from Takahashi et al. (1997).

3.2 European continental carbon balance

The carbon balance of the European continent equals -0.1 ± 0.4 GtC/year, with Europe being the sum of a group of regions (South, West, North and Cent in Fig. 1b; 15 million square kilometers) close to geographic Europe. With a denser network of 12 stations over Europe compared to seven stations in Gurney et al. (2003), our continental-scale C balance is closer to the Janssens et al. (2003) bottom-up and top-down estimate (JBU and JTD in Fig. 2) with a small carbon sink. Two European mean inversion flux estimates are shown in Fig. 2, one obtained with the five transport models (mean sink of -0.1 ± 0.4 GtC/year) and the other one with only TM3, LMDZ and REMO models (mean sink of -0.35 ± 0.25 GtC/year). This distinction allows isolation of DEHM and HANK, which were run without any CO_2 incoming flux at their equatorial boundary, a potential source of bias in the estimated European carbon balance (Section 6.1 for further discussion).

The largest between-model error is found over Europe (Fig. 2), as expected, given the distinct regional models influence functions over that region. For all the NH regions, the between-models error is smaller than the within-model error returned by the inverse procedure, as found by Gurney et al. (2005). This result indicates that uncertainties arising from modeled transport differences are smaller than the other sources of inverted flux uncertainty (sparse atmospheric network, observation errors).

3.3 European regional fluxes

Having at hand atmospheric CO_2 data from 12 stations across Europe, we can reanalyze the regional budgets to gain details on the carbon cycle. One must keep in mind that with ten optimized European regions each month, and data from 12 unevenly distributed stations, the inversion problem still remains poorly constrained. Figure 3 shows for each model/region (five regions of Fig. 1b) the estimated flux and its 1-σ error (within model). The continental carbon sink is located mostly in the southern and western regions, each absorbing $\sim 0.5 \pm 0.1$ GtC/year. In contrast, the northern and eastern regions are small sources and the central region is a large source of $\sim 0.68 \pm 0.23$ GtC/year. This regional flux dipole (south-west/north-east) is found through all the transport models (but less pronounced in HANK). The error reduction on the regional fluxes is larger for western and southern Europe (24% of the prior error) than for central and eastern Europe (44% of the prior error). This reflects the lower density of the observing network in the eastern half of the continent. To test whether this flux dipole (south-west versus north-east) is sensitive to the assimilation of CO_2 data from particular stations, we performed a bootstrap analysis where each of the 12 European stations is taken one by one out of the inversion. None of the 12 stations was solely responsible for the inverted flux dipole, suggesting that this regional pattern is not directly controlled by the geometry of the network. This flux dipole may reflect a difference in NEP between southwest and northeast Europe or alternatively be caused by a common bias to all the inversions,

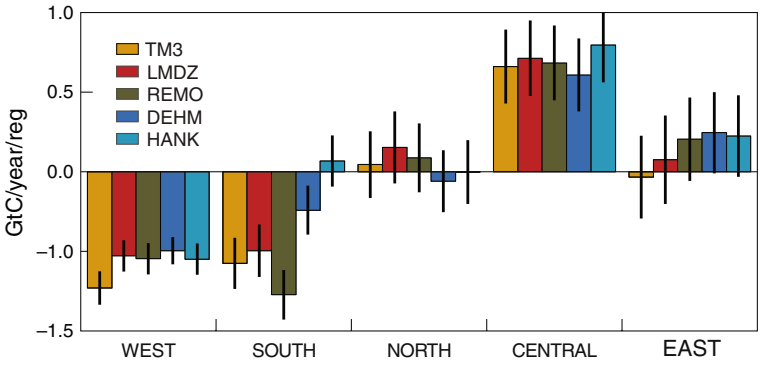

Fig. 3 Net carbon flux and 1σ error (*vertical bar*) estimates for five sub-continental European regions from the five different transport models. See regional map in Fig. 1

linked for instance to the representation of mountain stations, or to a bias in the pre-subtracted fossil fuel emission field (Gurney et al. 2005).

4 Results: seasonal fluxes

4.1 Seasonal cycle of NEP compared to ecosystem models

We now analyze the seasonal cycle of the estimated NEP for the European domain, sum of the regions WEST, SOUTH, NORTH, and CENT in Fig. 1b. Figure 4 compares the monthly seasonal cycle of NEP of the five inversions (five transport models) with independent estimates from four process-based ecosystem models recently compared in the CARBOEUROPE-IP project (Vetter et al. 2007). The four ecosystem models were integrated over the continent using the same simulation protocol, forced by meteorological data from the REMO regional climate model at 25 km spatial resolution and with rising CO_2, over the period 1948–2005. We kept the four models that cover the 1998–2001 period (ORCHIDEE, LPJ, JULES, and BIOME-BGC) out of the even analyzed in Vetter et al. (2007). None of the models include land use change or ecosystem management effects, and only BIOME-BGC has a nitrogen cycle, so that their annual carbon sink cannot be directly compared to the inversion results. These models capture only the land carbon sink because of changing climate and increasing atmospheric CO_2 concentration over time. The NEP range from the four ecosystem models is shown in Fig. 4 as a gray area.

First, we see that the prior NEP from the TURC model (the prior for the inversions) is comparable in amplitude and phase with the results of the four process-based models. In the inversion, the monthly NEP gets corrected toward a larger peak-to-peak amplitude (1.25 times the prior on average), in all transport model cases. The timing of the maximum seasonal uptake is shifted over the continent by 1 month, from June in the prior flux (TURC) toward July in the estimated fluxes. This correction is independent of the transport model and appears to be driven by the phase of the atmospheric CO_2 concentration signal. Comparison with the ecosystem models show that three out of four models present a maximum uptake in May (two months earlier than the inversion NEP). Only the BIOME-BGC model

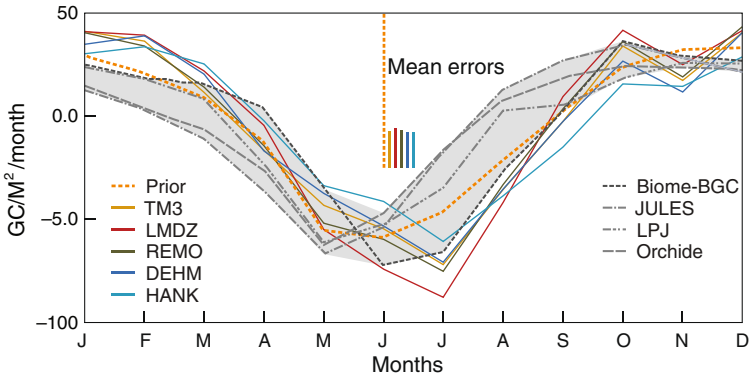

Fig. 4 Mean net monthly fluxes over European regions SOUTH + WEST + CENT + NORTH of Fig. 1 (averaging time period is 1998 to 2001); units are in grams C per square meter per month. The *thick black dotted line* is the prior curve used in the inversions. Results from bottom-up biospheric models (Biome-BGC, JULES, LPJ, Orchidee are represented by a *gray polygon*)

is in agreement with the inversions, showing a broad maximum of uptake between June and July.

The same comparison for the sub-European regions (graphs not shown), reveals similar patterns but with more spread between the inversions and between the ecosystem models. The shift of the maximum uptake in the inverse estimates is observed for all regions.

Further investigations are needed to definitely conclude that the seasonal cycle of NEP is more realistic in the inversions than in the ecosystem models. A possible bias of the inversion derived NEP is the use of a non-seasonal fossil fuel emission flux field (Section 2.1), whereas emissions are in reality higher in winter than in summer in Europe (Vestreng et al. 2005).

This bias would translate into a too-high amplitude of NEP, which may explain, at least partly, why the inversion NEP has a 25% larger amplitude than the ecosystem model NEP in Fig. 4. Other sources of bias for the inversion NEP are linked to error in the transport model and the sparse and uneven network of stations (Fig. 1), which does not allow separation between land and ocean and between land regions.

However, it is unlikely that all the five transport models would bias in the same direction the estimated NEP seasonality by 2 months. Thus, inversions can be seen as a useful verification of ecosystem models. One should note that if the timing of GPP (i.e., the growing season) can be well characterized using global satellite vegetation index data (Turner et al. 2005; Zhou et al. 2001) and used to tune the models, the timing of seasonal respiration is much more loosely constrained (Piao et al. 2007) in ecosystem models, thus adding uncertainty in the phasing of NEP.

4.2 Spatial distribution of summer NEP compared to ecosystem models

We now compare the spatial distribution of the inversion fluxes to that of the ecosystem models, during the peak of the growing season (July). Figure 5 shows, for July, the mean fluxes and standard deviations for the five inverse results and the four ecosystem models. In temperate and northern Europe (above 40° N), the inversions

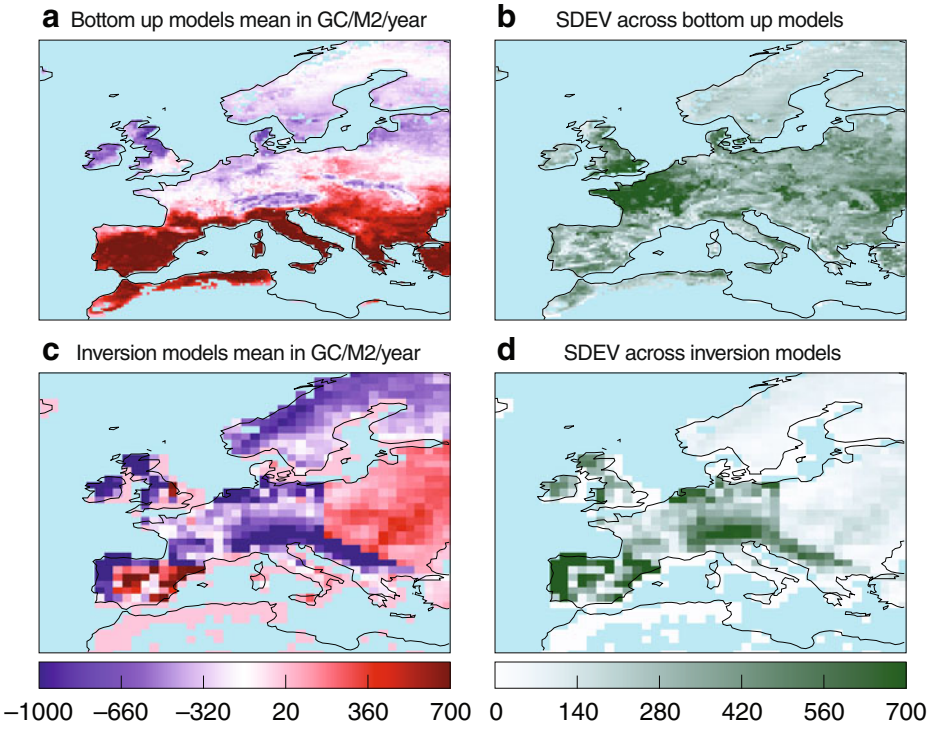

Fig. 5 Spatial distribution for July of the mean fluxes (**a**, **c**) and of the standard deviation (**b**, **d**) across the four ecosystems models results (**a**, **b**) and the five inversions (**c**, **d**)

and ecosystem models estimate a strong carbon uptake, close to 1 kgC/m^2 per year. In the southern part of Europe, around the Mediterranean Basin, the ecosystem models simulate a large carbon release in July (of the order of 0.7 kgC/m^2 per year) while the inversions have a neutral flux or even a small carbon sink. Note that these results are not contradictory to the annual NEE carbon fluxes discussed above, as they only concern the peak of the growing season. If we now consider the standard deviations (SDs), we clearly see that the spread of the four ecosystem models is quite large, especially in the temperate zone where SDs are close to 700 gC/m^2 per year, a value only slightly smaller than the mean uptake over the same region in July. These large SDs indicate that current ecosystem models (including process-based and more diagnostic approaches) still significantly differ in their estimation of NEP from a given climate forcing. The SDs across the five inversions shows on average a smaller spread of the inverse flux estimates except for few locations in western Europe (i.e., north of Spain). However, the fine structures of the inversion SDs (Fig. 5, bottom right plot) are tightly linked to the a priori flux spatial distribution (TURC model in this case, see Section 2.5, Net Ecosystem Productivity). Thus, they cannot be interpreted as a spread induced solely by different atmospheric transport models.

Overall, the inversions tend to estimate a lower carbon loss in southern Europe in July compared to the ecosystem models which explain part of the shift of the maximum uptake period from June to July discuss previously.

5 Sensitivity of European fluxes to inverse setup

We investigate the robustness of the estimated fluxes through the results of the different sensitivity tests described in Section 2.6 (Table 2). Table 3 synthesizes these results with the variations of the annual total European flux (in GtC) between each test and the control case (CNT). The tests have been ranked according to their impact on the inverse solution, from the largest to the smallest (left to right in Table 3) and are discussed in that order below.

Spatial discretization, number of regions The optimal level of spatial discretization for the fluxes is still rather uncertain and tightly linked to the accuracy of prior fluxes and to the number of observations (see Section 2.1). To assess the sensitivity of the results to the number of regions, we performed some inversions with only six regions (SR-LO) and with 20 regions (SR-HI) for Europe compared to 11 in the control case (CNT) (see contours Fig. 1). Changes of the total European sink are small with the ungrouped SR-HI case (∼0.13 GtC/year) but much larger for the SR-LO case (∼0.33 GtC/year) where all models tend to strongly reduce the sink with the LMDz model, even producing a source. This test highlights the importance of prior spatial discretization and the risk of systematic biases with large regions like those involved in the Transcom experiment.

Station network (number of sites) The use of additional European stations from the AEROCARB project is believed to be critical to improving the regional flux estimates. We performed a test without the five European stations (SN-LO, Table 2), keeping only the 71 sites used in the TRANSCOM experiment. As a direct consequence, the errors estimated on the European fluxes are much larger than in the CNT case (+36% on average). The total annual European flux varies by 0.25 GtC/year on average (mean absolute deviation) but with opposing effects between models: a decreased sink for the two global models (0.10 and 0.24 GtC/year for TM3 and LMDZ) and an increased one for the mesoscale models, up to 0.38 GtC/year for REMO. Sub-European flux variations are even more sensitive to the observing network but with no systematic effect between the five models. Increasing the number of station appears to be critical to investigating regional carbon balances.

Observation uncertainty The relative weight of each station in the inversion is critical to partitioning the sources and sinks regionally. Scaling the observation errors for a set of European stations ('HUN', 'MHD', 'CMN', 'PRS', 'SCH', 'WES')

Table 3 Synthesis of sensitivity tests: induced variations on the geographical European flux compared to the control case (absolute difference averaged over the models TM3, LMDZ, REMO, in GtC)

Sensitivity to	Spatial discretization		Number of sites	Uncertainties at stations	Prior flux errors
	SR-LO	SR-HI			
Variation on European flux compared to control case	0.33 (0.40 0.48 0.10)	0.13 (0.13 0.22 0.04)	0.25 (0.1 0.26 0.38)	0.11 (0.13 0.08 0.13)	0.06 (0.06 0.09 0.03)

In parenthesis are the absolute differences for the three individual models TM3, LMDZ, REMO

with a factor of 0.5 (SD-LO test) or 2 (SD-HI test) induce similar flux changes for the different transport models. Total European biospheric sink increases by ~0.1 GtC/year when the errors on the European stations decrease in SD-LO (i.e., a better fit is required at these sites compared to the other northern hemisphere sites) and vice versa in SD-HI.

Prior flux errors We tested a case with the same error for each sub-European region, 0.5 GtC per year evenly spread between months (SP-EQ case) compared to GPP-based error distribution in the CNT inversion (With a minimum of 0.3 GtC/year per region and a maximum of 1 GtC/year per region). Changes in the flux estimates for each model in SP-EQ appear to be smaller on average than the flux differences between models and the total annual European flux variations is only around 0.06 GtC/year (see Table 3).

Overall, the most critical component of the inverse setup that has been tested is the number of independent regions to be resolved. Among the different tests, some choices also tend to have a different impact on the different transport models (like the atmospheric network). Major features like the phase/amplitude of the mean seasonal cycle of the estimated NEP and the mean NEE carbon flux dipole (southwest sink versus northeast source) remain stable across the different tests.

6 Closing remarks

6.1 The use of regional models in an inversion

To use the regional domain models to optimize CO_2 fluxes, one ideally needs to nest them into a "mother" global model, as explained in Section 2.4. For DEHM and HANK hemispheric domain models, we did not implement such a nesting, hoping that neglecting the inflow of CO_2 at the equator would only cause a small error. To check this assumption, we compare the five model concentration time series resulting from the pre-subtracted fossil fuel source at two stations: Mace Head a surface site in Ireland (MHD) and Plateau Rosa a mountain site in Italy (PRS) (Fig. 6). The runs were performed for 3 years with fossil emissions during the first year (6.6 GtC/year) and zero flux the following years. For computational reasons, the DEHM and HANK models were only run for 1 year and the simulated concentrations were further extrapolated over time at each station to the asymptotic value (3.1 ppm equivalent to 6.6 GtC evenly spread in the atmosphere).

Significant concentration differences between DEHM or HANK and the other models appear after around 10 and 6 months of simulations at MHD and PRS, respectively. The differences are larger for the mountain site (PRS) and reach nearly 50% after 1 year. They clearly indicate that the loss of mass at the equatorial boundary has a non-negligible impact after only several months of simulation even at the European stations far from the boundary of the domain. This issue explains a large part of the differences obtained between DEHM or HANK and the other models. The pre-subtracted fossil fuel contribution at the Northern Hemisphere stations was significantly smaller for these two models. The impact is probably smaller for the land and ocean influence functions given that they were extrapolated to the exact asymptotic value after only 3–4 months of simulations. Note that as

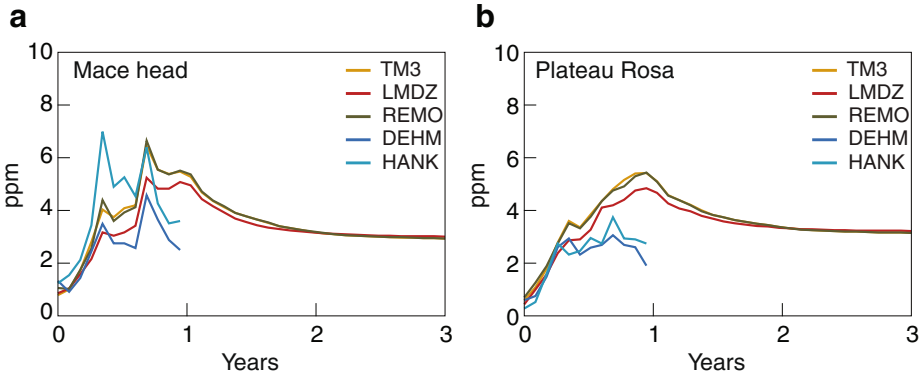

Fig. 6 Values in parts per million of the fossil fuel CO_2 signal at the coastal station MHD (Mace Head in Ireland) on the *left* and the mountain station PRS (Plateau Rosa in Italian Alps) as a function of time shown in years. For computational reason, the mesoscale models DEHM and HANK were only run for 1 year (and extrapolated after that time)

a result, the estimated total northern hemisphere land and ocean carbon uptake is decreased in DEHM and HANK by 0.22 and 0.41 GtC/year, respectively, as compared to the other models.

Note finally that using either TM3 or LMDZ as a global model to complete the influence functions for the mesoscale models (i.e., for stations outside their domain, as explained in Section 2.4), only significantly impact the estimated fluxes outside the mesoscale model domain that is mostly outside of Europe (as all the mesoscale models cover at least whole of Europe). Over Europe, the results are well constrained by the influence functions of the mesoscale models themselves.

6.2 Time-length computation for the "influence function"

The "matrix" formulation used to solve the inverse problem requires to the influence of each source to be computed (i.e., a given region and time step) to the concentration at each station for the whole time period covered by the inversion. In practice, the transport models are usually run for a shorter period so that we need to extrapolate forward in time the model concentrations to the asymptotic value (0.47 ppm for a source of 1 GtC). In this study, we invert for a quasi-stationary state of the NEE carbon fluxes over a 4-year period, while the mesoscale and global models were run only for 3 and 4 months, and 2 years, respectively (see Section 2.4). Different extrapolation procedures have been used:

- A linear extrapolation between the last model concentration and the asymptotic value that is supposed to be reached after a given time step (4 years in our case)
- An exponential fit using the last two model concentrations to estimate the curvature of the exponential function

We tested the impact of these technical choices on the inverse results with the TM3 model. Figure 7 shows, for different sub-European regions, the flux differences between the control case where TM3 is run for 2 years and cases where it is run only 12, 6, or 3 months and then linearly or exponentially extrapolated. On

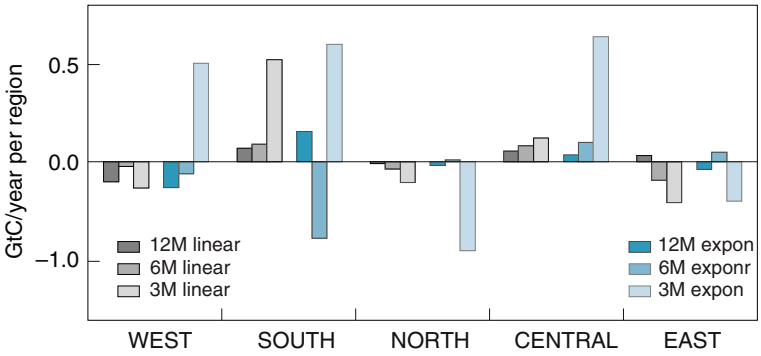

Fig. 7 Annual net fluxes over Europe. Influence of the duration of the computation of the response functions. TM3 result where response functions are truncated after respectively 12, 6, and 3 months are shown subtracted from the reference run where TM3's response function are taken with their full duration. In *dark* (*light*) *gray*, results are shown for a linear (exponential) extrapolation

average, significant biases affect the regional fluxes when the computation length of the influence function is limited to few months only (3 or even 6). For the exponential case, a large bias occurs when the length of the model simulations is restricted to 3 months (compared to the reference), while the results are less affected with the linear extrapolation. The difference between the two approaches probably only reflects the difficulty in defining an exponential curve using two points (the least) far from the asymptotic value. Overall, a 6-month period seems to be a minimum to avoid potential biases in the flux estimates, with 12 months being a preferred value. In this study, the impact of using only 3 and 4 months for the REMO/DEHM and HANK, is probably limited, given of our choice of a linear extrapolation scheme. This result is in line with Bruhwiler et al. (2005) where using a very different inversion technique ("improved Kalman Smoother") it is concluded that this technique shows "excellent agreement with the standard Bayesian synthesis batch technique by retaining transport information in the basic functions for as little as 6 months."

7 Conclusions

In this study, we use both global (LMDZ, TM3) and mesoscale models (REMO, HANK, DEHM) to perform a CO_2 monthly inversion for the years 1998–2001. A special focus is given to sub-continental regions of Europe as a first attempt given the high density of CO_2 concentration measurements in this region (nine sites, part of the AEROCARB and CARBOEUROPE network). The carbon balance of the European continent equals -0.1 ± 0.4 GtC/year, with Europe being the sum of a group of regions (South, West, North and Cent in Fig. 1b; 15 M km^2). With a denser network of 12 stations over Europe compared to seven stations in Gurney et al. (2003), our continental-scale C balance is closer to the Janssens et al. (2003) bottom-up and top-down estimate (JBU and JTD in Fig. 2) with a small carbon sink. Two European mean inversion flux estimates are shown in Fig. 2, one obtained with the five transport models (mean sink of −0.1 GtC/year) and the other one with only TM3,

LMDZ and REMO models (mean sink of −0.35 GtC/year). This distinction allows isolation of DEHM and HANK, which were run without any CO_2 incoming flux at their equatorial boundary, a potential source of bias in the estimated European carbon balance (Section 6.1 for further discussion). With only three models, the European carbon sink increases from 0.1 to 0.35 GtC/year.

The continental carbon sink is located mostly in the southern and western regions, each absorbing ∼0.5 ± 0.1 GtC/year. In contrast, the northern and eastern regions are small sources and the central region is a large source of ∼0.68 ± 0.23 GtC/year. This regional flux dipole (South-West/North-East) is found through all the transport models (but less pronounced in HANK). The error reduction on the regional fluxes is larger for western and southern Europe (24% of the prior error) than for central and eastern Europe (44% of the prior error). This reflects the lower density of the observing network in the eastern half of the continent. To test whether this flux dipole (south-west versus north-east) is sensitive to the assimilation of CO_2 data from particular stations, we performed a bootstrap analysis where each of the 12 European stations is taken one by one out of the inversion. None of the 12 stations was solely responsible for the inverted flux dipole suggesting that this regional pattern is not directly controlled by the geometry of the network. This flux dipole may reflect a difference in NEP between south-west and north-east Europe or alternatively be caused by a common bias to all the inversions, linked for instance to the representation of mountain stations or to a bias in the pre-subtracted fossil fuel emission field (Gurney et al. 2005).

Over Europe the spread of results between the different models is rather large (i.e., around 65% of the mean posterior error for yearly totals). Optimized monthly fluxes show a maximum uptake over Europe that is shifted by 1 month compared to the prior TURC model (from June to July). This correction is robust across all transport models and seems to be driven by the atmospheric data. It could be viewed as a crucial new independent source of information to validate or falsify ecosystem model results.

In this paper we also attempt to compare our regional European flux estimates to other "independent" approaches, such as bottom-up results. A major source of error in the inversion process arises from systematic biases in the atmospheric transport. However, when considering intra-annual flux variations, theses biases might cancel out, leading to more accurate flux variation estimates (see timing of the maximum biosphere uptake in Section 4.1). Improving model transport and increasing the network density should help to overcome the current inversion limitations.

Important methodological results have also been derived from this study. To perform the inversion with the limited domain models, we used a global model (1) to account for the lateral mass fluxes at the limit of their domain (done for REMO) and (2) to complete the set influence functions at all stations. Correctly addressing the boundary conditions of mesoscale models, even if these are hemispherical, appeared to be important to properly simulate CO_2 concentration variations at European stations (especially high-altitude stations). We also showed that a minimum period of 6 months is required for the computation of the influence functions, before any interpolation, in order to obtain robust results. However a period of 12 months is preferred.

Finally, for the first time, mesoscale models with limited domains have been used to estimate monthly mean surface CO_2 fluxes (mean over 1998–2001) and compared

with estimates using conventional global models. Geels et al. (2007) have shown the potential of mesoscale models to better represent concentrations at European continental sites. In this study, we do not obtain systematic differences between the mesoscale and global models flux estimates for Europe. However, the simplification of the boundary condition treatment for the two mesoscale models (DEHM and HANK) raises some caution about any quantitative interpretation of the benefit of mesoscale model in an inverse mode. Further investigations in that direction are required.

Acknowledgements We acknowledge participants of the AEROCARB project and especially all the experimentalists that contributed to the high precision measurements used in this paper. We also acknowledge P. Hess for his help in running the HANK model.

References

Baker DF et al (2001) Sources and sinks of atmospheric CO_2 estimated from batch least-squares inversions of CO_2 concentration measurements. PhD dissertation, Princeton University, NJ

Bocquet M (2005) Grid resolution dependence in the reconstruction of an atmospheric tracer source. Nonlinear Process Geophys 12:219–234

Bousquet P, Peylin P, Ciais P, Le Quere C, Friedlingstein P, Tans P (2000) Regional changes in carbon dioxide fluxes of land and oceans since 1980. Science 290:1342–1346

Bruhwiler LMP, Michalak AM, Peters W, Baker D, Tans P (2005) An improved Kalman Smoother for atmospheric inversions. Atmos Chem Phys 5:2691–2702

Carouge C, Bousquet P, Peylin P, Rayner P, Ciais P (2008) What can we learn from European continuous atmospheric CO_2 measurements to quantify regional fluxes, part 1: potential of the network. ACPD 8(5):18591–18620

Chevillard A, Karstens U, Ciais P, Lafont S, Heimann M (2002) Simulation of atmospheric CO_2 over Europe and western Siberia using the regional scale model REMO. Tellus B 54:872–894

Christensen JH (1997) The Danish Eulerian hemispheric model—a three-dimensional air pollution model used for the arctic. Atmos Environ 31:4169–4191

Enting I (2002) Inverse problems in atmospheric constituent transport. Cambridge University Press, Cambridge

Fan S, Gloor M, Mahlman J, Pacala S, Sarmiento J et al (1998) A large terrestrial carbon sink in North America implied by atmospheric and oceanic CO_2 data and models. Science 282:442–446

Frohn LM, Christensen JH, Brandt J (2002) Development of a high resolution nested air pollution model—the numerical approach. J Comput Phys 179(1):68–94

Geels C, Gloor M, Ciais P, Bousquet P, Peylin P, Vermeulen AT, Dargaville R, Aalto T, Brandt J, Christensen JH, Frohn LM, Haszpra L, Karstens U, Rödenbeck C, Ramonet M, Carboni G, Santaguida R (2007) Comparing atmospheric transport models for future regional inversions over Europe—part 1: mapping the atmospheric CO_2 signals. Atmos Chem Phys 7:3461–3479

Gerbig C, Lin JC, Wofsy SC, Daube BC, Andrews AE, Stephens BB, Bakwin PS, Grainger CA (2003) Toward constraining regional-scale fluxes of $CO_2$with atmospheric observations over a continent: 1. Observed spatial variability from airborne platforms. J Geophys Res 108(D24):4756. doi:10.1029/2002JD003018

GLOBALVIEW-CO_2 (Cooperative Atmospheric Data Integration Project—Carbon Dioxide) (2005) CD-ROM, NOAA CMDL, Boulder, Colorado. Available online via anonymous FTP to ftp.cmdl.noaa.gov, Path: ccg/CO2/GLOBALVIEW

Gloor M, Fan S, Sarmiento J, Pacala S (1999) A model-based evaluation of inversions of atmospheric transport, using annual mean mixing ratios, as a tool to monitor fluxes of nonreactive trace substances like CO_2 on a continental scale. J Geophys Res 14:245–260

Grell GA, Dudhia J, Stauffer DR (1995) A description of the fifth-generation Penn State/NCAR mesoscale model (MM5) NCAR/TN-398+STR. NCAR Technical Note, Mesoscale and Microscale Meteorology Division. National Center for Atmospheric Research, Boulder, p 122

Gurney K et al (2003) TransCom 3 CO_2 inversion intercomparison: 1. Annual mean control results and sensitivity to transport and prior flux information. Tellus 55B:555–579

Gurney KR, Chen YH, Maki T, Kawa SR, Andrews A, Zhu Z (2005) Sensitivity of atmospheric CO_2 inversion to seasonal and interannual variations in fossil fuel emissions. J Geophys Res 110(D10):10308–10321

Heimann M (1996) The global atmospheric transport model TM2. Tech Rep 10, Max-Planck-Institut für Meteorologie, Hamburg, Germany

Hess PG, Flocke S, Lamarque J-F, Barth MC, Madronich S (2000) Episodic modeling of the chemical structure of the troposphere as revealed during the spring MLOPEX intensive. J Geophys Res 105(D22):26809–26839

Holton JR (1987) Issues in atmospheric and oceanic modeling. Dyn Atmos Ocean 11:204–206 (review)

Holton JR (1992) An introduction to dynamic meteorology, 3rd edn. Academic, New York

Janssens IA et al (2003) Europe's terrestral biosphere absorbs 7 to 12% of European anthropogenic CO_2 emissions. Science 300:1538–1541

Kaminski T, Heimann M, Giering R (1999) A coarse grid three dimensional global inverse model of the atmospheric transport 1. Adjoint model and Jacobian matrix. J Geophys Res 104:18535–18553

Kaminski T, Rayner PJ, Heimann M, Enting IG (2001) On aggregation errors in atmospheric transport inversions. J Geophys Res 106(D5):4703–4715

Knorr W, Heimann M (1995) Impact of drought stress and other factors on seasonal land biosphere CO_2 exchange studied through an atmospheric tracer transport model. Tellus 47B:471–489

Lafont S, Kergoat L, Dedieu G, Chevillard A, Karstens U, Kolle O (2002) Spatial and temporal variability of land CO_2 fluxes estimated with remote sensing and analysis data over western Eurasia. Tellus 54B:820–833, 3719

Lauvaux T, Uliasz M, Sarrat C, Chevallier F, Bousquet P, Lac C, Davis KJ, Ciais P, Denning AS, Rayner P (2007) Mesoscale inversion: first results from the CERES campaign with synthetic Data. Atmos Chem Phys Discuss 7:10439–10465. SRef-ID: 1680-7375/acpd/2007-7-10439

Law RM et al (1996) Variations in modelled atmospheric transport of carbon dioxide and the consequences for CO_2 inversions. Glob Biogeochem Cycles 10:783–796

Law RM et al (2008) TransCom model simulations of hourly atmospheric CO_2: experimental overview and diurnal cycle results for 2002. Glob Biogeochem Cycles 22:GB3009. doi:10.1029/2007GB003050

Majewski D (1991) The Europa-Modell of the Deutscher Wetterdienst. In: Seminar proceedings ECMWF, ECMWF Shinfield Park, Reading, Berks, United Kingdom, vol 2, pp 147–191

Olivier JGJ, Berdowski JJM (2001) Global emissions sources and sinks. In: Berdowski J, Guicherit R, Heij BJ (eds) The climate system. A.A. Balkema/Swets & Zeitlinger, Lisse, pp 33–78. ISBN 90 5809 255 0

Pacala SW, Hurtt GC, Baker D, Peylin P, Houghton RA, Birdsey RA, Heath L, Sundquist ET, Stallard RF, Ciais P, Moorcroft P, Caspersen JP, Shevliakova E, Moore B, Kohlmaier G, Holland E, Gloor M, Harmon ME, Fan SM, Sarmiento JL, Goodale CL, Schimel D, Field CB (2001) Consistent land- and atmosphere-based US carbon sink estimates. Science 292:2316–2320

Page SE et al (2002) The amount of carbon released from peat and forest fires in Indonesia during 1997. Nature 420:61–65

Patra PK et al (2006) Sensitivity of inverse estimation of annual mean CO_2 sources and sinks to ocean-only sites versus all-sites observational networks. Geophys Res Lett 33:L05814. doi:10.1029/2005GL025403

Peters W et al (2007) An atmospheric perspective on North American carbon dioxide exchange: carbontracker. Proc Natl Acad Sci 104:18925–18930

Peylin P, Bousquet P, Ciais P (2001) Inverse modeling of atmospheric carbon dioxide fluxes—response. Science 294(5550):2292–2292

Peylin P, Rayner P, Bousquet P, Carouge C, Hourdin F, Heinrich P, Ciais P, AEROCARB contributors (2005) Daily CO_2 flux over Europe from continuous atmospheric measurements: 1, inverse methodology. Atmos Chem Phys 5:3173–3186. ISI:000233610300001

Piao SL, Ciais P, Friedlingstein P, Peylin P, Reichstein M, Luyssaert S, Margolis H, Fang JY, Barr L, Chen AP, Grelle A, Hollinger D, Laurila T, Lindroth A, Richardson AD, Vesala (2007) Net carbon dioxide losses of northern ecosystems in response to autumn warming. Nature 451:49–52. doi:10.1038/nature06444

Rodenbeck C, Houweling S, Gloor M, Heimann M (2003) CO_2 flux history 1982–200. Inferred from atmospheric data using a global inversion of atmospheric transport. Atmos Chem Phys 3:2575–2659

Sadourny R, Laval K (1984) January and July performance of the LMD general circulation model. In: Berger A, Nicolis C (eds) New perspectives in climate modeling. Elsevier, New York, pp 173–197

Takahashi T, Feely RA, Weiss R, Wanninkhof RH, Chipman DW, Sutherland SC, Takahashi TT (1997) Global air–sea flux of CO_2: an estimate based on measurements of sea–air pCO_2 difference. Proc Natl Acad Sci 94:8292–8299

Tarantola A (1987) Inverse problem theory. Elsevier, Amsterdam

Turner DP et al (2005) Site-level evaluation of satellite-based global terrestrial GPP and NPP monitoring. Glob Chang Biol 11:666–684

Van Der Werf GR et al (2004) Continental-scale partitioning of fire emissions during the 1997 to 2001 El Nino/La Nina period. Science 303(5654):73–76

Vestreng V, Breivik K, Adams M, Wagener A, Goodwin J, Rozovskkaya O, Pacyna JM (2005) Inventory review 2005, emission data reported to LRTAP Convention and NEC Directive, Initial review of HMs and POPs, MSC-W 1/2005 ISSN 0804-2446, EMEP

Vetter M, Churkina G, Jung M, Reichstein M, Zaehle S, Bondeau A, Chen Y, Ciai P, Feser F, Freibauer A, Geyer R, Jones C, Papale D, Tenhunen J, Tomelleri E, Trusilova K, Viovy N, Heimann M (2007) Analyzing the causes and spatial pattern of the European 2003 carbon flux anomaly in Europe using seven models. Biogeosciences 5:561–583

Zhou LM, Tucker CJ, Kaufmann RK, Slayback D, Shabanov NV, Myneni RB (2001) Variations in northern vegetation activity inferred from satellite data of vegetation index during 1981 to 1999. J Geophys Res (Atmospheres) 106:20069–20083

Zupanski D, Denning AS, Uliasz M, Zupanski M, Schuh AE, Rayner PJ, Peters W, Corbin KD (2007) Carbon flux bias estimation employing Maximum Likelihood Ensemble Filter (MLEF). J Geophys Res 112:D17107. doi:10.1029/2006JD008371 12 September 2007

Climatic Change (2010) 103:117–136
DOI 10.1007/s10584-010-9920-8

Remotely sensed soil moisture integration in an ecosystem carbon flux model. The spatial implication

Willem W. Verstraeten · Frank Veroustraete · Wolfgang Wagner · Tom Van Roey · Walter Heyns · Sara Verbeiren · Jan Feyen

Received: 5 January 2009 / Accepted: 15 June 2010 / Published online: 22 July 2010

Abstract While remote sensing is able to provide spatially explicit datasets at regional to global scales, extensive application to date has been found only in the reporting and verification of ecosystem carbon fluxes under the Kyoto Protocol. One of the problems is that new remote sensing datasets can be used only with models or data assimilation schemes adapted to include a data input interface dedicated to the type and format of these remote sensing datasets. In this study, soil water index data (SWI), derived from the ERS scatterometer (10-daily time period with a spatial resolution of 50 km), are integrated into the ecosystem carbon balance model C-Fix to assess 10-daily Net Ecosystem Productivity (NEP) patterns of Europe from the remote sensing perspective on an approximate 1-by-1 km^2 pixel scale using NDVI-AVHRR data. The modeling performance of NEP obtained with and without the assimilation of remotely sensed soil moisture data in the carbon flux model

W. W. Verstraeten (✉)
Geomatics Engineering, Katholieke Universiteit Leuven (K.U. Leuven),
W. de Croylaan 34, 3001 Heverlee, Flanders
e-mail: willem.verstraeten@biw.kuleuven.be

F. Veroustraete · T. Van Roey · W. Heyns · S. Verbeiren
Flemish Institute for Technological Research (VITO),
Boeretang 200, 2400 Mol, Flanders

W. Wagner
Institute of Photogrammetry and Remote Sensing,
Vienna University of Technology (T.U. Wien),
Gusshausstrasse 27–29, 1040 Vienna, Austria

J. Feyen
Laboratory for Soil and Water Management,
Katholieke Universiteit Leuven (K.U. Leuven),
Celestijnenlaan 200E, 3001 Heverlee, Flanders

C-Fix is evaluated with EUROFLUX data. Results show a general decrease of the RRMSE of up to 11 with an average of 3.46. C-Fix is applied at the European scale to demonstrate the potential of this ecosystem carbon flux model, based on remote sensing inputs. More specifically, the strong impact of soil moisture on the European carbon balance in the context of the Kyoto Protocol (anthropogenic carbon emissions) is indicated at the country level. Results suggest that several European countries shift from being a carbon sink (i.e., NEP > 1) to being a carbon source (i.e., NEP < 0) whether or not short-term water availability (i.e., soil moisture) is considered in C-Fix NEP estimations.

1 Introduction

The measurement of carbon stocks in soils and vegetation as a method of reporting and verifying greenhouse gas emissions and carbon removals is a challenging task, and moreover is subject to high uncertainties. Nilsson et al. (2001) expressed their concern that the high uncertainties in the estimation of greenhouse gas removals in the forestry and agricultural sectors veil the emission reduction efforts to which the signatory countries of the Kyoto Protocol have committed themselves.

Since the early stages of Kyoto Protocol implementation, remote sensing has been considered as an important method of providing basic input data to establish inventories and to quantify ecosystem carbon fluxes. However, though remote sensing enables the provision of regional to global scale datasets, it cannot yet be considered operational in more than a handful of applications related to the Kyoto Protocol (Rosenqvist et al. 2003). This is expressed in the *Good Practice Guidance for Land Use, Land Use Change and Forestry* report, adopted by the Intergovernmental Panel on Climate Change (IPCC) (Penman et al. 2003). This report repeatedly points out the potential of remote sensing to help the signatory parties fulfil their inventory requirements. However, it provides neither concrete advice on how to use remote sensing nor incentives for doing so (Wagner et al. 2005).

There are many reasons, including technological and economic ones, for the slow implementation of remote sensing methodology for inventory and verification objectives of greenhouse gas emissions and removals by the forestry and agricultural sectors. From the methodological point of view, a major problem area is the fact that assimilation of remotely sensed geophysical products (land cover, forest biomass, soil moisture, etc.) into carbon models, is a complex process. Typically, it is not sufficient to simply exchange conventional input data for their remotely sensed counterparts. Rather, it is necessary to develop new models and data assimilation systems.

Spaceborne soil moisture data became available only quite recently (Wagner et al. 2007). They are expected to shed light on the coupling between carbon assimilation and water availability. In this paper, an integrated approach to estimating ecosystem carbon fluxes based on remotely sensed soil moisture data assimilation across Europe is presented. The impact of 10-daily soil moisture data assimilation derived from the ERS scatterometer with a spatial resolution of 50 km in the ecosystem carbon balance model C-Fix (Veroustraete et al. 2002; Verstraeten et al. 2006b) is evaluated based on EUROFLUX data (Valentini et al. 2000) sampled at the local spatial scale. The potential of soil moisture data provision and integration in remote sensing ecosystem carbon models at the European scale is demonstrated with a resolution of

1.1 km^2, as NOAA-AVHRR data were used. The demonstration was performed by running C-Fix with and without soil moisture data input and by an assessment of the carbon exchange output data of the model. The two moisture input scenarios were compared with anthropogenic carbon emissions at national levels, thereby assessing the impact of soil moisture in the context of the Kyoto Protocol implementation procedure. Finally, our results are discussed within the framework of the workshop on Uncertainty in Greenhouse Gas Inventories (IIASS 2007).

2 Assessing ecosystem carbon fluxes using satellite data

The carbon balance of a terrestrial ecosystem is determined by the difference in carbon uptake and release or the ecosystem carbon fluxes—Gross Primary Productivity (GPP), Net Primary Productivity (NPP) considering autotrophic respiration (A_d), both above and below the surface, heterotrophic respiration (R_h), and Net Ecosystem Productivity (NEP). Total ecosystem carbon release is denominated as ecosystem respiration (ER). According to Valentini et al. (2000), ecosystem respiration varies with latitude and is the strongest component of the European net carbon balance. Grace and Rayment (2000) suggest that in moist soils, microbial flora adapts to low temperature regimes and therefore remains active over long periods during the growing season as long as soil moisture content does not constrain soil organic matter decomposition. Ciais et al. (2005) show that pronounced soil moisture deficits counteract the effect of high temperatures by a reduction of soil respiration (SR). Clearly, carbon uptake is significantly driven not only by plant water availability, but also by drivers like solar radiation, ambient temperature, and nutrients. To put it another way, it is the (differential) sensitivity of ecosystem processes to temperature and moisture that makes certain components of the carbon balance more or less important. Despite this, global carbon budget, analysis is often limited to studies of temperature effects only (Nemani et al. 2002).

The spatial dimension of soil moisture impacts on carbon uptake and release can be assessed, for instance, by the application of the production efficiency model C-Fix. This model has been applied earlier to simulate carbon mass fluxes on a daily basis from local (Veroustraete et al. 2004; Verstraeten et al. 2006b), through regional (Veroustraete et al. 2002; Chhabra and Dhadwall 2004; Lu et al. 2005) to global scales. The temporal evolution of the absorption efficiency of photosynthetically active radiation is directly inferred from spaceborne observations of the Normalized Difference Vegetation Index (NDVI), which allows the fraction of Absorbed Photosynthetically Active Radiation ($fAPAR$) data and radiation use efficiency (RUE) to be estimated. RUE is the integrated efficiency of the photosynthetic metabolism which converts radiation into assimilated carbon (or dry matter). Using the CLC2000 land cover map of Bartholomé and Belward (2005), RUE is stratified, that is, it produces a spatially explicit RUE database by assigning RUE values to different vegetation type classes. If NDVI data is used only to estimate $fAPAR$ without soil moisture data, long-term water limitation is taken into account when ecosystem carbon fluxes are estimated. As the NDVI refers to vegetation greenness and indirectly to leaf chlorophyll content, and as chlorophyll metabolism depends on long-term plant water availability, only pronounced drought periods will affect chlorophyll metabolism. Pronounced droughts may cause the degradation of chlorophyll and

hence there is a decrease in the greenness (and hence the NDVI and $fAPAR$) of a vegetation cover.

We define this scenario as the partially water limited (PWL) scenario applied to C-Fix in contrast to the fully water limited (FWL) scenario where short-term water limitations are considered directly. Short-term water limitation cannot be observed from vegetation greenness. Thus, other ecosystems attributes have to be determined to meet the requirements for the estimation of short-term water limitation.

Daily net ecosystem productivity (NEP) is estimated based on estimates of daily gross primary productivity (GPP). This is formalized by subtracting autotrophic respiration as well as soil respiration from photosynthesis (Maisongrande et al. 1995). Quite importantly, short-term soil moisture limitation of carbon uptake and release by ecosystems in the C-Fix approach is accounted for at the levels of photosynthesis (evapotranspiration) and soil respiration (Verstraeten et al. 2006b):

1. Here RUE depends on water limitation. At the GPP level, water limitation of photosynthesis by evapotranspiration is a prime determinant.
2. Moreover, soil moisture content affects the growth of soil micro-fauna and flora and thus the magnitude of soil respiration.

Changes in water availability for plant transpiration and hence photosynthesis:

1. Are due to water and CO_2 fluxes controlling stomatal closure. Increasing soil moisture deficits cause stomata to close, thereby inducing a reduction in the rate of photosynthesis. In C-Fix soil moisture deficit is formalized with a stomatal regulating factor F_s (Eq. 4) which is controlled by soil moisture availability.
2. Are influenced by soil aeration, an important limiting factor for the oxidative processes of soil respiration. Soil aeration is in turn also related to soil water content. In C-Fix this is formalized with a soil aeration stress factor (SAS) (Eq. 5).

Finally, daily net ecosystem productivity (NEP) (gC m^{-2} day^{-1}) is estimated as:

$$NEP_d = \left(1 - \xi \cdot A_d(T_c)\right) \cdot GPP_d - \check{S}\left[SRF.R_h(T_s) + ((1-\xi) \cdot A_d(T_c)) \cdot GPP_d\right] \tag{1}$$

$$GPP_d = p(T_c) \cdot CO_{2,\,fert} \cdot RUE_{wl} \cdot fAPAR \cdot c \cdot S_{g,d} \tag{2}$$

$$fAPAR = a \cdot NDVI_{toc} + b \tag{3}$$

$$RUE_{wl} = \left[RUE_{\min} + (F_s) \cdot (RUE_{\max} - RUE_{\min})\right] \tag{4}$$

$$\begin{aligned} SAS &= 1 - (\theta_{sat} - \theta).(\theta_{sat} - \theta_{crit})^{-1},\ \theta > \theta_{crit} \\ SAS &= 0, \qquad \theta \le \theta_{crit} \end{aligned} \tag{5}$$

$$SSS = BDF \cdot \sin\left[(\theta - \theta_{wp}) \cdot \left(\theta_{fc} - \theta_{wp}\right)^{-1}\right] \tag{6}$$

$$SRF = \left[SR_{\min} + (1 - SAS) \cdot (SSS) \cdot \left(SR_{\max} - SR_{\min}\right)\right] \tag{7}$$

In Eqs. 1–7:

NEP_d	is daily net ecosystem productivity [g C m^{-2} day^{-1}];
GPP_d	is daily gross primary productivity [g C m^{-2} day^{-1}];
ξ	is an allometric factor dividing autotrophic carbon release in above-ground (leaves) and below-ground (roots) components [−];
A_d	is the autotrophic respiratory fraction (Goward and Dye 1987) [−];
T_c and T_s	are canopy and soil temperature respectively [°C];
$p(T_c)$	is a normalized temperature dependency factor {0:1} [−] (Veroustraete et al. 1994);
CO_{2fert}	is a normalized CO_2 fertilization factor (Veroustraete et al. 1994);
RUE_{WL}	is RUE with water limitation taken into account (Verstraeten et al. 2006b) [gC MJ(APAR)$^{-1}$];
RUE_{min} and RUE_{max}	are minimum and maximum RUE [gC.MJ(APAR)$^{-1}$];
fAPAR	is the fraction of absorbed PAR {0:1} [−], a and b are regression coefficients;
$NDVI_{toc}$	is the NDVI at the top of canopy {−1:1} [−];
$S_{g,d}$	is daily incoming global solar radiation [MJ m^{-2} day^{-1}];
c	is climatic efficiency equaling 0.48 (McCree 1972) [−];
R_h	is heterotrophic respiration (Veroustraete et al. 2004) [gC m^{-2} day^{-1}];
F_s	is a stomatal regulating factor controlled by soil moisture availability [−];
SAS	is soil aeration stress depending on soil moisture content [−];
θ_{sat}	is the volumetric moisture content at saturation point [m^3 m^{-3}];
θ_{crit}	is the volumetric moisture content at a critical point [m^3 m^{-3}];
SSS	is a soil strength stress depending on soil moisture content [−];
BDF	is a bulk density factor [−];
θ_{wp}	is the volumetric moisture content at wilting point [m^3 m^{-3}];
θ_{fc}	is the volumetric moisture content at field capacity[m^3 m^{-3}];
SRF	is a soil stress respiration factor [−]; SR_{max} and SR_{min} are minimum and maximum soil respiration factors (between 0 and 1) [−];

Figure 1 schematically illustrates the involved inputs, the remote sensing contribution, and where soil moisture is assimilated into the C-Fix model. A detailed description of the C-Fix model can be found in Verstraeten et al. (2006b).

The C-Fix model was actually developed to accommodate the spatial heterogeneity of fully water limited (FWL scenario) ecosystem-related carbon fluxes from regional to continental scales (Verstraeten et al. 2006b). However, C-Fix is not a SVAT model and is developed neither to accommodate the multi-temporal detail offered by deterministic stand scale carbon models, nor to offer prognostic capability.

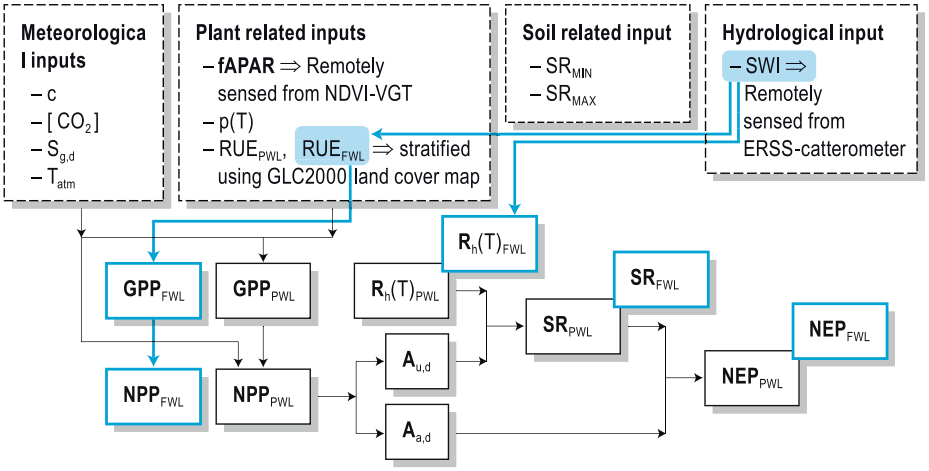

Fig. 1 Meteorological and climatic, vegetation-related and hydrological inputs and process sequences to assess net ecosystem productivity (NEP) from gross primary productivity (GPP), net primary productivity (NPP), and soil respiration (SR). Distinction is made between Partially Water Limited (PWL) and Full Water Limited (FWL) model modes and how soil moisture is involved in the different carbon fluxes, as indicated by the *blue lines*. The equations involved are Eqs. 1–7. Remote sensing-based data are marked. *fAPAR*: fraction of absorbed photosynthetic active radiation; *p(T)*: normalized temperature dependency factor; *RUE*: radiation use efficiency; *c*: climatic efficiency; *[CO_2]*: normalized CO_2 fertilization factor; $S_{g,d}$: daily incoming Global Solar Radiation; A_d: autotrophic respiratory fraction ($A_{u,d}$: underground; $A_{a,d}$: above); R_h: heterotrophic respiration; *SWI*: soil water index; *GPP*: gross primary productivity; *SR*: soil respiration; *NEP*: net ecosystem productivity

Nor does it contain a formalization of the decomposition mechanisms of soil organic matter.

3 Datasets: soil water index, *f*APAR, meteorology, anthropogenic carbon emissions, and EUROFLUX

To analyze the effect of partial and full water limitation on spatially explicit NEP for Europe, C-Fix was used to calculate NEP for the year 1997 with and without the assimilation of ERS scatterometer-derived soil moisture profile data (10-daily Soil Water Index, SWI) in C-Fix. SWI data for Europe were retrieved from ERS scatterometer observations based on the work of Wagner et al. (1999). The ERS scatterometer is an active microwave sensor operating at a frequency of 5.3 GHz (C-band) with a spatial resolution of 50 km. Radar waves penetrate only a few centimeters into the soil, which means that only information about soil moisture in the soil surface layer (2–5 cm) is collected. However, because of the frequent temporal coverage of the ERS scatterometer, the temporal evolution of the surface wetness conditions is known, which allows for soil moisture content estimation (Ceballos et al. 2005). Validation studies over different climatic regions have shown that soil moisture retrieval errors range from 0.03 to 0.06 m^3 m^{-3} (Ceballos et al. 2005; Pellarin et al. 2006; Verstraeten et al. 2006a; Wagner et al. 1999, 2003)

indicating a 15–20% relative error depending on the average SMC in time. Other data sets on water availability can also be used (Verstraeten et al. 2008a).

In addition to spaceborne retrieved soil water content, NOAA-AVHRR Normalized Difference Vegetation Index (NDVI) observations were used to estimate fAPAR according to the NDVI-fAPAR relationship established by Myneni and Williams (1994).

Meteorological data originate from the World Meteorological Organization (Veroustraete et al. 2002), and anthropogenic carbon emission data from the UNFCC (2005) report.

EUROFLUX datasets (Valentini et al. 2000; Wilson et al. 2002a, b; Dolman et al. 1998, 2003) acquired in 1998 at nine network sites (see also Table 1) were used as an independent validation dataset of the C-Fix model. Fortunately, in situ soil moisture data for 1998 were made available by the University of Tuscia (except for the NL1 site made available by Wageningen University and the BE2 site obtained from Verstraeten et al. 2005).

4 Improvement of NEP estimation based on the integration of SWI data in C-Fix. Evaluation at the EUROFLUX sites

To evaluate the improvement in NEP assessment when SWI time series are assimilated in C-Fix, NEP estimates based on the two water limitation scenarios are compared with EUROFLUX measurements. The first scenario is the partially water limited (PWL) case, where only long-term water limitations are taken into consideration by using fAPAR only. The second model scenario is the fully water limited (FWL) case where short-term water limitation is accounted for by integration of remotely sensed SWI data into C-Fix.

A multi-statistic performance test was applied for this purpose (Table 1). Hence, different statistics were used, eliciting different characteristics of modeled and measured datasets (Chow et al. 1993). Apart from the linear correlation coefficient (R^2), the slope (ideally equal to one) and intercept (ideally equal to zero) of modeled versus observed values are compared in a scatter graph; the relative root mean square error (RRMSE), model efficiency (ME), and the coefficient of determination (CD) were used for performance evaluation of both PWL as FWL C-Fix scenario runs. The RRMSE is of random error and should be as low as possible (ideally zero). R^2 (ideally one), and ME (should be positive and ideally take a value between zero and one). ME is a measure for both random and systematic errors in the predictions. CD is a measure related to the simulation of peak values and is optimally one. The formulas are given below:

$$RRMSE = \sqrt{\frac{\sum_{i=1}^{n}(O_i - P_i)^2}{n} \cdot \frac{1}{\overline{O}^2}} \tag{8}$$

$$ME = 1 - \frac{\sum_{i=1}^{n}(O_i - P_i)^2}{\sum_{i=1}^{n}(O_i - \overline{O})^2} \tag{9}$$

Table 1 Estimated average daily Net Ecosystem Productivity (NEP) for 1997 and for nine EUROFLUX sites for the PWL and FWL modes of C-Fix

EUROFLUX sites, coordinates, elevation, species	PWL						FWL					
	Slope	Interc	R^2	ME	CD	RRMSE	Slope	Interc	R^2	M E	CD	RRMSE
SW1, Flakaliden, 64° 07′ N 19° 27′ E, 225 m, *Picea abies*	0.95	0.97	0.58	0.25	0.61	4.04	0.26	0.37	0.57	0.33	5.28	3.81
FI1, Hyytiala, 61° 51′ N 24° 17′ E, 170 m, *Pinus sylvestris*	0.78	−0.74	0.78	0.48	0.94	1.72	0.93	−0.02	0.76	0.73	0.88	1.26
SW2, Norunda, 60° 05′ N 17° 28′ E, 45 m, *Pinus sylvestris Picea abies*	1.10	−0.69	0.65	0.22	0.51	3.01	1.05	−0.52	0.64	0.32	0.56	2.81
DK1[a], Soroe, 55° 20′ N 11° 30′ E, 40 m, *Fagus sylvatica*	/	/	/	/	/	/	/	/	/	/	/	/
NL1, Loobos, 52° 10′ N 05° 45′ E, 25 m, *Pinus sylvestris*	1.15	0.04	0.49	−0.43	0.34	2.35	0.70	0.07	0.47	0.35	0.90	1.58
BE2, Brasschaat, 51° 18′ N 04° 31′ E, 10 m, *Pinus sylvestris*	1.46	1.48	0.43	−2.81	0.17	5.87	0.51	0.03	0.40	0.33	1.46	2.46
GE2, Tharandt, 50° 58′ N 13° 34′ E, 380 m, *Picea abies*	1.46	0.06	0.52	−1.45	0.24	2.2	0.87	0.04	0.53	0.29	0.69	1.18
BE1, Vielsalm, 50° 18′ N 06° 00′ E, 450 m, *Picea abies*	1.01	−0.4	0.50	−0.04	0.49	1.48	1.04	−0.33	0.55	0.1	0.51	1.38
GE1, Bayreuth, 50° 09′ N 11° 52′ E, 780 m, *Picea abies*	1.05	1.00	0.27	−2.43	0.22	7.37	0.55	0.07	0.34	0.19	1.07	3.58
FR1, Hesse, 48° 40′ N 07° 05′ E, 300 m, *Fagus sylvatica*	1.54	0.94	0.57	0.62	0.24	6.46	0.84	0.03	0.56	0.63	0.78	0.47
FR2[a], Bordeaux, 44° 42′ N 00° 46′ E, 60 m, *Pinus pinaster*	/	/	/	/	/	/	/	/	/	/	/	/
Pooled	0.88	0.06	0.49	0.62	0.24	6.46	0.83	0.19	0.52	0.92	1.24	3.00

[a]These EUROFLUX sites are not used in the evaluation of the SWI contribution with respect to the 1997 NEP estimation from C-Fix since the sites are too close to vast water bodies (sea, ocean) disturbing the ERS Scatterometer signal

$$CD = \frac{\sum_{i=1}^{n} (O_i - \overline{O})^2}{\sum_{i=1}^{n} (P_i - \overline{O})^2} \tag{10}$$

In Eqs. 8–10:

O_i is the i^{th} measured or observed value;
P_i is the i^{th} simulated or predicted value;
n is the number of measurements in the time interval considered;
$\overline{O}$ is the average value of the observations.

Table 1 illustrates that the FWL scenario run of C-Fix to estimate NEP_{FWL} significantly improves the quantitative accuracy of the model estimates when NEP_{FWL} is compared with EUROFLUX tower NEP measurements. Correlation coefficients do not differ much between the two NEP series. In contrast to R^2, ME increases significantly and becomes positive for all sites considered in the analysis. This suggests that the bias between NEP_{FWL} and measured EUROFLUX NEP is quite low. We can observe that peaks in NEP measurements are reproduced more realistically when running C-Fix with the FWL scenario (CD closer to one). An exception is the SW2 site, where an underestimation of EUROFLUX NEP peaks can be observed. Additionally, RRMSE values for the NEP_{FWL} estimates are consistently

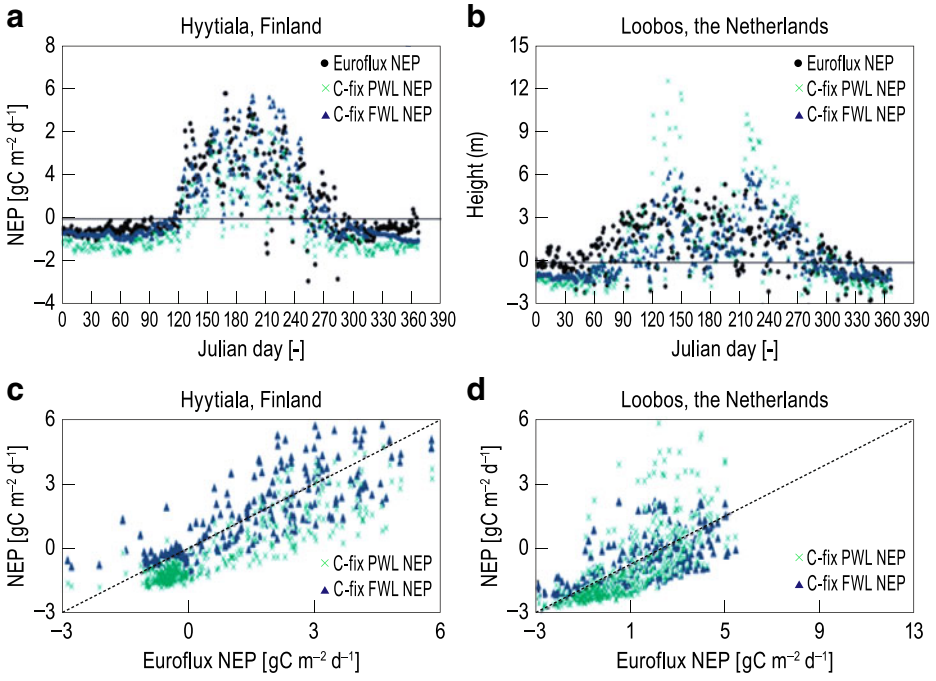

Fig. 2 Time series and scattergrams of measured NEP, modelled Partially Water Limited (PWL), and Fully Water Limited (FWL) NEP using C-Fix for 1997 at the EUROFLUX site of Hyytiala (Finland) and Loobos (Netherlands)

lower than for NEP_{PWL}. Although the intercepts and slopes of the linear equation between measured NEP and modeled NEP_{FWL} are less consistently close to zero and one respectively, the results for the slopes and intercepts in Table 1 indicate that the FWL scenario C-Fix estimates clearly improved compared with the PWL scenario estimates. From Verstraeten et al. (2006b), it can be observed that in the FWL scenario as opposed to the PWL one, NEP estimates fit EUROFLUX NEP observations more optimally. The FWL mode has a RRMSE (R^2) of 3.00 (0.52) for NEP estimated during 1997. The PWL mode has a RRMSE (R^2) value of 6.46 (0.49).

Figure 2 illustrates time series and scattergrams of measured and modeled NEP in the PWL and FWL scenario C-Fix runs for 1997 for the EUROFLUX sites of Hyytiala (Finland) and Loobos (the Netherlands). This figure clearly suggests that the FWL scenario at both sites produces better results compared to the PWL scenario, considering the better match of the FWL time series with the NEP measurements of the EUROFLUX sites and the closer position of the values toward the one-to-one line of the scattergrams. It can be observed in Fig. 2 that the NEP model simulation fits the site measurements better at Hyytiala than at Loobos. The site land use homogeneity or heterogeneity definitely affects the satellite data used in C-Fix. This can be one reason (of many) why C-Fix performance is better in the homogenous site of Hyytiala and less optimal in the much more heterogeneous site of Loobos. The different behavior of the NEP time series might be due to different climates and tree species, as indicated in Table 1. With the FWL scenario, NEP is reduced with the pooled dataset, with more than 20% compared to the PWL scenario. This suggests that the impact of water limitation leads to a decreased (or increased) NEP, depending on whether soil respiration increases (or decreases) or whether GPP decreases, or both.

5 The accuracy of C-Fix estimates of carbon uptake and respiration fluxes considering local soil moisture data

EUROFLUX datasets (Valentini et al. 2000; Wilson et al. 2002a, b; Dolman et al. 1998, 2003) acquired in 1998 at nine network sites (Table 1) were used as an independent validation dataset to evaluate the impact of soil moisture, and hence the short-term water availability on the C-Fix estimated ecosystem carbon flux. In Table 2 the differences between NEP_{PWL} and NEP_{FWL}, between SR_{PWL} and SR_{FWL}, and between ER_{PWL} and ER_{FWL} are illustrated for the year 1998 for the EUROFLUX sites.

- At the FR1 site, the difference between NEP_{PWL} and NEP_{FWL} is positive due to a significant decrease in SR.
- For the FR2 and GE2 sites, the difference between NEP_{PWL} and NEP_{FWL} is positive due to a larger increase in GPP than in ER and SR.
- For the FI1 and NL1 sites, despite a strong decrease of GPP in the FWL scenario, the difference between NEP_{PWL} and NEP_{FWL} remains positive due to a strong drop in heterotrophic and autotrophic respiration.
- At the SW1 site, a positive difference is due to a strong decrease in SR.
- For the BE1 site, the NEP_{PWL} and NEP_{FWL} difference is negative due to higher SR and AR values.

Table 2 Estimated average daily Net Ecosystem Productivity (NEP) in gC m^{-2} day^{-1} for 1998 and for nine EUROFLUX sites for the FWL and difference between the FWL and PWL scenarios run with C-Fix

EUROFLUX	NEP_{FWL} (gC m^{-2} day^{-1})	$\Delta NEP_{FWL-PWL}$ (gC m^{-2} day^{-1})	SR_{FWL} (gC m^{-2} day^{-1})	$\Delta SR_{FWL-PWL}$ (gC m^{-2} day^{-1})	ER_{FWL} (gC m^{-2} day^{-1})	$\Delta ER_{FWL-PWL}$ (gC m^{-2} day^{-1})
FI1	0.80	*0.04*	1.83	*−0.13*	2.07	*−0.73*
SW1	−0.02	*0.13*	0.99	*−0.47*	2.46	*−0.13*
DK1	0.12	−0.01	2.55	*−0.01*	3.89	*−0.03*
NL1	0.62	*0.03*	1.75	*−0.33*	3.04	*−0.54*
BE2	−0.25	−0.04	2.12	*−1.34*	3.07	*−2.10*
GE2*	1.70	*0.04*	1.84	0.71	3.38	1.03
BE1	1.18	−0.04	1.53	0.81	2.89	1.20
FR1	0.29	*0.34*	3.68	*−1.30*	5.35	*−1.79*
FR2**	0.83	*0.26*	0.77	0.08	0.88	0.04
Pooled	0.67	−0.18	1.80	*−0.42*	2.85	*−0.55*

NEP, SR, and ER are given as pooled values as well, by using all nine EUROFLUX site data. Positive (resp. negative) NEP values indicate uptake (resp. release) of CO_2 by an ecosystem. The SW2 and GE1 EUROFLUX sites were not used here, as some in situ data were not available for this study

- When all sites are pooled, the difference between NEP_{PWL} and NEP_{FWL} is negative despite a decrease in AR and SR. This is due to lower GPP values in the FWL scenario.

These observations suggest that soil moisture limitation decreases soil respiration more explicitly than photosynthesis. This is particularly true for mineral soils, as in organic soils respiration will increase under water-limiting conditions (Schils et al. 2008).

6 Soil water integration into a remote sensing-based ecosystem carbon assimilation model: possible implications for the carbon balance at a European scale

6.1 Water limited carbon uptake for Europe

When C-Fix runs are performed by assimilating only remotely sensed $fAPAR$ (PWL scenario), the effects of long-term water relations (stress) in vegetation are only indirectly accounted for. However, when $fAPAR$ as well as soil moisture are assimilated in C-Fix, both short- and long-term impacts of water limitation on carbon fluxes are accounted for (the PWL versus the FWL scenario). SWI is an input in the C-Fix model, as expressed in Eqs. 4 and 5. Spatially explicit NEP estimates at the European scale are shown in Fig. 3. Figure 3a, b illustrate the NEP estimates with the partially water limited scenario (NEP_{PWL}) and the fully water limited scenario (NEP_{FWL}), respectively. Figure 3c illustrates the difference between the NEP's from the two scenarios ($NEP_{PWL} - NEP_{FWL}$). It can be observed that the effect of soil moisture on NEP estimates is spatially very variable. However, some conspicuous patterns can be observed. In most parts of Europe, the results of the FWL scenario elicit a reduced NEP, although positive values are still retained. In other areas, soil moisture increases NEP. The spatial patterns of Fig. 3b are related to high or low soil moisture relative to soil texture properties. Very low soil moisture values reduce and ultimately completely inhibit soil micro-organism activity so that SR is either decreased or brought to a standstill. This is a condition where NEP evidently increases strongly. On the other hand, in water depleted soils, GPP decrease can be sharper than that of SR. In that case, the result is an NEP decrease. Unlike very dry soils, water saturated soils indicated by very high soil moisture values, are affected by soil anaerobiosis and a significant inhibition of soil micro-organism respiratory activity due to anaerobiosis. Photosynthesis is also inhibited, as water and mineral uptake by roots requires oxygen to supply the active water and mineral uptake process with the required biochemical energy.

6.2 Balancing NEP and anthropogenic carbon fluxes for several European countries

To put the magnitude of soil moisture impact on NEP into a Kyoto Protocol implementation context, an analysis of the difference between estimated NEP and anthropogenic carbon emissions (ACE) was made. The result of this exercise is shown in Table 3 for 26 European countries. As inventories of ACE values are available only at European national levels, the analysis of the balance of NEP

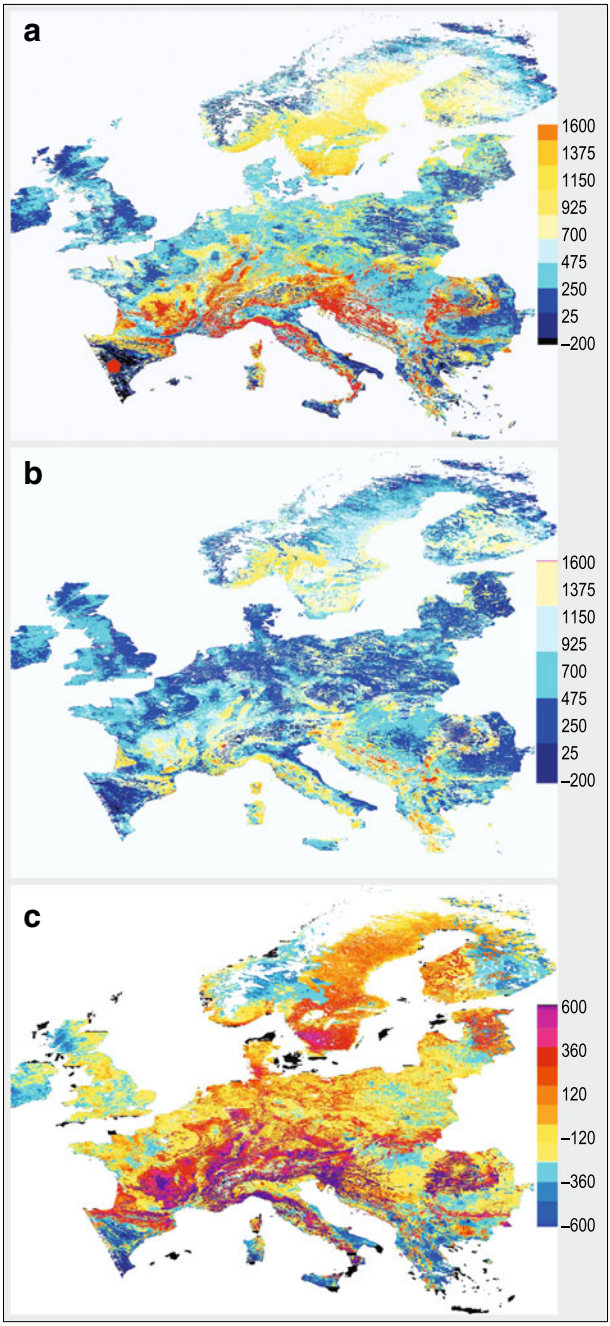

Fig. 3 Estimated average daily net ecosystem productivity (in 10^1 g C m^{-2} d^{-1}; thus divide by 10 to get the real value) for 1997 for Europe using the production efficiency model C-Fix. **a** Partially water limited model run (NEP_{PWL}) and **b** fully water limited model run (NEP_{FWL}). Negative NEP values indicate carbon sources; positive values indicate carbon sinks. Panel **c** illustrates the difference between the NEP of **a** and **b** ($NEP_{PWL} - NEP_{FWL}$)

and ACE also had to be limited to the different European national levels and unfortunately could not be scaled down to higher spatial resolutions.

When the PWL scenario is selected, 14 of the 26 European countries, representing 47.5% of the European continental surface area (±4,300,000 km^2), elicit a negative

Table 3 The difference between Net Ecosystem Productivity (NEP) and anthropogenic carbon emissions (ACE) at European country national level for 1997 (in Tg C a^{-1})

Country	ACE (Tg C a^{-1})	$NEP_{PWL}-ACE$ (Tg C a^{-1})		$NEP_{FWL}-ACE$ (Tg C a^{-1})	
Austria	66.5	61.7	*90.4*	−15.4	*51.8*
Belgium	122.2	−105.0	*15.9*	−118.3	*7.6*
Bulgaria	61.6	10.2	*100.9*	−23.7	*52.9*
Czech/Slovakia	137.4	−77.7	*60.9*	−114.9	*33.0*
Denmark	65.7	−49.3	*16.4*	−43.6	*10.1*
Estonia	20.2	11.6	*24.7*	−14.7	*23.1*
Finland	62.3	125.7	*149.0*	56.7	*145.5*
France	403.1	206.5	*590.4*	−161.9	*293.5*
Germany	893.5	−548.0	*279.5*	−813.4	*139.0*
Greece	94.3	−18.2	*131.9*	2.2	*90.1*
Hungary	60.5	−12.2	*75.5*	−37.0	*34.1*
Ireland	38.3	−42.6	*16.7*	−37.6	*10.1*
Italy/San Marino	443.1	−103.3	*424.7*	−283.7	*195.7*
Latvia	8.7	30.5	*36.6*	1.4	*35.8*
Lithuania	16.2	1.1	*29.0*	−6.9	*21.8*
Luxembourg	9.5	−9.1	*0.8*	−9.5	*0.3*
Monaco	44.7	−44.7	*0.0*	−44.7	*0.0*
Netherlands	170.2	−149.7	*19.1*	−167.1	*10.0*
Norway	40.6	219.5	*257.4*	199.7	*220.4*
Poland	361.6	−222.0	*180.2*	−300.2	*120.1*
Romania	123.8	76.4	*278.2*	−63.5	*137.4*
Slovenia	16.1	32.6	*21.9*	1.7	*9.9*
Spain/Andorra[a]	262.6	−198.4	*583.2*	−217.4	*286.3*
Sweden	56.8	390.1	*251.5*	152.0	*178.7*
Switzerland	43.2	13.9	*42.7*	−26.0	*20.6*
United Kingdom	548.4	−511.7	*77.7*	−533.2	*41.5*
Sum	4,176.8	−912.1		−2,619.0	

Standard deviations are listed in italics. Zero or positive difference (NEP−ACE): The countries' ecosystems can recapture anthropogenic carbon emissions. Negative difference: Anthropogenic carbon emissions are higher than terrestrial ecosystems can recapture

[a]For Spain NEP estimates are representative only for northeastern Spain (28.6% of the total country area); standard deviations are based on ecosystem carbon fluxes, not on errors for anthropogenic emission estimates

carbon flux budget. When the FWL scenario is selected, the number of countries with a negative carbon budget increases to 20 and the area with a negative carbon budget to 73.2%. Based on NEP_{FWL} data, we estimate that European countries recapture roughly one-third (37.2%) of ACE.

When comparing NEP_{PWL} and NEP_{FWL} respectively with ACE:

- The CO_2 recapturing capacity of Denmark, Ireland (negative NEP_{PWL} in Table 3) and northeastern Spain increases. The carbon flux balance, however, remains negative.
- For Greece, the difference between NEP_{PWL} and ACE is negative but shifts to a positive value when NEP_{FWL} and ACE are compared. Hence, Greece shifts from a CO_2 flux source to a sink.

- Austria, Bulgaria, Estonia, France, Lithuania, Romania and Switzerland—eliciting positive differences between NEP_{PWL} and ACE—shift to negative differences under the FWL scenario, namely, from CO_2 flux sinks to sources.
- Though the difference between NEP_{FWL} and ACE for Finland, Latvia, Norway, Slovenia, and Sweden is positive, the CO_2 uptake magnitude decreases, as shown in Fig. 3.
- When including soil moisture effects, for example, running the FWL scenario, the decrease in NEP is marginal for the Benelux countries, Spain/Andorra, and the UK.

NEP, as estimated with remote sensing measurements, can be converted into Net Biome Productivity (NBP) using a simple a NBP/NEP conversion factor. Through this, a rough assessment of the terrestrial carbon balance at the level of European countries can be made. Though strongly under debate at the IPCC, NBP is the most representative indicator for emitted carbon recapturing capacity for a terrestrial ecosystem as additional processes like forest clearing, logging, forest fires, crop harvesting or, in general, land use/land cover changes, are accounted for. This is of course in contrast to the NEP level. The NBP/NEP factor is estimated to be 0.10 to 0.20 at the level of the global terrestrial carbon cycle (Steffen et al. 1998). It amounts to 0.47 for European forest ecosystems (Janssens et al. 2003) and 0.23 for European grasslands (Soussana et al. 2004). For all European ecosystems (considering their land cover fractions) a NBP/NEP factor of 0.15 is an acceptable conversion factor value. When this factor is applied, it results in an annual European NBP using the FWL scenario of 229 ± 109 Tg C. This represents 5% of the European ACE, taking account of an error of 38% in the NBP/NEP factor applied. This estimate is quite similar to that of Janssens et al. (2003). Our estimate for 1997 for the NBP of forest ecosystems is 227 ± 101 Tg C a^{-1}. This is lower than the terrestrial NBP estimate of 363 ± 159 Tg C a^{-1} of Janssens et al. (2003) who considered the total area of Europe and not the limited area used in this study (±4,300,000 km^2), as indicated on the map shown in Fig. 3.

7 Referencing C-Fix in a GHG inventory framework: including its limits and potential improvements

The major strength of the remote sensing-based model C-Fix is its explicit spatiotemporal scale of operation in assessing GHG related data such as GPP, NEP, and ER. As a simple Production Efficiency Model (PEM), however, C-Fix is lacking the incorporation of detailed physiological processes. C-Fix is also not a SVAT-like model; hence, quantifying latent, sensible, and kinetic energy exchanges at the surface of soils and plants is out of the scope of this model. Nor is C-Fix a dynamic global vegetation model such as, for instance, DGVM (e.g., Cramer et al. 2001) and thus it is not capable of simulating vegetation dynamics. C-Fix does not accommodate the multi-temporal detail offered by deterministic stand-scale carbon models either, nor does it offer prognostic capability. Finally, it does not provide for the unravelled decomposition mechanisms of soil organic matter (Davidson and Janssens 2006).

On the other hand, the added value of remote sensing-based raster point models such as C-Fix, is situated in the capacity to describe the spatiotemporal heterogeneity of water limited ecosystem carbon fluxes in an operational way. This is due to the

semi-empirical modelling simplicity and therefore computational efficiency of such remote sensing-based raster point models. By assimilating high temporal resolution imagery, C-Fix can enable the analysis of spatially explicit seasonal and inter-annual effects of water availability and temperature on ecosystem carbon uptake and release. This spatialization of carbon fluxes can be performed from the regional to the continental scales (Verstraeten et al. 2006b). C-Fix therefore provides a significant added value by offering the possibility of scaling up from stand to regional and continental scales (see Black 2007), or of acting as a driver to calibrate out-of-phase phenological cycles in a DGVM or stand-scale model. Moreover, NEP spatial patterns, for example, often serve as validation fields for physically fully explicit models. Finally, remote sensing-based approaches benefit from local carbon sink and carbon mass accumulation studies and inventories (see Hawkins et al., 2007) as well as the reverse. Most inventories focus on well characterized ecosystems; they overlook the more fuzzy ecosystems such as tropical forests, savannas, shrublands, and tundra and evidently the large quantities of mixed land cover pixels in strongly fragmented landscapes. The application of remote sensing therefore provides a solution for many of the shortcomings of physically explicit approaches (see Field 2007).

The current C-Fix model is still amenable to many improvements, additional parameterizations, validations, and comparisons with other vegetation types (more broad-leaved forest species, agricultural crops, more Mediterranean and continental flux sites, sites on organic soils, etc.), data and approaches (for instance, as indicated in ClimSoil by Schils et al. 2008). More analysis over longer inter-annual time scales is also recommended. If available, remotely sensed SMC at finer spatial as well as temporal resolutions may also contribute to a better estimation of the carbon fluxes by C-Fix (Veroustraete et al. 2009). Integrating *fAPAR* data from other sources and methods is without doubt useful. For instance, *fAPAR* derived from MERIS or SeaWiFS imagery (Gobron et al. 2006) which offers a higher accuracy and more detailed values, thus reflecting the heterogenic character of terrestrial vegetation. Another nominee for further improvements is the RUE parameter. A finer stratification of this parameter according to vegetation type can be recommended; and also a closer and more direct link of RUE with the phenological stage of the vegetation is advisable. Other physiologically related parameters, suitable for improvement, are the normalized temperature dependency factor and the carbon dioxide fertilization factor (Eq. 2). They might also benefit from differentiation accordingly to vegetation type. Last, but not least, the heterotrophic respiration module in C-Fix can be replaced by more detailed sub-models, especially because (as expected, Verstraeten et al. 2008b) the largest variance in NEP estimates originates from soil processes (Black 2007). From GPP, to NPP, SR, and finally NEP, the model errors evolve from small fractions toward significant chunks of average daily NEP values. As soil moisture has a strong impact on the uncertainty of SR estimates (Verstraeten et al. 2008b), accurate SMC values are a must. RMSE values of ERS scatterometer-derived soil moisture vary between 0.022 and 0.158 $m^3\ m^{-3}$ for a wide range of soil types and climatic regions with a R^2 up to 0.75 (Wagner et al. 1999, 2003; Ceballos et al. 2005; Scipal et al. 2005). Illustratively, a quantitative example of the effect of error in SMC on carbon fluxes is given for the Brasschaat pixel (BE2). Assuming an absolute average error of SMC of 0.024 $m^3\ m^{-3}$ on daily averages of GPP, NPP, SR, and NEP with values of 3.10, 1.83, 1.80, and −0.18 $gC\ m^{-2}\ d^{-1}$, respectively

(a model simulation for 1997), the corresponding errors are 1.73, 0.88, 0.85 and 1.85 gC m^{-2} d^{-1}, respectively (Verstraeten et al. 2008b).

Moreover, a recent uncertainty revision of carbon fluxes for Russia indicates higher uncertainties for NPP and heterotrophic respiration than earlier estimates (Gusti and Jonas 2010) with lower absolute values. At the NBP level, Ciais (2010) reports values with an uncertainty of (181 ± 129 Tg a^{-1}) for the EU which shows similarity to the assessment presented in this paper, based on an assumption with respect to the conversion factor to estimate NBP from NEP for a slightly different area (229 ± 109 Tg a^{-1}). This conversion factor is both critical toward assessing the total carbon cycle and difficult to establish. Hence, wood harvesting studies and the associated uncertainty, as given by Dias et al. (2007), can be used to derive this conversion factor.

To obtain a balance between vegetation and anthropogenic carbon fluxes, it is necessary to have on hand reliable and complete emission data in terms of the uncertainty estimates involved. Wetlands and water bodies emit carbon (methane) and must also be considered in the carbon balance (Pandey et al., 2007), as must land cover and land cover changes (Schils et al. 2008). This also includes the methane emissions of solid waste disposal sites (Szemesová and Gera 2010). Leip (2010) estimates the uncertainty of agricultural emissions (including, for instance, fermentation, manure management, etc.) in the EU15. Another important issue is the requirement for methodology that converts annual country-based data (like PM10, SO_2, NO_x, NH_3) into data with a high temporal (e.g., hourly) and spatial resolution (van Oijen and Thomson 2010; Theloke et al., 2007). Not only the inventories itself, but also the uncertainties involved in them are estimated with a relatively low accuracy (Nahorski and Horabik 2010). This impacts policy (Winiwarter and Muik 2010). Nevertheless, system integration of available information sources and models of different types may decrease the uncertainties regarding, for instance, NEP and NBP estimates (Shvidenko and Nilsson 2010).

8 Conclusions

Even though in recent years the use of remote sensing to assess and verify ecosystem carbon fluxes has grown, the technique is still not being implemented to its full extent within the context of Kyoto Protocol implementation. One of the reasons is that, typically, new models and data assimilation schemes have to be developed that allow the incorporation of recently acquired or processed remotely sensed datasets. This paper gives an account of a primary study based on the integration of remotely sensed soil moisture data derived from ERS scatterometer data in an ecosystem carbon balance model, C-Fix. This model was applied to assess the impact of water limitation on the carbon balance between Net Ecosystem Productivity (NEP) and Anthropogenic Carbon Emission (ACE) for Europe. Regarding integrating soil moisture data, it was demonstrated that soil moisture has quite an important impact on the magnitude as well as on the spatial patterns of carbon exchange fluxes. Implementation of C-Fix suggests that NEP decreases in many areas when soil moisture is fully taken into account in the long and short term. Moreover, some European countries shift from being a sink to becoming a source, according to the findings obtained with the C-Fix model scenario runs.

Acknowledgements The authors acknowledge the Flemish Institute for Technological Research (Vito) for the scholarship, the financial support offered by the GLOVEG contract (VG/00/01). The authors also strongly acknowledge the work performed by ALL the collaborators of the EUROFLUX project. Without them, many validation datasets would never have been collected.

References

Bartholomé E, Belward AS (2005) GLC2000: a new approach to global land cover mapping from Earth observation data. Int J Remote Sens 26:1959–1977

Black K (2007) Scaling up from the stand to regional level: an analysis based on the major forest species in Ireland. Proceedings of the 2nd International Workshop on Uncertainty in Greenhouse Gas Inventories, International Institute for Applied Systems Analysis A-2361 Laxenburg, Austria 27–28 September 2007, p. 9–20

Ceballos A, Scipal K, Wagner W, Martínez-Fernández L (2005) Validation of ERS scatterometer-derived soil moisture data in the central part of the Duero basin. Hydrol Process 19(8):1549–1566

Chhabra A, Dhadwall VK (2004) Estimating terrestrial net primary productivity over India using satellite data. Curr Sci 86(2):269–271

Chow VT, Maidment DR, Mays LW (1993) Applied hydrology. McGraw-Hill, Singapore, pp 572

Ciais P (2010) Atmospheric inversions for estimating CO2 fluxes: methods and perspectives. doi:10.1007/s10584-010-9909-3

Ciais P, Reichstein M, Viovy N et al (2005) Europe-wide reduction in primary productivity caused by the heat and drought in 2003. Nature 437:529–533

Cramer W, Bondeau A, Woodward FI et al (2001) Global response of terrestrial ecosystem structure and function to CO2 and climate change: results from six dynamic global vegetation models. Glob Chang Biol 7(4):357–373

Dias AC, Louro M, Arroja L, Capela I (2007) Uncertainties in the estimates of carbon in harvested wood products for Portugal. Proceedings of the 2nd International Workshop on Uncertainty in Greenhouse Gas Inventories, International Institute for Applied Systems Analysis A-2361 Laxenburg, Austria 27–28 September 2007, p. 41–48

Davidson EA, Janssens IA (2006) Temperature sensitivity of soil carbon decomposition and feedbacks to climate change. Nature 440:165–173

Dolman AJ, Moors EJ, Elbers JA, Snijders W (1998) Evaporation and surface conductance of three temperate forests in the Netherlands. Ann Sci For 55:255–270

Dolman AJ, Moors EJ et al (2003) Factors controlling forest atmosphere exchange of water, energy and carbon in European forests. In: Valentini R (ed) Fluxes of carbon, water and energy of European forests. Springer, Heidelberg

Field CB (2007) Natural versus anthropogenic control of ecosystem carbon stocks. Proceedings of the 2nd International Workshop on Uncertainty in Greenhouse Gas Inventories, International Institute for Applied Systems Analysis A-2361 Laxenburg, Austria 27–28 September 2007, p. 59–60

Gobron N, Pinty B, Aussedat O et al (2006) Evaluation of fraction of absorbed photosynthetically active radiation products for different canopy radiation transfer regimes: methodology and results using joint research center products derived from SeaWiFS against ground-based estimations. J Geophys Res 111:D13110. doi:10.1029/2005JD006511

Goward SN, Dye DG (1987) Evaluating North-American net primary production with satellite observations. Adv Space Res 7:165–174

Grace J, Rayment M (2000) Respiration in the balance. Nature 404:819–820

Gusti M, Jonas M (2010) Terrestrial full carbon account for Russia: revised uncertainty estimates and their role in a bottom-up/top-down accounting exercise. doi:10.1007/s10584-010-9911-9

Hawkins M, Black K, Gallagher G, Connolly J (2007) Resolution of stochastic issues in estimating forest biomass carbon stock changes using non-linear mixed models. Proceedings of the 2nd International Workshop on Uncertainty in Greenhouse Gas Inventories, International Institute for Applied System Analysis A-2361 Laxenburg, Austria 27–28 September 2007, p. 97–100

IIASS (2007) 2nd international workshop on uncertainty in greenhouse gas inventories, 27–28 September 2007, International Institute of Applied Systems Analysis (IIASA). Laxenburg, Austria, p 233

Janssens IA, Freibauer A, Ciais P et al (2003) Europe's terrestrial biosphere absorbs 7 to 12% of European anthropogenic CO_2 emissions. Science 300:1538–1542

Leip (2010) The uncertainty of the uncertainty... on the example of the quality assessment of the greenhouse gas inventory for agriculture in Europe. doi:10.1007/s10584-010-9915-5
Lu L, Li X, Veroustraete F (2005) Terrestrial productivity and its spatio-temporal variability in Western China. Acta Ecol Sinica 25:1–12
Maisongrande P, Ruimy A, Dedieu G, Saugier B (1995) Monitoring seasonal and interannual variations of gross primary productivity, net primary productivity and ecosystem productivity using a diagnostic model and remotely sensed data. Tellus 47(B):178–190
McCree KJ (1972) Test of current definitions of photosynthetically active radiation against leaf photosynthesis data. Agric For Meteorol 10:442–453
Myneni RB, Williams DL (1994) On the relationship between fAPAR and NDVI. Remote Sens Environ 49:200–211
Nahorski, Horabik (2010) Compliance and emission trading rules for asymmetric emission uncertainty estimates. doi:10.1007/s10584-010-9916-4
Nemani R, White M, Thornton P, Nishida K, Reddy S, Jenkins J, Running S (2002) Recent trends in hydrologic balance have enhanced the terrestrial carbon sink in the Unite States. Geophys Res Lett 10:106-1–106-4
Nilsson S, Jonas M, Obersteiner M, Victor DG (2001) Verification: the gorilla in the struggle to slow global warming. For Chron 77:475–478
Pandey JS, Wat SR, Devotta S (2007) Development of emission factors for GHGs and Associated uncertainties. Proceedings of the 2nd International Workshop on Uncertainty in Greenhouse Gas Invetories, International Institute for Applied Systems Analysis A-2361 Laxenburg, Austria 27–28 September 2007, p. 163–168
Pellarin T, Calvet J-C, Wagner W (2006) Evaluation of ERS scatterometer soil moisture products over a half-degree region in southwestern France. Geophys Res Let 33(17):L17401
Penman J, Gytarsky M, Hiraishi T, Krug T, Kruger D, Pipatti R, Buendia L, Miwa K, Ngara T, Tanabe K, Wagner F (2003) Good practice guidance for land use, use change and forestry. IPCC National Greenhouse Gas Inventories Programme, Technical Support Unit
Rosenqvist Å, Milne A, Lucas R, Imhoff M, Dobson C (2003) A review of remote sensing technology in support of the Kyoto Protocol. Environ Sci Policy 6:441–455
Theloke J, Pfeiffer H, Pregger T, Scholz Y, Köble R, Kummer U, Nicklass D, Thiruchittampalam B, Friedrich R (2007) Development of a methodology for temporal and spatial resolution of greenhouse gas emission inventories for validation. Proceedings of the 2nd International Workshop on Uncertainty in Greenhouse Gas Inventories, International Institute for Applied Systems Analysis A-2361 Laxenburg, Austria 27–28 September 2007 p. 203–206
Schils R, Kuikman P, Liski J et al (2008) Review of existing information on the interrelations between soil and climate change. ClimSoil report, Alterra. Wageningen, The Netherlands
Scipal K, Scheffler C, Wagner W (2005) Soil moisture–runoff relation at the catchment scale as observed with coarse resolution microwave remote sensing. HESS 9:173–183
Shvidenko A, Nilsson S (2010) Can the uncertainty of full carbon accounting of forest ecosystems be made acceptable to policymakers? doi:10.1007/s10584-010-9918-2
Soussana J-F et al (2004) Greenhouse gas emissions from European grasslands. In: Discussion paper originated from a workshop in Clermont-Ferrand, France, pp 1–93
Steffen W, Noble I, Canadell J, Apps M et al (1998) The terrestrial carbon cycle: implications for the Kyoto protocol. Science 280:1393–1394
Szemesová J, Gera M (2010) Uncertainty analysis for estimation of landfill emissions and data sensitivity for the input variation. doi:10.1007/s10584-010-9919-1
UNFCC (2005) Report on national greenhouse gas inventory data for the period 1990–2003 and status of reporting. FCCC/SBI/2005/17, pp 1–23
Valentini R, Matteucci G, Dolman AJ et al (2000) Respiration as the main determinant of carbon balance in European forests. Nature 404:861–865
van Oijen M, Thomson AM (2010) Toward Bayesian uncertainty quantification for forestry models used in the United Kingdom Greenhouse Gas Inventory for land use, land use change, and forestry. doi:10.1007/s10584-010-9917-3
Veroustraete F, Patyn J, Myneni RB (1994) Forcing of a simple ecosystem model with fAPAR and climate data to estimate regional scale photosynthetic assimilation. In: Veroustraete F (ed) Modelling and climate change effects. Academic, The Hague
Veroustraete F, Sabbe H, Eerens H (2002) Estimation of carbon mass fluxes over Europe using the C-Fix model and Euroflux data. Remote Sens Environ 83:376–399
Veroustraete F, Sabbe H, Rasse DP, Bertels L (2004) Carbon mass fluxes of forests in Belgium determined with low resolution optical sensors. Int J Remote Sens 25:769–792

Veroustraete F, Li Q, Verstraeten WW, Xi C, Bao A, Dong Q-H, Liu T, Willems P (2009) Soil moisture content retrieval based on apparent thermal inertia for the Xinjiang province in China. Int J Remote Sens (in press)

Verstraeten WW, Muys B, Feyen J, Veroustraete F, Minnaert M, Meiresonne L, De Schrijver A (2005) Comparative analysis of the actual evapotranspiration of Flemish forest and cropland, using the soil water balance model WAVE. HESS 9(3):225–241

Verstraeten WW, Veroustraete F, van der Sande CJ, Grootaers I, Feyen J (2006a) Soil moisture retrieval using thermal inertia, determined with visible and thermal spaceborne data, validated for European forests. Rem Sens Environ 101(3):299–314

Verstraeten WW, Veroustraete F, Feyen J (2006b) On temperature and water limitation in the estimation net ecosystem productivity: Implementation in the PEM C-Fix. Ecol Model 199:4–22

Verstraeten WW, Veroustraete F, Feyen J (2008a) Assessment of evapotranspiration and soil moisture content across different scales of observation. Sensors 8:70–117

Verstraeten WW, Veroustraete F, Heyns W, Van Roey T, Feyen J (2008b) On uncertainties in carbon flux modelling and remotely sensed data assimilation: the Brasschaat pixel case. Adv Space Res 41:20–35

Wagner W, Lemoine G, Rott H (1999) A method for estimating soil moisture from ERS scatterometer and soil data. Rem Sens Environ 70:191–207

Wagner W, Scipal K, Pathe C (2003) Evaluation of the agreement between the first global remotely sensed soil moisture data with model and precipitation data. J Geophys Res 108(D19):4611–4619

Wagner W, Jonas M, Hoffmann C, Gangkofner U, Hasenauer S, Hollaus M, Schiller C, Kressler F (2005) The role of earth observation in the good practice guidance for reporting land use, land use change and forestry activities as specified by the Kyoto Protocol. In: Abstracts of the ENVISAT & ERS symposium, Salzburg, Austria, 6–10 September 2004, ESA SP-572

Wagner W, Blöschl G, Pampaloni P, Calvet J-C, Bizzarri B, Wigneron J-P, Kerr Y (2007) Operational readiness of microwave remote sensing of soil moisture for hydrologic applications. Nord Hydrol 38(1):1–20

Wilson KB, Baldocchi B, Aubinet M et al (2002a) Energy partitioning between latent and sensible heat flux during the warm season at FLUXNET sites. Water Resour Res 38(12):1294–1323

Wilson K, Goldstein A, Falge E et al (2002b) Energy balance closure at FLUXNET sites. Agric For Meteorol 113:223–243

Winiwarter W, Muik B (2010) Statistical dependence in input data of national greenhouse gas inventories: effects on the overall inventory uncertainty. doi:10.1007/s10584-010-9921-7

Climatic Change (2010) 103:137–157
DOI 10.1007/s10584-010-9918-2

Can the uncertainty of full carbon accounting of forest ecosystems be made acceptable to policymakers?

Anatoly Shvidenko · Dmitry Schepaschenko · Ian McCallum · Sten Nilsson

Received: 5 January 2009 / Accepted: 15 June 2010 / Published online: 14 July 2010

Abstract In accordance with the concept that only full accounting of major greenhouse gases corresponds to the goals of the United Nations Framework Convention on Climate Change and its Kyoto Protocol, this paper considers uncertainties of regional (national) terrestrial biota Full Carbon Accounting (FCA), both those already achieved and those expected. We analyze uncertainties of major components of the FCA of forest ecosystems of a large boreal region in Siberia ($\sim 300 \times 10^6$ ha). Some estimates for forests of other regions and Russia as a whole are used for comparison. The systems integration of available information sources and different types of models within the landscape-ecosystem approach are shown to have enabled an estimation of the major carbon fluxes (Net Primary Production, NPP, and heterotrophic respiration, HR) for the region for a single year at the level of 7–12% (confidential interval, CI, 0.9), Net Ecosystem Production (NEP) of 35–40%, and Net Biome Production (NBP) of 60–80%. The most uncertain aspect is the assessment of change in the soil carbon pool, which limits practical application of a pool-based approach. Regionalization of global process-based models, introduction of climatic data in empirical models, use of an appropriate time period for accounting and reporting, harmonization and multiple constraints of estimates obtained by different independent methods decrease the above uncertainties of NEP and NBP by about half. The results of this study support the idea that FCA of forest ecosystems is relevant in the post-Kyoto international negotiation process.

1 Introduction

Carbon accounting for terrestrial ecosystems that is "partial," that is, limited to direct human activities, was introduced into international practice by the Kyoto

A. Shvidenko (✉) · D. Schepaschenko · I. McCallum · S. Nilsson
International Institute for Applied Systems Analysis,
2361, Laxenburg, Austria
e-mail: shvidenk@iiasa.ac.at

Protocol and the subsequent decisions of the Conferences of Parties to the United Nations Framework Convention on Climate Change (UNFCCC). The 10-year period following the signing of the Protocol clearly demonstrated that the partial carbon accounting approach has a number of major shortcomings and that these are an impediment to achieving the UNFCCC goals. The shortcomings of partial carbon accounting are:

1. It distorts the real picture of the role of individual countries in climate change mitigation efforts in the sense that many emissions and greenhouse gas removals are not included in the accounting regime.
2. It excludes "climate-friendly" investment in fields of the biosphere where there is great potential: that is, in the language of the Kyoto Protocol, the Land Use, Land Use Change, and Forestry (LULUCF) sector;
3. It poses a threat to the protection of some categories of "unmanaged" ecosystems (e.g., old growth forests);
4. It gives insufficient consideration to large sources of emissions (e.g., wild fires); and
5. It restricts opportunities for developing countries to participate in the international processes of climate change mitigation.

Moreover, partial accounting does not allow for a comprehensive analysis of uncertainties, as considering the impacts on only a part of a system is not sufficient for assessing the responses and feedbacks of the entire system in any complete form. Substantial problems also arise from the large difficulties (and often, the impossibility) of strict definitions and unambiguous implementation of some of the key terms of the post-Kyoto language (e.g., managed land, anthropogenic impacts, base-lines and additionality, etc.), which raises doubt concerning some incentives and results.

Such a situation leads to the relevance of transition to a terrestrial ecosystems full carbon account (FCA), as a principal part of a full greenhouse gas account, (independently of future political decisions after the first commitment period), in terms of how these estimates should be used, either for "accounting" in the Kyoto Protocol sense or only for an "estimation" as auxiliary information for policymakers.

However, a number of studies illustrate a high level of uncertainty of biosphere carbon accounting from the regional to the global scale (Chen et al. 2000; Houghton 2003; Nilsson et al. 2007). Furthermore, two interconnected questions become crucially important: (1) what is the acceptable level of uncertainty at which the introduction of FCA results into the international accounting regime would be allowed? and (2) is there a scientifically solid, practically applicable methodology that would deliver a reasonable assessment of uncertainties at that level?

Finding the correct answer to the first question is not simple. The potential cost-effectiveness of carbon sequestration seems to be a major criterion here. However, as aiming for high accuracy significantly increases the cost of accounting, the elaboration and maximization of functions describing the difference between the benefit of carbon sequestration and the cost of the accounting is theoretically the soundest approach. In reality, however, this does not work because of: (1) the overwhelming difficulty and practical inexpediency of separating carbon issues from other ecosystem services; (2) the many unresolved economic problems involved in

carbon crediting and offsetting; and (3) the existence of substantial but difficult-to-quantify political components. This leads to the conclusion that any formally defined "perfect accuracy" does not actually exist, but should be rather "acceptable" for scientific considerations, evaluation of "global utility" of ecosystems services, including carbon credits, and that it ultimately crucially depends upon the requirements and preferences of stakeholders (cf. Waggoner 2009). Through analysis of limited studies on the topic (GCP 2003; Newell and Stavins 2000), supported by simplified calculations for pared-down, averaged conditions of northern Eurasia, we may conclude that the relative uncertainty of Net Biome Production (NBP) at 20–30%, with confidence interval (CI) = 0.9, assuming that mean NBP differs substantially from 0, could be satisfactory in terms of average carbon prices and the main tendencies of the post-Kyoto market.

With respect to the second question, appropriate methodologies should consider the possibility of changing to *verified* FCA (i.e., the accounting should provide a comprehensive and reliable assessment of uncertainties at all stages and for all modules of the account). General features of such an approach have been published (Nilsson et al. 2007). As a further step, an analysis of uncertainties recognized for major components of FCA for forests of a large boreal region in Central Siberia was undertaken. For comparison, we also discuss results obtained for forests of other boreal regions of Russia and of the country as a whole. Results obtained within a landscape-ecosystem approach were further compared with available estimates obtained using other methods. Forests as an informative case study were selected because: (1) forest is the largest land class within the boreal zone and a major player in ecosystems carbon cycling; and (2) the complex structure of forest ecosystems allows us to assume that uncertainty levels achieved for forests could be achieved for other vegetation land classes.

All definitions of forest land cover classes and biometric characteristics used in this study correspond to Russian forest inventory and forest management manuals (FFS'RF 1995; Shvidenko et al. 2008b). In particular, forest (forested area) is represented by stands with relative stocking >0.35 for young and >0.25 for other age groups, and growing stock is the sum of volumes of the stems of all living trees that constitute a stand.

2 Methods and material

2.1 Major features of FCA

Four major approaches are currently used for terrestrial carbon accounting: (1) inventory-based (landscape-ecosystem) approaches; (2) measurements of net ecosystem exchange (eddy covariance method); (3) process-based terrestrial biosphere models; and (4) inverse modeling. All these methods have inherent strengths and weaknesses. However, none—if individually applied—is able to provide comprehensive and reliable assessment of uncertainties because estimation of structural uncertainties cannot be based only on the consideration of an "individual" case. This leads to the conclusion that only an integration of different methodologies is capable of generating a promising solution (e.g., Nilsson et al. 2007). To provide integration of different FCA methods, one of them should be selected as the basis

of the accounting system. We assume that a landscape-ecosystem approach (LEA) is most appropriate for this goal for the following important reasons: (1) LEA presents a comprehensive geo-referenced description of ecosystems and landscapes (i.e., the information necessary for intelligent applications of any other methods of carbon accounting); (2) the information background of the LEA—an Integrated Land Information System (ILIS)—is an appropriate tool for monitoring temporal changes of land use–land cover (Nilsson et al. 2007).

Within the LEA, the accounting schemes for carbon budget are a combination of flux-based and pool-based approaches. The flux-based method is applied as a recurrent chain:

$$\mathrm{NEP} = \mathrm{NPP} - \mathrm{HSR} - \mathrm{DEC} - \mathrm{FLIT} - \mathrm{FHYD}, \mathrm{NBP} = \mathrm{NEP} - \mathrm{DC}, \quad (1)$$

where *NBP*, *NEP*, *NPP*, are, respectively, Net Biome Production, Net Ecosystem Production, and Net Primary Production, *HSR* is heterotrophic soil respiration, *DEC* is flux due to the decomposition of dead wood, *FLIT* is flux to the lithosphere, *FHYD* is flux to the hydrosphere, and *DC* is fluxes caused by natural and human-induced disturbances, including consumption of forest products. For the pool-based approach:

$$\Delta(\mathrm{C}) = \mathrm{C}_{\mathrm{syst,t+\Delta t}} - \mathrm{C}_{\mathrm{syst,t}}, \quad (2)$$

where $\Delta(C)$ is the change of carbon pools and $C_{syst,t+\Delta t}$ and $C_{syst,t}$ are carbon pools considered in the accounting system at the end and at the beginning of the period Δt, respectively.

In this study, carbon pools were classified as carbon of live biomass, dead wood, and soils. In turn, live biomass of forest ecosystems was estimated by seven fractions (stem wood over bark, bark, wood of branches, foliage, roots, understory, and green forest floor) using a set of multidimensional models developed according to tree species and including age, site index, and relative stocking of stands (Shvidenko et al. 2007). The stock of above-ground dead wood (snags, logs, and dead branches of live trees) was estimated based on sets of available measurements on sample plots in taiga regions of Northern Eurasia, estimates of forest inventory aggregated by forest enterprises, and data on mortality derived from empirically based models of growth of modal stands (Shvidenko et al. 2005). A special method was developed for assessing NPP of forest ecosystems (Shvidenko et al. 2007). The remaining major fluxes (*HSR*, *DEC*, *DC*, *FLIT*, *FHYD*) were estimated using state statistical data, various inventories, surveys, and empirical models. A detailed description of the methodology can be found in (Shvidenko et al. 2005).

2.2 Study region

FCA was provided for a region totaling 313 million hectares in Central Siberia (including 299.8×10^6 ha vegetated land, of which 177.6×10^6 ha are represented by closed forests), divided in 25 ecological regions (Schmullius and Santoro 2005) and about 31,000 polygons (Fig. 1). The region includes almost all the bioclimatic zones of Northern Eurasia, diverse land forms, land classes, and ecosystems. The

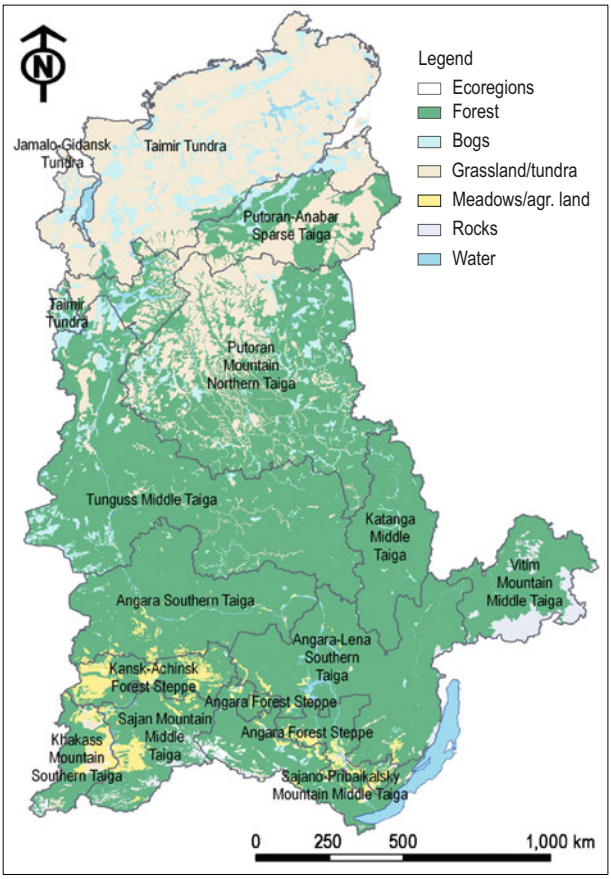

Fig. 1 Study region. Land cover of Central Siberia

integrated land information system (ILIS) for the region is represented by a comprehensive geographic information system (GIS) description of climate, landscape, soil, vegetation, disturbances, etc. (Shvidenko et al. 2005). All components of the FCA were estimated by polygons. The polygons were developed based on a combination of multi-sensor remote sensing (using 12 instruments from eight satellites) and all available ground information (State Land Account data, forest inventory, monitoring of disturbances, etc.). Major classes of land cover at the first (upper) level of the classification included unproductive areas, agricultural land, forest land, natural grassland, shrubs, and wetlands. At the second level, forest land was divided into closed forests, burn areas, dead stands, and (unregenerated) harvested areas. A more detailed classification of forests was carried out based on all available information, mainly using updated forest inventory data. Finally, the comprehensive parameterization of forest polygons included species composition, age, average height, and diameter by species, site index, relative stocking, and growing stock volume.

Characteristics of soil were extracted from a soil map at a 1:1 million scale, which was produced for the region and overlapped with the polygon map.

2.3 Assessment of uncertainties

Assessment of uncertainties is based on the understanding that FCA is a large dynamic fuzzy system that comprises a sophisticated interplay between many stochastic elements and processes (Nilsson et al. 2007). In a practical implementation, such systems cannot be directly validated or verified in any strict or formal way. This means that, before the uncertainties are assessed, there are a number of prerequisites and requirements to be observed.

1. A strict system design for the FCA is a mandatory prerequisite. Explicit structuring of the accounting schemes is needed, as well as delineation both of the intrasystem and the outer boundaries that have different dimensions (spatial, temporal, processes that should be considered, etc.). This will allow strict algorithms to be developed, permit potential application of error propagation theory, and provide the basis for consideration of the structural uncertainty of the models or accounting systems used.
2. A comprehensive analysis is needed of how "full" the carbon accounting is. There are two interconnected aspects to this problem, both of which impact the estimation of results and uncertainties. The first deals with the selection of processes and modules to be included in the accounting. This is closely tied to recognizing the structural uncertainties of the FCA and, in essence, is limited by heuristic approaches and expert estimates. The second defines the "working area" of the FCA, for example, whether or not consumption of plant products or the carbon budget of inland bodies of water should be considered as part of the accounting scheme.
3. All input information should be presented in a quantitative way; this requirement also assumes the formal use of personal probabilities and corresponding confidence intervals for different assumptions and expert estimates.
4. A preliminary harmonization of major terms and definitions is needed, particularly taking into account the multidisciplinary character of the FCA.
5. Uncertainties of the initial data need to be assessed based on an analysis of the entire chain of measurement, collection, and upscaling of data. This is a very time-consuming stage, as it is very difficult to get reliable quantitative conclusions on the topic.
6. Analysis and quantification of temporal and spatial trends of data sets and empirical models used in the accounting are needed. Avoiding this step could substantially change the results (Lapenis et al. 2005).
7. A methodology should be used to assess uncertainty that takes into account the fuzzy character of FCA (Nilsson et al. 2007).

Note that the above requirements have the same goal as that declared in IPCC "Good Practice Guideline, 2006" on GHG inventories: such inventories "are those which contain neither over- nor underestimates so far as can be judged, and in which uncertainties are reduced as far as practical" (IPCC 2006, p. 1.6).

Within the landscape-ecosystem approach, the following method of uncertainty estimation was used:

1. Assessment of precision within the landscape-ecosystem approach using the error propagation theory according to the algorithms developed;
2. Provision of a standard sensitivity analysis by applying either the Monte Carlo method or systems of numerical differentiation;
3. Transition from precision to uncertainties by expert modification of formal results; and
4. Comparative analysis, harmonization, and multiple constraints of results achieved by independent methods. In this study, this step was limited by expert estimates and professional judgments.

Overall, this approach can be applied to all methods and all stages of FCA, particularly where strict formalization of uncertainty assessment is difficult or impossible. All estimations below have been made under the assumption that the models and methods used have no unrecognized biases. Obviously, such an assumption should be used with caution: much of the input data has uncertainties in terms of unknown combinations of random and systematic errors.

As all calculations are based on a strict algorithm, standard errors of a function $Y = f(X_i)$, where X_i is a random quantity with standard error m_i, $i = 1, 2, \ldots, k$, could be calculated approximately at each hierarchical stage of the FCA by using functional:

$$m_y^2 = \sum_{i=1}^{k} \left(\frac{dY}{dX_i} m_i \right)^2 + 2 \sum_{i>j} \left(\frac{dY}{dX_i} \right) \left(\frac{dY}{dX_j} \right) r_{ij} m_{X_i} m_{X_j}, \tag{3}$$

where dY/dX_i—partial derivatives of Y by X_i, and r_{ij}—is the correlation coefficient between X_i and X_j. Usually, inclusion of the second item of Eq. 3 is important because many X_i in Eq. 3 are statistically interdependent.

3 Results and discussion

3.1 Uncertainties of carbon pools

The average *live biomass* (LB) *of forested areas* is estimated for the region at 56.5 ± 2.2 Mg C ha^{-1}, that is, with a relative precision of 3.9% (here and below, CI = 0.9). Uncertainty of biomass of stems is ~4.5%, and below-ground LB is ~8%. Note that this result was obtained because of the availability of:

1. Long-term spatially distributed forest inventory data at the level of individual forest stands—primary units of forest inventory;
2. Remote sensing information to allow updating of obsolete forest inventory data;
3. Information on the actual species composition by polygon;
4. More precise estimation of growing stock in comparison with routine forest inventory data;

5. Statistically valid and regionally distributed multidimensional nonlinear regression equations for transition from indicators measured by forest inventory to live biomass estimates by components; and
6. Accounting methodology used for recognition of temporal trends in allometric interdependences in forest ecosystems (Lapenis et al. 2005).

Uncertainties of inventory-based estimates of LB depend upon:

1. Reliability of delineation of polygon boundaries;
2. Uncertainty of biometric indicators of forest ecosystems within polygons;
3. Accuracy and adequacy of models used for assessing LB;
4. Variability of model parameters such as amount of carbon in plant tissues (Mitrofanov 1977); and
5. Assumptions and simplifications in the accounting systems.

In this study, the major simplification included an aggregation of primary units of forest inventory in more heterogeneous polygons at scale 1:1 million. For this reason, compared with the requirements of the forest inventory manual (FFS'RF 1995), a twofold increase in random errors of biometric characteristics of polygons for individual stands (inventory primary units) was provided. Based on detailed analysis of uncertainties of biometric indicators by polygon (Shvidenko et al. 2005), a prerequisite about absence of statistically significant bias of growing stock volume was used.

An attempt to harmonize the uncertainties of forest LB assessed for Central Siberia led to the following conclusions:

1. Assuming that growing stock volume on polygons does not have systematic errors and taking into account that the number of forest polygons exceeds 10,000, the summarized error of the total average is negligible.
2. It was shown that there were temporal trends in partition of live biomass fractions (Lapenis et al. 2005) during the 1960s–2000s, and that these trends do not coincide for different live biomass components. If this trend is disregarded, the live forest biomass of Russia for the early 2000s will be overestimated by between 7% and 10% (Shvidenko et al. 2008a).
3. The non-random character of experimental data used for development of the LB models does not allow the impacts of stem and root decay to be estimated. The latter comprise on average 5–7% of the growing stock in mature and overmature stands of European Russia and 12–15% (sometimes more) in the mostly unmanaged taiga forests of Asian Russia.
4. As discussed above, precision of the total live biomass was estimated at about ±4%. The present analysis leads to a final uncertainty estimate of live biomass at the ±5–7% limit. We must stress that here (and throughout the paper) we operate with "summarized" errors (i.e., errors that have some combination of random and systematic errors, assuming that the bias is relatively small).

An independent assessment of LB for the region's forests was based on data from the State Forest Accounting (SFA) of 2003 carried out by forest enterprises. This comparison is of interest because traditional forest inventory data remain a basic

information source for live biomass inventories at different scales. Uncertainties of forest inventory data in the region are basically defined by:

1. Accuracy of methods of forest inventory and reference information (models and tables) used;
2. Existence of extensive areas with obsolete inventories;
3. Simplified structure of information presented in aggregated data of SFA by forest enterprises (e.g., use of dominant species instead of actual species composition).

Forest inventory data for the region (and the entire country) use a combination of three major methods of forest inventory:

1. Ground forest inventory and planning;
2. Remote sensing technologies of different types; and
3. Aerial survey, or *aerotaxation*.

A detailed consideration of the problem is given in Shvidenko and Nilsson (2002). Here we enumerate its main conclusions.

1. Ground forest inventory and planning has underestimated the growing stock of immature, mature, and overmature forests from by about 8% to 15%;
2. Technologies based on remote sensing applications do not have statistically significant systematic errors;
3. Aerotaxation was used several decades ago, with the result that growing stock was overestimated by 20–25% depending on the date and geographical location of the survey. However, the area where this method was initially applied (and where new inventories were not subsequently done) currently comprises about 60 million hectares of remote land in the northern region. By 2003, 40% of the region had been inventoried by ground forest inventory and planning, 55% by different types of remote sensing technology, and 5% by aerotaxation. Overall, the FSA slightly underestimated the area of forests of the study region (172.1 versus 176.6×10^6 ha, or 2.5%, mostly at the expense of land reserve areas where SFA is not provided), and also underestimated average growing stock (and, correspondingly, forest live biomass) by −10 to −13%.

Another source of possible uncertainties follows from the methodologies of live biomass modeling and the structure of models used. From among several methods of live biomass assessment that were suggested in Russia in recent decades, we consider an approach developed by Usoltsev (1998, 2007). Usoltev developed a set of models of biomass expansion factor $BEF_{s,h,i}$ by tree species s, geographical region h, and live biomass fraction i as a function:

$$\mathrm{BEF_{s,h,i}} = \mathrm{f}\,(\mathrm{A},\ \mathrm{H_{100}}, \mathrm{N},\ \mathrm{D})\,, \tag{4}$$

where A, D, N, and H_{100} are age, average diameter, number of trees, and average height of a stand at age of 100 years (i.e., the latter can be scaled as a site index class). In our opinion, this method, from a scientific and information point of view,

is more appropriate than others (e.g., Zamolodchikov and Utkin 2000). However, some specific features of the method impact its reliability.

1. Allometry is used as the analytical form of the equations (i.e., the components of the models are presented by a combination of logarithms of variables of Eq. 4). Allometric forms for assessing live biomass of individual stands and their combinations (as opposed to individual trees) have no solid theoretical background;
2. Allometric equations are monotonous by all variables; this is not the case for some species and live biomass components (Shvidenko et al. 2007).
3. Usoltsev (1998, 2007) used a method of a "recursive analysis" where the final results follow from a step-by-step estimation of intermediate results using a limited number of variables, and these intermediate results serve as input to the subsequent equations of the recursive chain. Clearly, such an approach does not allow uncertainties to be defined by formal statistical methods and substantially increases an expert component of modeling (i.e., the reliability of results is strongly dependent upon the qualification of the modeler). We compared the results of live biomass assessment by Usoltsev's (2007) method and by the approach examined in our study for Central Siberia using forest inventory data for 150 forest enterprises of the Urals region covering a total forested area of 68 million hectares (Fig. 2). The results are close; the total live biomass estimated by Usoltsev's method was 3% less than ours and had 5% less above-ground LB.

Several conclusions follow from this analysis:

1. Biomass expansion factors depend upon region, tree species, age, and other biometric characteristics of stands; simplified representation of BEF (e.g., as an average for forests of large regions) generates substantial uncertainties and uncontrolled biases.
2. LB of the lower layers of forest ecosystems (green forest floor, understory) could comprise up to 15–20% of the total, particularly for forests that have low productivity in high latitudes. Thus, models and approaches that account for only tree LB underestimate the results.

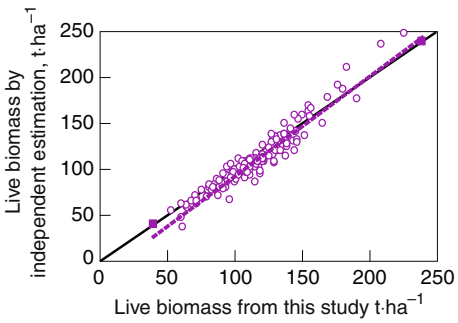

Fig. 2 Comparisons of total live biomass for forests of the Urals region (average densities by forest enterprises, expressed in tons per hectare of dry matter) obtained by different methods: *x*-axis indicates estimate received by Shvidenko et al. (2007) and line 2 (*solid*) corresponds to these estimates; *pink circles*, data received by Usoltsev's method (1998, 2007); and line 1 (*dashed*) indicates mean of these data

An assessment of two pools of *dead biomass* (coarse woody debris [CWD] and dead roots [DR]) is less certain: average estimates of uncertainty provided by two independent methods amounted to ±16 and 24%, respectively. Thus, taking into account that the LB, CWD, and DR in forests of the study region comprise 81%, 8%, and 11% of the total forest biomass, the uncertainty of the total biomass stock (for a single year of the account) is estimated at ~±4–5%. From this, the change in biomass stock between two inventories is estimated with an average uncertainty of ~±6 to 7%. Results delivered by other methods, such as radar and optical satellite instruments and dynamic global vegetation models (DGVMs), are more uncertain. In addition, these methods face large methodological problems regarding a formal definition of uncertainties.

Formal assessment of the uncertainty of the *soil carbon pool* for the region is difficult because of lack of data, which ideally would be temporally and spatially distributed, particularly over the vast remote territories. A soil map of Russia (Fridland 1989) at 1:2.5 million scale with a dataset of average characteristics by soil types still remains a major source of soil information for the country. For the study region, the soil map was subsequently modified to 1:1 million scale using additional information from different sources. However, drawing up the original sheets of the 1:1 million scale soil map took a long time up to half a century ago. This makes use of expert assumptions for assessing the uncertainties inevitable, and those assumptions might substantially affect the conclusions. Our calculations show that uncertainties of assessment of the soil carbon pool are at the level of 15–20%. The estimation of the soil carbon pool for the region is about 31 Pg C. This gives uncertainties of about ±5 Pg C, with unknown systematic errors; moreover, the signal of change between two consequent estimates can be detected if this exceeds ~7 Pg C. Clearly, this makes such results impractical for verified FCA. Another way of detecting change in the soil carbon stock is by using appropriate process-based models. However, the uncertainty of the latter cannot be properly quantified. Assumption of an equilibrium state of soil organic carbon generates a substantial bias of an unknown value. Attempts to quantify such a bias using aggregated indicators of transformation of forest land and disturbance regimes lead to significant but very approximate values (Shvidenko and Nilsson 2003). Thus, although currently available information allows useful results to be obtained from the pool-based method, it cannot satisfy the main requirements for verified FCA. Note that the above considerations put in doubt any application in the post-Kyoto world of the "Average Carbon Stock" method recommended by some publications (e.g., Kirschbaum and Cowie 2004), at least for vast boreal regions.

3.2 Uncertainties of major fluxes

In theory, Net Primary Production (NPP) is defined as the difference between gross photosynthesis and autotrophic respiration of ecosystems. However, the numerous methods of field measurement of NPP in Northern Eurasian forests not only were almost all based on consecutive destructive measurements with a time interval of weeks and months but also measured only part of NPP in the plant tissues allocated. Much NPP (root exudates, volatile organic compounds, others), comprising up to 20–25% of the total NPP (Isidorov and Povarov 2001; Vogt et al. 1986), was not measured. Other barely quantified uncertainties are also inherent in these data

(Usoltsev 2007). Thus, the available datasets of NPP field measurements in Russian forests, which include more than 1,000 sample plots, contain a bias of unknown value. The above information problems and the use of different methods led to threefold differences in the reported estimates of the average NPP of Russian forests: from 204 to 614 g C m^{-2} $year^{-1}$ (Shvidenko et al. 2008b).

Attempting to gain unbiased estimates, we developed a new semi-empirical method for assessing forest NPP. This method is based on a spatially distributed system of models of biological productivity of forest ecosystems by major forest-forming species (Shvidenko et al. 2007). We assume that this method has no recognized bias. Uncertainty of the method is defined by: (1) spatial and parametric incompleteness of the modeling system used for NPP simulation (regional representation of models by regions, tree species, and forest types; reliability of forest inventory data, etc.); (2) accuracy of ecological indicators used in the model (e.g., life span of fine roots and needles; share of disturbed part of NPP; etc.); and (3) difference in seasonal weather of an individual year from the many-year average climatic indicators.

The method is sufficiently resilient to varied input information; the most sensitive parameters are the life span of fine roots and needles. The application of the system above to the land cover of 2003 at the polygon level and aggregation of the results by ecoregion and the region as a whole gave the following results: total forest NPP 3.06 ± 0.15 (here and below, in Mg C ha^{-1} $year^{-1}$), that is, the relative uncertainty is $\sim\pm5\%$. Of this total, above-ground wood, green parts, and below-ground live biomass are assessed at 0.550 ± 0.032; 1.293 ± 0.106; and 1.222 ± 0.130, respectively. This means that annual forest NPP is defined, quite reliably, at the level of $\pm6\%$ for the part allocated in above-ground live biomass and $\pm11\%$ for below-ground. However, it should be pointed out that all models used were parametrized based on many-year average data of measurements. Thus, these results do not include the impacts of seasonal climate specifics on forest NPP.

A comparison of the results mentioned above with recent NPP estimates by different modeling approaches for 150 forest enterprises in the Urals region (the same area used above for live biomass assessments) reveals interesting results (Fig. 3). Application of multi-dimensional equations developed by Usoltsev (2007) gave a result very close to that obtained by the method applied in this study—only 8% lower (line 2 in Fig. 2). For this area, Usoltsev (2007) examined a simplified method developed in Russia (Utkin et al. 2003; Zamolodchikov and Utkin 2000)

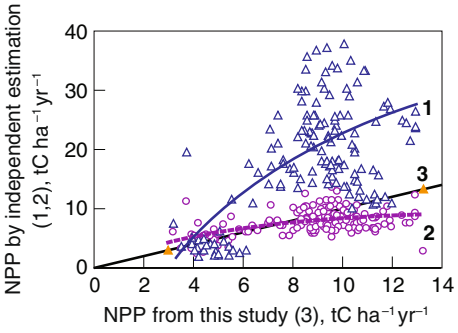

Fig. 3 Estimates of forest NPP obtained by different methods (average densities for 150 forest enterprises, tons per hectare per year of dry matter). *1 Triangle markers* method of Zamolodchikov and Utkin (2000) calculated by Usoltsev (2007); *2 circle markers* method of Usoltsev (2007); *3 solid line* method of Shvidenko et al. (2004)

and obtained the results averaged by line 1. This latter estimate produced a roughly twofold overestimation (+118%) for the result of this study.

Heterotrophic respiration of forest ecosystems includes two components: heterotrophic soil respiration (HSR) and the flux caused by decomposition of coarse woody debris (DEC). Average values of HSR were calculated by soil type, dominant species, and ecoregion based on the IIASA database which contains ~650 sets of field measurements in Northern Eurasia. A substantial part of the study region has not been subject to measurement, and we used all available measurements from similar soil and forest classes of other regions of the country (for example, Kurganova 2002; Mukhortova 2008 etc.). We made the assumption that the variation in the HSR fluxes measured outside the region is 30% higher than the variability of the fluxes measured within the region. For corrections of HSR for each forest polygon, the regression between NPP and HSR by dominant species within each ecoregion was used. Uncertainty of estimation of HSR depends on:

1. Amount, seasonal and parametric completeness, and spatial distribution of in situ measurements;
2. Understanding of the processes that control total soil respiration and its separation into autotrophic and heterotrophic parts (where substantial uncertainties exist. See, for example, Bond-Lamberty et al. (2004); and
3. Reliability of spatial delineation of basic units of calculation (soil polygons) and their compatibility with vegetation polygons. The overall average forest HSR for the region was estimated to be 2.16 ± 0.19 Mg C ha^{-1} year^{-1} (i.e., relative uncertainty is ~±9%) Uncertainty of HSR in this study was substantially lower than in studies for the whole of Russia defined by Gusti and Jonas (this volume) which can be explained by the availability of more detailed information and different methods of uncertainty estimation.

Uncertainty of *the decomposition flux* was estimated based on a simple model, $DEC = M_{CWD} \bullet \delta_{ji}$, where M_{CWD} is storage of coarse woody debris (CWD) in a polygon and δ_{ij} ($i = 1, \ldots, 9$; $j = 1, 2$) is a coefficient of decomposition by nine bioclimatic zones and two classes of CWD. Uncertainties of these two components were estimated at ±16% and 14% based on results of measurements and different auxiliary sources, that gave the estimate of DEC at 0.219 ± 0.047 Mg C ha^{-1} year^{-1} (i.e. the relative uncertainty is ~±22%).

The assessment of *the fluxes to the hydrosphere* (FHYD) was made by combining two methods: (1) based on measurements of the amount of dissolved and particulate organic carbon in rivers and other water reservoirs; and (2) by using measurements of carbon concentration in the soil solution. The average estimate was 0.049 ± 0.011 Mg C ha^{-1} year^{-1} (23%). Direct empirical data for assessing *the fluxes to the lithosphere* (FLIT) were scarce, and the assessment of this indicator was mostly made in a heuristic way based on all available data from the boreal biome. The estimated uncertainty of FLIT (0.017 ± 0.005 Mg C ha^{-1} year^{-1} or ~30%) contains substantial assumptions and expert components.

Major types of *disturbances* (DC) included in the analysis were fire, insect and disease outbreaks, and harvest and consumption of wood products. Carbon emissions due to natural and human-induced disturbance (D) and corresponding uncertainties were estimated by the method described in Shvidenko and Nilsson (2000), Kajii et al. (2002), Soja et al. (2004), French et al. (2004) and McRae et al. (2006).

The main factors affecting uncertainties of the emissions caused by disturbances, include area by type of D; severity of D and its impact on the amount of consumed organic matter; reliability of estimation of gas composition, particularly, after fire; and way of estimating post-disturbance fluxes (most publications on the topic do not consider this flux). The impacts of these factors vary for different types of D. Estimated uncertainties were: direct emissions due to fire 37.3 ± 8.6 Tg C year^{-1} (or 23%); harvest (including impacts of logging, wood removal, and decomposition of previously produced wood products) 20.6 ± 5.0 Tg C year^{-1} (24%); and direct emissions due to insect and disease outbreaks 2.2 ± 0.8 Tg C year^{-1} (36%). This means that uncertainty of the total flux due to all accounted-for D is estimated to be 60.1 ± 10.1 Tg C year^{-1} (17%). The average value of the flux DC for all forest area in 2003 is estimated to be 0.337 ± 0.057 Mg C year^{-1} ha^{-1}, or 17%. Note that the extent of wild fire for the year considered (2003) was about three times higher than the many-year average for the region.

3.3 Uncertainty of aggregated fluxes

As follows from the results above, Net Ecosystem Production (NEP) of the region's forest ecosystems is estimated to be 0.62 ± 0.23 Mg C ha^{-1} year^{-1} (the relative uncertainty ∼37%) and Net Biome Production (NBP) 0.28 ± 0.25 Mg C ha^{-1} year^{-1} (89%) or ∼49 Tg C year^{-1} for the region The total NBP for all vegetation of the region comprises 75 Tg C year^{-1}, if the complete technological lifecycle of plant products is considered, and 110 Tg C year^{-1} if the consumption of plant products (that is common in ecological estimations) is not included in the accounting (Shvidenko et al. 2005). Thus, forest NBP comprises two-thirds of the total. All these estimates are calculated for an individual year, while the parametrization of the models used was provided based on measurements over a long period of time (sometimes several decades). This eliminates an unaccounted-for part of the variability of NEP and NBP that depends on differences in weather conditions during the year of the accounting and average long-period indicators. Responses of plant and ecosystem physiology to weather conditions are indicated in many studies and used in numerous models of various types (Dunn et al. 2007). Most interactive vegetation-climate models usually represent respiration as a strongly increasing function of temperature, with photosynthesis assumed to be a function of light, subject to limitation by temperature, length of growing season, and availability of water and nutrients. Some studies indicate the crucial impact of temperature in cold regions, for example, Liski et al. (2003); Lucht et al. (2002). This encourages the use of seasonal climatic indicators to correct major components of the FCA, primarily NPP and HR.

We provided statistical analysis of dependencies of NPP and HSR of both the Siberian and entire Russian forests on different climatic indicators. About 20 indicators, such as average annual temperature and precipitation; length of growth season with daily temperature >0°C, >5°C and >10°C; sum of temperature, precipitation and hydro-thermal coefficient by Seljaninov for the above three periods; temperature of the warmest month, etc., were examined. As a general conclusion, corresponding regressions are statistically significant, but the correlations are low. For example, the multiple correlation coefficients for total soil respiration were within the limits of 0.5–0.7 (Mukhortova 2008). One of the probable explanations for this result may

stem from the incompleteness of simplified functional representations or the need to use more frequent (e.g., daily) climatic indicators.

Climatic variation is directly responsible for short- but not long-term variation in forest-atmosphere carbon exchange (Richardson et al. 2007). Factors acting over long time scales, for example, soil moisture regime and water table depth, substantially control the carbon budget on annual time scales in boreal forests and peatlands. In particular, elevated soil moisture causes a decrease in overall respiration, which leads to decreased NEE; the long-term ecosystem water balance, and particularly, the water table depth may explain much of the interannual variability and trends observed (Dunn et al. 2007). Nevertheless, our analysis shows that the introduction of seasonal weather corrections decreases the uncertainty of major carbon fluxes by about one-third.

Selection of a reasonable length of period for reporting results of the FCA is also important. Gathering information for large regions on an annual basis is expensive and resource-consuming. The operational supply of some data (e.g., changes in land use–land cover) is difficult and requires the development and implementation of integrated observing systems, which still do not exist in Northern Eurasia. Conversely, in order to be used in different climate change negotiations and decisions, FCA results are required for given periods (e.g., 5 years) rather than annually, as the latter contain additional noise and seasonal variation caused by weather and other specific features of individual years. To conclude, the improved estimates for a 5-year period have uncertainties at the level of 15% for NEP and 30% for NBP of forest ecosystems of the region studied.

We would like to point out that all relative uncertainties above (expressed as percentages of estimated means) are reasonable for illustrative purposes. Overall, they could have a limited meaning in measuring the reliability of the account, as they properly characterize variability of fluxes that differ substantially from 0.

3.4 Comparative analysis with other approaches

The results of carbon accounting obtained by the landscape-ecosystem approach are impacted by a number of assumptions and expert estimates that hinder a strict statistical validation of uncertainties. Thus, independent control of the intermediate and final results is an important procedure for assessing the uncertainty. One way to do this is a non-contradictory closing of the balance of the carbon budget. The second way is to build independent estimates into the comparative analysis. Unfortunately, there are very few independent results for the study region. To illustrate the variation among the results, we use some comparisons (below) for the entire Russian forests.

Dynamic Global Vegetation Models (DGVMs) explicitly describe major physiological processes in ecosystems. Basically, only DGVMs or other process-based models can serve as a tool to predict the interaction between vegetation and the environment. However, there are a number of reasons why it is not feasible to use DGVMs for formal assessment of the uncertainties, for instance:

1. They provide an over-simplified description of the land cover (as most models have a very limited number of plant functional types, they cannot give a proper description of ecosystem diversity at a regional level);
2. Most of the models are oriented toward potential rather than actual vegetation cover;

3. They lack or have an incomplete description of disturbances and "artificial" (e.g., agricultural) systems. Nevertheless, recent developments show substantial progress and promising prospects for the future (Grace et al. 2007).

The application of 17 DGVMs previously analyzed by Cramer et al. (1999), to all Russian forests gave the average NPP at 338 g C ha^{-1} $year^{-1}$ (M. Gusti, personal communication), while a landscape-ecosystem estimate is 297 g C ha^{-1} $year^{-1}$ (Shvidenko et al. 2008a), that is, about 14% higher. However, the variability of estimates given by the individual models was very high—from 20% to 70% depending on the climatic zone. Based on a "regionalized" version of the Lund–Potsdam–Jena model (including actual land cover, impact of fire, and a new permafrost-hydrological module), Beer et al. (2006) produced estimates of important components of the carbon budget that were very close to the results based on forest inventory data (Shvidenko and Nilsson 2003).

The eddy covariance method presents a unique possibility to directly measure Net Ecosystem Productivity (in the form of accumulated Net Ecosystem Exchange), as well as fluxes of water and energy in response to variability in environmental conditions. Although the method has a clear strength in terms of uncertainty estimation (the net flux is the sum of individual half-hourly or hourly flux measurements rather than a small difference between several large fluxes), the results are impacted by a sophisticated interconnection of random and systematic errors (Falge et al. 2001; Goulden et al. 1996; Moncrieff et al. 1996; Papale et al. 2006; Papale and Valentini 2003). The eddy covariance method is accurate when atmospheric conditions are steady, the underlying vegetation is homogeneous, and towers are situated on flat terrain for an extended distance upwind. Under such ideal conditions the error of annual NEE of CO_2 was reported to be less than $\pm$ 50 g C m^{-2} $year^{-1}$ (Baldocchi 2003). Some elements of field measurement techniques (e.g., nighttime fluxes in dense canopies, flow distortion over heterogeneous terrain, filling in measurement gaps) need to be developed in the future to achieve a more reliable estimation of uncertainties. Complete model validation, particularly over the full annual cycle, requires additional information on the balance between assimilation and decomposition processes (Friend et al. 2007). The method does not measure NPP directly, and rather complicated calculation schemes that exploit unjustified assumptions are used (e.g., Schwalm et al. 2007). One of the biggest methodological problems of eddy covariance measurements is upscaling the results to large areas. The footprint of an individual tower is typically 1 km $\times$ 1 km, and within Russia there were only 17 measuring points for all vegetation types in 2007. A number of advanced methods for upscaling results of measurements have been suggested (e.g., Papale and Valentini 2003). However, they cannot compensate for the lack of spatially distributed information. That is why the major value of eddy covariance methodology is considered to be the supply of data for global cycle modeling and evaluation process representation, rather than in providing unbiased estimates of NEP for large territories (Friend et al. 2007).

Inverse modeling of atmospheric concentration is the sole approach that presents the possibility of a top-down assessment of exchange between land and the atmosphere. The estimates of CO_2 fluxes include mainly the land use change and net ecosystem uptake for land regions. Uncertainties of the approach are basically defined by the amount and distribution of measurement stations and by the imperfection of the transport models used. The errors for observation over the land

Table 1 Assessment of fluxes for boreal Asia by inverse modeling

Source	Flux (Pg C year^{-1})	Period	Comments
Maksyutov et al. (2003)	-0.63 ± 0.36[a]	1992–1996	Includes observations in Siberia
Gurney et al. (2003)	-0.58 ± 0.53	1992–1996	Average flux from 17 transport models
Baker et al. (2006)	-0.37 ± 0.24	1988–2003	
Patra et al. (2006)	-0.33 ± 0.45	1999–2001	All sites; 16 transport models were used; uncertainties "within" models were ± 0.78
Average flux	-0.48 ± 0.41		Upscaling the result of this study for all boreal Asia gives ~ 0.40 Pg C year^{-1})

[a]The reported uncertainties are "between" models

are generally larger than those for observation over the ocean (Patra et al. 2006). The amount of measurements in boreal Asia is very small, which substantially impacts assessed uncertainties at the regional level. Recently, a number of results from inverse modeling have been reported for terrestrial ecosystems of boreal Asia, namely, the area of the continent north of latitude 50 (Table 1). The results are rather consistent, ranging from -0.33 to -0.63 Pg C year^{-1}, with the overall average being about -0.48 Pg C year^{-1}, while the uncertainties, both "within-model" (the multi-model root mean square of the flux uncertainties) and "between-model" (1 standard deviation of the estimated fluxes by different transport models) remain high. Assuming the approximate area of boreal Asia of 1.1×10^9 ha and taking into account the area of the study region, we gain results that are very close to the average obtained by inverse modeling (Table 1).

Overall, it can be concluded that comparison of the results obtained by the LEA with published data derived from flux measurements, some global vegetation models, and by inverse modeling showed a general consistency in terms of the sign and magnitude of NBP. This is in line with papers published on the consistency of results derived from process-based models, remote-sensing-based observations, and inversion of atmospheric data (Friend et al. 2007). For a number of reasons, our comparison is approximate; for example, the regions and time periods of the assessments did not coincide exactly; there was a lack of explicit gradients for upscaling of flux measurements in situ; and there were differences in some of the main definitions used.

4 Conclusion

Overall, this study concludes that verified FCA for forests of large boreal regions, while possible, requires a systems approach and a substantial effort to carry through. However, some precautions should be taken and a number of questions need to be resolved. The information for large regions already in existence tends to be unsatisfactory for an accurate assessment of the final results (i.e., for NBP and, to some extent, NEP) for individual years; moreover, the reported period should be compatible with the practical possibilities of detecting changes in land use and the distribution of natural and human-induced disturbances. Empirical and semi-empirical models are based on multi-year sets of measurements and require envi-

ronmental and climatic indicators of individual seasons and temporal trends to be introduced.

The process of multiple constraints requires a "convergence" of different methodologies, for example: proper regionalization of dynamic process-based vegetation models; search for common gradients to upscale flux measurements; advances in field measurement techniques. The results of the study, together with recent methodological developments in carbon accounting of terrestrial ecosystems reveal substantial potential for future improvements. There is an evident convergence of empirical (e.g., landscape-ecosystem) approaches and process-based models. However, the major approaches to carbon accounting have different strengths and weaknesses. Although the landscape-ecosystem approach, may have been suitable as a past and present background for accounting, only process-based models are able to provide satisfactory predictions in today's changing world. Geo-referenced and quantitative descriptions of land cover classes, an obligatory component of the landscape-ecosystem approach, could serve as a spatial gradient for upscaling the "point" flux measurements.

The idea of verified FCA and understanding of the fuzzy essence of FCA for large territories has substantial implications for the overall philosophy and major methodological decisions behind carbon accounting as a whole. It is vital to understand that heuristic methods and expert estimates cannot be avoided within FCA, which demonstrates the need for further developments in assessing uncertainties. Indeed, analysis of the "uncertainties of uncertainties" becomes no less important than assessing uncertainties of the major components of FCA exercises themselves. The estimation of uncertainties by "conventional" methods of mathematical statistics (e.g., by those recommended by IPCC in Best Practice Guidelines 2006) could provide conclusions that are quite far from reality.

Some theoretical improvements and developments are needed. Harmonizing and the mutual constraints of individual results delivered by different methods should be provided by strict mathematical methods. This is an important task for the future.

Relevant economic problems ("cost-effectiveness of uncertainties") are extremely important in terms of understanding the required FCA certainty levels. Limits of relevant use of standard normal theory for assessing heterogeneous and "contaminated" data sets should be clearly defined and appropriate statistical approaches introduced. Some "conventional" statistical agreements should be reconsidered. For instance, the typically used high confidential intervals (0.9 or even 0.95) seem excessive for carbon accounting, because this could generate the impression of an unsatisfactory accounting level in the wider public, specifically policymakers.

This paper considered uncertainties of a forest carbon budget. The inclusion of other greenhouse gases and other land classes in the accounting leads to particular problems (especially for land classes for which there are no long-term series of biometric inventories). A way of transitioning to verified accounting of terrestrial carbon budgets and other major greenhouse gases would be to develop integrated observing systems combined with existing national systems for the accounting of natural resources, such as land, forest, and wetlands.

References

Baker DF, Law RM, Gurney KR, Rayner P, Peylin P, Denning AS, Bousquet P, Bruhwiler L, Chen YH, Ciais P, Fung IY, Heimann M, John J, Maki T, Maksyutov S, Masarie K, Prather M, Pak

B, Taguchi S, Zhu Z (2006) TransCom 3 inversion intercomparison: impact of transport model errors on the interannual variability of regional CO_2 fluxes, 1988–2003. Glob Biogeochem Cycles 20(1):GB1002.1–GB1002.17
Baldocchi DD (2003) Assessing the eddy covariance technique for evaluating carbon dioxide exchange rates of ecosystems: past, present and future. Glob Chang Biol 9:479–492
Beer C, Lucht W, Schmullius C, Shvidenko A (2006) Small net carbon dioxide uptake by Russian forests during 1981–1999. Geophys Res Lett 33:L15403
Bond-Lamberty B, Wang C, Gower ST (2004) A global relationship between the heterotrophic and autotrophic components of soil respiration? Glob Chang Biol 10:1756–1766
Chen W, Chen J, Liu J, Cihlar J (2000) Approaches for reducing uncertainties in regional forest carbon balance. Glob Biogeochem Cycles 14:827–838
Cramer W, Kicklighter DW, Bondeau A, Moore Iii B, Churkina G, Nemry B, Ruimy A, Schloss AL (1999) Comparing global models of terrestrial net primary productivity (NPP): overview and key results. Glob Chang Biol 5:1–15
Dunn AL, Barford CC, Wofsy SC, Goulden ML, Daube BC (2007) A long-term record of carbon exchange in a boreal black spruce forest: means, responses to interannual variability, and decadal trends. Glob Chang Biol 13:577–590
Falge E, Baldocchi D, Olson R, Anthoni P, Aubinet M, Bernhofer C, Burba G, Ceulemans R, Clement R, Dolman H, Granier A, Gross P, GruM€nwald T, Hollinger D, Jensen NO, Katul G, Keronen P, Kowalski A, Lai CT, Law BE, Meyers T, Moncrieff J, Moors E, Munger JW, Pilegaard K, Rannik U, Rebmann C, Suyker A, Tenhunen J, Tu K, Verma S, Vesala T, Wilson K, Wofsy S (2001) Gap filling strategies for defensible annual sums of net ecosystem exchange. Agric For Meteorol 107:43–69
FFS'RF (1995) Manual of forest inventory and planning in the forest fund of Russia, field work, vol 1. Federal Forest Service, Moscow (in Russian)
French NHF, Goovaerts P, Kasischke ES (2004) Uncertainty in estimating carbon emissions from boreal forest fires. J Geophys Res 109:D14S08
Fridland VM (1989) Soil map of the USSR. Committee on Cartography and Geodesy, Moscow
Friend AD, Arneth A, Kiang NY, Lomas M, Ogee J, Roedenbeck C, Running SW, Santaren JD, Sitch S, Viovy N, Ian Woodward F, Zaehle S (2007) FLUXNET and modelling the global carbon cycle. Glob Chang Biol 13:610–633
GCP (2003) Global Carbon Project 2003 Science framework and implementation. Earth System Science Partnership IGBP, IHDP, WCRP, DIVERSITAS. In: Global carbon project report no 1
Goulden ML, Munger JW, Fan SM, Daube BC, Wofsy SC (1996) Measurements of carbon sequestration by long-term eddy covariance: methods and a critical evaluation of accuracy. Glob Chang Biol 2:169–182
Grace J, Nichol C, Disney M, Lewis P, Quaife T, Bowyer P (2007) Can we measure terrestrial photosynthesis from space directly, using spectral reflectance and fluorescence? Glob Chang Biol 13:1484–1497
Gurney KR, Law RM, Denning AS, Rayner PJ, Baker D, Bousquet P, Bruhwiler L, Chen YH, Ciais P, Fan S, Fung IY, Gloor M, Heimann M, Higuchi K, John J, Kowalczyk E, Maki T, Maksyutov S, Peylin P, Prather M, Pak BC, Sarmiento J, Taguchi S, Takahashi T, Yuen CW (2003) TransCom 3 CO_2 inversion intercomparison: 1. Annual mean control results and sensitivity to transport and prior flux information. Tellus Ser B Chem Phys Meteorol 55:555–579
Houghton RA (2003) Why are estimates of the terrestrial carbon balance so different? Glob Chang Biol 9:500–509
IPCC (2006) 2006 IPCC guidelines for national greenhouse gas inventories. Agriculture forestry and other land use. In: Eggleston S, Buendia L, Miwa K, Ngara T, Tanabe K (eds) IPCC National Greenhouse Gas Inventories Programme and IGES, vol 4. Japan
Isidorov VA, Povarov VG (2001) Phytogenic volatile organic compounds emission by Russian forests. Ecol Chem 9:10–21
Kajii Y, Kato S, Streets DG, Tsai NY, Shvidenko A, Nilsson S, McCallum I, Minko NP, Abushenko N, Altyntsev D, Khodzer TV (2002) Boreal forest fires in Siberia in 1998: estimation of area burned and emissions of pollutants by advanced very high resolution radiometer satellite data. J Geophys Res 107(D24):4745
Kirschbaum MUF, Cowie AL (2004) Giving credit where credit is due. A practical method to distinguish between human and natural factors in carbon accounting. Clim Change 67: 417–436
Kurganova I (2002) Carbon dioxide emissions from soils of Russian terrestrial ecosystems. In: Interim report IR-02-070, International Institute for Applied System Analysis, Laxenburg, Austria

Lapenis A, Shvidenko A, Shepaschenko D, Nilsson S, Aiyyer A (2005) Acclimation of Russian forests to recent changes in climate. Glob Chang Biol 11:2090–2102

Liski J, Nissinen A, Erhard M, Taskinen O (2003) Climatic effects on litter decomposition from arctic tundra to tropical rainforest. Glob Chang Biol 9:575–584

Lucht W, Prentice IC, Myneni RB, Sitch S, Friedlingstein P, Cramer W, Bousquet P, Buermann W, Smith B (2002) Climatic control of the high-latitude vegetation greening trend and Pinatubo effect. Science 296:1687–1689

Maksyutov S, Machida T, Mukai H, Patra PK, Nakazawa T, Inoue G (2003) Effect of recent observations on Asian CO_2 flux estimates by transport model inversions. Tellus Ser B Chem Phys Meteorol 55:522–529

McRae DJ, Conard SG, Ivanova GA, Sukhinin AI, Baker SP, Samsonov YN, Blake TW, Ivanov VA, Ivanov AV, Churkina TV, Hao WM, Koutzenogij KP, Kovaleva N (2006) Variability of fire behavior, fire effects, and emissions in Scotch pine forests of central Siberia. Mitig Adapt Strategies Glob Chang 11:45–74

Mitrofanov DP (1977) Chemical composition of forest plant in Siberia. Russian Academy of Sciences, Novosibirsk (in Russian)

Moncrieff JB, Malhi Y, Leuning R (1996) The propagation of errors in long-term measurements of land-atmosphere fluxes of carbon and water. Glob Chang Biol 2:231–240

Mukhortova L (2008) Decomposition of organic matter and carbon fluxes in forest ecosystems of Siberia. In: Unpublished manuscript, International Institute for Applied Systems Analysis, Laxenburg, Austria

Newell RG, Stavins RN (2000) Climate change and forest sinks: factors affecting the costs of carbon sequestration. J Environ Econ Manage 40:211–235

Nilsson S, Shvidenko A, Jonas M, McCallum I, Thomson A, Balzter H (2007) Uncertainties of a regional terrestrial biota full carbon account: a systems analysis. Water Air Soil Pollut Focus 7:425–441

Papale D, Valentini R (2003) A new assessment of European forests carbon exchanges by eddy fluxes and artificial neural network spatialization. Glob Chang Biol 9:525–535

Papale D, Reichstein M, Aubinet M, Canfora E, Bernhofer C, Kutsch W, Longdoz B, Rambal S, Valentini R, Vesala T, Yakir D (2006) Towards a standardized processing of net ecosystem exchange measured with eddy covariance technique: algorithms and uncertainty estimation. Biogeosciences 3:571–583

Patra PK, Gurney KR, Denning AS, Maksyutov S, Nakazawa T, Baker D, Bousquet P, Bruhwiler L, Chen YH, Ciais P, Fan S, Fung I, Gloor M, Heimann M, Higuchi K, John J, Law RM, Maki T, Pak BC, Peylin P, Prather M, Rayner PJ, Sarmiento J, Taguchi S, Takahashi T, Yuen CW (2006) Sensitivity of inverse estimation of annual mean CO_2 sources and sinks to ocean-only sites versus all-sites observational networks. Geophys Res Lett 33(5):L05814.1–L05814.5

Richardson AD, Hollinger DY, Aber JD, Ollinger SV, Braswell BH (2007) Environmental variation is directly responsible for short- but not long-term variation in forest-atmosphere carbon exchange. Glob Chang Biol 13:788–803

Schmullius C, Santoro M (2005) SIBERIA-II. Multi-sensor concepts for greenhouse gas accounting of Northern Eurasia. Contract number EVG1-CT-2001-0048, EC Deliverable, Final Report, In EC Environment and Climate Program

Schwalm CR, Black TA, Morgenstern K, Humphreys ER (2007) A method for deriving net primary productivity and component respiratory fluxes from tower-based eddy covariance data: a case study using a 17-year data record from a Douglas-fir chronosequence. Glob Chang Biol 13:370–385

Shvidenko A, Nilsson S (2000) Fire and the carbon budget of Russian forests. In: Kasischke ES, Stock BJ (eds) Fire, climate change, and carbon cycling in the boreal forest. Springer, Berlin, pp 289–311

Shvidenko A, Nilsson S (2002) Dynamics of Russian forests and the carbon budget in 1961–1998: an assessment based on long-term forest inventory data. Clim Change 55:5–37

Shvidenko A, Nilsson S (2003) A synthesis of the impact of Russian forests on the global carbon budget for 1961–1998. Tellus Ser B Chem Phys Meteorol 55:391–415

Shvidenko A, Schepaschenko D, Nilsson S, Bouloui Y (2004) A system of models of growth and productivity of forests of Russia. Tables and models of bioproductivity. Forestry Management 2:40–44 (in Russian)

Shvidenko A, McCallum I, Nilsson S (2005) Data, results and assessment of full greenhouse gas accounting for the major GHG's for 2002/2003. In: Siberia II (Multi-sensor concept for greenhouse gas accounting in Northern Eurasia) 5th Framework Programme, Generic

Activity 72: Development of Generic Earth Observation Technologies, Laxenburg, Austria
Shvidenko A, Schepaschenko D, Nilsson S, Bouloui Y (2007) Semi-empirical models for assessing biological productivity of Northern Eurasian forests. Ecol Model 204:163–179
Shvidenko A, Schepaschenko D, Nilsson S (2008a) Materials for learning current biological production of Russian forests. In: International seminar on sustainable management of Russian forests, December 6 to 7, 2007, Proceedings, Krasnoyarsk, Russia, pp 7–37 (in Russian)
Shvidenko AZ, Schepashchenko DG, Vaganov EA, Nilsson S (2008b) Net primary production of forest ecosystems of Russia: a new estimate. Dokl Earth Sci 421:1009–1012
Soja AJ, Cofer WR, Shugart HH, Sukhinin AI, Stackhouse PW Jr, McRae DJ, Conard SG (2004) Estimating fire emissions and disparities in boreal Siberia (1998–2002). J Geophys Res 109:D14S06
Usoltsev VA (1998) Forming databanks about live biomass of forests. Russian Academy of Sciences, Ekaterinburg
Usoltsev VA (2007) Biological productivity of Northern Eurasia's forests. Russian Academy of Sciences, Ekaterinburg
Utkin AI, Zamolodchikov DG, Pryazhnikov AA (2003) Methods for determining carbon deposition in phytomass and net productivity of forests: an example of Belarus. Lesovedenie 1:48–57
Vogt KA, Grier CC, Vogt DJ (1986) Production, turnover, and nutrient dynamics of above- and belowground detritus of world forests. Adv Ecol Res 15:303–377
Waggoner, PE (2009) Forest inventories. Discrepancies and uncertainties. Discussion paper RFF DP 09-29. Resources for the Future, Washington DC. Available at http://www.rff.org/RFF/Documents/RFF-DP-09-29.pdf
Zamolodchikov DG, Utkin AI (2000) A system of conversion relations for calculating net primary production of forest ecosystems by growing stocks. Lesovedenie 6:54–63

Climatic Change (2010) 103:159–174
DOI 10.1007/s10584-010-9911-9

Terrestrial full carbon account for Russia: revised uncertainty estimates and their role in a bottom-up/top-down accounting exercise

M. Gusti · M. Jonas

Received: 5 January 2009 / Accepted: 15 June 2010 / Published online: 20 July 2010

Abstract Our research addresses the need to close the gap between bottom-up and top-down accounting of net atmospheric carbon dioxide (CO_2) emissions. Russia is sufficiently large to be resolved in a bottom-up/top-down accounting exercise, as well as being a signatory state of the Kyoto Protocol. We resolve Russia's atmospheric CO_2 balance (1988–1992) in terms of four major land-use/cover units and eight bioclimatic zones. On the basis of our results we conclude that the Intergovernmental Panel on Climate Change (IPCC) must revise its carbon balance for northern Asia. We find a less optimistic, although more realistic, bottom-up versus top-down match for northern Asia than the IPCC authors. Nonetheless, in spite of the larger uncertainties involved, our research shows that (1) there is indeed an added value in linking bottom-up and top-down carbon accounting because our dual-constrained regional carbon balance is incomparably more rigorous; and that (2) the need persists for more atmospheric measurements, including atmospheric inversion experiments, over Russia.

Electronic supplementary material The online version of this article (doi:10.1007/s10584-010-9911-9) contains supplementary material, which is available to authorized users.

M. Gusti (✉) · M. Jonas
International Institute for Applied Systems Analysis, Schlossplatz 1, 2361, Laxenburg, Austria
e-mail: gusti@iiasa.ac.at

M. Gusti
Lviv National Polytechnic University, 12 Bandery Str., 79013, Lviv, Ukraine

1 Introduction

The terrestrial biosphere is strongly bound up with climate via biophysical and biochemical processes. In particular, the terrestrial biosphere absorbs about 25% of the anthropogenic carbon dioxide (CO_2) emissions into the atmosphere, thus mitigating human-induced climate change. Currently the net land uptake, especially its distribution within the northern hemisphere, is the most uncertain component in the global carbon budget (Denman et al. 2007).

CO_2 fluxes into the atmosphere can be estimated by using either ground-based measurements and accounting (bottom-up) or by measuring concentrations of atmospheric CO_2 and inferring the fluxes causing the concentration field (top-down).[1] There is a mismatch between the two kinds of estimates, caused by incomplete accounting and uncertainties peculiar to the methods used. The two methods are independent to a certain degree and can thus be used for verification purposes if the gap between the estimates is reduced and better understood. If the top-down method is advanced to yield reliable estimates at a country scale, it can be used for verification of countries' reports of GHG emissions under current and future climate agreements like the United Nations Framework Convention on Climate Change and the Kyoto Protocol.

Our research addresses the need to close the gap between bottom-up and top-down accounting of net atmospheric CO_2 emissions to support the (dual-constrained) verification of CO_2 emissions. House et al. (2003), Nilsson et al. (2003a, b) and Rödenbeck et al. (2003a, b) pinpointed a "CO_2 accounting gap" across subglobal (continental and smaller) scales in 2003. The geographical focus of our study is on Russia, a signatory state of the Kyoto Protocol, which is large enough to be resolved in a bottom-up/top-down accounting exercise. An initial, uncertainty-focused cyclo-stationary atmospheric inversion experiment carried out at Le Laboratoire des Sciences du Climat et l'Environnement (LSCE), France, indicated that the potential exists to improve atmospheric top-down estimates if bottom-up accounting is complete (full) and uncertainties are reliable and better known. Moreover, full carbon accounting is important for implementation of policies to mitigate climate change (like the Kyoto Protocol) that can be inferred from a number of studies, particularly, by Steffen et al. (1998), Shvidenko et al. (2010), and Ciais et al. (2010).

As a basis for bottom-up estimation of the atmospheric CO_2 budget (only CO_2 fluxes of the terrestrial biosphere) we use the Full Carbon Account for Russia (Nilsson et al. 2000), hereafter FCA 2000. In new studies (since publication of FCA 2000), it has been found that some processes were not known and thus not taken into account when net primary production (NPP)[2] and heterotrophic soil respiration (HR) were being estimated. However, we expect that the process of improving estimation of these two big fluxes will, and will have to, continue, as they and their uncertainties govern the uncertainty of Russia's atmospheric CO_2 balance.

[1] For details on bottom-up versus top-down estimates of CO_2 budget see (Lemke et al. 2007, p 521).

[2] For forest and arable land.

The objective of this study was to revise uncertainties[3] of the FCA 2000, taking into account recent studies,[4] compose a revised bottom-up atmospheric CO_2 budget for bioclimatic zones in Russia (Polar Desert, Tundra, Pre-Tundra and Northern Taiga, Middle Taiga, Southern Taiga, Temperate, Forest, Steppe, Semi-Desert and Desert) for use as prior information in the atmospheric inversion experiments, upscale it to Eurasia and the extratropical northern hemisphere for comparison with top-down estimates, and thereby advance the IPCC's understanding of the land–atmosphere CO_2 fluxes over northern Asia (Denman et al. 2007: Figure 7.7). This study incorporates some of the findings of a thorough study of a region in Central Siberia, which is discussed by Shvidenko et al. (2010), and is complementary to the European carbon budget assessment, presented by Ciais et al. (2010), and the North American Carbon Program.

We start the Methodology (Section 2 with subsections) by modifying the bottom-up estimate of the CO_2 fluxes over northern Asia from (Denman et al. (2007): Figure 7.7) and uncertainty estimate of the net land–atmosphere CO_2 fluxes for Russia, then consider the CO_2 balance fluxes in more detail. In the Results and Discussion section (Section 3) we present results and short discussions for each flux followed by general discussion on the uncertainty estimates; we then present modified bottom-up estimate of the CO_2 fluxes over northern Asia followed by discussion. In the fourth section we summarize our findings and make conclusions.

2 Methodology

2.1 General methodology overview

We modified the North Asia section in Figure 7.7 of the IPCC Fourth Assessment Report (FAR) (Denman et al. 2007: Figure 7.7). We substituted our current estimate for land-use/cover (Jonas and Gusti 2010) for the bottom-up CO_2 flux estimate by Shvidenko and Nilsson (2003: Table 6). We added together the national total net CO_2 flux for Russia and an estimate by Fang et al. (2001: Table 2) for China taking into account uncertainties. We compared the bottom-up estimate with top-down estimates by Gurney et al. (2002, 2003); Peylin et al. (2005) and Rödenbeck et al. (2003a, b), which correspond to the post-Pinatubo period, 1992–1996, shown in the figure as green symbols.

We estimated total bottom-up fluxes of CO_2 by bioclimatic zone as an arithmetic sum of the following fluxes: NPP, HR, disturbance, and consumption. To estimate the uncertainties we assumed that correlation between the disturbance and consumption fluxes equals one within each bioclimatic zone and that the correlation between other

[3]Under uncertainty we consider combination of random errors (inaccuracy), systematic errors (biases or imprecision), and lack of knowledge. For details on the uncertainty concept see for example (Jonas and Nilsson 2007).

[4]For example, comparative studies of soil respiration measurement methods; new methods for NPP estimation; new estimates of Russian carbon budget; new studies of soil autotrophic respiration; results of numeric simulation experiments; new studies on uncertainties of forest fire emission estimates, etc.

fluxes is negligible. The methodology of the uncertainty estimation of the fluxes is considered in Subsections 2.2 to 2.5.

We assume that the uncertainties of the parameters studied follow Gaussian distribution. All systematic errors found were corrected, while remaining uncertainties were estimated from a conservative point of view (i.e., we tried to reveal all major sources of uncertainties and estimate their influence on the result; we also adhered to the principle that lack of knowledge or information assimilates to an increase in uncertainty). The uncertainties are estimated for a 90% confidence interval (C.I.).

2.2 NPP

2.2.1 Forest

It was found that the FCA 2000 estimate of forest NPP is biased because a few processes of organic matter production (fine root life span and root exudates) were not grasped by the methods for NPP estimation on the plot level (Shvidenko et al. 2008). Thus, for further analysis we use the new estimate of forest NPP by Shvidenko et al. (2006, 2008) and Shvidenko (2007, personal communication), which is based on a new modeling approach described in Shvidenko et al. (2007). The new estimate is on average 36% higher than the FCA 2000 estimate. Shvidenko et al. (2006, 2008) and Shvidenko (2007, personal communication) do not provide forest NPP for bioclimatic zones. We distribute the national total by the bioclimatic zones using additional information, namely, the forest NPP estimates by bioclimatic zones for the Siberia-II region (Schmullius et al. 2005; Nilsson et al. 2000) and a composition of model estimates (Cramer et al. 1999). To assess the uncertainty of the distributed NPP we found the relative distance of the new NPP to the respective NPP from the Siberia-II region, NPP from the FCA 2000, and average NPP from the models for each bioclimatic zone and chose the largest of them. We assumed that the probability that the uncertainty intervals contain true NPP is 90%. For details of the NPP distribution, see Supplementary Material.

2.2.2 Agriculture

Russia's arable land (one of the land-cover classes [LC] considered) is resolved at the national level in terms of (1) cropland comprising grain crops and crops other than grains (for which annual and perennial grass is used as a surrogate) and (2) pastures. The overall basic assumption underlying all NPP calculations is that the agricultural life cycle is 1 year (i.e., production equals phytomass).

NPP at the national scale The sources listing the statistical data (areas, yield, dry matter-to-carbon conversion factors, etc.) that were employed by Nilsson et al. (2000, p 38) for their FCA 2000 study were found appropriate. Additional knowledge with respect to relative uncertainties and their ranges could be derived from the Austrian Carbon Database, made available by Jonas and Nilsson (2002) after completion of the FCA 2000 study. The regression equations suggested by Rodin and Krylatov (1998: Table 7) using yield as input, allow the remaining parts of the plants (i.e., their above and below-ground contributions) to be estimated.

Our recalculations based on the original data and a revision of Russian harvest conditions around 1990 featured three things: (1) dry matter of annual grass had, by

mistake, been overestimated by a factor of 10; (2) spring wheat indeed serves as a good surrogate for grains and a combination of "60% perennial plus 40% annual grass" is a very good surrogate for crops other than grains; and (3) harvest losses that were considerable at that time (grains, 10–50%; crops other than grains, 15–45%; pastures, 0%) were not taken into account.

NPP at the scale of bioclimatic zones Disaggregating the recalculated, national-scale NPP value, and its uncertainty across bioclimatic zones involved three main steps: (1) an "oblast–land cover–bioclimatic zones" map overlay ("oblast" is the administrative unit to which harvest statistics refer) to determine NPP for individual bioclimatic zones; (2) deriving the linear regression NPP = f(yield) on the basis of all oblasts and assuming that it also holds for bioclimatic zones, which allows establishment of the mathematical framework to calculate consistent NPP uncertainties at that scale; and (3) applying the assumption that yield uncertainties are equal across bioclimatic zones in relative terms, an important but still missing input for this mathematical framework.

2.2.3 Wetlands, grasslands, and shrubs

Russia's wetlands comprise swamps and bogs, while grasslands and shrubs are not further disaggregated. For reasons of insufficient data, our NPP calculations followed the same simplified structure that had already been applied by Nilsson et al. (2000): NPP density X area X carbon conversion factor. However, we considered additional results that had become available concomitant with and after the FCA 2000 study, notably those from a 17-model global intercomparison experiment with the focus on NPP and its uncertainty (Cramer et al. 1999). The NPP that was modeled and the uncertainty data were assessed using a "model grid–bioclimatic zone–land cover" map overlay to derive the corresponding values for Russia and its eight bioclimatic zones (Table 1). The comparison with the FCA 2000 NPP values on the national scale shows that the model-derived NPP value is as great for swamps, greater for bogs, and smaller for grasslands and shrubs. The spread of NPP values (and uncertainties) for both Russia and its bioclimatic zones allowed us to derive uncertainties at these scales and to achieve consistency.

2.3 Soil heterotrophic respiration

Heterotrophic soil respiration (HR) is one of the fluxes that are difficult to estimate over large unpopulated areas. HR is not measured directly in field campaigns but is estimated as a difference between total soil respiration and autotrophic respiration

Table 1 Comparison of NPP and its uncertainty estimated in FCA 2000 (FCA 2000, Tables 31 and 68) and NPP and intermodel variability derived from the model intercomparison data (Cramer et al. 1999) on the national scale

Data source/ vegetation cover	Cropland	Pastures	Forest	Bogs	Swamps	Grasslands and shrubs	Total
FCA 2000 NPP, gC/m^2 year	498	379	224	226	213	278	267
FCA 2000 uncertainty, %	18	18	18	27	27	18	10
Models' NPP, gC/m^2 year	448	389	348	346	248	227	322
Intermodel variability, %	17	19	21	21	24	25	21

(or root contribution, RC). We identified and quantified the following uncertainty components in the estimation of the heterotrophic soil respiration for Russia:

- Measurement uncertainty;
- Uncertainties resulted from weak spatial representation of the Russian territory by the measurements;
- Uncertainties caused by time of the measurements;
- Uncertainties of the autotrophic soil respiration;
- Uncertainties of productive areas;
- Uncertainties due to correlations;
- Uncertainties resulting from different estimation and aggregation methods.

For the study we used a database of total soil respiration (SR) measurements compiled by Kurganova (2002) from published data. We distributed the data in a bioclimatic zone–soil–vegetation matrix to take into account major factors controlling HR (climate, soil type, and vegetation type). In each matrix element the uncertainty components were estimated.

Random errors of measurements are not included in the analysis because in the database there are only average values extracted from publications. Usually the uncertainties are low because a series of measurements is taken and the average is estimated to minimize random errors. Systematic errors (biases) depend on the measurement method. Biases have substantial influence on the result if they are not eliminated. We estimated the biases by summing up the systematic errors peculiar to the measurement methods (Hutchinson and Rochette 2003; Jensen et al. 1996; Pumpanen et al. 2004; Yim et al. 2000) used in each matrix cell.

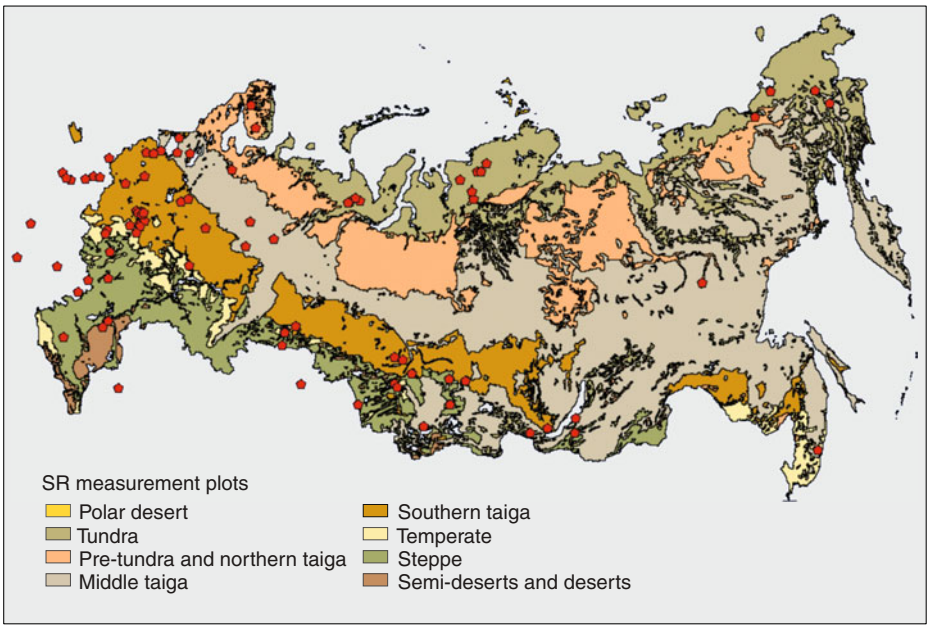

Fig. 1 Soil respiration measurement plots over bioclimatic zones

The amount of SR measurements (350 measurements are considered) is very little for the Russian territory. The measurements are distributed non-uniformly (see Fig. 1). Most of the measurements are located in the European part of Russia while, at the same time, there are no measurements in vast territory of Siberia. Some measurements are used from outside Russian territory (Byelorussia, Ukraine, and Kazakhstan). In many bioclimatic zone–soil–vegetation classes, one measurement or no measurements were taken. For such classes occupying more than 1% of country productive area, we used measurements from a similar soil–vegetation class in a neighboring bioclimatic zone or the same bioclimatic zone and vegetation type but close soil type, thereby increasing estimated uncertainty by 20%. Thus, the uncertainty is partially taken into account.

Most of the measurements were taken in 1955–1975. Use of the measurements for estimation of heterotrophic soil respiration in 1990 causes some uncertainty because of different climatic conditions. The uncertainty of a measurement presented in the database is assumed to be similar to interannual and spatial variabilities of SR that is more than 20% (Kurganova et al. 2003; Lopes de Gerenyu et al. 2005). When a few measurements are being averaged, the uncertainty decreases and has little influence on the total uncertainty. Only when a single measurement for the matrix element (bioclimatic zone–soil–vegetation) exists or all the measurements are published in 1 year an expert decision made to account for the uncertainty.

We estimated precision of the autotrophic soil respiration for different vegetation types from published measurements of the autotrophic respiration (Hanson et al. 2000; Kurganova 2002; Bond-Lamberty et al. 2004; and others; for details see Jonas and Gusti 2010). In general we selected 150 RC estimates representing different vegetation types and climate conditions. We also compared autotrophic soil respiration values using estimates of other authors on different levels of aggregation (Raich and Tufekcioglu 2000; Kurganova 2002).

Productive areas within the bioclimatic zones are uncertain, which is shown as inconsistencies when overlapping maps of bioclimatic zones, land use, and soil types or when comparing with areas used in earlier estimates of the heterotrophic soil respiration (Nilsson et al. 2000; Kurganova 2002; Stolbovoi 2003). When we estimate area-weighted averages, the area uncertainties (we consider only internal inconsistencies) contribute very little to the resulting uncertainty and are not taken into account. When estimating total fluxes of heterotrophic soil respiration from territories of bioclimatic zones in Russia, the area uncertainties are of greater importance and are taken into account. However, the area uncertainties do not influence total uncertainty substantially, as in general they are much smaller than the heterotrophic soil respiration uncertainties.

We estimated uncertainty due to application of common autotrophic respiration attributed to similar vegetation types within the bioclimatic zones and in many cases across the bioclimatic zones. This has the effect of correlating for the uncertainty estimates and is accounted for by taking a common parameter out of the parentheses when estimating the uncertainty.

Aggregated heterotrophic soil respiration (for bioclimatic zones or the entire territory) depends on the way the aggregated fluxes are calculated because of the incomplete spatial coverage of the measurements. Nilsson et al. (2000), Kurganova (2002), and Jonas and Gusti (2010) used similar SR measurement data but applied different approaches that led to different results. We combine all the estimates

on the level of the bioclimatic zones (because such values are reported by all the authors), including different aggregation techniques. We determined the accuracy (the uncertainty caused by the use of different estimation methods) and combined it with the internal uncertainty of the HR for the bioclimatic zones as two independent components. For details see Supplementary Material.

2.4 Consumption

The estimation of agricultural consumption and its uncertainty was part of our NPP calculations at the national scale. We distributed CO_2 fluxes from consumption of agricultural products, forest products, peat, and grasslands, and shrubs by domestic animals, national totals, and uncertainties given in Nilsson et al. (2000), proportionally to population in respective bioclimatic zones. CO_2 fluxes from consumption of grassland and shrubs by wild animals are distributed proportionally to areas of grassland and shrubs in respective bioclimatic zones. Uncertainty of the flux caused by consumption of grassland and shrubs by wild animals is assumed to be 50% in each bioclimatic zone. Uncertainty of the flux caused by consumption of grasslands and shrubs by domestic animals and usage of peat is assumed to be 50% for national totals. The squared uncertainty of distribution of the fluxes by bioclimatic zone is estimated as the sum of squares of the national total uncertainty and uncertainty of the population in respective bioclimatic zones. The uncertainty of population in bioclimatic zones is estimated as the difference between the population estimated by two methods—overlaying of bioclimatic zone and population grids or overlaying of polygons (all maps are from the Russian CD-ROM, Stolbovoi and McCallum 2002), multiplied by 1.65 (for details see Jonas and Gusti 2010).

2.5 Disturbances

Nilsson et al. (2000) estimated C-CO_2 fluxes and their uncertainties at national scale for the following disturbances: direct fire carbon emissions (DFCE) and post-fire carbon emissions (PFCE), industrial transformation of grasslands and shrubs, insect invasion, forest abiotic disturbances, disturbances of forests by harvesting. We distributed the national totals by bioclimatic zone and estimated the uncertainties of the distributions.

We estimated fire emissions by bioclimatic zone using data on fire types and areas of different fire types in bioclimatic zones by Shvidenko and Nilsson (2000a, b). To estimate the uncertainty of the DFCE we used the result of the uncertainty study by French et al. (2004) carried out for boreal forests (Alaska) using a similar fire emission model. For the 4-year average carbon flux, French et al. (2004) finds 24% CV which corresponds to 40% for 90% confidence interval uncertainty.

To estimate the uncertainty of the PFCE we used a simplified PFCE model by Shvidenko and Nilsson (2000b) and applied a Monte Carlo technique (10,000 solutions) to propagate the parameter uncertainties (for details, see Jonas and Gusti 2010).

The resulting uncertainty of the PFCE for 1990 is 40% (90% C.I.). We do not differentiate between 1990 uncertainty and 5-year average uncertainty because the same model (and most of the parameters) is used for each year; thus the estimates are not independent.

Uncertainty of the total carbon flux (FCE = DFCE + PFCE) is estimated to be 40% (90% C.I.), taking into account that both DFCE and PFCE depend on the same area burned. Emissions resulting from burning of organic matter mainly consist of a few gases containing carbon (CO_2, CO, and CH_4). Using estimations by French et al. (2004) we found that the CO_2 emissions make up about 85% of direct fire carbon emissions.

We distributed emissions caused by "industrial transformation of grasslands and shrubs" and "forest abiotic disturbances" proportionally to the population of the bioclimatic zones. The uncertainty of the distributed flux is estimated in a similar way to consumption flux.

Flux from disturbances of forests by harvesting is distributed proportionally to actual harvest by forest enterprises (we overlaid the bioclimatic zone map and Forestry Database from the Russia CD-ROM, Stolbovoi and McCallum 2002). The square uncertainty of the distribution is estimated by summing the squares of total national uncertainty reported by Nilsson et al. (2000) and the uncertainty of the harvest distribution by bioclimatic zone, which is estimated as misclassified harvest divided by harvest in each bioclimatic zone and multiplied by 1.65. We distributed flux caused by forest insect invasion proportionally to "Insect index": an index incorporating total forest area in a bioclimatic zone and severity of insect damage (compiled from the "insect map" from the Russia CD-ROM). For details, see Jonas and Gusti (2010).

3 Results and discussion

The 1988–1992 NPP estimate for Russia's arable land as specified by Nilsson et al. (2000: Tables 30 and 68) and Nilsson et al. (2003a, c: background data to Fig. 1) was about 957 TgC/year with an uncertainty ranging from ~5% to 18%. The new NPP estimate is smaller by 23% but exhibits a greater uncertainty, 739 TgC/year ±25%. In the bioclimatic zones the changes are different—from a 14% increase in Semi-Desert and Desert to a 50% decrease in Tundra. The main reasons for the bias and increased uncertainty are uncertain yield (at oblast level) and yield losses (see Table 2).

Table 2 NPP and uncertainties for bioclimatic zone and LC, TgC/year

BCZ	Arable land			Forest			Wetlands + grasslands and shrubs[a]		
	NPP	U90	R_U90	NPP	U90	R_U90	NPP	U90	R_U90
Polar desert	0	0	0	0	0	0	0	0–0.1	−100–+112
Tundra	2	2	80	8	2	17	341	143	42
Pre-Tundra and Northern Taiga	3	2	69	334	102	31	196	62	31
Middle Taiga	35	18	52	1,440	436	30	626	243	39
Southern Taiga	119	54	45	411	156	38	206	96	47
Temperate forest	108	44	41	98	40	41	28	14	50
Steppe	393	157	40	35	10	26	165	116	70
Semi-desert and desert	80	51	64	3	2	58	33	13	38
Total	739	187	25	2,329	350	15	1,594	513	32

[a]In the case of Polar Desert we provide 90% confidence intervals to avoid negative NPP and HR

The new estimate of forest NPP is greater than the previous one by 36%. The main reason is as follows. The FCA 2000 forest NPP estimate was based on the use of field measurements of tree NPP, which did not consider fine roots and root exudates properly (state of the art at the time of measurements). The difference between the NPP estimates for the bioclimatic zones varies from −21% in Steppe to more than 40% in Middle Taiga and Pre-Tundra and Northern Taiga. The uncertainty of the national total is approximately on the same level. The uncertainties of the NPP for bioclimatic zones represent our knowledge about distribution of the total NPP between the bioclimatic zones and are of a different nature than the uncertainty of the national NPP estimate.

The 1988–1992 NPP estimates for Russia's wetlands as specified by Nilsson et al. (2000: Tables 30 and 68) and Nilsson et al. (2003a, c: background data to Fig. 1) were about 487 TgC/year, with an uncertainty ranging from <5% to 27%. The corresponding values for grasslands and shrubs are 1,202 TgC/year, with an uncertainty range from <5% to 18%. The re-derived NPP estimates are 539 TgC/year ±53% for wetlands and 1,055 TgC/year ±40% for grasslands and shrubs.

The results of estimations of other terrestrial ecosystem CO_2 fluxes into and out of the atmosphere, the net atmospheric CO_2 flux, and their uncertainties are presented in Table 3.

The new estimate of the soil heterotrophic respiration is 9% smaller than the FCA 2000 estimate, and the uncertainty has increased from 16% to 24% in total. Decrease of the HR in bioclimatic zones ranges from 7% in the Steppe to 50% in Polar Desert. The main reason for the high uncertainty is the lack of spatial and temporal coverage of SR and RC measurements.

The estimated uncertainty of the HR is considerably greater than the uncertainty estimates published by other researchers, for example, Stolbovoi (2003) −6–7% (for SR); Kurganova (2002) and Zavarzin (2007) −10–12% (for HR and 6–8% for SR). Unfortunately, the authors do not present their uncertainty analyses, but only the final numbers. Taking into account the small amount and irregular distribution of

Table 3 Major CO_2 fluxes from and to the atmosphere and atmospheric CO_2 budget, including their uncertainties (U90; (assuming correlation between disturbance and consumption = 1), TgC/year (minus = net out of the atmosphere)

BCZ	NPP[a]		HR[a]		Disturbances		Consumption		Total	
	$\overline{NPP}$	U90	$\overline{HR}$	U90	$\overline{D}$	U90	$\overline{Con}$	U90	$\overline{Total}$	U90
Polar desert	0.05	0–0.1	0.10	0–0.25	0.00	0.00	0.00	0.00	0.05	0.16
Tundra	351	143	236	140	10	4	10	4	−96	200
Pre-Tundra and Northern Taiga	533	119	253	150	49	18	16	8	−215	193
Middle Taiga	2,101	499	1,063	578	75	16	70	21	−893	764
Southern Taiga	737	191	611	136	62	10	191	39	127	240
Temperate forest	233	61	188	38	23	5	90	44	68	86
Steppe	593	195	523	114	19	3	157	31	106	228
Semi-desert and desert	116	53	48	29	2	1	12	4	−55	60
Total	4,662	648	2,920	687	240	50	545	101	−957	957

[a]In the case of Polar Desert we provide 90% confidence intervals to avoid negative NPP and HR

the SR measurements, which are sporadic rather than statistically planned, the lack of RC studies, the difference between the estimates of HR, etc., we can conclude that most probably, the researchers underestimated the uncertainties.

Use of imperfect techniques for measurement of soil respiration leads (most probably) to substantial biases in measurements up to 30% in some bioclimatic zone–soil classes. Aggregation of the classes by soil types or bioclimatic zones decreases the biases to a maximum of 22% for soil types and only 9% for bioclimatic zones because the biases are of different signs. Country aggregation almost eliminates the bias, bringing it down to 3%. Estimation and elimination of the biases improves our knowledge about soil respiration, especially on sub-country scales.

Accounting for inside-bioclimatic zone and inter-bioclimatic zone correlation of HR (as common RC is used in a few bioclimatic zones) is important when studying flux uncertainties. The correlation reaches 32% in case of Middle Taiga and Forest Tundra and Northern Taiga. By not accounting for the correlations, one underestimates the uncertainties (in our case the correlation increases the HR uncertainty by 4% in total, but for some bioclimatic zone–soil classes the increase is much greater).

Uncertainty of the national total of disturbance fluxes increased slightly because of the re-estimated uncertainty of fire emissions (fire emission uncertainty increased from 23% to 40%). Uncertainty of the national total of consumption fluxes increased mainly because of a re-estimated consumption of agriculture products. Uncertainties of the flux estimates for the bioclimatic zones rise because of imperfect spatial data on population in the bioclimatic zones, insect invasion, and forest harvest (uncertainty of the assumptions on the flux distributions by bioclimatic zones are not taken into account). However, as the disturbance and consumption fluxes in general are much smaller than the HR and NPP fluxes (except for the Temperate Forest where consumption is two times greater than the HR) their uncertainties do not influence the uncertainties of the net atmospheric fluxes of the bioclimatic zones to a great extent. Our uncertainty estimate of the CO_2 balance fluxes is higher than the estimate by Shvidenko et al. (2010) for Central Siberia (estimate around 2003). This can mainly be explained by the much more detailed information used in their study.

The assumption that uncertainties of the parameters studied follow Gaussian distribution leads to approximate results for positively defined parameters in the case of uncertainties >33% because there is a (low) probability that some population values are negative. In reality, this does not occur, so a part of the probability "leaks" through the unrealistically long tail of the theoretical distribution with negative values. This could lead to a slight overestimation of the uncertainties. Where there was lack of information for checking an estimate and assessing its uncertainty, we assumed high uncertainty to reflect the shortage of knowledge.

It must be noted that we follow only a bottom-up approach, which is not (yet) constrained top-down. The uncertainty of our uncertainty estimate is considerable, and includes many assumptions and expert estimates. Our uncertainty estimates show the upper order of the uncertainties.

We applied our estimate of the atmospheric CO_2 budget to reconstruct a section for northern Asia in Figure 7.7 of Denman et al. (2007). The bottom-up value becomes −850 TgC/year against −360 TgC/year in the original figure and corresponding uncertainty interval [−1,700–0] against [−730–0] TgC/year. In general,

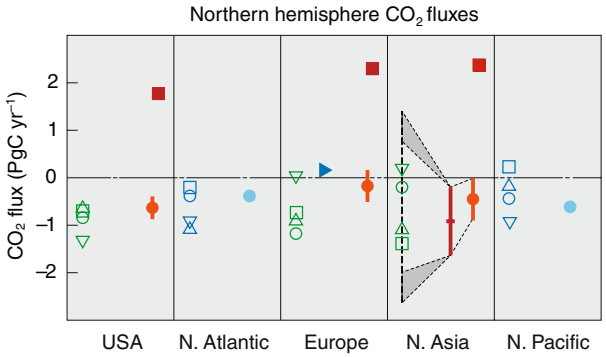

Fig. 2 Regional ocean–atmosphere and land–atmosphere CO_2 fluxes for the northern hemisphere from inversion ensembles and bottom-up studies. Fluxes to the atmosphere: positive; uptake: negative. Inversion results correspond to the post-Pinatubo period, 1992–1996. In the focus here: Northern Asia. *Orange line* bottom-up terrestrial fluxes from Shvidenko and Nilsson (2003) for Asian Russia, and Fang et al. (2001) for China. *Green symbols*: terrestrial fluxes from inversion (Gurney et al. 2002, 2003; Peylin et al. 2005; Rödenbeck et al. 2003a, b); their errors range between 500 and 1,000 TgC/year. *Red square* fossil fuel emissions. Source: IPCC FAR (Denman et al. 2007: Figure 7.7), modified. Additionally entered: *red line* our revised bottom-up estimate for the whole of Russia (68% C.I.) expanded by the flux estimate of Fang et al. (2001) for China; *gray-shaded triangles* to facilitate better comparison of this expanded bottom-up net flux estimate with the aforementioned inversion estimates, with and without considering their errors

uncertainty of the bottom-up estimate for Asia is smaller than the range of estimates given by top-down methods.

We find a less optimistic, although more realistic, bottom-up versus top-down match for northern Asia than the IPCC authors (see Fig. 2), confronting us with the crucial question of what the added value is of combining full carbon accounts bottom-up and top-down? It is correct to say that this question remained and remains subject to thorough research, as each approach carries considerable uncertainties. Nonetheless, a first bottom-up/top-down linking exercise with LSCE in 2007 based on our less optimistic, though more realistic, bottom-up uncertainty for Russia showed that an added value still seems to exist. Using a 12– and 77-station network as representative for ~1988 and ~2000, Rayner et al. (1999, 2007) demonstrate that our bottom-up uncertainty remains the main control for the a posteriori error reduction over Russia. That is, an increased need for atmospheric measurements over Russia continues to exist.

4 Conclusions

We revised uncertainties in estimates of CO_2 fluxes for 1988–1992 in FCA 2000, taking into account recent studies. Much attention was paid to NPP and HR as they are the main determinants of the uncertainty of the atmospheric CO_2 budget. All fluxes were estimated for bioclimatic zones for comparison with the results of atmospheric inverse modeling and use of the fluxes as prior information for the inverse modeling. Systematic errors found were corrected, while remaining uncertainties were estimated from a conservative point of view. Our estimate of

the uncertainty should be perceived as an upper estimate, which it was possible to make with the data available. Taking into account the uncertainty of the uncertainty estimate we are confident in the order of magnitude of the uncertainty but not in the exact number. The re-estimated Russian carbon budget alters the total Eurasian carbon budget considerably, and thus substantially changes the numbers presented in the IPCC FAR.

Our revision of the FCA 2000 leads to HR and NPP uncertainties that are greater than those derived previously. It was also found that uncertainties determined at the spatial scale of bioclimatic zones are still robust, while HR and NPP uncertainties typically exceed 100% (90% C.I.) at finer resolutions.

The new NPP estimate for Russia's arable land is smaller by 23% (957 versus 739 TgC/year) but exhibits a greater uncertainty—25% versus 18% in the FCA 2000. The main reasons for the bias and increased uncertainty are uncertain yield (at oblast level) and yield losses.

The new estimate of forest NPP is greater than the previous one by 36% in total (2,329 versus 1,707 TgC/year). The main reason for that is lack of knowledge of fine root NPP (state of the art at the time of measurements). The uncertainty of the national total (15%) is approximately on the same level.

The 1988–1992 NPP estimates for Russia's wetlands as specified by Nilsson et al. (2000) and Nilsson et al. (2003a, c) were about 487, with an uncertainty ranging from <5% to 27%. The corresponding values for grasslands and shrubs are 1,202 TgC/year with an uncertainty range from <5% to 18%. The re-derived NPP estimates for Russia's wetlands, grasslands, and shrubs are 539 TgC/year ±53% and 1,055 TgC/year ±40%, respectively.

The new estimate of the HR is 9% smaller than the FCA 2000 estimate (2,920 versus 3,197 TgC/year) and the uncertainty increased from 16% to 24% in total. The main reason for high uncertainty is the lack of spatial and temporal coverage of SR and RC measurements. One can use the developed bioclimatic zone–soil–vegetation matrix for planning future measurement campaigns to reduce the uncertainty.

The uncertainty of Russia's net atmospheric balance is approximately 100% (90% C.I.), as a consequence of the increases in both the uncertainty underlying HR and the uncertainty underlying NPP.

The results obtained allow a section for northern Asia in Figure 7.7 in the IPCC FAR (Denman et al. 2007) to be updated. The updated bottom-up value is −850 TgC/year against −360 TgC/year in the original figure and corresponding uncertainty interval [−1,700–0] against [−730–0] TgC/year.

The bottom-up/top-down linking exercise with LSCE based on our less optimistic, though more realistic, bottom-up uncertainty for Russia showed that an added value still seems to exist. Our bottom-up uncertainty remains the main control for the a posteriori error reduction over Russia, showing that there is a need for additional atmospheric CO_2 measurements over Russia.

The high uncertainty of the terrestrial carbon budget makes difficult to use it in policy agreements; at the least, the terrestrial carbon budget should be treated differently than the less uncertain emissions (IIASA 2007). Reduction of the uncertainties of either bottom-up or top-down estimates to the level that can be acceptable by policymakers, namely, 35–40% for net ecosystem production and 60–80% for net biome production, as found by Shvidenko et al. (2010) requires more systematic long-term observations. Future measurements have only a limited influence on reducing

uncertainties of the estimates of the carbon budget in the past, and this should be taken into account when selecting the base year for emission reductions.

Acknowledgements We are grateful to Anatoly Shvidenko for the fruitful discussions and help in revealing the methodological details of the FCA 2000. The work was supported by the Austrian Science Fund (FWF; project no. P17569-N04).

References

Bond-Lamberty B, Wang Ch, Gower S (2004) The contribution of root respiration to soil surface CO_2 flux in a boreal black spruce chronosequence. Tree Physiol 24(12):1387–1395

Ciais P, Rayner P, Chevallier F, Bousquet P, Logan M, Peylin P, Ramonet M (2010) Atmospheric inversions for estimating CO_2 fluxes: methods and perspectives. Clim Change (this issue). doi:10.1007/s10584-010-9909-3

Cramer W, Kicklighter DW, Bondeau A, Moore B III, Churkina G, Nemry B, Ruimy A, Schloss AL, the participants of the Potsdam NPP Model Intercomparison (1999) Comparing global models of terrestrial net primary productivity (NPP): overview and key results. Glob Chang Biol 5(S1):1–15

Denman K, Brasseur G, Chidthaisong A, Ciais P, Cox P, Dickinson R, Hauglustaine D, Heinze C, Holland E, Jacob D, Lohmann U, Ramachandran S, da Silva Dias P, Wofsy S, Zhang X (2007) Couplings between changes in the climate system and biogeochemistry. In: Solomon S, Qin D, Manning M, Chen Z, Marquis M, Avery K, Tignor M, Miller H (eds) Climate change 2007: the physical science basis. Contribution of working group I to the fourth assessment report of the intergovernmental panel on climate change. Cambridge University Press, Cambridge, pp 499–587. Available at: http://ipcc-wg1.ucar.edu/wg1/wg1-report.html

Fang J, Chen A, Peng C, Zhao S, Ci L (2001) Changes in forest biomass carbon storage in China between 1949 and 1998. Science 292:2320–2322

French NHF, Goovaerts P, Kasischke ES (2004) Uncertainty in estimating carbon emissions from boreal forest fires. J Geophys Res 109:D14S08. doi:10.1029/2003JD003635

Gurney KR, Law RM, Denning AS, Rayner PJ, Baker D, Bousquet P, Bruhwhiler L, Chen Y-H, Ciais P, Fan S, Fung IY, Gloor M, Heimann M, Higuchi K, John J, Maki T, Maksyutov S, Masarie K, Peylin P, Prather M, Pak BC, Randerson J, Sarmiento J, Taguchi S, Takahashi T, Yuen C-W (2002) Towards robust regional estimates of CO_2 sources and sinks using atmospheric transport models. Nature 415(6872):626–630

Gurney KR, Law RM, Denning AS, Rayner PJ, Baker D, Bousquet P, Bruhwhiler L, Chen Y-H, Ciais P, Fan S, Fung IY, Gloor M, Heimann M, Higuchi K, John J, Kowalczyk E, Maki T, Maksyutov S, Peylin P, Prather M, Pak BC, Sarmiento J, Taguchi S, Takahashi T, Yuen C-W (2003) TransCom 3 CO_2 inversion intercomaprison: 1. Annual mean control results and sensitivity to transport and prior flux information. Tellus 55B:555–579

Hanson PJ, Edwards NT, Garten CT et al (2000) Separating root and soil microbial contributions to soil respiration: a review of methods and observations. Biogeochemistry 48:115–146

House JI, Prentice IC, Ramankutty N, Houghton RA, Heiman M (2003) Reducing apparent uncertainties in estimates of terrestrial CO_2 sources and sinks. Tellus 55B:345–363

Hutchinson GL, Rochette P (2003) Non-flow-through steady-state chambers for measuring soil respiration: numerical evaluation of their performance. Soil Sci Soc Am J 67:166–180

IIASA (2007) Uncertainty in greenhouse gas inventories. IIASA Policy Brief #1, December. International Institute for Applied Systems Analysis, Laxenburg, Austria. Available at http://www.iiasa.ac.at/Admin/PUB/policy-briefs/pb01-web.pdf

Jensen LS, Mueller T, Tata KR, Ross DJ, Magid J, Nielsen NE (1996) Soil surface CO_2 flux as an index of soil respiration in situ: a comparison of two chamber methods. Soil Biol Biochem 28:1297–1306

Jonas M, Gusti M (2010) Reassessing uncertainty in IIASA's bottom-up full CO_2-C account of Russia's terrestrial biosphere: toward closing the accounting gap with top-down atmospheric inversion. Interim Report, International Institute for Applied Systems Analysis, Laxenburg, Austria (forthcoming)

Jonas M, Nilsson S (2002) Austrian carbon database (ACDb). International Institute for Applied Systems Analysis, Laxenburg. A brief project report covering that subject already exists: Jonas et al (2008) Assessing Uncertainty in Bottom-up Full Carbon Accounting for Russia. Brief Project Report (revised and expanded after acceptance by the Austrian Science Fund), Interna-

tional Institute for Applied Systems Analysis, Laxenburg, Austria, p 8. Available on the Internet: http://www.iiasa.ac.at/Research/FOR/acdb.html

Jonas M, Nilsson S (2007) Prior to economic treatment of emissions and their uncertainties under the Kyoto Protocol: scientific uncertainties that must be kept in mind. Water Air Soil Pollut Focus 7:795–511

Kurganova I (2002) Carbon dioxide emission from soils of Russian terrestrial ecosystems. Interim Report IR-02-070, International Institute for Applied Systems Analysis, Laxenburg, Austria, p 64. Available at http://www.iiasa.ac.at/Publications/Documents/IR-02-070.pdf

Kurganova I, Lopes de Gerenyu V, Rozanova L, Myakshina T, Kudeyarov V (2003) Effect of hydrothermal conditions on CO_2 emissions from soils of forest zone: analysis of long-term field observations. Abstracts of the second international conference "Emissions and Sink of Greenhouse Gases on the Territory of Northern Eurasia Territory", pp 70–71

Lemke P, Ren J, Alley RB, Allison I, Carrasco J, Flato G, Fujii Y, Kaser G, Mote P, Thomas RH, Zhang T (2007) Observations: changes in snow, ice and frozen ground. In: Solomon S, Qin D, Manning M, Chen Z, Marquis M, Avery K, Tignor M, Miller H (eds) Climate change 2007: the physical science basis. Contribution of working group I to the fourth assessment report of the intergovernmental panel on climate change. Cambridge University Press, Cambridge

Lopes de Gerenyu VO, Kurganova IN, Rozanova LN, Kudeyarov VN (2005) Effect of soil temperature and moisture on $\tilde{N}O_2$ evolution rate of cultivated Phaeozem: analysis of a long-term field experiment. Plant Soil Environ 51(5):213–219

Nilsson S, Shvidenko A, Stolbovoi V, Gluck M, Jonas M, Obersteiner M (2000) Full carbon account for Russia. Interim Report IR-00-021, International Institute for Applied Systems Analysis, Laxenburg, Austria, p 180. Available at http://www.iiasa.ac.at/Publications/Documents/IR-00-021.pdf

Nilsson S, Jonas M, Stolbovoi V, Shvidenko A, Obersteiner M, McCallum I (2003a) The missing "missing sink". For Chron 79(6):1071–1074. Available at http://www.iiasa.ac.at/~jonas/CV%20IIASA/CV.pdf

Nilsson S, Jonas M, Shvidenko A, Stolbovoi V, McCallum I (2003b) Monitoring, verification and permanence of carbon sinks. In: CarboEurope conference "The continental carbon cycle". 3rd CarboEurope Conference, 19–21 March, Abstracts, Lisbon, Portugal. Available at http://www.bgc.mpg.de/public/carboeur/workshop/speaker/nilsson.htm

Nilsson S, Vaganov EA, Shvidenko AZ, Stolbovoi V, Rozhkov VA, McCallum I, Jonas M (2003c) Carbon budget of vegetation ecosystems of Russia. Dokl Earth Sci 393A(9):1281–1283. Translated from Dokl Akad Nauk USSR 393(4):541–543

Peylin P, Bousquet P, Le Quéré C, Sitch S, Friedlingstein P, McKinley G, Gruber N, Rayner P, Ciais P (2005) Multiple constraints on regional CO_2 flux variations over land and oceans. Glob Biogeochem Cycles 19:GB1011. doi:10.1029/2003GB002214

Pumpanen J, Kolari P, Ilvesniemi H, Minkkinen K, Vesala T, Niinisto S, Lohila A, Larmola T, Morero M, Pihlatie M, Janssens I, Yuste JC, Grunzweig JM, Reth S, Subke JA, Savage K, Kutsch W, Oestreng G, Ziegler W, Anthoni P, Lindroth P, Hari P (2004) Comparison of different chamber techniques for measuring soil CO_2 efflux. Agric For Meteorol 123:159–176

Raich JW, Tufekcioglu A (2000) Vegetation and soil respiration: correlations and controls. Biogeochemistry 48:71–90

Rayner PJ, Enting IG, Francey RJ, Langenfelds R (1999) Reconstructing the recent carbon cycle from atmospheric CO_2, δ13C and O_2/N_2 observations. Tellus 51B:213–232

Rayner PJ, Law RM, Allison CE, Francey RJ, Pickett-Heaps C (2007) The interannual variability of the global carbon cycle (1992–2005) inferred by inversion of atmospheric CO_2 and $\delta^{13}CO_2$ measurements. Glob Biogeochem Cycles 22:GB3008

Rodin AZ, Krylatov AK (eds) (1998) Dynamic of humus balance on cropland of the Russian Federation. Goskomzem, Moscow, Russia, p 60 (in Russian)

Rödenbeck C, Houweling S, Gloor M, Heimann M (2003a) Time-dependent atmospheric CO_2 inversions based on interannually varying tracer transport. Tellus 55B:488–497

Rödenbeck C, Houweling S, Gloor M, Heimann M (2003b) CO_2 flux history 1982–2001 inferred from atmospheric data using a global inversion of atmospheric transport. Atmos Chem Phys 3:1919–1964

Schmullius C, Santoro M (eds), Balzter H, Bartsch A, Beer C, Cramer W, Delbart N, George C, Gerard F, Gerlach R, Grippa M, Handoh I, Hese S, Kidd R, Lehmann E, Le Toan T, Lucht W, Luckman A, McCallum I, Mognard N, Nilsson S, Pathe C, Petrocchi A, Quegan S, Robertson N, Rowland C, Shvidenko A, Skinner L, Thomson A, Voigt S, Wagner W, Wegmüller U, Wiesmann

A (2005) SIBERIA-II Final Report, Contract Number EVG1-CT-2001-00048, EC Deliverable: EC17, Reporting Period 1.1.2002–30.09.2005, October, 69 pp
Shvidenko AZ, Nilsson S (2000a) Extent, distribution, and ecological role of fire in Russian forests. In: Kasischke ES, Stocks BJ (eds) Fire, climate change, and carbon cycling in the boreal forest. Springer, New York, pp 132–150
Shvidenko A, Nilsson S (2000b) Fire and the carbon budget of Russian forests. In: Kasischke ES, Stocks BJ (eds) Fire, climate change, and carbon cycling in the boreal forest. Springer, New York, pp 289–311
Shvidenko A, Nilsson S (2003) A synthesis of the impact of Russian forests on the global carbon budget for 1961–1998. Tellus 55B:391–415
Shvidenko AZ, Schepaschenko DG, Nilsson S, Vaganov EA (2006) Dynamics of net primary production of Russian forests in a changing world: a new estimate. International Conference: Climate Changes and Their Impact on Boreal and Temperate Forests, 5–7 June, Abstracts, Ural State Forest Engineering University, Ekaterinburg, Russia, 90
Shvidenko A, Schepschenko D, Nilsson S, Bouloui Y (2007) Semi-empirical models for assessing biological productivity of Northern Eurasian forests. Ecol Model 204:163–179
Shvidenko AZ, Schepaschenko DG, Vaganov EA, Nilsson S (2008) Net primary production of forest ecosystems of Russia: a new estimate. Dokl Akad Nauk USSR 421(6):822–825
Shvidenko A, Schepaschenko D, McCallum I, Nilsson S (2010) Can the uncertainty of full carbon accounting of forest ecosystems be made acceptable to policymakers? Clim Change (this issue). doi:10.1007/s10584-010-9918-2
Steffen W, Noble I, Canadell J, Apps M, Schulze E-D, Jarvis P (1998) CLIMATE: the terrestrial carbon cycle: implications for the Kyoto protocol. Science 280(5368):1393–1394. doi:10.1126/science.280.5368.1393
Stolbovoi V (2003) Soil respiration and its role in Russia's terrestrial C flux balance for the Kyoto baseline year. Tellus 55B:258–269
Stolbovoi V, McCallum I (2002) CD-ROM "Land resources of Russia". International Institute for Applied Systems Analysis and the Russian Academy of Science, Laxenburg, Austria. Available at http://www.iiasa.ac.at/Research/FOR/russia_cd/index.htm?sb=17
Yim MH, Joo SJ, Nakane K (2000) Comparison of field methods for measuring soil respiration: a static alkali absorption method and two dynamic closed chamber methods. For Ecol Manag 170:189–197
Zavarzin GA (ed) (2007) Carbon pools and fluxes in terrestrial ecosystems of Russia. Nauka, Moscow, p 315

Climatic Change (2010) 103:175–213
DOI 10.1007/s10584-010-9914-6

Comparison of preparatory signal analysis techniques for consideration in the (post-)Kyoto policy process

Matthias Jonas · M. Gusti · W. Jęda · Z. Nahorski · S. Nilsson

Received: 5 January 2009 / Accepted: 15 June 2010 / Published online: 27 July 2010

Abstract Our study is a preparatory exercise. We focus on the analysis of uncertainty in greenhouse gas emission inventories. Inventory uncertainty is monitored, but not regulated, under the Kyoto Protocol to the United Nations Framework Convention on Climate Change. Under the Convention, countries publish annual or periodic national inventories of greenhouse gas emissions and removals. Policymakers use these inventories to develop strategies and policies for emission reductions and to track the progress of these policies. However, greenhouse gas inventories contain uncertainty for a variety of reasons, and these uncertainties have important scientific and policy implications. For most countries, the emission changes agreed under the Protocol are of the same order of magnitude as the uncertainty that underlies their combined (carbon dioxide equivalent) emissions estimates. Here we apply and compare six available techniques to analyze the uncertainty in the emission changes that countries agreed to realize by the end of the Protocol's first commitment period 2008–2012. Any such technique, if implemented, could "make or break" claims of compliance, especially in cases where countries claim fulfillment of their commitments to reduce or limit emissions. The techniques all perform differently and can thus have a different impact on the design and execution of emission control policies. A thorough comparison of the techniques has not yet been made but is needed when expanding the discussion on how to go about dealing with uncertainty under the Kyoto Protocol and its successor.

M. Jonas (✉) · M. Gusti · S. Nilsson
International Institute for Applied Systems Analysis,
Schlossplatz 1, 2361 Laxenburg, Austria
e-mail: jonas@iiasa.ac.at

M. Gusti
Lviv Polytechnic National University, Lviv, Ukraine

W. Jęda · Z. Nahorski
Systems Research Institute, Polish Academy of Sciences, Warsaw, Poland

Acronyms and nomenclature

Adj	Adjustment
C&C	Contraction and convergence
CH_4	Methane
crit	Critical (index)
CRU	Critical relative uncertainty
CI	Confidence interval
CO_2	Carbon dioxide
FCCC	Framework Convention on Climate Change
F_N	Standardized cumulative normal distribution
Gap	Gap (index)
GHG	Greenhouse gas
GSC	Gillenwater, Sussman, and Cohen
HFC	Hydrofluorocarbon
IPCC	Intergovernmental Panel on Climate Change
KP	Kyoto Protocol
KT	Kyoto (emissions) target
LULUCF	Land use, land-use change, and forestry
N_2O	Nitrous oxide
p	Fractional amount
P	Probability
PFC	Perfluorocarbon
RelDiff	Relative difference
SA	Signal analysis
SD	Standard deviation (index)
SF_6	Sulfur hexafluoride
t	Time ($t_1 \leq t \leq t_2$)
t	True (index)
u	Upper (index)
U	Undershooting
U_{GAP}	Initial obligatory undershooting
UN	United Nations
Und	Undershooting
VT	Verification time
x	Emissions
X	Random variable
z	Standardized emissions
Z	Standardized random variable
α	Risk ($0 \leq \alpha \leq 0.5$)
δ_{crit}	Critical emission limitation or reduction
δ_{KP}	Committed (normalized) emissions change under the KP
δ_{mod}	Modified emission limitation or reduction target
δ'_{crit}	Auxiliary variable
Δt	Verification time
ε	Absolute uncertainty
ρ	Relative uncertainty
ρ_{crit}	Critical relative uncertainty

υ	Uncertainty correlation coefficient
1	Referring to base year (index)
2	Referring to commitment year (index)

1 Introduction

The focus of our study is on the analysis of uncertainty in greenhouse gas (GHG) emission inventories. Inventory uncertainty is monitored, but not regulated, under the Kyoto Protocol (KP) to the United Nations Framework Convention on Climate Change (FCCC 1992). Under the Convention, countries publish annual or periodic national inventories of GHG emissions and removals, encompassing carbon dioxide (CO_2), methane (CH_4), nitrous oxide (N_2O), hydrofluorocarbons (HFCs), perfluorocarbons (PFCs), and sulfur hexafluoride (SF_6) (FCCC 1998, Annex A). Policymakers use these inventories to develop strategies and policies for emission reductions and to track the progress of these policies.

However, GHG inventories (whether at the global, national, corporate, or other level) contain uncertainty for a variety of reasons, for example, the lack of availability of sufficient and appropriate data and of the techniques to process them. Uncertainty has important scientific and policy implications. Until recently, relatively little attention has been devoted to how uncertainty in emissions estimates is dealt with and how it might be reduced. Now this situation is changing, with uncertainty analysis increasingly being recognized as an important tool for improving inventories of GHG emissions and removals (e.g., IPIECA 2007; Lieberman et al. 2007).

At present, parties to the UNFCCC are obliged, to include in the reporting of their annual inventories direct or alternative estimates of the uncertainty associated with these emissions and removals, consistent with the Intergovernmental Panel on Climate Change's (IPCC) good practice guidance reports (Penman et al. 2000, 2003). Yet, it makes a big difference in the framing of policies whether or not uncertainty is considered—both reactively, because there is a need to do so; or proactively, because difficulties are anticipated.

Our tenet is that uncertainty estimates are not intended to dispute the validity of national GHG inventories. Although the uncertainty of emissions estimates underscores the lack of accuracy that characterizes many source and sink categories, its consideration can help to establish a more robust foundation on which to base policy. According to the IPCC good practice guidance reports (notably, Penman et al. 2000, p. 6.5), uncertainty analysis is intended to help "improve the accuracy of inventories in the future and guide decisions on methodological choice." Uncertainty analyses function as indicators of opportunities for improvement in data measurement, data collection, and calculation methodology. Only by identifying elements of high uncertainty can methodological changes be introduced to address them. Currently, most countries that perform uncertainty analyses do so for the express purpose of improving their future estimates; and the rationale is generally the same at the corporate and other levels. Estimating uncertainty helps to prioritize resources and to ensure precautions are taken against undesirable consequences.

Our rationale for performing uncertainty analysis is to provide a policy tool, a means to adjust inventories or analyze and compare emission changes in order to

determine compliance or the value of a transaction. The aim of our study is to provide a preparatory guide for dealing with uncertainty in the (post-)Kyoto policy process. We apply and compare six available techniques to analyze uncertain emission changes (also called emission signals) that countries agreed to achieve by the end of the Protocol's first commitment period, 2008–2012. A thorough comparison of the techniques has not yet been made available. Even more problematical is the fact that techniques to analyze uncertain emission signals from various points of view, ranging from signal quality (defined adjustments, statistical significance, detectability, etc.) to the way uncertainty is addressed (trend uncertainty or total uncertainty), although highly needed, are not in place. For most countries under the Protocol (Annex B countries) the agreed emission changes are of the same order of magnitude as the uncertainty that underlies their combined (carbon dioxide equivalent) emission estimates (Table 1: compare last column on the left with first column on the right). Any such technique, if implemented, could "make or break" claims of compliance, especially in cases where countries claim fulfillment of their commitments to reduce or limit emissions.

Moreover, as demonstrated by Jonas et al. (2004b, c), Bun and Jonas (2006), Hamal and Jonas (2008a, b) and Bun et al. (this issue), these techniques could also be used for monitoring purposes. Emission changes since 1990 (the base year used by most Annex B countries) that are reported annually can be evaluated in an emissions change-versus-uncertainty context rather than an emissions change-only context. This advanced monitoring service is also not provided under the Protocol.[1]

Jonas et al. (2004a) distinguish between preparatory signal analysis, midway signal analysis, and signal analysis in retrospect (see also http://www.iiasa.ac.at/Research/FOR/unc_changes.html). Preparatory signal analysis is the most advanced. It allows useful information to be generated in advance as to how great uncertainties can be dependent on the level of confidence of the emission signal or the signal one wishes to detect, and on the risk that one is willing to tolerate in not meeting an agreed emission limitation or reduction commitment. We are aware of at least six different preparatory signal analysis techniques, some of which were presented at the 1st International Workshop on Uncertainty in GHG Inventories (Gillenwater et al. 2007; Jonas and Nilsson 2007; Nahorski et al. 2007). These techniques need to be scrutinized further, now in a comparative mode, before a discussion on which of them to select can take place. They all agree that uncertainty analysis is a key component of GHG emission analysis. However, the techniques all perform differently and can thus have a different impact on the design and execution of emission control policies. Going through this comparative exercise and making this knowledge available is a legacy of the 1st International Workshop on Uncertainty in GHG Inventories held in 2004 in Warsaw, Poland. This exercise is required prior to advancing the discussion on how to go about dealing with uncertainty under the KP and its successor.

This comparison is technical in nature, which is why we provide non-technical introductions and explanations for each section. We provide an overview of the techniques and their characteristics, and the conditions under which they are applied and compared in Section 2. In Section 3 we describe each technique in

[1]For an overview of IIASA's emissions change-versus-uncertainty monitoring (reports and countries) see http://www.iiasa.ac.at/Research/FOR/unc_overview.html.

Table 1 Left: Countries included in Annex B to the Kyoto Protocol (KP) and their emission limitation and reduction commitments.[2] Sources: FCCC (1996: Decision 9/CP.2, 1998: Article 3.8, Annex B, 1999: Decision 11/CP.4, 2009: National Inventory Submissions 2008); COM (2006: Section 2.b). Right: Emissions and/or removals of greenhouse gases (GHGs), or combinations of GHGs, classified according to their relative uncertainty ranges. The bars of the arrows indicate the dominant uncertainty range for these emissions and removals, while the tops of the arrows point at the neighboring uncertainty ranges, which cannot be excluded but appear less frequently. LULUCF stands for the direct human-induced land use, land-use change, and forestry activities stipulated by Articles 3.3 and 3.4 under the KP (FCCC 1998). The arrows are based on the total uncertainties that are reported annually by the member states of the EU25 (most recently: EEA 2009) and the expertise available at IIASA's Forestry Program (cf. http://www.iiasa.ac.at/Research/FOR/unc_bottomup.html) and elsewhere (e.g., Watson et al. 2000: Sections 2.3.7, 2.4.1; Penman et al. 2003: Section 5.2). Source: Jonas and Nilsson (2007: Table 1), modified

Country Group	Annex B Country	Base Year(s) for CO_2, CH_4, N_2O (for HFCs, PFCs, SF_6)	Commitment Period	KP Commitment %
1a	see below[a] see below[b]	1990 (1995) 1990 (1990)	2008–12	92
1b	RO	1989 (1989)	2008–12	
1c	BG	1988 (1995)	2008–12	
1d	SI	1986 (1995)	2008–12	
2	US[c]	1990 (1990)	2008–12	93
3a	JP CA	1990 (1995) 1990 (1990)	2008–12	94
3b	PL	1988 (1995)	2008–12	
3c	HU	1985–87 (1995)	2008–12	
4	HR	1990 (1995)	2008–12	95
5a	RU	1990 (1995)	2008–12	100
5b	NZ, UA	1990 (1990)	2008–12	
6	NO	1990 (1990)	2008–12	101
7	AU	1990 (1990)	2008–12	108
8	IS	1990 (1990)	2008–12	110

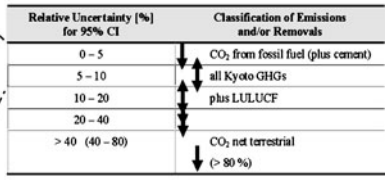

[a]Country Group 1a: BE, CZ, DE, DK, EC (= EU15; the EU27 does not have a common Kyoto target), EE, ES, FI, GR, IE, LT, LU, LV, MC, NL, PT, SE, UK. Member States of the EU27 but without individual Kyoto targets: CY, ML. Listed in the Convention's Annex I but not included in the Protocol's Annex B: BY and TR (BY and TR were not parties to the Convention when the Protocol was adopted). BY asked to become an Annex B country by amendment to the KP at CMP 2 in 2006. BY's base years and KP commitment are 1990 (1995) and 92%, respectively

[b]Country Group 1a: AT, CH, FR, IT, LI, SK

[c]Country Group 2: The US has indicated its intention not to ratify the KP. The US reports all its emissions with reference to 1990. However, information on 1990 in its national inventory submissions does not reflect or prejudge any decision that may be taken in relation to the use of 1995 as base year for hydrofluorocarbons (HFCs), perfluorocarbons (PFCs) and sulfur hexafluoride (SF_6) in accordance with Article 3.8 of the KP

a standardized fashion. We make available mathematical details and numerical results for all techniques as support for online material (SOM) at http://www.iiasa.ac.at/Research/FOR/unc_prep.html.[3] We summarize our findings in Section 4.

[2]ISO country code: AT Austria; AU Australia; BE Belgium; BG Bulgaria; BY Belarus; CA Canada; CH Switzerland; CY Cyprus; CZ Czech Republic; DE Germany; DK Denmark; EC European Community; EE Estonia; ES Spain; FI Finland; FR France; GR Greece; HR Croatia; HU Hungary; IE Ireland; IS Iceland; IT Italy; JP Japan; LI Liechtenstein; LT Lithuania; LU Luxembourg; LV Latvia; MA Malta; MC Monaco; NL Netherlands; NO Norway; NZ New Zealand; PL Poland; PT Portugal; RO Romania; RU Russian Federation; SE Sweden; SI Slovenia; SK Slovak Republic; TR Turkey; UA Ukraine; UK United Kingdom; US United States.

[3]At Web site http://www.iiasa.ac.at/Research/FOR/unc_prep.html click on *mathematical background* (referred to in the text as SOM_Math) and *numerical results* (referred to in the text as SOM_Num) to Jonas and Nilsson (2007) under *Overview over six preparatory emissions change analysis techniques*.

Table 2 The spatiotemporal and thematic conditions under which the six preparatory signal analysis techniques listed in Table 3 are applied and compared

Dimension	Methodological restriction	Focus in this study on
Spatial	None	National: countries as listed in Annex B to the KP (FCCC 1998) The country scale is the principal reporting unit requested for reporting GHG emissions and removals under the KP. For convenience, we group these countries according to their (i) emission limitation or reduction commitments; and (ii) the base years for their emissions of CO_2, CH_4, and N_2O, resulting in 8 country groups (see left side of Table 1). As the Annex B countries' emissions of CO_2, CH_4, and N_2O by far exceed those of the fluorinated (HCFs, PCFs, SF_6) gases, we use the combined emissions of CO_2, CH_4, and N_2O as reference.
Temporal	None	Two-points-in-time approach: base year (t_1)—commitment year/period (t_2) We use the year 2010 as commitment year with t_2 referring to the temporal average in net emissions over the commitment period 2008–2012.
Thematic	None	Annual CO_2 or CO_2 equivalent emissions: GHG emissions and/or removals of the six Kyoto GHGs as listed in Annex A to the KP (FCCC 1998), individually or combined

2 Overview of techniques and their characteristics and conditions of application

In Section 1 we apply and compare six techniques to analyze the uncertainty in the emission changes that countries agreed to achieve by the end of the Protocol's first commitment period, 2008–2012. Table 2 summarizes the spatiotemporal and thematic conditions under which the application and comparison are carried out. The conditions are shaped by the KP and imply the country scale and countries' annual emissions of the six GHGs listed in Appendices A and B to the Protocol (FCCC 1998). Box 1 recapitulates the relevant uncertainty terms and concepts that we refer to and make use of in our study.

Box 1 The relevant uncertainty terms and concepts that we refer to and make use of in our study

Uncertainty (inventory definition): A general and imprecise term which refers to the lack of certainty (in inventory components) resulting from any causal factor such as unidentified sources and sinks, lack of transparency, etc. (Penman et al. 2000: A3.19).
Total and trend uncertainty: The total (or level) uncertainty reflects our real diagnostic emissions accounting capabilities, that is, the uncertainty that underlies our past (base year) as well as our current accounting and that we will have to cope with in reality at some time in the future (commitment year/period). The trend uncertainty reflects the uncertainty of the difference in net emissions between two years (base year and/or commitment year/period) (Jonas and Nilsson 2007: Section 4).
Confidence interval: The true value of the quantity for which the interval is to be estimated is a fixed but unknown constant, such as the annual total emissions in a given year for a given country. The confidence interval (CI) is a range that encapsulates the true value of this unknown fixed quantity with a specified confidence (probability). Typically, a CI of 95% is used in GHG inventories (IPCC 2006: Section 3.1.3).
Relative uncertainty: To make all preparatory signal analysis techniques easily applicable, we build on relevant findings of earlier studies which suggest resolving relative uncertainty of inventory sources and sinks only in terms of intervals or classes and referring to their medians. Our definition of relative uncertainty classes (Class 1: 0–5%; Class 2: 5–10%; Class 3: 10–20%; Class 4: 20–40%; and Class 5: >40%) is arbitrary but appears robust. For further details we refer the reader to Jonas and Nilsson (2007: Section 2.4) and right side of Table 1.

Table 3 lists the six signal analysis techniques and summarizes their major characteristics which are explained in detail in Section 3. These are (1) the critical relative uncertainty (CRU) concept; (2) the verification time (VT) concept; (3) the undershooting (Und) concept; (4) the undershooting and VT (Und&VT) concepts combined; (5) the adjustment of emissions (Gillenwater, Sussman and Cohen—GSC #1) concept; and (6) the adjustment of emission reductions (Gillenwater, Sussman and Cohen—GSC #2) concept.

To ensure that all techniques are comparable, they refer to GHG emissions at two points in time, base year, and commitment year, of each country group (see Tables 1 and 2), and are operated under relative emission limitation or reduction (commitment) conditions, with uncertainty expressed in relative terms. Relative uncertainty can range widely depending on the system of GHGs studied (see Box 1 and right side of Table 1).

The major difference between the techniques is whether they follow the concept of trend or total uncertainty (see first and second row in Table 3 and Box 1 for explanations). This determines whether we classify a technique capable of pursuing an "intra-systems view" or even an "intra-systems view that is suited to support an inter-systems (top-down) view" (see third and fourth row in Table 3). The KP can be used as a good example for explaining the difference. The Protocol splits the terrestrial biosphere into directly human-impacted (managed) and not directly human-impacted (natural) parts. However, this artificial separation makes it impossible to estimate the reliability of any system output if only part of the system is considered. The tacit assumptions underlying this approach are that human impact on nature, the unaccounted-for remainder under the Protocol, is irrelevant and inventory uncertainty matters from only a relative point of view over space and time, not an absolute one. But such an approach is highly problematic because biases

Table 3 Major characteristics of the six preparatory signal analysis (SA) techniques compared in this study

Taken into account by the technique	Preparatory SA Technique					
	1	2	3	4	5	6
Trend uncertainty			✓			✓
Total uncertainty	✓	✓		✓	✓	
Intra-systems view			✓			✓
Intra-systems view but suited to support inter-systems (top-down) view	✓	✓		✓	✓	
Emissions difference (between t_1 and t_2 or at t_2)	✓		✓		✓	✓
Emissions gradient (between t_1 and t_2)		✓		✓		
Detectability of when an emission signal outstrips total uncertainty	✓	✓		✓		
Undershooting			✓	✓		
Upward adjustment of reported emissions					✓	✓
Risk with reference to the concept of significance			✓		✓	✓
Risk with reference to the concept of detectability				✓		

Sources: Jonas et al. (2004a: Table 3), Bun (2008: Table 2); modified

1 critical relative uncertainty concept (Gusti and Jęda 2002); *2* verification time concept (Jonas et al. 1999); *3* undershooting concept (Nahorski et al. 2003); *4* undershooting and verification time concepts combined (Jonas et al. 2004a); *5* Gillenwater, Sussman and Cohen #1 concept (Gillenwater et al. 2007); *6* Gillenwater, Sussman and Cohen #2 concept (Gillenwater et al. 2007)

(i.e., discrepancies between true and reported emissions), typically resulting from partial accounting, are not uniform across space and time. In addition, human impact on nature need not be constant or negligible.[4]

3 Preparatory signal analysis techniques

This section is technical in nature. It compares the six preparatory signal analysis techniques listed in Table 3. They allow the emission changes that countries agreed to achieve by the end of the Protocol's first commitment period 2008–2012 to be analyzed in an uncertainty context, with uncertainty expressed in relative terms and taking on the median values of the intervals specified in Box 1. Each technique is described using a standard template which addresses: the technique's starting point for its application; the assumptions made; the systems view followed; the main question(s) addressed; the approach taken; the answer expressed in mathematical terms; and the numerical results; followed by a verbal description of the technique's mathematical-numerical behavior. For both the more detailed mathematical background (SOM_Math) and the more complete set of numerical results (SOM_Num) the reader is referred to the supporting online material.[3]

3.1 CRU concept

The CRU concept is the easiest of the techniques and most straightforward. It centers on the commitment year and asks what the maximal (or critical) relative uncertainty is that a country can report in order to ensure favorable detection at that point in time. Here and in the remainder of the study, "detection" means that the absolute change in net emissions outstrips absolute uncertainty in the commitment year.

Starting Point: Annex B countries comply with their emission limitation or reduction commitments under the KP.

Assumptions:
(1) The relative uncertainty (ρ) of a country's net emissions (x) shall be symmetrical and not change over time, that is, $\rho_1 = \rho_2 (:= \rho)$.[5]
(2) The absolute change in net emissions shall outstrip absolute uncertainty (ε) at t_2, that is, $|x_1 - x_2| > \varepsilon_2$.

Systems View: Intra-systems view suited to supporting inter-systems (top-down) view: only our real diagnostic capabilities of grasping emissions at

[4] In their study Canadell et al. (2007: Table 1), making use of global carbon budget data between 1959 and 2006, show that the efficiency of natural carbon sinks in terms of removing atmospheric CO_2 has declined by about 2.5% per decade. Although this decline may look modest, it represents a mean net "source" to the atmosphere of 0.13 PgC year^{-1} during 2000–2006. In comparison, a 5% reduction in the mean global fossil emissions during the same time period yields a net "sink" of 0.38 PgC year^{-1}. Thus, deteriorating natural carbon sinks as a result of climate change or direct human impact exhibit the potential to offset efforts to reduce fossil fuel emissions. This shows that human impact on nature is indeed not negligible and stresses the need to look at the entire system, that is, to develop a full carbon systems view in which emissions and removals and their trends are monitored in toto.

[5] The CRU concept only considers uncertainty in the commitment year/period, not in the base year (i.e., formally $\varepsilon_1 = 0$). However, for reasons of comparability, we continue to abide by the condition of constant relative uncertainty.

any point in time individually—by absolute uncertainty ε(t)—are of interest. Correlation of uncertainty over time does not matter.

Question: What are the critical relative uncertainties (CRUs) that can be reported by Annex B countries to ensure favorable detection in the commitment year?

Approach: Deterministic (see Fig. 1).

Answer: The answer is given by Eq. A-6 in SOM_Math: Appendix A

$$\rho_{\text{crit}} := \frac{|\delta_{\text{KP}}|}{(1-\delta_{\text{KP}})}, \tag{A-6}$$

where ρ_{crit} is the CRU; and δ_{KP} the normalized emissions change committed under the KP between t_1 and t_2 ($\delta_{\text{KP}} > 0$: emission reduction; $\delta_{\text{KP}} \leq 0$: emission limitation).

Result: The numerical result is given by Table 4 (see also Table A-1 in SOM_Math and worksheet *Crit Rel Unc 1* in SOM_Num).

Table 4 lists δ_{KP} and ρ_{crit} for all Annex B countries under the KP. A country of group 1, for example, has committed itself to reducing its net emissions by 8% (second column). In the case of compliance and under the condition of constant relative uncertainty, the country's net emissions in the commitment year (t_2) only satisfy this concept if they are estimated with a relative uncertainty smaller than 8.7% (third column). With reference to the total uncertainty estimates that are reported annually by the European Union (EU) member states for all Kyoto gases (most recently: EEA 2009), it must be expected that these countries exhibit in the commitment year relative uncertainties in the range of 5–10% and above, rather than below (excluding land use, land-use change, and forestry [LULUCF] and Kyoto mechanisms). Thus, achieving a relative uncertainty smaller than 8.7% appears difficult for quite a few, especially data-poor, Annex B countries.

The CRU concept exhibits a dissimilarity between emission limitation ($\delta_{\text{KP}} < 0$) and reduction ($\delta_{\text{KP}} > 0$). This can be immediately seen when comparing the CRUs that belong to δ_{KP} values that are equal in absolute terms (see, e.g., country groups 1 and 7: ±8.0%). This has consequences when stricter or more lenient Kyoto emission targets are being defined. For instance, in the case of increasingly stricter Kyoto emission targets (let $\delta_{\text{KP}} < 0$ increase), Annex B countries that are committed to emission limitation must decrease their uncertainties according to this concept; their

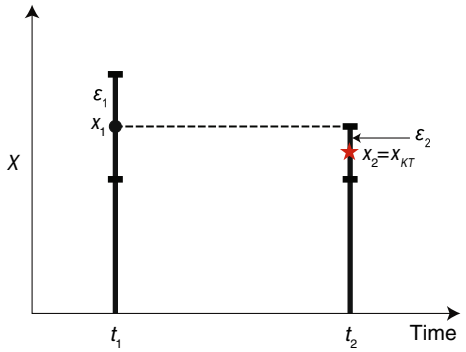

Fig. 1 Illustration of the CRU concept ($\rho_1 = \rho_2$): The absolute change in emissions outstrips uncertainty at t_2. (The absolute change in emissions is given by $|x_1 - x_2| = |\delta_{KP}|x_1$: see Eq. A-2 in SOM_Math: Appendix A). Kyoto (emissions) target (KT). Source: Jonas et al. (2004a: Fig. 8)

Table 4 The CRU concept (Eq. A-6) applied to Annex B countries

Country group	KP commitment δ_{KP}[a] %	CRU ρ_{crit} %	If the CRU concept had been applied
1a–d	8.0	8.7	(a) Compliance with the Kyoto emission target: Annex B countries must be expected to exhibit relative uncertainties in the range of 5–10% and above rather than below (excluding
2	7.0	7.5	emissions/removals due to LULUCF and
3a–c	6.0	6.4	Kyoto mechanisms). Thus, it is impossible for a number of countries in groups 1–4 to meet the condition that their overall relative
4	5.0	5.3	uncertainty is smaller than their CRU ($\rho < \rho_{crit}$).
–	4.0	4.2	(b) Toward more lenient Kyoto emission targets:
–	3.0	3.1	To unambiguously attest a decrease in emissions,
–	2.0	2.0	Annex B countries have to fulfill increasingly
–	1.0	1.0	smaller CRUs.
			(c) Toward stricter Kyoto emission targets: CRUs increase and can be met more easily.
5	0.0	0.0	(a) Compliance with the Kyoto emission target:
6	−1.0	1.0	Same conclusion for countries in groups 5–8 as
–	−2.0	2.0	for countries committed to emission reduction
–	−3.0	2.9	(see a) above.
–	−4.0	3.8	(b) Toward more lenient Kyoto emission targets:
–	−5.0	4.8	CRUs increase and can be met more easily.
–	−6.0	5.7	(c) Toward stricter Kyoto emission targets:
–	−7.0	6.5	To unambiguously attest a decrease in emissions
7	−8.0	7.4	Annex B countries have to fulfill increasingly
–	−9.0	8.3	smaller CRUs.
8	−10.0	9.1	

In the last column, we assess the hypothetical situation that the CRU concept had been applied prior to/during negotiation of the KP. Note the dissimilarity between countries committed to emission reduction ($\delta_{KP} > 0$) and emission limitation ($\delta_{KP} \leq 0$) with the introduction of more lenient or stricter Kyoto emission targets

[a]The countries' emission limitation and reduction commitments under the KP are expressed with the help of δ_{KP}, the normalized change in emissions between t_1 and t_2: $\delta_{KP} > 0$—emission reduction; $\delta_{KP} \leq 0$—emission limitation

CRUs decrease. In contrast, countries committed to emission reduction do not need to do so (let $\delta_{KP} > 0$ increase); their uncertainties can even increase because their CRUs also increase and can be met more easily. The opposite is true in the case of increasingly more lenient Kyoto emission targets. Annex B countries committed to emission reduction must decrease their uncertainties in order to satisfy decreasing CRUs (let $\delta_{KP} > 0$ decrease), while countries committed to emission limitation can even increase their uncertainties because their CRUs also increase and can be met more easily (let $\delta_{KP} < 0$ decrease).

According to this concept the stabilized emissions case ($\delta_{KP} = 0$) should not be allowed—it presupposes zero uncertainty—unless it is ascertained beforehand that relative uncertainties are, or can be expected to be, at least small.

3.2 VT concept

The VT concept goes beyond the CRU concept. In its most simplified version (as employed here) it takes the linear dynamics of the emission signal between base year and commitment year into account and can thus be used to qualify in relative terms the degree of detectability achieved in the commitment year.

Starting Point: Annex B countries comply with their emission limitation or reduction commitments under the KP.

Assumptions:
(1) The relative uncertainty (ρ) of a country's net emissions (x) shall be symmetrical and not change over time, that is, $\rho_1 = \rho_2 (:= \rho)$.
(2) The absolute change in net emissions shall outstrip absolute uncertainty at time t (which can be $\leq$ or $>t_2$), that is, $|\Delta x(t)| > \varepsilon(t)$.

Systems View: Intra-systems view suited to support inter-systems (top-down) view: only our real diagnostic capabilities of grasping emissions at any point in time individually—reflected by absolute uncertainty $\varepsilon(t)$—are of interest. Correlation of uncertainty over time does not matter.

Question: What are the times (also called verification times or VTs) at which the countries' emission signals outstrip uncertainty?[6]

Approach: Deterministic (see Fig. 2).

Answer: The answer is given by Eq. B-7a in SOM_Math: Appendix B

$$\frac{\Delta t}{t_2 - t_1} > \frac{\rho}{|\delta_{KP}| + \delta_{KP}\rho}, \tag{B-7a}$$

where Δt is the VT; and $t_2 - t_1$ the time between base year and commitment year/period upon which the VT is normalized.

Result: The numerical result is given by Table 5 (see also Table B-1 in SOM_Math and worksheet *Verification Time 1* in SOM_Num).

Table 5 lists normalized VTs for all Annex B countries under the KP. The VT concept provides a more detailed detection perspective for negotiators of the Protocol than the CRU concept presented in Section 3.1. It quantifies in detail what the consequences are in the form of normalized VTs if countries report emissions with relative uncertainties that are $\leq$ or $> \rho_{crit}$. Here we explore the range from 2.5% to 30% relative uncertainty, which is given by the medians of classes 1 and 4 (see Box 1 and right side of Table 1).

Moreover, the VT concept corroborates the dissimilarity between emission limitation and reduction, which has already been found for the CRU concept and which is a direct consequence of not demanding a uniform δ_{KP} for all countries under the Protocol. While both the VT concept and the CRU concept favor stricter over more lenient Kyoto emission targets in the case of emission reduction ($\delta_{KP} > 0$), this is not

[6]The term "verification time" was first used by Jonas et al. (1999) and has been used by other authors since then. A more correct term is "detection time" as signal detection does not imply verification. However, we continue to use the original term, as we do not consider it inappropriate given that signal detection must, in the long-term, go hand in hand with bottom-up/top-down verification of emissions (see Jonas and Nilsson 2007: Section 4).

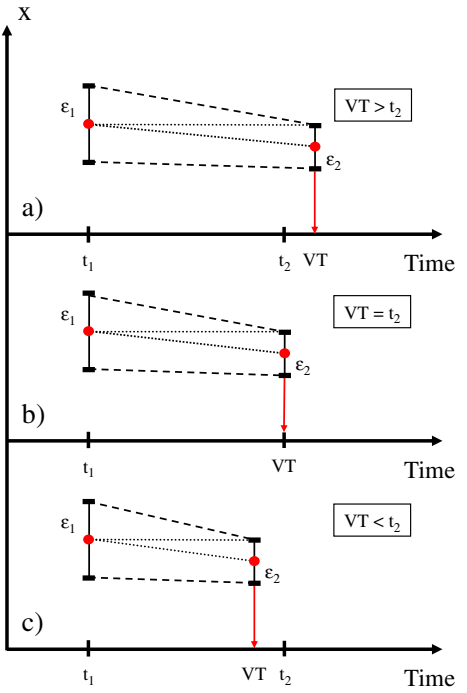

Fig. 2 Illustration of the VT concept ($\rho_1 = \rho_2$): The absolute change in emissions outstrips uncertainty at **a** VT > t_2, **b** VT = t_2 and **c** VT < t_2. (The absolute change in emissions is given by $|x_1 - x_2| = |\delta_{KP}|x_1$: see Eq. A-2 in SOM_Math: Appendix A). Source: Jonas and Nilsson (2007: Fig. 7), modified

so in the case of emission limitation ($\delta_{KP} < 0$) where the two concepts favor more lenient over stricter Kyoto emission targets (because compliance with normalized VTs ≤ 1 becomes less difficult in either case). This is not in line with the spirit of the KP.

3.3 Und concept

Inventoried emissions of GHGs are uncertain, and this uncertainty translates into a risk that true emissions are greater than those estimated and reported. Undershooting helps to limit, or even reduce, this risk, which is what the Und concept allows. In contrast to both the CRU concept and the VT concept, the Und concept also accounts for the uncertainty in the emission estimates in the base year when assessing compliance with the countries' commitments in the commitment year.

The Und concept follows the footsteps of statistical significance in quantifying the aforementioned risk. It correlates uncertainty between base year and commitment year and also allows change in uncertainty to be factored in that can be due to learning and/or result from structural changes in the emitters. However, here we assume that our knowledge of uncertainty stays constant over time in relative terms (first-order approach). This is because researchers are only beginning to diagnose

Table 5 The VT concept (Eq. B-7a) applied to Annex B countries

Country group	Max. allow. VT[a]	KP commit.	Normalized VTs if countries report with $\rho =$				If the VT concept had been applied
	$t_2 - t_1$ yr	δ_{KP}[b] %	2.5%	7.5%	15%	30%	
1a	20	8.0	0.3	0.9	1.6	2.9	(a) Compliance with the Kyoto emissions target: Annex B countries must be expected to exhibit relative uncertainties in the range of 5–10% and above rather than below (excluding emissions/removals due to LULUCF and Kyoto mechanisms). Thus, it is impossible for a number of countries in groups 1–4 to meet the condition $\rho < \rho_{crit}$ or, equivalently, achieve normalized VTs≤1. (b) Toward more lenient Kyoto emission targets: To unambiguously attest a decrease in emissions, Annex B countries have to fulfill increasingly smaller CRUs or, equivalently, find it more difficult to comply with normalized VTs ≤ 1. (c) Toward stricter Kyoto emission targets: CRUs increase and can be met more easily or, equivalently, compliance with normalized VTs ≤ 1 becomes less difficult.
1b	22						
1c	21						
1d	24						
2	20	7.0	0.3	<1.0	1.9	3.3	
3a	20	6.0	0.4	1.2	2.2	3.8	
3b	24						
3c	22						
4	20	5.0	0.5	1.4	2.6	4.6	
–	–	4.0	0.6	1.7	3.3	5.8	
–	–	3.0	0.8	2.3	4.3	7.7	
–	–	2.0	1.2	3.5	6.5	11.5	
–	–	1.0	2.4	7.0	13.0	23.1	

estimated changes in the uncertainty of GHG emissions (notably, CO_2 emissions from fossil fuel burning; Hamal 2010) and to separate their causes.

Starting Point: Annex B countries comply with their emission limitation or reduction commitments under the KP.

Assumptions:
(1) Uncertainties at t_1 and t_2 are given in the form of intervals, which take into account that a difference (ε) might exist between the true (t) but unknown net emissions (x_t) and their best estimates (x).
(2) The relative uncertainty (ρ) of a country's net emissions is symmetrical and does not change over time, that is, $\rho_1 = \rho_2 (:= \rho)$.

Systems View: Intra-systems view: correlation of uncertainty over time matters.

Question: Taking into account the combined uncertainty at t_2 and considering that the true emissions are not known, how much undershooting

Table 5 (continued)

Country group	Max. allow. VT[a] $t_2 - t_1$ yr	KP commit. δ_{KP}[b] %	Normalized VTs if countries report with $\rho =$ 2.5%	7.5%	15%	30%	If the VT concept had been applied
5	20	0.0	Infinite				(a) Compliance with the Kyoto
6	20	−1.0	2.6	8.1	17.6	42.9	emissions target: Same conclusion
–	–	−2.0	1.3	4.1	8.8	21.4	for countries in groups 5–8 as for
–	–	−3.0	0.9	2.7	5.9	14.3	countries committed to emission
–	–	−4.0	0.6	2.0	4.4	10.7	reduction (see (a) above).
–	–	−5.0	0.5	1.6	3.5	8.6	(b) Toward more lenient Kyoto
–	–	−6.0	0.4	1.4	2.9	7.1	emission targets: CRUs increase
–	–	−7.0	0.4	1.2	2.5	6.1	and can be met more easily or,
7	20	−8.0	0.3	>1.0	2.2	5.4	equivalently, compliance with
–	–	−9.0	0.3	0.9	2.0	4.8	normalized VTs≤ 1 becomes
8	20	−10.0	0.3	0.8	1.8	4.3	less difficult.
							(c) Toward stricter Kyoto emission targets: To unambiguously attest a decrease in emissions, Annex B countries have to fulfill increasingly smaller CRUs or, equivalently, find it more difficult to comply with normalized VTs≤ 1.

The table has to be read as follows: The maximal allowable VT ($t_2 - t_1$) for an Annex B country is given for $\rho = \rho_{crit}$ (see second column). For a country of group 1a the maximal allowable VT is 20 years or 1, if normalized. Normalized VTs equal to or smaller than 1 (see green fields for emission reduction and orange fields for emission limitation) are compatible with the KP, that is, countries report with $\rho \leq \rho_{crit}$; normalized VTs greater than 1 (see red fields) are not, that is, countries report with $\rho > \rho_{crit}$. In the last column, we assess the hypothetical situation that the VT concept was applied prior to/during negotiation of the KP. Note the dissimilarity between countries committed to emission reduction ($\delta_{KP} > 0$) and emission limitation ($\delta_{KP} \leq 0$) with the introduction of more lenient or stricter Kyoto emission targets

[a]The maximal allowable VT is calculated for each country group as the difference between 2010 (as the temporal mean over the commitment period 2008–2012) and its base year, or mean base year, for its emissions of CO_2, CH_4, and N_2O (cf. also Table 2)

[b]The countries' emission limitation and reduction commitments under the KP are expressed with the help of δ_{KP}, the normalized change in emissions between t_1 and t_2: $\delta_{KP} > 0$—emission reduction; $\delta_{KP} \leq 0$—emission limitation

(Und) is required to limit the risk α that countries overshoot their true emission limitation or reduction commitments?

Approach: Quasi-statistical, based on interval calculus (see Fig. 3).

Answer: The answer is given by Ineq. C-13 in combination with Eqs. C-15 and C-18 in SOM_Math: Appendix C

$$x_{t,2} \geq (1 - \delta_{KP}) x_{t,1} \text{ with risk } \alpha \Leftrightarrow$$

$$\frac{x_2}{x_1} \leq (1 - \delta_{KP}) \frac{1 - (1 - 2\alpha)(1 - \nu)\rho}{1 + (1 - 2\alpha)(1 - \nu)\rho} = 1 - \delta_{mod}, \qquad \text{(C-13a,c)}$$

where ν approximates (first-order approach) the net (effective) correlation between ε_1 and ε_2; and δ_{mod} is the countries' modified

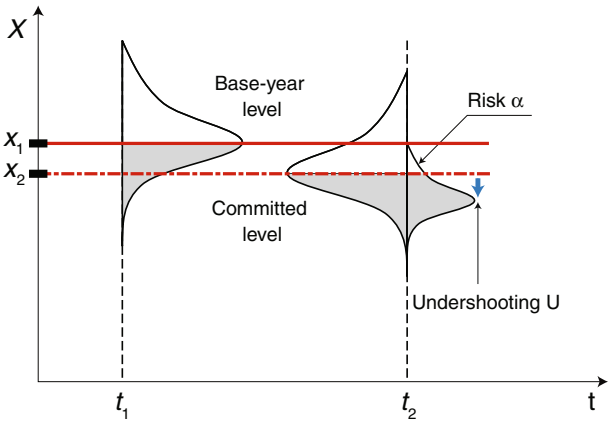

Fig. 3 Illustration of the Und concept ($\rho_1 = \rho_2$) with the help of normal probability density functions: undershooting helps to limit the risk α that countries overshoot their true emission limitation or reduction commitments. Source: Jonas and Nilsson (2007: Fig. 11); modified

(mod) emission limitation or reduction targets defined by

$$\delta_{\text{mod}} = \delta_{\text{KP}} + \text{U} \tag{C-15}$$

and U the undershooting given by

$$\text{U} = 2(1 - \delta_{\text{KP}}) \frac{(1 - 2\alpha)(1 - \nu)\rho}{1 + (1 - 2\alpha)(1 - \nu)\rho}. \tag{C-18}$$

Result: The numerical result is given by Table 6 (see also Table C-1 in SOM_Math and worksheet *Undershooting 4a* in SOM_Num).

Table 6 lists δ_{mod} values as a result of applying Eq. C-15 in combination with Eq. C-18. δ_{KP}, ρ and α are treated as parameters, while the correlation ν is 0.75 (typical for currently reported uncertainties; most recently: EEA 2009: Table 1.20).[7] Table 6 shows that the Und concept is difficult to justify politically in the context of the KP. Under the Protocol, non-uniform emission limitation or reduction commitments (see δ_{KP} values in the second column) were determined "off the cuff," meaning that they were derived via horse trading and that they did not result from rigorous scientific considerations. The outcome is discouraging. Varying δ_{KP} while keeping the relative uncertainty ρ and the risk α constant exhibits that Annex B countries that must comply with a smaller δ_{KP} (they exhibit a small δ_{mod}) are better off than countries that must comply with a larger δ_{KP} (they exhibit a large δ_{mod}). (See, e.g., δ_{mod} values in red for $\rho = 7.5\%$ and $\alpha = 0.3$.) The choice of δ_{KP} dominates Eq. C-15, while the influence of δ_{KP} on U (see Eq. C-18: U$\uparrow$ for $\delta_{\text{KP}} \downarrow$ and vice versa) is negligible and does not compensate for agreed deviations in the δ_{KP} values. Such a situation is not in line with the spirit of the KP.

This situation would be different if the non-uniformity of the emission limitation or reduction commitments were the outcome of a rigorously based process resulting in a straightforward rule that applies equally to all countries, as would be the case, for instance, under the widely discussed contraction and convergence (C&C) approach

[7] Applying Eq. C-7b in SOM_Math: Appendix C with $\varepsilon_{12} \approx 0.03$ (typically reported), $\delta_{\text{KP}} = 0.08$ (valid for many Annex B countries) and $\varepsilon_1 = \varepsilon_2 \approx 0.075$ (see right side of Table 1) results in $\nu \approx 0.79$.

Table 6 The Und concept (Eq. C-15 in combination with Eq. C-18 and a correlation of $\nu = 0.75$ typical for currently reported uncertainties) applied to Annex B countries

Country group	KP commit.	Modified emission or reduction target δ_{mod} in % for limitation					If the Und concept had been applied
	δ_{KP} [a]	$\alpha =$	$\rho =$				
	%	1	2.5%	7.5%	15%	30%	
1a–d	8.0	0.0	9.1	11.4	14.7	20.8	(a) For given δ_{KP} and α:
		0.1	8.9	10.7	13.4	18.4	The greater the ρ, the greater
		0.3	8.5	9.4	10.7	13.4	the modified emission reduction
		0.5	8.0	8.0	8.0	8.0	target δ_{mod} must be to keep the
2	7.0	0.0	8.2	10.4	13.7	20.0	"$x_{t,2}$-greater-than-$(1-\delta_{KP})x_{t,1}$"
		0.1	7.9	9.7	12.4	17.5	risk α at a constant level (see, e.g.,
		0.3	7.5	8.4	9.7	12.4	country group 1: third line:
		0.5	7.0	7.0	7.0	7.0	δ_{mod} values for $\alpha = 0.3$).
3a–c	6.0	0.0	7.2	9.5	12.8	19.1	(b) For given ρ and α:
		0.1	6.9	8.8	11.5	16.6	The smaller the δ_{KP}, the smaller
		0.3	6.5	7.4	8.8	11.5	the modified emission reduction
		0.5	6.0	6.0	6.0	6.0	target δ_{mod} can be to keep the
4	5.0	0.0	6.2	8.5	11.9	18.3	"$x_{t,2}$-greater-than-$(1-\delta_{KP})x_{t,1}$"
		0.1	5.9	7.8	10.5	15.8	risk α at a constant level (see, e.g.,
		0.3	5.5	6.4	7.8	10.5	δ_{mod} values for $\rho = 7.5\%$ and
		0.5	5.0	5.0	5.0	5.0	$\alpha = 0.3$). As a consequence,
–	4.0	0.0	5.2	7.5	10.9	17.4	countries that must comply with
		0.1	5.0	6.8	9.6	14.9	a small δ_{KP} (they exhibit a
		0.3	4.5	5.4	6.8	9.6	small δ_{mod}) are better off than
		0.5	4.0	4.0	4.0	4.0	countries that must comply with
–	3.0	0.0	4.2	6.6	10.0	16.5	a large δ_{KP} (they exhibit a
		0.1	4.0	5.9	8.7	14.0	large δ_{mod}).
		0.3	3.5	4.4	5.9	8.7	
		0.5	3.0	3.0	3.0	3.0	
–	2.0	0.0	3.2	5.6	9.1	15.7	
		0.1	3.0	4.9	7.7	13.1	
		0.3	2.5	3.5	4.9	7.7	
		0.5	2.0	2.0	2.0	2.0	
–	1.0	0.0	2.2	4.6	8.2	14.8	
		0.1	2.0	3.9	6.8	12.2	
		0.3	1.5	2.5	3.9	6.8	
		0.5	1.0	1.0	1.0	1.0	
5	0.0	0.0	1.2	3.7	7.2	14.0	(a) For given δ_{KP} and α: Same
		0.1	1.0	3.0	5.8	11.3	conclusion for country groups 5–8
		0.3	0.5	1.5	3.0	5.8	as for countries committed to
		0.5	0.0	0.0	0.0	0.0	emission reduction (see (a) above).
6	−1.0	0.0	0.3	2.7	6.3	13.1	(b) For given ρ and α: Same
		0.1	0.0	2.0	4.9	10.4	conclusion for country groups 5–8
		0.3	−0.5	0.5	2.0	4.9	as for countries committed to
		0.5	−1.0	−1.0	−1.0	−1.0	emission reduction (see (b) above).
–	−2.0	0.0	−0.7	1.8	5.4	12.2	
		0.1	−1.0	1.0	3.9	9.5	
		0.3	−1.5	−0.5	1.0	3.9	
		0.5	−2.0	−2.0	−2.0	−2.0	

Table 6 (continued)

Country group	KP commit.	Modified emission or reduction target δ_{mod} in % for limitation					If the Und concept had been applied
	δ_{KP} [a]	$\alpha =$	$\rho =$				
	%	1	2.5%	7.5%	15%	30%	
–	−3.0	0.0	−1.7	0.8	4.4	11.4	
		0.1	−2.0	0.0	3.0	8.7	
		0.3	−2.5	−1.5	0.0	3.0	
		0.5	−3.0	−3.0	−3.0	−3.0	
–	−4.0	0.0	−2.7	−0.2	3.5	10.5	
		0.1	−3.0	−0.9	2.1	7.8	
		0.3	−3.5	−2.5	−0.9	2.1	
		0.5	−4.0	−4.0	−4.0	−4.0	
–	−5.0	0.0	−3.7	−1.1	2.6	9.7	
		0.1	−4.0	−1.9	1.1	6.9	
		0.3	−4.5	−3.4	−1.9	1.1	
		0.5	−5.0	−5.0	−5.0	−5.0	
–	−6.0	0.0	−4.7	−2.1	1.7	8.8	
		0.1	−4.9	−2.9	0.2	6.0	
		0.3	−5.5	−4.4	−2.9	0.2	
		0.5	−6.0	−6.0	−6.0	−6.0	
–	−7.0	0.0	−5.7	−3.1	0.7	7.9	
		0.1	−5.9	−3.8	−0.8	5.1	
		0.3	−6.5	−5.4	−3.8	−0.8	
		0.5	−7.0	−7.0	−7.0	−7.0	
7	−8.0	0.0	−6.7	−4.0	−0.2	7.1	
		0.1	−6.9	−4.8	−1.7	4.2	
		0.3	−7.5	−6.4	−4.8	−1.7	
		0.5	−8.0	−8.0	−8.0	−8.0	
–	−9.0	0.0	−7.6	−5.0	−1.1	6.2	
		0.1	−7.9	−5.8	−2.7	3.3	
		0.3	−8.5	−7.4	−5.8	−2.7	
		0.5	−9.0	−9.0	−9.0	−9.0	
8	−10.0	0.0	−8.6	−6.0	−2.0	5.3	
		0.1	−8.9	−6.7	−3.6	2.5	
		0.3	−9.5	−8.4	−6.7	−3.6	
		0.5	−10.0	−10.0	−10.0	−10.0	

The table lists modified emission limitation or reduction targets δ_{mod} for all Annex B countries, where the "$x_{t,2}$-greater-than-$(1-\delta_{KP})\,x_{t,1}$" risk α is specified to be 0, 0.1, 0.3, and 0.5. If an Annex B country complies with its emission limitation or reduction commitment ($x_2 = (1-\delta_{KP})\,x_1$), the risk that its true, but unknown, emissions $x_{t,2}$ are equal to or greater than its true, but unknown, target $(1-\delta_{KP})\,x_{t,1}$ is 50%. Undershooting decreases this risk. For instance, a country of group 1 has committed itself to reduce its net emissions by 8%. If it reports with a 7.5% relative uncertainty, it needs to reduce emissions by 11.4% to decrease the risk from 50% to 0%. In the last column, we assess the hypothetical situation that the Und concept was applied prior to/during negotiation of the KP. Note the unfavorable situation, which arises when δ_{KP} varies while ρ and α are kept constant

[a]The countries' emission limitation and reduction commitments under the KP are expressed with the help of δ_{KP}, the normalized change in emissions between t_1 and t_2: $\delta_{KP} > 0$—emission reduction; $\delta_{KP} \leq 0$—emission limitation

(e.g., WBGU 2003: Section 2.3; Pearce 2003). Under such conditions, it would be the undershooting U that matters, not the modified emission limitation or reduction target δ_{mod}.

3.4 Und&VT concepts combined

The Und&VT concept seeks to combine the strengths of both the introduction of risk by the Und concept and the explicit consideration of time by the VT concept in detecting an emission signal. That is, the Und&VT concept also allows undershooting to limit, or even reduce, the risk that the true emissions are greater than those estimated and reported; and it addresses the degree of detectability achieved in the commitment year. The Und&VT concept, like the VT concept, accounts for the linear dynamics of the emission signal between base year and commitment year, and uncertainty at the latter. In contrast to the Und concept, it thus follows the footsteps of signal detection in quantifying the aforementioned risk. Concomitantly, the Und&VT seeks to overcome some of the undesirable properties of both the VT concept (countries committed to equal emission limitation and reduction targets in absolute terms are treated dissimilarly) and the Und concept (countries committed to different emission changes under the KP are assigned different modified emission limitation or reduction targets)

Starting Point: Annex B countries comply with their emission limitation or reduction commitments under the KP.

Assumptions:
(1) Uncertainties at t_1 and t_2 are given in the form of intervals, which take into account that a difference (ε) might exist between the true (t) but unknown net emissions (x_t) and their best estimates (x).
(2) The relative uncertainty (ρ) of a country's net emissions is symmetrical and does not change over time, that is, $\rho_1 = \rho_2 (:= \rho)$.[8]
(3) The absolute change in net emissions shall outstrip uncertainty at time $t \leq t_2$, that is, the VT shall be equal to, or smaller than, the maximal allowable VT ($\Delta t \leq t_2 - t_1$).

Systems View: Intra-systems view suited to support inter-systems (top-down) view: only our real diagnostic capabilities of grasping emissions at any point in time individually—reflected by absolute uncertainty $\varepsilon(t)$—are of interest. Correlation of uncertainty over time does not matter.

Question: If risk is the strength of the Und concept and time in detecting an emission signal is the strength of the VT concept, can these concepts be combined (Und&VT) to take advantage of the two?

Approach: Quasi-statistical, based on interval calculus (see Fig. 4).

Answer: The answer comprises four cases depending on how δ_{crit}, the critical emission limitation or reduction, and δ_{KP} relate to each other (see Fig. 4). δ_{crit} allows a distinction to be made between detectable and

[8] The Und&VT concept only considers uncertainty in the commitment year/period, not in the base year (i.e., formally $x_{t,1} = x_1$ and $\nu = 0$). However, for reasons of comparability, we continue to abide by the condition of constant relative uncertainty.

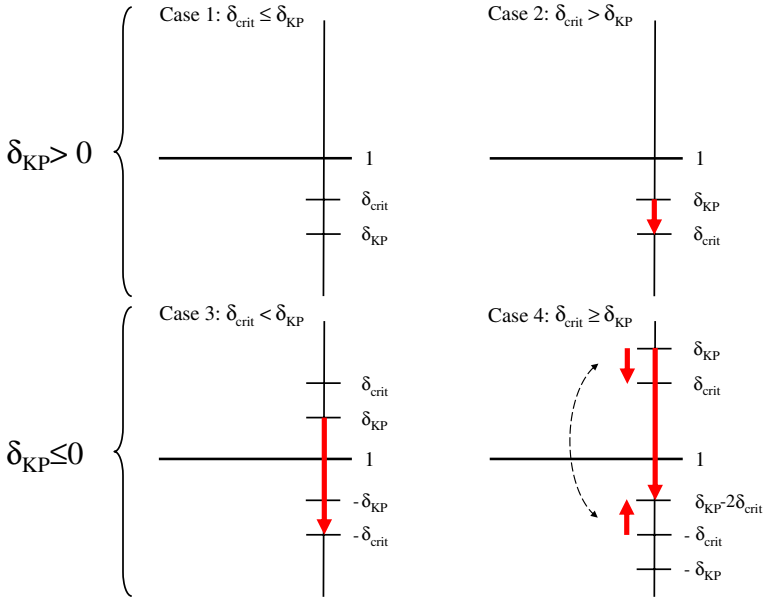

Fig. 4 Illustration of the Und&VT concept ($\rho_1 = \rho_2$). This preserves risk as the strength of the Und concept and detectability as the strength of the VT concept. Depending on how δ_{crit} and δ_{KP} relate to each other, four cases can be distinguished (see text). These differ in terms of detectability (Cases 1 and 4) versus non-detectability (Cases 2 and 3) and an initial obligatory undershooting U_{Gap} that is introduced (Cases 2–4) to ensure that detectability of emission reductions, not increases, is given before Annex B countries are permitted to make economic use of potential excess emission reductions. Emission reduction: $\delta_{KP} > 0$; emission limitation: $\delta_{KP} \leq 0$. Source: Hamal and Jonas (2008b: Fig. 4)

non-detectable emission changes.[9] The complete answer is given by (see SOM_Math: Appendix D for the inequalities and equations mentioned below)

Case 1: $\delta_{KP} > 0$: $\delta_{crit} \leq \delta_{KP}$:

$$x_{t,2} \geq (1 - \delta_{KP}) x_{t,1} \text{ with risk } \alpha \Leftrightarrow$$

$$\frac{x_2}{x_1} \leq (1 - \delta_{KP}) \frac{1}{1 + (1 - 2\alpha)\rho} = 1 - \delta_{mod}, \quad \text{(D-3), (C-13c)}$$

where δ_{mod} is defined as above (see Eq. C-15) and U is given by

$$U = (1 - \delta_{KP}) \frac{(1 - 2\alpha)\rho}{1 + (1 - 2\alpha)\rho}. \quad \text{(D-5)}$$

[9]Compliance with δ_{crit} ensures detectability in the commitment year. δ_{crit} is given by Eq. D-1 in SOM_Math: Appendix D; it is $\rho/(1 + \rho)$ in the case $\delta_{KP} > 0$ (emission reduction) and $-\rho/(1 - \rho)$ in the case $\delta_{KP} = 0$ (emission limitation). To overcome the dissimilarity between these two cases—δ_{crit} is smaller in absolute terms for emission reduction than for emission limitation—it is adjusted by Eq. D-2 in SOM_Math: Appendix D to $\rho/(1 + \rho)$ in the case $\delta_{KP} > 0$ (emission reduction) and $-\rho/(1 + \rho)$ in the case $\delta_{KP} = 0$ (emission limitation); that is, detectability as under emission reduction is declared as standard (in absolute terms).

Case 2: $\delta_{KP} > 0$: $\delta_{crit} > \delta_{KP}$:

$x_{t,2} \geq (1 - \delta_{crit}) x_{t,1}$ with risk $\alpha \Leftrightarrow$

$$\frac{x_2}{x_1} \leq (1 - \delta_{crit}) \frac{1}{1 + (1 - 2\alpha)\rho} = 1 - \delta_{mod}, \quad \text{(D-6), (C-13c)}$$

where δ_{mod} is defined as before (see Eq. C-15) and U is given by

$$U = U_{Gap} + (1 - \delta_{crit}) \frac{(1 - 2\alpha)\rho}{1 + (1 - 2\alpha)\rho} \tag{D-8}$$

with

$$U_{Gap} = \delta_{crit} - \delta_{KP}. \tag{D-9}$$

Case 3: $\delta_{KP} \leq 0$: $\delta_{crit} < \delta_{KP}$:

$x_{t,2} \geq (1 + \delta_{crit}) x_{t,1}$ with risk $\alpha \Leftrightarrow$

$$\frac{x_2}{x_1} \leq (1 + \delta_{crit}) \frac{1}{1 + (1 - 2\alpha)\rho} = 1 - \delta_{mod}, \text{ (D-10), (C-13c)}$$

where δ_{mod} is defined as above (see Eq. C-15) and U is given by

$$U = U_{Gap} + (1 + \delta_{crit}) \frac{(1 - 2\alpha)\rho}{1 + (1 - 2\alpha)\rho} \tag{D-12}$$

with

$$U_{Gap} = -(\delta_{KP} + \delta_{crit}). \tag{D-13}$$

Case 4: $\delta_{KP} \leq 0$: $\delta_{crit} \geq \delta_{KP}$:

$x_{t,2} \geq \left(1 + \delta'_{crit}\right) x_{t,1}$ with risk $\alpha \Leftrightarrow$

$$\frac{x_2}{x_1} \leq \left(1 + \delta'_{crit}\right) \frac{1}{1 + (1 - 2\alpha)\rho} = 1 - \delta_{mod}, \text{ (D-14), (C-13c)}$$

where δ_{mod} is defined as before (see Eq. C-15) and U is given by

$$U = U_{Gap} + \left(1 + \delta'_{crit}\right) \frac{(1 - 2\alpha)\rho}{1 + (1 - 2\alpha)\rho} \tag{D-16}$$

with

$$U_{Gap} = -2\delta_{crit} \tag{D-17}$$

$$-\delta'_{crit} = \delta_{KP} - 2\delta_{crit}. \tag{D-18}$$

U_{Gap} in Cases 2–4 is an initial obligatory undershooting, which is introduced to ensure that detectability is achieved before Annex B countries are permitted to make economic use of potential excess emission reductions.

Result: The numerical is given by Table 7 (see also Table D-3 in SOM_Math and worksheet *Und&VT 2a* in SOM_Num).

Table 7 lists δ_{mod} values as a result of applying Eq. C-15 in combination with: Eq. D-5 (Case 1), Eq. D-8 to D-9 (Case 2), Eq. D-12 to D-13 (Case 3), and Eqs. D-16 to D-18 (Case 4). δ_{KP}, ρ and α are treated as parameters. By employing δ_{crit} as a

Table 7 The Und&VT concept (Eq. C-15 in combination with: Eq. D-5 [Case 1: green fields], Eqs. D-8 to D-9 [Case 2: red fields], Eqs. D-12 to D-13 [Case 3: red fields], and Eqs. D-16 to D-18 [Case 4: orange fields]) applied to Annex B countries

Country group	KP commit.	Modified emission limitation of reduction target δ_{mod} in % for					If the Und&VT concept had been applied
	δ_{KP}[a]	α =	ρ =				
	%	1	2.5%	7.5%	15%	30%	
1a–d	8.0	0.0	10.2	14.4	24.4	40.8	Case 1 (green-colored area): $\delta_{crit} \leq \delta_{KP}$:
		0.1	9.8	13.2	22.4	38.0	No necessity to introduce U_{Gap}; the δ_{mod}
		0.3	8.9	10.7	18.0	31.3	values from Table 6 are still valid.
		0.5	8.0	8.0	13.0	23.1	Case 2 (red-colored area): $\delta_{crit} > \delta_{KP}$:
2	7.0	0.0	9.3	13.5	24.4	40.8	Increase of δ_{KP} by U_{Gap} to reach δ_{crit},
		0.1	8.8	12.3	22.4	38.0	the relevant reference for undershooting.
		0.3	7.9	9.7	18.0	31.3	Undershooting depends only on ρ and α
		0.5	7.0	7.0	13.0	23.1	and no longer on δ_{KP} (see Eqs. D-8 to
3a–c	6.0	0.0	8.3	13.5	24.4	40.8	D-9 in combination with Eq. C-15). This
		0.1	7.8	12.2	22.4	38.0	explains why δ_{mod} appears uniform for
		0.3	6.9	9.7	18.0	31.3	given ρ and α. Thus, the Und&VT
		0.5	6.0	7.0	13.0	23.1	concept rectifies the Und concept under
4	5.0	0.0	7.3	13.5	24.4	40.8	which countries complying with a small
		0.1	6.9	12.2	22.4	38.0	δ_{KP} exhibit a small δ_{mod}, while countries
		0.3	5.9	9.7	18.0	31.3	complying with a large δ_{KP} exhibit a large
		0.5	5.0	7.0	13.0	23.1	δ_{mod} (cf. Table 6).
–	4.0	0.0	6.3	13.5	24.4	40.8	
		0.1	5.9	12.2	22.4	38.0	
		0.3	5.0	9.7	18.0	31.3	
		0.5	4.0	7.0	13.0	23.1	
–	3.0	0.0	5.4	13.5	24.4	40.8	
		0.1	4.9	12.2	22.4	38.0	
		0.3	4.0	9.7	18.0	31.3	
		0.5	3.0	7.0	13.0	23.1	
–	2.0	0.0	4.8	13.5	24.4	40.8	
		0.1	4.4	12.2	22.4	38.0	
		0.3	3.4	9.7	18.0	31.3	
		0.5	2.4	7.0	13.0	23.1	
–	1.0	0.0	4.8	13.5	24.4	40.8	
		0.1	4.4	12.2	22.4	38.0	
		0.3	3.4	9.7	18.0	31.3	
		0.5	2.4	7.0	13.0	23.1	

Table 7 (continued)

Country group	KP commit.	Modified emission limitation of reduction target δ_{mod} in % for					If the Und&VT concept had been applied
	δ_{KP}[a]	$\alpha =$	$\rho =$				
	%	1	2.5%	7.5%	15%	30%	
5	0.0	0.0	4.8	13.5	24.4	40.8	Case 3 (red-colored area): $\delta_{crit} < \delta_{KP}$: Increase of δ_{KP} by U_{Gap} to reach $-\delta_{crit}$, the relevant reference for undershooting. Undershooting depends only on ρ and α and no longer on δ_{KP} (see Eqs. D-12 to D-13 in combination with Eq. C-15). This explains why δ_{mod} appears uniform for a given ρ and α. Thus, the Und&VT concept rectifies the Und concept under which countries complying with a small δ_{KP} exhibit a small δ_{mod}, while countries complying with a large δ_{KP} exhibit a large δ_{mod} (cf. Table 6). Case 4 (orange-colored area): $\delta_{crit} \geq \delta_{KP}$: Increase of δ_{KP} by U_{Gap} to reach $\delta_{KP} - 2\delta_{crit}$, the relevant reference for undershooting. In contrast to Case 3 ($\delta_{crit} < \delta_{KP}$) above, undershooting still depends on δ_{KP} (see Eqs. D-16 to D-18 in combination with Eq. C-15). This is a consequence of how the undershooting is achieved: detectability on the emissions limitation side is used to decrease the reference for undershooting ($\delta_{KP} - 2\delta_{crit}$) on the emission reduction side.
		0.1	4.4	12.2	22.4	38.0	
		0.3	3.4	9.7	18.0	31.3	
		0.5	2.4	7.0	13.0	23.1	
6	−1.0	0.0	4.8	13.5	24.4	40.8	
		0.1	4.4	12.2	22.4	38.0	
		0.3	3.4	9.7	18.0	31.3	
		0.5	2.4	7.0	13.0	23.1	
–	−2.0	0.0	4.8	13.5	24.4	40.8	
		0.1	4.4	12.2	22.4	38.0	
		0.3	3.4	9.7	18.0	31.3	
		0.5	2.4	7.0	13.0	23.1	
–	−3.0	0.0	4.3	13.5	24.4	40.8	
		0.1	3.8	12.2	22.4	38.0	
		0.3	2.8	9.7	18.0	31.3	
		0.5	1.9	7.0	13.0	23.1	
–	−4.0	0.0	3.3	13.5	24.4	40.8	
		0.1	2.8	12.2	22.4	38.0	
		0.3	1.9	9.7	18.0	31.3	
		0.5	0.9	7.0	13.0	23.1	
–	−5.0	0.0	2.3	13.5	24.4	40.8	
		0.1	1.8	12.2	22.4	38.0	
		0.3	0.9	9.7	18.0	31.3	
		0.5	−0.1	7.0	13.0	23.1	
–	−6.0	0.0	1.3	13.5	24.4	40.8	
		0.1	0.9	12.2	22.4	38.0	
		0.3	−0.1	9.7	18.0	31.3	
		0.5	−1.1	7.0	13.0	23.1	
–	−7.0	0.0	0.4	13.4	24.4	40.8	
		0.1	−0.1	12.2	22.4	38.0	
		0.3	−1.1	9.7	18.0	31.3	
		0.5	−2.1	7.0	13.0	23.1	

uniform detectability criterion, the Und&VT concept overcomes the dissimilarity of both the VT concept and the CRU concept between countries committed to emission reduction ($\delta_{KP} > 0$) and emission limitation ($\delta_{KP} \leq 0$), which arises if more lenient or stricter Kyoto emission targets are introduced (cf. with Tables 4 and 5). Moreover, the Und&VT concept also rectifies Cases 2 and 3, the cases of non-detectability (before correction), that is, the politically unfavorable situation under

Table 7 (continued)

Country group	KP commit.	Modified emission limitation of reduction target δ_{mod} in % for					If the Und&VT concept had been applied
	δ_{KP}[a]	$\alpha =$	$\rho =$				
	%	1	2.5%	7.5%	15%	30%	
7	−8.0	0.0	−0.6	12.5	24.4	40.8	
		0.1	−1.1	11.3	22.4	38.0	
		0.3	−2.1	8.7	18.0	31.3	
		0.5	−3.1	6.0	13.0	23.1	
–	−9.0	0.0	−1.6	11.6	24.4	40.8	
		0.1	−2.1	10.3	22.4	38.0	
		0.3	−3.1	7.7	18.0	31.3	
		0.5	−4.1	5.0	13.0	23.1	
8	−10.0	0.0	−2.6	10.7	24.4	40.8	
		0.1	−3.1	9.4	22.4	38.0	
		0.3	−4.1	6.8	18.0	31.3	
		0.5	−5.1	4.0	13.0	23.1	

The table lists modified emission limitation or reduction targets δ_{mod} for all Annex B countries, where the "$x_{t,2}$-greater-than-$(1-\delta_{KP})\,x_{t,1}$" risk α (Case 1), the "$x_{t,2}$-greater-than-$(1-\delta_{crit})\,x_{t,1}$" risk α (Case 2), the "$x_{t,2}$-greater-than-$(1+\delta_{crit})\,x_{t,1}$" risk α (Case 3), and the "$x_{t,2}$-greater-than-$(1-(\delta_{KP}-2\delta_{crit}))\,x_{t,1}$" risk α (Case 4), respectively, are specified to be 0, 0.1, 0.3, and 0.5. In the last column, we assess the hypothetical situation that the Und&VT concept was applied prior to/during negotiation of the KP. The Und&VT concept rectifies Cases 2 and 3, the cases of non-detectability (before correction), that is, the unfavorable situation under the Und concept under which countries complying with a small δ_{KP} exhibit a small δ_{mod}, while countries complying with a large δ_{KP} exhibit a large δ_{mod} (cf. Table 6)

[a]The countries' emission limitation and reduction commitments under the KP are expressed with the help of δ_{KP}, the normalized change in emissions between t_1 and t_2: $\delta_{KP} > 0$—emission reduction; $\delta_{KP} \leq 0$—emission limitation

the Und concept whereby countries complying with a small δ_{KP} exhibit a small δ_{mod}, while countries complying with a large δ_{KP} exhibit a large δ_{mod} (cf. Table 6).

However, this concept reveals a crucial difficulty from a political perspective. The Und&VT concept requires the KP's emission targets to be corrected through the introduction of an initial obligatory undershooting (U_{Gap}) so that the countries' emission reductions, not limitations, become detectable (i.e., meet the maximal allowable VT) before the countries are permitted to make economic use of their excess emission reductions. (See, e.g., group 1 countries in Table 7 ($\delta_{KP} = 8\%$) under Case 2 conditions: the δ_{mod} value for $\rho = 15\%$ and $\alpha = 0.5$ is $\delta_{mod} = \delta_{KP} + U_{Gap} = 13\%$ ($U = U_{Gap}$); that is, the initial obligatory undershooting is $U_{Gap} = 13\% - 8\% = 5\%$.) It remains to be seen whether this strict interpretation of signal detection will be accepted by Annex B countries, as it forces them to strive for detectability, that is, to first invest before they can profit from their economic actions. Notwithstanding, opponents of this concept must realize that the countries' detectability, that the "$x_{t,2}$-greater-than-$(1-\delta_{KP})x_{t,1}$" risk (Case 1), the "$x_{t,2}$-greater-than-$(1-\delta_{crit})x_{t,1}$" risk (Case 2), the "$x_{t,2}$-greater-than-$(1+\delta_{crit})x_{t,1}$" risk (Case 3), and the "$x_{t,2}$-greater-than-$(1-(\delta_{KP}-2\delta_{crit}))x_{t,1}$" risk (Case 4) of their emission signals can be grasped and thus priced—although the countries' true net emissions at t_1 and t_2 are unknown!

3.5 GSC #1 concept

GSC #1 refers to the first of the two concepts that Gillenwater et al. presented in 2007, following the notion of adjusting countries' national emissions in response to, and in accordance with, the estimated uncertainties and a statistically valid method. The GSC #1 concept centers on the commitment year and requires confidence that when countries report emissions inventories that nominally are in agreement with their commitments under the Protocol, the countries truly are, if not in compliance, then at least within a given tolerance of compliance with their commitments. That is, the GSC #1 concept considers a relative upward adjustment that seeks to attain a reasonable level of confidence that countries have actually achieved the target emissions stated in their commitments under the KP and are in compliance. Ultimately, countries must reduce their emissions in the commitment year by the amount of their upward adjustment to remain in compliance.

Starting Point: Annex B countries comply with their emission limitation or reduction commitments under the KP.[10]

Assumptions:
(1) It is accepted a priori that the true, but unknown, net emissions at t_2 ($x_{t,2}$) can exceed (overshoot) the target emissions commitment (x_2) by some fractional or percentage amount (p or p%, respectively).
(2) The relative uncertainty (ρ) of a country's net emissions is symmetrical and does not change over time, that is, $\rho_1 = \rho_2 (:= \rho)$.[11]
(3) The probability distributions for estimated emissions are normal and the shape of the emissions probability distribution for each country does not change significantly as emissions change.

Systems View: Intra-systems view suited to support inter-systems (top-down) view: only our real diagnostic capabilities of grasping emissions at any point in time individually—reflected by absolute uncertainty $\varepsilon(t)$—are of interest. Correlation of uncertainty over time does not matter.

Question: Can we attain a reasonable level of confidence that countries will have actually achieved the target emissions levels stated in their commitments under the KP and are in compliance? That is: (1) Would we consider it acceptable if true emissions exceed (overshoot) the target emissions commitment by some fractional or percentage amount? (2) How much is that amount? (3) How confident do we want to be in our result?

[10] The two emission adjustment methods presented by Gillenwater, Sussman and Cohen (GSC #1 and GSC #2) were meant to be applied in retrospect (Gillenwater et al. 2007). However, their methods can also be used to generate information that one would like to discuss in advance; that is, they can also be perceived as preparatory signal analysis techniques and thus be compared with the other four techniques discussed so far.

[11] The GSC #1 concept considers uncertainty only in the commitment year/period, not in the base year. However, for reasons of comparability, we continue to abide by the condition of constant relative uncertainty.

Approach: Statistical (see Fig. 5).

Answer: Depending on whether or not excess emissions are accepted and favorable compliance conditions exist a priori, the modified GSC #1 concept of Gillenwater et al. (2007) comprises three cases (see Fig. 5). The complete answer is given by (see SOM_Math: Appendix E for the equations mentioned below)

Cases 1 and 2: $\delta_{KP} > 0$: $p = \delta_{crit}$:

$$\text{Adj} = \begin{cases} 1 & 1 + z_{u,2}(F_N)\dfrac{\rho}{1.96} \le 1 + \rho_{crit} \\ & \text{(excess emissions accepted)} \\ & \text{for} \\ \dfrac{1 + z_{u,2}(F_N)\frac{\rho}{1.96}}{1 + \rho_{crit}} & 1 + z_{u,2}(F_N)\dfrac{\rho}{1.96} > 1 + \rho_{crit} \\ & \text{(excess emissions accepted)} \end{cases} \quad \text{(E-7,8)}$$

Case 3: $\delta_{KP} \le 0$: $p = 0$:

$$\text{Adj} = 1 + z_{u,2}(F_N)\frac{\rho}{1.96} \text{ (excess emissions not accepted)}, \quad \text{(E-9)}$$

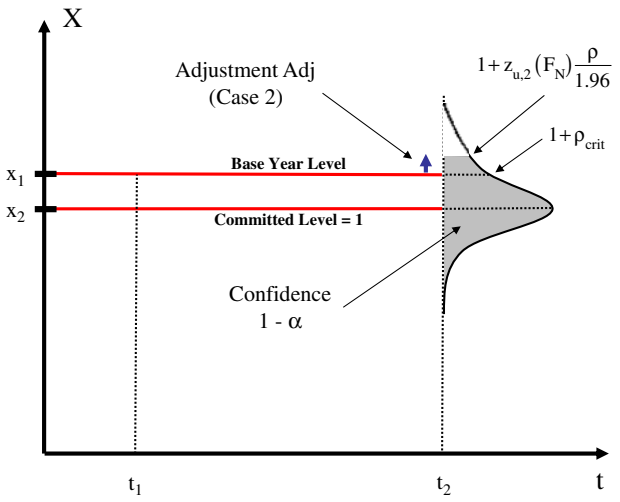

Fig. 5 Illustration of the GSC #1 concept ($\rho_1 = \rho_2$) with the help of the standard normal probability density function. This allows the confidence $(1-\alpha)$ to be specified via F_N that a country's true, but unknown, emissions comply with its Kyoto emissions target. Depending on whether or not excess emissions are accepted and favorable compliance conditions exist a priori, three cases are distinguished. Here, Case 2 is shown. Given an uncertainty of ρ%, this case requires a country's emissions estimate to be adjusted at t_2 upward if we want to be $(1-\alpha)$% confident that its true emissions do not exceed its KT (here referred to as 1) by more than ρ_{crit}%. Emission reduction: $\delta_{KP} > 0$; emission limitation: $\delta_{KP} \le 0$

where p specifies the accepted (fractional) amount by which true emissions can exceed target emissions commitments; $\rho/1.96$ is the standard deviation; F_N the standardized cumulative normal distribution; $z_{u,2}$ the standardized accepted upper (u) emissions limit at t_2; ρ_{crit} the CRU introduced in Section 3.1; and Adj the resulting upward adjustment of the country's emissions estimate relative to its KT (i.e., de facto an emission reduction by this amount more than the country's commitment in order to remain in compliance with that commitment).

Result: The numerical result is given by Table 8 (see also Table E-1 in SOM_Math and worksheet *GSC_I 1a* in SOM_Num).

Table 8 lists adjustment (Adj) values as a result of applying Eq. E-7 (Case 1), Eq. E-8 (Case 2) and Eq. E-9 (Case 3). They specify the required upward adjustment of the country's emissions estimate or, equivalently, the de facto emission reduction by this amount more than the country's commitment, in order to remain in compliance with that commitment. For any given δ_{KP} value (thus, ρ_{crit} value; see Eq. A-6 in Section 3.1), inventory uncertainty (ρ) is treated as parameter as well as the confidence $(1-\alpha)$ that true emissions do not exceed (overshoot) target emissions by more than $p = \delta_{crit}$ (Cases 1 and 2: this value for p ensures that, relative to committed target emissions, base year emissions are not exceeded) and $p = 0$ (Case 3: excess emissions are not accepted in the case of emission limitation). The confidence $(1-\alpha)$ is specified to be 0.9, 0.7, and 0.5. The table shows that the GSC #1 concept is not easy to handle because it requires strict enforcement under the KP. Emission reduction ($\delta_{KP} > 0$) under the GSC #1 concept behaves mirror-inverted to the Und concept as a consequence of non-uniform emission reduction commitments: varying δ_{KP} while keeping the relative uncertainty ρ and the confidence $(1-\alpha)$ constant exhibits that Annex B countries that must comply with a large δ_{KP} (they exhibit a small Adj) are better off than countries that must comply with a small δ_{KP} (they exhibit a large Adj). (See, e.g., Adj values in red for $\rho = 15\%$ and $1-\alpha = 0.9$.) However, this is only true if adjustments must be compensated for by additional emission reductions (undershooting mode) and if they are not misused by policy and decision makers just for establishing a country comparison in terms of confidence (confidence mode) that does not result in a compulsory undershooting. In the latter case, countries that must comply with a small δ_{KP} (they exhibit a large Adj) are better off than countries that must comply with a large δ_{KP} (they exhibit a small Adj). This situation would not be in line with the spirit of the KP.

3.6 GSC #2 concept

GSC #2 refers to the second of the two concepts that Gillenwater et al. presented in 2007. In contrast to GSC #1, their second concept also accounts for the uncertainty in the emission estimates in the base year when assessing compliance with countries' commitments in the commitment year. The GSC #2 concept requires confidence that, when countries report emissions inventories that are nominally in agreement with their commitments under the Protocol, emissions have actually been reduced by an amount equal to the difference in emissions between base year and commitment

Table 8 The GSC #1 concept (Eq. E-7 [Case 1: green fields; here, the Adj<1 values have not been set to 1], Eq. E-8 [Case 2: orange fields], and Eq. E-9 [Case 3: red fields]) applied to Annex B countries

Country group	KP commit.	CRU	Adjustment factor Adj (absolute) for					If the GSC #1 concept had been applied
	δ_{KP}[a]	ρ_{crit}	$1-\alpha=$	$\rho=$				
	%	%	1	2.5%	7.5%	15%	30%	
1a–d	8.0	8.7	1.0					Case 1 (green-colored area):
			0.9	0.935	0.965	1.010	1.100	$p = \delta_{crit}$ Adj ≤ 1: Favorable
			0.7	0.926	0.938	0.957	0.994	compliance conditions; no need
			0.5	0.920	0.920	0.920	0.920	for an adjustment (Adj can be
2	7.0	7.5	1.0					set to 1).
			0.9	0.945	0.976	1.021	1.112	Case 2 (orange-colored area):
			0.7	0.936	0.949	0.967	1.005	$p = \delta_{crit}$, Adj > 1:
			0.5	0.930	0.930	0.930	0.930	The greater the ρ, the
3a–c	6.0	6.4	1.0					uncertainty surrounding the
			0.9	0.955	0.986	1.032	1.124	emissions inventory estimate,
			0.7	0.946	0.959	0.978	1.015	or the greater $(1-\alpha)$, the
			0.5	0.940	0.940	0.940	0.940	degree of confidence that is
4	5.0	5.3	1.0					required, the greater the
			0.9	0.966	0.997	1.043	1.136	adjustment Adj. However,
			0.7	0.956	0.969	0.988	1.026	the smaller δ_{KP} the greater
			0.5	0.950	0.950	0.950	0.950	the adjustment Adj to keep
–	4.0	4.2	1.0					the confidence$(1-\alpha)$ at a
			0.9	0.976	1.007	1.054	1.148	constant level (see, e.g., Adj
			0.7	0.966	0.979	0.999	1.037	values for $\rho = 15\%$ and
			0.5	0.960	0.960	0.960	0.960	$1-\alpha = 0.9$). As a
–	3.0	3.1	1.0					consequence, countries that
			0.9	0.986	1.018	1.065	1.160	must comply with a large δ_{KP}
			0.7	0.976	0.989	1.009	1.048	(they exhibit a small Adj) are
			0.5	0.970	0.970	0.970	0.970	better off than countries
–	2.0	2.0	1.0					that must comply with a small
			0.9	0.996	1.028	1.076	1.172	δ_{KP} (they exhibit a large Adj).
			0.7	0.987	1.000	1.019	1.059	This is only true if adjustments
			0.5	0.980	0.980	0.980	0.980	must be compensated for by
–	1.0	1.0	1.0					additional emission reductions
			0.9	1.006	1.039	1.087	1.184	(undershooting mode).
			0.7	0.997	1.010	1.030	1.069	However, the opposite is true
			0.5	0.990	0.990	0.990	0.990	if this compensation is not
								compulsory and adjustments
								are only used to establish a
								country comparison
								in terms of confidence
								(confidence mode) without
								compulsory undershooting. In

Table 8 (continued)

Country group	KP commit.	CRU	Adjustment factor Adj (absolute) for					If the GSC #1 concept had been applied
	δ_{KP}[a]	ρ_{crit}	$1-\alpha=$	$\rho=$				
	%	%	1	2.5%	7.5%	15%	30%	
								the latter case countries that must comply with a small δ_{KP} (they exhibit a large Adj) are better off than countries that must comply with a large δ_{KP} (they exhibit a small Adj).
5	0.0	0.0	1.0					Case 3 (red-colored area): p = 0,
			0.9	1.016	1.049	1.098	1.196	Adj ≥ 1:
			0.7	1.007	1.020	1.040	1.080	The fractional factor p which
			0.5	1.000	1.000	1.000	1.000	allows true emissions to exceed
6	−1.0	1.0	1.0					target emissions commitments
			0.9	1.016	1.049	1.098	1.196	is unconditionally set to 0.
			0.7	1.007	1.020	1.040	1.080	No excess emissions, that is,
			0.5	1.000	1.000	1.000	1.000	additional emission increases are
–	−2.0	2.0	1.0					accepted. As a consequence, all
			0.9	1.016	1.049	1.098	1.196	countries exhibit identical
			0.7	1.007	1.020	1.040	1.080	adjustments Adj.
			0.5	1.000	1.000	1.000	1.000	
–	−3.0	2.9	1.0					
			0.9	1.016	1.049	1.098	1.196	
			0.7	1.007	1.020	1.040	1.080	
			0.5	1.000	1.000	1.000	1.000	
–	−4.0	3.8	1.0					
			0.9	1.016	1.049	1.098	1.196	
			0.7	1.007	1.020	1.040	1.080	
			0.5	1.000	1.000	1.000	1.000	
–	−5.0	4.8	1.0					
			0.9	1.016	1.049	1.098	1.196	
			0.7	1.007	1.020	1.040	1.080	
			0.5	1.000	1.000	1.000	1.000	
–	−6.0	5.7	1.0					
			0.9	1.016	1.049	1.098	1.196	
			0.7	1.007	1.020	1.040	1.080	
			0.5	1.000	1.000	1.000	1.000	
–	−7.0	6.5	1.0					
			0.9	1.016	1.049	1.098	1.196	
			0.7	1.007	1.020	1.040	1.080	
			0.5	1.000	1.000	1.000	1.000	

Table 8 (continued)

Country group	KP commit.	CRU	Adjustment factor Adj (absolute) for					If the GSC #1 concept had been applied
	δ_{KP}[a]	ρ_{crit}	$1-\alpha =$	$\rho =$				
	%	%	1	2.5%	7.5%	15%	30%	
7	−8.0	7.4	1.0					
			0.9	1.016	1.049	1.098	1.196	
			0.7	1.007	1.020	1.040	1.080	
			0.5	1.000	1.000	1.000	1.000	
–	−9.0	8.3	1.0					
			0.9	1.016	1.049	1.098	1.196	
			0.7	1.007	1.020	1.040	1.080	
			0.5	1.000	1.000	1.000	1.000	
8	−10.0	9.1	1.0					
			0.9	1.016	1.049	1.098	1.196	
			0.7	1.007	1.020	1.040	1.080	
			0.5	1.000	1.000	1.000	1.000	

The table lists the required adjustments Adj for all Annex B countries, where the confidence $(1-\alpha)$ that true emissions do not exceed (overshoot) target emissions by more than $p = \delta_{crit}$ (Cases 1 and 2) and $p = 0$ (Case 3) is specified to be 0.9, 0.7, and 0.5. In the last column, we assess the hypothetical situation that the GSC #1 concept was applied prior to/during negotiation of the KP. Note the potentially unfavorable situation in Case 2, which arises when δ_{KP} varies while ρ and $(1-\alpha)$ are kept constant

[a]The countries' emission limitation and reduction commitments under the KP are expressed with the help of δ_{KP}, the normalized change in emissions between t_1 and t_2: $\delta_{KP} > 0$—emission reduction; $\delta_{KP} \leq 0$—emission limitation

year (i.e., estimated emission reductions should not be "off" by more than a certain amount). That is, GSC #2 concept considers a relative upward adjustment that seeks to attain a reasonable level of confidence that countries have actually achieved the emission reductions, measured relative to the base-year emissions stated in their commitments under the KP, and that they are in compliance. Ultimately, countries must reduce their emissions in the commitment year by the amount of their upward adjustment to remain in compliance.

Starting Point: Annex B countries comply with their emission limitation or reduction commitments under the KP.[10]

Assumptions:

(1) It is accepted a priori that true emission reductions (increases) fall below (above) the committed level of reductions (increases) by some fractional or percentage amount (p or p%, respectively).

(2) The relative uncertainty (ρ) of a country's net emissions is symmetrical and does not change over time, that is, $\rho_1 = \rho_2 (:= \rho)$.

(3) The probability distributions for estimated emissions and emission changes are normal, and the shape of the emissions and emission change probability distributions for each country do not change significantly, as emissions change.

Systems View: Intra-systems view: correlation of uncertainty over time matters.

Question: Can we attain a reasonable level of confidence that countries will have actually achieved the emission changes, measured relative to base year emissions, stated in their commitments under the KP and that they are in compliance? That is: (1) Would we consider it acceptable if true emission reductions (increases) fall below (above) the committed level of reductions (increases) by some fractional or percentage amount? (2) How much is that amount? (3) How confident do we want to be in our result?

Approach: Statistical (see Fig. 6).

Answer: Depending on whether or not diminished reductions (additional increases) are accepted and favorable compliance conditions exist a priori, the modified GSC #2 concept of Gillenwater et al. comprises four cases (see Fig. 6). The complete answer is given by (see SOM_Math: Appendix F for the equations mentioned below)

Cases 1 and 2: $\delta_{KP} > 0$: $p = 0.1$:

$$\text{Adj} = \begin{cases} 1 & 2(1-\nu)\dfrac{z_{u,2}(F_N)\rho}{1.96\,\rho_{crit}} \le 0.1 \\ & \text{diminished reduction accepted} \\ \dfrac{1-\left(1-2(1-\nu)\dfrac{z_{u,2}(F_N)\rho}{1.96\,\rho_{crit}}\right)\delta_{KP}}{1-0.9\delta_{KP}} & 2(1-\nu)\dfrac{z_{u,2}(F_N)\rho}{1.96\,\rho_{crit}} > 0.1 \\ & \text{diminished reduction accepted} \end{cases} \quad \text{for} \tag{F-7,8}$$

Case 3: $\delta_{KP} = 0$: $p = 0$:

$$\text{Adj} = 1 \qquad \begin{pmatrix} \text{additional increase} \\ \text{not accepted} \end{pmatrix} \tag{F-9}$$

Case 4: $\delta_{KP} < 0$: $p = 0$:

$$\text{Adj} = \frac{1-\left(1+2(1-\nu)\dfrac{z_{u,2}(F_N)\rho}{1.96\,\rho_{crit}}\right)\delta_{KP}}{1-\delta_{KP}} \quad \begin{pmatrix} \text{additional increase} \\ \text{not accepted} \end{pmatrix}, \tag{F-10}$$

where p specifies the accepted (fractional) amount by which true emission reductions (increases) can fall below (above) the committed level of reductions (increases); ν approximates the net (effective) correlation between the absolute uncertainties ε_1 and ε_2 (cf. Section 3.3); and the other quantities are as explained above for the GSC #1 concept.

Result: The numerical result is given by Table 9 (see also Table F-1 in SOM_Math and worksheet *GSC_II 2a* in SOM_Num).

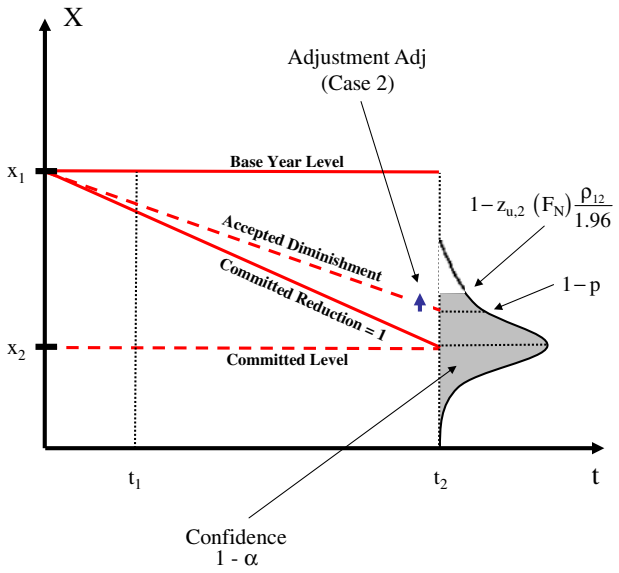

Fig. 6 Illustration of the GSC #2 concept ($\rho_1 = \rho_2$ and $\rho_{12} = 2(1-\nu)\rho/\rho_{crit}$ with $\rho_{crit} \neq 0$) with the help of the standard normal probability density function. This allows the confidence $(1-\alpha)$ to be specified via F_N that a country's true, but unknown, emissions change complies with its committed change. Depending on whether or not diminished reductions (additional increases) are accepted and favorable compliance conditions exist a priori, four cases are distinguished. Here, Case 2 is shown: Given an uncertainty of ρ%, this case requires a country's emissions estimate to be adjusted at t_2 upward if we want to be $(1-\alpha)$% confident its true emission reduction equals at least $(100-p)$% of the committed reduction (here referred to as 1). Emission reduction: $\delta_{KP} > 0$; emission limitation: $\delta_{KP} \leq 0$

Table 9 lists adjustment (Adj) values as a result of applying Eq. F-7 (Case 1), Eq. F-8 (Case 2), and Eqs. F-9 and F-10 (Cases 3 and 4). They specify—based on the country's reported emissions change between base year and commitment year—the required adjustment of the country's emissions estimate in the commitment year or, equivalently, the de facto emission reduction by this amount over and above the country's commitment to remain in compliance with commitments. For any given δ_{KP} value (thus, ρ_{crit} value; see Eq. A-6 in Section 3.1), inventory uncertainty (ρ) is treated as parameter as well as the confidence $(1-\alpha)$ that true emission reductions (increases) will not fall below (above) the committed level of reductions (increases) by more than $p = 0.1$ (Cases 1 and 2: arbitrary choice of p) and $p = 0$ (Cases 3 and 4: additional emission increases are not accepted in the case of emission limitation). The confidence $(1-\alpha)$ is specified to be 0.9, 0.7, and 0.5. The correlation (ν) is 0.75 (as in Section 3.3). The table shows that the GSC #2 concept is not easy to handle because it also requires strict enforcement under the KP. Emission reduction ($\delta_{KP} > 0$) under the GSC #2 concept behaves, as under the GSC #1 concept, mirror-inverted to the Und concept as a consequence of non-uniform emission reduction commitments. That is, the GSC #2 concept would not run counter to the spirit of the KP if it were applied in the undershooting mode (adjustments must be compensated for by additional emission reductions). But it must be mentioned that, for the given

Table 9 The GSC #2 concept (Eq. F-7 [Case 1: green fields; here, the Adj < 1 values have not been set to 1], Eq. F-8 [Case 2: orange fields], and Eqs. F-9 and F-10 [Cases 3 and 4: red fields]) applied to Annex B countries

Country group	KP commit.	CRU	Adjustment factor Adj (absolute) for					If the GSC #2 concept had been applied
	δ_{KP}[a]	δ_{crit}	$1-\alpha=$	$\rho=$				
	%	%	1	2.5%	7.5%	15%	30%	
1a–d	8.0	8.7	1.0					Case 1 (green-colored area):
			0.9	0.999	1.016	1.040	1.089	p = 0.1, Adj ≤ 1: Favorable
			0.7	0.995	1.001	1.011	1.031	compliance conditions;
			0.5	0.991	0.991	0.991	0.991	no need for an adjustment
2	7.0	7.5	1.0					(Adj can be set to 1).
			0.9	1.001	1.017	1.041	1.090	Case 2 (orange-colored area):
			0.7	0.996	1.002	1.012	1.032	p=0.1, Adj>1: The greater
			0.5	0.993	0.993	0.993	0.993	the ρ, the uncertainty
3a–c	6.0	6.4	1.0					surrounding the emissions
			0.9	1.002	1.018	1.042	1.091	inventory estimate, or the
			0.7	0.997	1.004	1.014	1.034	greater $(1-\alpha)$ the degree of
			0.5	0.994	0.994	0.994	0.994	confidence that is required,
4	5.0	5.3	1.0					the greater the adjustment
			0.9	1.003	1.019	1.044	1.092	Adj. However, the smaller
			0.7	0.998	1.005	1.015	1.035	the δ_{KP}, the greater the
			0.5	0.995	0.995	0.995	0.995	adjustment Adj to keep
–	4.0	4.2	1.0					the confidence $(1-\alpha)$ at a
			0.9	1.004	1.020	1.045	1.094	constant level (see, e.g.,
			0.7	0.999	1.006	1.016	1.036	Adj values for ρ=15%
			0.5	0.996	0.996	0.996	0.996	and $1-\alpha=0.9$). As a
–	3.0	3.1	1.0					consequence, countries that
			0.9	1.005	1.021	1.046	1.095	must comply with a large
			0.7	1.000	1.007	1.017	1.037	δ_{KP} (they exhibit a small
			0.5	0.997	0.997	0.997	0.997	Adj) are better off than
–	2.0	2.0	1.0					countries that must comply
			0.9	1.006	1.022	1.047	1.096	with a small δ_{KP} (they
			0.7	1.001	1.008	1.018	1.038	exhibit a large Adj). This
			0.5	0.998	0.998	0.998	0.998	is only true if adjustments
–	1.0	1.0	1.0					must be compensated
			0.9	1.007	1.023	1.048	1.097	for by additional emission
			0.7	1.002	1.009	1.019	1.039	reductions (undershooting
			0.5	0.999	0.999	0.999	0.999	mode). But it must be
								mentioned that, for the
								given set of parameters
								(notably, p = 0.1 and ν =
								0.75), the span between
								smallest and largest Adj
								values is negligible.
								However, the opposite is
								true if this compensation is
								not compulsory and adjustments

Table 9 (continued)

Country group	KP commit.	CRU	Adjustment factor Adj (absolute) for					If the GSC #2 concept had been applied
	δ_{KP}[a]	δ_{crit}	$1-\alpha=$	$\rho=$				
	%	%	1	2.5%	7.5%	15%	30%	
								are only used to establish a country comparison in terms of confidence (confidence mode) without compulsory undershooting. In the latter case countries that must comply with a small δ_{KP} (they exhibit a large Adj) are better off than countries that must comply with a large δ_{KP} (they exhibit a small Adj).
5	0.0	0.0	1.0					Cases 3 and 4 (red-colored area):
			0.9	1.000	1.000	1.000	1.000	$p = 0$, Adj ≥ 1:
			0.7	1.000	1.000	1.000	1.000	The fractional factor p which
			0.5	1.000	1.000	1.000	1.000	allows true emission increases to
6	−1.0	1.0	1.0					fall above the committed level
			0.9	1.008	1.025	1.049	1.098	of increases is unconditionally
			0.7	1.003	1.010	1.020	1.040	set to 0. No excess emissions,
			0.5	1.000	1.000	1.000	1.000	that is, additional emission
–	−2.0	2.0	1.0					increases, are accepted. As a
			0.9	1.008	1.025	1.049	1.098	consequence, all countries exhibit
			0.7	1.003	1.010	1.020	1.040	identical adjustments Adj.
			0.5	1.000	1.000	1.000	1.000	
–	−3.0	2.9	1.0					
			0.9	1.008	1.025	1.049	1.098	
			0.7	1.003	1.010	1.020	1.040	
			0.5	1.000	1.000	1.000	1.000	
–	−4.0	3.8	1.0					
			0.9	1.008	1.025	1.049	1.098	
			0.7	1.003	1.010	1.020	1.040	
			0.5	1.000	1.000	1.000	1.000	
–	−5.0	4.8	1.0					
			0.9	1.008	1.025	1.049	1.098	
			0.7	1.003	1.010	1.020	1.040	
			0.5	1.000	1.000	1.000	1.000	
–	−6.0	5.7	1.0					
			0.9	1.008	1.025	1.049	1.098	
			0.7	1.003	1.010	1.020	1.040	
			0.5	1.000	1.000	1.000	1.000	
–	−7.0	6.5	1.0					
			0.9	1.008	1.025	1.049	1.098	
			0.7	1.003	1.010	1.020	1.040	
			0.5	1.000	1.000	1.000	1.000	

Table 9 (continued)

Country group	KP commit.	CRU	Adjustment factor Adj (absolute) for					If the GSC #2 concept had been applied
	δ_{KP}[a]	δ_{crit}	$1-\alpha=$	$\rho=$				
	%	%	1	2.5%	7.5%	15%	30%	
7	−8.0	7.4	1.0					
			0.9	1.008	1.025	1.049	1.098	
			0.7	1.003	1.010	1.020	1.040	
			0.5	1.000	1.000	1.000	1.000	
–	−9.0	8.3	1.0					
			0.9	1.008	1.025	1.049	1.098	
			0.7	1.003	1.010	1.020	1.040	
			0.5	1.000	1.000	1.000	1.000	
8	−10.0	9.1	1.0					
			0.9	1.008	1.025	1.049	1.098	
			0.7	1.003	1.010	1.020	1.040	
			0.5	1.000	1.000	1.000	1.000	

The table lists the required adjustments Adj for all Annex B countries, where the confidence $(1-\alpha)$ that true emission reductions (increases) will not fall below (above) the committed level of reductions (increases) by more than $p = 0.1$ (Cases 1 and 2) and $p = 0$ (Cases 3 and 4) is specified to be 0.9, 0.7, and 0.5. The correlation ν is 0.75 (as in Section 3.3). In the last column, we assess the hypothetical situation that the GSC #2 concept was applied prior to/during negotiation of the KP. Note the potentially unfavorable situation in Case 2, which arises when δ_{KP} varies while ρ and $(1-\alpha)$ are kept constant. However, for the given set of parameters (notably, $p = 0.1$ and $\nu = 0.75$) the span between the smallest and largest Adj values is negligible

[a]The countries' emission limitation and reduction commitments under the KP are expressed with the help of δ_{KP}, the normalized change in emissions between t_1 and t_2: $\delta_{KP} > 0$—emission reduction; $\delta_{KP} \leq 0$—emission limitation

set of parameters (notably, $p = 0.1$ and $\nu = 0.75$), the span between smallest and largest Adj values is negligible.

4 Conclusions

We scrutinized six preparatory signal analysis techniques in a comparative mode. The purpose of this exercise was to provide a basis for discussing how to go about dealing with uncertainty under the KP and its successor, and which of the technique(s) to eventually select. It was well known that all the techniques presented prior to and at the 1st International Workshop on Uncertainty in GHG Inventories perform differently (see below and Table 10 for a summary), but a rigorous quantitative and qualitative comparison was still outstanding. In carrying out this comparative exercise, the aim was to understand the techniques holistically in the context of the KP (i.e., beyond their technical performance against mere disciplinary criteria). To this end we specified, for example, the systems view adopted by a technique, the important assumptions that underlie a technique (and typically go unmentioned), and whether or not a technique contributes to the ultimate objective of the KP

Table 10 Summary overview: the six signal analysis techniques and the characteristics of their numerical responses

Technique	Given	Numerical response	In the spirit of the KP?[a]
CRU, VT	δ_{KP}	Dissimilarity between countries committed to emission reduction ($\delta_{KP} > 0$) and limitation ($\delta_{KP} \leq 0$) depending on whether more lenient or stricter KTs are introduced: $\delta_{KP} > 0$: Stricter over more lenient KTs are favored $\delta_{KP} \leq 0$: More lenient over stricter KTs are favored	No
Und, GSC #2	δ_{KP}	Risk $\alpha \downarrow \Rightarrow$ undershooting Und $\uparrow$ Confidence (1-α) $\uparrow \Rightarrow$ adjustment Adj $\uparrow$ For any uncertainty ρ	Yes
	δ_{KP}	Uncertainty $\rho \uparrow \Rightarrow$ undershooting Und $\uparrow$ Uncertainty $\rho \uparrow \Rightarrow$ adjustment Adj $\uparrow$ For any risk α or confidence $(1-\alpha)$	Yes
	ρ and α (or $1-\alpha$)	$\delta_{KP} \downarrow \Rightarrow$ undershooting Und $\uparrow$ but modified KT $\delta_{mod} \downarrow$ $\delta_{KP} \downarrow \Rightarrow$ adjustment Adj $\uparrow$ or Adj = const (but relative to KT)	Und: No GSC #2: Yes[b]
Und&VT, GSC #1	δ_{KP}	As under Und and GSC #2	Yes
	δ_{KP}	As under Und and GSC #2	Yes
	ρ and α (or $1-\alpha$)	$\delta_{KP} \downarrow \Rightarrow$ modified KT δ_{mod} is made 'detectable' (according to Cases 2–4 in Fig. 4)[c] $\delta_{KP} \downarrow \Rightarrow$ adjustment Adj $\uparrow$ or Adj = const (but relative to KT)	Und&VT: Yes[c] GSC #1: Yes[b]

To facilitate comparison, the techniques are grouped into pairs of two. In the last column, we judge whether or not a technique is in line with the spirit of the KP, mainly determined by the shortfalls with which the techniques have to cope and which are related to the way the KP has been framed and implemented politically (see text). Kyoto (emissions) target (KT)

[a]On the assumption that accounting GHG emissions bottom-up and top-down do not exhibit biases

[b]If applied in the undershooting mode

[c]Statement does not refer to the case of detectability under emission reduction ($\delta_{KP} \geq \delta_{crit} > 0$: Case 1) which has been left unaltered; it behaves like the Und concept from a numerical point of view

of reducing anthropogenic GHG emissions to the atmosphere measurably, that is, above and beyond uncertainty.

The authors of these techniques all agree that uncertainty analysis is a key component of GHG emissions analysis even though their perceptions range from (1) using an investigation-focused approach to uncertainty analysis to improve only inventory quality to (2) actually applying a technique, or a combination of techniques, to check compliance. All authors also agree that it makes a big difference to the framing of emission control policies as to whether or not uncertainty is considered. Of course, as a consequence of the techniques' different performance, they can have a different impact on the design and execution of such policies.

However, as it stands, a single best technique cannot yet be identified (and most likely, does not exist); the main reason for this is that the techniques suffer

from shortfalls that are not scientific but are related to the way the KP has been framed and implemented politically. The two most important shortfalls on the side of policymaking can be identified as: (1) the overall neglect of uncertainty confronting experts resulting in agreed emission changes for most Annex B countries being of the same order of magnitude as the uncertainty that underlies their combined CO_2 equivalent emissions; and (2) the introduction of non-uniform emission reduction commitments from country to country. The techniques manifest these shortfalls differently.

CRU and VT These two concepts exhibit a dissimilarity between countries committed to emission reduction (stricter Kyoto emission targets are preferred to the more lenient ones) and emission limitation (more lenient Kyoto emission targets are preferred to the stricter ones).

Und and GSC #2 Varying δ_{KP}, the normalized emissions change committed to under the KP, while keeping the relative uncertainty ρ and the risk α constant, exhibits that under the Und concept countries that must comply with a small δ_{KP} (they exhibit a small modified emission limitation or reduction target δ_{mod}) are better off than countries that must comply with a large δ_{KP} (they exhibit a large modified emission limitation or reduction target δ_{mod}). This situation is not in line with the spirit of the KP. Emission reduction under the GSC #2 concept attempts to avoid this situation if applied in the undershooting mode. Countries that must comply with a large δ_{KP} (they exhibit a small Adj) are better off than countries that must comply with a small δ_{KP} (they exhibit a large Adj). However, it must be mentioned that, for the given set of parameters (notably, $p = 0.1$ and $\nu = 0.75$), the span between the smallest and largest Adj values is negligible. So far, emission reduction and emission limitation under the GSC #2 concept have not been treated uniformly. The GSC #2 concept still lacks clear guidelines as to whether or not, and to what extent, diminished (enhanced) emission reductions (increases) will be accepted under these two regimes.

Und&VT and GSC #1 The Und&VT overcomes situations that run (Und concept), or can run, counter to the spirit of the KP (GSC #1 and GSC #2 concepts if applied in the confidence mode). By requiring a priori detectable emission reductions, not limitations (see Cases 2–4 in Fig. 4), the Und&VT concept corrects the Protocol's emission limitation or reduction targets through the introduction of an initial or obligatory undershooting so that a country's emission signal becomes detectable before it is permitted to make economic use of its excess emission reductions. This, de facto, nullifies the politically agreed targets under the KP! However, we do not consider this a realistic scenario. By way of contrast, the GSC #1 concept builds on the notion of confidence, not detectability. If applied in the undershooting mode it would not run counter to the spirit of the KP. Nonetheless, it would enforce additional emission reductions, which though smaller than those under the Und&VT concept, would still be considerable and thus also difficult to sell politically. To date, emission reduction and emission limitation under the GSC #1 are not treated uniformly. The GSC #1 concept still lacks clear guidelines as to whether or not, and to what extent, excess emissions will be accepted under these two regimes.

It appears very probable that the first shortfall (emission changes and uncertainty are of the same order of magnitude) will vanish soon with increasing political

pressure to adopt a longer-lasting perspective and to achieve greater emission reductions in the mid to long term. However, we suggest that policymakers revisit the second shortfall. If non-uniform, country-specific emission reduction commitments are favored, then these must be decided on the basis of a straightforward rule that applies equally and rigorously to all countries and should not be determined "off the cuff." Only then can scientists finalize their discussion and give meaningful feedback on which technique(s) to select for the preparatory analysis of uncertainty in the countries' emission changes—not least, which numerical advantages and disadvantages between countries we then have to accept and tolerate. Such an unsatisfying situation should be overcome in the next round of political "post-Kyoto' negotiations." The knowledge to accomplish this is available.

Acknowledgements We like to thank the two anonymous reviewers for their valuable comments and suggestions for improving our paper.

References

Bun A (2008) The Kyoto policy process in perspective: long-term concentration targets versus short-term emission commitments. Interim Report IR-08-034, International Institute for Applied Systems Analysis, Laxenburg, Austria. http://wwws.iiasa.ac.at/Publications/Documents/IR-08-034.pdf

Bun A, Jonas M (2006) Preparatory signal detection for the EU-25 member states under EU burden sharing—advanced monitoring including uncertainty (1990–2003). Interim Report IR-06-054, International Institute for Applied Systems Analysis, Laxenburg, Austria. http://www.iiasa.ac.at/Publications/Documents/IR-06-054.pdf

Canadell JG et al (2007) Contributions to accelerating atmospheric CO^2 growth from economic activity, carbon intensity, and efficiency of natural sinks. PNAS 104(47):18866–18870. doi:10.1073/pnas.0702737104

COM (2006) Report from the commission. Assigned amount report of the European union. Report COM(2006) 799 final, Commission of the European Communities, Brussels, Belgium (15 December). http://eur-lex.europa.eu/LexUriServ/LexUriServ.do?uri=COM:2006:0799:FIN:EN:PDF

EEA (2009) Annual European community greenhouse gas inventory 1990–2007 and inventory report 2009. Technical Report No 4, European Environment Agency (EEA), Copenhagen, Denmark. http://www.eea.europa.eu/publications/european-community-greenhouse-gas-inventory-2009

FCCC (1992) United Nations convention on climate change. Document FCCC/INFORMAL/84, UN Framework Convention on Climate Change (FCCC), Bonn, Germany. http://unfccc.int/resource/docs/convkp/conveng.pdf

FCCC (1996) Report of the conference of the parties on its second session, held at Geneva from 8 to 19 July 1996. Addendum. Part two: action taken by the conference of the parties at its second session. Document FCCC/CP/1996/15/Add.1, UN Framework Convention on Climate Change (FCCC), Bonn, Germany. http://unfccc.int/resource/docs/cop2/15a01.pdf

FCCC (1998) Report of the conference of the parties on its third session, held at Kyoto from 1 to 11 December 1997. Addendum. Part two: action taken by the conference of the parties at its third session. Document FCCC/CP/1997/7/Add.1, UN Framework Convention on Climate Change (FCCC), Bonn, Germany. http://unfccc.int/resource/docs/cop3/07a01.pdf

FCCC (1999) Report of the conference of the parties on its fourth session, held at Buenos Aires from 2 to 14 November 1998. Addendum. Part two: action taken by the conference of the parties at its fourth session. Document FCCC/CP/1998/16/Add.1, UN Framework Convention on Climate Change (FCCC), Bonn, Germany. http://unfccc.int/resource/docs/cop4/16a01.pdf

FCCC (2009) National inventory submissions 2008. Website of the secretariat to the UN Framework Convention on Climate Change (FCCC), Bonn, Germany. http://unfccc.int/national_reports/annex_i_ghg_inventories/national_inventories_submissions/items/4303.php. Accessed 16 November 2009

Gillenwater M et al (2007) Practical policy applications of uncertainty analysis for national greenhouse gas inventories. In: Lieberman D et al (eds) Accounting for climate change. Uncertainty in

greenhouse gas inventories—verification, compliance, and trading. Springer, Dordrecht (Hardbound edition of Water Air Soil Pollut: Focus 7(4–5):31–54). doi:10.1007/s11267-006-9118-2

Gusti M, Jęda W (2002) Carbon management: a new dimension of future carbon research. Interim Report IR-02-006, International Institute for Applied Systems Analysis, Laxenburg, Austria. http://www.iiasa.ac.at/Publications/Documents/IR-02-006.pdf

Hamal K (2010) Reporting GHG emissions: change in uncertainty and its relevance for the detection of emission changes. Interim Report IR-10-003, International Institute for Applied Systems Analysis, Laxenburg, Austria. http://www.iiasa.ac.at/Publications/Documents/IR-10-003.pdf

Hamal K, Jonas M (2008a) Preparatory signal detection for the EU-25 member states under EU burden sharing—advanced monitoring including uncertainty (1990–2004). Interim Report IR-08-036, International Institute for Applied Systems Analysis, Laxenburg, Austria. http://www.iiasa.ac.at/Publications/Documents/IR-08-036.pdf

Hamal K, Jonas M (2008b) Preparatory signal detection for the EU-27 member states under EU burden sharing—advanced monitoring including uncertainty (1990–2005). Interim Report IR-08-037, International Institute for Applied Systems Analysis, Laxenburg, Austria. http://www.iiasa.ac.at/Publications/Documents/IR-08-037.pdf

IPCC (2006) 2006 IPCC guidelines for national greenhouse gas inventories, vol 1: general guidance and reporting. In: Eggleston HS et al (eds) National greenhouse gas inventories programme. Institute for Global Environmental Strategies, Hayama. http://www.ipcc-nggip.iges.or.jp/public/2006gl/index.html

IPIECA (2007) Greenhouse gas emissions estimation and inventories. Addressing uncertainty and accuracy. Summary report, International Petroleum Industry Environmental Conservation Association, London. http://www.ipieca.org/activities/climate_change/downloads/publications/Uncertainty.pdf

Jonas M, Nilsson S (2007) Prior to economic treatment of emissions and their uncertainties under the Kyoto Protocol: scientific uncertainties that must be kept in mind. In: Lieberman D et al (eds) Accounting for climate change. Uncertainty in greenhouse gas inventories—verification, compliance, and trading. Springer, Dordrecht (Hardbound edition of Water Air Soil Pollut: Focus 7(4–5):75–91). doi:10.1007/s11267-006-9113-7

Jonas M et al (1999) Verification times underlying the Kyoto Protocol: global benchmark calculations. Interim Report IR-99-062, International Institute for Applied Systems Analysis, Laxenburg, Austria. http://www.iiasa.ac.at/Publications/Documents/IR-99-062.pdf

Jonas M et al (2004a) Preparatory signal detection for annex I countries under the Kyoto Protocol—a lesson for the post-Kyoto policy process. Interim Report IR-04-024, International Institute for Applied Systems Analysis, Laxenburg, Austria. http://www.iiasa.ac.at/Publications/Documents/IR-04-024.pdf

Jonas M et al (2004b) Preparatory signal detection for the EU member states under the EU burden sharing—advanced monitoring including uncertainty (1990–2001). Interim Report, IR-04-029, International Institute for Applied Systems Analysis, Laxenburg, Austria. http://www.iiasa.ac.at/Publications/Documents/IR-04-029.pdf

Jonas M et al (2004c) Preparatory signal detection for the EU member states under the EU burden sharing—advanced monitoring including uncertainty (1990–2002). Interim Report, IR-04-046, International Institute for Applied Systems Analysis, Laxenburg, Austria. http://www.iiasa.ac.at/Publications/Documents/IR-04-046.pdf

Lieberman D et al (2007) Accounting for climate change: introduction. Springer, Dordrecht (Hardbound edition of Water Air Soil Pollut: Focus 7(4–5):1–4). doi:10.1007/s11267-006-9120-8

Nahorski Z et al (2003) Coping with uncertainty in verification of the Kyoto obligations. In: Studzinski J et al (eds) Zastosowania informatyki i analizy systemowej w zarzadzaniu (Application of computer sciences and systems analysis in management). Systems Research Institute of the Polish Academy of Sciences, Warsaw, pp 305–317 (in English)

Nahorski Z et al (2007) Compliance and emissions trading under the Kyoto Protocol: rules for uncertain inventories. In: Lieberman D et al (eds) Accounting for climate change. Uncertainty in greenhouse gas inventories—verification, compliance, and trading. Springer, Dordrecht, The Netherlands (Hardbound edition of Water Air Soil Pollut: Focus 7(4–5):119–138). doi:10.1007/s11267-006-9112-8

Pearce F (2003) Saving the world, plan B. New Sci 2425:6–7. http://environment.newscientist.com/article/mg18024251.100-saving-the-world-plan-b.html

Penman J et al (eds) (2000) Good practice guidance and uncertainty management in national greenhouse gas inventories. Institute for Global Environmental Strategies, Hayama. http://www.ipcc-nggip.iges.or.jp/public/gp/english/

Penman J et al (eds) (2003) Good practice guidance for land use, land-use change and forestry. Institute for Global Environmental Strategies, Hayama. http://www.ipcc-nggip.iges.or.jp/public/gpglulucf/gpglulucf.htm

Watson RT et al (eds) (2000) Land use, land-use change, and forestry. Cambridge University Press, Cambridge. http://www.ipcc.ch/ipccreports/sres/land_use/index.htm

WBGU (2003) Climate protection strategies for the 21st century: Kyoto and beyond. Special Report, German Advisory Council on Global Change (WBGU), Bremerhaven, Germany, ISBN: 3-936191-04-2. http://www.wbgu.de/wbgu_sn2003_engl.html

Climatic Change (2010) 103:215–225
DOI 10.1007/s10584-010-9906-6

Verification of compliance with GHG emission targets: annex B countries

A. Bun · K. Hamal · M. Jonas · M. Lesiv

Received: 5 January 2009 / Accepted: 15 June 2010 / Published online: 14 July 2010

Abstract The focus of this study is on the preparatory detection of uncertain greenhouse gas (GHG) emission changes (also termed emission signals) under the Kyoto Protocol. Preparatory signal detection is a measure that should be taken prior to/during negotiation of the Protocol. It allows the ranking of countries under the Protocol according to their realized versus their agreed emission changes and in terms of both certainty and credibility. Controlling GHGs is affected by uncertainty and may be costly. Thus, knowing whether each nation is doing its part is in the public interest. At present, however, countries to the United Nations Framework Convention on Climate Change (UNFCCC) are obliged to include in the reporting of their annual inventories direct or alternative estimates of the uncertainty associated with these, consistent with the Intergovernmental Panel on Climate Change's (IPCC) good practice guidance reports. As a consequence, inventory uncertainty is monitored, but not regulated, under the Kyoto Protocol. Although uncertainties are becoming increasingly available, monitored emissions and uncertainties are still dealt with separately. In our study we analyze estimates of both emission changes and uncertainties to advance the evaluation of countries and their performance under the Protocol. Our analysis allows supply and demand of emissions credits to be examined in consideration of uncertainty. For the purpose of our exercise, we make use of the Undershooting and Verification Time concept described by Jonas et al. (Clim Change doi:10.1007/s10584-010-9914-6, 2010).

A. Bun (✉) · K. Hamal · M. Lesiv
Lviv National Polytechnic University, P.O. Box 5446, Lviv, 79031, Ukraine
e-mail: andr.bun@gmail.com

M. Jonas
International Institute for Applied Systems Analysis, Schlossplatz 1, 2361 Laxenburg, Austria

1 Introduction

Past industrial development has resulted in an increase in concentrations of greenhouse gases (GHG) in the atmosphere (Canadell et al. 2007), and this is believed to be the major reason for the climate change observed today. The Kyoto Protocol to the United Nations Framework Convention on Climate Change (UNFCCC) aims to reduce the magnitude of the impacts resulting from climate change, and the impacts themselves. The Protocol stipulates accounting for and reporting of GHG emissions at the scale of countries in order to track progress and keep emissions below agreed limits.

To inventory GHG emissions, the Intergovernmental Panel on Climate Change (IPCC) developed standardized guidelines for national agencies to follow (IPCC 1997); they are supported by a software program (IPCC 1998). It is recommended that these tools are used when national GHG inventories are being conducted. However, as shown by Bun et al. (2010), these are too general and in many cases too simplified to reflect reality, resulting in a GHG inventory that is perceptibly different from "the truth." This inaccuracy adds to the inventory's inherent uncertainty, which results from imprecision. The greater the uncertainty, however, the lower the credibility of the inventory results is, thus lowering the credibility needed to use inventory results as a basis for emission allocations that can be traded.

Different concepts exist to assess GHG emission changes in terms of uncertainty (Gillenwater 2004; Jonas et al. 2004; Nahorski et al. 2007; Jonas et al. 2010). In our study we make use of the Undershooting and Verification Time (Und&VT) concept of Jonas et al. (2010) to investigate the potential supply of and demand for emission allocations, and we assume an emissions market that considers uncertainty. The Und&VT concept has been developed to rank countries under the Protocol according to their realized versus agreed emission changes and in terms of both certainty and credibility. Under commitment conditions, this concept requires that a country undershoot its true emission limitation or reduction commitment by a certain amount so that the risk of overshooting it is limited. Although true emissions are unknown—thus, also the targets derived from them—the concept allows the aforementioned risk to be grasped (Jonas et al. 2010).

We advance the monitoring of GHG emissions and uncertainties that are reported annually by signatory countries to the Kyoto Protocol (so-called Annex B countries) by jointly evaluating their emission changes and uncertainties. This combined evaluation allows countries' credibility as emission sellers to be assessed. Trading emission credits is believed to control GHG emissions, a costly exercise that is affected by uncertainty. Thus, knowing whether each nation is doing its part is in the public interest.

Here, we apply the Und&VT concept in a monitoring mode, that is, with reference to linear path emission targets between base year and commitment year (see Hamal and Jonas 2008). In our study we examine emissions for the period 1990–2004 (i.e., the emission reduction efforts of Annex B countries with reference to their linear emission targets as of 2004). As a result of applying the Und&VT concept, GHG emissions that are required for meeting and undershooting these targets can be derived. Undershooting reduces the risk that the countries' true emissions exceed their linear path emission targets (true emission targets) in 2004. Analysis of time series for the period (1990–2004) allows trends to be detected and short-term projections into the future to be made.

Section 2 of our study briefly recalls the mathematical background of the Und&VT concept and how it is applied. Section 3 analyzes and compares the countries' emissions estimates with and without uncertainty. The analysis of time series of GHG emissions and projected trends for the near future are presented in Section 4.

2 Methodology

The idea of the Und&VT concept is to apply undershooting which helps to reduce the risk that countries' true (but unknown) emissions in the commitment year/period exceed their (true) Kyoto target. This requires undershooting of the latter. In this way a new, modified target is calculated which falls below the official Kyoto target. By meeting the modified target, the country reduces the aforementioned risk of unintended overshooting (see Fig. 3 in Jonas et al. 2010). The introduced undershooting encompasses an initial or obligatory undershooting, where necessary, to make sure that the countries' emission signals become detectable (i.e., that they exceed the emissions' total uncertainty at a given point in time: here, at the time of commitment) before the countries are permitted to make economic use of their excess emission reductions.

Assumptions made in this method are:

- Uncertainties at base year (BY) and commitment year (CY) are given in the form of intervals, which take into account that a difference might exist between the true but unknown net emissions and their best estimates;
- Only the relative uncertainty ρ of a country's net emissions in the commitment year is used.

We make use of the critical emission reduction/limitation target δ_{crit}, which depends on relative uncertainty:

$$\delta_{crit} = \begin{cases} \dfrac{\rho}{1+\rho}, & \text{for } E_{CY} < E_{BY} \ (\delta_{KP} > 0) \ ; \\ -\dfrac{\rho}{1-\rho}, & \text{for } E_{CY} \geq E_{BY} \ (\delta_{KP} \leq 0) \ , \end{cases} \tag{1}$$

where δ_{KP} is the fractional emission reduction/limitation agreed under the Kyoto Protocol (reduction: $\delta_{KP} > 0$; limitation: $\delta_{KP} \leq 0$); and E_{BY} and E_{CY} are the emissions and agreed emission levels, respectively, referring to base year and commitment year. δ_{crit} indicates the smallest change in emissions that can be detected instead of uncertainty. Emission uncertainty in the base year is not considered here (see Fig. 1, Jonas et al. 2010).

With the help of δ_{KP} and δ_{crit}, four cases are distinguished depending on the sign of δ_{KP} and how δ_{crit} and δ_{KP} relate to each other (see Fig. 4, Jonas et al. 2010):

- Case 1—$\delta_{KP} > 0, \delta_{KP} \geq \delta_{crit}$;
- Case 2—$\delta_{KP} > 0, \delta_{KP} < \delta_{crit}$;
- Case 3—$\delta_{KP} \leq 0, \delta_{KP} > \delta_{crit}$;
- Case 4—$\delta_{KP} \leq 0, \delta_{KP} \leq \delta_{crit}$.

All these cases differ as to how the modified target is derived, which depends on the Kyoto target, the uncertainty involved, and the agreed level of risk countries are willing to accept. The latter is counterbalanced by ways of undershooting (U). Thus, the modified emissions limitation/reduction target (δ_{mod}) is calculated as follows, if the initial or obligatory undershooting ($\tilde{U}$) is addressed separately:

$$\delta_{\text{mod}} = \delta_{KP} + U + \tilde{U}. \tag{2}$$

Equation 2 is general and can be applied in all four cases. These differ, however, as to how the undershooting U and the initial or obligatory undershooting $\tilde{U}$ are calculated. U and $\tilde{U}$ depend on the Kyoto target δ_{KP}, relative uncertainty ρ, the critical emissions target δ_{crit}, and the aforementioned risk which is denoted by α. For example, in Case 1, the modified target is given by:

$$\delta_{\text{mod}} = \delta_{KP} + U = \delta_{KP} + (1 - \delta_{KP}) \cdot \frac{(1 - 2\alpha)\,\rho}{1 + (1 - 2\alpha)\,\rho}, \tag{3}$$

Where $\tilde{U}$ is zero, and α is the risk that a country's (true) emissions in the commitment year/period exceed its (true) target emissions ($0 < \alpha \leq 0,5$). The undershooting U increases if the risk α is to decrease. Hence, if a country's reported emissions meet δ_{mod} rather than δ_{KP}, the risk is α that the country's true (but unknown) emissions exceed its true (but unknown) Kyoto target. Nahorski et al. (2010) suggest using a risk of greater than 0.3, perhaps even as great as 0.4. Nevertheless, in our study we use 0.1 as a standard (if not otherwise stated) so as to analyze a greater range of possible values. Current compliance rules do not consider uncertainty, let alone risk. However, this situation might change, with uncertainty being considered important. Then, any risk $0,1 \leq \alpha \leq 0,5$ falls in between the upper case of "no undershooting" ($\alpha = 0.5$) and our lower case of an undershooting that satisfies $\alpha = 0,1$.

In a next step, required and actual emissions are compared. The maximum emissions level that exempts a country from buying emissions credits from another country is calculated as:

$$E_{r,y} = E_{BY} \cdot \left(1 - \delta_{\text{mod}} \frac{y - BY}{CY - BY}\right), \tag{4}$$

where E_{BY} are the country's base-year emissions; $E_{r,y}$ are its emissions required to satisfy a certain risk $0,1 \leq \alpha \leq 0,5$ at a given year y between base year and commitment year (i.e., $E_{r,y}$ fall below the linear emissions path); and the factor $(y - BY)/(CY - BY)$ is used to scale the emissions' path between base year and commitment year linearly. That is, here, the (standard) assumption made is that countries approach their Kyoto targets on a linear path.

A distance-to-target indicator (DTI) is introduced to measure the (normalized) difference between actual emissions E and required emissions $E_{r,y}$:

$$DTI = \left(E - E_{BY} \cdot \left(1 - \delta_{KP} \frac{y - BY}{CY - BY}\right)\right) \Big/ E_{BY} \tag{5}$$

while reference emissions follow a linear path between base year (E_{BY}) and commitment year ($E_{BY} \cdot (1 - \delta_{KP})$). That is, the DTI can be used to analyze a country's position relative to its linear reference path toward its target under the Kyoto Protocol. If the DTI is positive, the country's actual emissions exceed allowed levels, and vice versa.

A DTI that considers uncertainty is given by:

$$DTI_r = \left(E_{r,y} - E_{BY} \cdot \left(1 - \delta_{KP} \frac{y - BY}{CY - BY} \right) \right) \Big/ E_{BY}. \quad (6)$$

This indicates the undershooting that a country must fulfill in order to comply with its intermediate commitment under the condition that uncertainty is taken into account. Analyzing the DTI_r for all Annex B countries and their changes over time allows all-embracing conclusions to be drawn and even 1st-order projections about the emission trading situation in the future to be made.

Figure 1 shows the dependence of the modified target δ_{mod} on risk α for a country with a limitation target of 0% (e.g., New Zealand, Russia, and Ukraine) for four different levels of relative uncertainty. Here, Case 3 applies for all uncertainty levels, as δ_{crit} is always below 0. The modified target δ_{mod}, which expresses the magnitude of undershooting to satisfy risk α, decreases monotonously until α reaches its accepted maximum of 0.5. At this point the modified target δ_{mod} equals the country's official (here) limitation target δ_{KP}. Such graphs are useful when choosing and agreeing on accepted levels of risk. For a given relative uncertainty ρ in the reporting they display the relative change in the modified target that corresponds to a reduction in risk while the official target δ_{KP} is given (here: $\delta_{KP} = 0$).

Figures 2 and 3 display example plots of undershooting for countries that have agreed to emission reduction and limitation. The United Kingdom (UK) agreed to a reduction of 12.5% under the burden sharing of the European Union (EU) and reported, according to the EEA (2006), a (total) uncertainty of 14% (Tier 1) for the combined emissions of their Kyoto GHGs. Sweden agreed to a limitation target of 4% under the burden sharing of the EU and reported a (total) uncertainty of 5.8% (Tier 1) for all Kyoto GHGs according to EEA 2006), respectively. Figures 2 and 3 display these countries in the context of required undershooting or the DTI_r for different levels of uncertainty and risk α. Critical relative uncertainty (CRU) (here, the dashed line) is introduced to identify the uncertainty at which cases switch; hence another case applies and another formula is used for deriving the required undershooting and the DTI_r becomes more, or less, sensitive to a change in uncertainty. Each point on the plot represents a combination of relative uncertainty (x-axis)

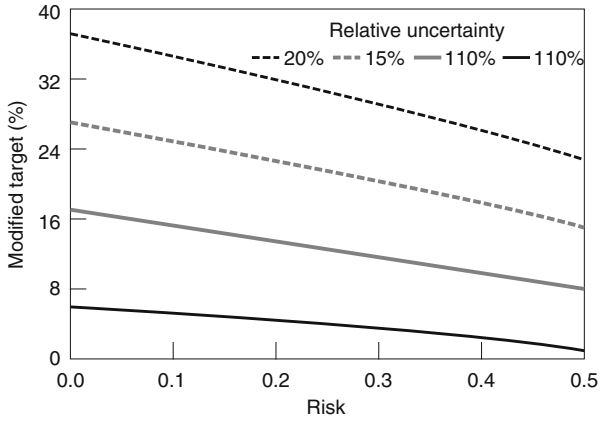

Fig. 1 Dependence of the modified target δ_{mod} on risk α (for given Kyoto target $\delta_{KP} = 0$)

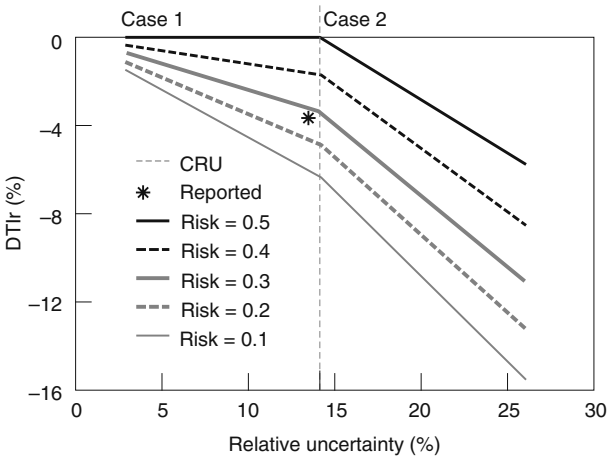

Fig. 2 Dependence of required DTI_r on relative uncertainty for the example of the UK ($r_{crit} = 14{,}3\%$ for Kyoto target $\delta_{KP} = 12{,}5\%$)

and required undershooting (y-axis). Points falling between any two lines shown in the figure refer to a situation when emission reduction is sufficient for current levels of relative uncertainty and risk as represented by the upper line; however, the emission reduction is not sufficient for current levels of relative uncertainty and risk as represented by the lower line. For instance, according to Fig. 2, UK emissions do not meet the required reductions to become detectable at a risk level well below 0.3 (i.e., total relative uncertainty is still greater than the reported emissions change in absolute terms). That is, although the country's DTI is negative (represented by black point), the UK can only sell its excess emission reductions as allowances with a risk of $\alpha \approx 0.3$ and greater, and not under a risk of $\alpha = 0.2$ and smaller. In this example, the UK needs to either reduce its emissions further (the black point moves downward) or decrease its total uncertainty (the black point moves to the left). Figures 2 and 3 show that neither of the countries that reported a negative DTI in 2004 can be considered as a highly credible emission sellers with α in the order of 0.1 and smaller), as their uncertainties were too large for the reported emissions.

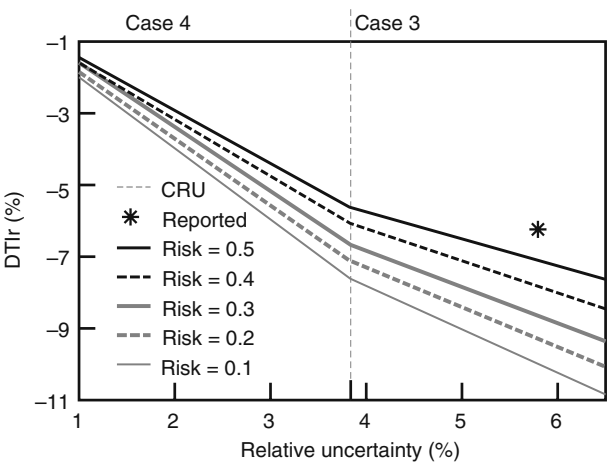

Fig. 3 Dependence of required DTI_r on the reported uncertainty for Sweden ($r_{crit} = 3.85\%$ for Kyoto target $\delta_{KP} = 4\%$)

3 National inventory results in consideration of uncertainty

The methodology described is applied for the emission change-uncertainty analysis of national GHG inventories reported by Annex B countries to the Kyoto Protocol. Calculations were carried out for the period 2002–2004. Emissions (total CO_2 equivalent excluding LULUCF) and uncertainty estimates were extracted from GHG inventory reports for all the countries investigated, in particular the EU (EEA 2006), the USA (USEPA 2006), Russia (Roshydromet 2006) and Ukraine (Arena-Eco 2006) and others. However, some countries (Estonia, Lithuania, Luxembourg, Portugal, and Romania) did not report uncertainties. Therefore, we assumed a relative uncertainty of 10% for the total GHG emissions of these countries.

Figure 4 displays both the DTI and the required DTI_r for some representative Annex B countries. These are calculated in accordance with the Und&VT concept (with risk $\alpha = 10\%$) for the year 2004. If a country's DTI is less than its DTI_r, its emissions fall below the required level and, even taking into account uncertainty, it can be a good emissions seller. Otherwise, the situation is as described above: the country must decrease its GHG emissions or the uncertainty underlying its emissions inventory or buy allowances from another country.

As can be seen from Fig. 4 some of the countries exhibit a positive DTI (i.e., their emissions exceed the levels agreed under the Protocol). Considering uncertainty in addition makes the situation even worse for these countries because the DTI_r is, by definition, negative. (See, e.g., Spain which reports a large uncertainty.) Nevertheless, for countries with a small uncertainty (e.g., Japan) the required undershooting is small.

Most of the New Independent States in Europe, new EU member states, and other countries exhibit some/considerable undershooting ($DTI \leq DTI_r \leq 0$), meaning that they are highly credible emission sellers. However, in some cases the situation is opposite ($DTI_r < DTI \leq 0$) (see Fig. 4, France and Sweden) meaning that the undershooting realized by a country meets its official commitment under the Kyoto Protocol but not with a risk of 0.1 (and smaller). Assuming that uncertainties are considered under an emission trading scheme and that all countries participate in it, such countries would be rated as less credible emission sellers because of the greater risk that true emissions exceed allowed (here: linear path) targets. That is, the consideration of uncertainty turns them into potential emission buyers (here,

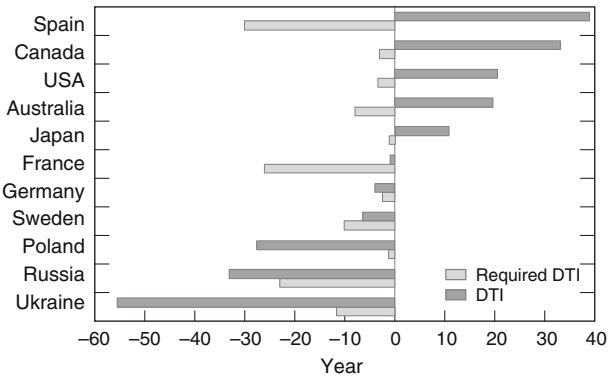

Fig. 4 Required DTI_r for current levels of uncertainty (for risk $\alpha = 10\%$) in comparison with the actual DTI (for 2004, in percent, relative to base year emissions)

for $\alpha = 0.1$) while they would appear as potential emission sellers if uncertainty is neglected all together.

Countries with $DTI \leq DTI_r \leq 0$ are/continue to stay excellent potential sellers as, in contrast to countries like France and Sweden, these countries' emissions are much lower than their targets.

4 Emission trends analysis

In the previous sections we described the DTI concept and introduced the required DTI_r. The present section deals with the outlook analysis of emission trading based on DTI data. We assume that inventory uncertainty, and its associated risk α, are explicitly accounted for in meeting compliance (see, e.g., Nahorski et al. 2007, 2010), and that these qualifiers are considered under an emission trading scheme. Here, we investigate the influence of uncertainty on the trading of emissions for a given risk α (e.g., 0.1). If a country's DTI is smaller than the requisite DTI (i.e., its emissions fall below the agreed level when uncertainty is considered), a country can potentially sell the amount of emissions:

$$E_{CS} = E_{BY} \cdot (DTI_r - DTI)\,, \tag{7}$$

where E_{CS}—emissions that a country can sell, CO_2 equivalent. If a country's DTI is greater than the required DTI_r, the country's emissions exceed the agreed level and it must buy emission allowances equal to:

$$E_{MB} = E_{BY} \cdot (DTI - DTI_r)\,, \tag{8}$$

where E_{MB}—emissions that country must buy from another country, CO_2 equivalents.

As can be seen from Figs. 5 and 6, overall GHG emissions in the Annex B countries showed a clear tendency to increase. Nevertheless, total GHG emissions in these countries were still below the Kyoto target in 2004 (see Fig. 5). However, taking into account the uncertainty of GHG inventories can change the situation to the opposite: the remaining undershooting of all countries after satisfying the risk of (here) 0.1 is not big enough to compensate for the emission allocations

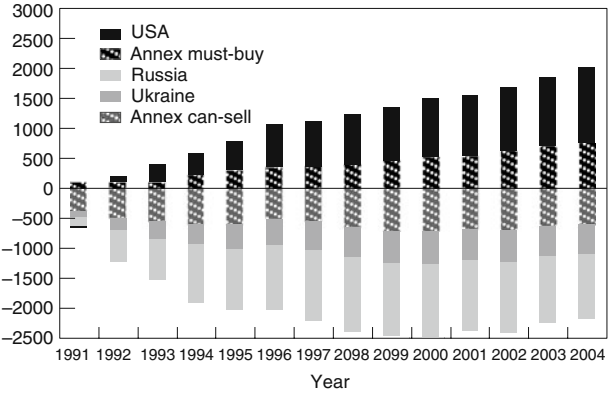

Fig. 5 Must-buy (positive) versus can-sell (negative) emissions of all Annex B countries to the Kyoto Protocol (in Tg CO_2-eq; some countries are resolved individually and are not included elsewhere)

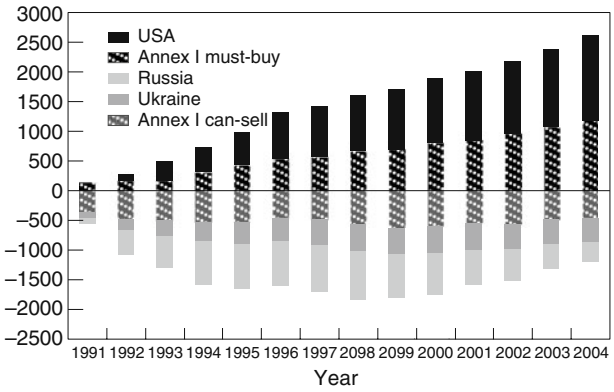

Fig. 6 Must-buy versus can-sell situation in consideration of uncertainty, in Tg CO_2 equiv (for risk $\alpha = 10\%$; some countries are resolved individually and are not included elsewhere)

that countries must buy in order to comply with the required undershooting (which satisfies $\alpha = 0.1$). Figure 6 shows that the amounts the Annex B parties need to buy are more than twice the amounts they can sell in 2004. At the same time Russia and Ukraine exhibited a significant undershooting so that even after the Und&VT concept is applied they still can sell much of their emission allowances, but the amounts of these two countries decrease from year to year.

Figure 5 indicates that the Russia, Ukraine, and the USA are the biggest participants in a potential GHG emissions market in which all Annex B countries would participate. Russia and Ukraine can sell more GHG emissions than the rest of Annex B countries together. However, this amount has been constantly decreasing since the late 1990s, while the remaining Annex B countries with DTI < 0 stay at about the same level. At the same time, countries with a positive DTI, hence those that must buy emission allowances, in general move away from their targets. Furthermore, the USA must buy more emissions than the rest of Annex B countries.

The total "can-sell" and "must-buy" values of Fig. 6 are presented in Fig. 7 as circles and squares, respectively. It can be observed from the figure that "must-buy" values increased almost linearly since 1990, while the "can-sell" values increased for

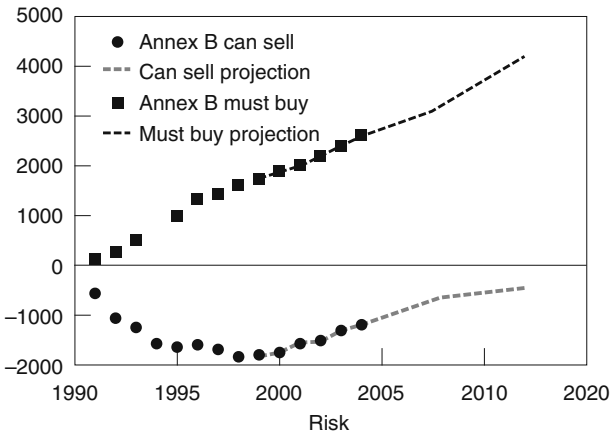

Fig. 7 Can-sell versus must-buy trends and projections

a time and then have been increasing since the late 1990s. The reason for this is the increase in GHG emissions in Russia as the biggest emitter among countries with a negative DTI, hence the increase in its DTI. The figure also displays trend lines for these indicators and projections until 2012.

It can be seen that if current trends prevail, the "can-sell" values will decrease until about 2008 when Russia will switch to being a country with a positive DTI. At this point the decrease in "can-sell" values will slow down while the increase in "must-buy" values will speed up.

5 Conclusions

The methodology presented in this paper allows national GHG inventories in an to be analyzed in an emissions change-uncertainty context rather than in an emissions-only context. There is a problem of design and implementation of the methodology for dealing with uncertainty of GHG emissions' inventory, as considering uncertainty is provided under the Kyoto Protocol, but the corresponding approach has not been implemented to date. We analyze emissions in the Annex B countries and their time series in consideration of uncertainty. Our analysis is based on the Undershooting and Verification Time concept described by Jonas et al. (2010). Emission inventory reports of the Annex B parties were used for this analysis. We show that not all of the countries with negative DTIs are credible emission sellers, as the risk remains that their emissions exceed allowed levels. Some countries (in particular Russia and Ukraine) can sell much of their emissions allowances, as GHG emissions in these countries are far below their Kyoto targets. However, analysis of time series of GHG emissions shows that overall emissions will continue to increase and exceed the Kyoto target by far. If the situation does not change, there will be no country with a negative DTI in the next decade. Hence, emissions in all countries will be above their Kyoto targets.

References

Arena-Eco (2006) Ukrainian national inventory report 1990–2004. Arena-Eco, Kiev, Ukraine (in Russian)

Bun R et al (2010) Spatial GHG inventory at the regional level: accounting for uncertainty. Clim Change. doi:10.1007/s10584-010-9907-5

Canadell P, Ciais P, Conway T, Field C, Le Quere C, Houghton S, Marland G, Raupach M, Buitenhuis E, Gillett N (2007) Recent carbon trends and the global carbon budget update to 2006. Global Carbon Project. http://www.globalcarbonproject.org/global/ppt/GCP_CarbonCycleUpdate.ppt

EEA (2006) Annual European community greenhouse gas inventory 1990–2004 and inventory report 2006. Technical Report No 6, European Environment Agency (EEA), Copenhagen Denmark. http://reports.eea.europa.eu/technical_report_2006_6/en/

Gillenwater M, Sussman F, Cohen J (2004) Practical applications of uncertainty analysis for national greenhouse gas inventories. GHG Uncertainty Workshop, Warsaw, p 14

Hamal KH, Jonas M (2008) Preparatory signal detection for the EU-27 member states under EU burden sharing—advanced monitoring including uncertainty (1990–2005). Interim Report IR-08-037, International Institute for Applied Systems Analysis, Laxenburg, Austria, pp 51. http://www.iiasa.ac.at/Admin/PUB/Documents/IR-08-037.pdf

IPCC (1997) Revised 1996 IPCC guidelines for national greenhouse gas inventories: reporting instructions. The workbook reference manual, vols 1–3. Intergovernmental Panel on Climate

Change (IPCC) Working Group I (WG I) Technical Support Unit, Bracknell, United Kingdom. http://www.ipcc-nggip.iges.or.jp/public/gl/invs4.htm

IPCC (1998) The IPCC software for estimating greenhouse gas emissions. IPCC version 1. http://www.ipcc-nggip.igres.or.jp/public/gl/software.htm

Jonas M, Nilsson S, Bun R, Dachuk V, Gusti M, Horabik J, Jęda W, Nahorski Z (2004) Preparatory signal detection for Annex B countries under the Kyoto Protocol—a lesson for the post-Kyoto policy process. Interim Report IR-04-024, International Institute for Applied Systems Analysis, Laxenburg, Austria, p 91. http://www.iiasa.ac.at/Publications/Documents/IR-04-024.pdf

Jonas M et al (2010) Comparison of preparatory signal analysis techniques for consideration in the (post-) Kyoto policy process. Clim Change. doi:10.1007/s10584-010-9914-6

Nahorski Z, Horabik J, Jonas M (2007) Compliance and emissions trading under the kyoto protocol: rules for uncertain inventories. Water Air Soil Pollut: Focus 7(4–5):20

Nahorski Z et al (2010) Compliance and emission trading rules for asymmetric emission uncertainty estimates. Clim Change. doi:10.1007/s10584-010-9916-4

Roshydromet (2006) National report on anthropogenic GHG emissions and sinks of 2002–2004. Federal Service for Hydrometeorology and Environment Monitoring (Roshydromet), Moscow, Russia, pp 139 [in Russian]

USEPA (2006) Inventory of US greenhouse gas emissions and sinks: 1990–2004. US Environmental Protection Agency, Washington DC, pp 448

Climatic Change (2010) 103:227–244
DOI 10.1007/s10584-010-9907-5

Spatial GHG inventory at the regional level: accounting for uncertainty

R. Bun · Kh. Hamal · M. Gusti · A. Bun

Received: 5 January 2009 / Accepted: 15 June 2010 / Published online: 15 July 2010

Abstract Methodology and geo-information technology for spatial analysis of processes of greenhouse gas (GHG) emissions from mobile and stationary sources of the energy sector at the level of elementary plots are developed. The methodology, which takes into account the territorial specificity of point, line, and area sources of emissions, is based on official statistical data surveys. The spatial distribution of emissions and their structure for the main sectors of the energy sector in the territory of the Lviv region of Ukraine are analyzed. The relative uncertainties of emission estimates obtained are calculated using knowledge of the spatial location of emission sources and following the Tier 1 and Tier 2 approaches of IPCC methodologies. The sensitivity of total relative uncertainty to change of uncertainties in input data uncertainties is studied for the biggest emission point sources. A few scenarios of passing to the alternative energy generation are considered and respective structural changes in the structure of greenhouse gas emissions are analyzed. An influence of these structural changes on the total uncertainty of greenhouse gas inventory results is studied.

1 Introduction

Emission inventories are the main parameters of various climate change models, atmospheric pollution investigations, and implementation of policy response options (Pacyna and Graedel 1995). The problems of greenhouse gases inventories and the

R. Bun (✉) · Kh. Hamal · M. Gusti · A. Bun
Lviv Polytechnic National University,
PO Box 5446, Lviv, 79031, Ukraine
e-mail: rost.bun@gmail.com

M. Gusti
International Institute for Applied Systems Analysis,
Schlossplatz 1, 2361 Laxenburg, Austria

quality of inventory results are especially relevant o the implementation mechanisms of the Kyoto Protocol. At present, parties to the United Nations Framework on Climate Change submit annual national inventories for six main greenhouse gases and are also encouraged to advise on the corresponding uncertainty levels.

For proper implementation of the Kyoto Protocol, greenhouse gas emission values at the commitment period alone are not sufficient. The quality of these emission data is also important in terms of verifying whether a country has really coped with its commitments in carbon trading processes, etc. The first and most important characteristic of data quality is their uncertainty, which ideally should take into account all possible errors and knowledge gaps. However, there is relatively little experience in the assessment and reporting of inventory uncertainties. Countries' compliance with emission targets cannot be scientifically proved when the emission reduction achieved is of the same order as, if not greater than, the emission reduction to which the country has committed. Analysis of compliance and emission trading rules under the Kyoto Protocol based on uncertainty of emission estimates has been performed in some recent studies, see Bun et al. (2010), Jonas et al. (2004), Jonas et al. (2010), Nahorski and Horabik (2010). Indeed, the uncertainties of inventory data and the problem of reduction of uncertainties are now of great interest in the scientific community.

Traditional methods of greenhouse gas inventory (used in countries' National Inventory Reports) are mainly focused on estimating GHG emissions and absorptions on a country scale. Country-scale inventory results are useful for tracing countries' adherence to international agreements, analyzing historical emission change trends, and grading countries according to their emission levels, etc. On the other hand it is an advantage for government bodies in all countries to have a tool that enables them to analyze the separate constituents of the many-sided processes of greenhouse gas emissions and absorptions and thereby find optimum ways of solving a number of economic or environment protection problems (Bun et al. 2006). Therefore, when we talk about emissions from the point of view of a single country, it is important to have knowledge about the spatial distribution of inventory data and their structure. Analysis of spatial distribution of atmospheric emissions has been performed in several studies using different approaches (for example, see Wang et al. 2005; Lindley et al. 1996). Spatial emission data can be useful for: (1) identifying appropriate land use planning strategies; (2) assessing sources that are likely to pose the greatest air quality problems and identifying suitable emission control targets; (3) providing a useful guide to the potential locations of further air quality monitoring sites (Lindley et al. 1996); (4) in various climate change models where spatially distributed (gridded) emission data can be compared with top-down inventories of atmospheric emissions, to determine the relevance of activity data used (for more information see Winiwarter et al. 2003; Horabik and Nahorski 2010). Spatial disaggregation of inventory data can also be treated as a way of improving data quality, and can thus be used in uncertainty analysis to provide guidelines for the most cost-effective ways of reducing uncertainty.

In this study, methods to estimate spatially resolved emissions (geo-referenced cadastres) of the main greenhouse gases using the spatially resolved "bottom-up" approach are developed. Uncertainty analysis based on knowledge of the spatial location of emission sources and following the IPCC Tier I and Tier II

approaches is carried out. Numerical results are obtained for the Lviv region of Ukraine. The study focuses on the spatial inventory in the energy sector in Ukraine, which is responsible for more than 80% of the country's total GHG emissions. Approaches to identifying the largest sources of greenhouse gas emissions at the regional level are shown and their contribution to the total uncertainty of inventory results is analyzed in two ways: by local transition to alternative sources and by reduction of the uncertainty of emission factors or activity data in given point sources.

2 Spatial inventory model for energy sector

For climatic models and for analysis of the territorial distribution of total GHG emissions, it is important to obtain emission values at the level of elementary plots of the same fairly small area. The spatial inventory approach we introduce has three main steps:

1. The territory under investigation is split into cells;
2. Statistical activity data are disaggregated between the corresponding grid cells using information on the geographical location of emission sources (big point sources can be pinpointed directly, while for area and line sources certain other assumptions need to be made and parameters with geographic information to be added); emission factors and other parameters used in the inventory process are established for each cell (preferable because certain areas or point sources have their own individual approach to fuel treatment);
3. The emission inventory is carried out for individual grid cells using the "bottom-up" approach (a "bottom-up" inventory provides emission estimates for a particular area by multiplying the activity data by appropriate emission factors).

The main point of the spatial inventory model is that the greenhouse gas inventory is carried out in turn for each plot following the traditional IPCC methodologies (IPCC 2006). The formal inventory model in the energy sector is presented in the following form:

$$Y = \sum_{n=1}^{N} \Delta Y_n = \sum_{n=1}^{N} \sum_{m=1}^{M} a_{nm} \Delta x_{nm}, \tag{1}$$

where a_{nm} is the emission factor for the m-th activity of the energy sector in the n-th elementary plot, N is the total number of elementary plots, Δx_{nm} is the data for the m-th anthropogenic activity in the energy sector in the n-th elementary plot, ΔY_n is the total inventory results for the n-th elementary plot, Y is the total emission estimate for the area under investigation. In such a model the input and output data relate to individual elementary plots and are presented in the form of a distributed (geo-referenced) database.

According to the traditional IPCC inventory methodology (IPCC 2006) and taking the specificity of Ukrainian statistics into account (Power 2002; Fuel 2005; Industry 2005; Statistical 2005) the energy sector is divided into five categories

of greenhouse gas sources (subsectors) ($M = 5$ in Eq. 1: (1) fuel treatment and electricity production (energy industries); (2) residential sector; (3) manufacturing industries and construction; (4) transport; (5) fuel treatment at other sectors. These are further divided into subcategories and individual emission sources (for example, the transport sector consists of road, railway, and off-road transport categories, and each of them may be expanded to individual emission source groups—buses, passenger cars, agricultural combines, locomotives, etc.). Subdivision into source categories is important, as it enables the distinctive features of fossil fuel treatment to be taken into account within the separate sectors when emission factors are being established. Moreover, the territorial distribution of emissions from different anthropogenic activities will differ. For example, in the transport sector emissions are concentrated in densely populated areas and main roadways, while methane emissions in agriculture are significant in rural and insignificant in urban areas; emissions from oil refining are concentrated mainly at refinery sites, etc.

Different emission sources are fully or partially located within the territory of each individual cell: large and small; mobile and stationary, etc. For the purposes of the spatial inventory, emission sources are grouped into three main types: line, area, and large point sources.

To the large point sources belong the large enterprises with significant annual emissions and occupying a fairly small area, for example, power stations, large industrial objects, refineries, etc. These sites are treated individually and corresponding activity data and emission factors are clearly defined by the geographical coordinates of the object. In this case it is important to obtain the activity data information at the level of each large point source (amount of fossil fuel used, amount of products manufactured etc.) as well as additional parameters that influence emission factors, such as the age and efficiency of plant equipment, chemical characteristics of fuel used, efficiency of pollution control systems, etc. Experience has shown that appropriate distribution of activity data on fossil fuel consumption in the energy sector (with the exception of the transport subsector) largely depends on the correct determination and location of sources on a point-source basis.

To the line emission sources belong sources that spatially have a line shape, for example, roadways, railroads, pipelines, etc. The spatial modeling of annual emissions for these is carried out by dividing each line source into segments with the help of l km $\times$ l km grid cells; further, for each segment the activity data and appropriate emission factors are established and the GHG emissions are calculated. The algorithms of distribution of general activity data on fossil fuel consumption to individual road segments differ depending on the subsector type.

Agricultural fields, forests, and oceans belong to area sources of GHG emissions/absorption. The territories in which many small point sources of emissions are concentrated, for example, urban road networks, households, small boiler plants, etc., are also included in the area sources. The methods of disaggregating activity data (which are available at the regional level) to the level of individual area sources are developed. The common feature of the disaggregation procedures for every type of area source is that the data are disaggregated using some territorially distributed surrogate parameters that characterize the intensiveness of a certain activity; for example, for the agricultural sector these parameters are: rural population distribution, amount of harvested production, amount of agricultural machinery, area of land under crop, etc. The ratio F_A^K of fuel F_A^R used solely in administrative region $\boldsymbol{R}$

for a certain activity subsector ***A*** in the individual area source ***K*** (which is located within region ***R***) is estimated as follows:

$$F_A^K = \frac{\left(F_A^R \cdot P_A^K\right)}{P_A^R}, \tag{2}$$

where P_A^K, P_A^R are values of the surrogate parameter (used to distribute activity data in subsector ***A***) in area source ***K***, and in region ***R***, respectively. At the level of the elementary plot, emissions are calculated as a sum of emissions from sources that are fully or partially located within a certain grid cell. If an area source is located in more than one cell, then its emissions are disaggregated proportionally to the area ratio.

For example, in the *road transport subsector* of the energy sector, the routes of passenger and cargo transportation (railroads, automobile roads, pipelines, etc.) are treated as line emission sources. Urban road networks are treated as area emission sources because of their high density (in cases where the selected grid cell size does not allow it to be allocated on a line basis). National statistical surveys contain information on fossil fuels used in road transport by fuel type, as well as information on vehicle miles traveled by car type and fuel type at the level of separate administrative regions and cities. These input data are disaggregated to individual road segments and parts of urban territories, which are formed using the l km $\times$ l km grid. The general approach to distributing the activity data is to disaggregate them proportionally to the length of road segment (also taking into account such parameters as road type and average capacity) for line sources and proportionally to the population in a certain grid cell for area sources. These parameters are available from digital maps of road networks and digital maps of settlements (which also contain information on their type and population). To take full consideration of very intensive traffic in suburban areas of big cities, three-level buffer zones were introduced around their administrative borders, the width of which depends on the area of the city. After this, the activity data disaggregating the emissions were calculated following "top-down" methodology. The total emissions in the road transport sector were calculated as the sum of cold start emissions and emissions that occurred when vehicles were operating with hot engines. Additionally the following parameters were considered in emission calculations for each road segment: ratio of car types, control technology distribution, average speed depending on road type, amount of cars in different age groups by regions and cities, etc.

It is desirable that, in inventories, "national" emission factors should be used that take into account the national peculiarities of fossil fuel in terms of its chemical characteristics and processing. Also important is the sectoral and spatial disaggregation of emission factors for other greenhouse gases besides carbon dioxide, as these may differ significantly among subcategories (because of their high dependence on fuel characteristics, combustion technology, operating and maintenance regimes, size of equipment, vintage of equipment, emission controls etc. See IPCC 2006). In this paper IPCC default emission factors were used in the main, with the exception of several point sources for which "national" emission factors were available. An uncertainty level for "national" coefficients is, of course, much lower than for the default values.

Spatial inventory technology allows all available information on emission factors at the level of individual emission sources to be used. Experiments regarding total inventory results and the change in their uncertainty caused by introducing emission control technologies in a given plant can also be easily carried out. In other words, spatially resolved inventory is very important when effective measures to emission mitigation and uncertainty reduction are being planned.

An important feature of such an inventory is that input and output data relate to elementary plots (i.e., they are not lumped). Presenting results in such a form accommodates various regional peculiarities and therefore provides government bodies with integrated information on the actual territorial distribution of greenhouse gas sources and absorbers (Bun et al. 2004). Moreover, summing the inventory results for all elementary plots within the boundaries of a given region will lead to general inventory results for the region.

3 Forming elementary plots

Before establishing the level of spatial resolution, the level for which the activity data and emission factors are available should be considered. In Ukraine statistical activity data relate to administrative regions. For better implementation of high-resolution inventory it is therefore better to divide each administrative region (rather than the entire territory under investigation) into elementary plots because: (1) statistical input data are available for separate regions; (2) further results could be aggregated for separate administrative units; (3) some specific features of administrative regions can be accounted for in input data and their uncertainty levels.

The territory investigated was divided into elementary plots ($l \times l$ km grid cells), which were also limited by the borders of administrative units. Separate objects, which refer to administrative cities, were formed. The total number of elementary plots in the region is $N = \sum_{r=1}^{R} N_r + N_M$, where N is the total amount of objects; r is the ordinal number of administrative unit, $r = 1, .., R$; R is the amount of units; N_r is the amount of elementary plots in the r-th unit; N_M is the number of objects that refer to administrative cities. A set of all elementary plots in the region V is a combination of sets of elementary plots at the regional level and objects V_m for administrative cities $V = \left[\bigcup_{r=1}^{R} \{v_{ri}, i = \overline{1, N_r}\} \right] \bigcup \{v_m, m = \overline{1, N_M}\}$.

For example, it is proposed that the territory of the Lviv region of Ukraine be "cut" into elementary plots of 10×10 km. As a result, a set of elementary plots is formed on the map of Lviv region. The total amount of objects $N = 420$. This includes objects of $R = 20$ administrative districts and $N_M = 9$ objects for cities.

4 Geo-information technology

The geo-information technology, GeoInventory, has been developed to realize the algorithms of a spatially referenced greenhouse gas inventory, automate the process of forming corresponding digital maps, and enable visual analysis of results obtained.

The technology is based on step-by-step inventory for all elementary plots which make up the territory under investigation.

For each subsector of the energy sector the programming modules are created in MapBasic language for GIS MapInfo which realize the models and algorithms of spatial GHG inventory for the specified by user inventory parameters, such as, the geographical territory, size of elementary plots, subcategory of economic activity, level of inventory and other parameters, specific to the given subsector. These modules use the following input information.

1. Excel tables, unified for each administrative unit, with statistical information on fuel extraction, treatment, and combustion in individual administrative units (regions or individual cities). This information is available from official statistical year-books and national statistical surveys (see, e.g., Power 2002; Fuel 2005; Industry 2005; Statistical 2005).
2. Statistical reference information, for example, on the current state of gasification of separate residential areas, population distribution, vehicle miles traveled on gasoline by individual administrative unit and by car type, etc. Depending on the kind of information it is, it can be presented as Excel tables or digital maps.
3. Territorially distributed data on net calorific values by fuel type and emission coefficient for separate activity sectors with reference to the geographical location of emission sources.

According to the activity sector selected, MapBasic modules also use a number of digital maps, which help to geographically allocate the amount of fuel used in individual grid cells. For example, digital maps of settlement locations with information on their type and population; road and railway digital maps; land use maps; maps with the information about gas, oil and coal extraction locations, including information on the amount of fuel extracted per year, etc.

The implementation of MapBasic modules allows the corresponding resulting digital map layers to be created. These maps are geographically divided into cells, each of which contains information about the object's geographical location, the sources of emissions fully or partially located within this cell, emission estimates and structure of emissions by GHG, fuel type, and emission source.

The technology developed also foresees analysis and visualization of the results obtained from the spatially referenced inventory using thematic maps, 3-D maps, graphics, and queries.

5 Spatial inventory results

Using the geo-information technology developed on the basis of the spatial GHG inventory, geo-distributed emission cadastres on the level of elementary plots are built for the territory of the Lviv region. The total emissions of direct acting greenhouse gases (CH_4, N_2O, CO_2) in the energy sector are calculated using the global warming coefficient. As an example, Fig. 1 presents the thematic map of the spatial distribution of total emissions in CO_2 equivalents in the energy sector of the Lviv region.

For a better visualization of the spatially referenced emission data, inverse distance weighted (IDW) interpolation is used. This interpolation takes into account the

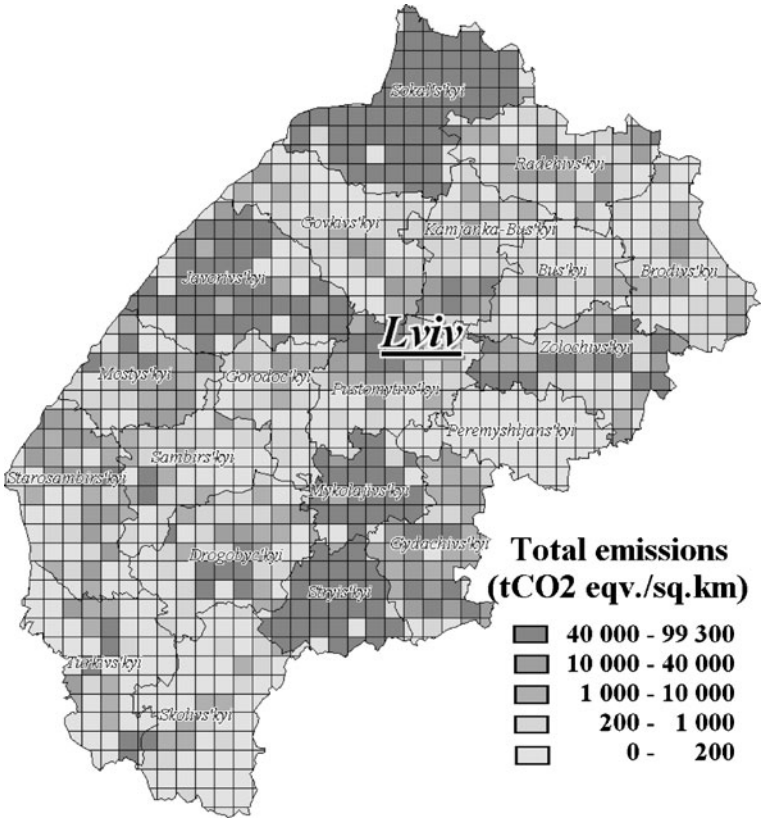

Fig. 1 Thematic map of specific GHG emissions in the energy sector (Lviv region, 2004; tCO_2-eqvivalent/km^2)

influence of neighboring grid cells. It gives—especially in the form of 3-D maps—an immediate indication of the leading emitters. Figure 2 depicts the interpolated GHG emission estimates for the Lviv region. However, this kind of map may be used only to derive the general situation regarding the spatial distribution of emission sources. That is, Fig. 2 shows that the location of emission sources is highly non-uniform in the Lviv region. More precisely, only one city (Lviv) is responsible almost for one-third of all emissions in the region (the territory of the Lviv city occupies only 7% of the territory of the whole region).

The geo-information technology of spatial inventory allows a investigation of the structure of greenhouse gas emissions by economic activity, by gas, or by fuel type at the level of elementary plots, administrative units, or the region as a whole. As an example, Fig. 3 shows the structure of emissions by sector for separate administrative regions and administrative cities. The main carbon dioxide and methane emissions occur in the energy industries. The leading greenhouse gas emitters are: Lviv agglomeration (31.7% of all emissions), Kamjanka-Bus'kiy district (16.5%), and Boryslav-Drogobych agglomeration (12%). Investments in the energy sector of these administrative units are needed to mitigate emissions. Emissions in the other administrative units do not exceed 500 Gg of CO_2 equivalent per year.

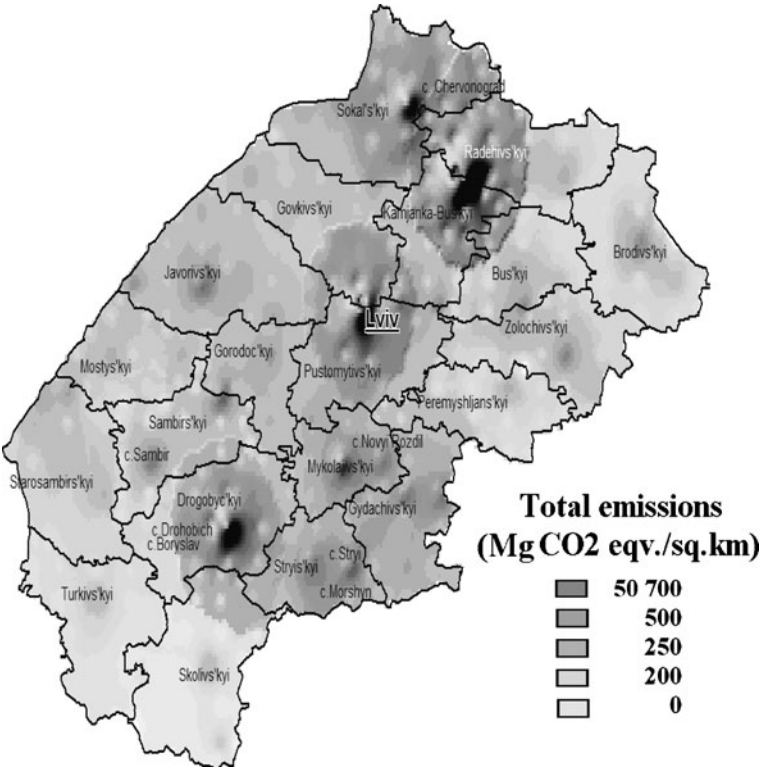

Fig. 2 Thematic map with IDW interpolation of CH_4, CO_2, and N_2O emissions in the energy sector (Lviv region 2004; Mg CO_2-eqv./km^2)

The consistency of two alternative spatially resolved emission estimates could be checked with the help of difference maps. Thematic maps can be compiled using color gradation to pinpoint places where the alternative emission estimates are very inconsistent.

For example, emissions in the transport sector can be estimated based on fuel consumption statistics or using the data on vehicle miles traveled. The total GHG emissions estimates (in CO_2 eqv.) based on these alternative input data differ significantly: for gasoline cars the difference is 6%, for diesel cars 3%, for natural gas cars, 23%. Comparison of emissions at the level of separate grid cells allows detection of the territory where the assessments obtained by different methods coincide and the territory where the assessments are significantly different. Using GIS technology in each grid cell, the difference in estimates is calculated as follows:

$$U_i = \frac{\left| E_{G,i}^{Tier1} - E_{G,i}^{Tier2} \right|}{E_{G,i}^{Tier1}} \cdot 100\% \tag{3}$$

where U_i is the relative difference between emission estimates based on alternative data in a grid cell i; $E_{G,i}^{Tier1}$, $E_{G,i}^{Tier2}$ represent emissions of gas G in cell i, calculated using the fuel use and mileage statistics, respectively.

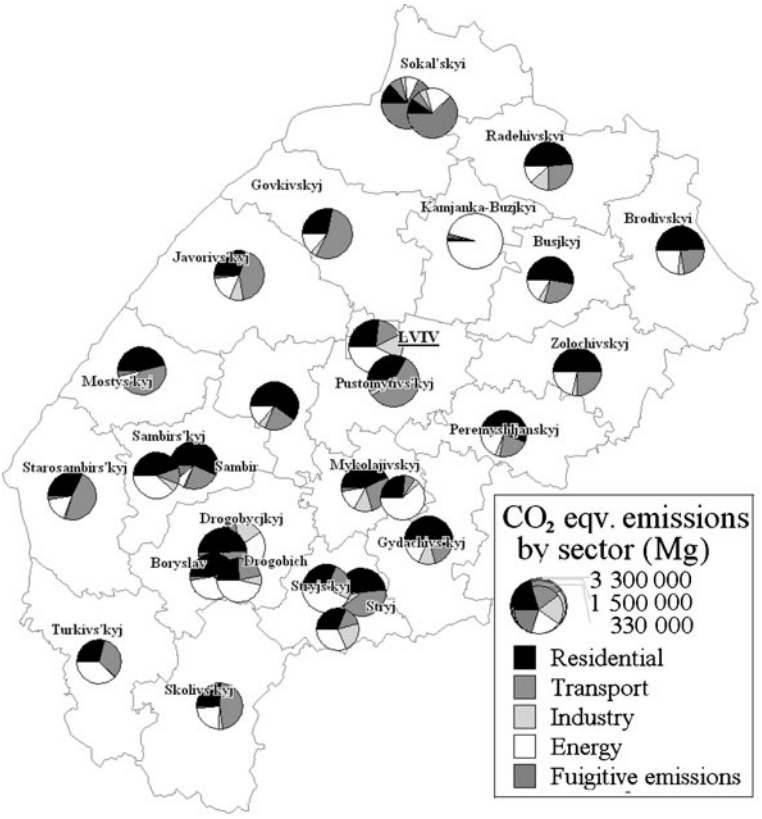

Fig. 3 The structure of GHG emissions by subcategory at the level of administrative regions and administrative cities (Lviv region 2004; Mg CO_2-eqv.) As emission distribution is very uneven, the circle sizes are scaled in logarithmic form

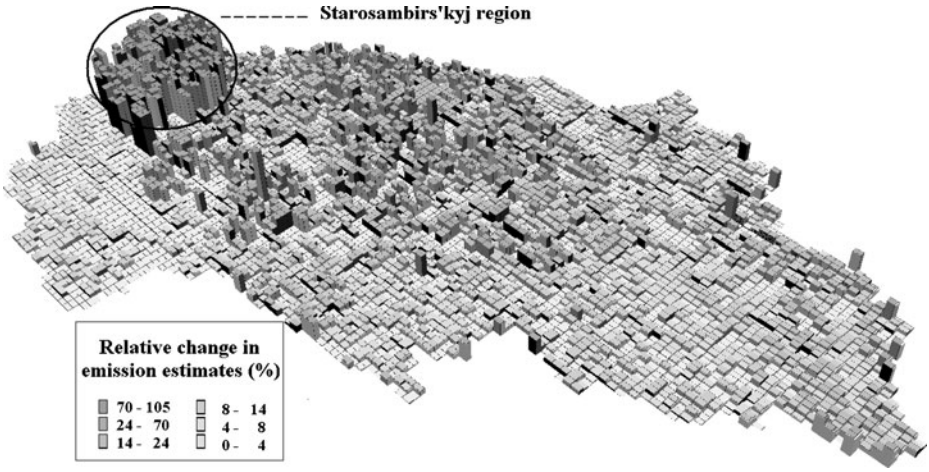

Fig. 4 Relative difference between GHG emission estimates in CO_2 eqv. in the road transport sector, obtained using two alternative statistical datasets (Lviv region; %)

As an example, the difference map of CO_2, CH_4, and N_2O emissions in CO_2 equivalents from the transport sector of Lviv region is built (see Fig. 4). The map shows a relatively good consistency of emission estimates based on fuel consumption and statistics on vehicle miles traveled for almost all cells (the difference does not exceed 24%) except for the cells located in the Starosambirskyj region. The estimates for this region do not coincide, mainly because of inconsistencies in the statistics on fuel consumption and vehicle mileage for this administrative district.

6 Uncertainty evaluation

As the input parameters in the emission inventorying process are not known exactly, best estimates are used. For an uncertainty analysis the probability density functions of parameters should be defined and then the error propagation law applied to combine the individual error estimates to provide uncertainty estimates for the entire inventory. The IPCC Guidelines (IPCC 2006) introduce two approaches (Tier 1 and Tier 2) for estimation of combined uncertainties. Tier 1 uses the simple error propagation Eqs. 4 and 5, and the main assumption is that the standard deviation divided by the mean is less than 0.3 and statistically independent (uncorrelated) inputs are used. To calculate the uncertainty of the product, expressed in percentage terms, the following formula is used:

$$U_{total} = \sqrt{(U_1)^2 + (U_2)^2 + \ldots + (U_n)^2}, \tag{4}$$

and for uncertainty of the sum:

$$U_{total} = \frac{\sqrt{(U_1 \cdot x_1)^2 + (U_2 \cdot x_2)^2 + \ldots + (U_k \cdot x_k)^2}}{x_1 + x_2 + \ldots + x_k}, \tag{5}$$

where x_i is the mean value of unknown parameter X_i, U_i is the relative uncertainty of parameter X_i, U_{total} is the resulting relative uncertainty.

All assumptions used in Tier 1 can be avoided in Tier 2, which is based on Monte Carlo simulation. The principle of Monte Carlo analysis is to select random values of emission factor, activity data, and other estimation parameters within their individual probability density functions (PDFs), and to calculate the corresponding emission values. This procedure is repeated many times and the results of each calculation run build up the overall emission probability density function. The Monte Carlo analysis can be performed at the category level for aggregations of categories or for the inventory as a whole (IPCC 2006).

Mean values and probability density functions were established for spatially distributed activity data and emission factors for grid cells covering the Lviv region of Ukraine. The methodology described allows different uncertainty levels to be used for separate emission source activity data and emission factors involved in inventory. It is important to use country-specific uncertainty data as the default and to use specific data referring to large point sources (these are available from specified technical editions, expert judgments, etc.).

The total uncertainty calculation of inventory results for the Lviv region is provided in two ways.

1. "Traditional" method of uncertainty calculation, using aggregated uncertainties of activity data and default emission factors within separate subcategories of the energy sector by gas type. Calculations were performed using IPCC Tier 1 and Tier 2 approaches.
2. Uncertainty calculation using knowledge of spatial distribution of activity data and emission factors. Monte Carlo simulations were provided for each grid cell using the geo-referenced databases with activity data and emission factors information.

The simulation in the second case has the following steps:

1. For each grid cell the means and PDFs referring to corresponding activity data and emission factors are set. For successful implementation of Monte Carlo uncertainty calculation, additional research should be provided to assess the mean values and PDFs of input data, which refer to large point emission sources. If the specific value of uncertainty is not available for the input data of certain grid cells the specific national (or regional) default values should be taken.
2. For each elementary plot the emission factors and activity data are selected randomly within their PDFs. After multiplying these generated values, one possible emission value for each grid cell is obtained. Summing of these emission values for all elementary plots results in an emission estimate for a region as a whole.
3. Step 2 is repeated many times. As a result, a set of emission estimates is obtained for the region, which is used to calculate the mean and the PDF of the total inventory result. Dependencies and correlations among different input data should be identified and taken into account (Rypdal and Winiwarter 2001).

7 Results of uncertainty assessments

Although we can highly specify the uncertainty values of activity data and emission factors for the calculations, we mainly used national default emission factors and uncertainty estimates, as the assessments of uncertainty values and emission factors for separate plants and other individual emission sources in Ukraine were poor. The focus is on emissions from the energy sector.

7.1 Uncertainty assessment using aggregated data within the Lviv region

Uncertainty of activity data on fuel consumption collected and published by the National Statistical Office of Ukraine is reported to be ±10% (Statistical 2005). This level of uncertainty corresponds to the activity data at the level of administrative region, but after spatial disaggregation, the uncertainty of the activity data used in each grid cell would differ depending on disaggregating methodology and source type (in general the uncertainty level of activity data is much lower for large point sources than for area or line sources).

Using the Monte Carlo approach the uncertainty estimates for total emissions in the Lviv region were simulated (Table 1: case 1). The calculations were based on

Table 1 Uncertainty assessments

		Greenhouse gas			Total
		CO_2	CH_4	N_2O	(Lviv region)
Emissions (Gg, CO_2-eqv.)		9,278.9	779.5	86.8	10,145.0
Case 1: "Traditional" approach					
Uncertainty, %	Tier 1	±9.0	±31.9	±42.2	±9.0
	Tier 2	−8.9..+9.4	−52.4..56.5	−48.5..93.1	−9.2..+9.7
Case 2: Separate grid cells' simulation approach					
Uncertainty, %	Tier 2	−7.4..+7.5	−49.6..+54.4	−33.5..+64.3	−7.3..+7.8

uncertainties of aggregated activity data and default emission factors. The lower and upper bound of relative uncertainty were calculated as 2.5% and 97.5% percentiles, respectively, of the obtained emissions distribution divided by the mean value.

7.2 Uncertainty assessment using spatially distributed data

Possible emission values are simulated using the Monte Carlo approach for each grid cell and summed for the whole territory under investigation. In calculations the correlation between grid cells caused by the use of common emission factors and activity data was not taken into account. After repeating the simulation many times the overall probability density function was built, and uncertainties are calculated as 2.5% and 97.5% percentiles divided by the mean value (Table 1: case 2).

Relative uncertainties, which refer to CH_4 and N_2O emissions, are relatively high (approximately 52% and 71%, respectively). The small share of CH_4 and N_2O in overall emissions explains the small difference between the uncertainty estimates when following the IPCC Tier 1 and Tier 2 approaches. This is because most of the total emissions consist of carbon dioxide emissions, which are believed to be best known, that is, the uncertainty of CO_2 emissions is small and the emission estimates follow a Gaussian distribution.

The uncertainties calculated using the approach where the uncertainties of aggregated activity data and default emission factors were used differ from those calculated using knowledge of the spatial allocation of activity data. Uncertainties of total emissions are ±9.4% using "traditional" methodology and approximately ±7.5% using developed geo-information technology. This is explained by the fact that in the geo-referenced approach, detailed data for large emission point sources were used. The ratio of emissions from large point sources is considerable in overall emissions and uncertainty of the activity data and emission factors is lower.

8 Uncertainty sensitivity analysis

The geo-information technology of spatial inventory and analysis of greenhouse gases is very useful for policymakers, as it gives additional information on the spatial distribution of emission sources. The technology makes it possible to identify (and localize) the greatest sources of emissions and then to investigate their influence on total regional emissions. This knowledge can be used in uncertainty analysis, asa very large part of inventory uncertainty can be attributed to a few sources (Winiwarter and Rypdal 2001).

8.1 Transition to alternative energy sources

As, in Ukraine, the biggest emissions occur from the processes of fuel burning for energy production, policymakers aspire to decrease emissions in this subsector (for example, by transition to alternative energy sources). This leads to considerable overall emission reduction, but in terms of change in their relative uncertainty, the effect of transition is not evident.

GHG inventory results from fossil fuel burning for energy production are characterized by comparatively small relative uncertainty. The transition to the other energy sources thus leads to structural changes in emissions and an increase in the relative uncertainty of total inventory results for the whole administrative region. In the Lviv region of Ukraine three major emission sources of greenhouse gases were identified; then, using the Monte-Carlo method, the simulation experiments were carried out to investigate the influence of these sources on total inventory results.

Figure 5 presents the change in relative uncertainty of total emissions due to the gradual transition to alternative energy sources for the Lviv region. The abscissa defines the grade of transition of the three emission leaders indicated (Lviv agglomeration, Kamjanka-Bus'kiy district, and Boryslav-Drogobych agglomeration) to alternative energy sources ($k = 0$ is traditional energy generation; $k = 100\%$ is full transition to alternative sources). For numerical experiments it was assumed that relative uncertainty of greenhouse gas emissions from fossil fuel burning is equal to 7%, 5%, and 3%, and the relative uncertainty of emission estimates in other subsectors is equal to 10%.

An interesting question arises as to the combined influence of the two effects: from one side, decrease in total emissions, and from the other side, increase in the relative uncertainty of emissions. Figure 6 demonstrates a decreasing of emissions caused by transition to alternative ways of energy generation for the three emission leaders) and a corresponding absolute uncertainty range around the emission line. The absolute uncertainties are mainly the same for all coefficients "k" in spite of relative uncertainty increasing.

Decreasing of uncertainty of inventory results for the biggest sources also leads to reduction in relative uncertainty of the total inventory results for administrative region as a whole. The relative uncertainty of the total inventory as a function of

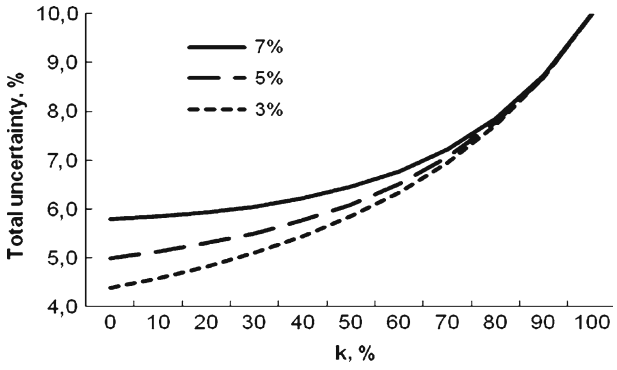

Fig. 5 Change in total relative uncertainty due to structural changes in emissions during transition to alternative energy sources

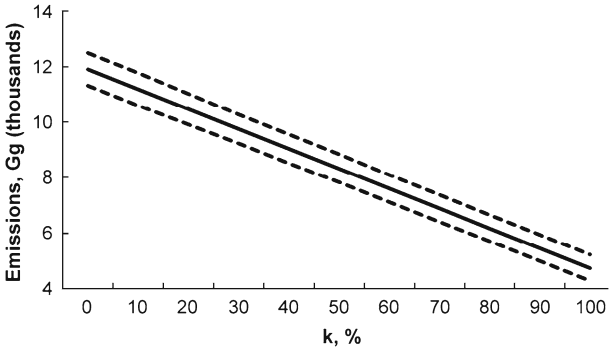

Fig. 6 Decreasing of emissions due to transition to alternative energy sources; and absolute uncertainty range

relative uncertainty of the three leaders for the Lviv region (for three values of transition coefficient) is presented in Fig. 7.

8.2 Input data uncertainty change

Another type of uncertainty analysis using the knowledge of spatial distribution of emission sources includes investigation of the impact of a change in uncertainty in the input data of point sources on the uncertainty of total inventory results. In practice this can reflect a situation where some investments are made to improve knowledge regarding fuel characteristics used at a certain plant or to improve the statistics on fuels used, etc. These actions will lead to reduced uncertainty in input data (for a certain emission source) used in inventory and thus to overall uncertainty reduction.

The Dobrotvir heat power plant was selected for the experiments. Some 85% of all coal used in the energy sector of the Lviv region is burned in the Dobrotvir heat power plant. Figure 8 shows the sensitivity of the overall uncertainty of emission estimates to knowledge improvements in separate input data on ***P*** percent. The calculations were performed using IPCC Tier 2 approach (based on Monte Carlo simulations).

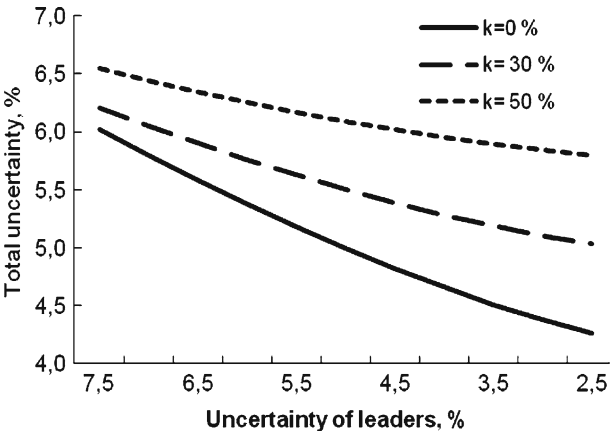

Fig. 7 The relative uncertainty of the total inventory results for region as a function of the relative uncertainty of emission leaders

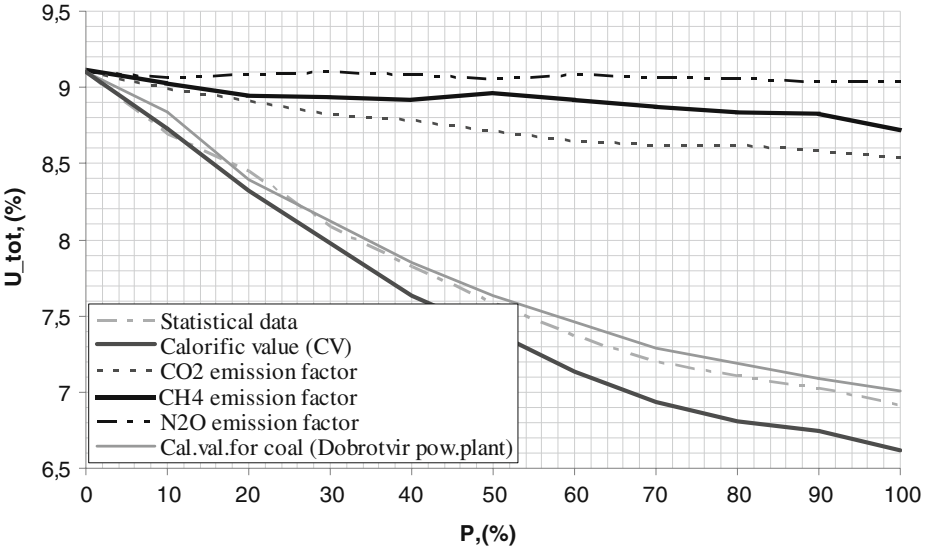

Fig. 8 Dependence of uncertainty of total inventory in the energy sector of the Lviv region from decreasing uncertainty of input data into ***P*** percent (Monte Carlo simulations)

The uncertainty of total emissions stays almost constant with the change in N_2O and CH_4 emission factors. For example, if, to reduce the uncertainty of CH_4 emission factors, the uncertainty of overall emissions did not change but the uncertainty of methane emissions decreased from 56% to 29%, the same would occur for N_2O: reduction of the uncertainty of this GHG emission factor leads to N_2O emission uncertainty reduction from 93% to 54% without affecting the uncertainty of overall emissions in CO_2 equivalents. This means that although the N_2O and CH_4 emissions are highly uncertain, reducing their uncertainty does not affect the uncertainty of overall emissions in the Lviv region. The most effective way of reducing the uncertainty of total emissions is to decrease knowledge improvement on fuel treatment statistical data and net calorific values for fuels used in different sectors.

The reduction of uncertainty of statistical data by half leads to a decrease in uncertainty of total emissions from 9.2% to 7.5%; and to 7.3% in the case of the same uncertainty reduction for net calorific values. What is more, knowledge improvement only about the chemical characteristics of coal (or its calorific values) used at one plant (Dobrotvir power plant) helped to significantly change the uncertainty of overall results (see Fig. 8: bold line). Such information is of great importance for the governmental bodies responsible for defining national or regional strategies for emission reduction and inventory quality improvements. It can significantly help to select the most cost-effective way of reducing the uncertainty in total inventory results.

9 Conclusions

The results of the spatial greenhouse gas inventory for the energy sector of the Lviv region of Ukraine confirm the assumption about the very uneven distribution of emissions in different administrative units and different economic subsectors. The results proved the importance of spatial inventory at the regional level. The spatial approach to greenhouse gas emission calculations is better at taking into account the differences in economic activities and specific features of fuel treatment at the level of separate administrative units and even for separate grid cells.

The spatial inventory methodology allows different uncertainties to be used for activity data and emission factors for the separate emission sources involved. Specific data referring to large point sources or economic areas can be used in the inventory process as well as in the uncertainty calculation. Uncertainties of emissions in the energy sector of the Lviv region are ±7.3% (in the case of a high-resolution inventory) and ±9.2% (in the case of a "traditional" inventory) using the Monte Carlo simulation approach. The difference is expected to be bigger if more specific uncertainty assessments of inputs become available.

The results of spatial inventory allow identification of the biggest sources of emissions and investigation of the influence of their uncertainties on the uncertainty of inventory results for the region as a whole. It enables better analysis and selection of the most cost-effective ways of reducing overall inventory uncertainty either by transition to alternative energy sources or by improving statistics or knowledge about the chemical characteristics of fuel used at a given plant. This gives policymakers an effective tool for supporting decisions on strategic baselines of economic development and environmental policy.

References

Bun R (ed) Gusti M, Dachuk V et al (2004) Information technologies for greenhouse gas inventories and prognosis of the carbon budget of Ukraine. Lviv, Ukraine, 376 pp. Needs call out in text Bun et al. 2004

Bun R, Gusti M, Bun A, Hamal Kh (2006) Multilevel model for greenhouse gas inventory and uncertainty analysis concerning the Kyoto Protocol implementation. In: Intern Conf on Ecological Modelling, "ICEM 2006." Yamaguchi, Japan

Bun A, Hamal K, Jonas M, Lesiv M (2010) Verification of compliance with GHG emission targets: Annex B countries. Clim Change. doi:10.1007/s10584-010-9906-6

Fuel (2005) Fuel and energy resources of Lviv Region. Reference book, Lviv, Statistical Department

Horabik J, Nahorski Z (2010) A statistical model for spatial inventory data: a case study of N_2O emissions in municipalities of southern Norway. Clim Change. doi:10.1007/s10584-010-9913-7

Industry (2005) Industry of Lviv Region. Reference book, Lviv Statistical Department

IPCC (2006) 2006 IPCC Guidelines for national greenhouse gas inventories. In: Eggleston HS, Buendia L, Miwa K, Ngara T, Tanabe K (eds) Prepared by the National Greenhouse Gas Inventories Programme. IGES, Japan

Jonas M, Gusti M, Jêda W, Nahorski Z, Nilsson S (2010) Comparison of preparatory signal analysis techniques for consideration in the (post-) Kyoto policy process. Clim Change. doi:10.1007/s10584-010-9914-6

Jonas M, Nilsson S, Bun R, Dachuk V, Gusti M, Horabik J, Jęda W, Nahorski Z (2004) Preparatory signal detection for Annex I countries under the Kyoto Protocol—a lesson for the post-Kyoto policy process. Interim Report IR-04-024 International Institute for Applied Systems Analysis. Laxenburg, Austria

Lindley SJ, Longhurst JWS, Watson AFR, Conlan DE (1996) Procedures for the estimation of regional scale atmospheric emissions. An example from the north-west region of England. Atmos Environ 30(17):3079–3091

Nahorski Z, Horabik J (2010) Compliance and emission trading rules for asymmetric emission uncertainty estimates. Clim Change. doi:10.1007/s10584-010-9916-4

Pacyna JM, Graedel TE (1995) Atmospheric emissions inventories: status and prospects. Annu Rev Energy Environ 20:265–300

Power (2002) Power industry of Ukraine: 1991–2000. Reference book, Kyiv, Ukrinformenergoservis

Rypdal K, Winiwarter W (2001) Uncertainties in greenhouse gas emission inventories—evaluation, comparability, and implications. Environ Sci Policy 4(2–3):107–116

Statistical (2005) Statistical year-book of Lviv Region on 2005 Part II: Administrative Units and Cities of Lviv Region Lviv Statistical Department Ukraine

Wang X, Mauzerall D, Hu J, Russel A, Larson E, Woo J, Streets D, Guenther A (2005) A high-resolution emission inventory for eastern China in 2000 and three scenarios for 2020. Atmos Environ 39:5917–5933

Winiwarter W, Rypdal K (2001) Assessing the uncertainty associated with national greenhouse gas emission inventories: a case study for Austria. Atmos Environ 35(32):5425–5440

Winiwarter W, Dore C, Hayman G, Vlachogiannis D, Gounaris N, Bartzis J, Ekstrand S, Tamponi M, Maffeis G (2003) Methods for comparing gridded inventories of atmospheric emissions—application for Milan province Italy, and the Greater Athens Area Greece. Sci Total Environ 303:231–243

Climatic Change (2010) 103:245–261
DOI 10.1007/s10584-010-9915-5

Quantitative quality assessment of the greenhouse gas inventory for agriculture in Europe

Adrian Leip

Received: 5 January 2009 / Accepted: 15 June 2010 / Published online: 17 July 2010

Abstract The greenhouse gas inventory of the European Communities and its estimation of the uncertainty is built from 15 individual and independent greenhouse gas inventories. This presents a particular challenge and is possible only if homogeneous information is available for all member states and if a proper evaluation of correlation between member states is performed. To this end, we present a methodology that estimates a quantitative measure for the aggregated Tier-level as well as the uncertainty for the main categories in the agriculture sector. In contrast to the approach suggested in the IPCC guidelines, which uses uncertainty estimates for activity data and emissions factors for each source category, the method presented uses quantitative information from individual parameters used in the inventory calculations, in combination with a well defined procedure to aggregate the information. Not surprisingly, N_2O emissions from agricultural soils are found to dominate the uncertainty. The results demonstrate the importance of correlation, if uncertainties are combined for the whole of Europe. The biggest challenge seems to be to conceptually harmonize the uncertainty estimates for the activity data (which tend to be underestimated) and emission factors (which tend to be overestimated).

1 Introduction

The use of a robust methodology to estimate the uncertainty in national greenhouse gas (GHG) inventories is becoming increasingly important as the role of the

A. Leip
European Commission Joint Research Centre, Institute for Environment and Sustainability, Ispra, Italy

A. Leip (✉)
John Research Center, Climate Change Unit T.P. 290, Via E. Fermi, 21027, Ispra, VA, Italy
e-mail: adrian.leip@jrc.ec.europa.eu

uncertainty estimates increases. In the past, the main purpose of uncertainty assessment (UA) was to prioritize future investments for the improvement of the national GHG inventory. Thus it was used to rank the source categories accordingly to obtain better data. Furthermore there is particular academic interest in comparing GHG inventory uncertainties across countries (e.g., Keizer et al. 2007; Monni et al. 2004; Rypdal and Winiwarter 2001), or the results of different methodologies used in the UA (e.g., Olsthoorn and Pielaat 2003; Ramiréz et al. 2006; Winiwarter 2007). It is now recognized that uncertainty estimates will be used to prove the achievement of GHG reduction commitments (Jonas et al. 2007; Monni et al. 2007; Nahorski et al. 2007) or to play a critical role in deciding on reduction projects (e.g., Grassi et al. 2008). Yet, while the quality of the GHG inventories has significantly improved in the last few years and is now generally accepted to be of comparable standard and quality (Leip et al. 2005), the estimates of the uncertainty are far from being comparable and are spread over a large quality range.

While there are several comparative studies on UA in GHG inventories, they are mainly in the framework of an improvement of national approach for UA (see, e.g., Winiwarter (2007) for Austria, Monni et al. (2007) for Finland, Ramiréz et al. (2006) for the Netherlands; Rypdal and Flugsrud (2001) for Norway, Passant (2003) for the United Kingdom). In this paper we present a compilation of uncertainty estimates of member states of the European Union (EU) for the agriculture sector. The European Commission (EC) is the only regional economically integrated organization that has joined the United Nations Framework Convention on Climate Change (UNFCCC) as a party and has thus the same reporting obligations. However, while data for GHG emissions and estimates for the relative uncertainty of activity data and emission factors were taken from the national GHG inventories of the respective member states, a common approach was applied to calculate sectoral and sub-sectoral uncertainty of the emissions. Additionally, we calculated the aggregated uncertainty for the 15 member states of the EU (EU15) which are part of the 'European bubble' (see EEA 2008, 2009). For the EC inventory, uncorrelated emission estimates of the individual countries reduce the level of uncertainty. It is thus important to make assumptions on the level of correlation between member states' emission estimates. We developed an approach that bases the degree of correlation between member states on the Tier level of the national emission inventories, being a further development of the approach already used in earlier EC GHG inventories (see EEA 2007). The term "Tier level" is used in analogy to the IPCC (2000) definition to describe the methodology used. The idea is that the higher the Tier level of the emission estimates, the higher the influence of national information on the emission calculations, and the smaller the degree of correlation among member states. Thus a correlation-matrix is obtained which is used for both an extended Tier 1 for uncertainty (simple error propagation with consideration of correlations) and a Tier 2 (Monte Carlo).

In the following I develop the methodology and show the results for the most recent EC inventory of the year 2008. I then identify necessary improvements to the UA and discuss some critical aspects such as likely over- or underestimation of uncertainties in inventory-input data and possible ways to achieve UAs of comparable content and quality for EU member states.

2 Method

The uncertainty estimates of member states are carried out by Tier 1 or Tier 2 methods following the IPCC guidance (IPCC 2000). As a further development of the approach used in the EC greenhouse gas inventory (EEA 2007), the method used for the UA of the agriculture sector of the combined EC inventory presented here involves several additions to the approaches described in the IPCC guidelines (IPCC 2000, 2006). This includes (1) a quantitative assessment of the Tier level of the emission estimate based on the individual factors and parameters used for all members states and the EC; (2) consistent aggregation of the available uncertainty information to the level of the categories including gap filling where necessary. This is done using both Tier 1 and Tier 2 methodology for both level and trend uncertainty; (3) aggregation of categorical uncertainty estimates to the EU level using quantitative information on the level of independence. As a proxy for the level of independence, the Tier level is used and is defined as follows: Tier 1 if only default IPCC data are used in the estimation equation and Tier 2 if the emissions estimate is based on country-specific data. Through the aggregation of emission data by categories and countries, intermediate values between Tier 1 and Tier 2 become possible.

2.1 Assessing the Tier level

The IPCC methodology estimates emissions E_s from a certain source category s as:

$$E_s = IEF_s \cdot AD_s \tag{1}$$

where AD_s is the activity data for the source category s and IEF_s is the implied emission factor for this category. There are three levels for estimating the emissions, called Tier 1, Tier 2, and Tier 3, moving from the use of default values through the inclusion of national information to the application of modeling tools. In order to define an EU-wide Tier level per source category and sector, two criteria must be met:

1. For each source category and member state a Tier level must be assigned.
2. To assess the quality of aggregated emissions derived at different Tier level, the Tier levels must be measured on an interval scale, allowing 'intermediate' Tier levels.

To do this, I developed standard procedures for each source category, based on the following principles:

1. The flow of nutrients in agriculture implies that the emission in one category can serve as an activity level in another. Therefore, the Tier level, for example, of the estimate for nitrogen excretion influences the Tier level for nitrous oxide (N_2O) emissions from manure management, and also N_2O emissions from manure application to soils, indirect N_2O emissions from volatilization of NH_3+NO_x, and N_2O emissions from nitrogen deposited by grazing animals.

2. A Tier level is assessed for each parameter by comparing the IPCC default value with the value used by the countries. If the default IPCC value is used, the Tier level is set to 1 and otherwise the Tier level is set to 2. Caution is taken for country-specific data that are identical to the default values. This has been checked "manually."
3. With a few exceptions, a country-specific estimation of the activity data is considered as "standard" for countries in Europe. Only for source categories where particular efforts are needed for a good estimate of the activity is the Tier level of the activity data considered, such as the area of cultivated histosols or the fraction of manure deposited by grazing animals.

For the sake of consistency with the IPCC usage, we evaluate Tier levels in the range [1,2], not considering emission estimates of higher Tier as Tier 2, which, however, have, to date, been very rare in the GHG inventories of European countries.

Tier levels are aggregated applying different aggregation rules:

a. The MEDIAN-rule is applied if the Tier level T of a *product* of different parameters P_i is to be evaluated ($T_{\prod_i Pi}$). The aggregation of the Tier level of these parameters to estimate the Tier level of the emission factor should follow the following principles. (1) If parameters at very different Tier levels are multiplied, the higher level should get more weight; (2) if parameters with different uncertainty are multiplied, it should be good practice to estimate the parameter which is associated with the higher uncertainty at a higher Tier level. Thus, the aggregation rule should reward the fact that efforts have been made to improve uncertain parameters. Where a comprehensive set of relative uncertainty estimates for the individual parameters is lacking, the following equation with an arbitrary weighting factors $w_{\mathrm{p,j}}$ has been introduced, based on expert judgment:

$$T_{\prod_i P_i} = 3 - \prod_i \left[(3 - T_{Pi})^{\frac{w_{p,i}}{\sum_j \{w_{p,j}\}}} \right] \tag{2}$$

with i and j indicating the individual parameters to be multiplied. The term $(3 - T_{Pi})$ assures that a higher weight is given to the parameter estimated with the higher Tier. For example, this formula is used to estimate the uncertainty of the emission factor for CH_4 emissions from manure management, which is calculated as the product of volatile solid excretion (VS), maximum CH_4 producing capacity (B_0), and CH_4 conversion factor (MCF). The following weights were used: VS: 0.75, B_0: 0.125, MCF: 0.125. The higher weight for VS is based on the observation that variations of B_0 and MCF are usually small and thus do not greatly contribute to uncertainty of the emission factor. A simplified rule has been applied to estimate the Tier level of CH_4 emissions from enteric fermentation, which in many cases is based on, or validated with, direct measurements.

b. The MEAN-rule if an emission estimate is calculated as the *sum* of two or more sub-categories. In this case, the Tier levels of the individual estimates are aggregated using an emission-weighted average. For example, the Tier level of indirect N_2O emissions from agriculture T_{4D3} is calculated from the Tier levels

determined for indirect emissions through volatilization of reactive nitrogen gases T_{4D3a} and leaching/run-off of nitrate T_{4Db} according to:

$$T_{\sum_i \mathrm{E_i}} = \frac{\sum_i T_\mathrm{i} \cdot E_\mathrm{i}}{\sum_i E_\mathrm{i}} \tag{3}$$

2.2 Assessing the uncertainty at member state level

The IPCC guidelines (IPCC 2000, 2006) describe two approaches for combining uncertainty in the GHG inventory models. The first approach uses the error propagation method. This method works fine as long as the probability density function (PDF) of the mean is normal and the relative standard deviation σ_r is not larger than 0.3. For larger relative standard deviations or skewed distributions IPCC (2006) also gives guidance on how a good estimate for combined uncertainty can nevertheless be achieved. I applied a Tier 1 (uncertainty propagation) and a Tier 2 (Monte Carlo) model to estimate combined uncertainty at member state and EC levels, where this was not yet reported at the required level of aggregation by the member state. For both approaches I considered potential dependencies, expanding the Tier 1 method for additive terms with the following equation:

$$\sigma^2_{X\pm Y} = \sigma^2_X + \sigma^2_Y \pm 2 \cdot COV_{X,Y} \tag{4}$$

$$\mathrm{COV_{X,Y}} = \rho_{X,Y} \cdot \sigma_X \cdot \sigma_\mathrm{Y} \tag{5}$$

if $\sigma^2 x$ is the variance of the parameter X, $\mathrm{COV_{X,Y}}$ is the covariance between the parameters X and Y, $\rho_{X,Y}$ is the coefficient of correlation. Both approaches were realized in Spreadsheet models using Visual Basic for Excel® functions. The information on the uncertainty estimates for agricultural sources differs significantly across the 15 member states for which the EC inventory has to be compiled. Some countries report uncertainties at the level of categories; other give detailed information, for example by main animal types or for the different types of nitrogen input contributing to direct N_2O emissions. For a meaningful comparison and further processing at the EU level, the numbers must be aggregated or gap-filled. As a rule, uncertainties below the subcategory are assumed to be correlated (e.g., when combining dairy and non-dairy cattle or different direct N_2O sources from agricultural soils), while for the combination of sub-categories (different animal types, direct and indirect N_2O emissions), the uncertainties were considered to be uncorrelated. The uncertainties of the categories within agriculture are considered to be uncorrelated as well. This is mainly due to the fact that the largest contribution of the uncertainties stems from the emission factors (Leip et al. 2005) so that the uncertainty of the activity data, which might be partly identical across categories, becomes less important. "Gap filling" is done for the combined uncertainty (AD*EF). For the analysis of the trend uncertainty, gap filling for AD_s and EF_s is also required. Here, AD uncertainties are gap-filled first on the basis of the model $\sum_i \{EF_i \cdot AD_i\} = IEF \cdot \sum_i \{AD_i\} = IEF \cdot AD$, and missing EF uncertainties are then calculated on the basis of the formula IEF = E/AD for both Tier 1 (with $(\sigma_{r,IEF} \cdot IEF)^2 = (\sigma_{r,E} \cdot E)^2 - (\sigma_{r,AD} \cdot AD)^2$) and Tier 2. Tables 1 and 2 show that there is large variability in uncertainty estimates for both activity

Table 1 Summary table for the relative uncertainty in percentage terms for activity data (source: national GHG inventories of EU member states for the year 2007, submitted in 2009, and own calculations)

	Total CH_4+N_2O	4A CH_4	4B CH_4	4B N_2O	4C CH_4	4D CH_4	4D N_2O
Austria	4	10	7	10			4
Belgium	12	5	10	10			30
Denmark	5	10	10	10			7
Finland[a]	12						
France	5	5	5	5			10
Germany[a]							
Greece	15	5	5	50	2		22
Ireland	1	1	1	11			
Italy	9	20	20	20	3		14
Luxembourg	4	2	2				9
Netherlands	8	4	9	10			17
Portugal	12	9	34	39	37		30
Spain	44	3	3	16			102
Sweden	9	5	20	20			16
United Kingdom	1	0	0	1			1

4A enteric fermentation, *4B* manure management, *4C* rice cultivation, *4D* agricultural soils

[a]Some countries do not report uncertainty estimates for AD, as the uncertainty assessment is done with a dedicated model and the combined uncertainty estimate is reported as EF-uncertainty

data (Table 1) and emission factors as they are reported in the national inventory reports of the member states of the European Union. The variability will be further discussed below.

Table 2 Summary table for the relative uncertainty in percentage terms for the implied emission factors (source: national GHG inventories of EU member states for the year 2007, submitted in 2009, and own calculations)

	Total CH_4+N_2O	4A CH_4	4B CH_4	4B N_2O	4C CH_4	4D CH_4	4D N_2O
Austria	41	22	50	100			101
Belgium	98	40	41	91			252
Denmark	18	13	100	100			24
Finland	45	32	16	82			75
France	100	40	50	50			200
Germany	158	6	12	21		50	307
Greece	63	30	50	112	40		95
Ireland	22	11	11	101			58
Italy	36	28	102	102	20		67
Luxembourg	82	30	145				159
Netherlands	41	15	70	100			83
Portugal	76	14	82	107	55		227
Spain	104	11	11	101			239
Sweden	41	25	54	54			71
United Kingdom	229	20	30	414			424

4A enteric fermentation, *4B* manure management, *4C* rice cultivation, *4D* agricultural soils

The Monte Carlo calculation includes a control on the likely PDF of the mean. If the relative uncertainty exceeds 0.4 then it is assumed that the mean is log-normally distributed and the distribution is transformed with $\mu_l = \log_{10}\{\mu_n\}$ and $\sigma_l = \log_{10}(1 + \sigma_n/100)$.

The trend uncertainty is calculated with both standard Tier 1 (IPCC 2006) and Monte Carlo calculation.

2.3 Assessing the uncertainty at the EU level

Uncertainties for source categories in the agriculture sector and for the sector as a whole are combined considering an assumed degree of dependence between each pair of countries. The quantitative assessment of the Tier levels outlined in Section 2.1 helps to derive a reasonable estimate for the correlation coefficient ρ_{XY} between two countries X and Y. To this end, the Tier levels T_X and T_Y are used in the following equation:

$$\rho_{X,Y} = \sqrt{(2 - T_X) \cdot (2 - T_Y)} \tag{6}$$

Equation 6 leads to the situation of no correlation ($\rho_{X,Y} = 0$) for two countries with a Tier 2 and full correlation ($\rho_{X,Y} = 1$) if both countries used a Tier 1. A correlation coefficient can be calculated for any intermediate situation. This information is further processed within the standard IPCC Tier 1 and Monte Carlo methods for both level and trend uncertainty.

3 Results

Table 3 summarizes the Tier levels calculated for EU15 countries for the main source categories in agriculture. Enteric fermentation and manure management emissions are largely based on a characterization of the animal performance. This is conducted for animal types relevant for CH_4 emissions from enteric fermentation. For CH_4 emissions from manure management other animals are relevant (swine, poultry) with the consequence that the Tier level for CH_4 emission estimates from manure management is, with Tier 1.6, somewhat lower than for CH_4 emissions estimates for enteric fermentation. Nitrogen excretion data are in many cases based on national studies, which makes the estimate for N_2O emissions from manure management of a higher Tier (Tier 1.7 for EU15). For N_2O emissions from agricultural soils, only few countries have developed national emission factors, even though national information for other parameters, particularly volatilization and leaching fractions, make the Tier level higher than 1. Very different approaches are used to estimate CH_4 emissions from agricultural soils; most countries do not report this source category. While two countries estimate CH_4 emissions from sewage sludge applied to soils, one country estimates this source category as uptake of CH_4 in aerobic soils.

The result of the uncertainty assessment (Tier 1) is shown in Table 4. For the EC uncertainty, five scenarios are calculated to give an idea for the range of possible uncertainty values. The first scenario calculates the uncertainty using the "most probable" correlation level as defined above. However, particularly for N_2O

Table 3 Summary table for the tier level assessment for EU15 countries, based on information for national GHG inventories for the year 2007, submitted in 2009

	Total CH_4+N_2O	4A CH_4	4B CH_4	4B N_2O	4C CH_4	4D CH_4	4D N_2O
Austria	Tier 1.6	Tier 1.9	Tier 1.8	Tier 1.7		Tier 2.0	Tier 1.3
Belgium	Tier 1.7	Tier 1.9	Tier 1.9	Tier 2.0		Tier 2.0	Tier 1.5
Denmark	Tier 1.7	Tier 2.0	Tier 1.9	Tier 1.9			Tier 1.5
Finland	Tier 1.6	Tier 1.9	Tier 1.6	Tier 1.4			Tier 1.5
France	Tier 1.4	Tier 2.0	Tier 1.2	Tier 1.5	Tier 1.0		Tier 1.1
Germany	Tier 2.0	Tier 2.0	Tier 1.9	Tier 2.0		Tier 2.0	Tier 2.0
Greece	Tier 1.2	Tier 1.6	Tier 1.1	Tier 1.7	Tier 1.0		Tier 1.1
Ireland	Tier 1.7	Tier 2.0	Tier 1.6	Tier 1.7			Tier 1.3
Italy	Tier 1.5	Tier 1.8	Tier 1.8	Tier 1.7	Tier 2.0		Tier 1.3
Luxembourg	Tier 1.5	Tier 2.0	Tier 1.8				Tier 1.2
Netherlands	Tier 1.9	Tier 1.9	Tier 2.0	Tier 1.7			Tier 1.9
Portugal	Tier 1.7	Tier 2.0	Tier 1.9	Tier 1.7	Tier 1.0		Tier 1.4
Spain	Tier 1.8	Tier 1.9	Tier 1.8	Tier 1.7			Tier 1.7
Sweden	Tier 1.8	Tier 1.9	Tier 1.9	Tier 1.7			Tier 1.8
United Kingdom	Tier 1.5	Tier 1.9	Tier 1.6	Tier 1.8			Tier 1.2
EU-15	Tier 1.6	Tier 1.9	Tier 1.6	Tier 1.7	Tier 1.6	Tier 2.0	Tier 1.4

4A enteric fermentation, *4B* manure management, *4C* rice cultivation, *4D* agricultural soils

Table 4 Summary table for the uncertainty assessment (relative uncertainties (Tier 1) in percentage of mean emission estimate, based on information for national GHG inventories for the year 2007, submitted in 2009)

	Total $CH_4+ N_2O$	4A CH_4	4B CH_4	4B N_2O	4C CH_4	4D CH_4	4D N_2O
Austria	40.5	22.4	50.1	100.5			100.6
Belgium	98.3	40.3	41.2	90.6			251.8
Denmark	18.4	12.8	100.5	100.5			24.1
Finland	44.8	32.1	15.9	82.0			74.9
France	100.2	40.3	50.2	50.2			200.2
Germany	158.4	5.9	11.6	20.9		50.0	306.6
Greece	63.2	30.4	50.2	111.8	40.0		95.0
Ireland	21.7	11.4	11.2	100.6			57.9
Italy	35.5	28.3	102.0	102.0	20.2		66.5
Luxembourg	82.1	30.1	144.6				158.7
Netherlands	40.5	15.2	69.7	100.5			82.8
Portugal	76.2	14.4	82.2	107.3	54.7		227.3
Spain	103.6	11.4	11.4	101.3			239.3
Sweden	40.8	25.5	53.9	53.9			70.5
United Kingdom	229.1	20.0	30.0	414.0			424.0
EU-15*	67.5	11.5	25.7	61.4	19.8	50.0	156.6
No correlation	45.4	10.5	18.0	41.6	18.7	50.0	93.1
Full correlation	102.4	22.6	40.7	101.0	27.9	50.0	209.9
Only 4D uncorr	46.4	22.6	40.7	101.0	27.9	50.0	93.1
Only 4D corr.	102.0	10.5	18.0	41.6	18.7	50.0	209.9

4A enteric fermentation, *4B* manure management, *4C* rice cultivation, *4D* agricultural soils

emissions from agricultural soils, the dependence on other exogenous factors that are not part of the inventory system might influence the uncertainty distribution, so that the "most probable" level of correlation does not necessarily reflect the reality. Therefore, a second scenario assumes no correlation between the uncertainty estimates of the individual countries, while the third scenario assumes full correlation. Obviously, this scenario leads to the highest overall uncertainty estimates of 102% for agriculture. Two additional scenarios calculate the bounds for the uncertainty estimate assuming that the member states' estimate for agricultural soils is uncorrelated, but the estimates of all other sub-categories is correlated (lower bound) and finally that only agricultural soil estimates are correlated (upper bound). The table shows that both bounds are shifted only slightly, the lower from 45.4% to 46.4% and the upper from 102.4% to 102.0%. This highlights again the importance of N_2O emissions from agricultural soils, which is further translated into the overall GHG inventory, as shown in Table 5, giving the uncertainty values as a percentage of the total GHG emissions, where it induces a range of the total uncertainty from 4% to 9%. If agriculture were not part of the GHG inventory, the uncertainty would be at a level of 1.4%! The analysis of the trend analysis yields similar results as calculated in EEA (2009), and shown in Table 6. The trend uncertainty is calculated following the methodology proposed in the IPCC (2000) guidelines. The table shows that agriculture contributes 1.2% to the total trend uncertainty of the EC GHG inventory of 8.4% (EEA 2009) and that, again, N_2O emissions from agricultural soils dominate.

Table 5 Member states' contribution of uncertainty in agriculture to the overall uncertainty estimate emission data from EEA (2009). Relative uncertainty in percentage of total emissions from agriculture, based on information for national GHG inventories for the year 2007, submitted in 2009

	Total CH_4+N_2O	4A CH_4	4B CH_4	4B N_2O	4C CH_4	4D CH_4	4D N_2O
Austria	3.7	0.8	0.5	1.0			3.4
Belgium	7.2	1.1	0.5	0.5			7.1
Denmark	2.8	0.5	1.6	0.9			2.0
Finland	3.2	0.6	0.1	0.5			3.0
France	18.1	2.2	1.3	0.6			17.9
Germany	8.5	0.1	0.1	0.1		0.0	8.7
Greece	5.4	0.7	0.2	0.2	0.0		5.4
Ireland	5.6	1.5	0.3	0.6			5.3
Italy	2.4	0.6	0.6	0.7	0.1		2.1
Luxembourg	4.5	0.6	1.1				4.2
Netherlands	3.6	0.5	0.9	0.4			3.4
Portugal	7.1	0.5	1.2	0.8	0.3		6.9
Spain	10.8	0.3	0.2	0.7			10.7
Sweden	5.3	1.1	0.4	0.4			5.1
United Kingdom	15.6	0.5	0.1	1.1			15.5
EU-15	6.2	0.3	0.3	0.3	0.0	0.0	7.0
EU-15 no corr	4.2	0.3	0.2	0.2	0.0	0.0	4.2
EU-15 full corr	9.4	0.7	0.5	0.6	0.0	0.0	9.4

4A enteric fermentation, *4B* manure management, *4C* rice cultivation, *4D* agricultural soils, *4D1* direct N_2O emissions, *4D2* N_2O emissions from grazing animals, *4D3* indirect N_2O emissions

Table 6 Trend uncertainty in percent-points of the overall EC GHG inventory, based on information for national GHG inventories for the year 2007, submitted in 2009

	Total CH_4+N_2O	4A CH_4	4B CH_4	4B N_2O	4C CH_4	4D CH_4	4D N_2O
Austria	0.02	0.01	0.00	0.00			0.01
Belgium	0.07	0.01	0.01	0.00			0.07
Denmark	0.03	0.01	0.01	0.00			0.02
Finland	0.02	0.00	0.00	0.00			0.02
France	0.49	0.06	0.02	0.02			0.48
Germany	0.34	0.01	0.00	0.00			0.34
Greece	0.08	0.01	0.00	0.01	0.00		0.08
Ireland	0.01	0.00	0.00	0.00		0.00	0.01
Italy	0.13	0.08	0.02	0.03	0.00		0.09
Luxembourg	0.00	0.00	0.00				0.00
Netherlands	0.08	0.01	0.01	0.00			0.08
Portugal	0.06	0.01	0.01	0.01	0.01		0.06
Spain	0.71	0.02	0.01	0.02			0.71
Sweden	0.03	0.01	0.00	0.00			0.03
United Kingdom	0.78	0.01	0.01	0.05			0.78
EU-15	1.2	0.1	0.0	0.1	0.0	0.0	1.2

4A enteric fermentation, *4B* manure management, *4C* rice cultivation, *4D* agricultural soils

4 Discussion

Generally, uncertainties in input data need to be derived from indirect sources or from expert judgments. A comparison of the uncertainty estimates of five inventories in the late 1990s (Rypdal and Winiwarter 2001), showed that the main reason for the difference in estimated uncertainty is the differences in the assessment of N_2O emissions from agricultural soils. We find striking differences in the uncertainty estimates from different countries, in that in many cases higher uncertainties are reported in countries where large efforts were put into the agricultural GHG inventory. Monni et al. (2004) also stress that differences in reported uncertainties are in large part due to different ways of assessing the uncertainty. Rypdal and Flugsrud (2001) describe two ways to handle correlations. One way is to aggregate the input data set in such a way that the dependencies are eliminated and the other solution is to explicitly model the dependencies in the analysis, if this is allowed by the method used. The IPCC Good Practice Guidance (IPCC 2000) notes that correlations, even if they exist, may not be important for the uncertainty assessment of a GHG inventory if the dependency is not sufficiently strong or the inventory is not sensitive to the dependent inputs. Nevertheless, consideration of correlation between countries is important as this lead to a significant reduction of the uncertainty of emission estimates when combined to the EC level. If countries are relying on default EF_s, the distribution of the true mean value is likely to be the same, unless national circumstances differ in important driving factors for that source category in which case the true mean would have to be sampled from a different probability distribution. New scientific evidence would lead to an upward or downward correction of the emission strength for all countries using this default emission factor. Therefore, the EC-IR (EEA 2009) assumed that the uncertainty of those countries are correlated which are using a Tier 1 methodology, while the countries using Tier 2 methodology were assumed to be

uncorrelated. This approach is not satisfactory, as it neglects that most calculations are conducted with several parameters so that the degree of "independence" varies with the amount of effort that has been put into the development of country-specific parameters. Hence, the analysis presented in this paper extends the approach of the EC-IR by quantifying a degree of independence between categories and countries on the basis of the Tier level as defined in the IPCC guidelines, but applying this definition not only to activity data or emission factors, but to each individual datum used in the calculation of the emissions.

The quantification of the degree of independence and its use for the combination of uncertainties was the main aim in developing the approach for aggregating the Tier levels; it has therefore been tailored to be an indicator of the influence of country-specific information on the emission estimates. It is thus a measure for the methodology used and does not automatically imply that a high "degree of independence" goes hand in hand with a high "quality level," as no evaluation of the data or the approach used has been performed. Nevertheless, an emission estimate that was derived with a higher Tier level should also be more accurate and less uncertain, and thus of a better quality, given the fact that all national GHG inventories considered here were subject to strict review by the UNFCCC Secretariat.

However, not all correlations between source categories could yet be considered. Important dependencies between the estimated amount of manure produced in a country and emissions of N_2O from various source categories "down the pipe" such as N_2O emissions from manure management, and direct and indirect N_2O following application of manure to soils, could not be quantified, as uncertainty values of N-excretion data are not reported by the countries. The large range of uncertainties reported for the N-input to agricultural soils (between 1% and 75%) suggests that these dependencies are inherently considered by some countries, but neglected by others. A common approach to handling these dependencies is important to increase the comparability of the uncertainty estimates across countries.

The comparison between the two approaches—error propagation with consideration of correlation versus the Monte Carlo analysis—confirms that both approaches yield very similar results (e.g., Monni et al. 2004; Ramiréz et al. 2006; Winiwarter 2007). Monte Carlo results are in most cases within 10% of the estimates obtained with the Tier 1 approach. Moreover, the aggregation of uncertainty estimates from country- to Europe-level yields only slight differences between the approaches, of a few percentage points. Differences, however, appear for emission estimates with high uncertainties such as N_2O emissions from agricultural soils (data now shown).

4.1 Activity data uncertainty is likely to be under-estimated

The final goal of the assessment was to obtain a realistic uncertainty estimate for the area covered by all 15 countries considered. However, this not only depends on an appropriate approach to combining the uncertainty estimates from the individual countries; it should also be checked whether these estimates themselves are comparable and/or realistic. For example, several countries use the same uncertainty value for the AD of CH_4 emissions from enteric fermentation and CH_4 and/or N_2O emissions from manure management (see Table 1). Taking the AD uncertainty in category 4A for describing the accuracy of the livestock population, the AD

uncertainty for category 4B(a) should, strictly speaking, include the uncertainties for the allocation of manure to climate regions and manure management systems. The AD uncertainty for N_2O emissions should include both the uncertainty for the allocation of manure to the manure management systems and the nitrogen excretion factors. For the latter, IPCC (2000) recommends an uncertainty range of ±50% if using default values, down to ±25% if country-specific information is used. In view of this recommendation, most countries appear to underestimate the uncertainty surrounding their estimate for the AD in category 4B(b).

The allocation of manure to the different manure management systems is a parameter which is highly controlled by the structure of the agricultural sector in a country (for example, increasing the average size and specialization of agricultural holdings in a country generally also implies that a higher percentage of the manure is managed in liquid systems) but also by environmental (e. g., NH_3 ceilings) and animal welfare policies (Leip 2005a; Petersen et al. 2007). This also makes this parameter highly dynamic for the time period since 1990, which can be observed for those countries that have estimated an increase/decrease in the importance of manure management systems by up to a factor of more than two (EEA 2009). However, even in these countries, statistics on the management systems for manure rarely exist and, having not usually been surveyed for the whole time period since 1990, are to a large degree based on expert judgment. Hence, in many cases the error made will vary significantly with time and it is unlikely that the distribution of manure management systems in a country is known with a higher accuracy than 20%. In Sweden, statistics on animal waste management systems have been available every 2 years since 1997, yet this country is among those with the highest estimate for the uncertainty for the AD in category 4B(a). We therefore consider it very likely that most countries are underestimating this uncertainty.

4.2 Correct allocation of sources of error to activity data and emission factors is important for estimating trend uncertainty

One explanation could be that these uncertainties are calculated into the estimate for the EF uncertainty (see Table 2). For category 4B(a), we find values ranging from 11% to over 100%. This should cover the uncertainties associated with the estimates of the content of volatile solid excretion, the maximum CH_4 producing capacity, and the methane conversion factor. The allocation of an uncertainty estimate to AD or EF remains important as long as standard rules are applied to evaluate correlation in time and therefore the trend uncertainty.

As a default, IPCC considers AD_s as uncorrelated in time and EF_s as correlated. The idea is straightforward: activity data are usually based on statistical surveys, and the error made in 1 year is independent of the error made in another year; thus no correlation in time is assumed. The uncertainty around emission factors is in most cases determined by scientific knowledge gaps (i.e., leading to a bias in unknown direction and quantity) or by high variability encountered in field measurements, as is the case, for example, for the N_2O emission factor for agricultural soils. However, the shift of the uncertainty surrounding, for example, the manure management system allocation (when this is not correlated in time) into the EF uncertainty estimates would lead to a significant underestimation of the trend uncertainty. A similar discussion also applies to the AD uncertainty estimates for N_2O emissions from

agricultural soils, where very large differences are observed (ranging from 1% to 102%, see Table 1).

4.3 Uncertainty of the emission factor for N_2O emissions from agricultural soils could be overestimated

One of the most important elements in today's uncertainty assessment of GHG inventories is the uncertainty of the emission factors used to estimate N_2O emissions from agricultural soils. The uncertainty range for direct N_2O emissions proposed in the IPCC (2000) is based on an assessment of Bouwman (1994) who analyzed a compilation of flux measurements and concluded that the best estimate ranges from 0.25% to 2.25% covering more than 90% of the published emission values (IPCC 1997). Even though the central value of the emission factor remained unchanged in the Good Practice Guidance, the uncertainty range was updated, accounting for the fact that measured N_2O emission factors have a skewed distribution and that the best estimate for the confidence limit ranges is set to one-fifth to five times the default emission factor of 1.25% (IPCC 2000). In the revised IPCC guidelines (2006), the N_2O emission factor for direct emissions was changed from 1.25% to 1% as a result of an analysis of the same, but updated, data by Bouwman et al. (2002) and Stehfest and Bouwman (2006). The confidence interval now ranges from one-third to three times the default emission factor. The reason for this high uncertainty for this source category is "natural variability, partitioning fractions, activity data, lack of coverage of measurements, spatial aggregation, and lack of information on specific on-farm practices. Additional uncertainty will be introduced in an inventory when emission measurements that are not representative of all conditions in a country are used" (IPCC 2006).

Natural variability of N_2O emissions is huge, both in time and space, and across scales from the micro-scale to the plot and regional scale. This means that good predictions of N_2O emissions are impossible unless the major factors influencing the fraction of the N-input which is transformed and emitted as N_2O are known and an appropriate model is available. For national GHG inventories, this natural variability is important only as far as the assembly of conditions encountered in the country does not compensate for it.

Several studies have shown that the IPCC emission factor seems to be fairly accurate if larger regions (countries or group of countries) are looked at. See, for example, Li et al. (2001), Leip et al. (2008), Del Grosso et al. (2005) and Butterbach-Bahl and Werner (2005) for model simulations in China, Europe, the United States, and Germany, respectively. This was also confirmed by the detailed analysis in Finland by Monni et al. (2007) who found that the yearly variation of N_2O emissions in Finland was relatively small (−104 to +171%) and suggested that climate-specific models should be developed that take soil properties into account (Freibauer 2003; Leip 2005b).

The analysis shows that N_2O emissions from agricultural soils are not only dominating the overall uncertainty of GHG emissions from agriculture, and in many cases also the overall uncertainty of GHG inventories, but they are also dominating the importance of correlation. This implies that particular attention has to be given to the construction of the GHG inventory for this source category with respect to correlations.

4.4 Improving methods to estimate emission to higher tiers could result in higher trend uncertainty

As discussed above, the concept of activity data and emissions factors as used in the IPCC guidelines gives room for interpretations, with consequences for the uncertainty assessment, particularly the trend assessment. This leads to a conceptual question/methodological problem: if a country goes from Tier 1-based approaches for quantifying emission factors to Tier 2 or even Tier 3-based approaches (i.e., calculated with process-based models); the assumption that these estimates are correlated in time will no longer hold. Thus, if the uncertainty of the emission factor (in one individual year) cannot be reduced under a certain threshold, the improvement of the methodology can lead to an increase in the trend uncertainty. This fact can have two consequences: (1) the country refrains from using higher Tier approaches until the models become sufficiently robust and are thoroughly validated so that the uncertainty of the emission factor falls below the threshold; (2) the models are used to improve the emission factor, but are not part of the inventory system. This could mean that the models run with a sufficiently large sample of weather conditions in order to derive one or more (regional) emission factors that are assumed to be valid for the whole time period (base year until end of commitment period). Both solutions have advantages. The first solution forces countries to check the models through a strict peer review for their own interest. The second solution would assure that emission trends remain controlled by anthropogenic drivers over a commitment period, thus giving a good ratio of benefit (in terms of incentives to implement mitigation measures) versus quality of the emission estimates.

4.5 Trend uncertainty is very important

The most important piece of information for the UA is the trend uncertainty. Therefore, the models should be tailored to suit that purpose (see also Monni et al. 2008). In practice, this means that a separation between AD and EF in the methodology proposed by IPCC (2000, 2006) should be replaced by a distinction of parameters which are correlated in time (the error thus being dominated by bias rather than by random error or inter-annual variability, as is the case for most default EF_s) and parameters which are not correlated in time (where random error or inter-annual variability dominate the uncertainty such as for most AD and other parameters derived with an accurate model).

5 Conclusion

We present a new methodology that estimates the uncertainty for the categories in the agriculture sector using information on the Tier level. In contrast to the approach suggested in the IPCC guidelines, that uses uncertainty estimates for activity data and emission factors for each source category, the method presented uses quantitative information from individual parameters used in the inventory calculations, in combination with a well defined procedure to aggregate, and comes

up with an—also quantitative—estimate for the Tier and finally the uncertainty. The methodology proposed is based on standard error propagation rules and additional rules for "Tier-level propagation." It considers possible correlation between source categories without the need for Monte Carlo calculations. The method allows a more transparent comparison of the uncertainty of GHG inventories across a group of countries and could thus be used to focus efforts to improve GHG emission estimates at a supra-national level. Not surprisingly, N_2O emissions from agricultural soils are found to be dominating the uncertainty of not only the agricultural sector, but also the overall GHG inventory for many countries. This suggests that further improvements should focus on programs to reduce the uncertainty of this source category. The analysis shows that differences in the uncertainty data are mainly based on different input data for the calculations, with a likely underestimation of the activity-data uncertainty and an overestimation of the uncertainty of the emission factors. Thus, the biggest challenge seems to be to put uncertainty estimates for AD and EF on a solid and common basis. Efforts should be invested in a harmonization of the concepts underlying the uncertainty assessment. At present, the combination of uncertainties is done with an improved Tier 1 that considers dependencies. The construction of a Monte Carlo model generally adds little accuracy to the uncertainty estimate. The method presented has been applied to the 15 member states that are part of the "European bubble." It could seamlessly be applied to estimate the uncertainty of the anthropogenic emissions at a larger scale, for example Annex I countries or all parties to the UNFCCC.

References

Bouwman AF (1994) Method to estimate direct nitrous oxide emissions from agricultural soils, report 773004004. National Institute of Public Health and Environmental Protection, Bilthoven

Bouwman AF, Boumans LJM, Batjes NH (2002) Emissions of N_2O and NO from fertilized fields: summary of available measurement data. Glob Biogeochem Cycles 16(4):1058

Butterbach-Bahl K, Werner C (2005) Upscaling of national N_2O emissions from soils with biogeochemical models—Germany. In: Leip A (ed) N_2O emissions from agriculture. Report on the expert meeting on "improving the quality for greenhouse gas emission inventories for category 4D," joint research centre, 21–22 October 2004, Ispra. Vol. EUR 21675. Office for Official Publication of the European Communities, Luxembourg, pp 138–134

Del Grosso SJ, Mosier AR, Parton WJ, Ojima DS (2005) DAYCENT model analysis of past and contemporary soil N_2O and net greenhouse gas flux for major crops in the USA. Soil Tillage Res 83(1):9–24

EEA (2007) Annual European community greenhouse gas inventory 1990–2005 and inventory report 2007. Submission to the UNFCCC Secretariat, European Environment Agency

EEA (2008) Annual European community greenhouse gas inventory 1990–2006 and inventory report 2008. Submission to the UNFCCC Secretariat, European Environment Agency

EEA (2009) Annual European community greenhouse gas inventory 1990–2007 and inventory report 2009. Submission to the UNFCCC Secretariat, European Environment Agency

Freibauer A (2003) Regionalised inventory of biogenic greenhouse gas emissions from European agriculture. Eur J Agron 19:135–160

Grassi G, Monni S, Federici S, Achard F, Mollicone D (2008) From uncertain data to credible numbers: applying the conservativeness principle to REDD. Environ Res Lett 3:035005

IPCC (1997) Houghton JT, Meira Filho LG, Lim B, Treanton K, Mamaty I, Bonduki Y, Griggs DJ, Callander BA (eds) Revised 1996 IPCC guidelines for national greenhouse gas inventories. IPCC/OECD/IEA, Paris

IPCC (2000) Penman J, Kruger D, Galbally I, Hiraishi T, Nyenzi B, Emmanuel S, Buendia L, Hoppaus R, Martinsen T, Meijer J, Miwa K, Tanabe K (eds) Good practice guidance and uncertainty management in national greenhouse gas inventories. IPCC/OECD/IEA/IGES, Hayama

IPCC (2006) Eggleston HS, Buendia L, Miwa K, Ngara T, Tanabe K (eds) 2006 IPCC guidelines for national greenhouse gas inventories, prepared by the national greenhouse gas inventories programme. IGES, Japan

Jonas M, Gusti M, Jeda W, Nahorski Z, Nilsson S (2007) Comparison of preparatory signal detection techniques for consideration in the (post-)Kyoto policy process. In: Proceedings of the 2nd international workshop on uncertainty in greenhouse gas inventories, international institute for applied systems analysis, Laxenburg, Austria, pp 107–134

Keizer Cd, Ramírez A, Sluijs JVd (2007) Uncertainty ranges and correlations assumed in tier 2 studies of several European countries. In: Proceedings of the 2nd international workshop on uncertainty in greenhouse gas inventories, international institute for applied systems analysis, Laxenburg, Austria, pp 35–39

Leip A (2005a) Greenhouse gas emissions from agriculture in Europe. In: Kuczynski T, Dämmgen U, Webb J, Myczko A (ed). Emissions from European agriculture. Wageningen Academic Publishers, The Netherlands, pp 35–49

Leip A (2005b) Executive summary and recommendations. In: Leip A (ed) N_2O emissions from agriculture. Report on the expert meeting on "improving the quality for greenhouse gas emission inventories for category 4D", joint research centre, 21–22 October 2004, Ispra, Vol. EUR 21675. Office for Official Publication of the European Communities, Luxembourg, pp 155–160

Leip A, Dämmgen U, Kuikman P, van Amstel AR (2005) The quality of European (EU15) greenhouse gas inventories from agriculture. Environ Sci 2(2–3):177–192

Leip A, Marchi G, Koeble R, Kempen M, Britz W, Li C (2008) Linking an economic model for European agriculture with a mechanistic model to estimate nitrogen and carbon losses from arable soils in Europe. Biogeosciences 5(1):73–94. Available at http://www.biogeosciences.net/5/73/2008/bg-5-73-2008.html

Li CS, Zhuang YH, Cao MQ, Crill P, Dai ZH, Frolking S, Moore B, III, Salas W, Song WZ, Wang XK (2001) Comparing a process-based agro-ecosystem model to the IPCC methodology for developing a national inventory of N_2O emissions from arable lands in China. Nutr Cycl Agroecosyst 60(1–3):159–175

Monni S, Syri S, Savolainen I (2004) Uncertainties in the Finnish greenhouse gas inventory. Environ Sci Policy 7:87–98

Monni S, Syri S, Pipatti R, Savolainen I (2007) Extension of EU emissions trading scheme to other sectors and gases: consequences for uncertainty of total tradable amount. Water Air Soil Pollut Focus 7(4):529–538

Monni S, Grassi G, Leip A (2008) Uncertainty estimation and management in AFOLU sector—background paper for the IPCC workshop on IPCC guidance on estimating emissions and removals from land uses, 13–15 May 2008. Helsinki, Finland

Nahorski Z, Horabik J, Jonas M (2007) Compliance and emissions trading under the Kyoto protocol: rules for uncertain inventories. Water Air Soil Pollut Focus 7(4):539–558

Olsthoorn X, Pielaat A (2003) Tier-2 uncertainty analysis of the Dutch greenhouse gas emissions 1999. Institute for Environmental Studies, Amsterdam

Passant NR (2003) Estimation of uncertainties in the national atmospheric emission inventory, AEAT/ENV/R/1039 Issue 1

Petersen SO, Sommer SG, Béline F, Burton C, Dach J, Dourmad JY, Leip A, Misselbrook T, Nicholson F, Poulsen HD, Provolo G, Sørensen P, Vinnerås B, Weiske A, Bernal M-P, Böhm R, Juhász C, Mihelic R (2007) Recycling of livestock manure in a whole-farm perspective. Livest Sci 112:180–191. doi:10.1016/j.livsci.2007.09.001

Ramiréz A, de Keizer C, van der Sluijs JP (2006) Monte Carlo analysis of uncertainties in the Netherlands greenhouse gas emission inventory for 1990–2004, NWS-E-2006-58. Department of Science, Technology and Society, Copernicus Institute for Sustainable Development and Innovation. Utrecht University, Utrecht, Netherlands

Rypdal K, Flugsrud K (2001) Sensitivity analysis as a tool for systematic reductions in greenhouse gas inventory uncertainties. Environ Sci Policy 4(2–3):117–135

Rypdal K, Winiwarter W (2001) Uncertainties in greenhouse gas emission inventories—evaluation, comparability and implications. Environ Sci Policy 4(2–3):107–116

Stehfest E, Bouwman AF (2006) N_2O and NO emissions from agricultural fields and soils under natural vegetation: summarizing available measurement data and modelling of global annual emissions. Nutr Cycl Agroecosyst V74(3):207–228

Winiwarter W (2007) Quantifying uncertainties of the Austrian greenhouse gas inventory. Final report to project no 1 S2.00116.0.0 contracted by Umweltbundesamt, Austrian Research Centres

Climatic Change (2010) 103:263–276
DOI 10.1007/s10584-010-9913-7

A statistical model for spatial inventory data: a case study of N_2O emissions in municipalities of southern Norway

Joanna Horabik · Zbigniew Nahorski

Received: 5 January 2009 / Accepted: 15 June 2010 / Published online: 14 July 2010

Abstract In this paper we apply a linear regression with spatial random effect to model geographically distributed emission inventory data. The study presented is on N_2O emission assessments for municipalities of southern Norway and on activities related to emissions (proxy data). Taking advantage of the spatial dimension of the emission process, the method proposed is intended to improve inventory extension beyond its earlier coverage. For this, the proxy data are used. The conditional autoregressive model is used to account for spatial correlation between municipalities. Parameter estimation is based on the maximum likelihood method and the optimal predictor is developed. The results indicate that inclusion of a spatial dependence component lead to improvement in both representation of the observed data set and prediction.

1 Introduction

This study focuses on a spatial aspect of inventories for atmospheric pollutants. The study tackles situations where emission inventory is to be expanded beyond its present coverage, where relevant activity data are missing. In the absence of measured data (activities) contributing to emissions, proxy data *about* activities can be used. The aim is to provide a tool to improve inventory developed with proxy data, by taking advantage of the spatial correlation of an emission process.

In the case of greenhouse gases, spatial resolution is usually not crucial for the emission effect as such. However, there are several situations where the spatial dimension is needed. In elaborated models of climate change, for instance, model HadAM3 of the British Meteorological Office (Pope et al. 2000), transport of

J. Horabik (✉) · Z. Nahorski
Systems Research Institute, Polish Academy of Sciences,
Newelska 6, 01-447 Warsaw, Poland
e-mail: Joanna.Horabik@ibspan.waw.pl

greenhouse gases is modeled in a similar way to other pollutants, e.g. (sulfur oxides) SO_x and NO_x. With growing resolution, for instance, in national models of this kind, the need for a finer inventory data mesh becomes important. The proposed method can be used for this purpose. Other examples include validations of regional inventories by field measurements or by inverse modeling in top-down approaches (Ciais et al. 2010; Rivier et al. 2010).

The topic of spatial heterogeneity of greenhouse gas (GHG) emissions and sequestration can be addressed in various ways. For instance, the spatial distribution of greenhouse gas emissions for Ukraine has been presented in Bun et al. (2010). Theloke et al. (2007) develop a methodology for spatial (and temporal) disaggregation of GHG annual country totals. Van Oijen and Thomson (2010) used a process-based forest model which accounts for spatial distribution of climate and soil; a Bayesian calibration was employed to quantify uncertainties.

When performing a statistical inference of spatial inventory data, we account for the fact that values at proximate locations tend to be more alike. This can be modeled by using spatial statistics. Moreover, as for each grid cell we have information on aggregated emission values, these are called areal data (also known as lattice data). A popular tool for incorporating this kind of spatial information is the conditional autoregressive (CAR) model proposed by Besag (1974). Unlike the geostatistical models with spatially continuous data, the CAR models have been developed to account for a situation where the set of all possible spatial locations is countable. The idea is to define a model in terms of the conditional distribution of the observation at one location given its values at other neighboring locations. Applications of the CAR model include, among others, mapping diseases in counties as well as modeling particulate matter air pollution in space and time (Kaiser et al. 2002).

The aim of the present paper is to demonstrate the usefulness of the CAR model to analyze data from spatially distributed emission inventories. With available proxy data related to emissions and an independent set of (modeled or measured) emission assessments, one can build a suitable regression model. Inclusion of a spatial component is intended to improve estimation results, compensating for the weaker explanatory power of proxy information. Based on the model, we develop the optimal predictor to extend the inventory.

The outline of the study is as follows. Section 2 presents an illustrative data set, including an initial non-spatial model. As a next step, the model is enriched with a spatial random effect. We use the conditional autoregressive structure to account for spatial correlation between neighboring areas (municipalities, in this case). The model is characterized in Section 3. It comprises model formulation, estimation and prediction. Results are presented in Section 4; we fit the spatial model and assess its predictive performance by means of a cross-validation procedure. Section 5 contains final remarks.

2 Preliminary explorations

Our illustration is provided with the data set on N_2O (nitrous oxide) emissions reported in 2006 for municipalities of southern Norway. In 2006 the main contributors to the country total N_2O emissions were as follows (National Inventory Report 2008). Forty-seven percent of emissions were attributed to agriculture, with agricultural soil

as the most important source. The second most important source was production of nitric acid in two plants, which accounted for 37%. Nitric acid is used in the production of fertilizer. Emissions from road traffic amounted to 4%. The remaining 12% included emissions from, for instance, manure management and waste-water handling.

The considered map of southern Norway covers 259 municipalities out of 431 in the whole of Norway. The data come from the StatBank (available at http://www.ssb.no) in Statistics Norway. According to the StatBank identification system, the area of our interest covers the municipalities numbered 0101 to 1449. One of the aforementioned nitric acid plants is operating in Porsgrunn municipality, which is a relatively small municipality located near the southern coast of the area considered, see also Perez-Ramirez (2007). Emissions from this kind of point source are usually reported and there is no need to model them. In our analysis we do not consider emissions from this source.

The municipalities have been chosen by StatBank as the smallest unit for geographical distribution of emissions. Details on the Norwegian emission model can be found in Sandmo (2009).

Of the statistics available in StatBank at the municipal level, we consider the following variables that might explain spatial distribution of N_2O emissions. Figures on livestock and detailed statistics on agricultural usage are the ones that are the most relevant to the N_2O emissions. However, these data sets contained a large number of missing values, and as such were of poor quality. Emissions from agriculture can generally be characterized with data on agricultural area in use as well as with data on persons employed in agriculture. Regarding emissions from stationary and mobile sources, data on population can be of use. Besides the Porsgrunn plant, emissions from fertilizer production occurs in a small number of municipalities. There is a lack of statistics on relevant production, financial data or employment at the municipal level (Statistics Norway personal communication).

To determine the independence of the above-mentioned variables from the emission data the inventory preparers from Statistics Norway were consulted (personal communication). We found out that for the municipal emission assessments they used figures from the agricultural statistics that are both more detailed and more comprehensive than those described above. In addition, a model that estimates emissions of ammonia from agriculture were used, as were figures on energy use.

Let us denote[1]

y_i N_2O emissions (tonnes) (Table 03535), $y = (y_1, \ldots, y_n)^T$
$x_{i,1}$ agricultural area in use (decare) (Table 06462), $x_1 = (x_{1,1}, \ldots, x_{n,1})^T$
$x_{i,2}$ persons employed in agriculture (Table 03324), $x_2 = (x_{1,2}, \ldots, x_{n,2})^T$
$x_{i,3}$ population (Table 05231), $x_3 = (x_{1,3}, \ldots, x_{n,3})^T$.

Figure 1 presents a scatterplot matrix for these data. We note that the relationship between y and x_1 is more pronounced than between y and x_2, and there is a weaker relation between y and x_3. Our aim is to explore opportunities for improvements of

[1]In brackets we report a number of the table containing the data set available from the StatBank Web site as of October 2009.

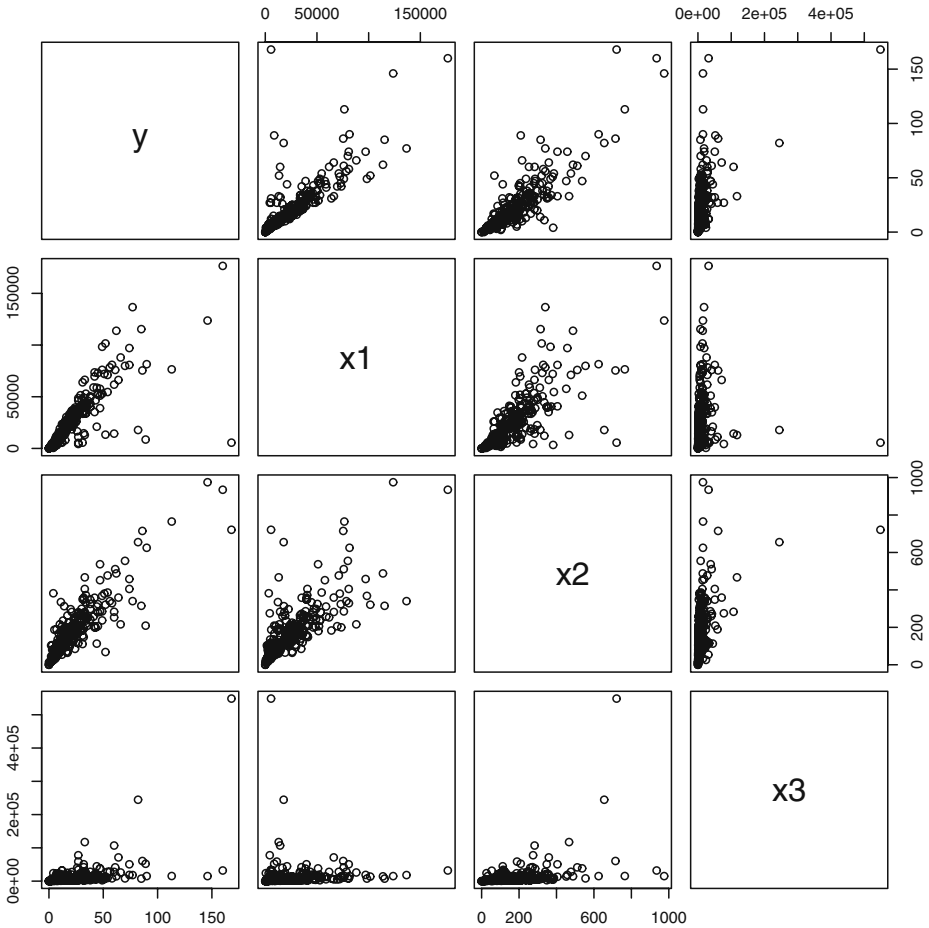

Fig. 1 Scatterplot matrix showing plausible relations between data on: N_2O emissions (y), agricultural area (x_1), persons employed in agriculture (x_2) and population (x_3) in municipalities

inventory prepared in the absence of information on agricultural area (x_1) activity, but using data on persons employed in agriculture (x_2) as its proxy. Therefore we define a multiple regression model

$$Y_i = \beta_0 + \beta_2 x_{i,2} + \beta_3 x_{i,3} + \varepsilon_i, \tag{1}$$

where ε_i are independent random variables following normal distribution with mean equal 0 and variance σ^2 and $i = 1, \ldots, 259$ indexes municipalities. In the sequel we compare results of the above model to the one with variable x_1 instead of x_2. We distinguish between an observation (y_i) and a random variable (Y_i) generating this observation. In the model (1) regression coefficients of the covariates x_2 and x_3 have p-values equal 2e–16 and 2.07e–09, respectively. The model explains 79% of variability in N_2O emissions—coefficient of determination is $R^2 = 0.79$.

Residuals of the model, that is, observations minus fitted values, are presented in Fig. 2: a residual plot (a) and a map (b). From a residual map we can identify the cluster of municipalities with underestimated emissions (yielding positive residuals) in the eastern part; moreover municipalities with highly overestimated emissions (yielding negative residuals) are located in the western region. In Fig. 2(a) residuals are plotted against municipality numbers. As municipalities are not randomly numbered and neighboring areas usually have close identification numbers, we again note that there are regions with underestimated and overestimated emissions.

We check spatial correlation in the residuals using the Moran's I statistic

$$I = \frac{n}{\sum_i \sum_j w_{ij}} \frac{\sum_i \sum_j w_{ij}(\varepsilon_i - \bar{\varepsilon})(\varepsilon_j - \bar{\varepsilon})}{\sum_i (\varepsilon_i - \bar{\varepsilon})^2},$$

where ε_i—a residual of linear regression in the area i, $\bar{\varepsilon}$—the mean of residuals, w_{ij}—the adjacency weights ($w_{ij} = 1$ if j is a neighbor of i and 0 otherwise, also $w_{ii} = 0$). We consider two municipalities as neighbors if they share common border. Moran's I can be recognized as a modification of the correlation coefficient. It accounts for correlation between residuals in area i and nearby locations and takes values approximately on the interval $[-1, 1]$. Higher (positive) values of I suggest stronger positive spatial association. Under the null hypothesis, where ε_i are independent and identically distributed, I is asymptotically normally distributed, with the mean and variance known (see e.g., Banerjee et al. 2004).

In the case of the residuals from model (1) with covariates on x_2 and x_3 Moran's I is equal to 0.2466. The corresponding test statistic z (Moran's I standardized with the asymptotic mean and variance) is equal to $z = 6.6953$ while $z_{cr} = 2.33$ at the significance level $\alpha = 0.01$. Thus we reject the null hypothesis of no spatial correlation of errors. Moran's I is, however, recommended as an exploratory information on spatial association, rather than a measure of spatial significance (Banerjee et al. 2004).

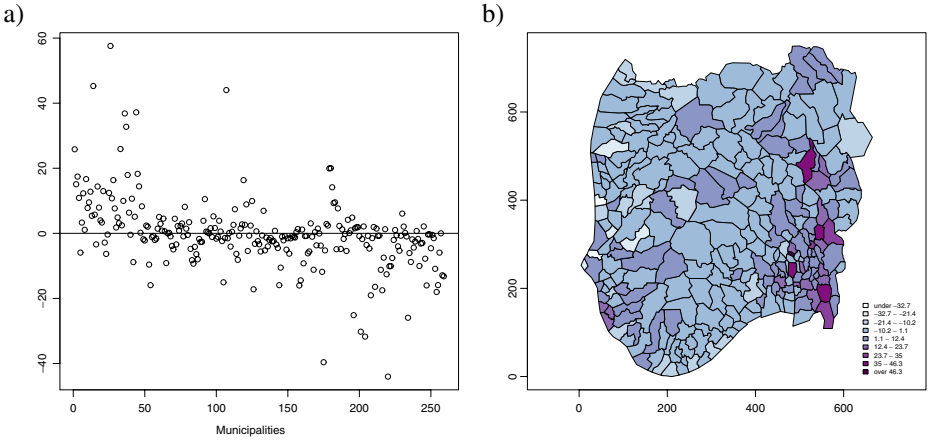

Fig. 2 Residuals from the linear model with covariates on persons employed in agriculture (x_2) and population (x_3)

3 Modeling spatial correlation

In this section we develop a model to characterize the spatial distribution of N_2O emissions in municipalities. Further, we provide details on the model estimation, prediction, and an applied cross-validation procedure. The calculations were accomplished using the statistical software `R` (R Development Core Team 2008).

3.1 The model

Following the notation already introduced, let Y_i denote a stochastic variable associated with the observed emission (y_i) defined at each spatial location i for $i = 1, \ldots, n$. It is assumed that the random variables Y_i for $i = 1, \ldots, n$ follow normal distribution with the mean μ_i and common variance σ^2

$$Y_i|\mu_i, \sigma^2 \sim \mathcal{N}\left(\mu_i, \sigma^2\right). \tag{2}$$

The collection of all Y_i is denoted as $\boldsymbol{Y} = (Y_1, \ldots, Y_n)^T$. Given the values of μ_i and σ^2, the stochastic variables Y_i are assumed independent, thus the joint distribution of the process $\boldsymbol{Y}$ conditional on the mean process $\boldsymbol{\mu} = (\mu_1, \ldots, \mu_n)^T$ is

$$\boldsymbol{Y}|\boldsymbol{\mu} \sim \mathcal{N}\left(\boldsymbol{\mu}, \sigma^2 \boldsymbol{I}_n\right), \tag{3}$$

where $\boldsymbol{I}_n$ is an identity $n \times n$ matrix.

Our approach to modeling the mean μ_i expresses the observation that available covariates explain part of the spatial pattern in observations, and the remaining part is captured through a regional clustering. To this extent we make use of the conditional autoregressive model. The CAR structure is given through specification of the full conditional distribution functions for $i = 1, \ldots, n$

$$\mu_i|\mu_{j,j\neq i} \sim \mathcal{N}\left(\boldsymbol{x}_i^T\boldsymbol{\beta} + \rho \sum_{j\neq i} \frac{w_{ij}}{w_{i+}}\left(\mu_j - \boldsymbol{x}_j^T\boldsymbol{\beta}\right), \frac{\tau^2}{w_{i+}}\right) \tag{4}$$

with $w_{i+} = \sum_j w_{ij}$ being the number of neighbors of area i; $\boldsymbol{x}_i$ is a vector containing 1 for the intercept β_0 and k explanatory covariates of area i, for example population; $\boldsymbol{\beta} = (\beta_0, \beta_1, \ldots, \beta_k)^T$ is a vector of regression coefficients and τ^2 is a variance parameter. The variance is inversely proportional to the number of neighbors w_{i+}. The second summand of the conditional expected value of μ_i (a remainder) is proportional to the average value of remainders $\mu_j - \boldsymbol{x}_j^T\boldsymbol{\beta}$ for those areas j which are the neighbors of the site i (that is $w_{ij} = 1$). The proportion is calibrated with parameter ρ. The parameter ρ is introduced into (4) in order to remedy singularity of the covariance function in the joint distribution of $\boldsymbol{\mu}$; for more details see for example Banerjee et al. (2004).

Given (4), the joint probability distribution of the process $\boldsymbol{\mu}$ is the following (Banerjee et al. 2004; Cressie 1993)

$$\boldsymbol{\mu} \sim \mathcal{N}\left(\boldsymbol{X}\boldsymbol{\beta}, \tau^2\left(\boldsymbol{D} - \rho\boldsymbol{W}\right)^{-1}\right), \tag{5}$$

where $\boldsymbol{X}$ is the (design) matrix containing transposed vectors $\boldsymbol{x}_i$, $i = 1, \ldots, n$

$$\boldsymbol{X} = \begin{bmatrix} 1 & x_{11} & \ldots & x_{1k} \\ 1 & x_{21} & \ldots & x_{2k} \\ \vdots & \vdots & & \vdots \\ 1 & x_{n1} & \ldots & x_{nk} \end{bmatrix};$$

$\boldsymbol{D}$ is an $n \times n$ diagonal matrix with w_{i+} on the diagonal; and $\boldsymbol{W}$ is an $n \times n$ matrix with adjacency weights w_{ij}.

3.2 Estimation

Estimation of unknown parameters $\boldsymbol{\beta}, \rho, \sigma^2$ and τ^2 is based on the maximum likelihood approach. From (3) and (5) we obtain the joint unconditional distribution of $\boldsymbol{Y}$

$$\boldsymbol{Y} \sim \mathcal{N}\left(\boldsymbol{X\beta}, \boldsymbol{M} + \boldsymbol{N}\right), \tag{6}$$

where for notational simplicity $\boldsymbol{M} = \sigma^2 \boldsymbol{I}_n$ and $\boldsymbol{N} = \tau^2 \left(\boldsymbol{D} - \rho \boldsymbol{W}\right)^{-1}$ were introduced. To see this let us write (3) as $\boldsymbol{Y} = \boldsymbol{\mu} + \boldsymbol{v}$, where $\boldsymbol{v} \sim \mathcal{N}\left(\boldsymbol{0}, \boldsymbol{M}\right)$ and (5) in the form of $\boldsymbol{\mu} = \boldsymbol{X\beta} + \boldsymbol{v}$, where $\boldsymbol{v} \sim \mathcal{N}\left(\boldsymbol{0}, \boldsymbol{N}\right)$. Together we obtain $\boldsymbol{Y} = \boldsymbol{X\beta} + \boldsymbol{v} + \boldsymbol{v}$, which is a sum of a constant and two independent normal random variables with the distribution $\boldsymbol{v} + \boldsymbol{v} \sim \mathcal{N}\left(\boldsymbol{0}, \boldsymbol{M} + \boldsymbol{N}\right)$. Compare also the lemma of Lindley and Smith (1972).

The log likelihood associated with (6) is, see, for example, Papoulis and Pillai (2002)

$$\begin{aligned} \mathcal{L}\left(\boldsymbol{\beta}, \rho, \sigma^2, \tau^2\right) = &- \frac{1}{2} \log\left(\left|\boldsymbol{M} + \boldsymbol{N}\right|\right) - \frac{n}{2} \log\left(2\pi\right) \\ &- \frac{1}{2} \left(\boldsymbol{y} - \boldsymbol{X\beta}\right)^T \left(\boldsymbol{M} + \boldsymbol{N}\right)^{-1} \left(\boldsymbol{y} - \boldsymbol{X\beta}\right), \end{aligned} \tag{7}$$

where $|\cdot|$ denotes the determinant and $\boldsymbol{y}$ is a vector containing the observations y_i, $i = 1, \ldots, n$. With fixed ρ, σ^2 and τ^2, the log likelihood (7) is maximized for

$$\hat{\boldsymbol{\beta}}\left(\rho, \sigma^2, \tau^2\right) = \left(\boldsymbol{X}^T \left(\boldsymbol{M} + \boldsymbol{N}\right) \boldsymbol{X}\right)^{-1} \boldsymbol{X}^T \left(\boldsymbol{M} + \boldsymbol{N}\right) \boldsymbol{y}, \tag{8}$$

which substituted back into (7) provides the profile log likelihood

$$\begin{aligned} \mathcal{L}\left(\rho, \sigma^2, \tau^2\right) = &- \frac{1}{2} \log\left(\left|\boldsymbol{M} + \boldsymbol{N}\right|\right) - \frac{n}{2} \log\left(2\pi\right) \\ &- \frac{1}{2} \left(\boldsymbol{y} - \boldsymbol{X} \left(\boldsymbol{X}^T \left(\boldsymbol{M} + \boldsymbol{N}\right) \boldsymbol{X}\right)^{-1} \boldsymbol{X}^T \left(\boldsymbol{M} + \boldsymbol{N}\right) \boldsymbol{y}\right)^T \\ &\times \left(\boldsymbol{M} + \boldsymbol{N}\right)^{-1} \\ &\times \left(\boldsymbol{y} - \boldsymbol{X} \left(\boldsymbol{X}^T \left(\boldsymbol{M} + \boldsymbol{N}\right) \boldsymbol{X}\right)^{-1} \boldsymbol{X}^T \left(\boldsymbol{M} + \boldsymbol{N}\right) \boldsymbol{y}\right). \end{aligned} \tag{9}$$

Further maximization of $\mathcal{L}\left(\rho, \sigma^2, \tau^2\right)$ is performed numerically. One also needs to ensure that the matrix $\boldsymbol{D} - \rho \boldsymbol{W}$ is non-singular. This is guaranteed if $\lambda_1^{-1} < \rho < \lambda_n^{-1}$,

where $\lambda_1 < \ldots < \lambda_n, \lambda_i \neq 0$, $i = 1, \ldots, n$ are the eigenvalues of $\boldsymbol{D}^{-1/2}\boldsymbol{W}\boldsymbol{D}^{-1/2}$, see Banerjee et al. (2004) and Cressie (1993). Our optimization procedure takes this constraint into account.

3.3 Prediction

Consider a random variable Y_0 associated with emissions at an unobserved location and let μ_0 denote its mean value. We assume that the distribution of $Y_0|\mu_0$ is of the form (2) and the distribution of $\mu_0|\boldsymbol{\mu}$ is of the form (4). The predictor of the observation Y_0, that is optimal in terms of minimum mean squared error, is given by $E(Y_0|\boldsymbol{y})$. It should be stressed that knowledge on covariates $\boldsymbol{x}_0$ is required to calculate the predictor in the location considered.

To begin with, we derive the conditional distribution of $\boldsymbol{\mu}|\boldsymbol{y}$ based on (3), (5) and (6) using the Bayes rules

$$\boldsymbol{\mu}|\boldsymbol{y} \sim \mathcal{N}(\boldsymbol{BC}, \boldsymbol{B}) \tag{10}$$

with $\boldsymbol{B} = \left(\boldsymbol{M}^{-1} + \boldsymbol{N}^{-1}\right)^{-1}$ and $\boldsymbol{C} = \boldsymbol{M}^{-1}\boldsymbol{y} + \boldsymbol{N}^{-1}\boldsymbol{X}\boldsymbol{\beta}$.

Next we develop the predictor $E(Y_0|\boldsymbol{y})$, see also Kaiser et al. (2002). In deriving the formula we will make use of the following property of the conditional expected value: $Y_0 = E(Y_0|\mu_0)$ and analogously $\mu_0 = E(\mu_0|\boldsymbol{\mu})$. We have

$$\begin{aligned} E(Y_0|\boldsymbol{y}) &= E\left[E\left(Y_0|\mu_0\right)|\boldsymbol{y}\right] = E\left[\mu_0|\boldsymbol{y}\right] = E\left[E\left(\mu_0|\boldsymbol{\mu}\right)|\boldsymbol{y}\right] \\ &= E\left[\boldsymbol{x}_0^T\boldsymbol{\beta} + \rho\sum_j \frac{w_{0j}}{w_{0+}}\left(\mu_j - \boldsymbol{x}_j^T\boldsymbol{\beta}\right)|\boldsymbol{y}\right] \\ &= \boldsymbol{x}_0^T\boldsymbol{\beta} - \rho\sum_j \frac{w_{0j}}{w_{0+}}\boldsymbol{x}_j^T\boldsymbol{\beta} + E\left[\rho\sum_j \frac{w_{0j}}{w_{0+}}\mu_j|\boldsymbol{y}\right]. \end{aligned} \tag{11}$$

We use the expression (10) to calculate the rightmost expectation in the last equality of (11) and denoting the jth element of the vector $\boldsymbol{BC}$ with l_j, we get the predictor

$$E(Y_0|\boldsymbol{y}) = \boldsymbol{x}_0^T\boldsymbol{\beta} + \rho\sum_j \frac{w_{0j}}{w_{0+}}\left(l_j - \boldsymbol{x}_j^T\boldsymbol{\beta}\right). \tag{12}$$

In order to assess the quality of the prediction we perform a leave-one-out cross-validation procedure. The idea is to fit a model to a data set from which a single observation was dropped. This observation is considered as unobserved and its value is calculated using the predictor (12). The operation is repeated for each observation (n times). The difference between the observation y_i and the prediction y_i^*, $d_i = y_i - y_i^*$, constitutes a base to quantify prediction error. We summarize it forming the mean squared error

$$\text{mse} = \frac{1}{n}\sum_i \left(y_i - y_i^*\right)^2, \tag{13}$$

Table 1 Model comparison for the linear regressions (LM) and the spatial model (CAR)

Model	$-\mathcal{L}$	AIC
LM(x_2, x_3)	1,622.27	3,252.55
CAR(x_2, x_3)	1,552.32	3,116.65
LM(x_1, x_3)	1,281.98	2,573.97

which should be as low as possible, indicating how well a model predicts data. We report also the minimum and maximum value of d_i, average values of the absolute differences $|d_i|$, and the sample correlation coefficient r between the predicted and observed values.

4 Results

The spatial CAR model has been applied to the emission data. In addition, we estimate the linear regression (1) denoted LM(x_2, x_3), as well as the model LM(x_1, x_3) with the variable on agricultural area (x_1) instead of the number of people employed in agriculture (x_2).

The results are compared using the Akaike Information Criterion (AIC), which is a suitable tool for comparison of models estimated with the maximum likelihood method. The AIC is calculated as a sum of twice the negative log likelihood $\mathcal{L}(\theta)$ and twice the number of parameters p:

$$AIC = -2\mathcal{L}(\theta) + 2p.$$

The term $-2\mathcal{L}(\theta)$ measures how well the model fits the data; the larger this value, the worse the fit. Model complexity is summarized by the number of parameters p. The idea of the AIC is to favor a model with a good fit and to penalize for the number of parameters. Thus models with smaller AIC are preferred to models with larger AIC.

For the estimated models both the negative log likelihood and AIC are displayed in Table 1. The applied spatial structure improved the results considerably. The negative log likelihood $-\mathcal{L}$ decreased from 1,622 for the linear regression LM(x_2, x_3) to 1,552 for the spatial model with the same set of covariates CAR(x_2, x_3). The spatial model includes only two parameters (ρ and τ^2) more than its linear regression counterpart. In terms of the AIC criterion the spatially enriched model is preferred (has a lower AIC), since the decrease in the negative log likelihood overwhelms increased model complexity.

To put this improvement into a perspective, we present results for the non-spatial model LM(x_1, x_3) with the variable on agricultural area. Spatially explicit model CAR(x_2, x_3) with the proxy is still much worse than the model LM(x_1, x_3). The latter has $-\mathcal{L} = 1{,}282$ and AIC $= 2{,}574$. In terms of the negative log likelihood $-\mathcal{L}$, the gain achieved by taking into account a spatial correlation can be summarized as a

Table 2 Estimated parameter values

Model	β_0	β_1	β_2	β_3	σ^2	ρ	τ^2
LM(x_2, x_3)	−1.882	–	0.129	0.00012	15.494	–	–
CAR(x_2, x_3)	−1.965	–	0.128	0.00013	15.127	0.9984	0.6186
LM(x_1, x_3)	0.177	0.0007	–	0.00031	15.494	–	–

Table 3 Cross-validation results

Model	mse	avg($\lvert d \rvert$)	min(d)	max(d)	r
LM(x_2, x_3)	134.67	7.06	−44.63	58.03	0.877
CAR(x_2, x_3)	115.38	6.87	−41.57	46.60	0.896

20.5% improvement over the initial model. Parameter estimates for the models are reported in Table 2.

We regard the method as a tool that can help to extend spatial coverage of inventories in a situation where the inventories are based on proxy data. The motivation behind it is that proxy data are more frequently available than measured data. This task calls for prediction. To evaluate the predictive performance of the method, we use a cross-validation technique. The procedure was applied to the spatial model and its non-spatial counterpart with the same set of proxy variables, see Table 3. We note again that observation y_i is not accounted for in the construction of the predictor y_i^*, thus a model is re-estimated for each observation separately. In the case of the spatial model, it is a time-consuming procedure.

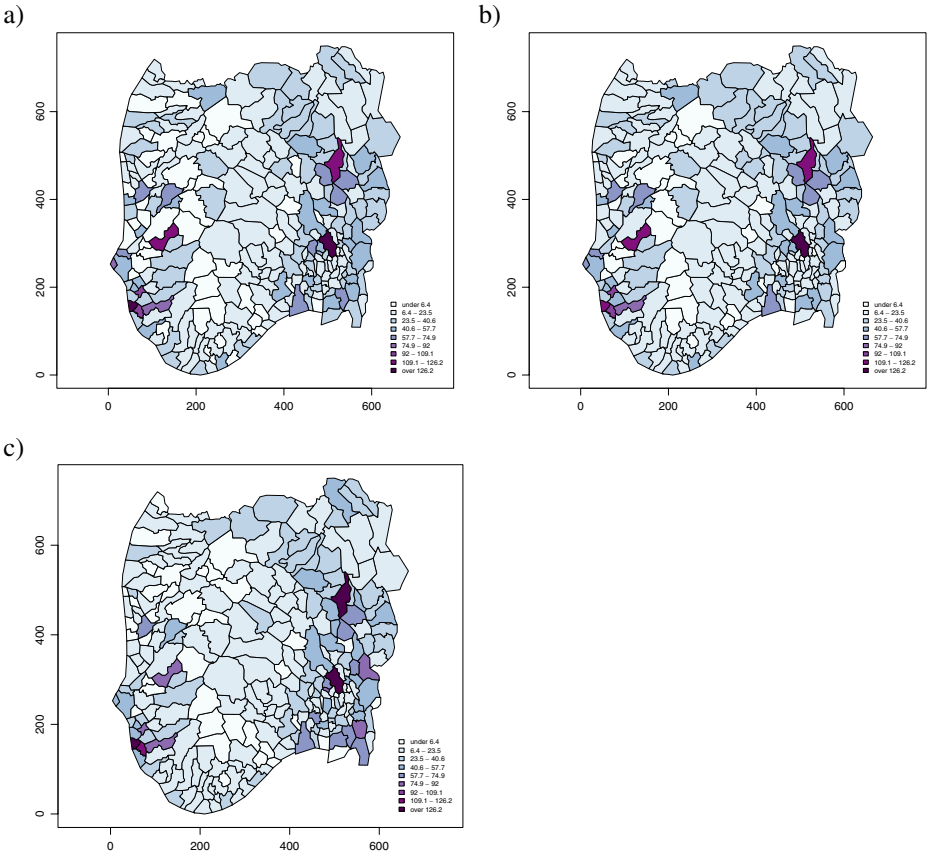

Fig. 3 Predicted values in the model CAR(x_2, x_3) (**a**); predicted values in the linear regression LM(x_2, x_3) (**b**); observed emission (**c**)

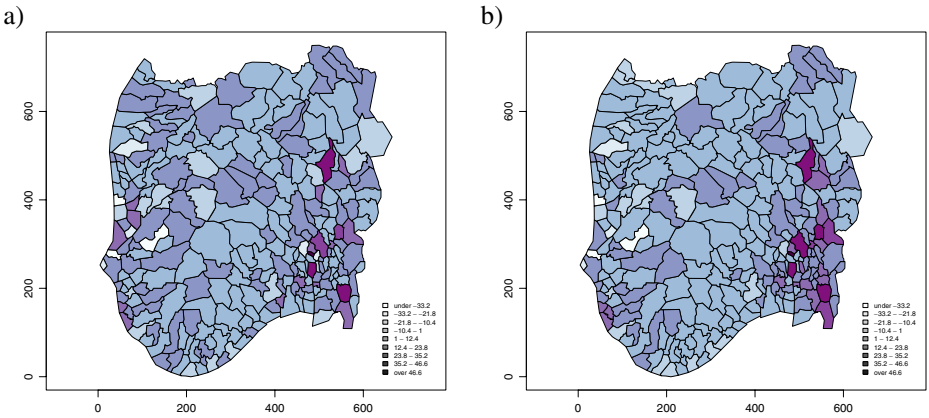

Fig. 4 Residuals from cross-validated values for the model CAR(x_2, x_3) (**a**); and for the model LM(x_2, x_3) (**b**)

Cross-validation results are also displayed in Fig. 3 as predicted values for the respective models, along with the observations. It can be noted that the spatial model predicts the original data slightly better. However, we suspect that some of the differences might have been masked because the mapped values are binned into nine classes. Therefore, in Fig. 4 we present the model residuals d_i. Here we can clearly see that for the linear regression in the eastern part there is a cluster of municipalities with highly underestimated values (positive residuals). Application of the spatial random effect to some extent remedied this deficiency.

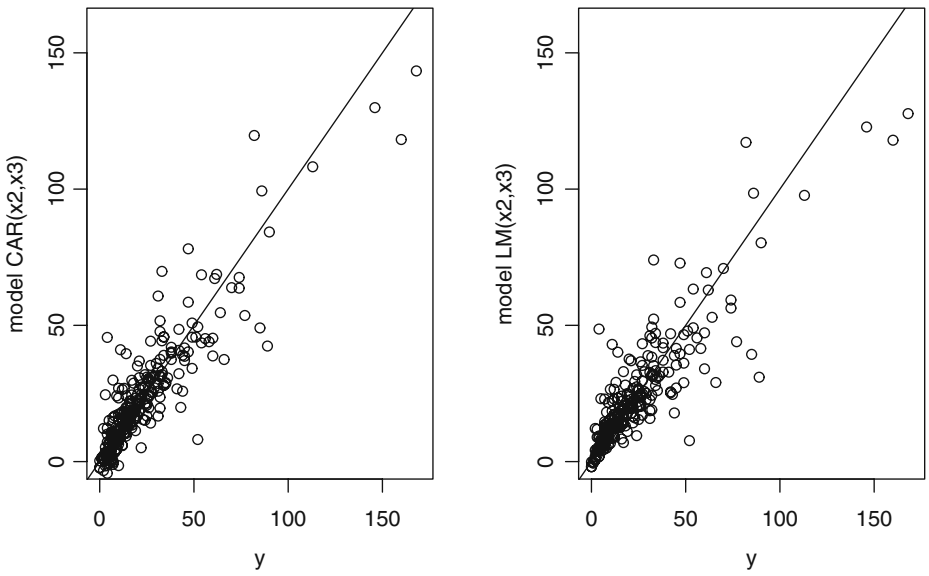

Fig. 5 Predicted values vs. observed values for the model CAR(x_2, x_3) (**a**); and for the model LM(x_2, x_3) (**b**)

Values for analysis of prediction error for the two models are given in Table 3. The spatial model showed noticeable improvement over the linear regression. In particular, the mean squared error was reduced by about 15% from 135 to 115. A smaller reduction is noted for the average in absolute residuals. With inclusion of spatial dependence we obtain higher minimum and lower maximum residuals, which yields a reduction of over 14% in a spread of differences d_i.

In Fig. 5 predicted values y_i^* are plotted against the observations y_i for the two models. An overall impression is that the spatial model provides better predictions. This is confirmed by a higher value of sample correlation coefficient r, see Table 3. It should be noted, however, that small value observations (i.e., below ca 10 tonnes) are predicted more accurately with a linear regression approach. This observation is related to a general feature of the conditional autoregressive models, which tend to over-smooth data.

5 Concluding remarks

The goal of this study was to demonstrate that emission inventories may be improved by making efficient use of spatial information. We consider a case study with a geographically distributed inventory for N_2O. Let us suppose that we wish to spatially expand the inventory beyond the present coverage. We have some proxy data available both for the present inventory area and in a predictive capacity. The proxy data is, however, of limited adequacy.

The idea is to take advantage of potentially existing spatial correlation to improve the outcome. First, the task includes model estimation based on available measured/modeled inventory. Second, an appropriately constructed predictor is used to produce an emission assessment from the proxy information. To model spatial dependencies we make use of the conditional autoregressive structure, which was introduced into a linear regression as a random effect.

The results indicate that inclusion of a spatial dependence component lead to improvement in both the representation of the observed data set and the prediction. Specifically, the introduction of spatial random effect into a model with less adequate covariate (on number of people employed in agriculture) improved estimation results by over 20% of what would have been obtained using more relevant activity data (on agricultural area). In terms of prediction, a 15% reduction in the mean squared error was achieved.

The presented application of the method seems to be particularly suitable to N_2O emissions, as N_2O emission pathways include, among other things, agriculture and soil emissions. These factors tend to be spatially correlated and have quite often been modeled with spatial tools, for example Sigua and Hudnall (2008). Based on a study of 15 national greenhouse gas inventories, Leip (2010) note that N_2O emissions from agricultural soils dominate the uncertainty of not only the agricultural sector, but also the overall greenhouse gas inventory for many countries.

Accounting for spatial scale of inventories may have one more aspect. One may compare estimation results for alternative proxy data used and try to conclude on their relevance. This kind of analysis has been already performed in some studies, see Winiwarter et al. (2003). In that study two sets of data on NOx (nitrogen oxides) emissions over the same spatial grid for the Greater Athens, Greece, were compared.

The authors examine significance of area, line, and point emission sources on the basis of statistical exploratory tools and a visual comparison of maps. In the case study presented here, we believe the problem is more of data availability than lack of knowledge on the relevant covariates. Therefore, our focus remains on prediction.

The applied spatial model proved to be especially successful when dealing with underestimated emission assessments. Further developments of the method would be required to deal with the problem of over-smoothed values for low emission observations.

Acknowledgements We are grateful to Ketil Flugsrud, Trond Sandmo and Kathrine Loe Hansen from Statistics Norway, Division of Environmental Statistics for comprehensive information on the inventory data. In addition, we are thankful to two anonymous reviewers for their valuable comments that considerably helped us to shape the final version of the manuscript.

References

Banerjee S, Carlin BP, Gelfand AE (2004) Hierarchical modeling and analysis for spatial data. Chapman and Hall, London

Besag J (1974) Spatial interactions and the statistical analysis of lattice systems (with discussion). J R Stat Soc Ser B 36:192–236

Bun R, Hamal K, Gusti M, Bun A (2010) Spatial GHG inventory at the regional level: Accounting for uncertainty. Clim Change. doi:10.1007/s10584-010-9907-5

Ciais P, Rayner P, Chevallier F, Bousquet P, Logan M, Peylin P, Ramonet M (2010) Atmospheric inversions for estimating CO_2 fluxes: methods and perspectives. Clim Change. doi:10.1007/s10584-010-9909-3

Cressie N (1993) Statistics for spatial data, revised edn. Wiley

Kaiser MS, Daniels MJ, Furakawa K, Dixon P (2002) Analysis of particulate matter air pollution using Markov random field models of spatial dependence. Environmetrics 13:615–628

Leip A (2010) The uncertainty of the uncertainty... On the example of the quality assessment of the greenhouse gas inventory for agriculture in Europe. Clim Change. doi:10.1007/s10584-010-9915-5

Lindley DV, Smith AFM (1972) Bayes estimates for the linear model. J R Stat Soc 34(B):1–41

National Inventory Report—Norway (2008) Greenhouse gas emissions 1990–2006 reported according to the UNFCCC reporting guidelines. Available at http://www.sft.no/publikasjoner/2416/ta2416.pdf

Papoulis A, Pillai SU (2002) Probablility, random variables and stochastic processes, 4th edn. McGraw Hill

Perez-Ramirez J (2006) Prospects of N_2O emission regulations in the European fertilizer industry. Appl Catal, B Environ 70:31–35

Pope VD, Gallani ML, Rowntree PR, Stratton RA (2000) The impact of new physical parametrizations in the Hadley Centre climate model: HadAM3. Clim Dyn 16:123–146

R Development Core Team (2008) R: a language and environment for statistical computing. R Foundation for Statistical Computing, Vienna, Austria. Available at www.r-project.org. ISBN 3-900051-07-0

Rivier L, Peylin Ph, Ciais Ph, Gloor M, Rödenbeck C, Geels C, Karstens U, Bousquet Ph, Brandt J, Heimann M (2010) European CO_2 fluxes from atmospheric inversions using regional and global transport models. Clim Change. doi:10.1007/s10584-010-9908-4

Sandmo T (ed) (2009) The Norwegian emission inventory 2009. Documentation of methodologies for estimating emissions of greenhouse gases and long-range transboundary air pollutants. Statistics Norway, Report 2009/10

Sigua GC, Hudnall WH (2008) Kriging analysis of soil properties. J Soils Sediments 8:192–202

Theloke J, Pfeiffer H, Pregger T, Scholz Y, Koble R, Kummer U, Nicklass D, Thiruchittampalam B, Friedrich R (2007) Development of a methodology for temporal and spatial resolution of

greenhouse gas emission inventories for validation. In: Proceedings of the 2nd international workshop on uncertainty in greenhouse gas inventories, IIASA 27–28.09.2007. Available at http://www.ibspan.waw.pl/ghg2007/GHG-total.pdf

Van Oijen M, Thomson A (2010) Towards Bayesian uncertainty quantification for forestry models used in the U.K. GHG inventory for LULUCF. Clim Change. doi:10.1007/s10584-010-9917-3

Winiwarter W, Dore Ch, Hayman G et al (2003) Methods for comparing gridded inventories of atmospheric emissions—application for Milan province, Italy and the greater Athens Area, Greece. Sci Total Environ 303:231–243

Climatic Change (2010) 103:277–289
DOI 10.1007/s10584-010-9910-x

Carbon emission trading and carbon taxes under uncertainties

Tatiana Ermolieva · Yuri Ermoliev · Günther Fischer · Matthias Jonas · Marek Makowski · Fabian Wagner

Received: 5 January 2009 / Accepted: 15 June 2010 / Published online: 16 July 2010

Abstract The idea of market-based carbon emission trading and carbon taxes is gaining in popularity as a global climate change policy instrument. However, these mechanisms might not necessarily have a positive outcome unless their value reflects socioeconomic and environmental impacts and regulations. Moreover, the fact that they have various inherent exogenous and endogenous uncertainties raises serious concerns about their ability to reduce emissions in a cost-effective way. This paper aims to introduce a simple stochastic model that allows the robustness of economic mechanisms for emission reduction under multiple natural and human-related uncertainties to be analyzed. Unlike standard equilibrium state analysis, the model shows that the explicit introduction of uncertainties regarding emissions, abatement costs, and equilibrium states makes it almost impossible for existing market-based trading and carbon taxes to be environmentally safe and cost-effective. Here we propose a computerized multi-agent trading model. This can be viewed as a prototype to simulate an emission trading market that is regulated in a decentralized way. We argue that a market of this type is better equipped to deal with long-term emission reductions, their direct regulation, irreversibility, and "lock-in" equilibria.

1 Introduction

The idea of carbon trading and taxation as a way of combating global climate change is gaining in popularity. At the same time, the uncertainties, both exogenous and endogenous (Rypdal and Winiwarter 2000; Winiwarter 2007; Lieberman et al. 2007; Marland 2008), inherent in carbon trading markets and taxes, raise serious concerns about their ability to contribute to controlling climate change in a cost-effective way.

T. Ermolieva (✉) · Y. Ermoliev · G. Fischer · M. Jonas · M. Makowski · F. Wagner
International Institute for Applied Systems Analysis,
Schlossplatz 1, 2361 Laxenburg, Austria
e-mail: ermol@iiasa.ac.at

The international emission trading scheme under the Kyoto Protocol was devised to lower the cost of achieving greenhouse gas emission reductions for different countries: emissions are reduced where it is cheapest, and emission certificates are then traded to meet the nominal targets in each country (EEA 2006). Thus, in order to minimize costs and make environmentally safe decisions, parties can engage in a bilateral emission exchange process that is independent of market structures.

In contrast, carbon trading markets, which have become popular, resemble stock markets. Carbon markets, like other commodity markets, are volatile and are the result of and react to stochastic "disequilibrium" spot prices, which may be affected by speculations and bubbles (Energy Business Review 2006). The existing emission trading, therefore, might not necessarily minimize abatement costs and achieve emission reduction goals promoting environmental safety.

There are two main approaches to cost-effective pollution control: centralized "command-and-control" methods and decentralized market simulation schemes. If the centralized agency is fully informed about the emissions and abatement cost functions of all parties, finding emission levels that meet given environmental standards in a cost-effective way is a straightforward task. Unfortunately, parties prefer to keep the information private and the costs of emission reductions remain unknown. In the absence of information, a decentralized approach to cost-effective emission reduction is required, as in the bilateral emission trading scheme outlined in Section 2. An alternative to this scheme may be a tax scheme (Section 3) or a price-based scheme (Section 5) simulating a decentralized market solution.

The aim of this paper is to discuss a basic model for analyzing robust decentralized emission control schemes, which treats various uncertainties and detectability (Jonas and Nilsson 2007) of emissions explicitly. The model describes a trading system that enables parties to achieve solutions that are cost-effective and environmentally safe. Section 2 introduces the emission trading schemes and argues that the uncertainties and the way they are represented in emission trading significantly influence equilibrium prices. For example, the standard deterministic representation of emission uncertainties by equal-sided intervals might overlook their essential characteristics. These can, in turn, affect the timing when emission changes become detectable (i.e., when they outstrip the uncertainty associated with them) and whether or not emission reduction targets satisfy agreed safety controls, as illustrated in Appendix 1 and 2. In the sequential bilateral trading scheme of Section 3, the trade at each step takes place toward the cost-effective and environmentally safe equilibrium price. Section 3 also discusses the disadvantages of taxation. Section 4 outlines a computerized, multi-agent and decentralized trading system that allows irreversibility of emission trading to be coped with. Section 5 analyses path-dependencies of myopic trading schemes relying on instantaneous market prices. Section 6 concludes.

2 Trade equilibrium under uncertainty

Carbon control policies, like other environmental policies, should ideally be introduced so as to be environmentally safe and cost-effective. The following model (1)–(4) provides a basis for designing rather different decentralized emission trading schemes. Let us consider in detail an exchange scheme which does not require the existence of a market.

Our model reflects the following key features. The participants (countries, companies, or other emitting entities) are given a right to emit a specific amount for which they must hold an equivalent number of allowances or emission permits. The amount of emissions allowed is limited to the "cap" (Kyoto or other targets). If participants emit more than the cap, they are required to buy additional credits from the parties who pollute less. The transfer of permits is called "trading." Let us briefly discuss the deterministic model proposed in Godal et al. (2003) that will be further extended to include a stochastic model with probabilistic safety constraints. Uncertainties in emission trading have also been addressed in Nahorski et al. (2003) and Nahorski et al. (2007) where, similar to Godal et al. (2003), the uncertainty is added to the emissions reported in the compliance year before the target compliance is checked.

The decision problem of each party can be separated into two interdependent sub-problems. First, for a fixed amount of permits, each party solves its individual problem by deciding whether to spend resources on abating emissions or on investing in uncertainty reduction to satisfy emission targets. This problem does not require information from any other party. Second, each party needs to decide whether or not to exchange permits with other parties. This decision problem involves the cost functions of other parties. In the model this information is private and therefore the methodology of decentralized optimization (Ermoliev et al. 2000) is required.

2.1 Model with interval uncertainty

Let us consider first a model with interval uncertainties. For the individual optimization problem, we define the least costs $f_i(y_i)$ for party i (to comply with imposed targets with fixed permits y_i and the target K_i) as the minimum of emission reduction costs $c_i(x_i)$ and uncertainty reduction costs $d_i(u_i)$:

$$f_i(y_i) = \min_{u_i, x_i} \left[c_i(x_i) + d_i(u_i) \right], \tag{1}$$

$$x_i + u_i \le K_i + y_i, \;\; x_i \ge 0, \;\; u_i \ge 0, \tag{2}$$

for all i, where x_i is the estimate of the reported emissions at source i, u_i is its uncertainty, and y_i is the amount of emission permits acquired by source i (y_i is negative if i is a net supplier of permits).

Remark 1 (*Long-term perspective*) In the model, we introduce a long-term perspective by explicit treatment of future uncertainties and a dynamic trading process. The environmental constraint (2) requires that estimated emissions plus their uncertainty undershoot the agreed emission target. This corresponds exactly to the detectability concept in Fig. 4.

The second optimization problem involves finding the permit vector $y = (y_1, ..., y_n)$ or distribution of permits minimizing the total or social costs

$$F(y) = \sum_{i=1}^{n} f_i(y_i) \tag{3}$$

subject to

$$\sum_{i=1}^{n} y_i = 0. \tag{4}$$

For illustration, let us assume that the cost functions $c_i(x_i)$ and $d_i(u_i)$ are positive, decreasing, convex in x_i and u_i, respectively, and continuously differentiable. Furthermore, if $f_i(y_i)$ is the minimum of two convex positive functions subject to a linear constraint, the function $f_i(y_i)$ is convex, positive, and decreasing. Then, from the Lagrangian minimization $\sum_{i=1}^{n} f_i(y_i) - \lambda \sum_{i=1}^{n} y_i$, a trade equilibrium can be defined as the vector $y = (y_1, ..., y_n)$ satisfying the following equations:

$$f_i'(y_i) = \lambda, \; i = \overline{1:n}. \tag{5}$$

The condition 5 states that, in equilibrium, the marginal value of a permit shall be equal to a specific unknown level (price) $\lambda = \lambda^*$ that is the same for all parties. At the equilibrium vector y^* the following condition holds true:

$$f_i(y) = \max_{x_i} \left[c_i(x_i) + d_i(K_i + y_i - x_i)\right] = \max_{u_i} \left[c_i(K_i + y_i - u_i) + d_i(u_i)\right].$$

Therefore from Eqs. 1, 2, it follows that at the equilibrium $y_i = y_i^*$, $\lambda = \lambda^*$, $x_i = x_i^*$, $u_i = u_i^*$:

$$c_i'(x_i) = d_i'(u_i) = \lambda, \tag{6}$$

where (x_i^*, u_i^*) is the solution of the sub-problem (1), (2) for (y^*, λ^*), and $y^* = (y_1^*, ..., y_n^*)$ satisfying Eq. 5. This equation states that in the cost-effective and environmentally safe equilibrium, the marginal cost of holding emissions down to x_i^* will be equal to the marginal cost of holding uncertainty down to u_i^*. It is important to note that the explicit introduction of uncertainty u_i, the detectability of emissions, and safety constraints (2) into emission trading schemes may significantly affect the equilibrium and hence the design of emission trading schemes. In particular, it means that market prices must reflect Eqs. 5 and 6.

The price λ^* can also be viewed as a cost-effective and environmentally safe carbon tax. However, it is difficult for an agency acting as a central planer to know the cost functions of all parties and thus find equilibrium λ^*. In particular, if adopted by the agency, there is no guarantee that any fixed (regulated) price (tax) λ satisfies Eqs. 5 and 6. In contrast, the scheme of sequential bilateral trade (see Section 3) allows the equilibrium x_i^*, u_i^*, λ^* to be recovered without information on cost functions of all parties being known.

2.2 Probabilistic safety constraints

In the simplified case, constraints (2) assume that the uncertainty of emissions is characterized by equal-sided intervals. These constraints discount the level of reported emissions x_i by their uncertainty u_i (see Fig. 1). As the reduction of uncertainty (6) involves costs, the interval representation may incur costlier or even worst-case solutions, because it may not capture the likelihoods and the preference structure of individual emissions values within the given interval ranges.

In fact, Figs. 2 and 3 illustrate rather complex asymmetric variabilities of emissions and cases in which the interval representation of uncertainty might be inadequate. The following stochastic model introduces probabilistic safety constraints with risk-based discounting of reported emissions, which is less conservative than interval-based discounting.

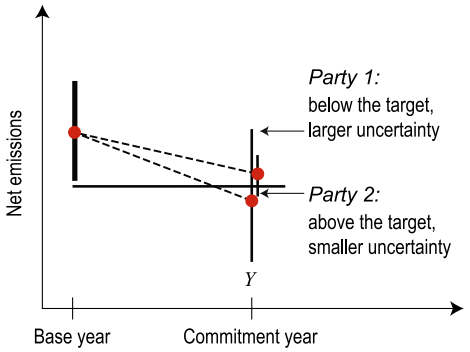

Fig. 1 Which party is more credible for emission trading? Party II reveals a smaller uncertainty interval, the mean of which, however, does not comply with the Kyoto target

Let us define the variability (uncertainty) of reported emission x_i as random variable $\xi_i(x_i, \omega_i)$. Then, the safety constraint can be written as a probabilistic version of the deterministic constraint (2):

$$P\left[x_i + \xi_i\left(x_i, \omega_i\right) \leq K_i + y_i\right] \geq Q_i \tag{7}$$

for all parties i, where Q_i is a safety level that ensures the probability of all potential emission paths to x_i, satisfying the emission target K_i exceeds Q_i.

A random variable $\xi_i(x_i, \omega_i)$ depends, in general, on x_i. In reality, the uncertainty ξ_i can be reduced by improvements to monitoring systems. Let us introduce for this purpose the variable u_i that may control the variability of emissions within the desirable safety level Q_i. If $z_i(x_i)$ is the minimal z such that

$$P\left[\xi_i\left(x_i, \omega_i\right) \leq z\right] \geq Q_i,$$

then the following equivalent constraints can be substituted for the safety constraint (7):

$$x_i + u_i \leq K_i + y_i, \;\; u_i \leq z_i\left(x_i\right). \tag{8}$$

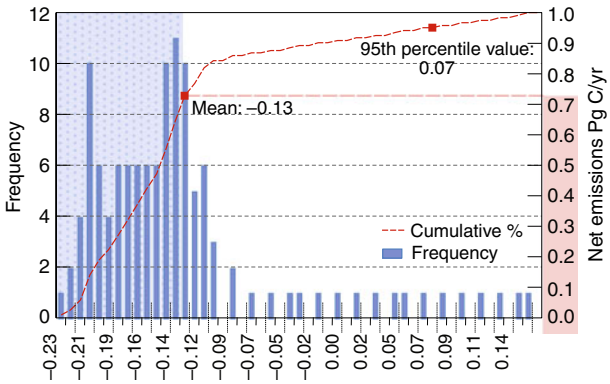

Fig. 2 Global CO_2 net terrestrial uptake, 1960–1970

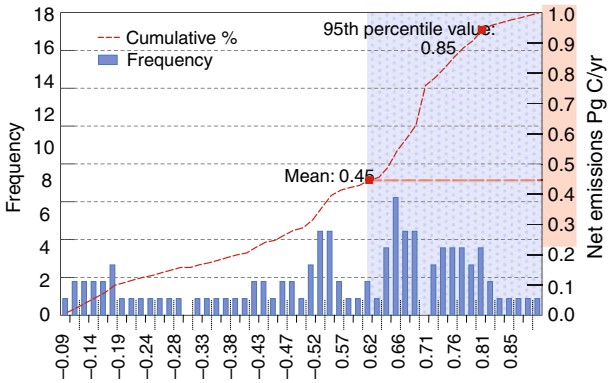

Fig. 3 Global CO_2 net terrestrial uptake, 1985–1995

For notational simplicity, the vector of all uncertainties affecting cost functions and emissions will be denoted by ω. We can redefine function $f_i(y_i)$ in Eq. 1 as

$$f_i(y_i) = \min_{x_i u_i} E\left[c_i(x_i, \omega) + d_i(u_i, \omega)\right], \tag{9}$$

where the minimization in Eq. 9 is subject to constraint (8).

Example 1 (*Deterministic safety constraints*) Assume that ξ_i does not depend on x_i. Then, the constraint (8) reduces to the constraint (2) of the original deterministic model which controls the safety of targets K_i only within a given safety level Q_i.

Example 2 (*Linear equivalent*) Often, $\xi_i(x_i, \omega_i)$ is represented as $\xi_i(x_i, \omega_i) = \gamma_i x_i + \varepsilon_i$, where $0 < \gamma_i < 1$, and ε_i is a random variable. The reduction of uncertainty is controlled by γ_i in the following manner. Let $\varepsilon_i(Q)$ be the minimal z such that $P[\varepsilon_i \le z] \ge Q_i$. Then the safety constraint (8) is reduced to linear constraints

$$x_i + u_i \le K_i - \varepsilon_i(Q_i) + y_i,\ u_i \le x_i.$$

After the individual sub-problems are solved, the optimal γ_i can be found as $\gamma_i = u_i/x_i$.

Remark 2 (*Risk indicator*) Safety constraints (7) are well known in financial applications as a Value-at-Risk indicator (Rockafellar and Uryasev 2000). Similar constraints are typically used in safety regulation by insurance companies, power plants, and in catastrophic risk management (Ermolieva and Ermoliev 2005).

The proposed models allow the comparative advantages of different emission control economic mechanisms to be analyzed.

3 Dynamic bilateral trading process and taxes

The overall goal of the parties participating in emission trading is to jointly achieve emission targets by redistributing the emission permits y_i, that is, to find a robust vector y that would minimize the risk-adjusted social costs of all parties (3) under safety constraints (8), where cost functions $f_i(y_i)$ are defined according to Eq. 9.

It is assumed that a party i knows its expected cost function $f_i(y_i)$, but that the expected social cost function $F(y)$ is unknown. As well as the uncertainty of the social cost function $F(y)$, this scheme takes into account uncertainties of cost functions $c_i(x_i)$, $d_i(u_i)$, which may be affected by market performance, production shocks, and technological uncertainties related to new technologies that cannot be known in advance.

The basic feature of the scheme (Ermoliev et al. 2000) is that two randomly selected parties exchange emission permits in a mutually beneficial way. A new pair is chosen and the procedure is repeated. The following simple equations illustrate that the bilateral exchange of emissions is beneficial for both parties. Let $y^k = \left(y_1^k, ..., y_n^k\right)$ be the vector of emission permits after k trades. Consider two parties i and j at step k with permits y_i^k and y_j^k.

According to Eq. 5, if any two parties i and j have different marginal costs on emission reduction $f_i'\left(y_i^k\right) \neq f_j'\left(y_j^k\right)$, then the permit vector $y^k = \left(y_1^k, ..., y_n^k\right)$ is not cost-efficient. Without loss of generality, assume that $f_i'\left(y_i^k\right) - f_j'\left(y_j^k\right) < 0$. Constraint (4) requires that the feasible exchange in permits has to be such that $y_i^{k+1} + y_j^{k+1} = y_i^k + y_j^k$. If we take $y_i^{k+1} = y_i^k + \Delta_k$ and $y_j^{k+1} = y_j^k - \Delta_k$, $\Delta_k > 0$, then the new feasible vector of permits y^{k+1} reduces the total costs of parties $f_i\left(y_i^k\right) + f_j\left(y_j^k\right)$ and hence the total cost $F(y^k)$:

$$\begin{aligned} F\left(y^{k+1}\right) - F\left(y^k\right) &= f_i\left(y_i^{k+1}\right) + f_j\left(y_j^{k+1}\right) - f_i\left(y_i^k\right) - f_j\left(y_j^k\right) \\ &= \Delta_k\left(f_i'\left(y_i^k\right) - f_j'\left(y_j^k\right)\right) + o\left(\Delta_k\right) < 0, \end{aligned} \tag{10}$$

for small Δ_k. This equation demonstrates that bilateral trade reduces the aggregate costs for sources i and j. We also have

$$f_i\left(y_i^{k+1}\right) - f_i\left(y_i^k\right) < f_j\left(y_j^k\right) - f_j\left(y_j^{k+1}\right). \tag{11}$$

That is, the new distribution of permits reduces costs of j more than increasing the cost of i. Hence j is able to compensate i for the increased costs in a mutually beneficial way.

A party j that decreases emission permit by $\Delta_k > 0$ may negotiate with party i such a level Δ_k that equalizes marginal costs, that is, $f_i'\left(y_i^k - \Delta_k\right) = f_j'\left(y_i^k + \Delta_k\right) = \lambda^k$, where λ^k is an equilibrium price (usually stochastic) at step k. Similar to Ermoliev et al. (2000) it can be proven that for convex functions $f_i(y_i)$, $f_j(y_j)$ the sequence of permits $y^k = \left(y_1^k, ..., y_n^k\right)$ and λ^k converges to an equilibrium satisfying Eq. 5. The computerized market system, described in the next section, allows more sophisticated global solutions for non-convex functions to be achieved.

It is important to compare the bilateral trading scheme outlined with price-based schemes and carbon taxes. A price or tax signal λ decentralizes the solution of overall minimization problem into individual sub-problems: find solutions $y_i(\lambda)$ minimizing functions $f_i\left(y_i\right) + \lambda y_i$. In general, solutions $y_i(\lambda)$ do not satisfy the balance Eq. 4, that is, as $\sum_{i=1}^n y_i\left(\lambda\right) \neq 0$, the price (tax) λ has to be adjusted toward the desirable balance. The common idea is to change current λ_k at time $k = 0,1,...$ proportionally to the imbalance, that is, $\lambda_{k+1} = \lambda_k + \rho_k \sum_{i=1}^n y_i\left(\lambda_k\right)$, with a proper step size ρ_k. It is unrealistic to assume that imbalances $\sum_{i=1}^n y_i\left(\lambda_k\right)$ can be evaluated exactly.

The inherent uncertainty of values $\sum_{i=1}^{n} y_i(\lambda_k)$ results in irregular adjustments of λ_k. It would thus be very difficult to establish an agency that is able to calculate imbalances and regularly update taxes to achieve harmonization across countries, thereby satisfying Eqs. 4–6. This would also include harmonization of taxes among all countries producing a similar product, which would be extremely difficult. Fundamental additional difficulties arise in the case of the market uncertainties analyzed in Section 5.

4 Computerized multi-agent decentralized trading system

Although during sequential bilateral trades, marginal costs and prices will differ for each sequential trade, the trading system will finally converge to an equilibrium where the marginal costs of all parties is equal to equilibrium price as in Eq. 5. This perfect trading system implies that trades being bilateral, sequential (dynamic), and random does not reduce the cost savings, even if sources only have information on their own abatement costs. However, there are major obstacles that can inhibit real markets from perfect functioning according to the proposed procedure. In a perfect market, a party that has sold permits at an early stage of the trading process would be able to renegotiate its earlier transaction. In the real emission trading market, this type of counteraction may be impossible because decisions are irreversible: investments may already have been made, and these investment costs are largely sunk costs. This is the fundamental obstacle involved in the design of cost-minimizing and environmentally safe emission trading markets. Available computer technology and numerically stable optimization procedures allow a computerized (say, Web-based) Multi-Agent Decentralized Trading System to be organized to resolve these issues.

One can imagine a distributed computer network that connects computers of parties with the computer of a central agency. The party anonymously stores information on its specific cost functions and other characteristics of the underlying optimization model 8, 9, including specific probability distributions. The central agency stores information on the emission detection model. The computer of the central agency generates a pair of parties i, j and anonymously "negotiates" with the computers of these partners a proper Δ_k that solves the sub-problem (12). This can easily be done without revealing parties' private information, and the process is repeated until equilibrium levels have been reached. This procedure allows an equilibrium solution to be found that can then be implemented in reality. It is important to stress that a network of interconnected computers is essential for the rapid, smooth, and robust functioning of the emission trading market. There would also be a clear separation between a first stage, in which provisional bids are made between the computers of the parties and a reconstruction of the decisions is still allowed, and a second stage, when contracts have been concluded and investments in emission control have been implemented.

It is well known (Baumol and Oates 1971) that the market will not usually generate desirable outcomes if market prices fail to reflect socioeconomic and environmental impacts. In such a case, it is typically necessary to establish negotiation processes between parties involved to determine desirable collective solutions. From this perspective, the computerized Multi-Agent Decentralized Trading system can

be viewed as a device for collective negotiations and decision making in the presence of inherent uncertainties and irreversibilities.

5 Myopic market processes

The basic model 3, 4, 8, 9 takes a long-term perspective on emission permit trading. Parties use rational expectations and safety constraints to achieve cost-effective and environmentally efficient outcomes that are robust against potential future eventualities. The resulting trading scheme is similar to a pure exchange economy. There are no demand and supply functions. Instead, the safety constraints oblige parties to invest in emission and uncertainty reductions and consequently act as suppliers of emission permits until a rational expectations equilibrium emerges, that is, sequential decisions on the part of parties generate a path of emission permit prices λ_k that converge to the equilibrium price.

The proposed model exists in a prototype "world" where in a perfect market the parties would be able to trade at equilibrium price. In the actual emission trading market, the emissions trades are accomplished at spot disequilibrium prices, and once done, cannot be redressed, which may involve potential lock-in irreversibility not only of trades but also of technological investments. The short- term price-driven market perspective orient parties to instantaneous information ω on prices and cost functions. At time interval k, parties observe uncertainty ω_k and thus know their own cost functions $c_i(x_i, \omega_k)$, $d_i(x_i, \omega_k)$. Based on this information, they trade permits until the next time interval $k+1$ when new information comes on stream. In other words, parties calculate cost functions

$$f_i\,(y_i, \omega_k) = \min_{u_i, x_i} \left[c_i\,(x_i, \omega_k) + d_i\,(u_i, \omega_k)\right]$$

subject to the safety constraints 8, and they minimize $\sum_{i=1}^{n} f_i\,(y_i, \omega_k)$ subject to $\sum_{i=1}^{n} y_i = 0$.

This yields ω_k-dependent decisions $x_i(k, \omega_k)$, $u_i(k, \omega_k)$, $y_i(k, \omega_k)$. At time interval $k+1$, a new observation $\omega_k + 1$ may contradict ω_k, requiring significant revisions to be made to these decisions, which may then be impossible because of their irreversibility. The sequence of myopic short-term decisions $x_i(k, \omega_k)$, $u_i(k, \omega_k)$, $y_i(k, \omega_k)$ would exhibit path-dependent random behavior without providing an equilibrium.

6 Concluding remarks

The feasibility of carbon emission trading and carbon taxes is usually discussed under strong assumptions that all actions are made simultaneously at known equilibrium prices, which implies the existence of a perfectly informed central agency. The proposed sequential bilateral trading scheme under uncertainties avoids this assumption. Sequential trades and resulting emission prices implicitly depend on cost functions and safety constraints for environmental targets. With probabilistic safety constraints, the parties set the level of their exposure to uncertainties and risks. The safety constraints discount the reported emissions to verifiable levels. Yet there is a serious concern that the irreversibility of trades prevents these schemes from achieving cost-effective and environmentally safe solutions. This calls for the

use of a computerized multi-agent emission trading system that provides a collective decentralized regulation of trades.

The computational effectiveness and counterintuitive effects of deterministic interval uncertainties on emission trading are analyzed in Godal et al. (2003) using data on the European Union countries, Russia, Ukraine, and the USA. The modification of these large-scale calculations for stochastic models is a straightforward but tedious task that is beyond the scope of this paper. In general, the stochastic model allows less conservative confidence intervals to be substituted for deterministic uncertainty intervals, leading to less conservative risk-adjusted conclusions.

Acknowledgements Authors are thankful to anonymous referees and the chief editor for numerous important comments and suggestions which led us to make considerable improvements of the paper.

Appendix 1: Uncertainties and trends of carbon fluxes

Here, we illustrate the role of emissions uncertainties and the need for their proper representation in the context of the Kyoto Protocol. The main question that Kyoto parties will face at the end of the commitment period is whether they have fulfilled their obligations. As can be seen from Fig. 1 (see also Jonas and Nilsson 2007), situations might arise when it is difficult to determine which Kyoto parties have genuinely met their Kyoto targets and which Kyoto parties are more "credible," especially when it comes to emission trading.

Uncertainties in Fig. 1 are represented by means of symmetrical intervals. In reality, however, emissions might have different likelihoods within these intervals (i.e., rather general skewed probability distributions). In this case, the use of equal-sided uncertainty representation means that essential patterns of emission changes might not be considered, as illustrated in Figs. 2 and 3. These figures show the variability in emissions of the global CO_2 net terrestrial uptake (see also Ermolieva et al. 2007, data source: http://lgmacweb.env.uea.ac.uk/lequere/co2/carbon_budget.htm). The histogram in Fig. 2 is skewed to the left (more frequent values are on the left-hand side). In the next study period, Fig. 3, the situation changes: more values are concentrated on the right-hand side. Between the two periods, the system changed from being a source to being a sink of CO_2. Moreover, while in Fig. 2, the rare values on the right-hand of the mean have probability only in the order of 15–20%, in Fig. 3, the values and their likelihoods on the right-hand of the mean have much heavier probability mass and, therefore, would be essentially more important for deciding about the level of emission permits to trade. It is clearly impossible to represent the uncertainty characteristics of the variable in Figs. 2 and 3 through intervals.

Appendix 2: Detectability of emissions

Apart from detecting natural variability and changes of emissions as illustrated in Figs. 2 and 3, the detectability of emission changes may also be applied to the analysis of human-related uncertainties, e.g., associated with underreported emissions. The simplest way to introduce the detectability concept into the emission trading schemes (models) is to make a straightforward representation of uncertainties by equal-sided intervals setting ranges of potential emissions as in Section 2.1 (for overview, see

Jonas et al. 1999). Such a representation allows only a conservative or, in a sense, "worst-case" conclusions to be derived, as it does not really give a clue as to the different likelihoods of emissions within the interval (i.e., rather different left- or right-skewed probability distributions; for example, as in Figs. 2 and 3, may be "covered" by the same interval). Let us illustrate the main idea of the interval-based detection techniques with a simple example in Fig. 4. Assume that uncertainty of emission e_1 in the base year t_1 is characterized by equal-sided interval $[e_1 - \varepsilon, e_1 + \varepsilon]$. The uncertainty of reported emission e_2 in the commitment year t_2 ($t_1 < t_2$) is characterized by the same type of interval $[e_2 - \varepsilon, e_2 + \varepsilon]$. We assume that $e_1 > e_2$, although the case $e_1 < e_2$ is also possible (e.g., as a result of emission trading). The emission changes are said to be detectable at time t_2, if the change in carbon emissions $\Delta e = e_1 - e_2$ at time t_2, with reference to time t_1, is greater than the uncertainty (e.g., $e_2^{\max} - e_2$, of the reported net carbon emissions at time t_2). Section 2.2 deals with this case within a stochastic emission trading model, where $e_1 \le K_i + y_i, e_2 \le x_i, \varepsilon = u_i$ in Eqs. 1 and 2.

Under the non-restrictive assumption that first-order linear approximations for emission $e(t)$ and uncertainty $\varepsilon(t)$ trends are applicable for $t_1 \le t \le t_2$, the detection time t^* is then defined as the first time moment at which net emission change Δe outstrips the uncertainty interval ε.

The deterministic detection concept allows describing the dynamics of emissions and their uncertainties, depending on data, up to any order. In Fig. 4 emissions are described up to the first order and uncertainties by a constant in absolute (or relative) terms. That is, the figure's focus is on two points in time, the base year and the commitment year. However, this concept always assumes a single scenario (here a straight line (e_1, e_2)) of how emissions and their uncertainties evolve from a value within an uncertainty interval at t_1 to a value within an uncertainty interval at t_2. As Figs. 2 and 3 show, emissions within uncertainty intervals may have rather different skewed probability distributions.

Remark 3 (*Stochastic detection models*) The detection of emission changes accounting for non-symmetrically distributed emissions is addressed by the stochastic detection technique (DT) proposed in Hudz (2002) and Hudz et al. (2003), and Ermolieva et al. (2007). Emission uncertainties and stochastic detection techniques are also discussed in Nahorski et al. (2003). The goal of the stochastic DT is to rank the trading parties by a safety indicator, which represents the percentile (probability) of emission

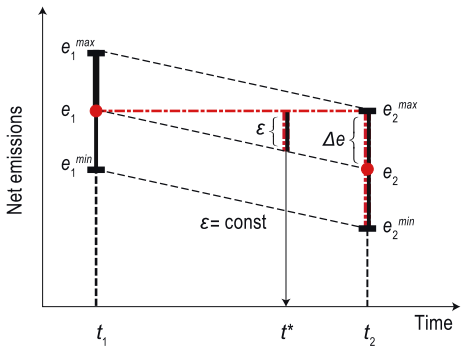

Fig. 4 Simplified illustration of detection time t^*

changes detectable in a given time period. Stochastic emission trading model in Section 2.2 allows the deterministic uncertainty intervals to be replaced by possibly much smaller, confidence (safety) intervals. Comparative analysis of deterministic and stochastic detection techniques using simplified version of the detection model can be found at http://www.iiasa.ac.at/Research/FOR/unc_prep.html and educational software at http://www.iiasa.ac.at/Research/FOR/vt_concept.html).

References

Baumol W, Oates W (1971) The use of standards and prices for protection of the environment. Swed J Econ 73:42–54

EEA (2006) Application of the emission trading directive by EU Member States. Technical Report No. 2/2006, European Environment Agency (EEA), Denmark, p 54. http://reports.eea.europa.eu/technical_report_2006_2/en/technicalreport_2_2006.pdf

Energy Business Review (2006) Volatility the only certainty in EU carbon market. http://www.energy-business-review.com/article_feature.asp?guid=FD09D7CA-3EFC-4229-BA86-1D968025DF5B

Ermoliev Y, Michalevich M, Nentjes A (2000) Markets for tradable emission and ambient permits: a dynamic approach. Environ Res Econ 15:39–56

Ermolieva T, Ermoliev Y (2005) Catastrophic risk management: flood and seismic risks case studies. In: Wallace SW, Ziemba WT (eds) Applications of stochastic programming. MPS-SIAM Series on Optimization, Philadelphia

Ermolieva T, Jonas M, Ermoliev Y, Makowski M (2007) The difference between deterministic and probabilistic detection of emission changes: toward the use of the probabilistic verification time concept. In: Proc. of the 2nd international workshop on uncertainty in greenhouse gas inventories, IIASA-Systems Research Institute of the Polish academy of Sciences. http://www.iiasa.ac.at/Research/FOR/unc_prep.html

Godal O, Ermoliev Y, Klassen G, Obersteiner M (2003) Carbon trading with imperfectly observable emissions. Environ Res Econ 25:151–169

Hudz H (2002) Verification times underlying the Kyoto protocol: consideration of risk. Interim Report IR-02-066, International Institute for Applied Systems Analysis, Laxenburg, Austria. http://www.iiasa.ac.at/Publications/Documents/IR-02-066.pdf

Hudz H, Jonas M, Ermolieva T, Bun R, Ermoliev Y, Nilsson S (2003) Verification times underlying the Kyoto protocol: consideration of risk. Background data for IR-02-066, International Institute for Applied Systems Analysis, Laxenburg, Austria. http://www.iiasa.ac.at/Research/FOR/vt_concept.html

Jonas M, Nilsson S (2007) Prior to economic treatment of emissions and their uncertainties under the Kyoto Protocol: scientific uncertainties that must be kept in mind. Water Air Soil Pollut Focus 7(4–5):495–511. doi:10.1007/s11267-006-9113-7

Jonas M, Nilsson S, Obersteiner M, Gluck M, Ermoliev Y (1999) Verification times underlying the Kyoto protocol: global benchmark calculations. Interim Report IR 99-062, International Institute for Applied Systems Analysis, Laxenburg, Austria, p 43. http://www.iiasa.ac.at/Publications/Documents/IR-99-062.pdf

Lieberman D, Jonas M, Nahorski Z, Nilsson S (eds) (2007) Accounting for climate change. Uncertainty in greenhouse gas inventories—verification, compliance, and trading. Springer, Dordrecht, pp 159, ISBN: 978-1-4020-5929-2 [Reprint: Water Air Soil Pollut.: Focus, 2007, 7(4–5), ISSN: 1567-7230]. http://www.springer.com/environment/global+change+-+climate+change/book/978-1-4020-5929-2

Marland G (2008) Uncertainties in accounting for CO_2 from fossil fuels. J Ind Ecol 12(2):136–139. doi:10.1111/j.1530-9290.2008.00014.x

Nahorski Z, Jeda W, Jonas M (2003) Coping with uncertainty in verification of the Kyoto obligations. In: Studzinski J, Drelichowski L, Hryniewicz O (eds) Zastosowania informatyki i analizy systemowej w zarządzaniu. Systems Research Institute PAS, Warsaw, pp 305–317

Nahorski Z, Horabik J, Jonas M (2007) Compliance and emissions trading under the Kyoto protocol: rules for uncertain inventories. In: Lieberman D, Jonas M, Nahorski Z, Nilson S (eds) Accounting for climate change: uncertainty in greenhouse gas inventories—verification, compliance, and trading. Springer, Heidelberg, pp 119–138

Rockafellar T, Uryasev S (2000) Optimization of conditional-value-at-risk. J Risk 2/3:21–41
Rypdal K, Winiwarter W (2000) Uncertainties in greenhouse gas emission inventories evaluation, comparability and implications. Environ Sci Policy 4:107–116
Winiwarter W (2007) National greenhouse gas inventories: understanding uncertainties versus potential for improving reliability. In: Lieberman D, Jonas M, Nahorski Z, Nilson S (eds) Accounting for climate change: uncertainty in greenhouse gas inventories—verification, compliance, and trading. Springer, Heidelberg, pp 23–30

Climatic Change (2010) 103:291–301
DOI 10.1007/s10584-010-9905-7

CO_2 emission trading model with trading prices

Jarosław Stańczak · Paweł Bartoszczuk

Received: 5 January 2009 / Accepted: 15 June 2010 / Published online: 14 July 2010

Abstract In this paper we consider the buying/selling prices of carbon dioxide (CO_2) emission permits in trading models with uncertainty. Permission prices, although usually omitted from standard models, may significantly influence the trading market. We thus undertook to construct a more realistic trade model and to compare it with the standard one. To do this, we introduced several important changes to the standard model, namely, (1) a new optimized quality function; and (2) transactions with price negotiations between regions. We also enhanced the model using methods described in the literature to allow it to deal with reported emissions uncertainty. Additionally, we used an original method of simulating this kind of market based on a specialized evolutionary algorithm (EA).

1 Introduction

It is claimed that the implementation of a tradable emission permit system can be an efficient strategy for achieving environmental goals. In permit systems a regulatory agency distributes emission permits to polluters in accordance with environmental goals. The permits are transferable among polluters, resulting in—to use simple, everyday trade model terminology—an equalization of marginal abatement costs among pollution sources.

J. Stańczak (✉)
Systems Research Institute, Polish Academy of Sciences,
01-447 Warszawa, ul. Newelska 6, Warsaw, Poland
e-mail: stanczak@ibspan.waw.pl

P. Bartoszczuk
Warsaw School of Economics, Enterprise Institute,
Al. Niepodleglosci 162, Warsaw, Poland
e-mail: pbarto1@sgh.waw.pl

National researchers build market models that optimize their ability to forecast the emission allowance process and the cost of emission reduction for different countries (Ermoliev et al. 2000) to stay fully informed about how obligations regarding greenhouse gas emissions will influence the world economy and about the rules governing the market. A major challenge is to build a transaction model and to solve many other problems associated with the credibility and uncertainty of emission level reports (Ermoliev et al. 1996; Godal 2000; Klaasen et al. 2001; Nahorski et al. 2007).

Earlier proposed models of emission permit trading for CO_2 do not really use transaction prices. Although the models calculate the equilibrium prices, they are not applied during the trade. The equilibrium permit price is used to calculate the emission reduction costs only. No negotiation of prices or any additional transaction costs are applied.

The problem-solving method proposed in earlier papers was original, but diverged from the real market situation. A more elaborated market model was thus considered, in which additional elements were included, such as the possibility of choice of price during negotiation and the influence of real prices on model solutions.

Application of the evolutionary algorithm (EA) method to simulate economic models is a very fast developing domain, mainly because it is quite easy to model economic systems using this tool. The evolutionary and agent-based approach to dynamic market modeling, which can be found in Bonatti et al. (1998), is used to simulate the very complicated information industry market. The evolutionary method is a natural way of performing computer simulations of the new model. This method is presented below.

2 New and earlier market models

The idea of emission permit trading is based on the assumption that some countries can save emission permits, which they can sell to countries wishing to emit more than their Kyoto obligations.

Trading is beneficial only when the price of permits is lower than the cost of emission reduction. Then, the country can reduce emissions below its obligation and sell the surplus as permits to another country (see Figs. 1 and 2).

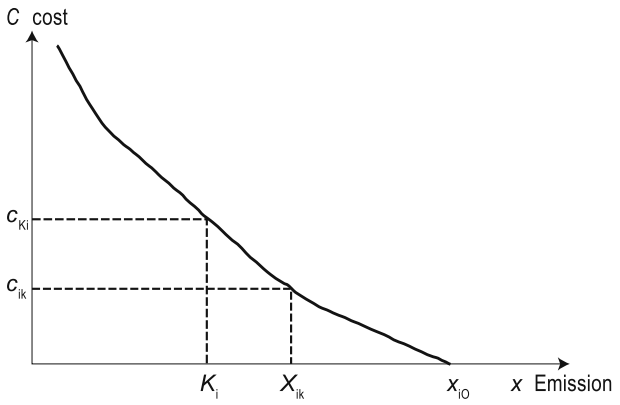

Fig. 1 CO_2 emission reduction cost: without trade (c_{Ki}), and with trade (c_{ik}) for buying country, K_i—Kyoto limit, x_{ik}—emission after trade, x_{i0}—initial emission

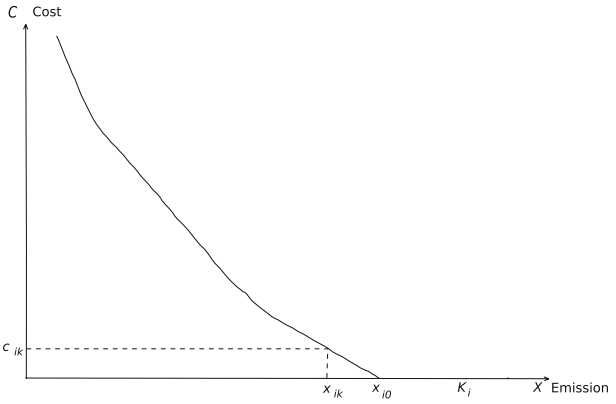

Fig. 2 Without trade, the emission reduction costs of CO_2 are zero; with trade for the selling country (c_{ik}), K_i—Kyoto limit, x_{ik}—emission after trade, x_{i0}—initial emission

In the base model the total cost of holding emissions in region i down to x_i, is denoted by $C_i(x_i)$, which represents the abatement cost function. We assume that the cost functions $C_i(x_i)$ are positive, decreasing, and continuously differentiable for each region. The Kyoto target for each region i is indicated by K_i. The number of emission permits acquired, by source, is expressed by y_i (y_i is negative if region i is a net supplier of permits),

$$E = \min_{x_i} \sum_{i=1}^{n} C_i\,(x_i) \tag{1}$$

with the constraints:

$$x_i \leq K_i + y_i \tag{2}$$

$$\sum_{i=1}^{n} y_i = 0 \tag{3}$$

where:

E	is the minimum cost of decreasing emissions for all countries in the standard model;
$C_i(x_i)$	is the cost of reducing emissions at region i down to x_i;
y_i	is the number of emission permits acquired by region i;
K_i	is Kyoto target for region i;
n	is the number of regions;
x_i	is current emissions.

The goal is to minimize the cost of emission reduction in order to cut emissions to the required level in compliance with the Kyoto target.

This basic model does not deal with the problem of uncertainty in emissions, but it can be extended to do so, for instance, using ideas described in Nahorski et al. (2007), Horabik (2005), or Bartoszczuk and Horabik (2007). The only modification

required to the standard model for considering uncertainty is to replace formula (2) with formula (4) (Nahorski et al. 2007; Horabik 2005).

$$x_i + (1 - \varsigma)(1 - 2\alpha)\, d_i n_i \leq K_i + y_i \tag{4}$$

where:

- ζ is the parameter that describes the correlation of emissions in the base year (1990) and the current year, usually $\zeta \in [0.65,0.7]$;
- α is the parameter that describes the risk of noncompliance with the Kyoto target, $\alpha \in [0,0.5]$;
- d_i is the inventory uncertainty for country i;
- n_i is the base year emission for country i.

The modified model minimizes the sum of total emission reduction costs; however, the limits imposed are lower than the Kyoto target in order to take into account possible unreported emissions.

Normally, prices (the shadow price) are defined as the cost derivatives at a given point. However, in the real world, neither sellers nor buyers are apt to disclose their emission reduction costs. Moreover, the cost reduction function are usually not precisely known. Finally, they are not the only component of emission permit prices. Therefore, in the solution described we assume that a transaction is finalized only when the permit price that is negotiated is lower than the average cost of emission reduction for the buyer and higher than the average cost of emission reduction for the seller. It is obvious that each party wishes to maximize its profit, and this assumption is the basis for our new quality function.

In the evolutionary approach, which will now be further described, maximization over y_{ji} and π_{ji} is performed in each transaction by genetic operators (which try to simulate the price negotiation process to make the transaction more beneficial and reject any outcomes that are unprofitable), while the total maximization over x_{ji} is the EA task (selection of better market solutions with lower emission reduction costs). As mentioned earlier, the model presented contains important changes in relation to previous models. The most important change is a different goal function (5) which maximizes the difference between cost with no trade and cost with trade, where the buying/selling price of the permit is included. It considerably influences transaction profitability and the decision regarding buying/selling permits, including the decision, whether it is more advantageous to reduce emissions than to buy permits. Unfortunately, in a single-criterion version a large part of the information specific to participating parties is lost after the total sum over i is calculated, but this information is used by genetic operators and can be stored to research the market behavior. The goal function (5) is only a single-criterion version of a more sophisticated model with many criteria: one for each party. A multicriteria model designed for an agent or multicriteria evolutionary system, has not yet been built; however, the first steps have been taken toward applying such a system, through modeling of the Cournot game (Stańczak 2009).

Formulae (6–11) are constraints which assure that the market model created has realistic properties:

- A party is not allowed to emit more than its Kyoto obligation plus acquired permits (6);

- Additional permits can be bought only from parties participating in the market, and no extra permits are available (8);
- Buying/selling permits changes the level of allowable emissions of a party (7);
- The number of permits traded in one transaction is limited to $y_{\max}$ to avoid major fluctuations in permit prices (9);
- The price of the permit in a transaction is identical for the selling and buying party (10);
- The numbers of traded permits are treated as negative values for the selling parties and positive for the buying ones, and their absolute values are equal (11).

In the new model the goal function is given by the following formula:

$$G = \sum_{j=1}^{T} \max_{x_{ji}} \sum_{i=1}^{n} \max_{y_{ji}\pi_{ji}} \left(C_i\left(x_{j-1,i}\right) - \left(C_i\left(x_{ji}\right) - y_{ji} \cdot \pi_{ji}\right)\right) \tag{5}$$

with the constraints:

$$x_{Ti} \leq K_i + \sum_{j=1}^{T} y_{ji} \tag{6}$$

$$x_{j-1,i} + y_{ji} = x_{ji} \text{ and } x_{0,i} = K_i \tag{7}$$

$$\sum_{i=1}^{n} \sum_{j=1}^{T} y_{ji} = 0 \tag{8}$$

$$0 \leq y_{ji} \leq y_{\max} \tag{9}$$

$$\pi_{ji} = \begin{cases} 0 & \text{for parties not trading in the transaction } j \\ \pi_{ji} & \text{for parties trading in the transaction } j \end{cases} \tag{10}$$

$$y_{ji} = \begin{cases} 0 & \text{for parties not trading in the transaction } j \\ -y_{ji} & \text{for party selling in the transaction } j \\ y_{ji} & \text{for party buying in the transaction } j \end{cases} \tag{11}$$

where:

G	is the minimum cost of decreasing emissions for all parties in the model;
T	is number of buying/selling transactions conducted;
$C_i(x_{ji})$	are the costs of reducing emissions by the party i to x_{ji} after j transactions;
K_i	is the Kyoto target for the party i;
n	is the number of parties;
x_{ji}	is the emissions of the party i after j transactions;
y_{ji}	is the number of emission permits acquired by the party i;
π_{ji}	is the price of permits bought/sold in transaction j by the party i.

Using function (5) we look for a solution to maximize the difference between the cost when no trading takes place and the cost when permits are exchanged, in other words, the profit from emission trading. In the previous goal function we minimized the cost of emission reduction without including buying prices and expenditures for this goal: note that the cost of buying can be considerably greater than expenditure on CO_2 reduction if there is no trade. In the new approach, we also assume slightly different methods of permit price setting. The authority or market must set a minimum price below which the permit price cannot go. This is to exclude cases where countries reporting emissions below the Kyoto level have zero marginal abatement costs (compare Fig. 2). Therefore, the marginal cost (e.g., shadow price) is no longer a derivative of the abatement cost, but a derivative with minimal value. In practical cases the price negotiations prevent a situation arising where the price of a permit drops to zero. While no country would wish to "sell" permits at no cost, the model described should have some kind of protection against such cases.

The second important change is the introduction of transactions. Transactions are conducted iteratively until there is no further benefit for participants and all parties have dropped out. Prices and amounts of transferred permits are negotiated. Thus, unlike the static base model, our market model is dynamic.

The real price of permits and the number of permit is not known before computer simulation of market activity is conducted and the process of price negotiations among parties is emulated. As an approach to negotiations, in computer simulations presented in this paper the number of permits sold is randomly chosen from some interval. In a similar way the permit price is chosen from the interval between the maximum price (shadow price) of the buyer and minimum price (modified shadow price) of the seller.

Similar to the base model, the new formulae (5–10) do not deal with the problem of the uncertainty of reported emissions; however, this can be changed by introducing a new formula (12) instead of a formula (6) to consider possible unreported emissions:

$$x_{Ti} + (1 - \varsigma)\,(1 - 2\alpha)\,d_i n_i \leq K_i + \sum_{j=1}^{T} y_{ji} \tag{12}$$

where all symbols have the same meaning as in formulae (4–11).

3 Evolutionary algorithm method in computer simulations

Although the standard evolutionary algorithm works as shown in Table 1, many problem-specific improvements are needed to make this simple scheme work efficiently. To adjust the genetic algorithm to the solved problem, there must be: (1) a proper encoding of solutions; (2) creation of specialized genetic operators for that problem and an accepted data structure; and (3) a fitness function that is optimized by the algorithm.

We thus use a specialized evolutionary algorithm to solve the problem: one individual contains information about all the parties participating in the market, making it a complete solution to our problem. Another method may also be applied whereby each party is treated as one independent individual (Alkemade et al. 2006; Clemens and Riechmann 2006). In the latter case we obtain only one solution, as

Table 1 The evolutionary algorithm

Random initialization of the population of solutions.
Reproduction and modification of solutions using genetic operators.
Valuation of the solutions obtained.
Selection of individuals for the next generation.
If a stop condition is not satisfied, return to step 2.

the population of solutions in evolutionary algorithm is limited to the number of parties participating in the trade. The case considered (five parties) is too small for an evolutionary algorithm to work efficiently, and is therefore not used.

We use the former approach. Thus, the whole individuals' population contains a number of solutions, as many as the number of individuals. The solutions need not be different, although they usually are. Thanks to this parallelism of evolutionary computations, we usually obtain several scenarios of possible market evolution.

The information needed to describe one party is as follows:

- Theoretical price of own permits (shadow price);
- The real price of current permits sold/bought;
- The value of current permits sold/bought;
- Number of permits currently sold/bought;
- The total sum of permits sold/bought;
- Current emissions;
- Previous emissions (before present transaction);
- Value of present and previous goal function.

To modify the solution, the following genetic operators were used:

- Competition: a chosen party offers a number of permits for sale, some other parties declare a willingness to buy them, next the best option is chosen, and the solution (the individual) is modified;
- Sale: the chosen parties conduct transactions.

The prices and numbers of permits traded are randomly chosen. The number of permits traded is chosen from the interval {1,..,5},[1] and the permit price is drawn from a given distribution as a value between the buying and selling offer, with the expected value of the distribution being the average of these two values.

In EA a goal function is called fitness function because it is often modified (scaled or moved) due to EA requirements. Thus the fitness function for EA is a direct goal function of a problem, as described by formula (5).

Population initializing procedures and genetic operators are designed so as to obey the constraints (6–12), and forbidden solutions cannot appear in the population of solutions.

As specialized genetic operators are used, some method of sampling them needs to be applied in all iterations of the algorithm. In the approach used (Mulawka and Stańczak 1999; Stańczak 2003), it is assumed that an operator that generates good

[1]The limitation on the maximum amount of permits sold is introduced, as trading too large a number of permits in one transaction can have a large impact on permit prices and undermine profitability. One permit is an equivalent of 1MtC.

Table 2 The data applied for calculations for various regions

Country	Initial emission (x_{i0}) MtC/year	Cost function parameter (a) MUSD/(MtC/year)^2	Limit Kyoto (K_i) MtC/year
USA	1,820.3	0.2755	1,251
EU	1,038.0	0.9065	860
Japan	350.0	2.4665	258
CANZ	312.7	1.1080	215
FSU	898.6	0.7845	1,314

results should have greater probability and affect the population more frequently. As every individual may have its own preferences, every individual has a vector of floating point numbers, beside the encoded solution. Each number corresponds to one genetic operation. It is a measure of quality of the genetic operator. The higher the number, the higher the probability of operator execution by the individual.

This set of probabilities or, in other words, the ranking of qualities is also a basis of the experience of every individual, and each individual chooses an operator in each epoch of the algorithm according to it. Through the experience gathered, individuals can maximize the chances of their offspring surviving.

4 Computer simulation results

Computer simulations were conducted on data set, in line with other authors' papers, mainly Bartoszczuk and Horabik (2007), Horabik (2005), and Nahorski et al. (2007). We consider a group of the following countries: United States (USA); European Union (EU); Japan; Canada, Australia and New Zealand (CANZ); and former Soviet Union with Eastern Europe (FSU). We assume that cost depends on emission reductions in the following way (quadratic cost function) (Horabik 2005; Bartoszczuk and Horabik 2007).

$$C(x_i) = \begin{cases} a * (x_{i0} - x_i)^2 & \text{for } x_i < x_{i0} \\ 0 & \text{for } x_i \geq x_{i0} \end{cases} \tag{13}$$

Table 3 Results in scenario assuming perfect permit market model

Region/ country	Final emission MtC/year	Final price USD/tC	Number of imported permits Mt/year	Permits expenditures MUSD/year	Emission reduction cost MUSD/year
USA	1,561.0	143	310	11,974.3	18,523.7
EU	959.0	143	100	15,790.6	5,515.1
Japan	321.0	143	63	29,987.6	2,074.3
CANZ	248.0	143	33	16,077.6	4,638.2
FSU	808.0	143	−506	−73,830.1	6,439.5
Total	–	–	0	0	37,190.8

Table 4 The results of simulation from the new model; uncertainty not considered

Region/ country	Final emission MtC/year	Final price USD/tC	Number of imported permits Mt/year	Permits expenditures MUSD/year	Emission reduction cost MUSD/year
USA	1,562.0	142.3	311	47,486.4	18,381.1
EU	959.0	143.2	99	15,823.3	5,657.5
Japan	321.0	143.1	63	18,521.7	2,074.3
CANZ	248.0	143.4	33	4,010.5	4,638.2
FSU	808.0	142.2	−506	−85,841.9	6,439.5
Total	–	–	0	0	37,190.6

where:

a cost function parameter;
x_{i0} initial emission;
x_i current emission.

In Table 2 we describe abatement cost function coefficients, which have special interpretation.

Table 5 Results obtained using the described new model; uncertainty considered with different values of risk parameter α, see formula (12)

Region	Reported emissions (MtC/year)	Final price USD/tC	Permits traded (Mt/year)	Cost of traded permits MUSD/year	Cost of emission reduction MUSD/year
Risk parameter $\alpha = 0.5$					
USA	1,559.0	144.0	308	44,834.0	18,810.5
EU	970.0	141.4	100	14,393.0	5,515.1
Japan	321.0	143.1	63	17,831.2	2,074.3
CANZ	249.0	141.2	34	4,049.0	4,495.9
FSU	809.0	140.6	−505	−81,107.2	6,298.1
$\alpha = 0.3$					
USA	1,538.0	167.1	287	45,975.4	25,340.5
EU	957.0	167.2	97	17,948.8	7,707.3
Japan	331.0	167.4	63	17,159.6	2,839.9
CANZ	242.0	168.2	27	5,406.2	6,384.3
FSU	840.0	167.5	−474	−86,489.9	8,936.8
$\alpha = 0.1$					
USA	1,514.0	191.9	263	51,350.1	33,414.8
EU	954.0	192.9	94	16,610.9	10,265.5
Japan	321.0	191.7	63	18,810.4	3,725.4
CANZ	237.0	190.8	22	2,737.3	8,216.9
FSU	872.0	192.8	−442	−89,508.7	11,842.5
$\alpha = 0.0$					
USA	1,502.0	204.3	251	51,801.7	37,870.0
EU	954.0	203.1	94	19,372.8	11,375.2
Japan	320.0	208.8	62	16,584.4	4,419.5
CANZ	234.0	203.3	19	1,403.0	9,321.1
FSU	888.0	205.4	−426	−89,161.9	13,448.4

In a traditional method (perfect market information) we obtain the results presented in Table 3.

In the case of new model application the results are presented in Table 4.

Application of the EA method to simulate the permits market provides some additional benefits, as the result is not just a single set of parameters, but a set of possible scenarios. EA operates on a population of mainly different individuals, and computations are conducted in a non-deterministic way. In particular, negotiation of permit prices is modeled as random number generation from a little modified normal distribution, cut to the desired interval—prices are generated from the interval that is profitable for both countries, and if there is no such interval, no transaction is made. Thus, different scenarios depend mainly on negotiated prices (i.e., prices randomly generated in the simulation).This non-deterministic aspect of EA can be seen if one compares results presented in Tables 4 and 5 for $\alpha = 0.5$: this value of risk parameterα makes the uncertainty component in (12) inactive, but results are not exactly the same. Thus, two different scenarios of market evolution can be observed. Such scenarios can be obtained and used as a basis for more sophisticated analyses of market behavior.

5 Conclusions

In contrast with the previous model (Bartoszczuk and Horabik 2007), our original permit market model is dynamic. The results show that including perfect permit prices is more cost-effective than in our dynamic market solution, but this fact is easy to explain—transactions are conducted at negotiated prices (free market assumptions), not at optimal prices calculated and imposed by some authority. The permit distribution is thus slightly different in the second model (column 4 in Tables 3 and 4), and the structure of buying parties is changed; it is more beneficial to reduce emissions than to buy permits in the case of the USA (column 6 in Tables 3 and 4. Obviously, the total cost of emission reduction in the second method (85,841.9 MUSD/year) is higher than in the first (73,830.1 MUSD/year), which can be explained by higher expenditure for permits and slightly higher necessary emission reduction. Results obtained using the new model with different values of risk parameter α show that in a case with full uncertainty, fewer permits are purchased and there is a greater reduction of emissions, which is more expensive. Moreover, the permit prices in the scenario with full uncertainty is 30% higher than in the scenario with parameter $\alpha = 0.5$ (no-uncertainty scenario). For all practical purposes we are able to anticipate that applying the dynamic model requires additional agreements among parties. While such activities are difficult to implement, our analysis proves that they are environmentally friendly, as they require emission reductions.

References

Alkemade F, La Poutre H, Amman M (2006) Robust evolutionary algorithm design for socio-economic simulation. Comput Econ 28:355–470

Bartoszczuk P, Horabik J (2007) Tradable permit systems: considering uncertainty in emission estimates, water air soil pollution. Focus 7:573–579

Bonatti M, Ermoliev Y, Gaivoronski A (1998) Modeling of multi-agent market systems in the presence of uncertainty: the case of information economy. Robot Auton Syst 24(3–4):93–113

Clemens C, Riechmann T (2006) Evolutionary dynamics in public good games. Comput Econ 28:399–420

Ermoliev Y, Klaassen G, Nentjes A (1996) Adaptive cost-effective ambient charges under incomplete information. J Environ Econ Manage 3:37–48

Ermoliev Y, Michalevich M, Nentjes A (2000) Markets for tradable emission and ambient Permits: a dynamic approach. Environ Resour Econ 15:39–56

Godal O (2000) Simulating the carbon permit market with imperfect observations of emissions: Approaching equilibrium through sequential bilateral trade. Interim Report IR-00-060, IIASA. Laxenburg, Austria

Horabik J (2005) On the costs of reducing GHG emissions and its underlying uncertainties in the context of carbon trading. Raport Badawczy RB/34/2005, IBS PAN

Klaasen G, Nentjes A, Smith M (2001) Testing the dynamic theory of emissions trading: experimental evidence for global carbon trading, Interim Report IR-01-063, IIASA. Laxenburg, Austria

Mulawka J, Stańczak J (1999) Genetic algorithms with adaptive probabilities of operator selection. In: Proceedings of ICCIMA '99. New Delhi, India, pp 464–468

Nahorski Z, Horabik J, Jonas M (2007) Compliance and emissions trading under the Kyoto protocol; rules for uncertain inventories. Accounting for climate change. Uncertainty in greenhouse gas inventories—verification, compliance, and trading. Springer, pp 119–138

Stańczak J (2003) Biologically inspired methods for control of evolutionary algorithms. Control Cybern 32(2):411–433

Stańczak (2009)) Evolutionary algorithm for market simulations. Evolutionary computation and global optimization 2009, Prace Naukowe PW, Elektronika, z. 169, Warszawa, pp 163–172

Climatic Change (2010) 103:303–325
DOI 10.1007/s10584-010-9916-4

Compliance and emission trading rules for asymmetric emission uncertainty estimates

Zbigniew Nahorski · Joanna Horabik

Received: 5 January 2009 / Accepted: 15 June 2010 / Published online: 14 July 2010

Abstract Greenhouse gases emission inventories are computed with rather low precision. Moreover, their uncertainty distributions may be asymmetric. This should be accounted for in the compliance and trading rules. In this paper we model the uncertainty of inventories as intervals or using fuzzy numbers. The latter allows us to better shape the uncertainty distributions. The compliance and emission trading rules obtained generalize the results for the symmetric uncertainty distributions that were considered in the earlier papers by the present authors (Nahorski et al., Water Air & Soil Pollution. Focus 7(4–5):539–558, 2007; Nahorski and Horabik, 2007, J Energy Eng 134(2):47–52, 2008). However, unlike in the symmetric distribution, in the asymmetric fuzzy case it is necessary to apply approximations because of nonlinearities in the formulas. The final conclusion is that the interval uncertainty rules can be applied, but with a much higher substitutional noncompliance risk, which is a parameter of the rules.

1 Introduction

Emission of greenhouse gases is a basic element of the climate change models. See, for example, Stern (2007) where results are presented in probabilistic terms. However, greenhouse gas inventories estimates are not calculated exactly. Possible error magnitudes depend on the types of gas considered, activities involved, and countries, ranging from a few to over 100 percent. Moreover, distributions of errors for different gases as well as for national inventories may be asymmetric (Ramirez

Electronic supplementary material The online version of this article (doi:10.1007/s10584-010-9916-4) contains supplementary material, which is available to authorized users.

Z. Nahorski (✉) · J. Horabik
Systems Research Institute, Polish Academy of Sciences,
Newelska 6, 01-447 Warsaw, Poland
e-mail: Zbigniew.Nahorski@ibspan.waw.pl

et al. 2006; Winiwarter and Muik 2007). The methods of checking compliance and, particularly, establishing rules for emission trading proposed to date for the uncertain inventories (Jonas et al. 2010; Jonas and Nilsson 2007; Nahorski et al. 2007; Nahorski and Horabik 2008) concern only the symmetric distributions and mainly the interval uncertainty models.

In Nahorski et al. (2007) the compliance and trading rules were considered for the interval uncertainties of emissions. In order to have a high enough likelihood of fulfilling the compliance, lower limit of reductions were required (undershooting), and an appropriate recalculation of the traded emissions needed to be performed. However, the interval uncertainty approach provides too conservative a reduction of limits and a recalculation of traded emissions. Although the stochastic case may be useful for the determination of new compliance rule, see also Gillenwater et al. (2007), only a complicated formula for recalculation of the traded emissions has been provided (Nahorski et al. 2007), which is practically useless because it is valid only for uncorrelated inventories. In this paper a fuzzy uncertainty is considered. The fuzzy set calculus basically inherits the rules from the interval calculus and thereby provides simpler calculations than that for the stochastic variables. At the same time the fuzzy variables may be shaped to have distributions that are more concentrated around observed values than in the interval case, where the information on distribution is lost. Thus, it can better approximate the real distributions. This paper also deals with the asymmetric cases, aiming to improve the precision of assessments as to whether the given emission limits or reductions are satisfied, and being able to guarantee (with a small prescribed risk) that this limit or reduction has been fulfilled in emission trading among parties and in other possible flexible mechanisms under the Kyoto Protocol. Improved precision, as compared with the interval case, means lower compliance costs and more reliable estimates of inventories for the climate change models.

We derive in this paper a new formula for recalculation of the trading quantities for the fuzzy and symmetric distributions, which is a generalization of that used for the interval approach. To obtain an analogous formula for the asymmetric fuzzy case, an approximation is required. The one proposed in this paper is a generalization of those for both the symmetric fuzzy case and the asymmetric interval approach.

Summing up, we derive here new rules for checking compliance and for emission trading, for asymmetric fuzzy distributions. They are generalizations of the rules presented in Nahorski et al. (2007) and Nahorski and Horabik (2008) for symmetric distributions and interval uncertainty and they reduce to them as special instances provided that appropriate parameters are taken. Comparison of the rules obtained for the fuzzy approach with those for the interval approach shows that the latter can be used equivalently, but with a much bigger substitutional parameter than originally designed for the noncompliance risk.

In Section 2 we formulate the problem and introduce some basic notation. Then, in Section 3, we deal with the asymmetric interval uncertainty and we derive conditions for checking compliance and formulas for so-called effective emissions, which can be directly traded, without taking into account the emission uncertainty. In Section 4 a family of fuzzy numbers is introduced. These are used to model the full inventory uncertainty and form the basis for derivations of generalized compliance and emission trading rules. These rules are compared with the interval approach rules, and their equivalence in applications considered in the paper, for appropriately chosen parameters, is shown. Section 6 concludes.

2 Problem formulation

Two systems for reducing greenhouse gases emissions have been applied. One, called *cap and trade*, as, for example, in the European Trade System, where the limits on emissions from chosen activities are distributed among member countries in the first stage and then finally between companies within the European Union. The problem here is to check, if L, the given emission limit for the company, expressed as emission permit, has not been exceeded, that is, if

$$x \leq L \tag{1}$$

where x is the real, unknown emission of a party in a given year. Unfortunately, x is not known exactly, as only its available estimate of the emission $\hat{x}$ can be calculated. The estimate of the total emissions by a party is calculated from an inventory of emissions from every contributing activity, including absorption by sinks. These are, however, highly uncertain, see (Winiwarter 2004; Monni et al. 2007). Moreover, uncertainties of inventories $\hat{x}$ differ among different activities both in terms of the range and distributions. Another system used under the Kyoto Protocol requires each participating country to reduce a pre-specified percentage of its base year emissions within the given period (from 1990 to 2008–2012 for most countries), although some countries are granted an opportunity to stabilize emissions at the base year level or even to increase its emissions in a limited way. Three so-called flexible mechanisms are connected with the Kyoto Protocol. These are: Joint Implementation, Clean Development Mechanism, and Permit Trading. All are related to buying the emissions saved by other parties. In all these cases, the problem is to check to see if the declared reduction has actually been achieved.

With emission reductions, the compliance checking is slightly more complicated than in the *cap-and-trade* system because the limit referred to is also uncertain. This leads to the problem of comparing two uncertain values. Here, however, this problem will be transformed to the form similar to (1), that is to the comparison of uncertain value with the exactly known limit. Let us denote by δ the fraction of the party's emissions to be reduced. The value of δ may be negative, for parties required to limit their emission increase. Denoting by x_b the basic emission and by x_c the emission to be checked, the following inequality should be satisfied

$$x_c - (1 - \delta)x_b \leq 0 \tag{2}$$

This inequality has the same form as (1), with the inspected variable $x_c - (1 - \delta)x_b$ and the limit $L = 0$. Similarly as earlier, neither x_c nor x_b are known precisely enough. Thus, only the difference in estimates can be calculated

$$\hat{x}_c - (1 - \delta)\hat{x}_b \tag{3}$$

where both $\hat{x}_c$ and $\hat{x}_b$ are known inaccurately. In the Kyoto Protocol context, x_b is the emission in the basic year and x_c the emission in the compliance period. We are not, however, interested here in reference and compliance times, but only in the values to be compared.

Moreover, the emission estimate of a party may be modified by selling or buying uncertain emissions, which adds to the final uncertainty on the left hand side. These problems are discussed in the sequel using two models of uncertainty: interval and fuzzy.

3 Interval uncertainty

Material in this section is a generalization of the results for the symmetric intervals given in Nahorski et al. (2007). The methodological concept is the same, but the results differ because of changed assumptions, although they do reduce to the previous results, when the symmetric intervals are considered in the equations. The derivations in this section are fundamental for the rest of the material and are therefore presented in a fairly complete way, even if they are more or less straight generalizations of the formulas for the symmetric intervals.

3.1 Compliance

Let us denote the lower spread of the uncertainty interval by d^l and the upper spread by d^u. Then, the real basic emission x_b and the real checked emission x_c are situated in the intervals

$$x_b \in \left[\hat{x}_b - d_b^l, \hat{x}_b + d_b^u\right], \qquad x_c \in \left[\hat{x}_c - d_c^l, \hat{x}_c + d_c^u\right]$$

Known limit We start with the simpler case of the limit L which is known exactly. To be completely sure that a party (typically a company) fulfills the limit, its emission inventory should satisfy the following condition, see Fig. 1a.

$$\hat{x}_c + d_c^u \le L \tag{4}$$

As the bounds can be quite large, a weaker condition will be used, see Nahorski et al. (2007). A party is compliant with the risk α if its emission inventory satisfies the condition

$$\hat{x}_c + d_c^u \le L + \alpha\left(d_c^l + d_c^u\right) \tag{5}$$

The risk is here understood as a likelihood that the party may not fulfill the agreed obligation regarding the emission limit or reduction because of the uncertainty of the emission inventory.

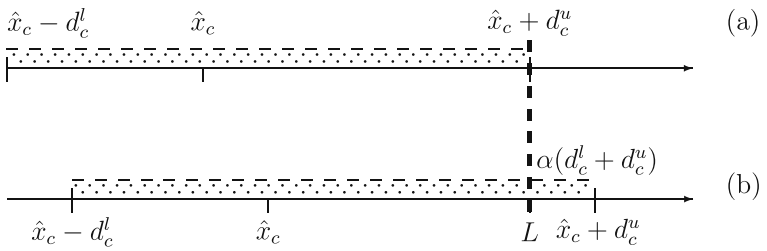

Fig. 1 Full compliance (**a**) and compliance with risk α (**b**) in the interval uncertainty approach for the known limit case

Condition (5) means that the αth part of the party's emission estimate (inventory) uncertainty interval is allowed to lie above the limit L, see Fig. 1b. After some algebraic manipulations the condition (5) can be also written in the following form

$$\hat{x}_c + \left[1 - \left(1 + \frac{d_c^l}{d_c^u}\right)\alpha\right] d_c^u \le L \tag{6}$$

The above condition shows that a part of the upper spread of the uncertainty interval is added to the emission estimate before compliance is checked. This can be also interpreted to mean that an unreported emission, due to uncertainty, is included in the condition to reduce the risk of non-compliance.

For the symmetric interval $d_c^l = d_c^u = d_c$ the condition (6) takes the form

$$\hat{x}_c + (1 - 2\alpha)d_c \le L$$

which has been derived in Nahorski and Horabik (2008).

Emission reduction A more difficult case of checking an emission reduction, when both the checked and the basic emission are uncertain, will be transformed to the problem of a known limit by considering the difference of the checked and reduced emissions, as mentioned earlier. Using the interval calculus rules, we get

$$x_c - (1 - \delta)x_b \in \left[D\hat{x} - d_{bc}^l,\, D\hat{x} + d_{bc}^u\right]$$

where

$$D\hat{x} = \hat{x}_c - (1 - \delta)\hat{x}_b \tag{7}$$

and the lower and upper spreads are

$$d_{bc}^l = d_c^l + (1 - \delta)d_b^u, \qquad d_{bc}^u = d_c^u + (1 - \delta)d_b^l \tag{8}$$

However, the inventories $\hat{x}_b$ and $\hat{x}_c$ are dependent and the values of d_{bc}^l and d_{bc}^u are usually much smaller than those resulting from the above expression. Nahorski et al. (2007) proposed to take this into account by modification of the formulas (8) to

$$d_{bc}^l = (1 - \zeta)\left(d_c^l + (1 - \delta)d_b^u\right) \tag{9}$$

$$d_{bc}^u = (1 - \zeta)\left(d_c^u + (1 - \delta)d_b^l\right) \tag{10}$$

where $0 \le \zeta \le 1$ is an appropriate chosen dependency coefficient. This will be also assumed in this paper.[1]

Now, to be fully credible, that is, to be sure that (2) is satisfied, the party should prove

$$D\hat{x} + d_{bc}^u \le 0 \tag{11}$$

This non-equality condition is analogous to (4), with the upper limit $L = 0$.

[1]Modification of the addition operator has a disadvantage. As far as the usual addition is commutative and associative (i.e. for the intervals A, B and C it holds $A + B = B + A$ and $A + B + C = (A + B) + C = A + (B + C)$), then the modified operator with operations (9) and (10), denoted below as $+_\zeta$, is only commutative and not associative, because then $(A +_\zeta B) +_\zeta C \ne A +_\zeta (B +_\zeta C)$. Thus, practically, the operator $+_\zeta$ can be used only for pairs of numbers. But this is actually exactly what is needed in the application considered in this paper.

When a party is compliant with risk α, then the part of its distribution that lies above zero is not bigger than α, see Fig. 2 for the geometrical interpretation. That is, it holds $D\hat{x} + d^u_{bc} \le 2\alpha d^u_{bc}$. After simple algebraic manipulations this gives the condition

$$\hat{x}_c + \left[1 - \left(1 + \frac{d^l_{bc}}{d^u_{bc}}\right)\alpha\right] d^u_{bc} \le (1-\delta)\hat{x}_b \tag{12}$$

This condition is analogous to (6). Thus, to prove the compliance with risk α the party has to fulfill its obligation with the inventory emission estimate increased by the value $\left[1 - \left(1 + \frac{d^l_{bc}}{d^u_{bc}}\right)\alpha\right] d^u_{bc}$, dependent on its uncertainty.

3.2 Emission trading

The above compliance-proving policy can be used to modify the rules of emission trading. The main idea presented in earlier papers (Nahorski et al. 2007; Nahorski and Horabik 2008) involves transferring the emission seller uncertainty to the emission buyer together with the quota of emissions traded and then including it in the buyer's emission balance. Here it is adapted to the asymmetric distributions.

Let us denote by $R^{uS}_c = d^{uS}_c / \hat{x}^S_c$ and $R^{lS}_c = d^{lS}_c / \hat{x}^S_c$ the respective relative upper and lower spreads of the uncertainty intervals of the seller and by $\hat{E}^S$ the amount of estimated emission traded. This emission is associated with lower and upper spreads of the uncertainty intervals $\hat{E}^S R^{lS}_c$ or $\hat{E}^S R^{uS}_c$, respectively.

Known limit First, let us consider the simpler case of known limit L. Before the trade the buyer has to satisfy the condition (6), which is reformulated to

$$\hat{x}^B_c + d^{uB}_c - \left(d^{lB}_c + d^{uB}_c\right)\alpha \le L^B$$

After buying $\hat{E}^S$ units of emissions from the seller and including the corresponding uncertainty in the formula, the new condition looks like

$$\hat{x}^B_c - \hat{E}^S + d^{uB}_c + \hat{E}^S R^{uS}_c - \left(d^{uB}_c + \hat{E}^S R^{uS}_c + d^{lB}_c + \hat{E}^S R^{lS}_c\right)\alpha \le L^B$$

The above conditions differ in the following value, which is called *the effective emission* (Nahorski et al. 2007)

$$E_{eff} = \hat{E}^S - \hat{E}^S R^{uS}_c + \hat{E}^S\left(R^{uS}_c + R^{lS}_c\right)\alpha$$

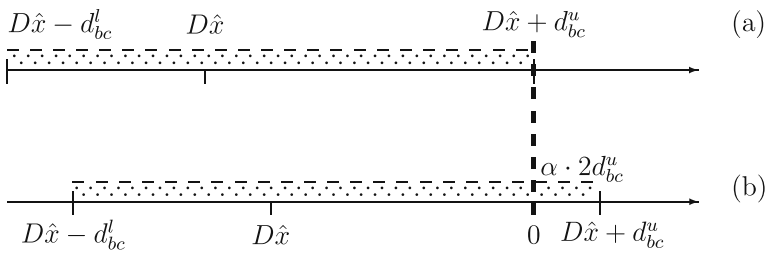

Fig. 2 Full compliance (**a**) and compliance with risk α (**b**) in the interval uncertainty approach for the emission reduction case

which can be transformed to the form

$$E_{eff} = \hat{E}^S \left\{ 1 - \left[1 - \left(1 + \frac{d_c^{lS}}{d_c^{uS}} \right) \alpha \right] R_c^{uS} \right\} \tag{13}$$

The effective emission is smaller than the estimated emission. The bigger the relative upper spread of the uncertainty interval of the seller is, the smaller the effective emission. But it also depends on the ratio d_c^{uS}/d_c^{lS}, and obviously on α.

Emission reduction When emission reduction is required, before the trade the buying party checks the following condition

$$\hat{x}_c^B + d_{bc}^{uB} - (d_{bc}^{uB} + d_{bc}^{lB})\alpha \leq (1 - \delta^B)\hat{x}_b^B$$

After the transaction the condition changes into

$$\hat{x}_c^B - \hat{E}^S + d_{bc}^{uB} + \hat{E}^S R_c^{uS} - (d_{bc}^{uB} + \hat{E}^S R_c^{uS} + d_{bc}^{lB} + \hat{E}^S R_c^{lS})\alpha \leq (1 - \delta^B)\hat{x}_b^B$$

Because of partial cancellation of the subtracted estimated emission and its uncertainty in the buyer's emission balance, the effective emission is

$$E_{eff} = \hat{E}^S \left\{ 1 - \left[1 - \left(1 + \frac{d_c^{lS}}{d_c^{uS}} \right) \alpha \right] R_c^{uS} \right\} \tag{14}$$

This is exactly the same formula as (13). The bigger the seller's upper spread of uncertainty interval is, the fewer the purchased units on the account of the buyer. Expressions (13) and (14) reduce emissions estimated with an arbitrary precision to globally comparable values, which can be directly subtracted from a country's estimated emission. This way it is possible to construct a market for the effective emissions, see Nahorski et al. (2007) and Nahorski and Horabik (2007) for details.

4 Fuzzy uncertainty

The interval uncertainty approach does not use any information on the distribution of inventory errors. Thus, its results are too conservative. Modeling the uncertainty using the stochastic approach causes problems related to the non-linearities of the underlying algebra. Instead, we propose to use the fuzzy approach in modeling uncertainty distribution. It allows for a good approximation of the distribution while keeping the algebra of the interval calculus simple. A short explanation of fuzzy sets and some related notions is given in the Appendix.

In this paper the fuzzy numbers (see Appendix for a definition) are used to model imperfect knowledge of uncertainty. A fuzzy number is a straight generalization of an ordinary number, whose value is uncertain: the situation that we note pertains to greenhouse gas inventories.

Usually, the main problem with the fuzzy set approach is to determine the membership function. Here, we introduce analytical membership functions dependent on parameters. To estimate the parameters, the function can be fitted to the distribution obtained from Monte Carlo simulations, as shown in the sequel. If there is a lack

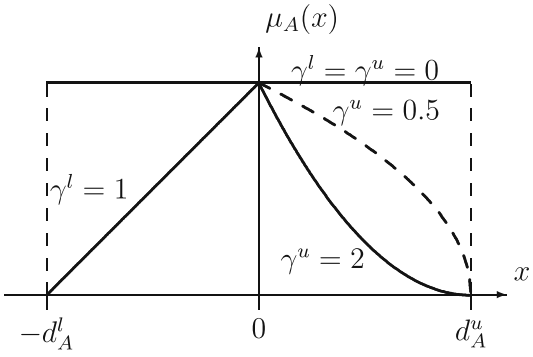

Fig. 3 Membership functions for different values of γ

of experimental distributions, the parameter can be fixed to fit the experimenter expectation.[2]

The most popular membership functions are the triangular or trapezoidal ones. These functions are, however, rather inconvenient for our purpose because of their bad approximations of the distribution tails, which are very important in the applications described here.

Consider a family of fuzzy numbers $A^\gamma = \{(x, \mu^\gamma_A(x)) | x \in \text{supp } A^\gamma\}$ indexed by a vector parameter $\gamma = [\gamma^u_1, \gamma^l_2] \in C^+ \times C^+$, with the support supp $A^\gamma = [-d^l_A, d^u_A]$. The proposed membership function has the form (see Fig. 3)

$$\mu^\gamma_A(x) = \begin{cases} a\left(1 - \frac{x}{d^u_A}\right)^{\gamma^u} & \text{for } 0 \le x \le d^u_A \\ a\left(1 + \frac{x}{d^l_A}\right)^{\gamma^l} & \text{for } d^l_A \le x < 0 \end{cases} \qquad \gamma^l, \gamma^u \neq 0 \tag{15}$$

where a is a normalizing factor used for fitting the membership function to empirical distributions. In the theoretical considerations it can be assumed that the membership function has been normalized and therefore $a = 1$ is taken in the sequel. Let us note that taking $\gamma^l = \gamma^u = 0$ we get the even distribution (see Fig. 3) and actually reduce the considerations to the interval case.

Figure 4 presents an estimate of an asymmetric distribution obtained using the Monte Carlo method and presented in Winiwarter and Muik (2007).

4.1 Compliance

It is assumed that the uncertainty of the estimate $\hat{x}_b$ is described by the membership function

$$\mu^\gamma_{\hat{x}_b}(x) = \begin{cases} \left(1 - \frac{x - \hat{x}_b}{d^u_b}\right)^{\gamma^u_b} & \text{for } \hat{x}_b \le x \le \hat{x}_b + d^u_b \\ \left(1 + \frac{x - \hat{x}_b}{d^l_b}\right)^{\gamma^l_b} & \text{for } \hat{x}_b - d^l_b \le x < \hat{x}_b \end{cases}$$

[2] It is perhaps worth mentioning at this point that we treat the fuzzy approach only as an approximation of distribution and algebraic rules for the variables and not to introduce the possibility function, see for example Bandemer (2006), which gives another possible approach to the problem.

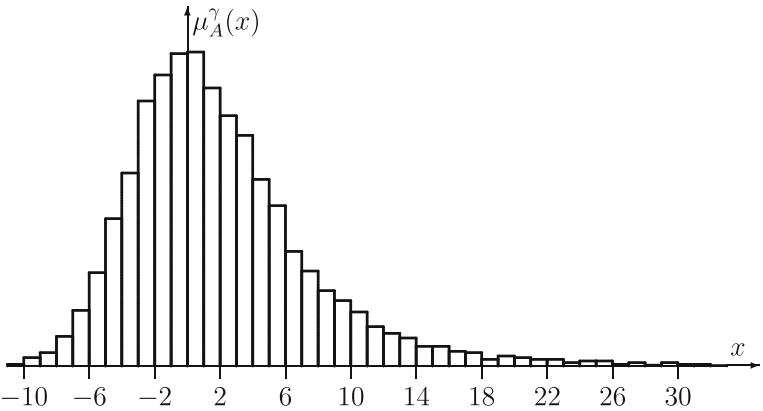

Fig. 4 An estimate of a membership function $\mu_A^{\gamma}(x)$ calculated using the Monte Carlo method

and of the estimate $\hat{x}_c$ by

$$\mu_{\hat{x}_c}^{\gamma}(x) = \begin{cases} \left(1 - \frac{x-\hat{x}_c}{d_c^u}\right)^{\gamma_c^u} & \text{for } \hat{x}_c \le x \le \hat{x}_c + d_c^u \\ \left(1 + \frac{x-\hat{x}_c}{d_c^l}\right)^{\gamma_c^l} & \text{for } \hat{x}_c - d_c^l \le x < \hat{x}_c \end{cases} \tag{16}$$

Known limit We start with the exactly known limit case. First, we calculate by integration the whole area A under the membership function. It is the sum of two areas, see Fig. 5

$$A = A^l + A^u$$

$$A^l = \int_{\hat{x}_c - d_c^l}^{\hat{x}_c} \left(1 + \frac{x - \hat{x}_c}{d_c^l}\right)^{\gamma_c^l} dx = \frac{d_c^l}{1 + \gamma_c^l}$$

$$A^u = \int_{\hat{x}_c}^{\hat{x}_c + d_c^u} \left(1 - \frac{x - \hat{x}_c}{d_c^u}\right)^{\gamma_c^u} dx = \frac{d_c^u}{1 + \gamma_c^u}$$

We now want to find the distance $x_{c\alpha}$ between $\hat{x}_c$ and $\hat{x}_c + x_{c\alpha}$, where the latter is the value cutting off the most right αth part of the area under the membership function, see Fig. 5. This area, denoted A_α, for $0 \le \alpha \le A^u/(A^l + A^u)$, where A^l is the area under the left branch of the membership function and A^u under the right branch is

$$A_\alpha = \int_{\hat{x}_c + x_{c\alpha}}^{\hat{x}_c + d_c^u} \left(1 - \frac{x - \hat{x}_c}{d_c^u}\right)^{\gamma_c^u} dx = \frac{d_c^u}{1 + \gamma_c^u} \left(1 - \frac{x_{c\alpha}}{d_c^u}\right)^{1+\gamma_c^u}$$

Now, it must hold

$$A_\alpha = \alpha A$$

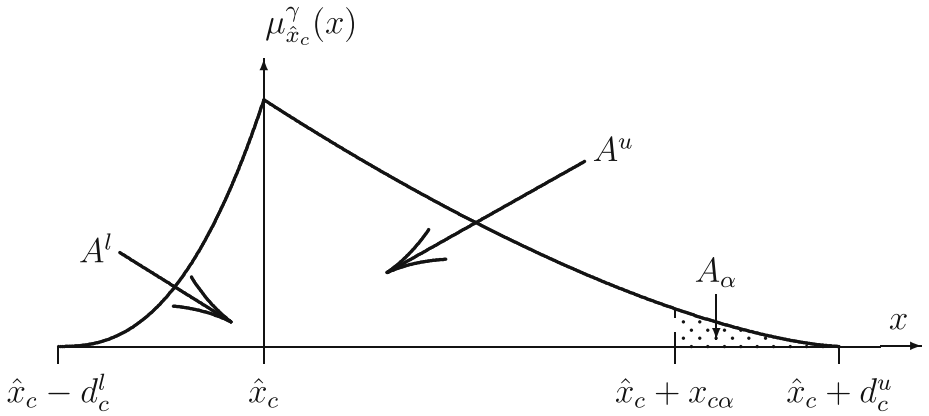

Fig. 5 Definition of areas under asymmetric fuzzy number membership function

which after some algebraic manipulations gives

$$x_{c\alpha} = \left\{1 - \left[\left(1 + \frac{d^l_c}{d^u_c}\frac{1+\gamma^u_c}{1+\gamma^l_c}\right)\alpha\right]^{\frac{1}{1+\gamma^u_c}}\right\} d^u_c$$

Finally, the compliance checking condition is

$$\hat{x}_c + \left\{1 - \left[\left(1 + \frac{d^l_c}{d^u_c}\frac{1+\gamma^u_c}{1+\gamma^l_c}\right)\alpha\right]^{\frac{1}{1+\gamma^u_c}}\right\} d^u_c \le L \tag{17}$$

For the interval uncertainty case $\gamma^u_c = \gamma^l_c = 0$. Then the above condition is the same as (6). For the symmetric case $d^l_c = d^u_c = d_c$ and $\gamma^l_c = \gamma^u_c = \gamma_c$, and the above condition takes the form

$$\hat{x}_c + \left[1 - (2\alpha)^{\frac{1}{1+\gamma_c}}\right] d_c \le L$$

This formula was derived in Nahorski and Horabik (2008).

For the symmetric case, only the range $0 \le \alpha \le 0.5$ is practically worth being considered, as for $\alpha = 0.5$ the above condition takes the form $\hat{x}_c \le L$, and for $\alpha > 0.5$ we would allow for exceeding the limit, that is, for $\hat{x}_c > L$. For the asymmetric case the range $0 \le \alpha \le A^u/(A^l + A^u)$ should be considered. Thus, the limiting α can take values greater or smaller than 0.5. For the interval uncertainty the range will be $0 \le \alpha \le d^u/(d^l + d^u)$.

In addition, let us note that for the right-skewed distributions, as in Fig. 4, the probability of non-compliance is greater than 0.5 when $\hat{x}_c$ is equal to the limit L. It is a consequence of the fact that in this case of asymmetry, it is more likely that the limit L is exceeded than that it is not attained.

Emission reduction For the emission reduction case, to find the membership function of the fuzzy number $D\hat{x} = \hat{x}_c - (1-\delta)\hat{x}_b$ as a linear combination of the fuzzy numbers $\hat{x}_b$ and $\hat{x}_c$, the η-cuts will be used, see Appendix for an explanation of this

notion. For the number $\hat{x}_c$ the upper $\hat{x}_c^{\eta u}$ and the lower $\hat{x}_c^{\eta l}$ ends of the η-cut are as follows, see Fig. 6. For $\hat{x}_c^{\eta u}$ we have

$$\left(1 - \frac{\hat{x}_c^{\eta u} - \hat{x}_c}{d_c^u}\right)^{\gamma_c^u} = \eta$$

Then, assuming $\gamma_c^u \neq 0$,

$$\hat{x}_c^{\eta u} = \hat{x}_c + d_c^u\left(1 - \eta^{\frac{1}{\gamma_c^u}}\right)$$

In the same way, for $\hat{x}_c^{\eta l}$, assuming $\gamma_c^l \neq 0$,

$$\left(1 + \frac{\hat{x}_c^{\eta l} - \hat{x}_c}{d_c^l}\right)^{\gamma_c^l} = \eta$$

and

$$\hat{x}_c^{\eta l} = \hat{x}_c - d_c^l\left(1 - \eta^{\frac{1}{\gamma_c^l}}\right)$$

For $\gamma_c^u = 0$ or $\gamma_c^l = 0$ we have $\eta = 1$. For this case the expression like $\eta^{\frac{1}{\gamma_c^u}}$ is not formally defined. Thus, we additionally define

$$\eta^{\frac{1}{\gamma_c^u}} = 0, \qquad \text{for} \quad \gamma_c^u = 0$$

$$\eta^{\frac{1}{\gamma_c^l}} = 0 \qquad \text{for} \quad \gamma_c^l = 0$$

The fuzzy number $\hat{x}_b$ can be treated analogously. But we consider the number $-(1-\delta)\hat{x}_b$. Taking analogous assumptions and additional definitions as above, we now look for $\hat{x}_b^{\eta u}$ satisfying

$$\left(1 - \frac{\hat{x}_b^{\eta u} + (1-\delta)\hat{x}_b}{(1-\delta)d_b^u}\right)^{\gamma_b^u} = \eta$$

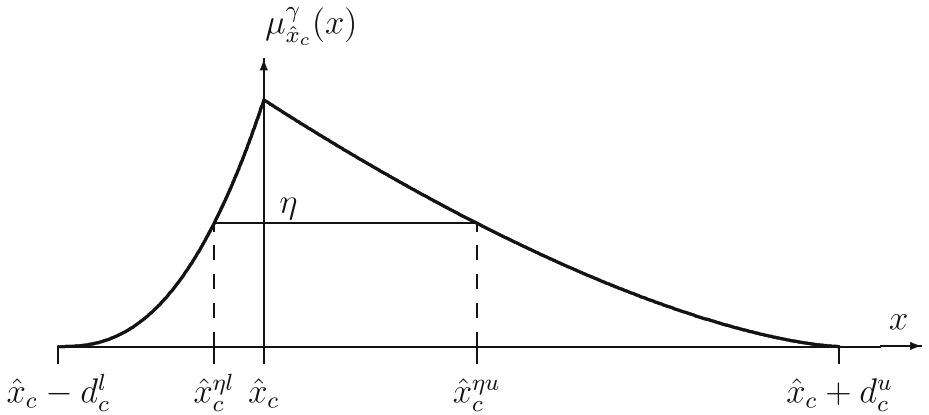

Fig. 6 Asymmetric fuzzy number and definitions of related parameters

from where the upper end $\hat{x}_b^{\eta u}$ of the η-cut is given by

$$\hat{x}_b^{\eta u} = -(1-\delta)\hat{x}_b + d_b^u(1-\delta)\left(1-\eta^{\frac{1}{\gamma_b^u}}\right)$$

For the lower end $\hat{x}_b^{\eta l}$ of the η-cut the equation

$$\left(1+\frac{\hat{x}_b^{\eta l}+(1-\delta)\hat{x}_b}{(1-\delta)d_b^l}\right)^{\gamma_b^l} = \eta$$

provides

$$\hat{x}_b^{\eta l} = -(1-\delta)\hat{x}_b - d_b^l(1-\delta)\left(1-\eta^{\frac{1}{\gamma_b^l}}\right)$$

Finally, the η-cut of the number $D\hat{x}$ is obtained by applying the modified interval calculus rules (9) and (10) for the sum of the η-cuts of the numbers $\hat{x}_c$ and $-(1-\delta)\hat{x}_b$. Thus

$$D\hat{x}^{\eta u} = D\hat{x} + (1-\zeta)\left[d_c^u\left(1-\eta^{\frac{1}{\gamma_c^u}}\right) + d_b^l(1-\delta)\left(1-\eta^{\frac{1}{\gamma_b^l}}\right)\right] \tag{18}$$

$$D\hat{x}^{\eta l} = D\hat{x} - (1-\zeta)\left[d_c^l\left(1-\eta^{\frac{1}{\gamma_c^l}}\right) + d_b^u(1-\delta)\left(1-\eta^{\frac{1}{\gamma_b^u}}\right)\right] \tag{19}$$

The above equations show dependences of $D\hat{x}^{\eta l}$ and $D\hat{x}^{\eta u}$ on η, that is, they are the reverse functions of the two branches of the membership function $\mu^{\gamma}_{D\hat{x}}(x)$, see Fig. 6.

Let us now transform (18) to

$$1-\frac{D\hat{x}^{\eta u}-D\hat{x}}{d_{bc}^u} = \frac{d_c^u\eta^{1/\gamma_c^u}+d_b^l(1-\delta)\eta^{1/\gamma_b^l}}{d_c^u+d_b^l(1-\delta)} \tag{20}$$

where d_{bc}^u is given by (10), and define γ_{bc}^u to satisfy the equation

$$\frac{d_c^u\eta^{1/\gamma_c^u}+d_b^l(1-\delta)\eta^{1/\gamma_b^l}}{d_c^u+d_b^l(1-\delta)} = \eta^{\frac{1}{\gamma_{bc}^u}}$$

From the above

$$\gamma_{bc}^u = \frac{1}{\log_\eta \frac{d_c^u\eta^{1/\gamma_c^u}+d_b^l(1-\delta)\eta^{1/\gamma_b^l}}{d_c^u+d_b^l(1-\delta)}} = \frac{\log\eta}{\log \frac{d_c^u\eta^{1/\gamma_c^u}+d_b^l(1-\delta)\eta^{1/\gamma_b^l}}{d_c^u+d_b^l(1-\delta)}} \tag{21}$$

In the spirit of earlier additional definitions we also define

$$\gamma_{bc}^u = 0 \qquad \text{for} \quad \gamma_c^u = 0 \quad \text{or} \quad \gamma_b^l = 0$$

Now it is possible to write the right branch of the membership function as

$$\mu^{\gamma u}_{\hat{x}_{bc}}(x) = \left(1-\frac{x-D\hat{x}}{d_{bc}^u}\right)^{\gamma_{bc}^u} \qquad D\hat{x} \le x \le D\hat{x}+d_{bc}^u \tag{22}$$

Likewise we get

$$\mu^{\gamma^l}_{\hat{x}_{bc}}(x) = \left(1 + \frac{x - D\hat{x}}{d^l_{bc}}\right)^{\gamma^l_{bc}} \qquad D\hat{x} - d^l_{bc} \le x \le D\hat{x} \tag{23}$$

where d^l_{bc} is given by (9), and

$$\gamma^l_{bc} = \frac{1}{\log_\eta \frac{d^l_c \eta^{1/\gamma^l_c} + d^u_b (1-\delta)\eta^{1/\gamma^u_b}}{d^l_c + d^u_b (1-\delta)}} = \frac{\log \eta}{\log \frac{d^l_c \eta^{1/\gamma^l_c} + d^u_b (1-\delta)\eta^{1/\gamma^u_b}}{d^l_c + d^u_b (1-\delta)}} \tag{24}$$

with

$$\gamma^l_{bc} = 0 \qquad \text{for} \quad \gamma^l_c = 0 \quad \text{or} \quad \gamma^u_b = 0$$

Now, the most right αth part of the area under the membership function (22) is

$$A_\alpha = \int_{D\hat{x}+x_\alpha}^{D\hat{x}+d^u_{bc}} \left(1 - \frac{x - D\hat{x}}{d^u_{bc}}\right)^{\gamma^u_{bc}} dx = \frac{d^u_{bc}}{1+\gamma^u_{bc}} \left(1 - \frac{x_\alpha}{d^u_{bc}}\right)^{1+\gamma^u_{bc}}$$

and the area under the entire membership function (22)–(23) is

$$\begin{aligned} A &= \int_{D\hat{x}-d^l_{bc}}^{D\hat{x}} \left(1 + \frac{x - D\hat{x}}{d^l_{bc}}\right)^{\gamma^l_{bc}} dx + \int_{D\hat{x}}^{D\hat{x}+d^u_{bc}} \left(1 - \frac{x - D\hat{x}}{d^u_{bc}}\right)^{\gamma^u_{bc}} dx = \\ &= \frac{d^l_{bc}}{1+\gamma^l_{bc}} + \frac{d^u_{bc}}{1+\gamma^u_{bc}} \end{aligned} \tag{25}$$

As $A_\alpha = \alpha A$, its solution for x_α, denoted $x_{bc\alpha}$, has the form

$$x_{bc\alpha} = \left\{1 - \left[\left(1 + \frac{d^l_{bc}}{d^u_{bc}} \frac{1+\gamma^u_{bc}}{1+\gamma^l_{bc}}\right)\alpha\right]^{\frac{1}{1+\gamma^u_{bc}}}\right\} d^u_{bc} \tag{26}$$

and finally the compliance condition is

$$\hat{x}_c + \left\{1 - \left[\left(1 + \frac{d^l_{bc}}{d^u_{bc}} \frac{1+\gamma^u_{bc}}{1+\gamma^l_{bc}}\right)\alpha\right]^{\frac{1}{1+\gamma^u_{bc}}}\right\} d^u_{bc} \le (1-\delta)\hat{x}_b \tag{27}$$

This condition is analogous to (17). For the interval case $\gamma^l_{bc} = \gamma^u_{bc} = 0$ and (27) reduces to (12). For the symmetric distribution $d^l_{bc} = d^u_{bc} = d_{bc}$ and $\gamma^l_{bc} = \gamma^u_{bc} = \gamma_{bc}$ and it reduces to

$$\hat{x}_c + \left[1 - (2\alpha)^{\frac{1}{1+\gamma_{bc}}}\right] d_{bc} \le (1-\delta)\hat{x}_b \tag{28}$$

The condition (28) has been derived in Nahorski and Horabik (2007).

4.2 Emission trading

The formula for the effective emission can be quite easily obtained for the symmetric distribution (28) using derivations similar to the interval case. Before the trade, the buying party has to satisfy the condition

$$\hat{x}_c^B + \left[1 - (2\alpha)^{\frac{1}{1+\gamma_{bc}^B}}\right] d_{bc}^B \leq (1-\delta^B)\hat{x}_b^B$$

and after buying $\hat{E}^S$ emission units from the seller it becomes

$$\hat{x}_c^B - \hat{E}^S + \left[1 - (2\alpha)^{\frac{1}{1+\gamma_{bc}^B}}\right] (d_{bc}^B + \hat{E}^S R_c^S) \leq (1-\delta^B)\hat{x}_b^B$$

Then the effective emission is

$$E_{eff} = \hat{E}^S \left\{1 - \left[1 - (2\alpha)^{\frac{1}{1+\gamma_{bc}^B}}\right] R_c^S\right\} \tag{29}$$

where $R_c^S = d_c^S/\hat{x}_c^S$ and for the symmetric distributions $d_c^S = d_c^{uS} = d_c^{lS}$.

However, the problem becomes more difficult for the asymmetric distributions, as then the uncertainty distribution bounds d_{bc}^l and d_{bc}^u enter non-linearly into the compliance condition (27). This is why linearization is now used to obtain the result. The exact derivation is presented in Electronic Supplementary Material. That way the following expression for the effective emission is obtained

$$E_{eff} = \hat{E}^S \left\{1 - \left\{1 - \left[\left(1 + \frac{d_c^{lS}}{d_c^{uS}}\right)\alpha\right]^{\frac{1}{1+\gamma_{bc}^{uB}}}\right\} R_c^{uS}\right\} \tag{30}$$

It generalizes expressions for simpler cases. In particular, for the known limit case the following substitution should be made: $\gamma_{bc}^{uB} \to \gamma_c^{uB}$. For the symmetric distributions the substitutions are: $d_c^{lS} \to d^S$, $d_c^{uS} \to d^S$, $\gamma_{bc}^{uB} \to \gamma_{bc}^B$, which provide (29). For the interval uncertainty: $\gamma_{bc}^{uB} \to 0$, which gives (14).

In comparison with the formula (14) for the interval uncertainty, the formulas (29) and (30) depend on parameters γ_{bc}^B or γ_{bc}^{uB} of the emission buyer uncertainty distributions. This would considerably complicate the market, as the traded quota depends in such a case both on the seller and the buyer uncertainty distributions. This problem will not be discussed in this paper.

4.3 Equivalence of approaches

We start here with a summary of results. Table 1 provides relevant formulas for compliance condition and effective emission in the case of known limit for various types of uncertainty models considered.

Let us note that, for a given case, the same compliance condition or the same effective emissions can be obtained for the interval model as for the fuzzy model, choosing an appropriate value of α in the former one. Let us denote by α_I the value for the interval model and by α_F for the fuzzy one. It can be noticed that actually it is enough to consider only the asymmetric cases, as the results for the symmetric cases are obtained taking specific values od parameters.

Table 1 Model review

Model	Compliance checking	Effective emission
Interval symmetric	$\hat{x}_c + (1-2\alpha)d_c \le L$	$E_{eff} = \hat{E}^s\left[1-(1-2\alpha)\,R_c^S\right]$
Interval asymmetric	$\hat{x}_c + \left[1-\left(1+\frac{d_c^l}{d_c^u}\right)\alpha\right]d_c^u \le L$	$E_{eff} = \hat{E}^s\left\{1-\left[1-\left(1+\frac{d_c^{lS}}{d_c^{uS}}\right)\alpha\right]R_c^{uS}\right\}$
Fuzzy symmetric	$\hat{x}_c + \left[1-(2\alpha)^{\frac{1}{1+\gamma_c}}\right]d_c \le L$	$E_{eff} = \hat{E}^s\left\{1-\left[1-(2\alpha)^{\frac{1}{1+\gamma_c^B}}\right]R_c^S\right\}$
Fuzzy asymmetric	$\hat{x}_c + \left\{1-\left[(1+\frac{d_c^l}{d_c^u}\frac{1+\gamma_c^u}{1+\gamma_c^l})\alpha\right]^{\frac{1}{1+\gamma_c^u}}\right\}d_c^u \le L$	$E_{eff} = \hat{E}^s\times\left\{1-\left\{1-\left[\left(1+\frac{d_c^{lS}}{d_c^{uS}}\right)\alpha\right]^{\frac{1}{1+\gamma_c^{uB}}}\right\}R_c^{uS}\right\}$

Equaling the effective emissions $E_{eff,F} = E_{eff,I}$, from the second and the fourth rows in the last column of the Table 1, after simple algebraic manipulations we arrive at the following condition

$$\left[\left(1+\frac{d_c^{lS}}{d_c^{uS}}\right)\alpha_I\right]^{1+\gamma_{bc}^{uB}} = \left(1+\frac{d_c^{lS}}{d_c^{uS}}\right)\alpha_F$$

If the cases $\alpha_F = 0$ (no noncompliance risk) and $\gamma_{bc}^{uB} = 0$ (interval uncertainty) are excluded, then

$$\frac{\alpha_I}{\alpha_F} = \left[\left(1+\frac{d_c^{lS}}{d_c^{uS}}\right)\alpha_I\right]^{-\gamma_{bc}^{uB}}$$

Thus we have

$$\alpha_I > \alpha_F \qquad \text{for} \quad \alpha_I \le \frac{d_c^{uS}}{d_c^{uS}+d_c^{lS}} \quad \text{and} \quad \gamma_{bc}^{uB} > 0$$

Both conditions are very mild. The second is obviously satisfied. Taking into account that in the up to now considered cases $d_c^{uS} \ge d_c^{lS}$, then in the first condition the upper limit is not smaller than 0.5, which is true for the symmetric case.

For the compliance checking, comparing formulas from the second and the fourth rows in the middle column we get

$$\left[\left(1+\frac{d_c^l}{d_c^u}\right)\alpha_I\right]^{1+\gamma_c^u} = \left(1+\frac{d_c^l}{d_c^u}\frac{1+\gamma_c^u}{1+\gamma_c^l}\right)\alpha_F$$

from where

$$\frac{\alpha_I}{\alpha_F} = \frac{1+\frac{d_c^l}{d_c^u}\frac{1+\gamma_c^u}{1+\gamma_c^l}}{1+\frac{d_c^l}{d_c^u}}\left[\left(1+\frac{d_c^l}{d_c^u}\right)\alpha_I\right]^{-\gamma_c^u}$$

Now, if $\alpha_I \le \frac{d_c^u}{d_c^u+d_c^l}$ and $\gamma_c^u \ge \gamma_c^l > 0$, and at least one of these conditions is strict, then again

$$\alpha_I > \alpha_F$$

Table 2 Dependence of α_I on α_F and γ_{bc}^{uB}

$\alpha_F \downarrow \gamma_{bc}^{uB} \rightarrow$	0.1	0.5	1	1.5	2	2.5
$d_c^l/d_c^u = 0.2$						
0.05	0.06	0.13	0.20	0.27	0.33	0.37
0.10	0.12	0.20	0.29	0.36	0.41	0.45
0.15	0.18	0.27	0.35	0.42	0.47	0.51
0.20	0.23	0.32	0.41	0.47	0.52	0.55
0.25	0.28	0.37	0.46	0.51	0.56	0.59
$d_c^l/d_c^u = 0.5$						
0.05	0.06	0.12	0.18	0.24	0.28	0.32
0.10	0.12	0.19	0.26	0.31	0.35	0.39
0.15	0.17	0.25	0.32	0.37	0.41	0.44
0.20	0.22	0.30	0.37	0.41	0.45	0.47
0.25	0.27	0.35	0.41	0.45	0.48	0.50
$d_c^l/d_c^u = 1$ (symmetric case)						
0.05	0.06	0.11	0.16	0.20	0.23	0.26
0.10	0.12	0.17	0.22	0.26	0.29	0.32
0.15	0.17	0.22	0.27	0.31	0.33	0.35
0.20	0.22	0.27	0.32	0.35	0.37	0.38
0.25	0.27	0.32	0.35	0.38	0.40	0.41

Thus, the noncompliance risk parameter α in the interval uncertainty model has to be greater than in the fuzzy model to get the same compliance conditions or effective emissions.

Dependence of α_I on α_F and γ_{bc}^{uB} for effective emissions is shown in Table 2. The results show that α_I rises quickly when γ_{bc}^{uB} rises. In cases considered in our calculations, estimates of γ_{bc}^{uB} close to or much higher than 1.5 were obtained. Then, practically it seems that $\alpha_I \geq 0.3$ should be taken even for small values of α_F.

An interpretation of these results is quite straightforward. Within the considered family of distributions, ignorance of the uncertainty distribution in the interval case requires a greater reduction. To obtain the same effective emissions as for the fuzzy uncertainties, a bigger substitutional non-compliance risk should be adopted in the interval approach. Thus, for α_I, at least the values 0.3 or higher should be taken

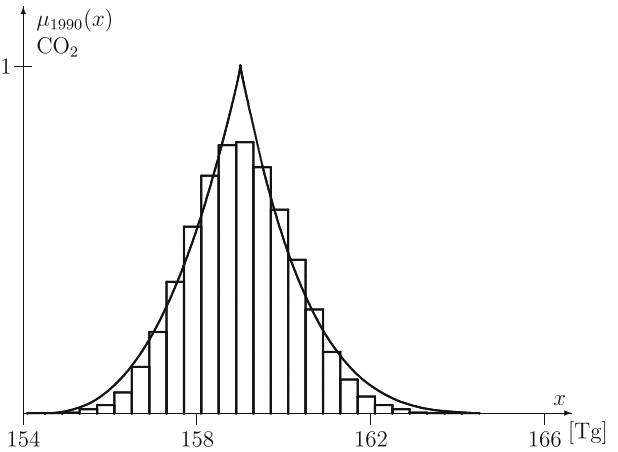

Fig. 7 Fit of a membership function $\mu_A^{\gamma}(x)$ to the histogram for emission of CO_2

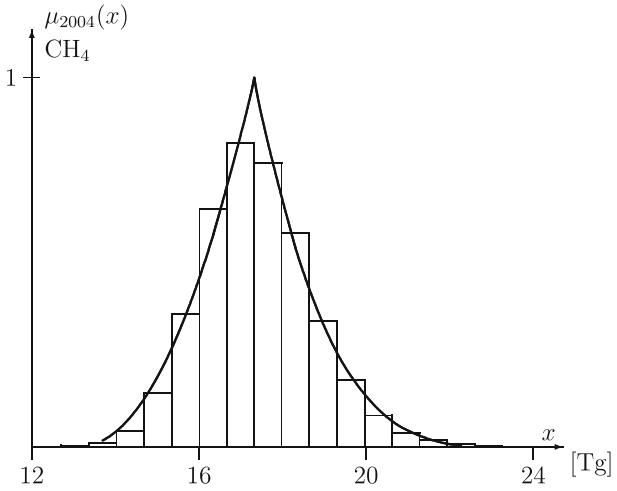

Fig. 8 Fit of a membership function $\mu_A^{\gamma}(x)$ to the histogram for emission of CH_4

to compensate for ignorance of the exact knowledge of the uncertainty interval distribution, even if a small non-compliance risk is actually meant.

5 An example

In the example the data from the Monto Carlo simulation presented in Ramirez et al. (2006) are used. Uncertainty distributions of emissions of three gases, carbon dioxide (CO_2), methane (CH_4), and fluorine (F), are considered. The uncertainty distributions were chosen to illustrate the proposed rules of trade and are depicted in Figs. 7, 8 and 9 together with fits of the distribution functions (15). It is assumed that each emission is related to different companies, called CO_2, CH_4 and F, respectively. Table 3 contains parameters of the distributions obtained from the fits.

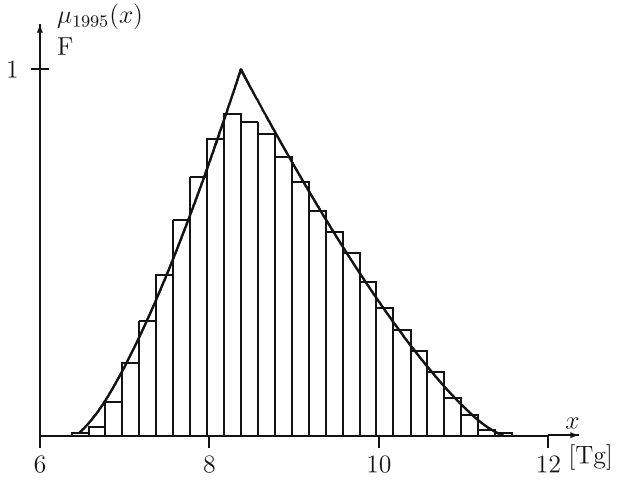

Fig. 9 Fit of a membership function $\mu_A^{\gamma}(x)$ to the histogram for emission of F

Table 3 Parameters of the distributions

Distribution	d^l [Tg]	γ^l	γ^u	d^u [Tg]
CO_2	4.8	2.6	4.5	6.9
CH_4	4.3	2.1	3.9	6.7
F	2.0	1.4	1.4	3.1

We do not consider the compliance, only the trade. Let us then suppose that the three companies mentioned: CO_2, CH_4, and F, want to trade with each other. The uncertainty of emissions in company CO_2 is small, less than 4 percent, while in the rest it is around 38 percent. On the other hand, the shape of the uncertainty distributions of CO_2 and CH_4 are similar, with values γ of the order of 2–2.5 for the lower and 4–4.5 for the upper branch, while the shape of F is close to triangular, with γ equal to 1.4. In Table 4 the values of E_{eff} are depicted for three assumed trades, when each company in turn is the seller while the others are buyers. Two values of the original non-compliance risk $\alpha = 0.05$ or 0.1 were assumed and substitutional values of α_I are given in the right-hand side of the table. Most of them are of the order of 0.4. For CO_2, with small uncertainty, the values E^1_{eff} are only slightly smaller than 1. The values E^2_{eff} and E^3_{eff} are much smaller, around 0.8–0.9.

Let us note that for the fuzzy distribution there is no unique substitutional risk parameter α_I related with the seller, because it also depends on who the buyer is. This is what causes problems in the trade as compared to the interval case. A way of avoiding this might be that a common value 0.4 or a smaller one, like 0.35, is taken for α_I to organize the market with a substitutional interval uncertainty. This way the market scheduled in Nahorski et al. (2007) can be applied. A market with substitutional risk parameters α_I dependent on the buyer is, however, an interesting question. It will be considered elsewhere.

6 Conclusions

The paper deals with the problem of checking compliance of pollutant emissions with a given limit in the case where the observed emission values are highly uncertain with asymmetric uncertainty distributions. High uncertainty should be also considered in trading in emission permits, which is frequently used to minimize the emission abatement cost, and this is also done in the paper. Asymmetric uncertainty is evidenced by recent investigations, and particularly by Monte Carlo simulations of uncertainty distributions.

Table 4 Effective emissions in the trade and substitutional values of α_I for interval uncertainty

Emission	R^u_c	E^1_{eff}	E^2_{eff}	E^3_{eff}	α^1_I	α^2_I	α^3_I
$\alpha = 0.05$							
CO_2	0.043	Seller	0.86	0.86	–	0.21	0.36
CH_4	0.385	0.98	Seller	0.85	0.39	–	0.36
F	0.371	0.97	0.75	Seller	0.39	0.37	–
$\alpha = 0.1$							
CO_2	0.043	Seller	0.89	0.90	–	0.28	0.41
CH_4	0.385	0.99	Seller	0.88	0.44	–	0.42
F	0.371	0.98	0.79	Seller	0.44	0.42	–

Asymmetry of distributions biases the compliance and trading results, and it constitutes an additional issue in troubles related to uncertainty of emission inventories. This is due to unequal probabilities of occurrence of the real emission below and above the nominal inventory value. The Monte Carlo simulations of national greenhouse gases inventories (Winiwarter and Muik 2007; Ramirez et al. 2006) show that the distributions are right-skewed, that is, real emissions higher that the nominal value are more likely than the smaller ones. This means that even if the nominal inventory value is exactly equal to the given limit and is considered to be compliant according to the present standard, it is actually more probable that the real emission is non-compliant than that it is compliant.

An interesting case[3] of an asymmetric distribution of uncertainty is connected with the risk of valuing forest carbon offsets caused by accidental losses, for example, due to wildfires (Hurteau et al. 2009). The uncertainty there has a specific one-sided distribution. This case has already entered the implementation stage in the United States forest carbon storage project (Mignone et al. 2009). However, the solutions applied there take into account that the related uncertainty is eventually resolved in the future, as the damages are known after they have happened. This is in contrast with the case discussed in this paper, where uncertainties are an inherent part of data considered at all stages of decision making.

The idea proposed in this paper is based on grounding the derivations in the fuzzy set approach. A family of fuzzy numbers depending on free parameters is introduced. These parameters can be chosen to appropriately shape the distribution of uncertainty. The approach provides the closed form formulas, which can be used for designing a market for effective emission permits. A market with the effective emission permits has been outlined in earlier papers (Nahorski et al. 2007; Nahorski and Horabik 2008) for the symmetric case. That construction is also valid in the asymmetric case discussed in this paper, after appropriate adaptation. However, for the most general case of asymmetric membership functions, a closed analytical solution could not be found. An approximate solution was considered for this case, and a generalized rule for compliance has been derived.

Application of the fuzzy numbers and consideration of asymmetric distributions enabled us to much more precisely determine the required level of reduced inventories to obtain a high likelihood of fulfilling the given limit or reduction. Moreover, better accuracy in terms of determining the level give rise to better scaling of the amounts of emission emitted by parties for use in trading, which has a measurable financial meaning. Approximating distribution by a function dependent on parameters allowed us to derive the analytical expressions for reduction of emissions and for scaling the traded emissions. The distribution parameters have been acquired by fitting the distribution functions to the data from the Monte Carlo simulations.

The results obtained are generalizations of the results derived for the interval and symmetric uncertainty models. However, it was shown that the rules for the interval case can be used instead of the generalized ones, provided that the appropriately higher value of the risk of non-compliance is substituted in the interval case.

Although the fits of the functions presented in this paper to the data are quite good, except perhaps in the central part of the uncertainty interval, the question of

[3]This direction of research has been brought to our attention by one of undisclosed reviewers.

a possibly better fit to the data has been raised by one of the anonymous reviewers. As this is certainly possible with a more flexible class of functions, the possibility of obtaining a close analytical solution may be challenging. It will be a subject of further investigations.

Appendix: Fuzzy sets and fuzzy numbers

To introduce the notion of a fuzzy set, let us first consider a classical set A from an universe U. This can be conveniently described by the characteristic function χ_A defined as

$$\chi_A(u) = \begin{cases} 1 \text{ if } u \in A \\ 0 \text{ if } u \notin A \end{cases}$$

which says that a point $u \in U$ belongs to the set, if $\chi_A(u) = 1$, or does not belong, if $\chi_A(u) = 0$.

In a fuzzy set the characteristic function χ_A is generalized to take any value from the interval [0, 1]. It is then called *a membership function* and is denoted μ_A. The value of a membership function $\mu_A(u)$ reflects the degree of acceptance of the point u to the set. Thus, *a fuzzy set* is characterized by the set A and the membership function μ_A. A usual set is then a special fuzzy set with the membership function being the characteristic function. A comparison of a membership function and a characteristic function of a set is shown in Fig. 10.

A fuzzy set can be also fully characterized by a family of so-called η-cuts[4] denoted by A_η, that is, points of U, for which the value $\mu_A(u)$ assumes at least the value η. See Fig. 10, where an example of a η-cut for $\eta = 0.5$ is depicted.

Two additional notions connected with a fuzzy set are worth mentioning. One is *the support*, called supp A, which is the set of points u, for which the membership function is positive, that is,

$$\text{supp } A = \{u \in U : \mu_A(u) > 0\}$$

Another definition of the support may be formulated using η-cuts, as

$$\text{supp } A = \lim_{\eta \to 0} A_\eta$$

The second notion is *the core* of the fuzzy set, called core A, which is the set of points, for which the membership function is equal 1, that is,

$$\text{core } A = \{u \in U : \mu_A(u) = 1\}$$

Using the notion of the η-cuts we may also write

$$\text{core } A = A_1$$

[4]Here we name the η-cut of a fuzzy set A the notion usually called the α-cut, i.e. the set $A_\eta = \{x \in \text{supp } A | \mu_A(x) \geq \eta\}$, for $\eta \in (0, 1]$.

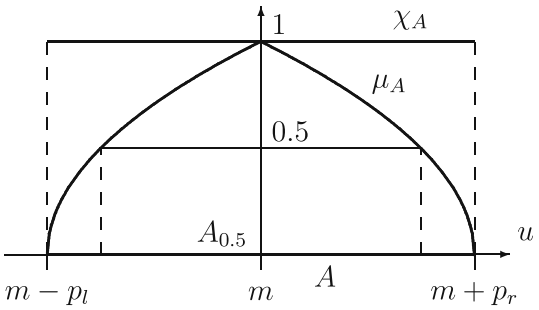

Fig. 10 The characteristic function and a membership functions of the set A

A fuzzy set A is called *a fuzzy number*, if it satisfies three additional conditions:

1. core A consists of only one point.
2. The membership function does not increase starting from the core point toward both sides.
3. Every η-cut is a (connected) closed interval.

A weaker definition of a fuzzy number is often used, with the first condition replaced by

1' There is a point belonging to the core A.

But in this paper we use the former stronger definition.

The η-cuts for a fuzzy number form a family of intervals. Each interval can be interpreted as our measure of knowledge of the core value. Values of the level η close to 1 mean that we are highly convinced that the core value is precise. Small values of η, close to 0, mean that our conviction is low. See also Dubois and Prade (2005) for more formal discussion of this subject. Calculations performed on fuzzy numbers allow us to process all of this knowledge together.

Technically, two functions defined for non-negative arguments may be introduced, L and R, (Bandemer 2006), such that they have the unique value 1 at 0, $L(0) = R(0) = 1$, equal zero for arguments greater or equal 1, $L(u) = R(u) = 0$ for $u \geq 1$, and are not increasing. Then, given that core $A = \{m\}$, the membership function of a fuzzy number may be constructed using the above functions as its left and right branches

$$\mu_A^l(u) = L\left(\frac{m-u}{p_l}\right) \quad \text{for } u \leq m \tag{31}$$

$$\mu_A^r(u) = R\left(\frac{u-m}{p_r}\right) \quad \text{for } u \geq m \tag{32}$$

where p_l and p_r are scale parameters, see Fig. 10. Let us denote the fuzzy number constructed this way as $A = (m, p_l, p_r)_{LR}$.

Although operations on fuzzy sets or fuzzy numbers can be defined in a more general context, they are first restricted only to fuzzy numbers described in the

above LR form. For two fuzzy numbers $A = (m, p_l, p_r)_{LR}$ and $B = (n, q_l, q_r)_{LR}$ the following operations are defined, see Dubois and Prade (1978):

1. Addition

$$A + B = (m + n, p_l + q_l, p_r + q_r)_{LR} \tag{33}$$

2. Multiplication by a positive real number c

$$cA = (cm, cp_l, cp_r)_{LR} \tag{34}$$

3. Multiplication by a negative real number c

$$cA = (cm, |c|p_r, |c|p_l)_{RL} \tag{35}$$

with interchange of the function L and R in (31) and (32)

$$\mu^l_{cA}(u) = R\Big(\frac{cm - u}{|c|p_r}\Big) \quad \text{for } u \le cm$$

$$\mu^r_{cA}(u) = L\Big(\frac{u - cm}{|c|p_l}\Big) \quad \text{for } u \ge cm$$

In the general case, the interval calculus for the η-cuts can be used to obtain the appropriate operation.

References

Bandemer H (2006) Mathematics of uncertainty. In: Studies in fuzziness and soft computing, vol 189. Springer Verlag, New York

Dubois D, Prade H (1978) Operations on fuzzy numbers. Int J Syst Sci 9:613–626

Dubois D, Prade H (2005) Fuzzy intervals versus fuzzy numbers: is there a missing concept in fuzzy set theory? In: Proc. 25th Linz seminar fuzzy set theory, Linz, Austria

Gillenwater M, Sussman F, Cohen J (2007) Practical policy applications of uncertainty analysis for national greenhouse gas inventories. Water, Air & Soil Pollution. Focus 7(4–5):451–474

Hurteaux MD, Hungate BA, Koch GW (2009) Accounting for risk in valuing forest carbon offset. Carbon Balance and Management 4:1. http://www.cbmjournal.com/content/4/1/1

Jonas M, Nilsson S (2007) Prior to economic treatment of emissions and their uncertainties under the Kyoto protocol: scientific uncertainties that must be kept in mind. Water, Air & Soil Pollution. Focus 7(4–5):495–511

Jonas M, Gusti M, Jęda W, Nahorski Z, Nilsson S (2010) Comparison of preparatory signal detection techniques for consideration in the (post-)Kyoto policy process. Clim Change. doi:10.1007/s10584-010-9914-6

Mignone BK, Hurteau MD, Chen Y, Sohngen B (2009) Carbon offsets, reversal risk and US climate policy. Carbon Balance and Management 4:3. http://www.cbmjournal.com/content/4/1/3

Monni S, Syri S, Pipatti R, Savolainen I (2007) Extension of EU emissions trading scheme to other sectors and gases: consequences for uncertainty of total tradable amount. Water, Air & Soil Pollution. Focus 7(4–5):529–538

Nahorski Z, Horabik J, Jonas M (2007) Compliance and emission trading under the Kyoto protocol: rules for uncertain inventories. Water, Air & Soil Pollution. Focus 7(4–5):539–558

Nahorski Z, Horabik J (2007) Compliance and emission trading rules for uncertain estimates of inventory uncertainty. In: Proc 2nd int workshop on uncertainty in greenhouse gas inventories. IIASA, Laxenburg, pp 149–161

Nahorski Z, Horabik J (2008) Greenhouse gas emission permit trading with different uncertainties in emission sources. J Energy Eng 134(2):47–52

Ramirez AR, de Keizer C, van der Sluijs JP (2006) Monte Carlo analysis of uncertainties in The Netherlands greenhouse gas emission inventory for 1990–2004. Report NWS-E-2006-58. Copernicus Institute for Sustainable Development and Innovation. Utrecht. http://www.chem.uu.nl/nws/www/publica/publicaties2006/E2006-58.pdf

Stern N (2007) The economics of climate change. In: The stern review. Cambridge University Press, Cambridge

Winiwarter W (2004) National greenhouse gas inventories: understanding uncertainties versus potential for improving reliability. Water, Air & Soil Pollution. Focus 7(4–5):443–450

Winiwarter W, Muik B (2007) Statistical dependences in input data of national GHG emission inventories: effects on the overall GHG uncertainty and related policy issues. In: Presentation at 2nd int workshop uncertainty in greenhouse gas inventories, IIASA, Laxenburg, Austria, 27–28 September 2007. http://www.ibspan.waw.pl/ghg2007/Presentation/Winiwarter.pdf

Climatic Change (2010) 103:327–338
DOI 10.1007/s10584-010-9912-8

The impact of uncertain emission trading markets on interactive resource planning processes and international emission trading experiments

Stefan Pickl · Erik Kropat · Heiko Hahn

Received: 5 January 2009 / Accepted: 15 June 2010 / Published online: 21 July 2010

Abstract Interactive resource planning is an increasingly important aspect of emission trading markets. The conferences of Rio de Janeiro, 1992, and Kyoto, 1997, originally focusing on environmental protection at both macro- and micro-economic levels, called for new economic instruments of this kind. An important economic tool in this area is Joint Implementation (JI), defined in Article 6 of the Kyoto Protocol. Sustainable development can be guaranteed only if JI is embedded in optimal energy management. In this contribution we describe and evaluate one international procedure within uncertain markets which helps to establish optimal energy management and interactive resource planning processes within uncertain emission trading markets.

1 Introduction

In Section 2 of this paper we present an overview of the impact of uncertain emission trading markets on interactive resource planning processes. The debate about climate change, Kyoto Protocol, other related agreements, and economic issues, as a basis for further consideration is introduced. Based on these considerations we describe in Section 3 the macro-economic dynamic game model, TEM, which was specifically developed to model an interactive resource planning process. As chaotic behavior may be observed—we describe this phenomenon at the end of Section 3—the aspect of uncertainty comes into play. In the main part of the paper we analyze uncertainty issues related to climate change in general and to economic agreements involving emission trades using the TEM model. We propose the extended interval valued model as a suitable solution procedure. The approach is demonstrated by several simulation applications.

S. Pickl (✉) · E. Kropat · H. Hahn
Universität der Bundeswehr München, 85577, Neubiberg-Munich, Germany
e-mail: stefan.pickl@unibw.de

2 Climate change and the Kyoto Protocol

2.1 The Kyoto Protocol

Since the industrial revolution, which began in around 1800, the burning of fossil fuels has caused a dramatic increase in carbon dioxide (CO_2) in the atmosphere, reaching levels unprecedented since records began. The increase in CO_2 and other greenhouse gas (GHG) emissions has been implicated as a primary cause of global warming (Kyoto 1997a).

The United Nations Framework Convention on Climate Change (UNFCCC) recognizes that the climate system is a shared resource and that its stability can be affected by industrial and other sources of GHG emissions. Its goal is to achieve "stabilization of greenhouse gas concentrations in the atmosphere at a level that would prevent dangerous anthropogenic interference with the climate system" (Article 2). The Convention enjoys near universal membership, with 194 countries having ratified, a notable exception being the United States.

Under the Convention, governments (Kyoto 1997b):

- Gather and share information on greenhouse gas emissions, national policies, and best practices;
- Launch national strategies for addressing greenhouse gas emissions and adapting to expected impacts, including the provision of financial and technological support to developing countries;
- Cooperate in preparing for adaptation to the impacts of climate change.

The 1997 Kyoto Protocol to the UNFCCC entered into force on 16 February 2005, following ratification by Russia on 18 November 2004. Countries ratifying the Protocol commit to reducing their emissions of CO_2 and five other GHGs. The industrialized countries that are signatories to the Kyoto Protocol have agreed to cut their combined emissions to 5% below 1990 levels by 2008–2012, with each country having its own target. Japan's target is to reduce its greenhouse gas emissions by 5% and EU countries by 8%. Some countries with low initial emissions are permitted to increase their emissions. Others, like China and India, which have ratified the Protocol, are not required to reduce carbon emissions under the present agreement.

Under the Convention, the developed country parties in Annex I and developed country parties in Annex II shall take all practicable steps to promote, facilitate and finance, as appropriate, the transfer of, or access to, environmentally sound technologies and know-how to other parties, particularly to developing countries to enable them to implement the provisions of the Convention (Article 4.5) (http://unfccc.int/technology/items/2681.php).

Economists have been trying to investigate the overall net benefit of Kyoto Protocol through a cost–benefit analysis. Just as in the case of climatology, there is disagreement due to large *uncertainties* in economic variables. The Copenhagen Consensus Project established to set priorities among a series of proposals for confronting ten great global challenges, including climate change, looked at three projects addressing climate change (optimal carbon tax, the Kyoto Protocol and value-at-risk carbon tax). The expert panel regarded all three proposals as having costs that were likely to exceed the benefits (Kyoto 1997a).

Estimates to date generally indicate either that (1) observing the Kyoto Protocol is more expensive than not observing the Kyoto Protocol or (2) the Kyoto Protocol has a marginal net benefit which exceeds the economic cost of adjusting to global warming.

2.2 Climate change

Climate change refers to changes in the variability or average state of Earth's atmosphere and global/regional climate over time scales ranging from decades to millennia. These changes are driven both by natural processes and human activities (Kyoto 1997a). In current usage, especially in the context of environmental policy, the term climate change is used to refer only to the ongoing changes in the climate, including the average rise in the Earth's surface temperature known as global warming. Sometimes, the term is also used with a presumption of human causation, for example, in the UNFCCC, which uses *climate variability* when referring to anthropogenic climate variations (Kyoto 1997a).

3 Simulation and analysis of the Kyoto Protocol and its greenhouse gas reduction instruments

3.1 Joint implementation programs and the TEM model

At the United Nations *Conference* on Environment and Development (UNCED) conference in Rio de Janeiro (1992) and the Climate Change *Conference at Kyoto* (1997) there were calls for new and important macro- and micro-economic instruments focusing on environmental protection, including measures to reduce global warming. An important economic tool under the Kyoto Protocol is the Joint Implementation (JI) mechanism (defined in Article 6 of the Kyoto Protocol) whose purpose is to strengthen international cooperation among countries or parties to the Protocol in order to reduce CO_2 and other GHG emissions.

The Joint Implementation mechanism allows a country with an emission reduction or limitation commitment under the Kyoto Protocol (Annex B Party) to earn emission reduction units (ERUs) from an emission-reduction or emission removal project in another Annex B Party. Each ERU is equivalent to 1 tonne of CO_2, which can count toward meeting Kyoto targets. Joint implementation offers Parties a flexible and cost-efficient means of fulfilling a part of their Kyoto commitments, while the host Party benefits from foreign investment and technology transfer (see http://unfccc.int/kyoto_protocol/mechanisms/joint_implementation/items/1674.php).

Sustainable development can only be guaranteed if JI is embedded in optimal energy management. In JI, such a system has to work on the micro level with minimal costs and should be protected against misuse on the macro level. For that reason, the Technology–Emissions–Means (TEM model), was developed by the first author of this paper, to allow simulation of this highly specific economic behavior. TEM considers the case of cooperative economic behavior, including co-funding in joint international projects, as well as the mathematical analysis of several trend scenarios. This leads to new results in the area of cooperative time-discrete dynamic games using discrete optimization techniques and exploiting the underlying combinatorial

structure. The successful implementation of the JI mechanism is subject to technical and financial constraints. Specifically, the concept of JI involves a bilateral or multilateral deal in which countries/operators can sell their unused emission quotas as carbon credits, while businesses that wish to exceed their quotas can buy the extra allowances as credits, privately or on the open market under a cap-and-trade program. The emission reductions resulting from technical cooperation are recorded at the Clearing House which was also established under the Kyoto Protocol.

The TEM model was developed to capture these constraints in an empirically practicable way. The kernel of the TEM model represents an underlying cost game that can be used to determine feasible economic sets describing a range of investments. As the TEM model is based only on empirical parameters, the scenarios can be compared with real data. TEM integrates economic and technical investments in a coupled time-discrete nonlinear (quadratic) system of equations. For instance, the question could be posed: how can the associated cost reductions be allocated in an optimal way? This approach is as well integrated into the TEM model as the possibility of looking at the influence of several cost allocations on the feasible set of control parameters. In the cost game played, a special solution called the "τ value", which stands for a rational allocation process, is examined (Branzei et al. 2005); it was introduced into CO_2 emission control in (Pickl 1999). The main question is: in what situations can the τ value be equivalent to the control parameters needed to reach the regions mentioned in the Kyoto Protocol.

3.2 The formulation of the TEM model

To provide a view of the behavior of the key elements of the Kyoto process, the TEM model describes economic interaction among several players ("actors") that is intended to maximize their reduction of emissions E_i caused by technologies T_i, by expenditure of money or by other financial means M_i. The index stands for the i-th player. The players are linked by technical cooperation and by the market. The effectivity measure parameter em_{ij} describes the effect on the emissions of the i-th player if the j-th actor invests money in the i-th player's technologies. In other words, it expresses how effective technology cooperation (like an innovation factor) is when it is the central element of a JI program (this will be the focus of our *uncertainty* approach in Section 4 for example in comparison to Ermolieva et al. 2010).

The variable φ can be regarded as a memory parameter of the financial investigations, whereas the value λ acts as a growth parameter. For a deeper insight see (Pickl 1999). The TEM model is represented by the following two equations:

$$E_i(t+1) = E_i(t) + \sum_{j=1}^{n} em_{ij}(t)\, M_j(t), \tag{1}$$

$$M_i(t+1) = M_i(t) - \lambda_i M_i(t)\left[M_i^* - M_i(t)\right]\{E_i(t) + \varphi_i \Delta E_i(t).\} \tag{2}$$

Furthermore, we force:

$$0 \le M_i(t) \le M_i^*, i = 1, \ldots, n \text{ and } t = 0, \ldots, N. \tag{3}$$

Additionally we assume:

$$-\lambda_i M_i(t)\left[M_i^* - M_i(t)\right] \le 0 \text{ for } i = 1, \ldots, n \text{ and } t = 0, \ldots, N. \tag{4}$$

We have then guaranteed that $M_i(t+1)$ increases if $E_i(t) + \varphi_i \Delta E_i(t) \leq 0$ and decreases if the term is positive. In the following, it is explained why this is necessary from a practical point of view. A detailed description is contained in Pickl (1999).

3.3 Empirical foundation

At the center of the TEM model is the so-called em-matrix. The possibility of being able to determine the em_{ij}-parameters empirically is a great advantage of the TEM model. The parameters offer a quantitative measure of climate risk under a range of potential outcomes. We now provide a short summary of the TEM model focusing on the problem of uncertainty.

In the first equation of the TEM model, the level of reduced emissions at the t + 1-th time step depends on the previous value plus a market effect. This effect is represented by the additive terms which might be negative or positive.

In general, $E_i > 0$ implies that the actors have not yet reached the demanded value $E_i = 0$ (normalized *Kyoto-level*). A value $E_i < 0$ expresses that the emissions are less than the emission targets set by the Kyoto Protocol. In the second equation we see that for such a situation the financial means will increase, whereas $E_i > 0$ will lead to a reduction of $M_i(t+1)$. The second equation contains the logistic functional dependence and the memory parameter φ which describes the effect of the preceding investment of financial means.

The dynamics does not guarantee that the parameter $M_i(t)$ lies in the interval, which can be regarded as a budget for the i-th actor. For that reason we have to impose the following additional restrictions on the dynamical representation:

$$0 \leq M_i(t) \leq M_i^*, i = 1, \ldots, n \text{ and } t = 0, \ldots, N. \tag{5}$$

These restrictions ensure that the financial investigations can neither be negative nor exceed the budget of each actor. Now, it is easy to show that:

$$-\lambda_i M_i(t)\left[M_i^* - M_i(t)\right] \leq 0 \text{ for } i = 1, \ldots, n \text{ and} \tag{6}$$

We have guaranteed that $M_i(t+1)$ increases if $E_i(t) + \varphi_i \Delta E_i(t) \leq 0$ and it decreases if the term is positive. Applying the memory parameter φ, we have developed a reasonable model for the money expenditure–emission interaction, where the influence of the technologies is integrated into the em-matrix of the system.

3.4 The control model: forecasting and scenario development

We can use the TEM model as a time-discrete model in which we start with a special parameter set and observe the resulting trajectories. Scenarios can be built using such an approach; several different situations can be compared. Usually, the actors start with a negative value (i.e., a value that is under the Kyoto Protocol baseline) and try to reach a positive value of E_i. By adding control parameters, we enforce this development by an additive financial term. For that reason the control parameters are added to the second equation of our model:

$$M_i(t+1) = M_i(t) - \lambda_i M_i(t)\left[M_i^* - M_i(t)\right]\{E_i(t) + \varphi_i \Delta E_i(t)\} + u_i(t). \tag{7}$$

The introduction of the control parameter $u_i(t)$ implies that each actor makes an additional investigation at each time step. In terms of environmental protection, the

aim is to choose the control parameters to reach a state, mentioned in the Kyoto Protocol, in which the emissions of each player are minimized. For details and the treatment as an approximation problem see Krabs and Pickl (2003). Approximation means that the solution will be approximated numerically.

The solution is the realization of the necessary optimal control parameters via a played cost game, which is determined through actor cooperation. We shall first discuss where and how this aspect can be integrated into the TEM model. For the analysis of uncertainty questions it may be necessary to integrate a qualitative measure under a range of potential outcomes. If the em_{ij}-parameters vary, this approach allows analysts to use this model to simulate potential financial behavior and the risk of different policies in the electricity sector. First numerical examples are in Pickl (1999).

3.5 Chaotic behavior

The numerical examinations which show that chaotic behavior can occur, emphasize the necessity for a control theoretic approach, which is implied by an additional control term in the second equation of the TEM model. In terms of environmental protection, the aim is to reach a state mentioned in the Kyoto Protocol by choosing the control parameters such that the emissions of each player are minimized. The focal point lies in the realization of the necessary optimal control parameters via a played cost game, determined through cooperation among the actors (Pickl 2002). According to the Kyoto Protocol, this approach means that each actor invests additional financial means. There are now several possible ways of solving the problem of controllability to increase the effectiveness of the instruments.

4 Measures of effectiveness

The Kyoto Protocol calls for reductions in GHGs by industrialized countries. On the other hand, the energy consumption of developing countries is increasing, leading to growing GHG levels. The preparation of an optimal management tool in that field requires several technological options to be identified, assessed, and compared.

The TEM mathematical model was elaborated to address this challenge. In line with the Kyoto Protocol, control parameters were incorporated into the model that have to be determined iteratively, depending on the negotiation process. The model integrates economic and technical investments within a coupled time-discrete nonlinear (quadratic) system of equations. The iterative solution of the TEM model, with implied time-discrete control variables, aims to successfully overcome the occurrence of chaotic behavior in the TEM model and, as a result, improve projections so as to better guide decision makers working toward sustainable development (Pickl 2002; Nahorski and Horabik 2010).

While environmental problems are among the main challenges of the twenty-first century, there are few innovative allocation principles for investments. Several approaches from game theory on this topic may be found. In addition, the improvement of technical *effectivity* through JI cooperation is attracting great interest. The TEM model to provide opportunities to combine these two aspects.

Both problems are concerned with uncertainty issues:

- Uncertainty in the building of Joint Implementation partnerships
- Uncertainty in the technical parameters (measures of effectivity)

We will overcome this uncertainty by characterizing stable/unstable regions. Stability reflects the fact that uncertainty does not have a major influence/impact. In the following section, we describe the TEM model and show how it can help us understand the uncertainty aspect in the Kyoto process.

4.1 The interval valued model

The TEM model presented in Section 3.2 depends on crisp data. To include various kinds of errors and uncertainty of both states and parameters, an interval-valued approach has been introduced and analyzed (Weber et al. 2009a, b). Here, uncertain states and parameters are represented by intervals. Aiming at time-discrete dynamics, the TEM model can firstly be structured in the following way:

$$\begin{pmatrix} E \\ M \end{pmatrix}^{(k+1)} = M^{(k)} \left(\begin{pmatrix} E \\ M \end{pmatrix}^{(k)} \right) \begin{pmatrix} E \\ M \end{pmatrix}^{(k)}. \tag{8}$$

Having added the control parameter, we obtain the time-discrete dynamics:

$$\begin{pmatrix} E \\ M \end{pmatrix}^{(k+1)} = M^{(k)} \left(\begin{pmatrix} E \\ M \end{pmatrix}^{(k)} \right) \begin{pmatrix} E \\ M \end{pmatrix}^{(k)} + \begin{pmatrix} 0 \\ u^k \end{pmatrix}, \tag{9}$$

which can be represented by:

$$(D\varepsilon)\, \mathrm{E}^{(k+1)} = \mathrm{M}^{(k)} \mathrm{E}^{(k)}. \tag{10}$$

Here, the matrices $\mathrm{M}^{(k)}$ incorporate the control variables.

In these extended space notations, the variable E and entire dynamics $(D\varepsilon)$ could be enriched by further environmental, technical, and financial items and relations. The shift vector $\left(0^T, \left(u^{(k)}\right)^T\right)^T$ can be regarded as parametric and as a realization of $V\left(E, \overset{\vee}{E}^{v}\right)$; then regions of stability and instability can be determined (Weber et al. 2009a, b). According to how those matrices (which express the uncertainty behavior) are adjusted, we arrive at different behaviors of stability or instability of $(D\varepsilon)$ in the sense of dynamical systems or of parameter estimation. As an alternative to the feedback-like realization by the vector $V\left(E, \overset{\vee}{E}^{v}\right)$ which becomes incorporated into the matrix $\mathrm{M}^{(k)}$, the control vectors $u^{(k)}$ could also become integrated into $\mathrm{E}^{(k)}$. The time-dependent parameters $em_{ij}^{(k)}$ can then, like the controls, be treated in similar ways. Each $\mathrm{M}^{(k)}$ is an element of a finite set of interval matrices and the optimized outcome of a time-discretization. Some of the parameters are estimated by means of a (generalized) Chebychev approximation and GSIP (Weber et al. 2009a, b). With the remaining set of parameters, we represent and study different economic and decision scenarios. For a deeper discussion of regulatory systems under uncertainty and further details about the related stability analysis we refer to the literature

(Weber et al. 2009a, b; Kropat et al. 2008). In our future work, we plan to integrate other representations of errors in terms of stochastic dependencies like Winiwarter and Muik (2010) and set theoretic aspects.

4.2 Simulation

The aim of the TEM model is to understand emission reduction activities and thereby to reduce countries' CO_2 emissions in line with the Kyoto Protocol. This refers to real-world processes with all their uncertainties, but until now research using the TEM model has been conducted using exact data (see, for example, TEMPI software, Fig. 1).

The software solution allows the uncertainties to be reconsidered as intervals. This leads to a very elegant way of modeling and simulating the uncertainty aspects within the Kyoto Protocol. The operator may vary the different parameter interactively (i.e., he can examine certain intervals for different values).

In the following section, uncertainty in general *transaction* relationships is discussed. We will conclude by stating that the integration of uncertainty aspects will become increasingly important for economic theory in the future, and we will accordingly integrate market characteristics into the TEMPI simulation software. We thus conclude with an outlook on *Uncertainty in general transaction* relationships.

4.3 Uncertainty in general transaction relationships

In the following, we focus on the problem of uncertainty which is inherent in many transaction relationships. Seen from a very general perspective, the problem of uncertainty arises because of the division of labor. As shown by Adam Smith, we all gain by specializing in what we can do best. However, we also depend on the outcome of other peoples' work (i.e., there needs to be technical and economic coordination

Fig. 1 Interactive software TEMPI (Technology Emissions Means Process Identification)

for a successful joint outcome). As a transition from one production stage to another causes friction, the interfaces between the different stages need to be managed. From the perspective of neoclassical economics, the currently dominant economic theory, there is no real coordination problem in the first place because there is no uncertainty, or if there is, it is of a very specific type. Referring to a distinction elaborated in Knight's (1921) dissertation, there can be either risk or uncertainty about the outcome of an event, and this has a (known) influence on the value of an economic activity like an investment. In the case of risk, we are dealing with the problem of randomness in the outcome, but we do know the probabilities involved. In the case of uncertainty, we are faced with the problem that we have no knowledge about the probabilities of the outcome. For normal neoclassical analysis, we are dealing either with deterministic outcomes or with risk and not with uncertainty. Even though the need to make a decision under uncertainty may be a difficult starting point for neoclassical analysis, it is a long way from being the worst case.

In a general and rather critical discussion of the treatment of uncertainty in neoclassical economic analysis, Langlois (1984) discusses two distinct kinds of uncertainty, that is, parametric and structural uncertainty. In the case of parametric uncertainty, we do know all the parameters of the decision problem, though not their probabilities. However, in the case of structural uncertainty we are faced with the more fundamental problem that we do not know the structure of the decision problem in the first place. Many parameters that could have a decisive influence on the outcome may only show up in later stages as the future unfolds, but may be completely unknown and unknowable at the outset. Going back to the problem of the coordination of different economic agents, economic theory knows several coordination mechanisms of which markets or hierarchies are the extremes, with cooperative and network organizations being examples of intermediate forms. Every form has not only advantages but also preconditions for being appropriate for certain situations. Derived from the analysis of contract law by MacNeil (1978), which also influenced Williamson's version of transaction cost economics, we can apply three criteria for analyzing the "marketness" of transaction relationships: presentation (i.e., completeness of ex ante coordination) discreteness of transactions, and (the possibility of) anonymity of the partners to a transaction.

The first criterion of presentation considers the possibility of comprehensively specifying the contract so that if it fails to materialize, remedies are easily found and sanction mechanisms enforced.

The second criterion, discreteness, refers to the interdependence between different transactions (i.e., if the different transactions are undertaken one by one, or if the first transaction already determines future transactions). The last criterion, anonymity, analyzes the relevance of the identity of the partners to a transaction.

For market transactions, the identity is of little importance because the service or product provider can be replaced to ensure that the criteria for the specification of the product are fulfilled. Thus, in a sense, only the first criterion is of consequence (Table 1) and compares the characteristics of market and non-market relationships, as described by the three criteria. For non-market relationships we face the situation that the criteria are not met and what is described in the table is either the effect of or the reaction to the uncertainty that arises or that causes it.

Taking the first criterion as a case in point, a lack of comprehensive specification tools makes a comprehensive specification impossible to reach. The hypothetical

Table 1 Characteristics of market and non-market transactions

Criteria	Market	Non-market
Presentation	Comprehensive specification tools	Specification after the signing of the contract
	Enforceable sanction mechanism	Iterative specification
Discreteness	Independent purchases	Carry-over effects
	No binding effect because of past transactions	Lock-in because of past transactions
		"Power asymmetry"
Anonymity of market participants	Who offers service/products has no relevance	Product/service provider differ in terms of competence/quality
	Trust in the institutional setting of the market place (e.g., sanction mechanism)	Trust in the relationship

market for a product potentially exchanged in it, in a sense, lacks the necessary specification infrastructure in terms of a body of shared standards. To be able to communicate with the seller, the firm that wishes to buy a product needs to know: (1) what the specification provided with the product offered in a market means, and (2) what kind of specification requirements the product (e.g., a high value component for a larger system) has to meet, given the specific demands of the firm. Hence, the customer needs to translate his or her needs into a specification language and compare it with the information that is provided along with the components. This information has to be specified or codified in the same specification language or at least in one the buyer is able to understand. Furthermore, the specification language must cover all the information that is important for that customer. Otherwise, an alternative medium (e.g., intensive business and long-lasting learning relationships or the use of system integrators) is needed to transmit this information which raises information and transaction costs for assessing qualities others than those covered by, for example, a specification standard. The less structured the technological dialog in a special domain is, the more likely there is to be a "semantic mismatch" and uncertainty because of possible incompatibilities arising. However, such specification languages (i.e., comprehensive standardization schemes) can be considered as the shared contractual infrastructure of the market place and must be provided by the market place or as a public good by the commercial community using such new markets. Nevertheless, before firms can agree on shared concepts underlying the specification language, they must be able to make their knowledge explicit and translate and codify it into a specification language that allows them and their business partners to communicate all relevant aspects. This is very important as, for example, emission trading markets are just at a constitutional phase.

Codification for a structured exchange to reduce the friction between different vendors, to increase the division of labor is often difficult to achieve, and there is a lively debate about the drivers and inhibitors of "knowledge codification" (c.f. and for different views on the codification debate, see Cowan et al. 2000 and Nightingale 2003). From the perspective of institutional economics, historically, the main condition for market-like transactions has been to embed transactions in an institutional framework. Institutions can be defined as "the humanly devised constraints that structure human interaction. They are made up of formal constraints

(e.g., rules, laws, standards) and informal constraints (e.g., norms of behavior, conventions, self-imposed codes of conduct), and their enforcement characteristics." The economic raison d'être of institutions is therefore that they reduce uncertainty by providing a more structured interaction between economic agents so that some stable expectations about the economic outcome and the behavior of the transaction partners can be formed. As Coase (1988) points out, coordination situations that come closest to the ideal of perfect markets (e.g. commodity and stock exchanges) are, in fact, highly regulated by the underlying institutional framework in which the transactions are embedded.

5 Conclusions

In this short discussion about the problem of uncertainty in transaction relationships, we have presented different understandings of uncertainty and related concepts (risk, parametric, and structural uncertainty) and the relationship with the coordination problem that arises because of the division of labor. We have then discussed markets as a coordination mechanism. Markets, however, presuppose a very structured and well defined exchange process. To reach such a state of maturity (see also Shvidenko et al. 2010), a body of standards as "contract infrastructure" is necessary.

We briefly discussed the knowledge codification aspect of establishing such an infrastructure and finished the discussion by presenting a decision process about the appropriate coordination mechanism to use based on the ability of the institutional infrastructure to reduce the uncertainty to an acceptable level. The less uncertainty there is, the more likely a market transaction is. High levels of uncertainty favor more cooperative transaction relationships. The decision to control the production process instead might be another option as long as it was justified by the relevance of the products and the costs involved. The establishment and constitution of emission trading markets will be influenced by such mechanisms. Together with the mathematical TEM model and the TEMPI software (which enables interactive decision support and the design of economic experiments in the context of Kyoto Protocol, Grabner et al. 2009), the aspect of uncertainty might be better understood; nevertheless, it is only a first approach toward a comprehensive understanding of uncertainty and, in a second step, toward successfully dealing with it.

References

Branzei R, Dimitrov D, Tijs S (2005) Models in cooperative game theory, crisp, fuzzy, and multi-choice games. Springer, Berlin

Coase RH (1988) The firm, the market, and the law. University of Chicago Press, Chicago, pp 1–31

Cowan R, David PA et al (2000) The explicit economics of knowledge codification and tacitness. Ind Corp Change 9(2):211–253

Ermolieva T, Ermoliev Y, Fischer G, Jonas M, Makowski M, Wagner F (2010) Carbon emission trading and carbon taxes under uncertainties. Clim Change. doi:10.1007/s10584-010-9910-x

Grabner C, Hahn H, Leopold-Wildburger U, Pickl S (2009) Analyzing the sustainability of harvesting behaviour and the relationship to personality traits in a simulated Lotka–Volterra biotope. Eur J Oper Res 193(3):761–767

Knight FH (1921) Risk, uncertainty and profit. Houghton Mifflin, Boston

Krabs W, Pickl S (2003) Controllability of a time-discrete dynamical system with the aid of the solution of an approximation problem. Control Cybernetics 32(4):57–74

Kropat E, Weber G-W, Akteke-Öztürk B (2008) Eco-finance networks under uncertainty. In: Proceedings of the international conference on engineering optimization, EngOpt 2008, Rio de Janeiro, Brazil (ISBN 978857650156, CD)

Langlois RN (1984) Internal organisation in a dynamic context: some theoretical considerations. In: Jussawalla M, Ebenfield H (eds) Communication and information economics: new perspectives. Elsevier, Amsterdam, pp 23–49

MacNeil IR (1978) Contracts: adjustment of long-term economic relations under classical, neoclassical, and relational contract law. Northwest Univ Law Rev 72(6):854–905

Nahorski Z, Horabik J (2010) Compliance and emission trading rules for asymmetric emission uncertainty estimates. Clim Change. doi:10.1007/s10584-010-9916-4

Nightingale P (2003) If Nelson and Winter are only half right about tacit knowledge, which half? A searlean critique of 'codification'. Ind Corp Change 12(2):149–183

Pickl S (1999) Der τ-value als Kontrollparameter. Modellierung und analyse eines joint-implementation programmes mithilfe der kooperativen dynamischen Spieltheorie und der diskreten Optimierung. Shaker, Aachen (in German)

Pickl S (2002) An iterative solution to the nonlinear time-discrete TEM model—the occurrence of chaos and a control theoretic algorithmic approach. AIP Conf Proc 627(1):196–205

Shvidenko A, Schepaschenko D, McCallum I, Nilsson S (2010) Can the uncertainty of full carbon accounting of forest ecosystems be made acceptable to policymakers? Clim Change. doi:10.1007/s10584-010-9918-2

Weber G-W, Alparslan-Gök SZ, Söyler B (2009a) A new mathematical approach in environmental and life sciences: gene-environment networks and their dynamics. Environ Model Assess 14(2):267–288. doi:10.1007/s10666-007-9137-z

Weber G-W, Kropat E, Akteke-Öztürk B, Görgülü Z-K (2009b) A survey on OR and mathematical methods applied on gene-environment networks. Cent Eur J Oper Res 17(3):315–341. doi:10.1007/s10100-009-0092-4 (special issue on "innovative approaches for decision analysis in energy, health, and life sciences")

Winiwarter W, Muik B (2010) Statistical dependence in input data of national greenhouse gas inventories: effects on the overall inventory uncertainty. Clim Change. doi:10.1007/s10584-010-9921-7

Lessons to be learned from uncertainty treatment: Conclusions regarding greenhouse gas inventories

M. Jonas,[1*] G. Marland,[2] W. Winiwarter,[3,1] T. White,[4] Z. Nahorski,[5] R. Bun,[6] S. Nilsson[1]

[1] International Institute for Applied Systems Analysis, Laxenburg, Austria
[2] Carbon Dioxide Information Analysis Center, Oak Ridge National Laboratory, Oak Ridge, TN, USA
[3] AIT Austrian Institute of Technology, Vienna, Austria
[4] B.C. Ministry of Environment, Victoria, Canada
[5] Systems Research Institute, Polish Academy of Sciences, Warsaw, Poland
[6] Lviv Polytechnic National University, Lviv, Ukraine
* Corresponding author: Dr. Matthias Jonas, IIASA, Schlossplatz 1, A-2361 Laxenburg, Austria; Tel: +43-2236-807-430; Fax: +43-2236-807-599; jonas@iiasa.ac.at

When assembling the 17 papers for this volume, the editors decided to put together general concluding thoughts on dealing with uncertainty in emission inventories. There is a wealth of research in this volume, and this has encouraged us to present both the systematic classification of contributions that is included in our introductory paper and also—here—a comprehensive overview of uncertainty treatment that contains broad take-home messages. It is hoped that this concluding perspective will help readers focus on the benefits, for science and for policy, of properly covering uncertainty.
In addition to the knowledge assembled in this book, we use several very recent events and publications to articulate this wider perspective. In particular, we consider:

- The 3rd International Workshop on Uncertainty in Greenhouse Gas Inventories, held 22–24 September 2010, in Lviv, Ukraine (http://ghg.org.ua/);
- The sixteenth Conference of the Parties (COP16) and the sixth Conference of the Parties serving as the Meeting of the Parties to the Kyoto Protocol (CMP6), held 29 November to 10 December 2010, in Cancún, Mexico; and
- Key articles published in the recent technical literature.

Our big picture comprises six take-home messages. These are outlined below, along with a short discussion of the outcomes we expect from each of them.

1. It must be clear beyond controversy that the Earth's atmosphere will benefit from actions taken to reduce greenhouse gas (GHG) emissions. When we tackle the problem of accounting for GHG emissions, we have to take the position of an observer of the atmosphere. That is, ultimately, the accounting must be top-down and reductions in emissions must be reflected in reductions in atmospheric GHG concentrations. This is in line with the more general challenge put forward by Reid et al. (2010) of developing, enhancing, and integrating appropriate observation systems into efforts to manage global and regional environmental change (see also Canadell et al. 2010; NRC 2010; WMO 2010). There are two main comments to make here.

   (i) We must accept that bottom-up accounting for GHG emissions, the approach that we currently use, is incomplete (e.g., Gregg 2010). Our bottom-up accounting for emissions is important in the sense that it shows which activities and which actors are responsible for emissions. Moreover, bottom-up accounting will be subject to

continued revision in the future and must remain flexible. However, this perception of emissions does run counter to the objectives of the emission trading schemes that have been put in place to date. To produce the desired results, these emission trading schemes need to be anchored, not least legally, within a reference system, and this is not the case with current bottom-up accounting. Emission permits by country, which the country can sell at a given point in time but whose number changes subject to continuous revisions in the estimates, fall outside conventional economic thinking. As traders have insufficient expertise to second-guess how emission markets have been designed, they must trust that the experts have set up a system that achieves real emission cuts so that the market can get on and do its job, namely deliver emission reductions at least cost. Traders have no need to understand the science, or even to believe in it, in order to trade in the market (Pearson 2010). This shortcoming between theory and practice has still not been resolved.

(ii) It is anticipated that within a few years scientists will be able to further narrow the gap that still exists between bottom-up and top-down accounting for Kyoto GHG emissions at the scale of continents. Scientists may even be able to downscale verified (dual constrained) emission estimates for countries or groups of countries. In other words, scientists will be able to detect incomplete or inappropriate accounting data reports submitted under the Kyoto Protocol or any successor (Jonas et al. 2009) well beyond current review procedures, which are limited to establishing consistency and the fulfillment of formal requirements and which, at best, permit bottom-up validation to be achieved.

2. It must be clearly understood that Earth's ecology, in contrast with our built environment (technosphere), acts as a complex and nonlinear system that is full of surprises and in a constant state of change. This system can be best understood over a long-term perspective (Seitzinger 2010).
   Consequently, we should not expect to be able to utilize nature to reduce GHG emissions in the same way that we can use technospheric opportunities. To avoid surprises we need to exercise caution in superposing subsystems with different emission-dynamic and uncertainty characteristics as, for example, in the energy system and in the terrestrial biosphere (see, e.g., Jonas and Nilsson 2007).

3. Experience shows that uncertainty analysis should be used to develop clear understanding and informed policy in the framing of international environmental agreements.
   To ensure that uncertainty analysis becomes a key component of national GHG inventory analysis in support of international environmental policy, advanced guidance is needed so that uncertainty can be dealt with appropriately, that is, in an internationally standardized way across countries, subsystems, sources and sinks, GHGs, and sectors. We recognize that the IPCC methodologies clearly stress the value of conducting uncertainty analyses and offer guidance on executing them, but the sort of guidance that we refer to must go well beyond current efforts.

4. It must be acknowledged that uncertainty is inherently higher for some GHGs and some sectors of an inventory than for others. The land use, land-use change, and forestry (LULUCF) sector and the landfill sector, for example, have higher uncertainties than the fossil fuel sector; and current estimates of nitrous oxide (N_2O) emissions are more uncertain than those of methane (CH_4) and carbon dioxide (CO_2). This raises the option that in designing future policy agreements some components of a GHG inventory could be treated differently from others.

The approach of treating subsystems individually and differently would allow emissions and uncertainty to be looked at simultaneously and would thus allow for differentiated emission reduction policies. This approach could have an advantage over treating all GHG emissions and removals collectively (i.e., in terms of CO_2-equivalence), which usually leads to increased uncertainty with potentially important scientific and policy implications. Under the Kyoto Protocol the agreed emission changes for most countries are of the same order of magnitude as the uncertainty that underlies their combined emission estimates. This renders compliance difficult to establish, especially in cases where countries claim that their commitments to reduce or limit emissions have been fulfilled.

It must be noted, however, that a differentiated approach would run counter to the emissions-only approach currently being followed. Under the current emissions-only approach, subsystems are treated collectively and equally (i.e., without distinction to their emission-dynamic and uncertainty characteristics), as well as over a wide range of mitigation options. This is intended to minimize costs or maximize benefits resulting from the joint reduction of GHG emissions, possibly in combination with air pollutants (e.g., Amann 2009). Not all emissions of GHGs and/or air pollutants are equally expensive to reduce. If emissions are restricted in a manner that allows flexibility, the least costly reductions tend to be undertaken first (e.g., CBO 2009).

5. Any differentiated approach to accounting must form a logical subset of a full GHG accounting approach. Full accounting is the only way to reach a proper understanding of the global climate system and is a prerequisite for reducing the uncertainties in that understanding.

   Providing reliable and comprehensive estimates of uncertainty cannot necessarily be achieved by applying the current approach under the UNFCCC and Kyoto Protocol, which provide for only partial accounting of GHG fluxes to and from the atmosphere. It is virtually impossible to estimate the reliability of any system output if only part of the system is considered.

6. The option of treating subsystems individually and differently, while at the same time following full GHG accounting, forces us to deal with subsystems more skillfully than we have in the past. The maxim to follow would be to treat both the technosphere and the biosphere individually but also holistically.

   Dealing with technosphere and biosphere individually and differently, although not independently, leads to agreement bifurcation but has clear advantages for emission inventories. First, it does not jeopardize verification—atmospheric measurements can discriminate between fossil-fuel, terrestrial biosphere, and ocean carbon by means of their carbon isotope fingerprints in combination with measurement of atmospheric O_2; but they cannot identify individual fluxes within any of these categories (e.g., Battle et al. 2000). Second, it offers the option of i) placing emissions from the technosphere, where uncertainty is believed to be smallest, under stringent compliance with clear rules for dealing with uncertainty, while ii) putting biospheric emissions and removals, with their greater uncertainties, under consistent reporting by means of a global monitoring framework.

   But the consequences for political action are demanding. Subsystem approaches that are believed attractive—for example, reducing emissions from deforestation and forest degradation (REDD; see, e.g., http://unfccc.int/methods_science/redd/items/4531.php)—should best be pursued if there is a master plan in existence for transforming these subsystem approaches into global full-system approaches. If we fail to meet this condition, it would

mean giving up (dual-constrained) verification as a scientific—and political—tool for controlling GHG emissions. In the case of REDD such a master plan, based on sound science and policy, has never existed and will most likely not exist in the foreseeable future. REDD will, at best, be controlled top-down with the help of instruments that measure surface-related (structural) parameters such as area and type of vegetation. However, what would be needed for dual-constrained verification are top-down observation systems that directly, not indirectly, measure flux-related (functional) parameters, such as ecosystem exchange, independently from any surface-related parameters. Even if the two tracks are in place and are applicable, they would need to be able to be compared one-to-one in terms of resolution—spatio-temporally and thematically—for the global full-systems picture to be achieved. The most likely outcome to expect is claims being made that GHG removals have been realized under REDD, with the global full-systems view at the same time seeing the overall terrestrial biosphere in toto differently, or even as a source of GHG emissions. Acceptance of REDD, therefore, is likely to require lower standards for acceptance of uncertainty in monitoring without any immediate prospect of scientific (top-down) verification.

By way of contrast, a subsystem approach related to country-specific emissions from the technosphere appears to be much more promising in terms of transformation into a global full-systems approach. Technospheric emissions are sky-rocketing; they involve uncertainties that are smaller and have scientific obstacles that are less fundamental from the scientific viewpoint; and approximate solutions can be found that, though insufficient, are not inconsistent and would still guarantee success. Gregg (2010), for example, suggests such an approximate step as an initial goal: uncertainties of less than 10 percent for the top 20 emitting countries (about three-quarters of global fossil-fuel CO_2 emissions) and less than 50 percent for the rest of the world. This goal could be achieved if countries had a more systematic, transparent, and standardized method for reporting energy consumption (and uncertainty, for that matter) and if international assistance in data collection were to be more readily available. Not least, it would be a realistic goal, not only scientifically but also politically.

Acknowledgements

This book was made possible through the generous financial support of the Polish Member Organization to IIASA.

References

Amann M (2009) Air pollutants and greenhouse gases – Options and benefits from co-control. In: Pleijel H, Karlsson PE, Simpson D (eds) Air pollution & Climate Change. Two sides of the same coin? Swed. Environ. Prot. Agency, Stockholm, Sweden, 99–108. ISBN: 978-91-620-1278-6

Battle M, Bender ML, Tans PP, White JWC, Ellis JT, Conway T, Francey RJ (2000) Global carbon sinks and their variability inferred from atmospheric O_2 and $\delta^{13}C$. Science 287(5462), 31 March:2467–2470. doi:10.1126/science.287.5462.2467

Canadell JG, Ciais P, Dhakal S, Dolman H, Friedlingstein P, Gurney KR, Held A, Jackson RB, Le Quéré C, Malone EL, Ojima DS, Patwardhan A, Peters GP, Raupach MR (2010) Interactions of the carbon cycle, human activity, and the climate system: a research portfolio. Curr Opin Environ Sust 2(4):301–311. doi:10.1016/j.cosust.2010.08.003

CBO (2009) The costs of reducing greenhouse-gas emissions. Economic and Budget Issue Brief, Congressional Budget Office (CBO), 23 November. Available at: http://www.cbo.gov/ftpdocs/104xx/doc10458/11-23-GreenhouseGasEmissions_Brief.pdf

Gregg J (2010) Counting carbon. Chinadialogue, 3 December. Available at: http://www.chinadialogue.net/article/show/single/en/3978-Counting-carbon

Jonas M, Nilsson S (2007) Prior to economic treatment of emissions and their uncertainties under the Kyoto Protocol: Scientific uncertainties that must be kept in mind. Water Air Soil Pollut: Focus. doi:10.1007/s11267-006-9113-7

Jonas M, White T, Marland G, Lieberman D, Nahorski Z, Nilsson S (2009) Dealing with uncertainty in GHG inventories: How to go about it? In: Marti K, Ermoliev Y, Makowski M (eds) Coping with Uncertainty: Robust Solutions. Springer, Berlin, Germany, 229–245. ISBN: 978-3-642-03734-4

NRC (2010) Verifying greenhouse gas emissions. National Research Council of the National Academies, National Academic Press, Washington, D.C., USA, pp 110. ISBN: 978-0-309-15211-2

Pearson NO (2010) Carbon math doesn't compute when scientists check gases in air. Bloomberg Businessweek, 22 November. Available at: http://www.businessweek.com/news/2010-11-22/carbon-math-doesn-t-compute-when-scientists-check-gases-in-air.html

Reid WV, Chen D, Goldfarb L, Hackman H, Lee YT, Mokhele K, Ostrom E, Raivio K, Rockström J, Schellnhuber HJ, Whyte A (2010) Earth system science for global sustainability: grand challenges. Science 330(6006), 12 November:916–917. doi:10.1126/science.1196263

Seitzinger S (2010) A sustainable planet needs scientists to think ahead. Nature 468(7324), 1 December:601. doi:10.1038/468601a

WMO (2010) Implementation plan for the global observing system for climate in support of the UNFCCC (2010 update). GCOS-138, World Meteorological Organization, Geneva, Switzerland, pp 180. Available at: http://www.wmo.int/pages/prog/gcos/Publications/gcos-138.pdf